LEABHARLANN CHOLÁISTE NA TRÍONÓIDE, BAILE ÁTHA CLIATH | TRINITY COLLEGE LIBRARY DUBLIN
Ollscoil Átha Cliath | The University of Dublin

Terms and Conditions of Use of Digitised Theses from Trinity College Library Dublin

Copyright statement

All material supplied by Trinity College Library is protected by copyright (under the Copyright and Related Rights Act, 2000 as amended) and other relevant Intellectual Property Rights. By accessing and using a Digitised Thesis from Trinity College Library you acknowledge that all Intellectual Property Rights in any Works supplied are the sole and exclusive property of the copyright and/or other IPR holder. Specific copyright holders may not be explicitly identified. Use of materials from other sources within a thesis should not be construed as a claim over them.

A non-exclusive, non-transferable licence is hereby granted to those using or reproducing, in whole or in part, the material for valid purposes, providing the copyright owners are acknowledged using the normal conventions. Where specific permission to use material is required, this is identified and such permission must be sought from the copyright holder or agency cited.

Liability statement

By using a Digitised Thesis, I accept that Trinity College Dublin bears no legal responsibility for the accuracy, legality or comprehensiveness of materials contained within the thesis, and that Trinity College Dublin accepts no liability for indirect, consequential, or incidental, damages or losses arising from use of the thesis for whatever reason. Information located in a thesis may be subject to specific use constraints, details of which may not be explicitly described. It is the responsibility of potential and actual users to be aware of such constraints and to abide by them. By making use of material from a digitised thesis, you accept these copyright and disclaimer provisions. Where it is brought to the attention of Trinity College Library that there may be a breach of copyright or other restraint, it is the policy to withdraw or take down access to a thesis while the issue is being resolved.

Access Agreement

By using a Digitised Thesis from Trinity College Library you are bound by the following Terms & Conditions. Please read them carefully.

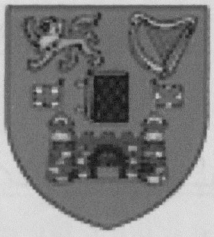
I have read and I understand the following statement: All material supplied via a Digitised Thesis from Trinity College Library is protected by copyright and other intellectual property rights, and duplication or sale of all or part of any of a thesis is not permitted, except that material may be duplicated by you for your research use or for educational purposes in electronic or print form providing the copyright owners are acknowledged using the normal conventions. You must obtain permission for any other use. Electronic or print copies may not be offered, whether for sale or otherwise to anyone. This copy has been supplied on the understanding that it is copyright material and that no quotation from the thesis may be published without proper acknowledgement.

Synthesis and physical studies of luminescent lanthanide and colorimetric chemosensors for ions and molecules

By

Joseph Leonard, B.Sc., M.Sc.

January 2003



University of Dublin
Trinity College

Based on research carried out under the direction of Dr. Thorfinnur Gunnlaugsson

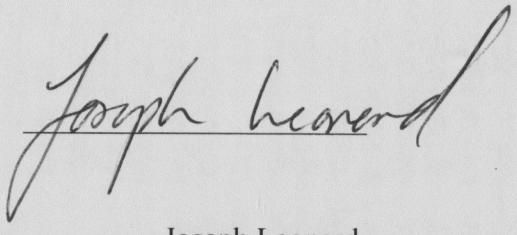
A thesis submitted to the Department of Chemistry, University of Dublin, Trinity College in fulfillment of the requirements for the degree of Doctor of Philosophy.

TRINITY COLLEGE
0 3 JUL 2003
LIBRARY DUBLIN
THESIS
~~7431~~
7342.

Declaration

This thesis is being submitted for the degree of Doctor of Philosophy in the University of Dublin, Trinity College, Dublin and has not been submitted before for any degree or examination in this or any other University. Except where acknowledgement is given, all work described is original and carried out by the author alone.

I give permission for the Library to lend or copy this thesis upon request.



Joseph Leonard

To all my Family

Acknowledgements

I would like to take this time to acknowledge and thank the many people who have helped or inspired me in the last three years or so. Firstly I would like to give a big thank you to all the members of the Gunnlaugsson research group, past and present. Claire, Caroline and Mark, the pioneers of the group who afforded me much assistance in the beginning when I was a bit rusty after my long absence from lab work. A big thank you must also go to Aoife and Sinead, who started with me back in 1999 and to the new crew emerging in the lab, Raman, Jilly, Andrew, Anne-Marie, Lin, and Lisa. Sincerest thanks definitely has to go to our Post doc contingent of Celine, Fred and Julie, you were all a great help especially in the final weeks when the pressure was on. Finally to the Big Boss himself, Thorri, thanks for all your support and motivation provided and the great trip to Switzerland, any more trips would be greatly appreciated.

I would like to thank the Department of Chemistry for all their help and assistance. To Corinne, Tess and Helen for there help in the many request made over the last three years. To the technicians in the Cocker lab and especially Martin and Patsy in the physical chemistry lab for their friendly and professional manner which made the job of demonstrating a bearable experience. Thank you to Theresa Mc Donald for her assistance in the many purchasing requests and quires that helped greatly in keeping my project on schedule. A big thank also must go to the many technical support staff, namely, John, Brendan, Paul, and Martin who on many occasions came to the rescue of our research group with their much appreciated technical talents. The biggest thanks must definitely be paid to Fred and Eddie in their limitless efforts in the chemistry stores.

Thanks to Dr. John O Brien for the NMR services provided and for teaching me to use the 400 myself and a big thank you to Martin Feeney for running my ESMS samples in the early days and for training me to run it myself. During my time in TCD all my X-ray crystallography was performed by Dr. Mark (Woody) Nieuwenhuyzen in Queens University Belfast, his excellent work was greatly appreciated. I would also like to thank Anthony Birchall and Dennis O' Connor who have both sorted out every computer problem I managed to get myself into.

I would like to thank the many people who have supported me financially. These include Bioresearch Ireland, Enterprise Ireland and Trinity College. In particular I would like to thank the friendly and very supportive members of Bioresearch Ireland, Professor Clive Williams, Dr. Margaret Woods, Mary and Gay. And finally a big thanks to my brother, Tom, for his many loans.

Well it wasn't all work. I did have a bit of fun while I was in TCD and I have to thank the many friends who made that possible, namely Dara, Jacqui, Tom Mc D, Tom, Claire N., Claire W., Caroline, Aoife, Celine, Katell, Gar, Brian, Rob, Yvonne and the many others that I just cant think of right now. May there be many more nights out and lots of beer drank. My family, have been very supportive of me over the many years (almost 10) spent in and out of college and I just want them to know how appreciative I am of them and all they have done for me. The final thanks goes to my partner, Linda for all of her love and support over the years. I realize what a strain the last three years has been and hopefully I can make up for it in the future.

"Organic chemistry… is enough to drive one mad. It gives me the impression of a primeval tropical forest, full of the most remarkable things, a monstrous and boundless thicket, with no way of escape, into which one may well dread to enter."

Wöhler, 19th Century chemist

Abstract

This thesis, entitled "Synthesis and physical studies of luminescent lanthanide and colorimetric chemosensors for ions and molecules" is divided into six chapters. Chapter One, the introduction, includes a brief summary of what chemosensors are, specifically optical chemosensors. These are discussed in terms of the major components that make up chemosensors and the methods by which they work using relevant examples from the literature. Following this, a review on the use of lanthanide complexes as signalling moieties in optical chemosensing is presented. The design of lanthanide complexes with good optical properties is discussed, as is the mechanism by which lanthanide luminescence is produced. Finally, a review of the most recently published reports of lanthanide based chemosensors is presented. The results of this review highlights that the exploration of lanthanide complexes as chemosensors is still in its infancy and the potential for the development of new chemosensors for ions and molecules is worthy of further investigation. Chapter Two deals with the design and synthesis of six lanthanide complexes, designed for the detection of intracellular concentrations of Na^+ and K^+ in aqueous solutions. The synthesis of these complexes involved incorporating either a 15-crown-5 or 18-crown-6 diaza crown receptor into a tris-alkylated cyclen ligand. Upon complexation with a lanthanide ion such as Tb(III) or Eu(III), photophysically active lanthanide complexes are produced, which can detect the presence of Na^+ and K^+ in solution *via* lanthanide luminescence upon excitation of the complex. During the synthesis of these complexes a new mild method of nitration was developed for the nitration of alkylated anilines, which was selective and high yielding. Physical studies on the Tb(III) complexes highlighted their ability to detect the presence of Na^+ and K^+ in aqueous solutions or buffered solutions at pH 7.4. The lanthanide complexes designed for detecting K^+ demonstrated good selectivity over other physiologically important group I and II cations. However, the operating range for these complexes was higher than the target range which was the intracellular concentration range. Chapter Three deals with the design and synthesis of two colorimetric chemosensors, designed for the detection of intracellular concentrations of Na^+ and K^+ in aqueous solutions. These chemosensors were developed from the diaza crown receptors discussed in Chapter Two. Incorporation of an azo dye in each case resulted in the successful synthesis of these colorimetric chemosensors. Physical studies showed that the 15-crown-5 colorimetric chemosensor could detect Na^+ at

intracellular concentrations with a high selectivity over other physiologically important group I and II cations. The 18-crown-6 colorimetric chemosensor was shown to have a high selectivity for K^+ at intracellular concentration, however, in this case the response to Na^+ was similar. Chapter Four deals with the attempted development of a lanthanide complex for the detection of Ca^{2+} at intracellular concentrations. This involved the development of a ligand structurally similar to those described in Chapter Two, except that the receptor was a Ca^{2+} chelator derived from BAPTA. Synthesis of this ligand and the subsequent Tb(III) complex was demonstrated with photophysical studies. However the final synthetic step, the hydrolysis of the ester groups of the Ca^{2+} receptor was not achieved. With subtle modifications to the design and synthesis of this lanthanide complex, a Ca^{2+} sensor could easily be achieved in the future. Chapter Five deals with the design and synthesis of lanthanide complexes that can be used for the detection of aromatic carboxylates. These complexes were produced from the complexation of Tb(III) and Eu(III) with tris alkylated cyclen ligands previously discussed in Chapter Two. These ligands are heptadentate and form lanthanide complexes with two vacant sites, which in solution and the solid state are bound by two water molecules. Physical studies showed that the Tb(III) complexes could bind to aromatic carboxylates upon displacement of the metal bound water molecules. Excitation of the bound aromatic carboxylate was found to cause sensitisation of the lanthanide cation resulting in lanthanide luminescence. Further studies showed that the Tb(III) complexes could selectively detect the presence of salicylic acid, the physiologically active form of Aspirin® in aqueous solution or in buffered solutions at pH 7.4. The final chapter, Chapter Six, is the experimental section were the synthetic procedures for the molecules discussed in Chapter Two, Three, Four and Five are presented.

Abbreviations

abs.	Absorbance
AcOH	Acetic acid
β	Binding constant
BAPTA	Bis amino phenoxy tetra acetic acid
Bpy	Bipyridine
Ca^{2+}	Calcium cation
CD_3OD	Deuterated methanol
$CDCl_3$	Deuterated chloroform
CH_2Cl_2	DCM – Dichloromethane
$CHCl_3$	Chloroform
CPL	Circularly polarised luminescence
DEPT	Distortionless Enhancement by Polarization Transfer
EDCI	1-(3-dimethylaminopropyl)-3-ethyl-carbodiimide hydrochloride
ESMS	Electro spray mass spectroscopy
ESR	Electron spin resonance
ET	Electron transfer
EtOAc	Ethyl acetate
EtOH	Ethanol
Eu(III)	Europium cation
ε	Molar absorptivity (Molar extinction coefficient) (cm^{-1} M^{-1})
ϕ	Qunatum yield
H_2SO_4	Sulphuric acid
HCl	Hydrochloric acid
Hex	Hexane
HNO_3	Nitric acid
HOBt	N-Hydroxybenzotriazole
ICT	Internal charge transfer
IR	Infrared spectroscopy
ISC	Inter system crossing
K^+	Potassium cation
Li^+	Lithium cation

LMCT	Ligand to metal charge transfer
MeCN	Acetonitrile
MeOH	Methanol
Mg^{2+}	Magnesium cation
MLCT	Metal to ligand charge transfer
NH_3	Ammonia
Na^+	Sodium cation
NMR	Nuclear magnetic resonance
NOE	Nuclear overhauser effect
Pd-C	Palladium on carbon catalyst
P_2O_5	Phosphorus pentoxide
ppm	Parts per million
PET	Photoinduced electron transfer
phen	Phenanthroline
pH	-log $[H_30^+]$
pK_a	-log (Ka), were Ka is the acidity constant
pM	-log (M), were M is a cation
q	Hydration state
τ	Lifetime
Tb(III)	Terbium cation
TEA	Triethylamine
TFA	Trifluoroacetic acid
THF	Tetrahydrofuran
TLC	Thin layer chromatography
TMACl	Tetramethylammonium chloride
TMAOH	Tetramethylammonium Hydroxide
TRIS Buffer	Tris(hydroxymethyl)aminomethane
TsCl	*para*- Toluene sulphonyl chloride

Table Of Contents

Page Number

Chapter 1.0 - Introduction

1.0 Introduction 1

1.1 Components of a sensor 1

1.2 Receptors 2

1.2.1 Cation receptors 2

1.2.2. Anion receptors 3

1.3 Signaling systems 4

1.3.1 Colorimetric 4

1.3.2 Fluorescent (PET) 5

1.3.3 Metal centered luminescence 7

1.4 Considerations for in vivo sensing 9

1.5 Lanthanide complexes: an alternative signaling system for in-vivo applications 10

1.5.1 How to produce lanthanide luminescence – considerations for developing signaling systems 11

1.5.2 Considerations when applying antennae effect in signaling applications 13

1.6 Complexation and sensitising of lanthanides: An overview 14

1.6.1 Podands 15

1.6.2 Cryptands 15

1.6.3 Calixarenes 19

1.6.4 Macro cyclic and bicyclic ligands 25

1.7 Lanthanide complexes as luminescent sensors..... 33

1.8 Conclusion 44

Chapter 2.0 - Synthesis, characterisation and photophysical studies of lanthanide luminescent sensors for the detection of sodium and potassium

2.1 Introduction 45

2.1.1 Synthesis strategy 46

2.2 Synthesis of monoaza and diaza cation receptors based on 2-methoxy aniline 47

2.2.1 Monoaza crown receptors – Synthesis and characterisation of **103** and **104**..... 47

2.2.2 Diaza crown receptors - Synthesis and characterization of **111** and **112** 49

2.2.2.1 Characterisation and physical studies of **111** and **112**..... 52

2.2.2.2 ^{1}H NMR analysis of the receptors..... 53

2.2.2.3 X-ray crystallographic investigation of **112**..... 55

2.3 Nitration and reduction of aza and diaza crown receptors **103**, **104**, **111** *and* **112** 59

2.3.1 Characterisation of the nitrated receptors..... 61

2.3.2 Crystallographic analysis of nitrated receptors **122** and **131**..... 62

2.3.3 Proposed mechanism for nitration using $NaNO_2$..... 63

2.3.3.1 Testing the versatility of the nitration method..... 65

2.3.4 Reduction of **122**, **123**, **124** and **125**..... 67

2.4 Synthesis of **145**, **146**, **147** *and* **148**..... 67

2.5 Synthesis of sensor ligands **99**, **100**, **101** *and* **102**..... 69

2.6 Synthesis of lanthanide complexes..... 71

2.6.1 *Characterisation of the Tb(III) and Eu(III) complexes* 72

2.6.1.1 Lifetime analysis *of the Tb(III) and Eu(III) complexes* 73

2.7 Photophysical analysis of **Eu.99, Eu.100, Tb.99, Tb.100, Tb.101** *and* **Tb.102** 74

2.7.1 Absorption investigations of Eu(III) and Tb(III) complexes..... 75

2.7.1.1 pH studies of Eu(III) and Tb(III) complexes..... 75

2.7.1.2 Metal ion studies of Eu(III) and Tb(III) complexes..... 77

2.7.2 Fluorescence investigations of Eu(III) and Tb(III) complexes..... 79

2.7.2.1 pH studies of Eu(III) and Tb(III) complexes..... 79

2.7.2.2 Metal ion studies of Eu(III) and Tb(III) complexes..... 81

2.7.3 Lanthanide luminescence investigations of Eu(III) and Tb(III) complexes..... 82

2.7.3.1 pH studies of Eu(III) and Tb(III) complexes..... 82

2.7.3.2 Metal ion studies of Eu(III) and Tb(III) complexes..... 87

2.8 Conclusion..... 94

Chapter 3.0 - Synthesis and photophysical studies of colorimetric sensors for the detection of sodium and potassium

3.1 Introduction..... 95

3.2 Synthesis of **153** *and* **154**..... 96

3.3 Characterisation of **153** *and* **154**..... 977

3.4 ^{1}H NMR complexation studies..... 98

3.5 Photophysical investigations of **111** *and* **112**..... 99

3.5.1 *pH studies of* **111** *and* **112**..... 100

3.5.2 Selectivity studies of **111** and **112** with Group I and II cations..... 102

3.6 Photophysical analysis of **153** 105

3.6.1 Determination of the pH dependence of **153** 106

3.6.2 Selectivity studies of **153** with Group I and II cations 107

3.7 Photophysical analysis of **154** 111

3.7.1 Determination of the pH dependence of **154** 111

3.7.2 Selectivity studies of **154** with Group I and II cations 113

3.8 Comparative studies of detection ranges of **111**, **112**, **153** *and* **154** 117

3.9 Conclusions 119

Chapter 4.0 - Attempted synthesis of a lanthanide luminescent sensor for the detection of Calcium

4.1 Introduction 120

4.2 Synthesis of **160** 121

4.3 Conclusion 132

Chapter 5.0 - Synthesis and photophysical studies of lanthanide luminescent sensors for the detection of aromatic carboxylates

5.1 Introduction 133

5.1.1Project Objective 135

5.2 Synthesis of **149** *and* **181** *and their Eu(III) and Tb(III) complexes* 136

5.3 Determination of bound water in lanthanide complexes by lifetime analysis 142

5.4 Crystallographic analysis of **Eu.149**, **Tb.149** *and* **Eu.181** 143

5.5 Photophysical analysis of **Eu.149**, **Tb.149**, **Eu.181** *and* **Tb.181** *with aromatic carboxylates* 146

5.5.1 Lifetime analysis of **Eu.149**, **Tb.149**, **Eu.181** and **Tb.181** with **191** 153

5.6 Photophysical evaluation of **Tb.149**, **Tb.181**, **Eu.149** *and* **Eu.181** *with physiological important aromatic carboxylates and their related derivatives* 155

5.6.1 Photophysical evaluation of **Tb.149**, **Tb.181**, **Eu.149** and **Eu.181** with **194** and **195** 155

5.7 Determination of binding mode for **194** *with* **Tb.149** 158

5.8 Conclusion 159

Chapter 6.0 - Procedures

6.0 General experimental details 161

6.1 Synthesis and photophysical data for Chapter 2 161

6.1.1 Photophysical studies 187

6.2 Synthesis and photophysical data for Chapter 3 189

6.2.1 Photophysical studies 190

6.3 Synthesis data for Chapter 4 191

6.4 Synthesis and photophysical data for Chapter 5 199

6.4.1 Lanthanide complexes – Photo physical studies 206

6.4.2 Lanthanide complexes – Life time studies 207

6.4.3 Anion selectivity experiment 208

6.4.4 Aromatic carboxylate absorption max values 208

Chapter 7.0 - References

7.0 - References 209

Appendix

Crystallography data for **112** 215
***Crystallography data for* 112•KPF_6** 221
***Crystallography data for* 122** 234
***Crystallography data for* 131** 241
Crystallography data for **Eu.149** 247
***Crystallography data for* Tb.149** 266
***Crystallography data for* Eu.181** 281

Publications

Syntheses of novel functionalised macrocyclic compounds as Na^+ and K^+ receptors: a mild and high yielding nitration in water of mono and bis 2-methoxyaniline functionalised crown ethers - *J. Chem. Soc., Perkin Trans. 1*, **2002**, 1954–1962.

Delayed lanthanide luminescence sensing of aromatic carboxylates using heptadentate tri-amide Tb(III) cyclen complexes: the recognition of salicylic acid in water under physiological conditions - *J. Chem. Soc., Chem. Commun.*, **2002,** 2134-2135.

Synthesis and evaluation of colorimetric chemosensors for monitoring sodium and potassium ions in the intracellular concentration range - *J. Chem. Soc., Perkin Trans. 2*, **2002**, 1980–1985.

List of Tables

Page Number

Chapter 1.0

Table 1.1 ***Effect of Cavity size on Cation Selectivity*** 3

Chapter 2.0

Table 2.1 ***Selected parameters for crystal structure of*** **112** ***in its "free" form*** 57

Table 2.2 ***Selected parameters from*** **112•** $K^+PF_6^-$ 59

Table 2.3 ***Accurate mass analysis summary of nitrated receptors*** 62

Table 2.4 ***Results of variation to new nitration method*** 67

Table 2.5 ***Summary of Lifetime studies on lanthanide complexes*** 74

Table 2.6 ***Summary of pKa values determined for*** **Tb.99** 85

Table 2.7 ***Maximum luminescent enhancement of*** **Tb.99** ***and*** **Tb.101** ***in the presence*** M^+ 90

Table 2.8 ***Maximum luminescent enhancement of*** **Tb.100** ***and*** **Tb.102** ***in the presence*** M^+ 93

Chapter 3.0

Table 3.1 ***Summary of physical properties of*** **111** ***and*** **112** 105

Table 3.2 ***Summary of physical properties of*** **153** ***and*** **154** 117

Table 3.3 ***Comparison of detection ranges of sensors*** 118

Chapter 4.0

Table 4.1 ***Summary of*** **Tb.178** ***Emission (Max. Intensity) vs.*** λ_{Excite} 131

Chapter 5.0

Table 5.1 ***Measured lifetimes, rate constants and computed q values for*** **Eu.149,** 142

Tb.149, Eu.181 ***and*** **Tb.181**

Table 5.2 ***Selected bond lengths and angles for Crystals of*** **Eu.149, Tb.149** ***and*** **Eu.181** 144

Table 5.3 ***Absorption analysis*** **Tb.181** ***with*** **191** ***and corrected emission (Emission/(I/I$_0$))*** 152

Table 5.4 ***Measured lifetimes, rate constants and computed q values for*** **Eu.149, Tb.149, Eu.181** ***and*** **Tb.181** ***in the presence of N,N-dimethylaminobenzoic acid*** **(191)** 154

Chapter 6.0

Table 6.1a ***Fluorimeter settings for pH and pM Studies*** 187

Table 6.1b ***Fluorimeter settings (Phosphorescence mode) for pH and pM Studies*** 188

Table 6.2 ***Fluorimeter settings for lifetime analysis*** 188

Table 6.3 ***General settings for luminescence studies (Perkin Elmer LS 50B)*** 207

Table 6.4 ***General settings for lifetime studies (Varian Carey Eclipse)*** 207

Table 6.5 ***Anion concentrations for selectivity studies*** 208

Table 6.6 ***λ max (H_2O) of aromatic carboxylates*** **189-199** 208

List of figures

Page Number

Chapter 1.0

Figure 1.1 ***Illustration of the common models used in sensor construction*** 1

Figure 1.2 ***Illustration of PET mechanism for* 3 *and* 4** 7

Figure 1.3 ***Illustration of metal centered luminescence mechanism for* 7** 8

Figure 1.4 ***Illustration of time gating*** 10

Figure 1.5 ***Photophysical pathway to produce lanthanide luminescence by sensitisation*** 12

Figure 1.6 ***Jablonski diagram of sensitisation for Tb(III)*** 12

Chapter 2.0

Figure 2.1 ^{1}***H NMR of* 103** ***[δ_H ($CDCl_3$: 400MHz)]*** 49

Figure 2.2 ^{1}***H NMR of* 112** ***[δ_H ($CDCl_3$: 400MHz)]*** 53

Figure 2.3 ^{1}***H NMR comparison [δ_H ($CDCl_3$: 400MHz)] of* 111** 54

Figure 2.4 ^{1}***H NMR comparison [δ_H ($CDCl_3$: 400MHz)] of* 112** 54

Figure 2.5 ***X-ray crystal structure of unbound receptor* 112** 55

Figure 2.6 ***Illustration of crystal structures of* 112** ***"free" and "bound with K^+"*** 56

Figure 2.7 ***X-ray crystal structure of* 112• $K^+PF_6^-$** 58

Figure 2.8 X***-ray crystal structure of* 122** 62

Figure 2.9 ***X-ray crystal structure of* 131** 63

Figure 2.10 ***Summary of successful nitrations*** 66

Figure 2.11 ***Summary of molecules used with nitration method that yielded no nitro product*** 66

Figure 2.12 ***Mass spectrum of* Eu.100** ***(Uncalibrated)*** 72

Figure 2.13 ***Mass spectrum of* Tb.99** ***(Uncalibrated)*** 73

Figure 2.14 ***Absorption of* Tb.99** ***as a function of pH*** 76

Figure 2.15 ***Absorbance of* Tb.99** at 279 nm ***as a function of pH*** 76

Figure 2.16 ***Absorption of* Tb.100** ***as a function of pK*** 78

Figure 2.17 ***Absorbance of* Tb.100** at 279 nm ***as a function of pK*** 78

Figure 2.18 ***Fluorescence of*** **Tb.99** ***as a function of pH*** 80

Figure 2.19 ***Fluorescence profile of*** **Tb.99** ***as a function of pH at 378 nm*** 80

Figure 2.20 ***Fluorescence study of*** **Tb.99** ***in the absence (brown line) or presence (red line) of NaOAc*** 81

Figure 2.21 ***Lanthanide emission of*** **Tb.99** ***as a function of pH*** 83

Figure 2.22 ***Lanthanide emission at 547 nm of*** **Tb.99** and **Tb.100** ***as a function of pH*** 83

Figure 2.23 ***Lanthanide emission of*** **Tb.101** ***as a function of pH*** 86

Figure 2.24 ***Lanthanide emission at 547 nm of*** **Tb.101** and **Tb.102** ***as a function of pH*** 87

Figure 2.25 ***Lanthanide emission at 547 nm of*** **Tb.99** ***as a function of pNa*** 88

Figure 2.26 ***Comparison of Lanthanide emission at 547 nm of*** **Tb.99** ***as a function of pM*** 89

Figure 2.27 ***Comparison of Lanthanide emission at 547 nm of*** **Tb.101** ***as a function of pM*** 89

Figure 2.28 ***Lanthanide emission at 547 nm of*** **Tb.100** ***as a function of pK*** 91

Figure 2.29 ***Comparison of Lanthanide emission at 547 nm of*** **Tb.100** ***as a function of pM*** 91

Figure 2.30 ***Lanthanide emission at 547 nm of*** **Tb.102** ***as a function of pK*** 92

Figure 2.31 ***Comparison of Lanthanide emission at 547 nm of*** **Tb.102** ***as a function of pM*** 93

Chapter 3.0

Figure 3.1 ***^1H NMR of*** **154** ***[δ_H ($CDCl_3$: 400MHz)]*** 98

Figure 3.2 ***^1H NMR study of*** **153** ***($CDCl_3$), before and after the addition of $NaPF_6$ in CD_3OD*** 99

Figure 3.3 ***Absorption of*** **112** ***as a function of pH (Absorption at 240 nm, 50:50 MeOH:H_2O)*** 101

Figure 3.4 ***Absorbance vs. pH of*** **112** ***(Absorption at 240 nm, 50:50 MeOH:H_2O)*** 101

Figure 3.5 ***Absorption of*** **112** ***as a function of added potassium acetate, pK = 0.7-5.9 (50:50 MeOH:H_2O, 0.1M Tris buffer, 0.1M TMACl, pH 7.4)*** 103

Figure 3.6 ***Absorbance vs. pK of*** **112** ***(50:50 MeOH:H_2O, 0.1M Tris buffer, 0.1M TMACl, pH 7.4)*** 103

Figure 3.7 ***Absorption vs. pNa of*** **112**, ***pNa = 0.85-5.9 (50:50 MeOH:H_2O, 0.1M Tris*** 104

buffer, 0.1M TMACl, pH 7.4)

Figure 3.8 *Absorbance vs. pM of* **112** *(50:50 MeOH:H_2O, 0.1M Tris buffer, 0.1M TMACl, pH 7.4)* 105

Figure 3.9 *Absorption of* **153** *as a function of pH, pH range = 1.41-12.32 (50:50 MeOH:H_2O)* 106

Figure 3.10 *Absorbance vs. pH of* **153** *(50:50 MeOH:H_2O)pK_a determination studies* 107

Figure 3.11 *Illustration of* **153** *as an active colorimetric sensor for* Na^+ 108

Figure 3.12 *Absorption of* **153** *as a function of added sodium acetate, pNa = 0.7-5.9 (50:50 MeOH:H_2O, 0.1M Tris buffer, 0.1M TMACl, pH 7.4)* 109

Figure 3.13 *Absorbance vs. pNa of* **153** *(50:50 MeOH:H_2O, 0.1M Tris buffer, 0.1M TMACl, pH 7.4)* 109

Figure 3.14 *Absorbance vs. pM of* **153** *- Selectivity group I and II cations (50:50 MeOH:H_2O, 0.1M Tris buffer, 0.1M TMACl, pH 7.4)* 110

Figure 3.15 *Absorption of* **154** *as a function of pH, pH range = 0.92-12.42 (50:50 MeOH:H_2O)* 112

Figure 3.16 *Absorbance vs. pH of* **154** *(50:50 MeOH:H_2O)pK_a determination studies* 112

Figure 3.17 *Illustration of* **154** *to indicate the assignment of pK_a values* 113

Figure 3.18 *Absorption of* **154** *as a function of added potassium acetate, pK = 0.85-5.9 (50:50 MeOH:H_2O, 0.1M Tris buffer, 0.1M TMACl, pH 7.4)* 114

Figure 3.19 *Absorbance vs. pK of* **154** *(50:50 MeOH:H_2O, 0.1M Tris buffer, 0.1M TMACl, pH 7.4)* 115

Figure 3.20 *Absorption of* **154** *as a function of added sodium acetate, pK = 0.85-5.9 (50:50 MeOH:H_2O, 0.1M Tris buffer, 0.1M TMACl, pH 7.4)* 116

Figure 3.21 *Absorbance vs. pM of* **154** *– Comparison of response of* **154** *to* Na^+ *and* K^+ *(50:50 MeOH:H_2O, 0.1M Tris buffer, 0.1M TMACl, pH 7.4)* 116

Figure 3.22 *Absorbance vs. pM of* **154** *- Selectivity study of Group I and II cations (50:50 MeOH:H_2O, 0.1M Tris buffer, 0.1M TMACl, pH 7.4)* 117

Chapter 4.0

Figure 4.1 ^1H *NMR of* **172** *- (Tetra ethyl ester BAPTA)* 124

Figure 4.2 ^1H *NMR comparison* **173** *with* **172** 126

Figure 4.3 *Comparison of ESMS spectra with the calculated isotopic model for* **176** 128

Figure 4.4 *Absorption spectrum of* **Tb.178** *in aqueous solution* 130

Figure 4.5 ***Lanthanide emission spectrum of*** **Tb.178** ***in aqueous solution*** 131

Chapter 5.0

Figure 5.1 ***X-ray crystal structure of*** **188** ***with*** $CHCl_3$ ***in unit cell*** 137

Figure 5.2 ^{1}***H NMR of*** **181** 139

Figure 5.3 ***ES Mass spectrum of*** **Eu.149** ***and comparison to its theoretical isotopic model*** 141

Figure 5.4 ***X-ray crystal structure of*** **Eu.149** ***showing the presence of two bound water molecules*** 145

Figure 5.5 ***X-ray crystal structure of*** **Tb.149** ***showing the presence of two bound water molecules*** 145

Figure 5.6 ***X-ray crystal structure of*** **Eu.181** ***showing the presence of two bound water molecules*** 146

Figure 5.7 ***Aromatic carboxylates and esters used in photophysical analysis of*** **Eu.149, Tb.149, Eu.181** ***and*** **Tb.181** 147

Figure 5.8 ***Lanthanide emission spectrum of*** **Tb.149** ***(16-17 μM) from titration with*** **191** *(0-0.4 mM)* ***in aqueous solution*** 148

Figure 5.9 ***Tb(III) emission intensity as a function of concentration – Titration of*** **Tb.149** ***(16-17 μM) with*** **191** ***(0-0.4 mM). [λ_{excite} = 300 nm]*** (Inset: Tb(III) emission intensity *vs.* equivalents) 149

Figure 5.10 ***Tb(III) emission intensity as a function of p[191] – Titration of*** **Tb.149** ***(16-17 μM) with*** **191** ***(0-0.4 mM)*** 149

Figure 5.11 ***Tb(III) emission intensity as a function of equivalents – Titration of*** **Tb.181** ***(16-17 μM) with*** **191** ***(0-0.4 mM)*** 151

Figure 5.12 ***Tb(III) emission intensity as a function of p[191] – Titration of*** **Tb.181** ***(16-17 μM) with*** **191** ***(0-0.4 mM)*** 151

Figure 5.13 ***Effect of aqueous vs. buffered solutions on titration of*** **Tb.149** ***(16-17 μM) with*** **191** ***(0-0.4 mM)*** 152

Figure 5.14. ***Corrected Tb(III) emission intensity as a function of [191] – Titration of*** **Tb.181** ***(16-17 μM Buffered solution) with*** **191** ***(0-0.35 mM).*** 153

Figure 5.15 ***Tb(III) emission intensity as a function of p[194] – Titration of*** **Tb.149** ***(16-17 μM Buffered solution) with*** **194** ***(0-0.4 mM)*** 156

Figure 5.16 ***Tb(III) emission intensity as a function of equivalents – Titration of*** 157

Tb.149 ***(16-17 μM Buffered solution) with*** **194** ***(0-0.4 mM)***

Figure 5.17 ***Methods of Binding for*** **194** ***with Tb(III)*** 159

List of schemes

Page Number

Chapter 1.0

Scheme 1 ***Attack on N-methyl phenanthradine by OH⁻ at the C-6 position in a reversible manner*** 37

Scheme 2 ***pH reversible coordination effect of*** **86a, 86b** ***and*** **86c** 39

Scheme 3 ***pH reversible coordination effect of*** **87** 40

Chapter 2.0

Scheme 1 ***Retro synthetic analysis – Towards a synthetic strategy*** 46

Scheme 2 ***Dales procedure towards aromatic monoaza crown receptors*** **103 & 104** 47

Scheme 3 ***Gokel's procedure towards aromatic monoaza crown receptors*** **103 & 104** 48

Scheme 4 ***Direct synthesis of*** **111 & 112** ***by aromatic nucleophilic substitution*** 49

Scheme 5 ***The synthesis of*** **111** ***and*** **112** 50

Scheme 6 ***Nitration and reduction of*** **103, 104, 111** ***and*** **112** 59

Scheme 7 ***Proposed mechanism for nitration of aza crown receptors*** 64

Scheme 8 ***Synthesis of*** **145, 146, 147** ***and*** **148** 68

Scheme 9 ***Synthesis of sensor ligands*** 70

Scheme 10 ***Synthesis of sensor ligands*** **101** ***and*** **102** 70

Scheme 11 ***Synthesis of lanthanide complexes using lanthanide triflate salts*** 71

Scheme 12 ***Proposed protonated and deprotonated forms of the aryl amide moiety of*** **Tb.99** ***and*** **Tb.100** 84

Scheme 13 ***Assignment of pK_a values of*** **Tb.99** 85

Chapter 3.0

Scheme 1 ***Synthesis of colorimetric sensors*** **153** ***and*** **154** 97

Scheme 2 ***Resonance forms of*** **153** ***and*** **154** ***to describe the charge repulsion effect proposed for the shift in detection range observed for each receptor*** 118

Chapter 4.0

Scheme 1 ***Proposed synthesis of 4-Amino BAPTA (169) using synthesis of*** Erdogan *et al.* 122

Scheme 2 ***Modified synthesis of*** **172** ***Tetra ethyl ester – BAPTA*** 123

Scheme 3 ***Nitration of Tetra ethyl ester BAPTA,*** **173** 125

Scheme 4 ***Synthesis of*** **176** ***and*** **177** 127

Scheme 5 ***Synthesis of*** **178** 128

Scheme 6 - ***Proposed synthesis of*** **Tb.178** ***and*** **Tb.160** 129

Chapter 5.0

Scheme 1 ***Illustration of*** **Zn.179** ***as an aromatic carboxylate sensor*** 133

Scheme 2 ***Complexes*** **Eu.149**, **Tb.149**, **Eu.181** and **Tb.181** ***and their proposed sensing function with aromatic carboxylates (R = implicit free site)*** 135

Scheme 3 ***Synthetic route 1: Synthesis of*** **149** ***and*** **181** ***by N-protection of*** **182** ***using p-methoxyphenylsulphonyl chloride*** **183** 136

Scheme 4 ***Synthetic route 2: Synthesis of*** **149** ***and*** **181** ***by direct alkylation*** 138

Scheme 5 ***Synthesis of*** **Eu.149, Tb.149, Eu.181** ***and*** **Tb.181** 140

Chapter 1

Introduction

1.0 Introduction

Sensing usually involves the continuous monitoring of the activity of a chemical species in a given matrix such as air, blood, tissue, waste effluents or drinking water. Sensing relies on an interaction occurring at the molecular level. This usually involves the binding of the analyte to a molecular fragment called a receptor. This process is defined as 'recognition', a process that occurs on the molecular level. The recognition process has to be fast and reversible. [1] Sensing does not involve recognition alone, but requires that the recognition event be signaled by the change of a given property that can be detected visually or instrumentally. [1] Signaling a recognition event in a sensor can be achieved with molecular properties such as optical, thermal, magnetic, electrical, mechanical, and chemical. The following sections of this Chapter deal with sensing by optical recognition. In the following sections the most common types of optical sensors will be discussed using examples of cation and anion sensors. This will then be followed by a detailed discussion into the development of lanthanide complexes as sensors.

1.1 Components of a sensor

As mentioned above a chemosensor (or chemical sensor) is comprised of two major components a receptor and a signaling system (also known as a signal transducer). A receptor is required which can selectively and reversibly interact with a target molecule of interest. A signaling system is required to report on the receptor signaling the presence or absence of a target molecule at the receptor site. Combining both of these components can be achieved in a number of ways, such as integrated, twisted or spaced, as shown in Figure 1.1.[2, 3, 4, 5, 6]

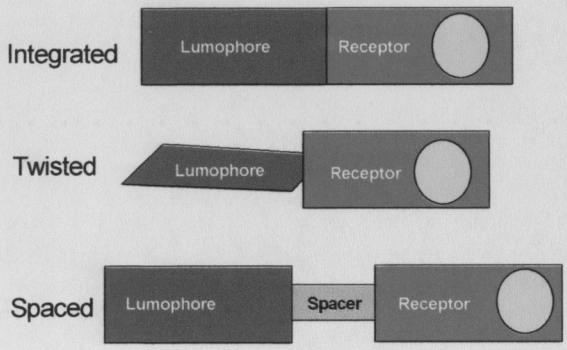


Figure 1.1 *Illustration of the common models used in sensor construction*

All of the above systems have been well detailed in literature.[5] The method of connection between receptor and the signaling moiety depend on the photophysical property being utilised. Sensors where the signaling moiety and the receptor are attached in an integrated manner typically involve photophysical processes in which an internal charge transfer (ICT) is required in the communication process.[5] Twisted systems are similar to the integrated system previously discussed. The method of communication is also by way of an internal charge transfer process. In this case the physical orientation of the two components is controlled to maximize the degree of charge separation. Spaced systems are quite common in sensing were the method of communication between the receptor and the lumophore occurs by way of electron transfer (ET) or energy transfer. In such cases the spacer must be present to prevent any π-π or σ-π orbital interactions between the two components. In the case of efficient electron transfer systems the spacer group must be as short as possible.[7]

1.2 Receptors

All chemical species can be categorized as cationic, anionic or neutral. Due to the major differences in physical and chemical properties of these classes of chemical species different types of receptors are required for their detection. The major theme of this thesis is cation and anion sensing. The following sections are a brief discussion on the requirements for such receptors.

1.2.1 Cation receptors

Detecting cations is of great interest in many fields of science. Cations such as Na^+, K^+, Mg^{2+} and Ca^{2+} are biologically important being involved in processes such as regulation of cell activity, muscle contraction and transmission of nerve impulses.[8] Other metal cations such as Hg^{2+}, Pb^{2+}, Al^{3+} or Cd^{2+} are toxic for biological organisms; therefore early detection is desirable to prevent accumulation of such cations to toxic levels.[9] Finally metal ions are more commonly being used in clinical treatments, for instance *cis*-platin is used in the treatment of testicular and ovarian cancer[10, 11] while Li^+ is used in the treatment of manic depression, however, levels need to be monitored carefully due to its toxicity [12, 13].

Cations vary in size, charge and charge density (This is especially true in the case of metals were all cations are spherical). A substantial amount of work has been carried out over the last 40 years into designing receptors that can bind a specific cation selectively.[14] Some of the most common cation receptors are crown ethers, cryptands,[15] aza crowns and calixarenes all being examples of macrocyclic receptor systems. Acyclic macromolecules are also well known for cation recognition. Many of these such as EDTA and BAPTA have very high selectivity for Ca^{2+} over other competitive physiological cations such as Mg^{2+}. In terms of cyclic macrocycles, selectivity for specific cations can be designed into such receptors usually in two ways.[16] Firstly, by tuning the ring size of the receptor to the radius of the cation of interest, [17] *e.g.*, 15-crown-5 is a crown ether designed to specifically bind to Na^+ while the slightly larger 18-crown-6 macrocycle is designed to specifically bind to K^+. (See Table 1.1) Secondly, addition of extra coordination sites to the chelating structure can help with selectivity for instance, lariat ethers. In aza crown macrocylces the use of additional ether groups add to the binding ability by becoming involved in coordination and improve selectivity to the target cations.[16, 17, 18, 19, 20]

Table 1.1 Effect of Cavity size on Cation Selectivity

Cations	Diameter (Å)	Crown Ether	Cavity Diameter (Å)
Li^+	1.36	[12] crown-4	1.2 – 1.5
Na^+	1.94	[15] crown-5	1.7 – 2.2
K^+	2.66	[18] crown-6	2.6 – 3.2
Cs^+	3.34	[21] crown-7	3.4 – 4.3

1.2.2 Anion Receptors

Anions play an important role in biology and living in general. Phosphates are found in cells and in circulating fluid and have many functions, which include acting as linking units for sugar esters of DNA and RNA. Furthermore it is found in phospholipids as diesters and in membranes as monoesters. Anions can also be toxic F^- which is useful in biominerals, but competes with OH^- in enzymatic reactions.[21] Designing receptors for detecting anions can be difficult because of their numerous shapes, sizes and geometries. The halides, Cl^-, F^-, Br^- are all monoatomic and spherical whereas carboxylate and nitrate anions are flat and trigonal planar in geometry, phosphates, sulphates and permanganates have tetrahedral geometries and

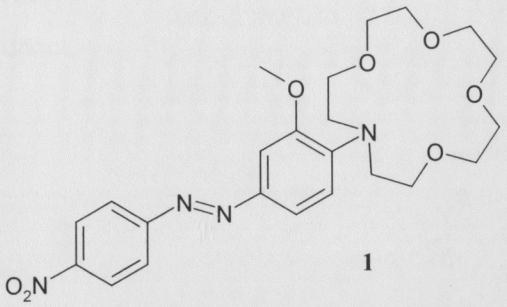
other anions such as OH^- or CN^- anions are linear in geometry. [22] Unlike the field of metal cation recognition, the design and synthesis of anion receptors has not been investigated as deeply, mainly because of problems such as low charge to radius ratio, pH sensitivity and range of geometries. Nonetheless, there are many examples of receptors for anion recognition. For instance it has been shown that halides can be encapsulated in protonated cryptands. [23] Another example of such receptors was shown by Graf and Lehn[24] in this case Cl^- and Br^- were shown to be able to efficiently bind with protonated cryptands. More recently the use calixarenes functionalised with (trimethylammonium)- methyl groups that can act as receptors for anions have been shown.[25]

1.3 Signaling systems

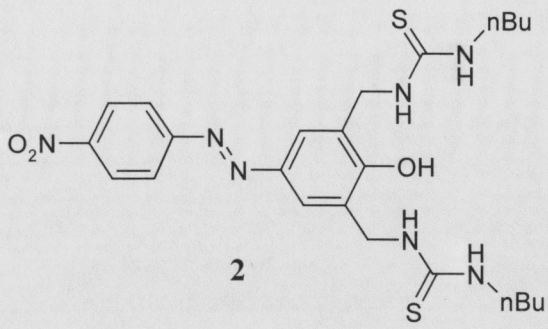
Signaling can be reported optically with a number of photophysical systems. The most common forms are: colorimetric, fluorescent (PET) and luminescence (metal centered). In the following sections example of such sensors will be discussed.

1.3.1 Colorimetric

Compounds can be classed as colorimetric sensors when perturbation of the electronic properties of the reporter groups upon complexation with an analyte produces a visually detectable response. Ideally such sensors do not require the use of a potentiostat or spectrometer since the recognition should be visible to the naked eye. **1** is the most recent example of a cation colorimetric sensor reported by Gunnlaugsson *et al.* [26, 27, 28] In this case the red colored dye changed to yellow upon addition of Na^+. The red colour of the uncomplexed aza crown occurs because the aza crown nitrogen lone pair are engaged in a charge push-pull mechanism with the nitro group (at the other end). This gives rise to an internal charge transfer (ICT) excited state. Upon complexation with Na^+ in 50:50, H_2O:MeOH, the nitrogen lone pair become engaged in binding reducing the ability to participate in the ICT process causing the hypsochromic shift to occur. Studies show that this sensor could selectively detect Na^+ over other physiologically important cations under near physiological conditions.



1



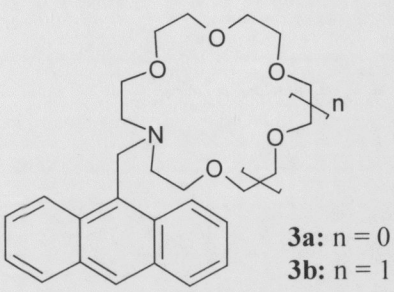
2

A recent example of a colorimetric anion sensor is **2**.[29] The four thiourea N-H groups are designed to geometrically fit anions, while the phenol group is involved in the recognition and reporting of the bound anion. Studies on a number of anions in $CHCl_3$ showed this sensor to be quiet active to the presence of F^-, $H_2PO_4^-$ and AcO^-. In the absence of any anions the absorption maximum was observed at 376 nm. In the presence of anions this shifted to 529 nm. In this case the ICT state is stabilized by anion binding resulting in a bathochromic shift.

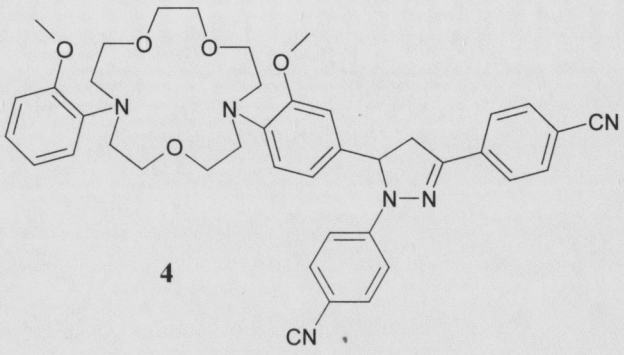
1.3.2 Fluorescent (PET) [30]

Fluorescence is the term that describes the emission when a ligand in its singlet excited state, S_1, deactivates to its ground state, S_0, with concomitant emission of light. Such photophysics has been shown to be quite useful as a method of signaling for optically based sensors. [3, 4, 5, 6, 12] Chemosensors **3(a-b)** and **4** are examples of such fluorescent sensors that utilize photoinduced electron transfer (PET) in signaling the presence of cations in solution. Sensors **3(a-b)** are early example from the group of de Silva, consisting of a 15-crown-5 (**a**) and 18-crown-6 aza crown (**b**) receptor with a 9-methyl anthracence moiety attached as a fluorophore. This is an example of a fluorophore-spacer-receptor system discussed previously where the spacer separates the two components and as such minimizes any π-π or σ-π orbital interactions between them.[30] In MeOH a very low fluorescent emission was observed and quantum yields of 0.003 and 0.009 were determined for **3a** and **3b** respectively. In the absence of any metal ions, (Figure 1.2 [A]) deactivation of the anthracence excited state is dramatically reduced by a PET process in which the lone pair of the nitrogen quenches the excited state of the anthracence moiety *via* electron transfer.[30] In contrast, upon addition of Na^+ in the case of **3a** or K^+ for **3b** the fluorescence emission is "switched on", (Figure 1.2[B]). The electrostatic effect of the metal ion causes a large increase in the oxidation potential of the

receptor and the PET process becomes thermodynamically unfavourable. Without PET deactivation of the excited state fluorescence becomes the dominant de-excitation pathway.[30]

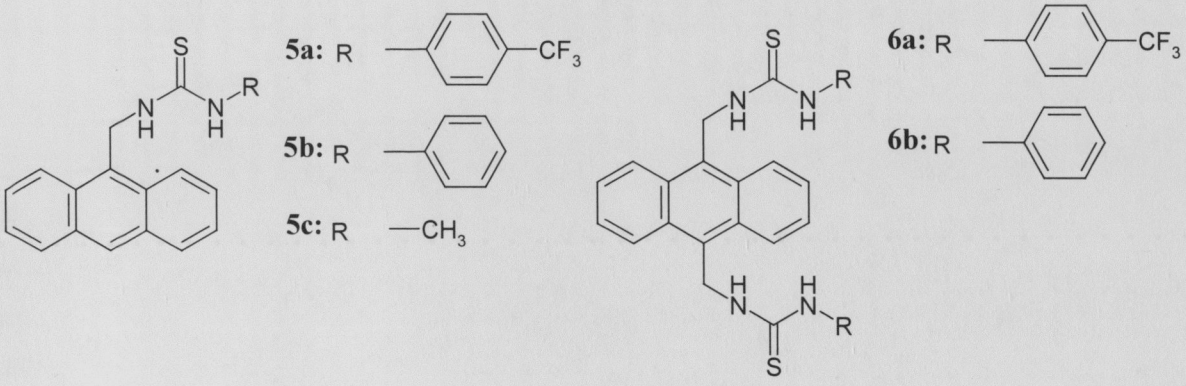


3a: n = 0
3b: n = 1



4

The crown ether functionalised chemosensor **4** is another example of a PET sensor for the detection of Na^+. In this case selectivity to Na^+ using a diaza crown receptor was achieved by functionalising the receptor with two methoxy moieties that can participate in the binding through a lariat ether effect. Crystallographic studies have shown that the methoxy groups are directly involved in binding. In this case the signaling system is a pyrazoline fluorophore that emits at long wavelengths, an essential feature for the design of chemosensors for physiological applications. Upon binding to Na^+ a 16-fold enhancement in fluorescence was observed with a quantum yield of 0.31.[31] The process by which this fluorescence is produced is the same as described for **3** and as illustrated in Figure 1.2.



5a: R = CF_3
5b: R = H
5c: R = CH_3

6a: R = CF_3
6b: R = H

Chemosensors **5(a-c)** [32] are recent examples of charge neutral anthracence based fluorescent sensors. **5(a-c)** showed ideal PET sensor behaviour in which the anthracence fluorescence emission was selectively quenched in DMSO in the presence of anions such as

AcO^-, $H_2PO_4^-$, and F^- but not by Cl^- and Br^-. In these sensors the binding of the anion is through a charge neutral thiourea receptor similar to that of **2**. The different R groups affect the acidity of the thiourea N-H protons that can be used to tune the selectivity of the receptor to different anions. Chemosensors **6a** and **6b** [33] are more recent and similar type fluorescent PET sensors to that of **5(a-c)** however, these sensors showed selectivity to pyrophosphate and bis-carboxylates. In this case, the anion recognition lead to the enhancement in the rate of electron transfer from the HOMO of the thiourea-anion complex to the anthracence excited state, which enhanced PET quenching.

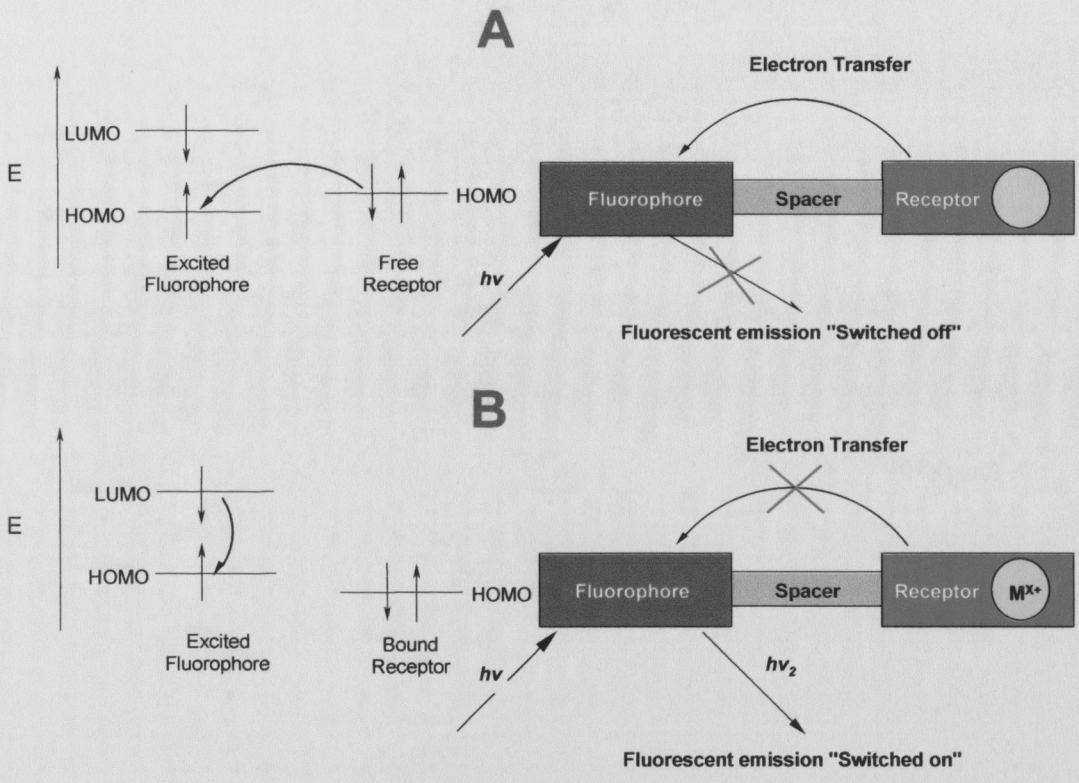


Figure 1.2 ***Illustration of PET mechanism for* 3** ***and* 4** [30, 12] ***A: when receptor is unbound electron transfer from the receptor HOMO can occur, preventing fluorescence. B: when receptor is bound oxidation potential of the receptor is increased and electron transfer becomes unfeasible resulting in deactivation of the fluorophore excited state by fluorescence.***

1.3.3 Metal centered Luminescence

Luminescent signaling can also be produced using metal complexes. The most common complexes are based on transition metal complexes such as Ruthenium, [34] Osmium [35] or

Rhenium. [36] An example of a Pb^{2+} sensor is **7**, which is comprised of an 18-crown-6-aza crown attached to a phenanthroline complexed with Rhenium tetra carbonyl.[36] Although the receptor of this sensor is typically used to sense K^+, this sensor was reported as a Pb^{2+} sensor. Upon titration of Pb^{2+} to an aqueous solution of **7** the fluorescent emission (between 500-700nm) is switched "on" with an increase in emission intensity. As shown in Figure 1.3, absorption of light produces a charge separated "singlet state", ($^1[d\pi^5\pi^{*1}]$), which decays *via* intersystem crossing. This ISC process is so fast that upon excitation all radiative and non-radiative decay occurs from the lowest excited "Triplet" state, ($^3[d\pi^5\pi^{*1}]$). It was proposed that an electron – transfer modulation process occurs in such systems when a cation is bound in the receptor. This affects the non-radiative intramolecular electron transfer process, which causes changes in the lifetime (τ) of the emission. Hence the lifetime, for this complex was measured to be 73 ns in N_2 degassed water at pH 6.0. Whereas when bound to $Pb^{2+}{}_{(aq)}$ the lifetimes of the complex increases to 123 ns. [36] This is in part due to an increase in the oxidation potential of the amine of the receptor of **7** upon metal binding indicating that this is a PET process. This prevents the intramolecular non – radiative electron transfer allowing luminescence to occur. [36]

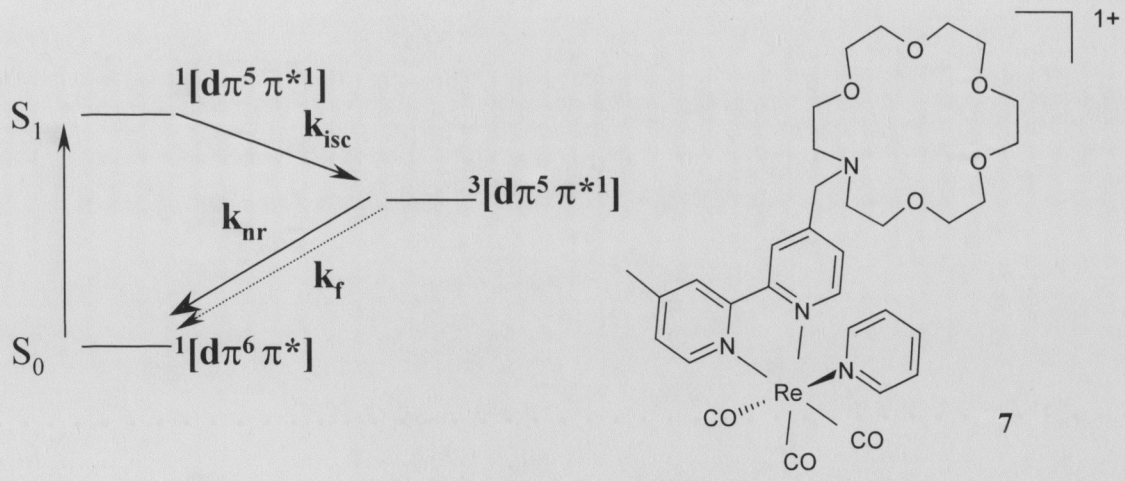
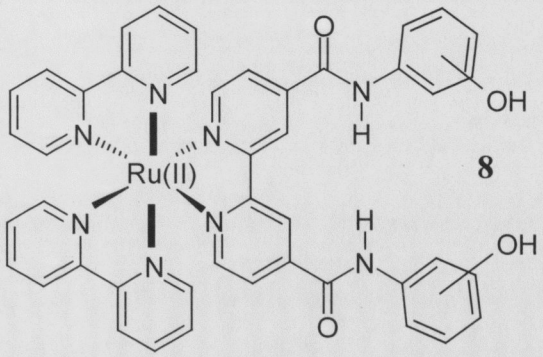


Figure 1.3 ***Illustration of metal centered luminescence mechanism for* 7 *(K_{ISC} = rate of intersystem crossing, K_{nr} = rate of non-radiative decay, K_f = rate of radiative decay)***[36]

The use of metal centered luminescence sensors for anion detection has also been reported.[37] The Ruthenium (II) tris (2,2'-bipyridyl) complex, **8** is an example of a Cl^- sensor.[37]

X-ray crystallography clearly shows hydrogen bonding occurring between Cl^- and the receptor amide hydrogen's. The addition of *meta* and *para* phenolic substituents was found to significantly enhance selectivity for Cl^- over Br^- and I^- through additional hydrogen bonding interactions. In this example addition of Cl^- to a MeCN solution resulted in an increase in the MLCT emission maxima.



8

1.4 Considerations for *in vivo* sensing

As mentioned previously, chemosensing can take place in many matrices. Of these we will consider *in vivo* only. Over the years, a substantial amount of work has been carried out on the use of fluorescence sensors for *in vivo* applications. This research has been spurred on by the requirement to replace radio labeling as a means of detection because of its many disadvantages such as radioactivity, handling license requirements, disposal costs, risk to health and short shelf life. [38, 39, 40] The use of fluorescence as a detection mode has been the major area of research because of its ability for detection to limit as low as 10^{-10} M, making it a good alternative to radioactive tracers. However, there are a number of drawbacks, which have led to the current interest in finding a better alternative. The main concerns with fluorescence sensors are the to excitation wavelengths used and the lifetime of the emissions.[39] Excitation *in vivo* can lead to autofluorescence in which biological species fluoresce, or cause Rayleigh scattering due to micro heterogeneous biological moieties. Using sensors that can be excited at longer wavelengths can elevate autofluorescence. This has been demonstrated successfully by Tsien *et al.* with many examples of Na^+, K^+ and Ca^{2+} probes, all of which have excitation wavelengths of *ca.* 350 nm or higher.[41, 42, 43] However the short lifetimes

(nanosecond scale) characteristic of fluorescent sensors cannot be overcome. Therefore the emissions of many fluorescent sensors cannot be distinguished from the emissions caused by autoflourescence. [39]

1.5 Lanthanide complexes: an alternative signaling system for *in-vivo* applications

In recent times, the use of lanthanide ions has been researched as an alternative means of signaling in biology and biotechnology.[38, 44] Results of some lanthanide complexes have resulted in commercially successful immuno-assays and DNA probes.[38] Lanthanide ions have a number of advantages that make them appealing as signaling systems *in-vivo*. In the case of lanthanides such as Eu (III) and Tb (III) lifetimes can range in the millisecond timescale. This is a considerable advantage over many existing flourophores. Such long lifetimes allows for the use of time resolved techniques that can overcome the problem of autofluorescence. This involves a process referred to as 'Time gating' as shown in Figure 1.4. By delaying the time between excitation and observation of the emission, the short-lived background fluorescence emission can be avoided.[43] Other advantages found with lanthanides include large stoke shifts of around 150-300 nm and emissions that normally consist of several narrow bands. [43]

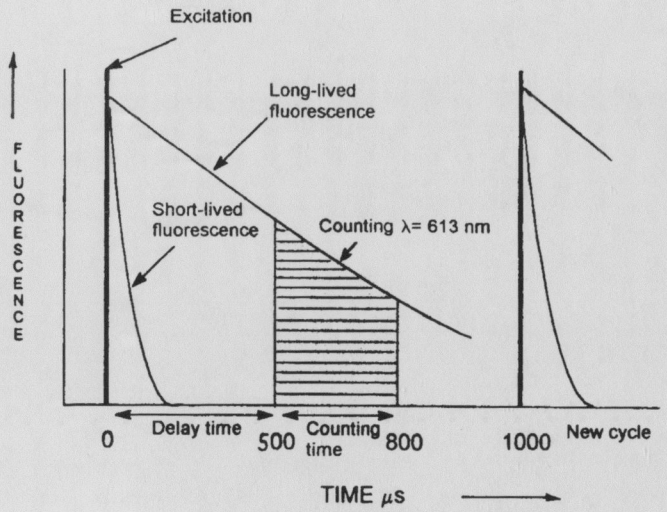


Figure 1.4 ***Illustration of time gating*** [43] ***After excitation a delay of up to 0.5 ms can be applied. This allows sufficient time for all fluorescent emissions to cease. Observation of the long-lived emission(in this example 613 nm for Eu(III)) can then take place.***

1.5.1 How to produce lanthanide luminescence – considerations for developing signaling systems

Lanthanide f-f transitions are Laporte-forbidden and very weak, with extinction coefficients of the order of only 0.5-3 $dm^3\ mol^{-1}\ cm^{-1}$.[45, 46] Direct excitation of the lanthanide ion is inefficient, and only practical with lasers, or at high ion concentrations. Such disadvantages can be overcome by using sensitisation. This involves incorporating a sensitising chromophore (often termed an 'antenna') into the lanthanide-coordinating ligand, allowing indirect excitation of the lanthanide ion, [47, 48] usually through an intramolecular energy transfer process.[46, 49] The process by which this photophysical emission is produced is described graphically in Figure 1.5 and 1.6.

As shown in Figure 1.5, lanthanide luminescence begins with the excitation of the antenna chromophore (sensitiser, denoted Ar in Figure 1.5) from the ground state, S_0, (Ar-Ln), to the singlet-excited state, S_1, (^{1}Ar-Ln). Following the formation of this excited state, deactivation to the ground state (Ar-Ln), with concomitant ligand fluorescence emission (hv') can occur. It is also possible for this excited state to be quenched ($k_q[Q]$) back to the ground state (Ar-Ln). A triplet excited state, T_1, (^{3}Ar-Ln) can also be formed by intersystem crossing (ISC). At this point ^{3}Ar-Ln can be lost by quenching from oxygen, ($k_q[O_2]$). It is also possible to transfer the excited state of the antenna (^{3}Ar-Ln) to the lanthanide excited state ($^5D_4$ and $^5D_0$ for Tb(III) and Eu(III) respectively) by way of an energy transfer process, resulting in Ar-Ln*. [50] The process by which this energy transfer occurs has two proposed mechanisms. [48] Firstly, the Dexter mechanism involves an exchange interaction that involves a mutual electronic exchange between the antenna and the metal center acceptor.[51, 52] Energy transfer occurs through overlapping orbitals of the antenna and the metal ion and hence requires physical contact between the two components. Secondly, energy transfer *via* the Förster [53] mechanism, which is due to a coulombic interaction that arises when the dipole of the excited antenna induces a dipole in the acceptor (lanthanide metal center). This is a through space process that does not require physical contact between the sensitiser and the acceptor. The rate of energy transfer (k) *via* the Förster mechanism is distance dependent as shown by equation **1**. (Where r is the intramolecular distance between the sensitising chromophore and the metal center)

$$k \propto r^{-6} \qquad (1)$$

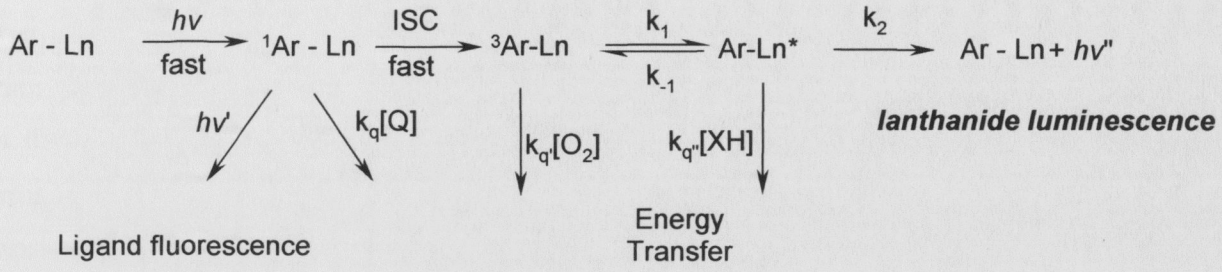


Figure 1.5 ***Photophysical pathway to produce lanthanide luminescence by sensitisation.***[45, 46]

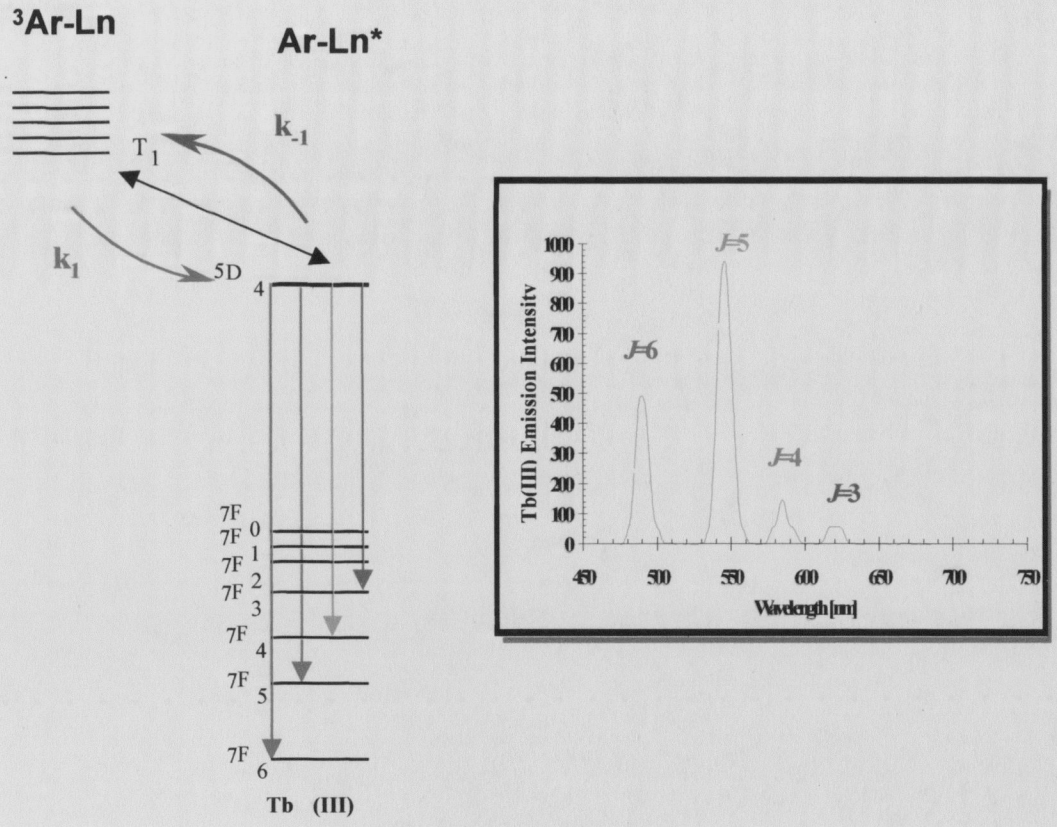


Figure 1.6 ***Jablonski diagram of sensitisation for Tb(III), showing the reversible formation of Ar-Ln*, by energy transfer from sensitiser triplet state to the lowest lanthanide excited state $^5D_4$(Inset: Typical Tb(III) emission spectrum showing most common transitions)*** [47, 54, 55]

As shown in Figure 1.5 and 1.6, the formation of the lanthanide excited state (Ar-Ln*) is a reversible process that can result in the reformation of the antenna triplet excited state (^{3}Ar-Ln). It is also possible to quench this lanthanide excited state by vibrational quenching from energy-matched oscillators, (k_q[XH]) such as OH, NH and CH. In situations were the energy transfer is efficient in forming Ar-Ln*, a lanthanide emission can occur. Figure 1.5 shows that in the case of Tb(III) energy transfer occurs to the lowest excited state, $^5D_4$. The resulting emission involves transitions from this state. For Tb(III) these transitions are $^5D_4 - ^7F_J$, the most common of these transitions observed are those of J = 6, 5, 4 and 3.

1.5.2 Considerations when applying antenna effect in signaling applications

This long photophysical pathway to the lanthanide emission, as shown above has a number of factors that must be considered when designing complexes to use for *in vivo* sensing. Firstly, we must consider the lanthanide ions that can be used and discuss them in terms of the energy gaps between their excited and ground states. Not all lanthanide ions can be used for signaling in *in vivo* applications. In some lanthanide ions the energy gap is so large that the emission wavelength appears in the ultra violet region *ca.* 300 nm as is the case for Gd(III). In other lanthanides with small energy gaps, O-H, N-H, C-H and O-D oscillators deactivate the excited state before luminescence can occur, since the energies of these oscillators match that of the lanthanide excited state. [48, 56, 57, 58, 59, 60] The photophysical properties of Eu(III) and Tb(III) have generated the most interest of all the lanthanides. In these lanthanides, emissions occur in the visible region. For example Eu(III) emits in the red and Tb(III) emits in the green and both have long lived emissions in the milliseconds range. Secondly, the triplet energy of the sensitising chromophore must be considered.[48] The lowest excited states of Eu(III) and Tb(III) are 17,200 cm^{-1} and 20,500 cm^{-1} respectively. The energy of the triplet excited state needs to be at least 1700 cm^{-1} above the excited state of the lanthanide, to prevent a thermally initiated back energy transfer process, from Ar-Ln* to ^{3}Ar-Ln. Finally the effect of O-H, N-H and C-H oscillators must be considered, for instance designing lanthanide complexes which are free from bound water molecules can greatly improve the lifetime and emission intensity of a complex. Metal bound water molecules can be determined in a complex by measuring the lifetime of the luminescent emission in H_2O (τ_{H2O}) and in D_2O (τ_{D2O}) respectively.

Determination of ***q***, the number of bound water molecules can be made using the equations derived by Horrocks *et al.*.[61] From studies by Parker *et al.* these equations have been refined further to take into account not only the deactivation by O-H oscillators but also deactivation by N-H and C-H oscillators. This results in equations (**2**) and (**3**), where A is a proportionality constant specific to a given lanthanide ion that mirrors the sensitivity of the ion to quenching from metal bound waters. In the case of Tb(III) and Eu(III) this is 5.0 ms and 1.2 ms respectively. [62]

$$[q \pm 0.5] : q^{Eu(III)} = A\,[(1/\tau_{H2O} - 1/\tau_{D2O}) - 0.25 - 0.075x] \qquad (2)$$

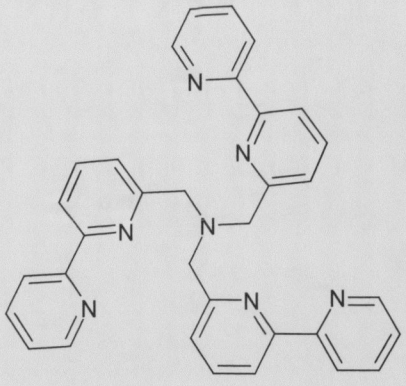
$$[q \pm 0.5] : q^{Tb(III)} = A\,[(1/\tau_{H2O} - 1/\tau_{D2O}) - 0.06] \qquad (3)$$

1.6 Complexation and sensitising of lanthanides: An overview

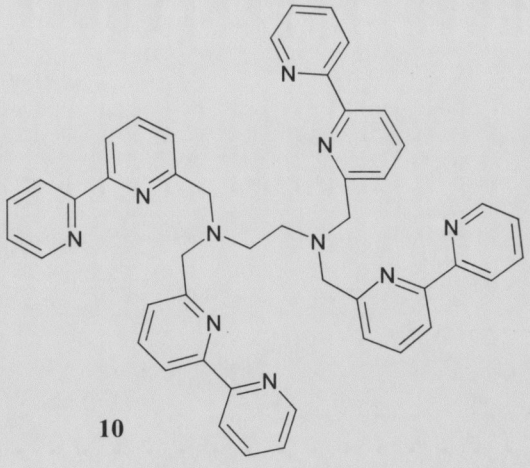
The Ln (III) ions can be classified as "hard acids". Coordination occurs *via* ionic bonding interactions, leading to a strong preference for negatively charged or neutral donor groups that possess large ground state dipole moments such as carboxylic acid and carboxyl amide oxygen's. Among the donor atoms most commonly used the binding preference are O > N > S. In aqueous solution, donor groups containing neutral oxygen or nitrogen atoms generally bind only when present in multidentate ligands, such as podands and cryptates. [51] In order to use lanthanide ions for *in vivo* chemosensing, stable complexes are required within which the metal sensor can be shielded from quenching moieties such as O-H, N-H and C-H oscillators as previously discussed. Lanthanide ions in solution require a high degree of coordination typically with coordination as high as 9-10. Complexation with multidentate ligands is a common method of forming highly coordinated complexes. Complexation is required as stated above for shielding and also to tether the lumophore (lanthanide complex) to the receptor. The following is a review of the development of ligands used in complexing lanthanides in recent years. This review looks at four of the most common types of multidentate ligands that have been utilized. These are *podands*, *cryptands*, *calixarenes* and *macrocycle / bicycle* ligands. The formation of lanthanide complexes of such ligands and their photophysical properties are discussed in the following sections.

1.6.1 Podands

Balzani *et al.* [63, 64, 65] have demonstrated the use of bypyridyl (bpy) based podand ligands for lanthanide complexation. A tris bpy, **9** and tetra bpy podand, **10** were reported. The lowest triplet energy of the bpy unit being ideal as a sensitiser ($^3\pi\pi^*$) at *ca.* 23,000 cm^{-1}. In both cases Eu(III) complexes were shown to be unstable in aqueous solution as demonstrated by monitoring the changes in the *UV-Visible* spectra overtime. In the case of the Eu(III) complex, **Eu.10**, (from herein lanthanide complexes of ligands presented in this text will be presented in the following format: **Ln.X**, were **X** is the number which denotes the ligand) this was observed as a slow decomposition over 1 hour, where as **Eu.9** was found to be stable in MeOH:H_2O, 4:1. A Eu(III) emission was observed when bpy was excited at 300 nm which was assigned to an energy transfer from the coordinated ligand to the metal center. Lifetime studies (As described in section 1.5.1) indicated two water molecules bound to **Eu.9**, and a quantum yield of $\phi = 0.1$. The complex, **Eu.10** showed a quantum yield of, $\phi = 0.003$ in water and 0.07 in MeOH. From lifetime studies OH quenching was very efficient and more severe in **Eu.10**. This indicates that **Eu.9** binds better improving the shielding of the lanthanide cation from the solvent environment.



9



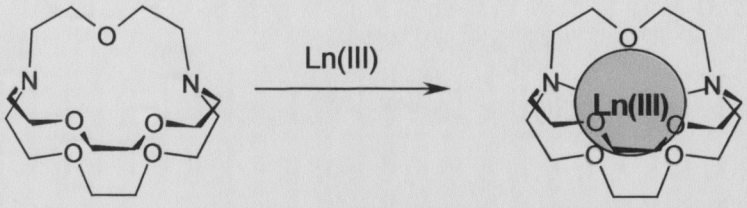
10

1.6.2 Cryptands

The formation of stable complexes with alkali cations by [2.2.1] and [2.2.2] cryptates has been well documented.[66, 67, 68] The formation of stable complexes with lanthanides are also possible as lanthanides have similar size cationic radii (Ln^{3+} - 1.05 – 0.85 Å) as the alkali and

alkali earth cations. Below, follows a brief review of a number of Eu(III) and Tb(III) cryptate complexes and their photophysical properties.

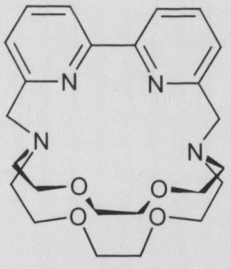
We begin this review with a look at the photophysical properties of the Eu(III) and Tb(III) complexes of **11**, a [2.2.1] cryptate. Sabbatini *et al.*[69] have shown that stable complexes can be formed and are stable in water unlike the podands discussed earlier (section 1.6.1). Lifetime studies indicated ***q*** values of 1.7 and 1.8 for the complexes of **Eu.11** and **Tb.11** respectively indicating that each complex has 2 water molecules associated with their structure. Photophysical studies of **Tb.11** showed no temperature effect indicating no effect from non-radiative decay.[70] In the case of **Eu.11** a charge transfer deactivation state resulted.[71] In further studies by Sabbatini *et al.*[72] it was shown that luminescent properties of both **Eu.11** and **Tb.11** could be enhanced by the addition of fluorine anions. In this study, F^- displaced the metal bound water molecules from the cryptate complexes, thus preventing O-H vibrational quenching. In the case of the **Eu.11** coordination of the F^- was found to shift the LMCT excited states of the cryptate to higher energies preventing the radiationless decay previously observed for **Eu.11**.



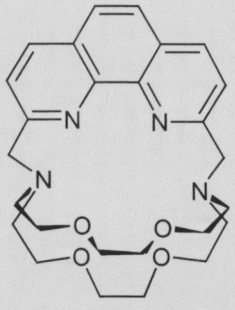
11 **Ln.11** (Ln = Eu(III) or Tb(III)

The synthesis of cryptates incorporating bpy moieties have also been reported.[73] The **Tb.12** and **Eu.12** complexes of **12** showed increases in the lifetime of the lanthanide emissions, of 0.72 ms and 0.41 ms respectively; upon excitation at 310 nm corresponding to excitation of the bpy moiety and energy transfer to the lanthanide center. Similar results are found in the phen version, **13**, with **Eu.13** having a lifetime of 0.27 ms when excited at 280 nm. A large number of modifications of these cryptates have been reported, all showing enhancements in the metal ion emission.[74] Two other examples are that of ligands made

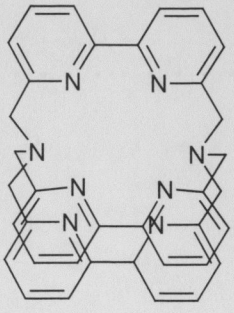
entirely of bpy, **14** or phen, **15** moieties.[73,75] Of these, the **Tb.14** and **Eu.14** complexes showed lifetimes similar to that of the **Tb.12** and **Eu.12** complexes.[74, 76, 77, 78, 79, 80] In the case of **Tb.14** a low-lying triplet state was present. The low luminescence emissions observed was partly due to poor shielding as indicated by the ***q*** value of 2.5. Attempts at improving the quantum yield (ϕ), of these Eu(III) and Tb(III) complexes with the use of *N*-oxide derivatives **16**, **17** and **18** have been reported.[75, 80, 81, 82, 83, 84] An improvement in the ***q*** values was observed. For example **Eu.16** had a $q = 1.4$ compared to $q = 2.5$ for **Eu.14**.[85] In terms of the **Eu.16** complex, the *N*-oxide was shown to have a higher quantum yield than its nitrogen precursor, **Eu.14**, of $\phi = 0.15$ for **Eu.16** and $\phi = 0.02$ for **Eu.14** respectively. This was described as being due to *N*-O increasing the efficiency in which the $^3\pi\pi^*$ was populated.[85, 86] In the case were the *N*-oxide bpy has been functionalised with methyl esters, **17**, reduction in the observed quantum yield, from $\phi = 0.15$ to $\phi = 0.09$ was observed. This was determined to be a low-lying triplet state in the bpy sensitizing chromophore.[85] Other examples of functionalisation on the *N*-oxide bpy have shown improvement to the quantum yield as was demonstrated by **18** from which a quantum yield of $\phi = 0.20$ was determined.[87] These good shielding characteristics and high quantum yields show *N*-oxide cryptates as promising ligands for the formation of sensitisable lanthanide complexes.



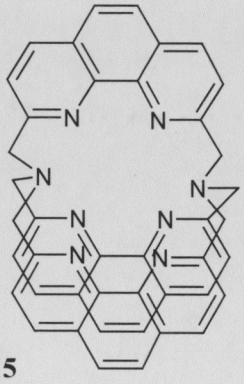
12



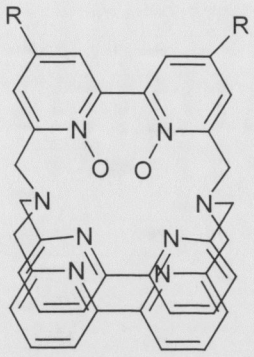
13



14

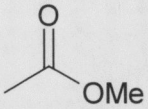


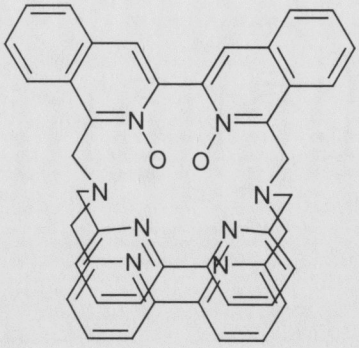
15



16 :R = H

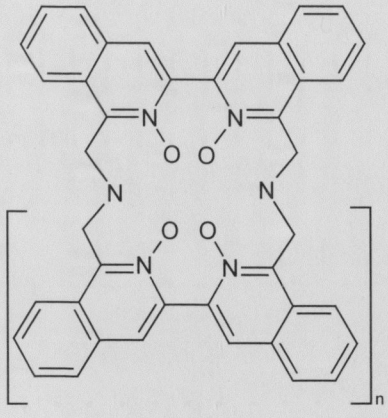
17: R =





18

From the above results it can be seen that the most efficient ligands to use for lanthanide complexes are aryl *N*-oxide cryptates. In a final example of this family of ligands a report on [2.2.2] aryl *N*-oxide ligand, **19** was reviewed.[83] However, the effect of the large number of *N*-oxide groups was found to be detrimental, resulting in the formation of unstable complexes. It was determined that the cavity of this cryptate had been reduced substantially resulting in inadequate complexation with Eu(III). This was reflected by a quantum yield of $\phi = 0.002$ for **Eu.19** in MeOH. [83]



19 (n=2)

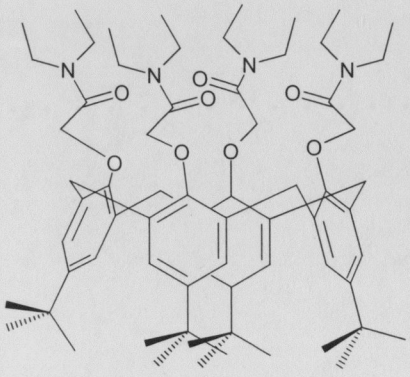
In summary the above review of podands has shown that their use as ligands for complexation and sensitization were unsuccessful due to the formation of unstable complexes and poor shielding from the solvent environments. The use of cryptands has shown that this

problem of stability and shielding can be overcome and by careful choice of the incorporated chromophore and their substituents, efficient ligands can be developed.

1.6.3 Calixarenes

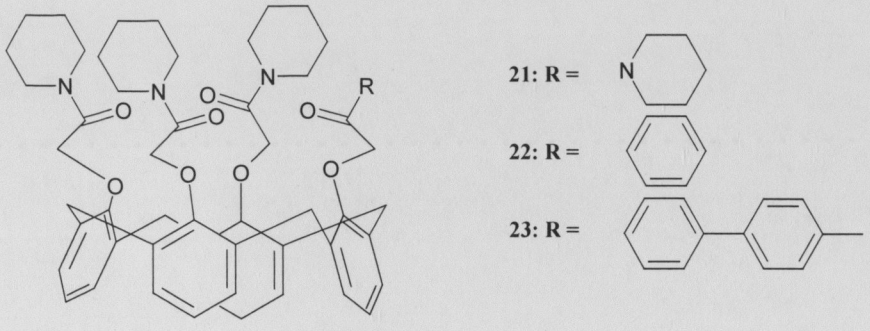
Calixarenes modified on the lower rim with, ether, acetate, ketone and amide functional groups have been shown to readily form complexes with ions and neutral molecules.[88] Calix[4]arene is a common calixarene that has the ability to bind Na^+. Lanthanides have similar size radii to that of Na^+ and Ca^{2+} and therefore can be bound in appropriately functionalised calix[4]arene ligands. For this reason calixarene lanthanide complexes have been synthesized and their photophysical properties examined. The following section is a review of some calixarene lanthanide complexes and their photophysical properties.

We begin with the reported work of Sabbatini *et al.* [89] in which **Tb.20** and **Eu.20** complexes were made from **20**. Ligand **20**, was an example of a Calix[4]arene that contained *t*-butyl groups on the upper rim and amido groups functionalised on the phenols of the lower rim. In this example the aromatic residues of the calix[4]arene were used as a sensitiser. These complexes were studied in water and MeOH. In both Eu(III) and Tb(III) complexes ***q*** values of *ca.* 1 were determined. Of these two complexes the **Tb.20** complex was found to be highly luminescent with a quantum yield of $\phi = 0.2$, compared to $\phi = 0.002$ for **Eu.20**. The high quantum yield was explained as being due to efficient ligand to metal energy transfer and good shielding from solvent deactivation. The short-lived **Eu.20** emission was attributed to a commonly observed deactivation process.

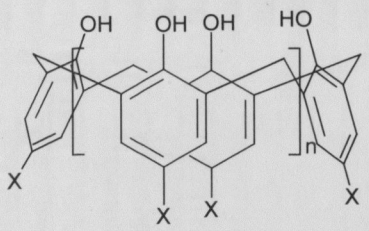


20

Sato and Shinkai [90] reported three ligands **21**, **22** and **23** similar to **20**. The ligand, **21** contained four piperidin amide groups on the lower rim, while **22** and **23** had one of these piperidin amide groups replaced by phenacyl and diphenacylcarbonyl sensitisers respectively. The Tb(III) and Eu(III) complexes of **21**, **22** and **23** were studied in MeOH and in MeCN. Almost all of the Tb(III) complexes showed higher quantum yields by one or two orders of magnitude. The quantum yields of the Tb(III) complexes ranged from ϕ = 0.27 – 0.16 compared to the Eu(III) complexes which ranged from ϕ = 0.06 – 0.0017. The high values for Tb.**21** were attributed to good metal encapsulation by the ligand as shown previously.[89] Sensitisation of Tb(III) in **Tb.21** was reported to occur by energy transfer from the phenol residues of the calixarene. However in the case of the **22** and **23** energy transfer was suggested to be possible from the attached sensitisers in some cases. Sensitisation of **Tb.22**, **Eu.22** and **Eu.23** are suggested to occur in this way. In contrast **Tb.23** showed only energy transfer from the phenol residue of the calixarene, the diphenyl acyl units lowest triplet energy T_1 was thought to be too low. For the Eu(III) complexes the highest quantum yields were found for **Eu.22** and **Eu.23** but were only 0.06 (after excitation at 270nm) and 0.061 (after excitation at 325 nm) respectively and only in MeCN. This clearly indicates that the choice of sensitiser is important in improving Eu(III) quantum yields. In work by Matsumoto and Shinkai, [91] Tb(III) and Eu(III) complexes of calixarene ligands similar to **21,** showed relatively high quantum yields could be produced by careful choice of sensitizing chromophores that have high triplet energies and carbonyl groups which facilitate intersystem crossing, (ISC).



Sato *et al.*[92] followed up the previous example of Sabbatini by synthesizing Calix[4]arene, **24**, Calix[6]arene, **25** and a Calix[8]arene, **26** and their Tb(III) complexes which were reported to be water soluble. In these ligands the phenolic moiety on the lower rim was not functionalised and the upper rim contained sodium sulphate groups. The quantum yields of **Tb.24** and **Tb.26** were found to be quite high and comparable with those mentioned for **Tb.20** shown previously. The high values were thought to be due to structural effects. In the case of the **Tb.24** it was found that a 1:2, metal:ligand complex was formed which allowed the lanthanide ion to be shielded through coordination by the eight phenol groups from the deactivating water molecules. In contrast the complex of **Tb.25** showed a 1:1, metal:ligand complex, which resulted in poor shielding from the surrounding solvent. The complex of **Tb.26** showed a 1:1, metal:ligand complex was formed. The relatively high quantum yield was attributed to a flexible ring that allowed for coordination with all eight of the phenol groups in this ligand. This example indicates that when designing luminescent complexes with calixarenes shielding can be achieved with large flexible ligands, it is not essential that the ligand is small and rigid



X = SO_3Na

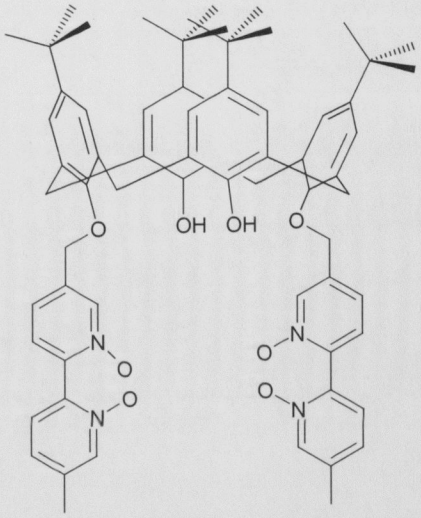
24: n = 1

25: n = 3

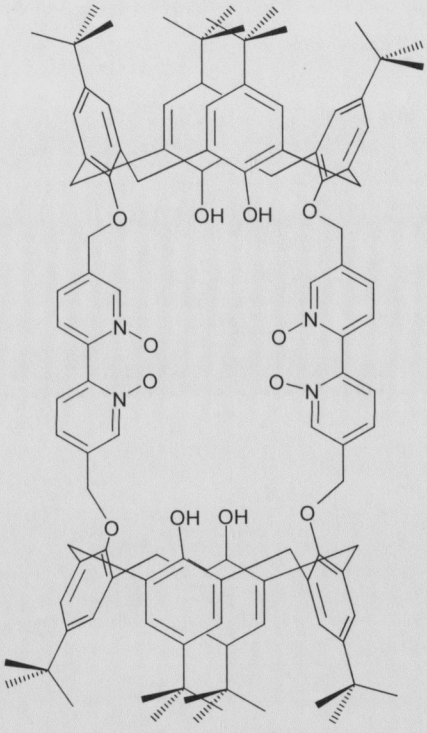
26: n = 5

Ulrich and Ziessel [93] reported the synthesis of a number of calix[4]arene based ligands that were functionalised on the lower rim in the phenol position with 5,5'-substituted-2,2'-bypyridine moieties that gave podand-like ligands capable of encapsulation of lanthanides. In these examples the calixarene was not used to coordinate with the lanthanide ion or to sensitise it. The substituted bpy units carried out both these functions. The calixarene was required in the design in order to hold the bpy units in place. Two examples reported based on this family of ligands were the *N*-oxide functionalised ligands **27** and **28**. [94] For these ligands

stable complexes were formed in MeOH and water. The luminescence of the Tb(III) complexes was reported to be weak at room temperature, as a result of a low-lying triplet state. In contrast the Eu(III) complexes showed high emissions with quantum yields of ϕ = 0.19 for **Eu.27** and ϕ = 0.10 for **Eu.28**. The luminescence of Eu(III) complexes was found to be unaffected by temperature or deuterated solvents thus showing good encapsulation of the metal.



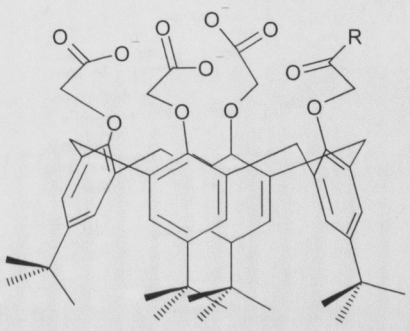
27



28

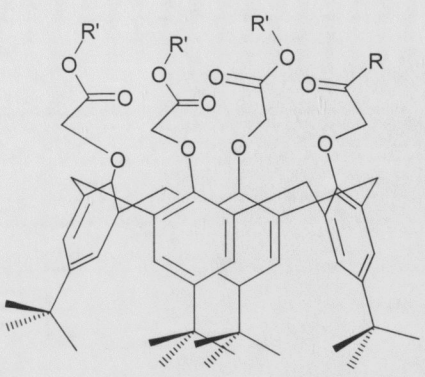
In 1995 Rudkevich *et al.*[95] showed the synthesis of functionalised calix[4]arene where three of the phenolic residues have been substituted with carboxylic acid groups and the fourth substituted with a carboxamido ester. In some of these cases a pyridine moiety was incorporated into the structure yielding **29**, **30**, **31** and **32**. All of the Tb(III) and Eu(III) complexes of these ligands were found to contain only one metal bound water molecule. Studies were carried out in MeOH for all these complexes. A conclusion based on the lifetimes reported for all these complexes with both Tb(III) and Eu(III) suggests that different

side groups attached as an 'R' group have no effect on the shielding efficiency of the encapsulated lanthanide cations. Excitation spectra indicated that efficient energy transfer occurred from the calixarene aromatic moieties as well as the pyridine groups. This report demonstrated the potential ability of developing neutral lanthanide complexes to which specific sensitizing chromophore can be added without effecting shielding properties, thus leading to control over possible excitation and energy transfer properties that can be designed into these complexes.



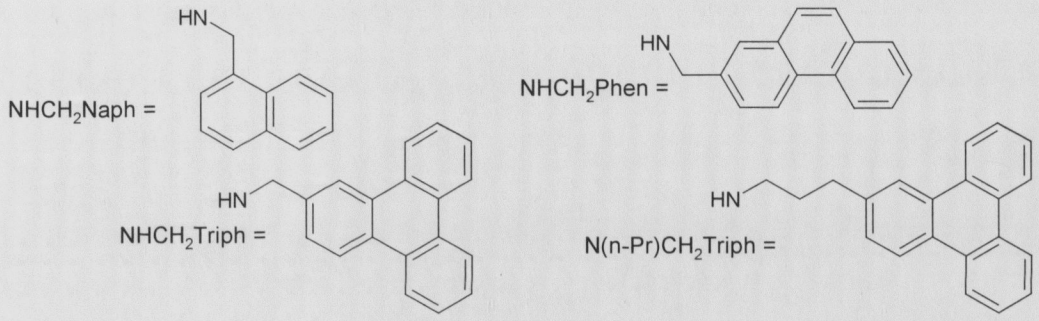
29: R= $NHPr^n$
30: R=$NH(CH_2)_2NHC(O)CH_3$
31: R= $NHCH_2Py$
32: R= $NH(CH_2)_2Py$

In a report by Steemers *et al.* [96] similar calix[4]arene tris esters, **33**, **34**, **35**, **36**, **37** and triacid **38**, **39**, **40**, **41** ligands were developed. The fourth phenol position was functionalised with naphthalene, phenanthrene, and triphenylene by way of an amide link or in the case of **36**, by an ester link. In all cases the Tb(III) and Eu(III) complexes were studied in MeOH. In the case of **Eu.38** (when excited between 300 and 320 nm) the Eu(III) emission was enhanced by a factor of 2.9. A more efficient sensitisation process had been expected as the absorption in this region was found to be strong. Better results were obtained for complexes that contained phen, **39** and triph, **40**. For **Eu.39** when excited at 300 nm a 33-fold enhancement in the emission was observed. In contrast **Eu.37**, showed no emission. However, when hydrolysed to its tri acid form, **Eu.41**, a weak emission was seen. Morever when the bridging sensitiser was functionalised through an ester linkage, **36**, instead of an amide linkage **35**, a stronger emission was observed, particularly in the case of **Eu.36** that was the most emissive complex studied. This result showed that the antennae effect was not really perturbed by other binding sites more so by the spacer. The Tb(III) complexes of these ligands were also tested and in these cases only triph based ligands showed lanthanide emissions.



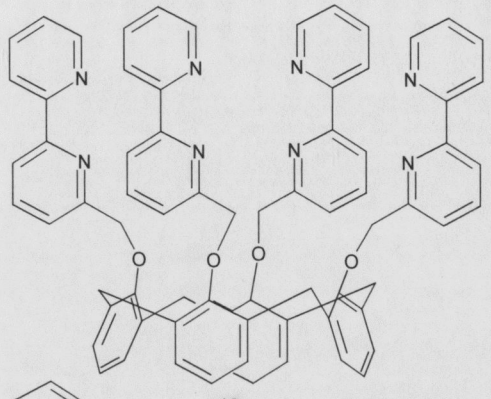
33: R = $NHCH_2Naph$, R' = C_2H_5
34: R = $NHCH_2Phen$, R' = C_2H_5
35: R = $NHCH_2Triph$, R' = C_2H_5
36: R = OCH_2Triph, R' = C_2H_5
37: R = N(n-Pr)CH2Triph, R' = C_2H_5

38: R = $NHCH_2Naph$, R' = H
39: R = $NHCH_2Phen$, R' = H
40: R = $NHCH_2Triph$, R' = H
41: R = N(n-Pr)CH2Triph, R' = H

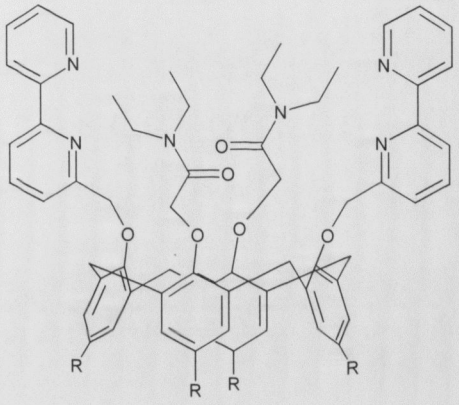


In a final review of calixarenes as complexing ligands for sensitization of lanthanides a report of Sabbatini *et al.* [97] was reviewed. The synthesis and photophysical studies of a calix[4]arene containing four bipyridine units namely **42, 43**, **44** and also examples with methylated phenanthroline moieties, **45**. Coordination and sensitisation of the complexed lanthanide cations occur through the bpy or phen units. All studies were carried out in MeCN. **Tb.42**, **Tb.43** and **Tb.44** gave long-lived emissions of 1.4 ms, 1.65 ms and 1.9 ms respectively, while **Eu.42**, **Eu.43** and **Eu.44** gave shorter values of 0.65 ms, 0.50 ms and 0.65 ms respectively. However, the quantum yields, ϕ were quite different. This was attributed to different metal-ligand interactions, *i.e.*, for the complexes with **42** low ϕ were attributed to steric hindrance preventing adequate metal ligand coordination. This hypothesis was helped with the results of CPK modeling. These examples showed more intense luminescence emissions than calixarenes with just acetamide appendages discussed earlier due to the higher molar absorption coefficients of the bypyridine chromophores over calixarene aromatic groups. Formation of lanthanide complexes with **45** was not possible, due probably to steric

hindrance caused by the methyl groups on the phen ligands. This steric hindrance prevents the phen units coming close enough to form stable complex with the lanthanide cation.

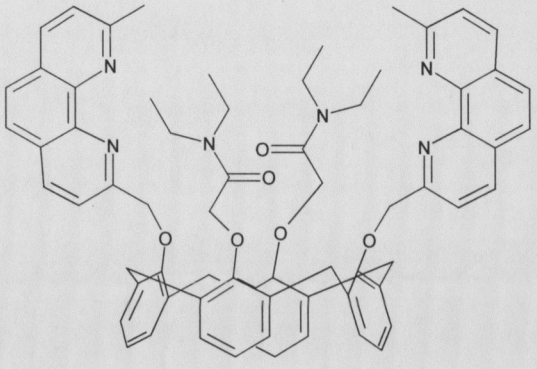


42



43: R = H

44: R = *t*-Bu



45

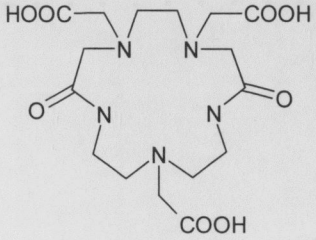
In summary, the development of lanthanide complexes using calixarenes has been shown. Efficient sensitisation of the lanthanide complexes can be achieved through the excitation of the calixarene phenol groups or by attachment of other sensitising chromophores. This incorporation of additional sensitising chromophores can allow for manipulation of the excitation wavelength used to produce the lanthanide emissions.

1.6.4 Macro cyclic and bicyclic ligands

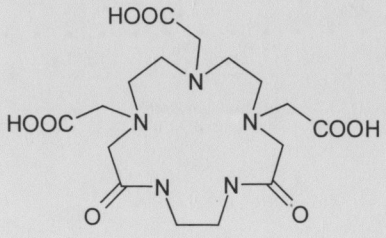
The formation of metal ligand complexes of Alkali earth and Alkali metals with crown ethers has been studied since their discovery by Pederson as discussed earlier.[98] Selectivity of the ligand to specific metals ions was controlled mainly by the size of the ring (cavity).[99, 100] We have presently only discussed other macrocyclic systems such as cryptands that could be

used for complexation. Further work on aza crown systems to which pendant arms can be attached, makes for an even larger array of coordinating ligands. It has been shown that small macrocycles such as cyclen that normally favour Na^+ can be functionalised with pendant arms such as alcohols or amides, which changes the selectivity towards larger metal ions such as Ca^{2+}, Cd^{2+} or Pb^{2+}.[101] The lanthanide ions having similar size radius to cations such as Na^+ or Ca^{2+} have also been shown to coordinate in such ligands.[102] The following section is a review of the use of functionalised aza macrocycles and bicyclic ligands for lanthanide complexes and their photophysical properties.

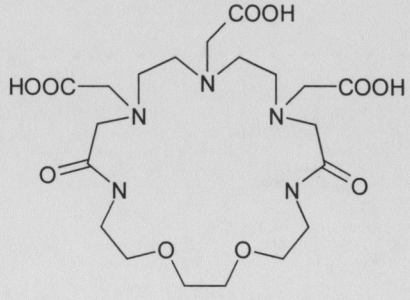
Frey *et al.* [103] have shown a number of amide macrocyclic ligands, **46-50**, which had carboxylate pendant arms attached to increase their coordination potential. This study demonstrated the effect that different size cavities and number of carboxylic appendages had on coordination and complexation of lanthanide ions. The first three ligands, **46-48** were all determined to form 1:1 complexes with Eu(III). The complexes, **Eu.46** and **Eu.47** had ***q*** values of 3.4 and 2.3 respectively indicating complexation but without adequate shielding despite the ligands being octadentate. The Eu(III) complex of **48** was found to be more shielded, showing a ***q*** value of 1.3. The Eu(III) complex of **49** showed similar shielding power to that of **48**, however, in this case a 2:1, metal:ligand complex was formed. The final example, **50** was not an amide-based macrocycle. In this case the ligand consisted of two cyclen ligands attached through an amide bridging moiety. Again **50** formed a 2:1, metal:ligand complex, with good encapsulation shown by a ***q*** value of 1.2. These examples have demonstrated that a variety of macrocyclic ligands can be used to form stable and well shielded lanthanide complexes.



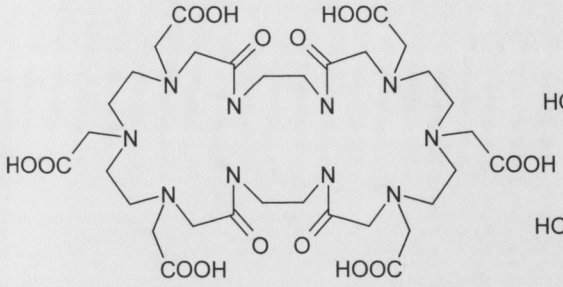
46



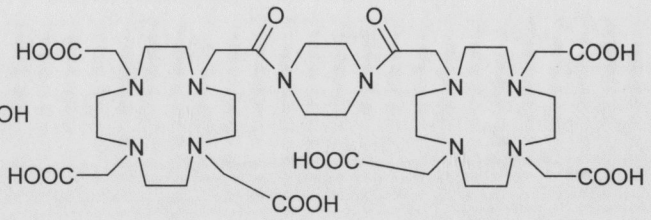
47



48

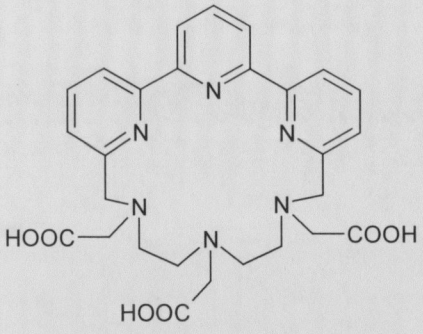


49



50

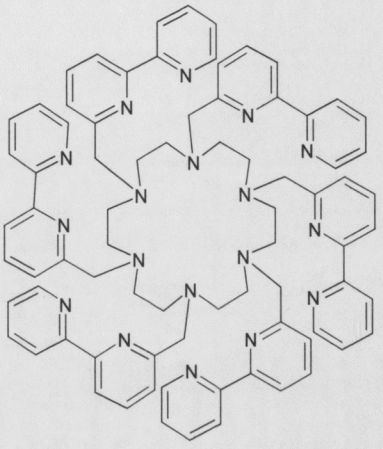
Galaup *et al.* [104] has shown that aza crown macrocycle ligands such as **51** can be used to produce stable, well-shielded lanthanide complexes that have good photophysical properties. In this ligand a terpyridine moiety was incorporated to act as a sensitiser. In the case of **Eu.51** and **Tb.51** quantum yields of $\phi = 0.18$ and $\phi = 0.21$ were determined in water respectively.



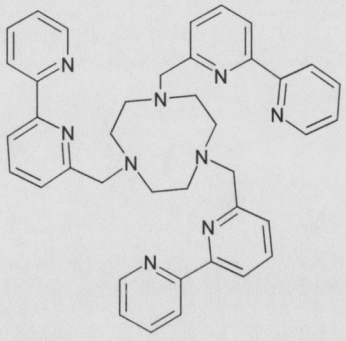
51

Ziessel *et al.* showed the synthesis [105] of a number of aza crown ligands including **52,** (18-crown–6) and **53** (12-crown-3) aza crowns functionalised with 9-methyl bpy as pendent coordination sites. In the case of **52** there are 18 coordination points, that resulted in the formation of 2:1 metal:ligand complexes. Ligand **53** being a smaller macrocycle was found to form 1:1 metal:ligand complexes. Studies were performed in water, MeCN or in a mixture of EtOH:MeOH (1:5). Tb(III) and Eu(III) complexes of **52** were shown to have poor photophysical properties. These were attributed to poor shielding of the lanthanide ions and also in the case of **Eu.52** to a low-lying LMCT deactivation process. [106] The complexes of **53** were found to be much better with a quantum yield of $\phi = 0.37$ reported for **Tb.53.** The Eu(III)

complex **Eu.53** was found to suffer from the same low-lying LMCT as **Eu.52**, resulting in a low quantum yield, $\phi = 0.05$. [49, 107]

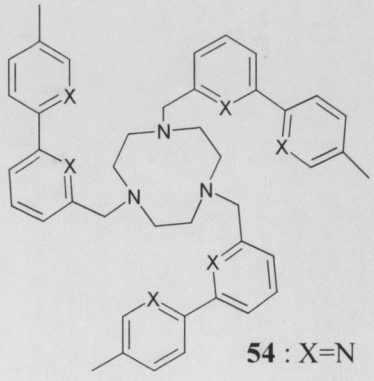


52



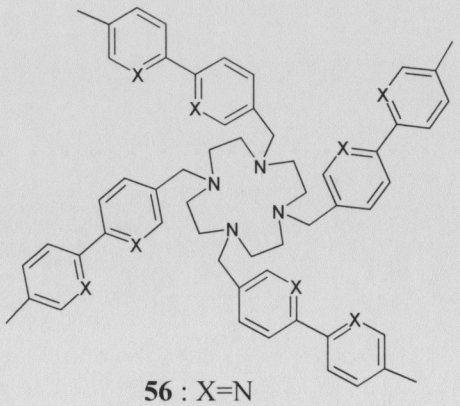
53

Ligands similar to **52** and **53** have been reported by Ulrich *et al.* [108] In these cases the use of methylated bpy chromophores functionalised to small aza crown macrocycles, ligands **54-57** were shown. A high quantum yield was observed for **Eu.54** in MeCN, $\phi = 0.35$. A lower value was obtained for **Eu.56** that was attributed to lower metal-ligand interaction due to steric hindrance. As shown in previous examples, such as **16** and **18**, the use of *N*-oxides can be beneficial at improving the quantum yields of lanthanide complexes. However in all the Tb(III) and Eu(III) complexes of **55** and **57** quantum yields and lifetimes were lower.



54 : X=N

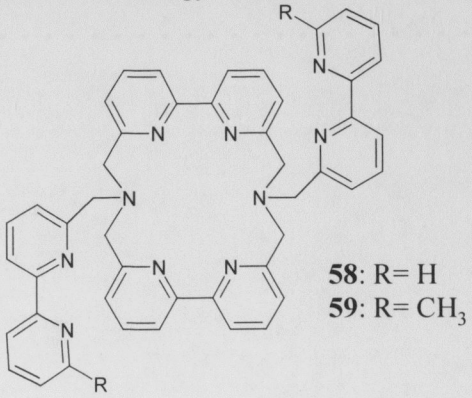
55: X=N-O



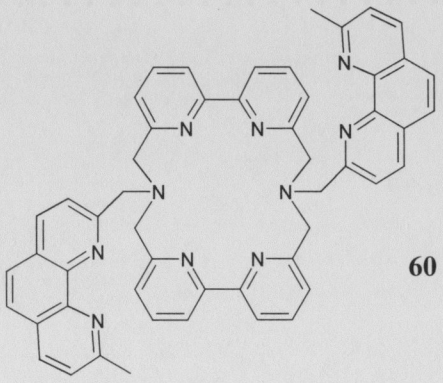
56 : X=N

57: X=N-O

Ziessel *et al.* have also shown [105] the synthesis of a number of ligands, **58-60** in which bpy units have been incorporated into the macrocycle ring as well as being functionalised as pendent arms. These ligands are similar to the [2.2.2] bpy cryptands, **14** and **15**, discussed earlier. In these new examples the extra bpy units were found to give higher molar absorption coefficients than that of their corresponding cryptand due to the extra chromophore. **Eu.58** was studied in both water and MeOH with a reported quantum yield in MeOH, $\phi = 0.1$, a noticeable improvement on its corresponding cryptand, **Eu.14** ($\phi = 0.02$). This was attributed to better shielding of the Eu(III) center. The complex, **Tb.58** was only studied in MeOH with a quantum yield reported to be, $\phi = 0.14$. Lifetime measurements showed temperature dependence, indicating a thermally activated decay process, possibly by a low-lying triplet state.[109] **59** was similar to **58** except for methylation in the 9' position of the two bpy pendent arms. The complex, **Eu.59** was found to be unstable in water and in measurements in MeOH the quantum yield was found to be lower than that of Eu.**58** (Eu.**58**, $\phi = 0.1$, Eu.**59**, $\phi = 0.01$). Both of these observations were attributed to steric hindrance in coordination of the sensitizing chromophore to the lanthanide ion center. Steric hindrance caused by the methyl groups preventing a close approach between the bpy pendent arms and the lanthanide ion center allowing water molecules to compete for ion complexation. Also the lack of close proximity between the bpy pendent arms and the lanthanide ion leads to a reduction in the metal-to-ligand energy transfer. [49] Further work on **60**, a similar ligand to **59** has been reported by Sabatini *et al.*[110] By changing the attached appendages from 2,2'- bypyridine to 1,10 phenanthroline, the Tb(III) and Eu(III) complexes become water soluble and stable. The authors suggested that this was be due to the rigidity of the complex. The resulting photophysical properties were found to be poor, due to inefficient shielding of the metal center and an inefficient energy transfer.

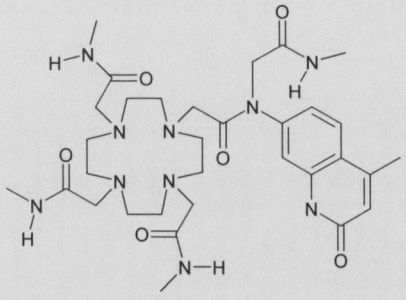


58: R= H
59: R= CH_3



60

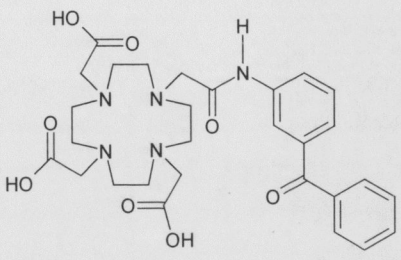
So far in this review of macrocylces it can be seen that the best quantum yield has been observed with small macrocycles that have sensitizing chromophores attached as pendent arms. The cyclen based ligand, **61** reported by Parker *et al.*, is an example of a cyclen macrocycle with 3 acetamide pendent arms and a chromophore sensitiser linked via an amide linkage that formed highly stable (kinetically and thermodynamically) lanthanide complexes.[111] Complexation occurs through coordination of the lanthanide ion with the four nitrogens of the cyclen ring and the carbonyl groups of the acetamide pendent arms, with good shielding properties reported. (This is just one of the many cyclen based ligands reported by this group for use in lanthanide complexation for biological probes, sensors and MRI contrast agent applications).[62] In this case the sensitizing chromophore was a functionalised 7-amino-4-methyl-2(1H) quinoline (also known as carbostyril 124). The quantum yields showed that sensitization of **Tb.61** was more efficient than for the **Eu.61**, ϕ = 0.044, and ϕ = 0.018 respectively. The low quantum yield of **Tb.61** was determined to be due to a low-lying triplet state, whereas the low value found for **Eu.61** was reported to be due to a competitive charge transfer deexcitation pathway.



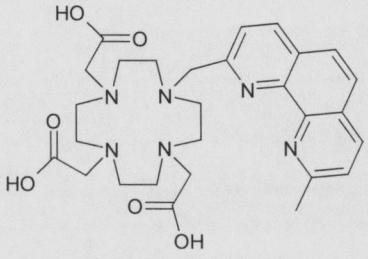
61

Beeby *et al.* [112] have reported **62**, a similar ligand to **61**. Ligand **62** was a cyclen based ligand functionalised with three carboxylic pendent arms and a benzophenone chromophore attached to the fourth cyclen nitrogen through an amide bridging group, which resulted in the formation of charge neutral lanthanide complexes. Quantum yields of ϕ = 0.095 for **Eu.62** and ϕ = 0.27 for **Tb.62** were found when measured in H_2O. By changing the sensitising chromophore to phen as in **63,** reported by Quici *et al.*, [113] it was shown that binding with both nitrogens of the phen substituent occurs making this a nonodentate ligand, resulting in optimal shielding of the lanthanide center. This good shielding ability is explained by the rigidity of

the phenanthroline chromophore and its spatial arrangement within the complex. Stability in water and high luminescence efficiencies were shown as well as an increase in the quantum yields reported for **Eu.63** of $\phi = 0.21$, compared to $\phi = 0.095$ for **Eu.62**.

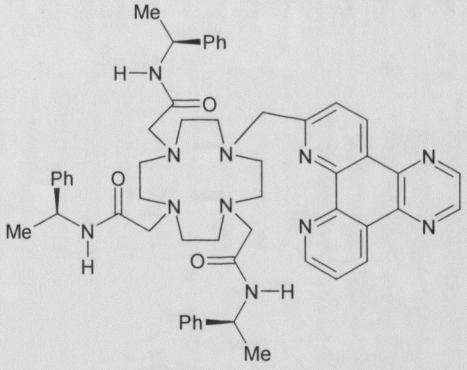


62

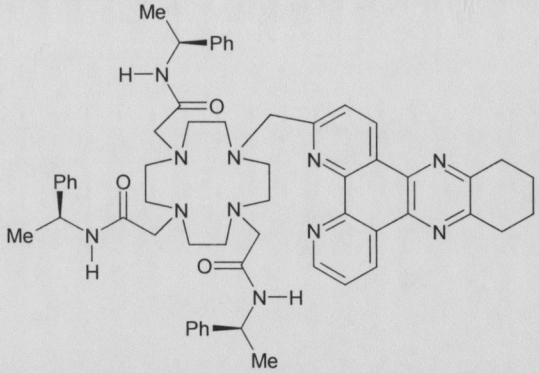


63

Other comparable examples of **63** were ligands **64** and **65** reported by Bobba *et al.*[114] The Eu(III) complex quantum yields for **64** and **65** were comparable with that of **63**, at $\phi = 0.21$ and $\phi = 0.16$ respectively. The quantum yields for the Tb(III) complexes of both these ligands was also shown to be very high at $\phi = 0.36$ and $\phi = 0.40$ respectively. These high values were attributed to high triplet states in the sensitizer



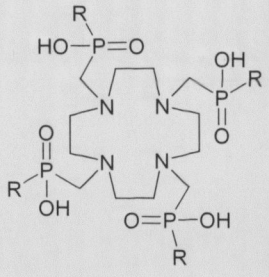
64



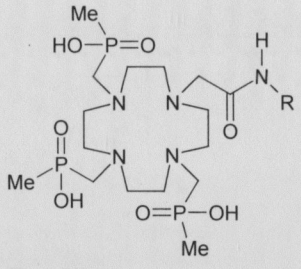
65

So far we have looked at ligands with organic sensitizing chromophores, typically aromatic and heterocyclic systems. In recent times it has been shown that alkylphosphonic groups attached to crown ethers also form kinetically stable complexes. [115] Sato *et al.*, have demonstrated that phosphonic acid can coordinate strongly to lanthanide cations and when phenylphosphonic acids are used efficient energy transfer occurred resulting in lanthanide luminescent emissions. [116] With this in mind we now look at macrocyclic ligands that use such appendages as both coordinating moieties as well as sensitising chromophores.

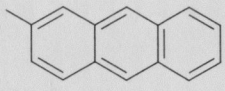
Stable Eu(III) and Tb(III) complexes using tetraaza phosphinate ligands has been shown by Murru *et al.* [117] All complexes were shown to be stable in aqueous solutions as well as *in vivo*. In the case of **67** the lanthanide complexes were sensitised by the benzyl moiety of the phosphinate appendages In **Tb.67** a quantum yield of $\phi = 0.44$ was reported, one of the highest reported for a lanthanide complex in this review to date. Modifications of these systems has resulted in the development of tris phosphinate complexes with one amide pendent arm, **68** and **69** are examples of such complexes. The shielding was less efficient for both **68** and **69** when complexed to Eu(III) and Tb(III) resulting in lower quantum yields. For **Tb.68** a quantum yield of $\phi = 0.16$ was determined which was less than half that determined for **Tb.67**. The value for the **Eu.68** complex was measured to be even lower at 0.0005, however this was partly due to a competitive charge transfer transition mechanism. In a similar complex that uses an anthracene sensitizer attached to the amide, **69**, low quantum yields for the **Eu.69** and **Tb.69** complexes were explained by competitive anthryl fluorescence.



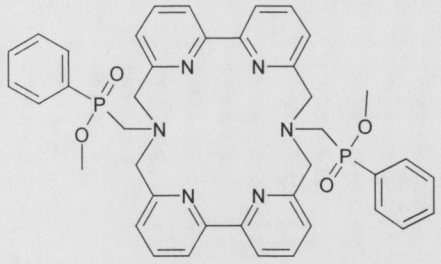
66: R = Me
67: R = CH_2Ph



68: R = Me
69: R =



The use of phosphinate esters has not been confined to cyclen based ligands. Sabbatini *et al.* have shown their uses in other ligands such as **70**. [118] Ligand, **70** was a bis 2,2' bpy based macrocycle, similar to earlier examples such as **58**, **59** or **60**, but in this case the bpy or phen pendent arms were replaced with phosphinate esters. In the case of **Eu.70** and **Tb.70**, good stability and shielding was observed in water in contrast to the lanthanide complexes of **58**, **59** or **60**. The quantum yields were also determined to be higher with values of $\phi = 0.08$ and $\phi = 0.10$ reported for **Tb.70** and **Eu.70** respectively.



70

In summary the review of Section 1.6 has shown that a large array of ligands can be used to produce stable, water-soluble and highly luminescent lanthanide complexes. In general the lanthanide complexes that displayed good photophysical properties, *i.e.*, high quantum yields, were those formed with high coordinating ligands with sensitising chromophores attached. Shielding of the lanthanide ion from the external environment, and close proximity to the sensitising chromophore were also important factors. It is also important to note that the photophysical properties of the lanthanide complexes produced vary greatly depending on the properties of the sensitising chromophore. In most cases highly luminescent Tb(III) complexes are possible when the sensitising chromophore contains a high triplet state energies sufficient to populate the lowest excited state $^5D_4$ (20,500 cm^{-1}). Highly luminescent Eu(III) complexes can also be produced with high triplet energy sensitisers through population of the Eu(III) lowest excited state $^5D_0$ (17,200 cm^{-1}). However, the Eu(III) lanthanide luminescent emission can be quenched by LMCT processes from some sensitisers.

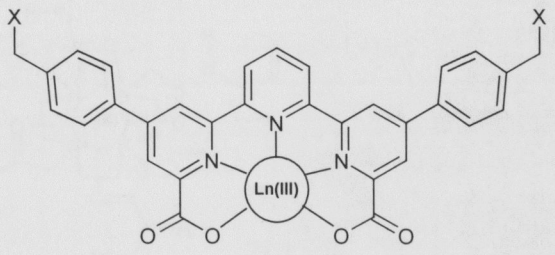
1.7 Lanthanide complexes as luminescent sensors

So far we have looked at examples of ligands that have the ability to coordinate to lanthanide cations, protecting them from their environment and by way of the 'antennae' effect producing long-lived lanthanide excited states that can emit at long wavelengths. In many cases the complexes already shown had been developed for potential use as biological probes. In order to use lanthanide lumophores as signaling systems in sensors their ability to cause a change in the luminescence emission as a direct consequence of the presence of an analyte would be a requirement. Therefore a receptor needs to be incorporated into the ligand complex system. Changes in the photophysical properties of such lanthanide complexes upon analyte recognition can occur in a number of ways such as changes in lifetime or emission

intensity. This is often referred to as modulation of the emission signal.[46] Recently studies have been reported into the design, synthesis and testing of lanthanide luminescent sensors. These studies have been somewhat driven by the desire to overcome the major issues found in fluorescent sensing for *in vivo* applications. Typical concerns have been short emission lifetimes, which have to compete in biological systems with autofluorescence as well as the problems of light scattering caused by biological moieties being micro heterogeneous.[119] Both these issues make the attainment of meaningful luminescent signals difficult. Luminescent emissions from lanthanides are long lived and for this reason can overcome the above problems by delaying the time of observation of the output signal to allow autoflourescence and light scattering emission to diminish. [120] In the following pages the application of lanthanide complexes as lumophores in sensing devices as reported in literature over the past seven years are reviewed.

We begin with the work of de Silva *et al.*, [121] on Tb(III) and Eu(III) complexes of ligands **71-74**, as pH sensors in H_2O based on a terpyridyl ligand, which have two proton receptor sites incorporated. These systems are based upon the use of terpyridine but similar ligands have been used before as DNA probes. [122] This ligand was chosen in the design of lanthanide luminescent sensors because of its ease of synthesis, and near ultraviolet absorption. It was also expected that this ligand would have a relatively electron deficient π - system when complexed to a lanthanide ion. To act as a sensor this ligand was modified with amino groups that could act as proton receptors and also as electron donors in a PET process with the electron deficient π - system of the ligand. The lanthanide complexes of these ligands were made *in situ* using 100-fold excess of lanthanide ions however these complexes were not stable in aqueous media. From lifetime studies the presence of four bound water molecules was determined. In the case of Tb(III) complexes of **71** and **72** dramatic changes were seen in the lanthanide emission during pH titrations in H_2O. These complexes showed proton induced luminescence enhancement factors of 16 for **Tb.71** and 10 for **Tb.72** with no reported shifts in wavelengths of the emission bands. Sigmoidal pH versus intensity plots for **Tb.71** showed pH dependence in the range 5.5 to 8.0 and for **Tb.72**, pH dependence was shown to occur in pH range 4 –7. In both cases when the amino receptors were protonated the quantum yields was measured to be *ca.* 0.5, dropping dramatically in basic conditions to *ca.* 0.04. As expected

Tb.73 and **Tb.74** was independent of pH since the ligand unit lacks the amino moiety. In these sensors protonation of the alkyl amino receptors suppresses electron transfer to the singlet excited state, which leads to enhancement in the lanthanide luminescent emission. Similar pH dependence was observed for **Eu.71** and **Eu.72** however, only weak emissions were observed.



71: X = NEt_2

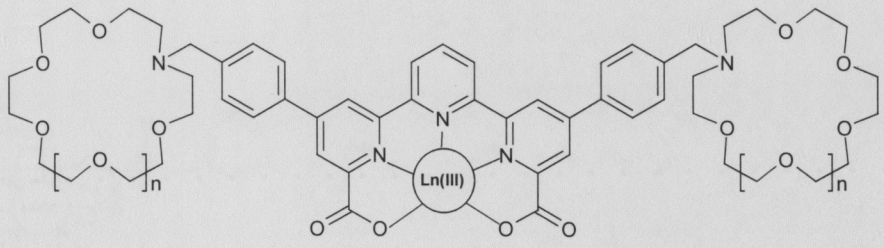
72: X = $N[(CH_2)_2]_2O$

73: X = N^+Me_3

74: X = H

Ln(III) = Eu(III) or Tb(III)

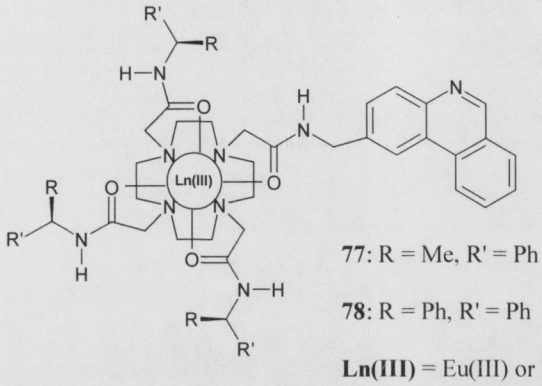
In 1997 one the first cation sensors to use lanthanide luminescence was shown by de Silva *et al.* The complexing ligand was similar to that used by them in the first pH sensor already discussed. In a continuation to this work the amino groups were functionalised with 18-crown-6 and 21-crown-7 mono aza crown ether to give **75** and **76** respectively. In both these cases enhancement in the luminescence of Eu(III) with **75** and **76** were demonstrated. This luminescent enhancement was over an order of magnitude in size. In MeOH the ϕ for **Eu.75** was found to be *ca.* ϕ = 0.47. The switching 'on' of luminescence was attributed to alkali cation – induced suppression of PET from the azacrown. Similar results were obtained for **Tb.75** and **Tb.76** but the ϕ were measured to be less than 0.0016 in both cases due to a low-lying triplet state. [123, 120]



75: n = 0
76: n = 1 **Ln(III)** = Eu(III) or Tb(III)

Parker *et al.* demonstrated the use of Eu(III) and Tb(III) based sensors for pH, pO_2, halide and hydroxide ion sensing. [46, 124] In these cases the ligand used was based on cyclen

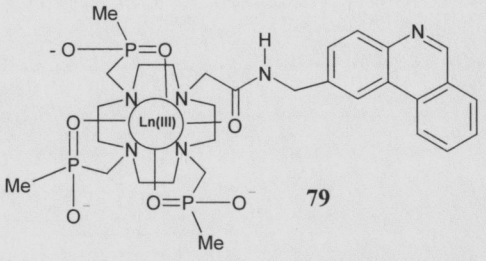
substituted in one of the four positions with phenanthridine, as the receptor. The other three positions were substituted with various pendent arms such as chiral amides as in the case of **77**, **78** and phosphinate esters in **79** respectively.



77: R = Me, R' = Ph

78: R = Ph, R' = Ph

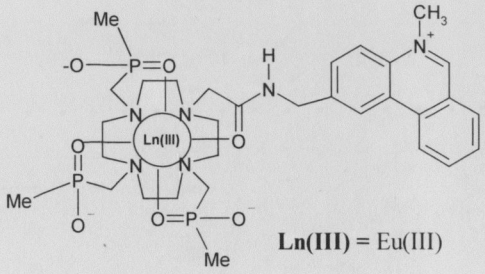
Ln(III) = Eu(III) or Tb(III)



79

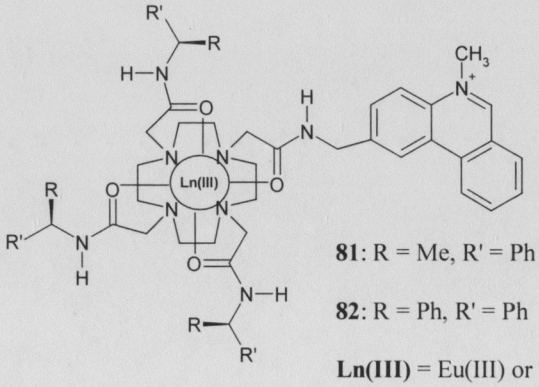
Ln (III)= Eu(III) or Tb(III)

All the above complexes showed lanthanide luminescent emissions that were dependent on pH in aqueous solution. A luminescence enhancement factor of over 500 was recorded for **Eu.79** when the phenanthridine was excited at 370 nm. In the case of **Tb.79** no emission was observed when protonated due to the phenanthridine low-lying triplet state. In a continuation to this work the phenanthridine ligand was methylated at the nitrogen position thus preventing its use as a pH sensor. In this instance **Eu.76**, **Eu.77** and **Eu.78** were found to be sensitive to chloride anions in the physiological range. Quenching of the luminescent emission occurring by way of charge transfer from the halide to the singlet excited state, S_1 of the electron poor cationic chromophore, which thus prevents population of the triplet excited state, T_1.[46]



80

Ln(III) = Eu(III)

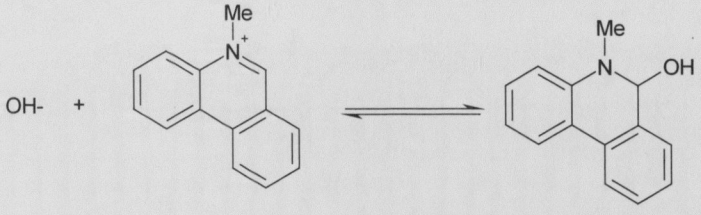


81: R = Me, R' = Ph

82: R = Ph, R' = Ph

Ln(III) = Eu(III) or Tb(III)

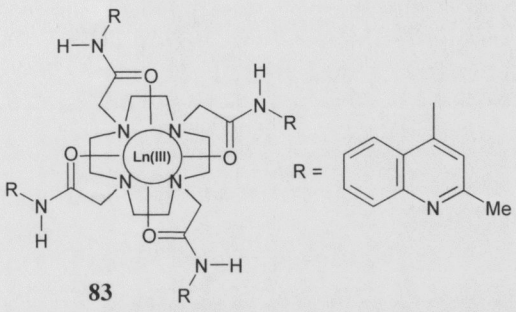
In Tb(III) complexes of **80** and **81** pH independence was found over the range of 1-10 however, a sensitivity to pO_2 in the pH range 2-9 was reported. This sensitivity being explained by quenching of the aromatic triplet state. Finally the sensitivity of Eu(III) emission of **80** and **81** to hydroxide anions was shown. The Eu(III) emission was found to decrease with increasing amounts of KOH. The Eu(III) emission was independent of pH up to pH 9 however, above this there was a significant decrease in the emission which was at zero by pH 13.5. This phenomenon was rationalized by the attack on the N- methyl phenanthradine by OH- at the C-6 position in a reversible manner that leads to the disappearance of the longest wavelength absorption band in the phenanthradine. In a similar study of Tb(III) complexes of **80** and **81**, the Tb(III) emission was found to be switched "on" with the addition of KOH at *ca.* pH 9 reaching a maximum at pH 11.2 decreasing by a factor of 2 to a limiting value beyond pH 13. The switching on of the Tb(III) emission was explained to be due to an increase in the triplet energy of the *N*-methylated phenanthradine moiety upon formation of the hydroxylated species (Scheme 1.0). No explanation was given for the decrease in Tb(III) emission beyond pH 11.2. However, this was found to be a reversible process over a number of acid/base cycles. [46, 124]



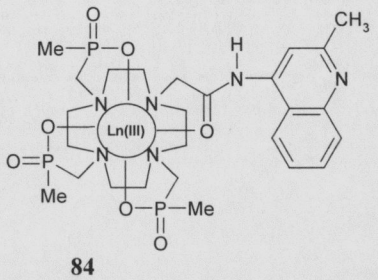
Scheme 1.0 ***Attack on N- methyl phenanthradine by OH⁻ at the C-6 position in a reversible manner***

In work by Gunnlaugsson *et al.*,[125] complexes of Eu(III) and Tb(III) were made with a cyclen based ligand that contained four quinoline receptors for pH sensing, attached through amide bridged pendent arms, **83** and also a modified version which contained only one receptor, **84**. In the case of **84** the cyclen was substituted in three of the four nitrogen positions with alkyl phosphonic acid groups resulting in a charge neutral lanthanide complex. The fourth position was substituted with this methylated quinoline proton receptor/sensitizing moiety. The pH profile of the **Eu.84** and **Eu.83** complexes showed sigmoidal characteristics, with excitation at 330nm. A pK_a was determined to be *ca.* 4.6 and *ca.* 5.8 respectively. In both

cases luminescence was switched on in acidic conditions. A more interesting result was that observed for the complex of **Tb.84**. It was found that lanthanide luminescence was only produced when the complex was in acidic conditions "and" in the absence of molecular oxygen. This development being the first example of a lanthanide luminescent molecular logic gate.



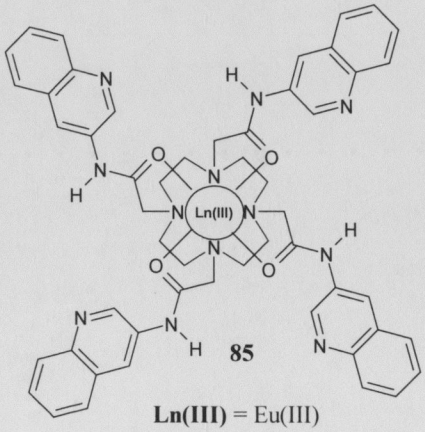
83



84

Ln(III) = Eu(III) or Tb(III)

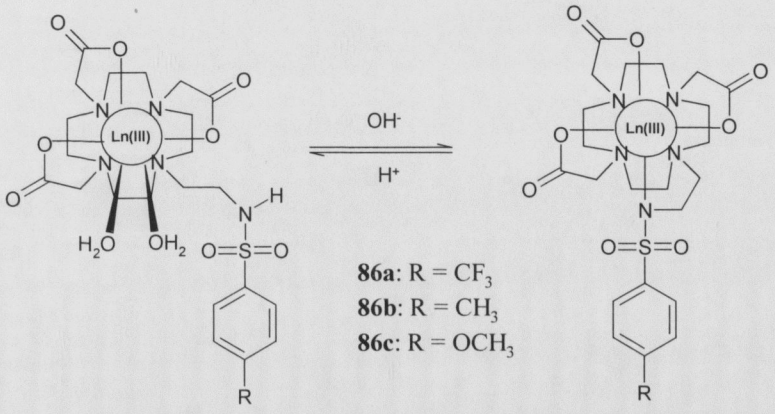
Another example of a lanthanide luminescent sensor by Gunnlaugsson was shown using ligand **85**.[126] This involved the synthesis of a tetra substituted cyclen ligand with four quinoline receptor moieties, capable of sensing protons, similar to **83**. The complex of **Eu.85** was found to be stable in water. In this case the excitation of the chromophore was found to occur at 350 nm. The lanthanide emission was found to be switched on at highly acidic conditions, with a luminescent enhancement of over 300 fold. A bell shaped pH profile was found to exist from pH 1.8 to pH 3.5. This is the first report of such a pH sensor being able to work in such harsh acidic conditions. Luminescent enhancement was attributed to enhancement in the population of the S_1 and subsequent T_1 excited states of the quinoline chromophore when in acidic media.



85

Ln(III) = Eu(III)

In 2000, Lowe and Parker [127] published work on Eu(III) and Tb(III) complexes, which showed modulation caused by changes in pH. This was demonstrated on a cyclen complex to which three carboxylate pendant arms were attached that allowed coordination to take place resulting in the formation of a charge neutral complex. The fourth position had a sulphonamide tethered via an ethyl carbon chain, **86a**, **86b** and **86c**.



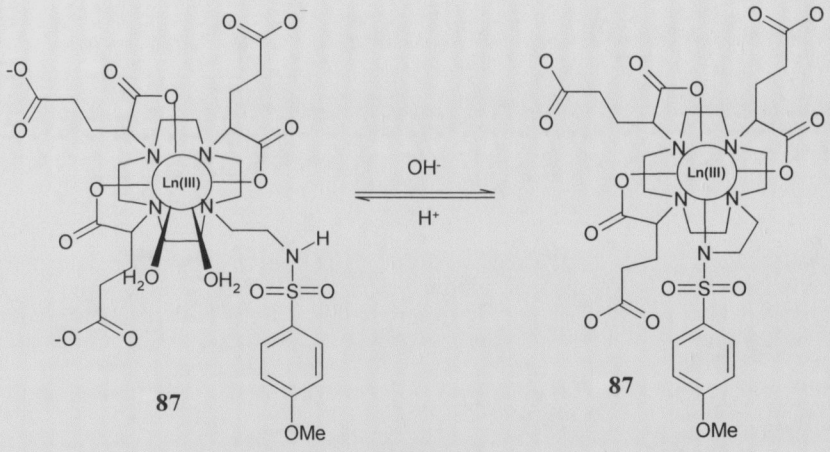
86a: R = CF_3
86b: R = CH_3
86c: R = OCH_3

Ln(III) = Eu(III) or Tb(III)

Scheme 2.0 ***pH reversible coordination effect of*** **86a, 86b** ***and*** **86c**

Studies showed that luminescence was switched "on" when the complexes were in alkaline conditions. This was found to relate to a situation in which the two metal bound waters ($q = 2$) were displaced. This led to a situation were the pendant aryl sulphonamide group was now coordinated ($q = 0$). Such coordination could only occur when the sulphonamide was deprotonated. When such coordination occurred sensitisation was greatly enhanced. This was probably due to the closer proximity of the aryl sulphonamide to the lanthanide as well as the reduction of q from 2 to 0. The pH range over which this 'on-off' luminescence occurs could be modulated by careful choice of the substituents on the aromatic ring of the sulphonamide. This was achieved by varying the electron withdrawing power of the *para* substituents on the aryl ring. For instance with **86a**, the high electron withdrawing effect of the CF_3 substituent causes the pK_a of the sulphonamide to be lowered to $pK_a = 5.7$. With **88c**, (R = OCH_3), the electron withdrawing effect from the ring was reduced considerably which resulted in a change in pK_a by one log unit. A considerable disadvantage to this system was found to be its

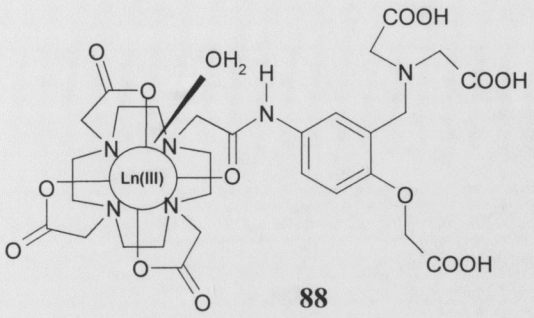
limited use under physiological type conditions where competition with other anions such as carbonates, lactates, citrates and phosphates exist. Secondly excitation of the sensitising ligand was carried out at 270 nm, well below the 350 nm threshold discussed for *in vivo* applications. These drawbacks were overcome in some way by modifying the coordinating arms of the complex to produce **87**. In **87**, three carboxyethyl substituent were attached α to the cyclen ring nitrogens. This had the effect of reducing the affinity towards competitive anions allowing coordination of the aryl sulphonamide to take preference. In a repeat pH titration in a simulated physiological environment, the response was shown to be identical to that in water, indicating the success of the modified arms at preventing competitive anion binding. The second problem of short excitation wavelengths was overcome as shown in further work by changing the sensitising ligand to a dansyl moiety were excitation was increased to 332 nm. [128]



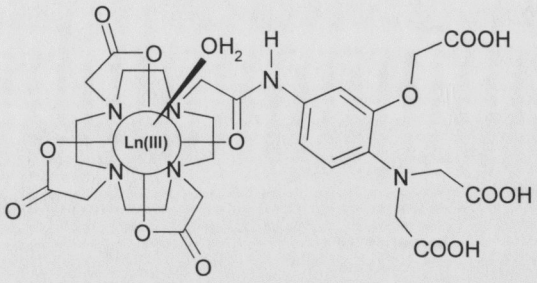
Ln(III) = Eu(III)

Scheme 3.0 ***pH reversible coordination effect of*** **87**

Parker *et al.*, [129, 130] have also shown examples of lanthanide complexes for sensing cations, with receptors selective to zinc (II). This was similar to the last few examples shown by this group in which a cyclen based encapsulating ligand is used to form a neutral lanthanide complex with a receptor covalently attached as a pendent arm. In both cases the receptors are structurally similar with one being synthesised from benzylamine, **88** and the other from aniline, **89**.



88



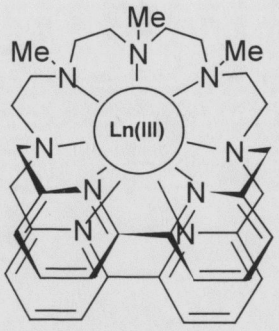
89

Ln(III) = Eu(III) and Tb(III)

On addition of Zn(II) to a solution of **Ln.88** under simulated physiological conditions, the luminescent emission of the lanthanide was enhanced. The **Tb.88** complex showed an enhancement of 26 %, while the **Eu.88** showed an enhancement of 42 %, These were much lower than that observed in most of the examples previously discussed above where the enhancement was an order of magnitude or larger. In the case of **Ln.89** it was suggested that binding of zinc resulted in deconjugation of the aniline nitrogen lone pair, which results in a suppression of PET, from or to the intermediate aryl singlet excited state of the aniline moiety, which leads to a luminescent enhancement.

In 2000, the first example of pH modulation of a Eu(III) cryptate was shown.[131] In this case a bis bypyridyl based cryptate with a poly *N*- methylated flexible arm, **90**, was synthesized. In aqueous solution **Eu.90** gave characteristic Eu(III) emissions arising from energy transfer from the bipyridyl moiety of the cryptate excited triplet state to the metal center. This emission was found to be dramatically affected by pH. The complex showed a maximum intensity around pH 7, decreasing in intensity above and below pH 7 by almost 50%, but showing a second maximum of lower intensity around pH 3.5. The drop in emission intensity in acidic environments was attributed to protonation of the aliphatic amines, which prevented them from being involved in coordination to the metal center. When conditions are made more basic, the amines are deprotonated and could contribute to the complexation of the metal center, thus leading to longer lifetimes and higher emission intensities. At very high pH loss of emission is attributed to the formation of a hydroxylated Eu(III) species. This hypothesis was confirmed by ***q*** value analysis. At pH 2 a ***q*** value of 2 was determined while at

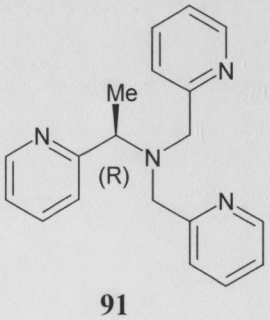
pH 6.8 a ***q*** value of 1 was determined showing that when deprotonated the complex does indeed shield the metal center more efficiently.



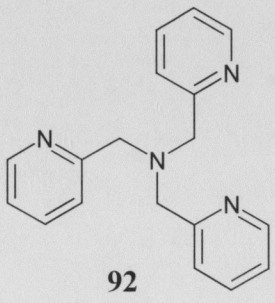
90

Ln(III) = Eu(III)

A more recent example of a lanthanide luminescence anion sensor was that of Yamada *et al.*. [132] This involved the use of a podand ligand, using pyridine moieties. Two examples were presented, **91** and **92**, **91** being a chiral ligand. In both cases the lanthanide complexes were studied in MeCN. Lanthanide luminescence was found to be switched 'on' when anions are added to solutions of these complexes. The anions were found to be displacing the bound water molecules that quench the excited state. A similar observation was made by Sabbatini *et al.* when F^- was added to [2.2.1] cryptates of Eu(III) and Tb(III).[72] **Eu.91** was found to be somewhat selective to NO_3^- over all other anions tested. The circular dichroisim signal of **Eu.91** was observed at 260 nm and was intensified on addition of NO_3^- to the complex causing modification to the 3-D arrangement of the pyridines. When the metal center was changed to Tb(III) , the anion selectivity of **Tb.91** was found to change to Cl^-. This indicated that the nature of the lanthanide ion dramatically effects anion sensing selectivity despite their similar ionic radii. Similar results have been reported for the achiral ligand complexes **Eu.92** and **Tb.92**.[132]

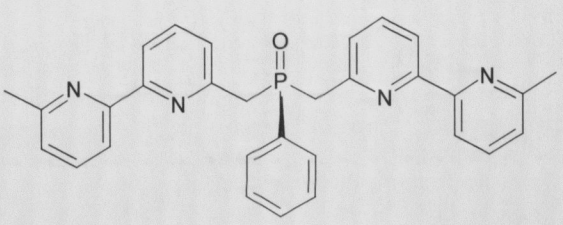


91

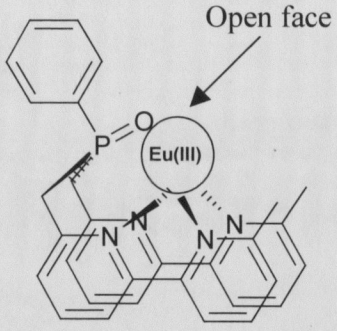


92

Similar work has recently been reported by Montalli *et al.*[133, 134] in which a bis-bpy-phenyl phosphine oxide ligand, **93** was designed as an anion sensor when complexed with Eu(III). This pentadentate ligand is unable to fully complex the lanthanide thus leaving an open face that acts as the receptor site for anion coordination. Luminescence was produced by energy transfer from the bpy moiety. The complexes were made *in situ* in MeCN with either Eu(III) triflate or nitrate salts. Mass spectroscopy and elemental analysis showed the formation of the 1:1 complex. Infrared analysis showed that the triflate anions were coordinated in the first coordination sphere. Water molecules were also shown to be present. In studies with a number of anions an 11-fold increase in emission intensity was seen on the addition of two equivalents of NO_3^-. A quantum yield of 0.30 was determined and the lifetime for the emission was found to be 1.45 ms. These values were found to be similar to the complex formed with **[Eu.93]**$(NO_3^-)_3$.



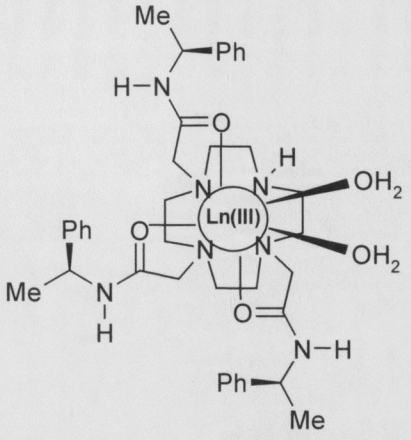
93



Ln(III) = Eu(III)

In the same year Parker *et al.*[135, 136] reported the synthesis of a heptadentate cyclen based lanthanide complexes. This consisted of cyclen alkylated in three of the four amine positions with [R]-*N*- (2-chloroethanoyl)-2- phenyl-ethylamine, **94**. The resulting **Tb.94** and **Eu.94** complexes were found to contain two water molecules that were bound directly to the metal center. In solution it was observed that both water molecules could be displaced in the presence of hydrogen carbonate resulting in the formation of a reversible 1:1 adduct which led to a large change in the lifetime measurements. Studies were carried out in solutions containing MES buffer with pH ranging between 6.4 and 7.3. This study demonstrated that stable lanthanide complexes can be produced that can sense the presence of species under near physiological conditions. In this example the excitation wavelength criteria was also met with λ_{excit} = 365nm. Further evidence for the formation of 1:1 adducts with lanthanide complexes of

this ligand were shown by Dickens *et al.*.[137] The results of these studies showed by way of a crystal structure (of the Yb (III)) the formation of a 1:1 adduct with (S) – lactate.



94

Ln(III) = Eu(III) and Tb(III)

1.8 Conclusion

The purpose of this chapter was to highlight the field of optical chemosensing. This involved a brief overview the most common types of optical sensors that have been developed; their method of function in terms of their photophysical properties and their limitations in biological applications. Stable lanthanide complexes have been shown to be possible with excellent photophysical properties for *in vivo* sensing applications. The recent incorporation of lanthanide complexes as signaling systems in chemosensors has also been demonstrated. As such these results show that the use of lanthanide complexes in the field of chemosensing is relatively new and the potential for more advances in their use in this field are promising.

The main focus of this thesis will be with the synthesis and physical studies of chemosensors for cation and anion detection. *Chapter Two* will deal with the design and synthesis of lanthanide based chemosensors for the detection of Na^+ and K^+ using receptors derived from 2-methoxy aniline. The synthesis of a number of complexes is described and their ability to function as sensors for the detection of cations is demonstrated. *Chapter Three* will show the design and synthesis of two colorimetric chemosensor for the detection of intracellular concentrations of Na^+ and K^+ respectively. *Chapter Four deals with the* attempts made at producing a lanthanide based chemosensors for detecting Ca^+ using a similar design strategy to that described in *Chapter Two*. Finally, *Chapter Five* shows the synthesis and photophysical studies of novel lanthanide complexes designed as anion sensors for aromatic carboxylate detection.

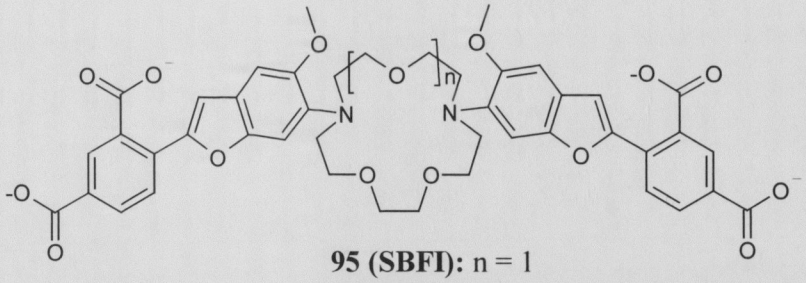
Chapter 2

Synthesis, characterisation and photophysical studies of lanthanide luminescent sensors for the detection of sodium and potassium

2.0 Synthesis, characterisation and photophysical studies of lanthanide luminescent sensors for the detection of sodium and potassium

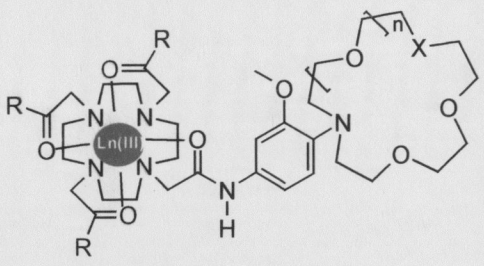
2.1 Introduction

Na^+ and K^+ are cations essential for maintaining life in animal cells through a number of cellular functions including nutrient uptake, regulation of intracellular ions and the transmission of electrical impulses. The concentration of both cations within and around cells differs greatly.[8] The concentration of Na^+ is found to exist at levels of 120-450 mM outside of cells compared to 10-40 mM within, whereas K^+ is found within cells at concentrations of 90-120 mM compared to 10 mM outside.[8, 27, 42,138] These values refer to the concentrations of each cation found in red blood cells and blood serum. In recent years there have been many examples of chemosensors that can measure intracellular and extracellular levels of Na^+ and K^+ [12] some of which have been discussed in Chapter 1. In terms on intracellular Na^+ and K^+ sensing, **95** [42] (SBFI) and **96** [42] (PBFI) have been shown to be efficient and are now commercially available.[139] Both of these examples are fluorescent sensors that employ a diaza crown receptor linked with methoxy aromatic units that help to improve the binding efficiency and selectivity of these receptors over similar size crown receptors.[42]



95 (SBFI): n = 1
96 (PBFI): n = 2

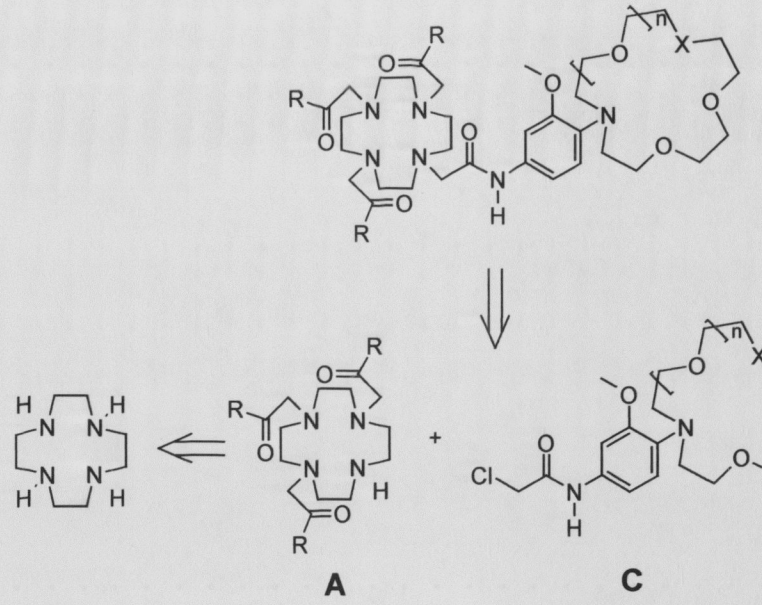
The objective of this project was to synthesize a series of lanthanide-based sensors using ligands **97-102**. Ligands **99-102** are based upon the receptors incorporated in **95** (SBFI) and **96** (PBFI), while **97** and **98** are the mono aza crown equivalents. Both **97** and **98** are expected to have the potential for extracellular detection of cations such as Na^+ and K^+ and **99-102** for intracellular detection. Ligands **99-102** consist of three major components that can be identified as a receptor, a spacer and a cyclen based ligand that is capable of forming thermodynamically and kinetically stable complexes with lanthanide cations.



97: R= NMe_2, n=1, X = O, Ln(III) = Eu(III) or Tb(III)
98: R= NMe_2, n=2, X = O, Ln(III) = Eu(III) or Tb(III)
99: R= NMe_2, n=1, X = NC_6H_4OMe, Ln(III) = Eu(III) or Tb(III)
100: R= NMe_2, n=2, X = NC_6H_4OMe, Ln(III) = Eu(III) or Tb(III)
101: R= OH, n=1, X = NC_6H_4OMe, Ln(III) = Eu(III) or Tb(III)
102: R= OH, n=2, X = NC_6H_4OMe, Ln(III) = Eu(III) or Tb(III)

2.1.1 Synthesis Strategy

A new strategy was developed for the synthesis of ligands **97-102** as shown by Scheme 1. From retro synthetic analysis it was determined that the formation of these ligands required the synthesis of tris alkylated cyclen macrocycles (**A**) that would later be used in the complexation of lanthanide cations thus forming the lanthanide lumophore. Synthesis of aza crown macrocycles (**B**) was also necessary that would function as the Na^+ or K^+ receptor.



97: R= NMe_2, n=1, X = O
98: R= NMe_2, n=2, X = O
99: R= NMe_2, n=1, X = NC_6H_4OMe
100: R= NMe_2, n=2, X = NC_6H_4OMe
101: R= OH, n=1, X = NC_6H_4OMe
102: R= OH, n=2, X = NC_6H_4OMe

Scheme 1 - ***Retro synthetic analysis – Towards a synthetic strategy***

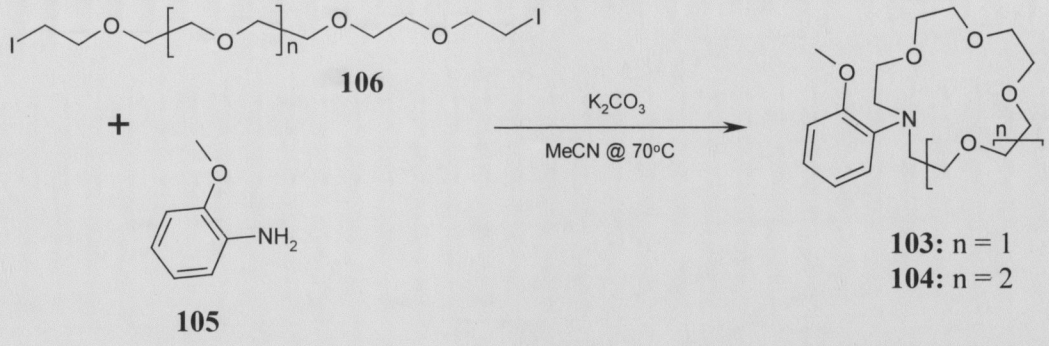
These two components **A** and **B** are the major fragments of the desired ligands **97-102**. In order to attach these two components together the aza crown macrocycles require the addition of an α-chloroamide functional group resulting in component **C**. Direct attachment of

components **A** and **C** would then result in the desired ligands **97-102**. The final stage following the attainment of ligands **97-102** requires the formation of their lanthanide complexes to afford the desired chemosensors for the detection of Na^+ and K^+ respectively. The synthesis of these ligands, their subsequent complexation with Eu(III) and Tb(III) and their photophysical properties as cation sensors are the subject of the following sections.

2.2 Synthesis of monoaza and diaza cation receptors based on *2*-methoxy aniline

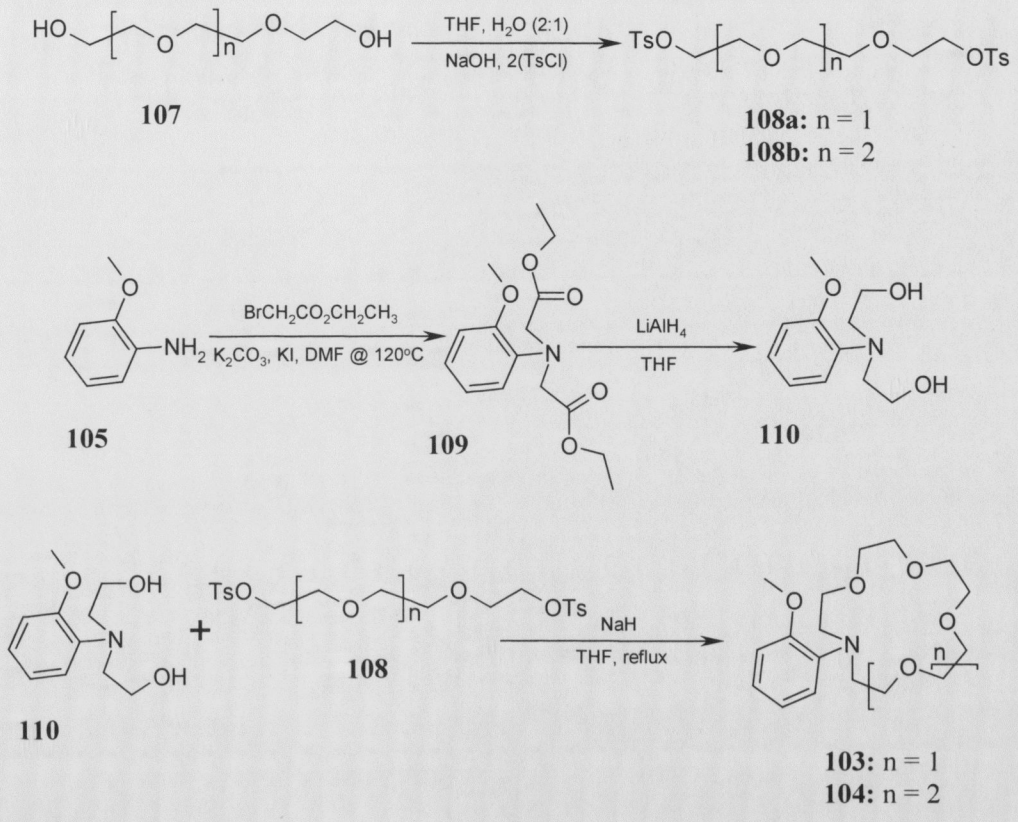
2.2.1 Monoaza crown receptors – Synthesis and characterisation of 103 and 104

Two separate routes have been reported for the synthesis of the *2*-methoxy aniline (**105**) based aza crown receptors **103** and **104**. The first route discussed was that of Dales *et al.*.[140] This involved the formation of the aza crown by way of a substitution reaction between a secondary amine, in this case *2*-methoxy aniline, **105** and a bis iodo ethereal chain, **106**. This procedure was carried out in the presence of a base in MeCN at high dilution to prevent the formation of polymers. (Scheme 2)



Scheme 2 - ***Dales procedure towards aromatic monoaza crown receptors 103 & 104*** [140]

The second route (Scheme 3) was that of Gokel *et al.*.[20, 141] This involved the formation of the aza crown using a high dilution cyclisation reaction in which a tosylated polyethylene glycol unit **108**, obtained by tosylation of **107**, was cyclised with **110** in the presence of a base. The amino bis alcohol, **110** was synthesized by reduction of **109**, a bis ethyl ester derived from alkylation of **105** using bromoethyl acetate.



Scheme 3 - ***Gokel's procedure towards aromatic monoaza crown receptors*** **103** & **104** [20, 141]

Gokel's procedure was used in this project, where yields as high as 70% were obtained for the synthesis of the 15-crown-5 aza crown, **103**. This high yield was attributed to modifications in the rate of addition of the reaction substituents. Comparison of the spectral data of **103** and **104** to previously published data showed good comparison for both. [20, 141] For instance, the ^{1}H NMR obtained for **103**, Figure 2.1 shows the presence of a doublet at 7.11 ppm, a triplet at 6.93 ppm, a doublet at 6.88 ppm and a triplet at 6.84 ppm representing the four aromatic hydrogen's. The aromatic methoxy group appeared as a singlet at 3.82 ppm, while the ether protons of the aza crown ring appeared as a multiplet at 3.69 - 3.63 ppm and a triplet at 3.45 ppm. Physical studies on both these receptors have been reported previously and show that both have good binding selectivity for Na^+ and K^+ respectively. [20, 141]

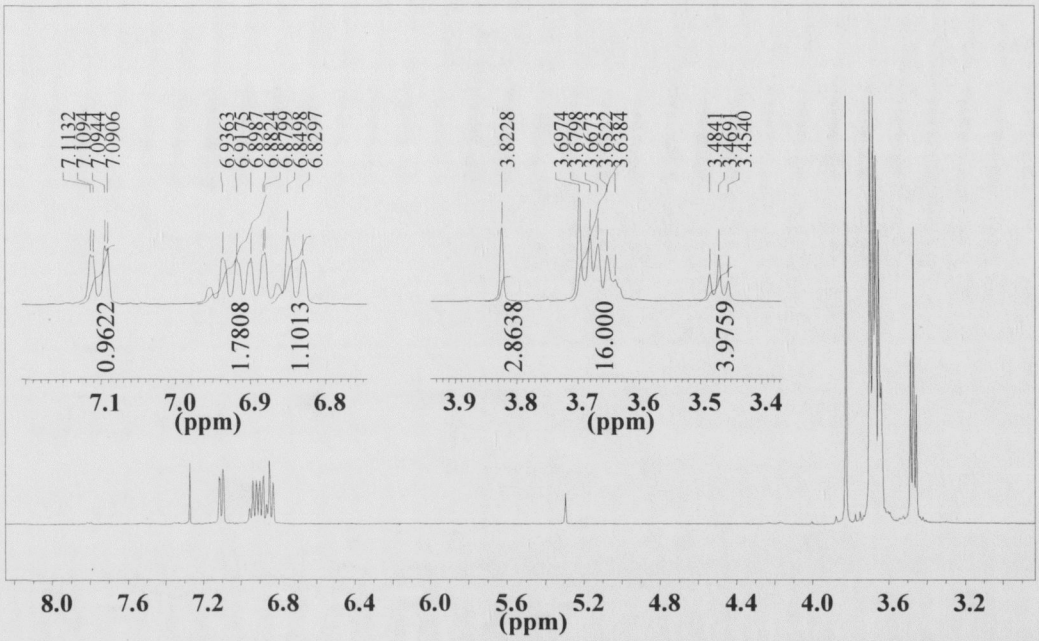
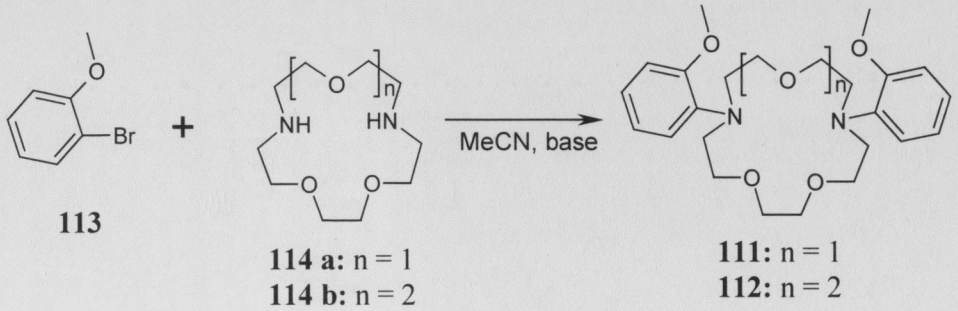


Figure 2.1 *^1H NMR of 103 [δ_H ($CDCl_3$: 400MHz)]: d, t, d, and t, in the region of 7.11-6.83 ppm represents the four aromatic hydrogen's. s, at 3.82 ppm represents OCH_3, m at 3.69 - 3.63 ppm, and t at 3.45 ppm represents aza crown ring.*

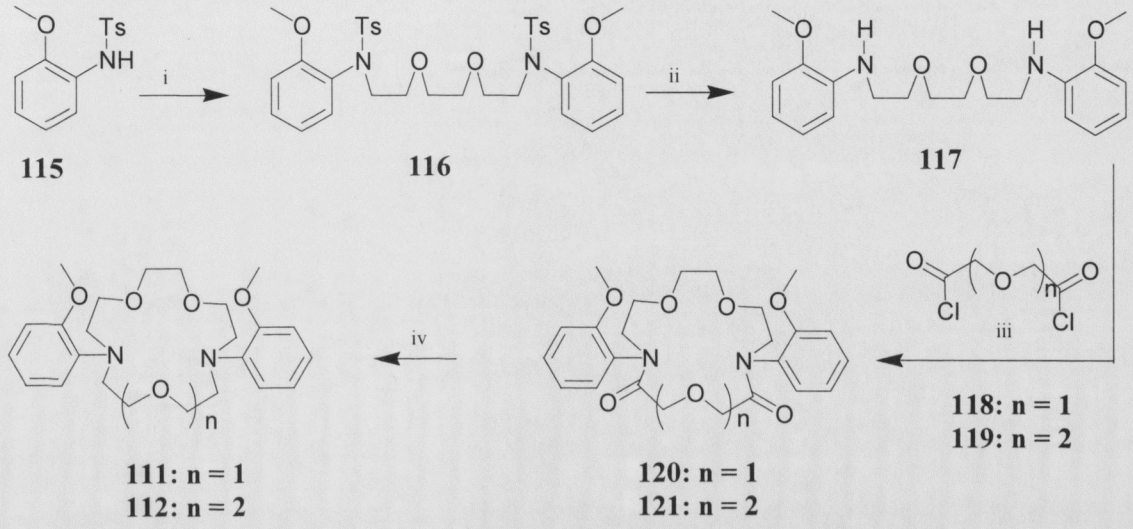
2.2.2 Diaza crown receptors - Synthesis and characterization of 111 and 112

The simplest method of synthesis of **111** and **112** appeared to be the direct substitution of 2-methoxy bromo benzene, **113** with the appropriate diaza crown, **114** (**a** or **b**) as shown in Scheme 4. Such reactions have been reported for monoaza crowns using **113** but the yields reported were low (40 %).[142] Reports of this synthesis using **114a** and 2-chloro-5-nitro-pyridine have been shown, [143] however, this method was shown to be quite ineffective at producing the desired product **111** and **112**.[144]



Scheme 4 - *Direct synthesis of* **111** *&* **112** *by aromatic nucleophilic substitution* [144]

An alternative method was used,[144] which involved the cyclisation of 1,10-bis-(2'-methoxyphenyl, 4''-methyl- benzenesulfonyl)-1,10-diaza-4,7-dioxa-decane, **117** and a diacid chloride, **118** or **119** (Scheme 5), [31, 144] using high dilution methods, **117** being synthesised initially in a 3 step synthesis from **105**.



Scheme 5. The synthesis of **111** and **112**. i) **115**, DMF, KI, K_2CO_3, $(ClCH_2CH_2OCH_2)_2O$, 70°C 3 days, 90 % . ii) (3:2) AcOH:H_2SO_4 (98% pure) 60°C, 24 hours, 32 %. iii) For **120**: $O(CH_2COCl)_2$, **118**, pyridine, benzene, high dilution at 75°C, 24 hours; for **121** $(ClCOCH_2OCH_2)_2$, **119**, 60-70 %. iv) B_2H_6, Boron triflouride etherate, THF , reflux, > 90%. [31, 144]

Synthesis of **117** began with the protection of **105** with 4-Methyl-benzenesulfonyl chloride (TsCl) to afford the desired *N*- (2-Methoxy-phenyl)-4-methyl-benzenesulfonamide, **115** in a 87 % yield after crystallisation from ethanol. Tosylation of **105** was carried out to protect the amino group from double alkylation and to make the nitrogen more active to substitution.[144] Characterisation of the translucent crystals by means of ^1H NMR ($CDCl_3$) indicated the desired product had been formed. The tosyl group was clearly distinguished two doublets at 7.65 ppm and 7.52 ppm respectively corresponding to the aromatic hydrogen's and a singlet at 2.35 ppm for the tosyl methyl group. The synthesis of 1,10-bis-(2'-methoxyphenyl, 4''-methyl- benzenesulfonyl)-1,10-diaza-4,7-dioxa-decane, **116** was achieved in yields of 90 % after recrystallisation from ethanol. The spectral characterization compared well with that of the original synthesis results.[144] The ^1H NMR of **116** showed three characteristic singlets at 3.38 ppm for the methoxy groups, a singlet at 2.41 ppm for the methyl group of the two tosyl

moieties and a singlet at 3.40 ppm and the two sets of methylene groups adjacent to the central oxygen of the diethyl ether respectively.[144] Detosylation of **116** to produce **117** proved difficult. Work by de Silva *et al.* showed that using a 2:1 mixture of acetic acid and sulphuric acid at 59-61°C for 24 hours gave yields for this reaction as high as 60 % after recrystallisation.[144] The synthesis was described as being sensitive to temperature and that the reaction only worked when kept at exactly 60 °C. This factor was strictly adhered to, but this quoted yield was not obtained. Through a number of experiments it was found that the quality of the acids used was also a major factor in the yields produced. By changing the quality of the concentrated sulphuric acid from 95 % to 98 % purity, the yields were increased from 20 % to 32 %. Further work was carried out to improve this yield, which included changing the ratio of the acids used and extending the reaction time, but with no success. It should be noted that mass spectral analysis of the remaining residues indicated that the mono tosylated product was the main byproduct identified from this reaction, but changing the reaction time did not result in the conversion of this product into the desired detosylated product. **117** was obtained in a crystalline state and was fully characterised. ^{1}H NMR showed four signals in the aromatic region, 6.92-6.65 ppm, two doublets and two triplets as expected for a 1,2 substituted aromatic moiety. The secondary amine was represented by the slightly broad singlet at 4.6 ppm and the aromatic methoxy substituent resonated at 3.85 ppm. Finally the protons of the ethereal chain appeared at 3.8-3.3 ppm as two triplets and a singlet. The most striking difference from the starting material is the absence of the tosyl aromatic doublets and the methyl singlet.

Synthesis of the macrocyclic amides **120** and **121** involved a high dilution cyclisation synthesis of **117** with the diacid chlorides **118** and **119** respectively as shown in Scheme 5. The attempted synthesis of **118** and **119** were made by a published procedure from the corresponding acids.[145] **118** was made from diethylene glycol by oxidation to the dicarboxylic acid using HNO_3 and formation of the acid chloride **118** from a reflux in $SOCl_2$. However, in this case the product could not be purified sufficiently and was acquired commercially. **119** was produced in a pure state by chlorination from the bis carboxylic acid by refluxing in $SOCl_2$ and purified by vacuum distillation at 170 °C. The high dilution method involved adding the two reagents (**117** and **118** or **119**) in dry benzene simultaneously into a mixture of benzene and dry pyridine at 70 °C with mechanical stirring. These reactions yielded **120** and

121 as mixtures of two isomers in yields of 60-70 %. Characterisation data for **120** compared well with the original synthesis.[144] Spectroscopic techniques confirmed the formation of **121** was successful. A small fraction of the mixture of two isomers of **121** was separated by silica gel column chromatography to obtain ^1H and ^{13}C NMR spectra. ^1H NMR showed four signals in the aromatic region, two doublets at 7.58 and 6.90 ppm and two triplets at 7.32 and 7.06 ppm representing the aromatic protons. A single singlet corresponding to the aromatic methoxy at 3.87 ppm was also clearly visible. The ^{13}C NMR spectra showed the presence of thirteen carbon signals as expected. The signal at 169.85 ppm was assigned to the carbonyl carbon of the newly formed amide. The desired receptors **111** and **112** were obtained by reduction of **120** and **121** respectively using B_2H_6 in THF, generated *in situ* from $NaBH_4$ and BF_3-Etherate. These products were produced in high yield; In the case of the **111** the product was an oil (98% yield) while **112** was produced as a white solid by tituration from ether (92% yield).

2.2.2.1 Characterisation and physical studies of 111 and 112

Comparison of **111** with the original synthesis data [144] with respect to ^1H and ^{13}C NMR, IR, accurate mass and ESMS analysis showed that this receptor had been formed. **112** had never been reported before and so was characterised fully. Figure 2.2 shows the ^1H NMR of this receptor. The C_2 symmetry of the molecule resulted in a relatively simple spectrum. As seen previously for **103**, the aromatic system shows four signals, two doublets and two triplets as expected for a 1,2 substituted aromatic system. The four signals were assigned to the four non-equivalent aromatic protons. The singlet at 3.84 ppm represented the six protons of the two equivalent aromatic methoxy groups. Two triplets and a singlet each integrating to eight hydrogens represented the twenty-four ethereal ring hydrogens. ^{13}C NMR showed the existence of ten carbon signals. The aza crown ring consisted of three signals at 70.54, 69.90 and 52.65 ppm respectively and the aromatic methoxy group appeared at 55.37 ppm shown by a DEPT experiment. The final six signals consisted of four C-H carbons at 122.45 – 111.78 ppm and two quaternary carbons at 153.07 and 139.28 ppm. Mass spectroscopy, accurate mass analysis, IR and elemental analysis were also carried out and all the evidence collected demonstrated that **112** had been synthesised.

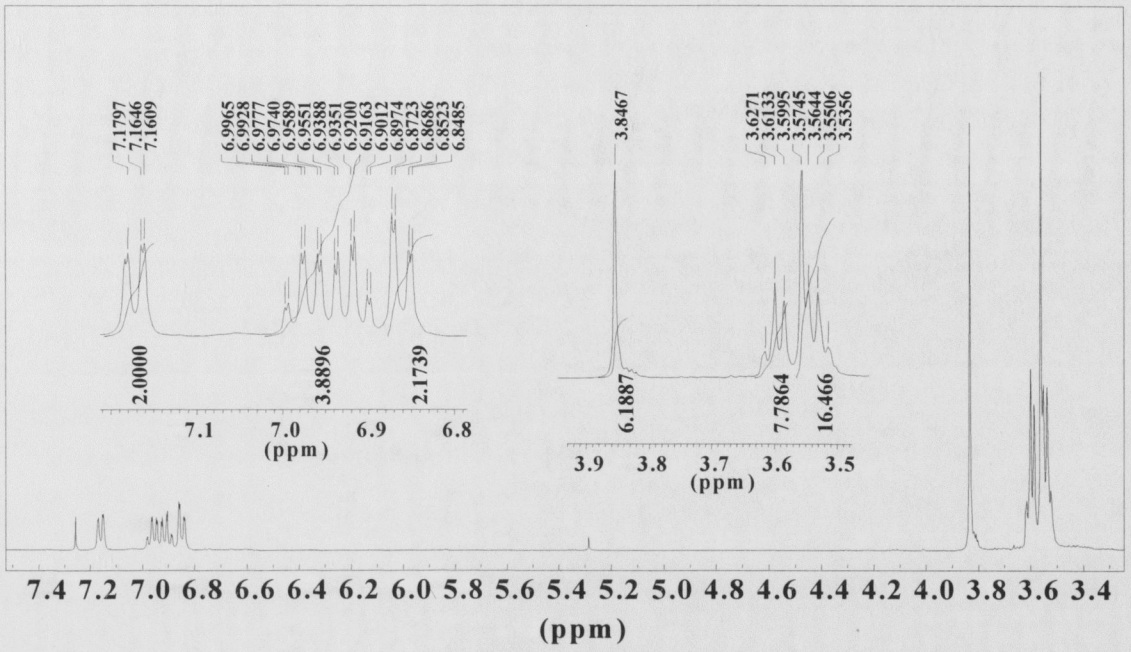


Figure 2.2 ***^1H NMR of* 112** ***[δ_H ($CDCl_3$: 400MHz)] d, t, t, and d in the region of 7.18-6.84 ppm represent the eight aromatic hydrogen's. s at 3.84 ppm represents OCH_3,t at 3.61 ppm and m in the region of 3.57 - 3.53 ppm represent aza crown ring.***

2.2.2.2 ^{1}H NMR analysis of the receptors

Further analysis of **111** and **112** was preformed by ^{1}H NMR studies in $CDCl_3$. These studies were used to demonstrate the effect of cations on the conformational arrangement of these receptors. In both cases the ^{1}H NMR of the free receptor was recorded prior to the addition of Na^+ and K^+ respectively followed by the addition of an excess of NaCN or KPF_6 in CD_3OD for **111** and **112** respectively. In both cases significant changes in chemical shift were observed for the receptors upon cation complexation. This is described by the ^{1}H NMR spectra in Figure 2.3 and 2.4 for **111** and **112** complexed with Na^+ and K^+ respectively. Figure 2.3 shows a comparison between the ^{1}H NMR spectra of the free receptor, **111**, (**A**) and the receptor in the presence of excess Na^+ (**B**). A significant change in the chemical shift of the methoxy singlet and the aza crown ring protons was observed. There were also minor changes in the positions of the four signals in the aromatic region. Figure 2.4 shows a comparison between the ^{1}H NMR spectra of the free receptor, **112** (**A**) and the receptor in the presence of excess K^+ (**B**). A similar result to that observed for **111** was seen. In both cases these observations demonstrate a conformational change in the receptors in the presence of the

cation. As expected the aza crown protons of the ring were the most affected. It should also be noted that in both studies shown the symmetry of the receptor was maintained after complexation. Furthermore, although the aromatic moieties are not directly involved in cation binding considerable changes occur in the observed chemical shifts upon cation binding.

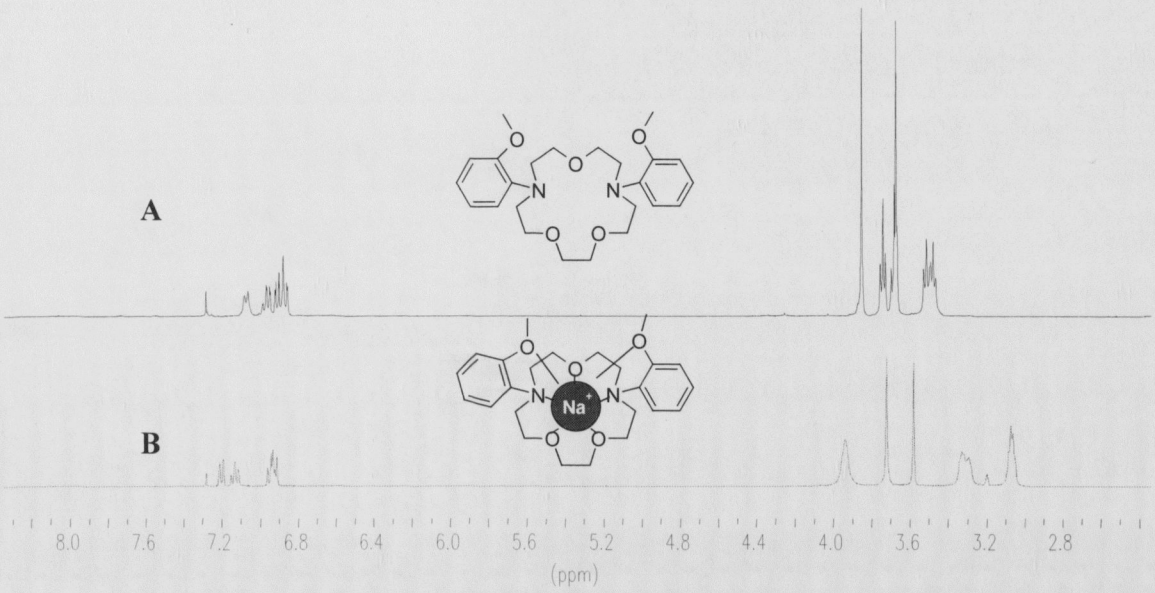


Figure 2.3 ***^1H NMR comparison [δ_H ($CDCl_3$: 400MHz)] of* 111.** ***A: without Na^+*** (methoxy singlet at 3.84 ppm and ethereal ring protons 3.72 – 3.42 ppm) ***B: Excess Na^+*** (methoxy singlet ethereal ring protons now shifted running from ~ 3.9 – 3.0 ppm)

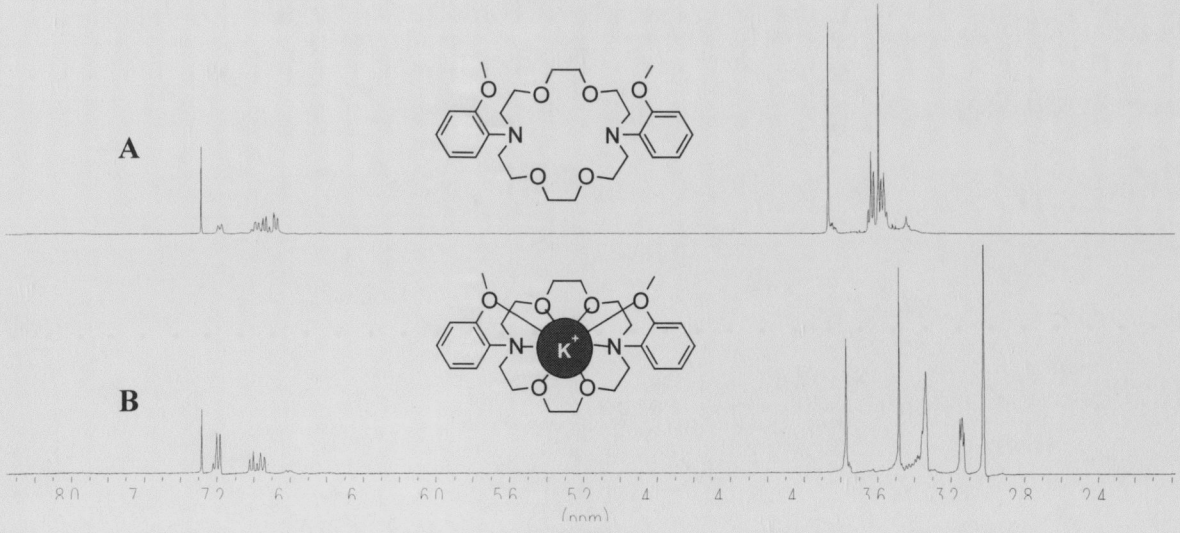


Figure 2.4 ***^1H NMR comparison [δ_H ($CDCl_3$: 400MHz)] of* 112.** ***A: without K^+*** (methoxy singlet at 3.85 ppm and ethereal ring protons 3.61 – 3.49 ppm) ***B: Excess K^+*** (methoxy singlet ethereal ring protons now shifted running from ~ 3.7 – 3.0 ppm)

2.2.2.3 X-ray crystallographic investigation of 112

The spectroscopic changes observed using ^1H NMR analysis on **111** and **112** suggest conformational changes had occurred in the receptors in the presence of Na^+ and K^+ respectively. Further evidence for this ion-induced conformational change were shown with the examination of the crystal structures of its free and complexed forms respectively. This has already been demonstrated for **111**. [31, 144] Crystals were obtained for **112** by slow evaporation from CH_2Cl_2 or $CHCl_3$ under ambient conditions over a 2-4 day period producing translucent crystals that were cubic in appearance. Crystals of the receptor bound to K^+ were also produced by slow evaporation from $CHCl_3$:MeOH (95:5) using KPF_6 over a seven day period. In both cases the crystals produced were suitable for X-ray crystallographic analysis. This analysis was preformed by Dr. Mark Niewenhuyzen in the school of chemistry, Queens University Belfast. The data was collected using a Siemens P4 four circle diffractometer with graphite monochromated Mo-K_α radiation. (More details can be seen in the Appendix) Crystal structure of the unbound receptor **112** is shown in Figure 2.5.

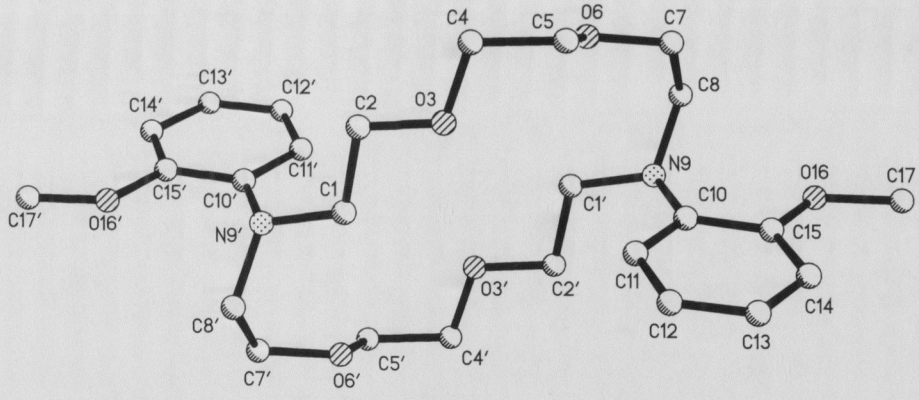


Figure 2.5. ***X-ray crystal structure of unbound receptor* 112 *(Hydrogen's omitted for clarity)***

Here the X-ray verified the presence of the C_2 symmetry in **112**. A number of features were noted regarding this structure. A view from above the ring as shown in Figure 2.6 (**A** and **B**) shows that the ring is held in a relaxed "rectangular shaped" planar conformation. The distance across space between the opposing oxygens and nitrogens of the ring vary considerably. The distance from O3 - O3' is calculated to be 4.337 Å, as opposed to 7.025 Å

for O6-O6'. The distance between the nitrogens was calculated to be 6.745 Å. All these values were obtained from analysis of the CIF files generated for the crystal or by using Mercury 1.1©. The methoxy aromatic appendages can be seen to be orientated above and below the plane of the ring *ca.* 90° with respect to the plane of the ring. Both methoxy groups point away from each other possibly to avoid repulsion from their oxygen lone pairs. From Figure 2.6 (**B**) it can be seen that both methoxy aromatic groups lie in the same plane. In this configuration, the methoxy oxygen's are as far apart as possible. The through space distance has been calculated to be 11.91(0) Å. All carbon – carbon bond lengths for the ring are *ca.* 1.4 Å with bond angles ranging from 106°-113°. Their values are probably due to the slight twisting within the ring due to its conformational freedom. The bond angles are not too extreme suggesting minimal strain to the ring.

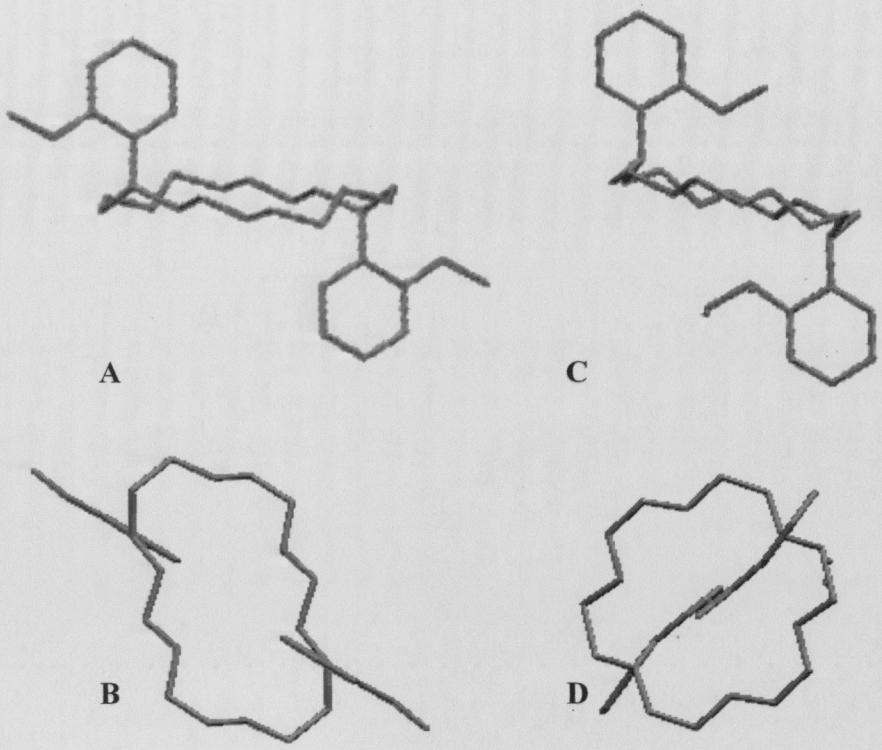


Figure 2.6. ***Illustration of crystal structures of* 112 *"free" and "bound with K^+": A and B are a side and top view of 112 in its free form. C and D are a side and top view of* 112 *"bound with K^+" respectively.***

Table 2.1 Selected parameters for crystal structure of 112 in its "free" form

Bond distance label	Bond distance (Å)	Bond angle Label	Bond angle (°)
C1 N9	1.465(2)	N9 C1 C2	112.23(17)
C1 C2	1.509(3)	O3 C2 C1	106.12(16)
C2 O3	1.420(2)	C4 O3 C2	113.62(15)
O3 C4	1.417(2)	O3 C4 C5	108.36(17)
C4 C5	1.499(3)	O6 C5 C4	108.18(17)
C5 O6	1.421(2)	C5 O6 C7	114.77(15)
O6 C7	1.425(2)	O6 C7 C8	110.00(16)
C7 C8	1.513(3)	N9 C8 C7	114.40(17)
C8 N9	1.475(2)	C10 N9 C1	116.86(16)
N9 C10	1.420(2)	C10 N9 C8	114.87(16)
C15 O16	1.369(2)	C1 N9 C8	113.83(16)
O16 C17	1.431(2)	C11 C10 C15	117.30(18)
		C11 C10 N9	122.46(17)
Through space distance		C15 C10 N9	120.24(17)
O3 O3'	4.337	O16 C15 C10	115.94(17)
O6 O6'	7.025	C14 C15 C10	120.74(18)
N9 N9'	6.974	C15 O16 C17	117.68(17)
O16 O16'	11.910		

In contrast the addition of K^+ to **112** can be seen to have a considerable effect on the conformational state of the receptor as shown in Figure 2.7 and Figure 2.6 (**C** and **D**). However, the C_2 symmetry is maintained upon complexation, an observation noted in the ^1H NMR studies shown previously (Section 2.2.2.2). The shape of the ring (**B**) changed upon complexation; the "rectangular shape" was replaced by a more circular ring. This feature is visually clear by comparison of Figure 2.6 (**B**) and Figure 2.6 (**D**). The bond distance between opposing oxygens and nitrogens in the ring also confirmed this observation. In this case the distance from O3-O3' was calculated to be 5.31(9) Å, and 5.52(5) Å for O6 - O6'. The distance between the nitrogens was calculated to be 5.907 Å. The K^+ is found to be lying directly at the center of the receptor almost equidistant to all of these coordination oxygen atoms. This was indicated by equal distances being calculated for the distance between K^+ and the opposing donor atoms (see Table 2.2). As shown by Figure 2.6 (**C**) the ring remains flat and in one plane. It is also clear, in comparison to the unbound structure of the receptor crystal **112** that considerable changes have occurred to the methoxy groups. A side view of

the crystal structure, Figure 2.6 (**C**) shows that the aromatic methoxy groups have rotated by 180° and are now directly involved in coordinating the K^+. The through space distance between the two methoxy oxygens has decreased from 11.91(0) Å to 5.05(3) Å. This conformational change leads to a pseudo cryptand like structure with all the coordinating moieties forming an orthogonal structure. This was confirmed by the bond angles for all opposing coordinating atoms being 180° for all ring contributors, with the methoxy groups lying at 90°. Unlike the unbound receptor in which the methoxy aromatic groups lie ca. 90° to the ring upon coordination to the K^+ the aromatic groups are pushed out slightly giving an angle slightly greater than 90°. Bond angles and bond lengths within the ring structure remain unchanged from that of the free receptor thus indicating that the ring size is sufficiently large enough to facilitate a cation the size of K^+, making **112** ideal for K^+ binding.

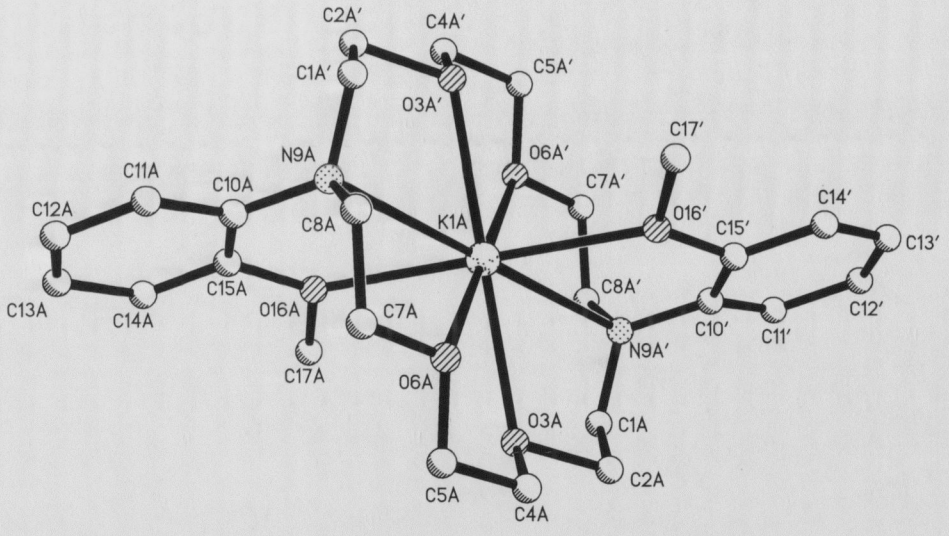


Figure 2.7. ***X-ray crystal structure of* 112• $K^+PF_6^-$ *(Hydrogen's omitted for clarity)***

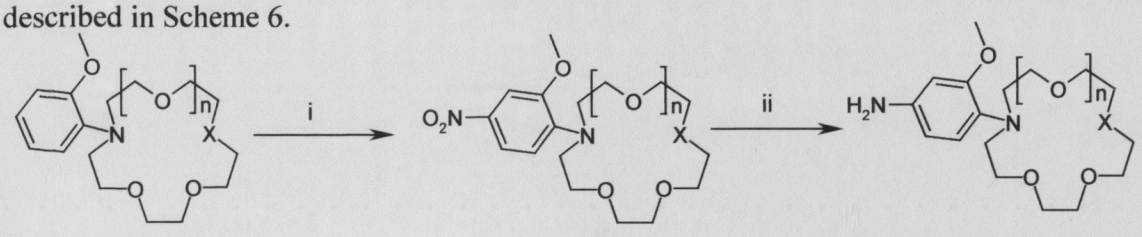
It should be noted that in the case of the **112•** $K^+PF_6^-$ crystals, two unique complexes (A and B) were seen in the unit cell. The previous discussion is based upon the crystal structure of A. The difference between the two complexes A and B was the orientation of the methoxy appendages. Like complex A, B shows coordination to the K^+ by the methoxy groups. However, for B the distance between the two methoxy oxygens is slightly longer (5.451 Å) than that for complex A (5.05(3) Å).

Table 2.2 Selected parameters from 112• $K^+PF_6^-$

Bond distance label	Bond distance (Å)	Bond angle Label	Bond angle (°)
K1A O16A	2.527(15)	O16A K1A O16'	180.000(2)
K1A O16'	2.527(15)	O16A K1A O3A	90.1(3)
K1A O3A	2.659(3)	O3A K1A O3A'	180
K1A O3A'	2.659(3)	O6A K1A O6A'	180
K1A O6A	2.763(2)	N9A K1A N9A'	180.00(9)
K1A O6A'	2.763(2)	O3A C2A C1A	100.5(7)
K1A N9A	2.953(3)	C4A O3A C2A	97.3(4)
K1A N9A'	2.953(3)	O3A C4A C5A	109.4(4)
C1A N9A'	1.449(15)	O6A C5A C4A	109.0(3)
C1A C2A	1.554(14)	C5A O6A C7A	112.1(3)
C2A O3A	1.547(8)	O6A C7A C8A	109.2(3)
O3A C4A	1.386(6)	N9A C8A C7A	112.3(3)
C4A C5A	1.474(6)	C10A N9A C8A	112.8(3)
C5A O6A	1.416(5)	C15A C10A N9A	120.0(4)
O6A C7A	1.429(5)	C14A C15A O16A	123.8(7)
C7A C8A	1.484(6)	C15A O16A C17A	116.7(12)
C8A N9A	1.468(6)		

2.3 Nitration and reduction of aza and diaza crown receptors 103, 104, 111 and 112

Following the synthesis of the azacrown receptors **103, 104, 111** and **112**, the addition of a nitrogen atom to the aromatic moiety was required to facilitate the attachment of an amide spacer for subsequent addition of the lumophore ligand. In this case the addition of a nitro or nitroso group onto the ring was a requirement followed by reduction to an amino group as described in Scheme 6.



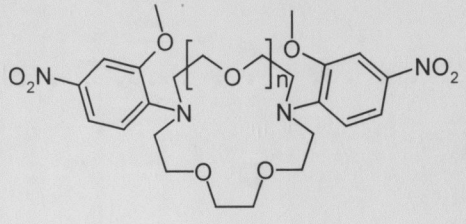
103: n=1, X=O
104: n=2, X=O
111: n=1, X=$NC_6H_4OCH_3$
112: n=2, X=$NC_6H_4OCH_3$

122: n=1, X=O
123: n=2, X=O
124: n=1, X=$NC_6H_4OCH_3$
125: n=2, X=$NC_6H_4OCH_3$

126: n=1, X=O
127: n=2, X=O
128: n=1, X=$NC_6H_4OCH_3$
129: n=2, X=$NC_6H_4OCH_3$

Scheme 6. ***Nitration and reduction of*** **103, 104, 111** and **112,** ***i)1.1 eq $NaNO_2$, 1:10 AcOH: H_2O, RT, > 70 % yield ii) EtOH, Pd-C (10%), H_2, RT, > 90% yield.***

Nitrations of aromatic molecules are quite common and can be achieved using many existing methods. The three most common methods are nitration with HNO_3:H_2SO_4, HNO_3:AcOH or using NO_2BF_4.[146, 147] Unfortunately, all attempts to nitrate receptor **103** using these methods failed. In the case of nitration with NO_2BF_4 the product was observed in a mass spectrum of the reaction solution. However, ^{1}H NMR and TLC showed only the starting material, **103**. The use of HNO_3:H_2SO_4 proved too harsh and led to decomposition of the starting material. In one instance when HNO_3:AcOH was dropped onto a solution of the **103** in $CHCl_3$ at – 60 °C, a yield of 32 % of **122** achieved. However, it was not possible to purify this product completely even with repeated attempts using column chromatography. With little success at nitration of **103** an attempt at nitrosation was made using **103** as an alternative method of introducing a nitrogen to the ring. The nitrosation procedure that was employed consisted of adding an aqueous solution of 1.1eq of $NaNO_2$ to an aqueous solution of **103** (10 % glacial acetic acid) that was being stirred at room temperature. Upon drop-wise addition of an aqueous solution of $NaNO_2$ an instantaneous colour change was observed from clear to orange which increased in intensity with every drop of solution added. Surprisingly, mass spectroscopy of the yellow oil produced indicated that the receptor contained a nitro group and not the nitroso group as expected. Comparison of the ^{1}H NMR with that of **122**, produced from the procedure described earlier showed this to be the case. This successful result was complemented by high yields of up to 89 % after a short alumina column using [99:1] CH_2Cl_2:MeOH. The only drawback was that on scale up from 0.6 g to 5.0 g, the yield fell to *ca.* 60 %. This procedure was repeated on all the other receptors with similar excellent results. In the case of the diazacrown receptors **111** and **112** the expected dinitro byproduct **130** and **131** were also isolated.



130: n = 1
131: n = 2

Using the method described above for **111**, a 48 % yield of **124** and 17% yield of **130** was achieved. In the case of the **112** this technique produced a 43 % yield of **125** and 36 % yield of **131**. Through further optimization of the method, for the diazacrown systems, preferential

synthesis of the mono nitrated product was accomplished. In the case of **112**, 4.7 g of the receptor was stirred in a 500 mL aqueous solution of 10 % glacial acetic acid. To this a 60 mL aqueous solution of (1.1eq) $NaNO_2$ was added over a four-hour period and left stirring over night. Following purification by alumina column chromatography using [99:1] CH_2Cl_2:MeOH the mononitrated receptor **125** was isolated in 70% yield.

2.3.1 Characterisation of the nitrated receptors

In all but one case, these nitrated products were characterised fully, the exception being **124**. In this case the product was an oil and attempts to obtain elemental analysis failed. In the case of **122** and **123** a distinguishable difference in the aromatic protons was observed. The four signals (two triplets and two doublets) seen for the unnitrated product **103** and **104** were replaced by three signals, a double doublet at 7.77 ppm, a doublet at 7.63 ppm and a doublet at 6.86 ppm. These are typical of a tri-substituted aromatic system. In the case of **123**, the resolution was lower and this resulted in the observation of a doublet, singlet, doublet with the same chemical shifts as described above respectively. In the case of the **130** and **131** the aromatic region was the same as described above. The ^1H NMR of **124** and **125** was more interesting. In both cases the symmetry of the molecule was lost and two distinct sets of aromatic peaks were observed. One set of signals were similar to the mononitrated monoaromatic receptors **122** and **123**; the other set was characteristic of the unnitrated aromatic receptor system. Changes were also seen on the methoxy groups of the receptor upon mononitration, since two distinct singlets were observed at 3.87 ppm and 3.82 ppm respectively for **124** and at 3.89 ppm and 3.83 ppm in the case of **125**. Changes were also seen in the ethereal ring protons. In both cases the number of peaks doubled. This was due to the asymmetry introduced by the mononitration. In all cases NOE experiments indicated substitution had occurred *para* to the aniline nitrogen. The evidence from ^1H NMR showed substitution had occurred on the aromatic groups but did not prove that the products produced were nitro aromatic. More substantial evidence was collected by way of ESMS, accurate mass, IR spectroscopy, elemental analysis and X-ray crystallography. In the case of accurate mass all compounds were found to be of the nitro derivatives, all showing exact weights within the 5-ppm tolerance threshold. (As shown in Table 2.3 below) IR analysis was also beneficial, since two characteristics peaks could be identified to support the formation of the nitro group.

A peak at around 1500 cm^{-1} representative of a symmetric $(N=O)_2$ stretch as well as a peak around 1350 cm^{-1} representative of an asymmetric $(N^{=}O)_2$ stretch which would not be seen in a nitroso aromatic product.[148]

Table 2.3 Accurate mass analysis summary of nitrated receptors

Compound	Formula [M+H]	Mass Calculated	Mass Observed	Tolerance (PPM)
122	$C_{17}H_{27}N_2O_7$	371.1818	371.1817	-0.4
123	$C_{19}H_{31}N_2O_8$	415.2080	415.2066	-3.4
124	$C_{24}H_{34}N_3O_7$	476.2397	476.2420	4.8
130	$C_{24}H_{33}N_4O_9$	521.2248	521.2260	2.4
125	$C_{26}H_{38}N_3O_8$	520.2659	520.2676	3.4
131	$C_{26}H_{37}N_4O_{10}$	565.2510	565.2507	-0.4

2.3.2 Crystallographic analysis of nitrated receptors 122 and 131

The final evidence for the nitration of these receptors and confirmation of its position on the receptor was derived from crystallographic analysis. Crystals were obtained for **122** and for **131**. In both cases crystals suitable for X-ray crystallographic analysis were grown by slow evaporation from CH_2Cl_2 solutions. Crystals obtained for **122** and **131** are shown in Figure 2.8 and Figure 2.9 respectively. In both cases nitration was shown to have occurred *para* to the aniline nitrogen on both aromatic moieties as was already determined by ^1H NMR analysis.

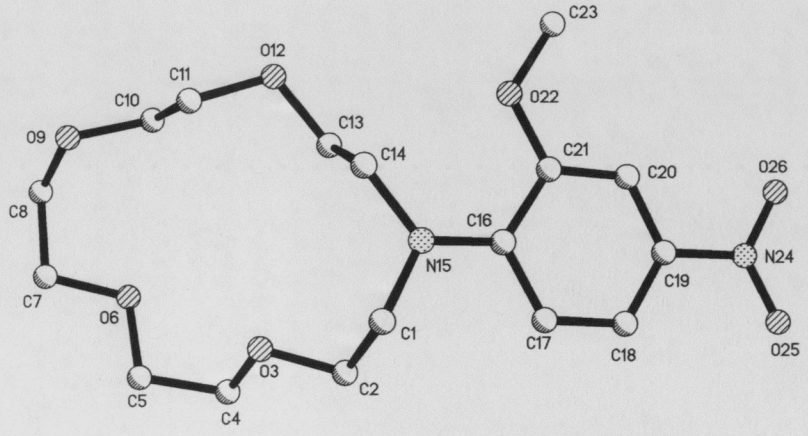


Figure 2.8. ***X-ray crystal structure of* 122 *(Hydrogen's omitted for clarity)***

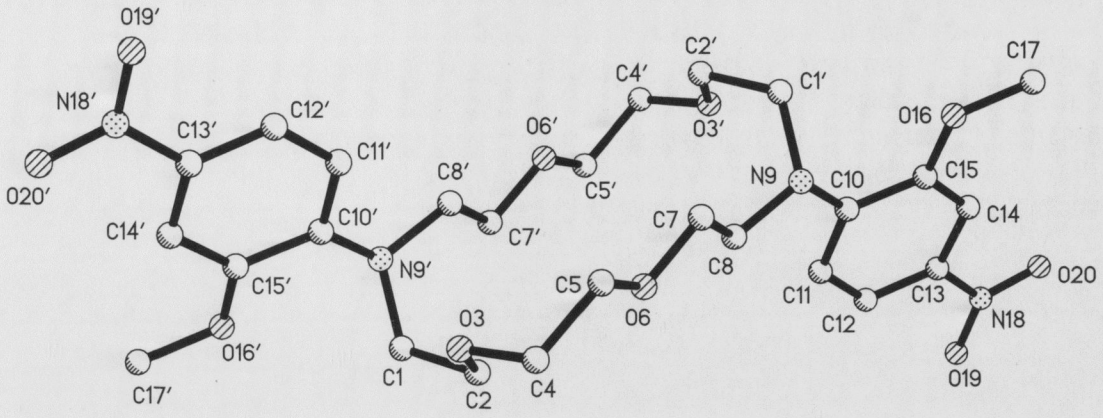


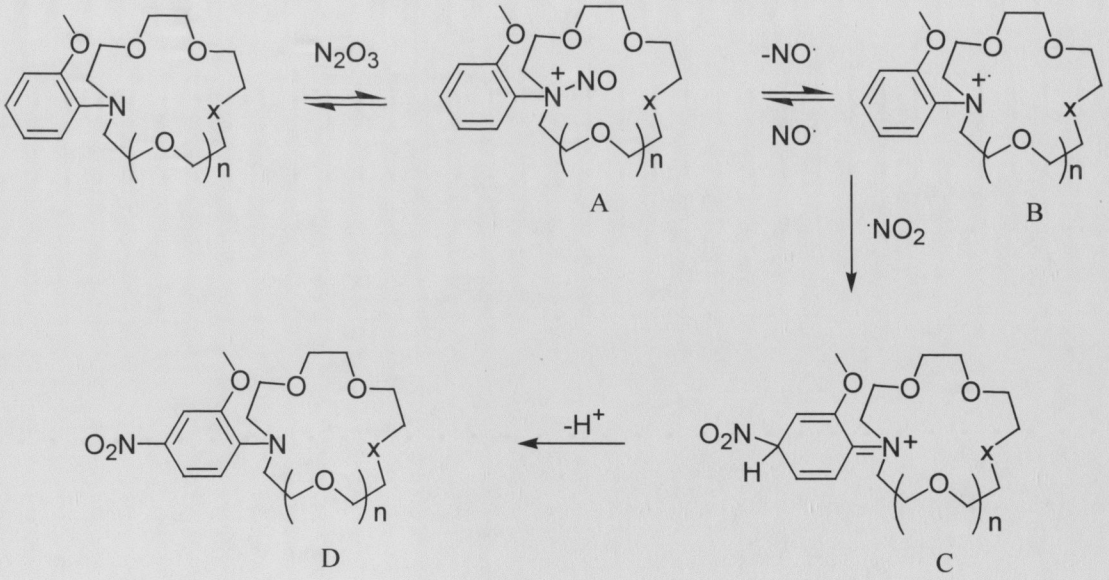
Figure 2.9. ***X-ray crystal structure of* 131*(Hydrogen's omitted for clarity)***

2.3.3 Proposed mechanism for nitration using $NaNO_2$

Following these unexpected results, a detailed literature search focusing on the nitration of aromatic amines with $NaNO_2$ was conducted with the aim of understanding why nitration had occurred when nitrosation was expected. From this search only a few examples were found in which this nitroso reagent produced nitro products but in all cases strong acids such as H_2SO_4 were used which could easily oxidize nitroso groups. A search spanning back as far as 1891 revealed mixed results with various but similar procedures with a number of aromatic systems.[149, 150, 151, 152, 153] The use of $NaNO_2$ with H_2SO_4/H_2O in the presence of (2-methoxy-phenyl)-dimethyl-amine resulted in a nitro compound, [151] as did the use of nitrous acid on the nitrosamine analogue. [152] When carried out on phenols such as 2-methoxy-phenol sodium salt, the use of $NaNO_2$ with H_2SO_4/H_2O produced the nitroso compound as well.[149] Further examples of triphenyl phosphine together with $NaNO_2$ and HCl/MeOH at –5 °C gave a nitroso product. [150] Nitroso products have also been produced with this method for mono and bis alkylated anilines with or without substituents on the ring. [153]

A greater understanding into what was happening came with a review that covered the work of Loeppky *et al.* and other research groups who have studied in detail the mechanisms of aromatic nitrations and nitrosations.[154] In this work, Loeppky *et al.* studied the reaction of 4-dimethylamino-benzoic acid ethyl ester with HNO_2 in acetic acid or acetic acid/ water buffered at pH 3.8. In this work the dominant product was almost always a nitrosoamine system with a nitro byproduct. Through kinetic studies the formation of a radical cation intermediate was

shown to occur; this observation was supported by earlier work in the field, [155] by other groups who examined *N, N* alkylated aniline compounds and methoxy phenols as substrates. Mechanisms were studied by a number of methods, [156] including ^{15}N NMR, electrochemical and ESR experiments. Evidence for NO, NO_3^- and hence NO_2^+ was found in the reaction media, thus a conventional electrophilic aromatic nitration was not occurring. The possibility of nitrosation followed by oxidation was shown not to be the case by Loeppky *et al.*. Instead formation of a radical cation was shown to occur by reaction of $NO^\bullet$ with the aniline nitrogen. Following formation of the cation radical intermediate, a nitration occurs through reaction with $NO_2^\bullet$. Subsequent deprotonation results in the aromatic nitro product. This nitrated product was always seen as a minor product except in the case where a fifteen-fold increase in HNO_2 was used. Under these more acidic conditions the major product became the nitro product. Another significant observation was that the nitration occurred on the aromatic ring, whereas nitrosations occurred on the aniline nitrogen through dealkylation. Based on these previous studies, the mechanism for the nitration of the aza crown receptors **103**, **104**, **111** and **112** was believed to occur in a similar fashion, as shown in Scheme 7.



Scheme 7 ***Proposed mechanism for nitration of aza crown receptors. n=1 or 2. X = O or $NC_6H_4OCH_3$***

As described in Scheme 7, radical cation formation, **B** is proposed to arise through homolysis of the nitroso ammonium ion, **A**, but could also be produced by an equivalent set of transformations involving oxidation by N_2O_3 or another NO^+ donor, or by NO_2 (N_2O_3 produced from $NaNO_2$, and radicals produced by homolytic cleavage). Under Loeppky conditions $NO_2^{\bullet}$ was generated by the facile homolysis of N_2O_3. Reaction of the intermediate, **B** with NO_2 generates the protonated nitro species, **C** which quickly deprotonates to yield the nitrated aromatic product, **D**.

2.3.3.1 Testing the versatility of the nitration method

Unlike the work of Loeppky *et al.* [154] and others,[155,156] the only products observed from the reaction of **103**, **104**, **111** and **112** were the nitrated aromatic products. This was the case even when a large excess (10 equivalents) of $NaNO_2$ was used. However for **103** and **104** mononitration was observed exclusively (multiple nitrations were never seen under any conditions). This fact along with high yields and the mild and environmentally friendly conditions makes this method potentially applicable for industrial use. With this in mind further investigations were carried out to determine if this method, or other variations could be employed on other aromatic systems. The use of this method on a number of aromatic systems was tested and the results are shown summarized in Figure 2.10 and 2.11.

Figure 2.10, shows that this reaction is indeed successful when various groups are substituted on the aniline nitrogen as seen with **132**, **134** and **135**. In all these cases the amine was tertiary. The same is true when substituents such as a methoxy group are present in either the *ortho* (**132**) or *para* (**133**) position. When the aromatic substituent was bromine, a nitro product was still produced (**136**). However, with no substituents present the desired product was not produced (**138**). This method also failed to produce the nitro product when the amino unit was secondary, such as in the case of **117**. Furthermore, the tosyl amide derivatives **115**, **116** or **137** gave no nitrated products, but the solubility of these starting materials was poor in the aqueous solution, which may have contributed to these results. Nitration of **140** and **141**, which lack the amino moieties, were also unsuccessful. This method was also found to be unsuccessful when attempted on substituted pyridines **142**, **143**, **144** and on phenol **139**. The effect of the solvent and choice of acid on the nitration product was also investigated. The

results were shown in Table 2.4. Using a mixture of water and glacial acetic acid gave on all occasions the desired product under either aerated or degassed conditions. However, no nitration occurred if MeOH was used instead of water or when HCl or H_2SO_4 was used as the acid. It is apparent from these results that the substitution pattern of the starting material is very important and that the reaction only yields the nitro compounds when tertiary amines are employed.

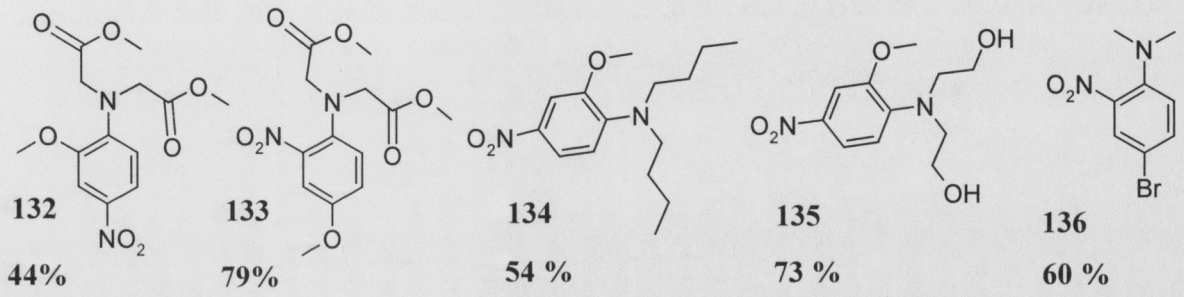


Figure 2.10. ***Summary of successful nitrations, (with yield of reaction inset)***

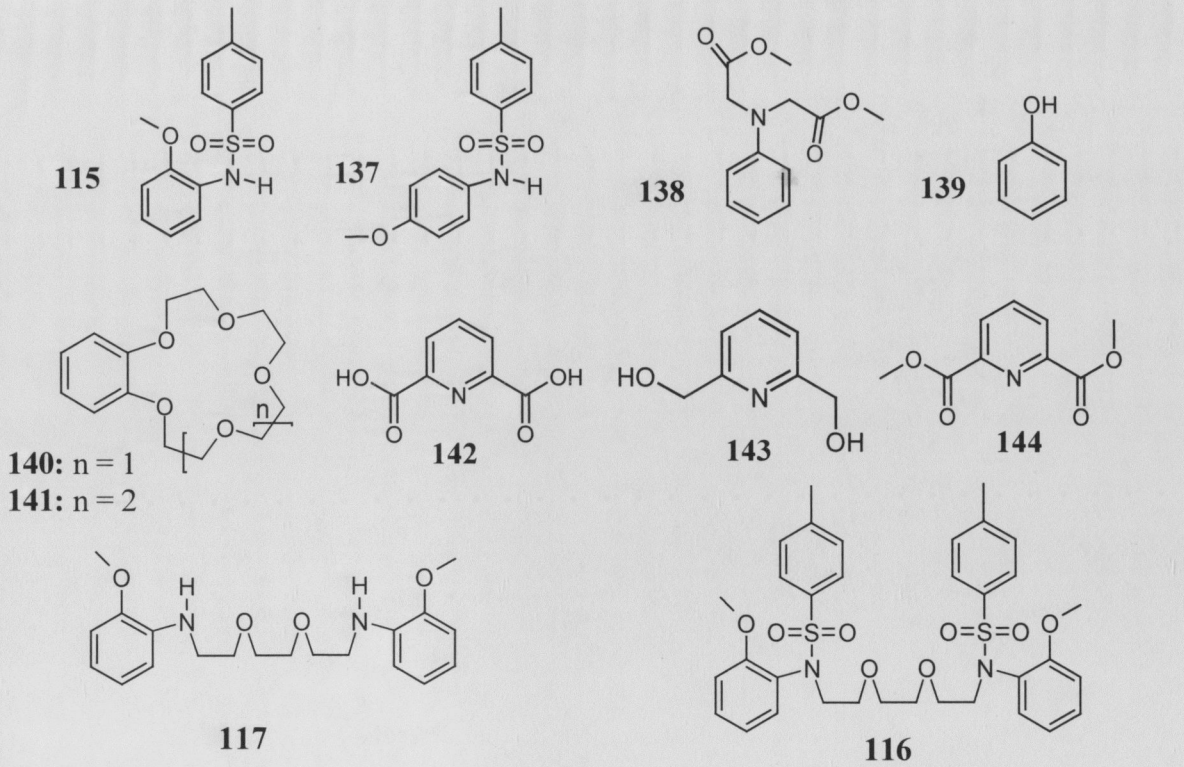


Figure 2.11. ***Summary of molecules used with nitration method that yielded no nitro product.***

Table 2.4 Results of variation to new nitration method

Method	Solvent *	Acid *	Atmosphere	Purged Or Unpurged	Product +
New Method	H_20	CH_3COOH [100%]	Air	Unpurged	Nitro
B	H_20	CH_3COOH [100%]	Argon	Unpurged	Nitro
C	H_20	CH_3COOH [100%]	Argon	Purged	Nitro
D	MeOH	CH_3COOH [100%]	Air	Unpurged	No reaction
E	MeOH	HCl [conc.]	Air	Unpurged	No reaction
F	H_20	HCl [conc.]	Air	Unpurged	No reaction
G	H_20	H_2SO_4 [conc.]	Air	Unpurged	No reaction
H	H_20	--------	Air	Unpurged	No reaction

In all cases ratio of solvent: acid was 10:1, + In all the cases model compound was **110 and product was **135**.*

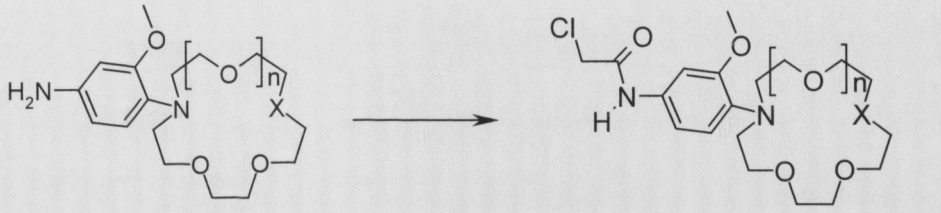
2.3.4 Reduction of 122, 123, 124 and 125

Following the synthesis of nitrated receptors **122**, **123**, **124** and **125**; these desired compounds had to be converted to the corresponding amines **126**, **127**, **128** and **129** respectively. This was achieved by stirring the nitro compounds in absolute EtOH with 10 %, Pd-C under an atmosphere of H_2. The desired products were isolated in good yields as viscous oils. In all cases ^1H NMR showed the presence of the NH_2 resonance and a shift in the aromatic peaks. All these amines were found to be quite stable. For instance, **126**, **128** and **129** were reinvestigated by ^1H, ^{13}C NMR and ESMS after the samples had been stored under ambient conditions for six months. In all cases, no decomposition had occurred over time.

2.4 Synthesis of 145, 146, 147 and 148

The attachment of the spacer groups to the amine functionalised receptors to produce **145**, **146**, **147** and **148** (Scheme 8) was found to be a challenge, employing a number of procedures. These will be discussed below. The introduction of the spacer group was first attempted on **126**, using of chloroacetyl chloride in CH_2Cl_2 in the presence of TEA [130] at - 40 °C, yielding

145 in a 40 % yield. The ^1H NMR of the desired product, **145** showed a peak at 9.18 ppm corresponding to an amide N-H peak and a singlet at 4.18 ppm corresponding to the α chloro methylene moiety. There were also further changes in the aromatic region. IR analysis revealed the presence of an amide carbonyl at 1685 cm^{-1}. Changing the base to Na_2CO_3, $NaHCO_3$ or Cs_2CO_3 did not improve this yield. A second method involving a peptide coupling was also investigated.[157] This procedure involved the use of α chloro acetic acid, HOBt and EDCI in CH_2Cl_2. [157] This reaction gave the desired product in a yield of 81 %, but required purification by way of alumina column chromatography. However, when this procedure was scaled up to over 0.3 g the yield decreased to 65-70 % yield.



126: n=1, X=O
127: n=2, X=O
128: n=1, X=$NC_6H_4OCH_3$
129: n=2, X=$NC_6H_4OCH_3$

145: n=1, X=O
146: n=2, X=O
147: n=1, X=$NC_6H_4OCH_3$
148: n=2, X=$NC_6H_4OCH_3$

Scheme 8 ***Synthesis of*** **145**, **146**, **147** ***and*** **148**

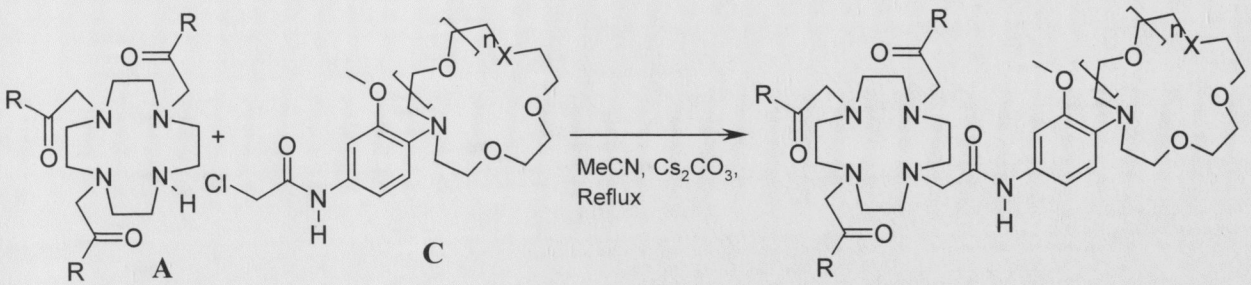
The peptide coupling reaction was also employed using the amine **127** to produce the amide **146** in a 73 % yield. As previously found for **145**, the ^1H NMR of **146** exhibited signals corresponding to the N-H amide and the α chloro methylene moiety, which were characteristic of this compound. The results confirmed that **146** had been formed. Unfortunately, the product contained a number of unidentified impurities that could not be removed by acid base extraction, or by column chromatography. In the synthesis of **147** and **148** from **128** and **129** respectively, none of the above methods were adequate and a new method had to be devised. In these cases, α chloro acetic anhydride was used in the presence of Na_2CO_3 in 1,4 dioxane. The desired receptors, **147** and **148**, were isolated after alumina column chromatography using a gradient dilution of CH_2Cl_2 to 70:30, CH_2Cl_2:MeOH. Yields of 45 % and 65 % were achieved for **147** and **148** respectively. The ^1H NMR spectra of **147** and **148** showed the presence of the

expected amide N-H peaks at 8.30 ppm and 8.39 ppm respectively and a singlet at 4.21 ppm and 4.18 ppm for the methylene spacer. ^{13}C NMR also proved successful in characterization showing a carbonyl quaternary peak at *ca.* 163 ppm for both as well as a α-Cl-CH_2 peak at *ca.* 42-43 ppm. In both cases IR spectroscopy showed the amide carbonyl peak at ca. 1680 cm^{-1}. In the ESMS of **147** and **148** the isotope pattern corresponding to a chlorine-containing compound was observed.[148]

2.5 Synthesis of sensor ligands 99, 100, 101 and 102

The last step in the synthesis of **99**, **100**, **101** and **102** (Scheme 9) involved a substitution reaction between component **A** (**149** or **150**) and component **B** (**147** and **148**). The cyclen based macrocycle **150** was synthesised in one step [158] by reacting cyclen with bromo *tert*-butyl acetate in MeCN in the presence of $NaHCO_3$ stirring at room temperature for 48 hours. The desired product, **150** was isolated in 42 % yield and characterisation of this product was in agreement with published data.[158] **149** was made in a similar way using cyclen and 2-chloro-*N,N*-dimethyl-acetamide in MeCN with $NaHCO_3$, stirring at 65 °C for 72 hours which afforded **149** in 52 % yield following alumina column chromatography. The characterisation of this product is discussed in great detail in Chapter 5.

The coupling of the two components was carried out in MeCN at reflux in the presence of Cs_2CO_3. [130] In all these reactions, oils were produced which, when analysed by conventional methods showed that the desired products had been formed. TLC indicated that there were a number of impurities. A number of purification techniques were employed in the purification of these ligands. In the case of **99** or **100**, silica or alumina column chromatography failed to afford the products in a sufficiently pure state. Attempts to purify these compounds using size exclusion chromatography were also unsuccessful. Partial purification was possible by washing solutions of **99** and **100** in $CHCl_3$ with water. The ^1H NMR spectrum was insufficient for characterisation. However, ^{13}C NMR was useful along with DEPT experiments at elucidating the structure of these ligands. In contrast, **151** and **152** were successfully purified by alumina column chromatography and were isolated as oils by elution with 70:30, DCM:THF, followed by slowly changing the solvent system to 60:30:10, CH_2Cl_2:THF:MeOH.



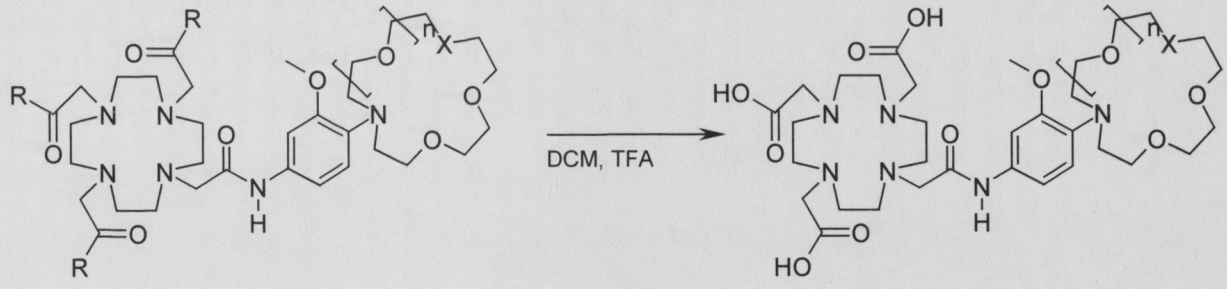
149: R= NMe_2
150: R= O*t*-Bu

147: n=1, X=$NC_6H_4OCH_3$
148: n=2, X=$NC_6H_4OCH_3$

99: R= NMe_2, n=1, X = NC_6H_4OMe
100: R= NMe_2, n=2, X = NC_6H_4OMe
151: R= O*t*-Bu, n=1, X = NC_6H_4OMe
152: R= O*t*-Bu, n=2, X = NC_6H_4OMe

Scheme 9 ***Synthesis of sensor ligands*** [130]

Characterisation of both these ligands was best achieved using ^{13}C NMR, ESMS, accurate mass and IR spectroscopy. The ^{13}C NMR spectra showed four quaternary peaks for the carbonyl groups as well as seven aromatic C-H's. The presence of the aromatic methoxy carbon and the cyclen and aza crown ring CH_2 carbon signals were also apparent. Resonance corresponding to the *tert*-butyl ester carbons were also very prominent, the quaternary carbons of **151** appeared *ca.* 81 ppm and the CH_3 carbons appeared at *ca.* 27 ppm. Similar results were observed for **152**. Finally for both **151** and **152**, the *tert*- butyl ester groups were removed using TFA in CH_2Cl_2 (Scheme 10) yielding **101** and **102** respectively. [158]



151: R= O*t*-Bu, n=1, X = NC_6H_4OMe
152: R= O*t*-Bu, n=2, X = NC_6H_4OMe

101: n=1, X = NC_6H_4OMe
102: n=2, X = NC_6H_4OMe

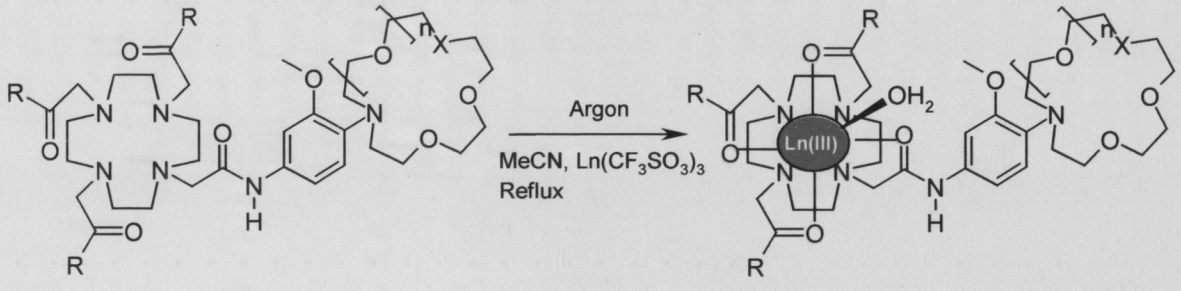
Scheme 10 ***Synthesis of sensor ligands*** **101** ***and*** **102** [158]

Ligands **101** and **102** were both obtained in a pure form by precipitation of the crude ligand with diethyl ether. Both ligands were characterised by ^1H and ^{13}C NMR, ESMS, accurate mass

and IR analysis. Examination of the ^1H NMR indicated that the *tert*-butyl groups had been clearly removed as the *tert*-butyl signal at *ca.* 1.27 ppm had disappeared. Carboxylic OH groups were also observed as broad singlets at 10.88 ppm and 8.41 ppm for **101**, and at 10.88 ppm and 8.64 ppm for **102** respectively. In both ligands a broad OH peak at *ca.* 3429 $cm^{-1}$was observed in the IR spectra.

2.6 Synthesis of lanthanide complexes

The final synthesis required to produce the desired Na^+ and K^+ chemosensors of ligands **99, 100, 101** and **102** required the synthesis of their respective Europium (III) and Terbium (III) complexes. This was achieved using a method described in Scheme 11, [130] resulting in the formation of six lanthanide complexes, **Eu.99**, **Eu.100**, **Tb.99**, **Tb.100**, **Tb.101** and **Tb.102**. The synthesis of all these complexes consisted of stirring the ligand and 1.1 equivalents of the appropriate lanthanide (III) triflate salt in freshly distilled MeCN for approximately fifteen hours, under an atmosphere of dry argon. After cooling to room temperature the reaction mixture was dropped onto ether from which a gum or solid material was recovered. The complexes, **Eu.99**, **Eu.100**, **Tb.99** and **Tb.100** were purified by alumina column chromatography using 30:70, THF:CH_2Cl_2, the products were eventually isolated by increasing the polarity to 30:60:10, THF:CH_2Cl_2:MeOH. In all cases a yield in excess of 40% was achieved. The Tb(III) complexes, **Tb.101** and **Tb.102** were obtained in yields of *ca.* 80 % by precipitation from ether and did not require further purification.



99: R= NMe_2, n=1, X = NC_6H_4OMe, Ln(III) = Eu(III) or Tb(III)
100: R= NMe_2, n=2, X = NC_6H_4OMe, Ln(III) = Eu(III) or Tb(III)
101: R= OH, n=1, X = NC_6H_4OMe, Ln(III) = Tb(III)
102: R= OH, n=2, X = NC_6H_4OMe, Ln(III) = Tb(III)

Scheme 11 - ***Synthesis of lanthanide complexes using lanthanide triflate salts*** [130]

2.6.1 Characterisation of the Tb(III) and Eu(III) complexes

The six lanthanide complexes, **Eu.99**, **Eu.100**, **Tb.99**, **Tb.100**, **Tb.101** and **Tb.102** were characterized by ^1H and ^{19}F NMR as well as other conventional characterizing techniques. The ^1H NMR spectra of **Eu.99**, **Eu.100**, **Tb.99** and **Tb.100** were all very similar, showing large chemical shifts due to the presence of the paramagnetic lanthanide ions. The ^{19}F NMR spectra clearly showed the presence of triflate counter anions. Of all the analysis carried out on these complexes, ESMS and accurate mass proved to be the most valuable. In all cases the ESMS showed a number of peaks related to the complexes. As shown in Figure 2.12 and 2.13 the isotopic patterns of the Eu(III) and Tb(III) were clearly distinguishable. The **Tb.101** and **Tb.102** complexes were characterised in the same way and gave similar results to those discussed above. The obvious difference was seen in the absence of any triflate counter anions, as these complexes were charge neutral.

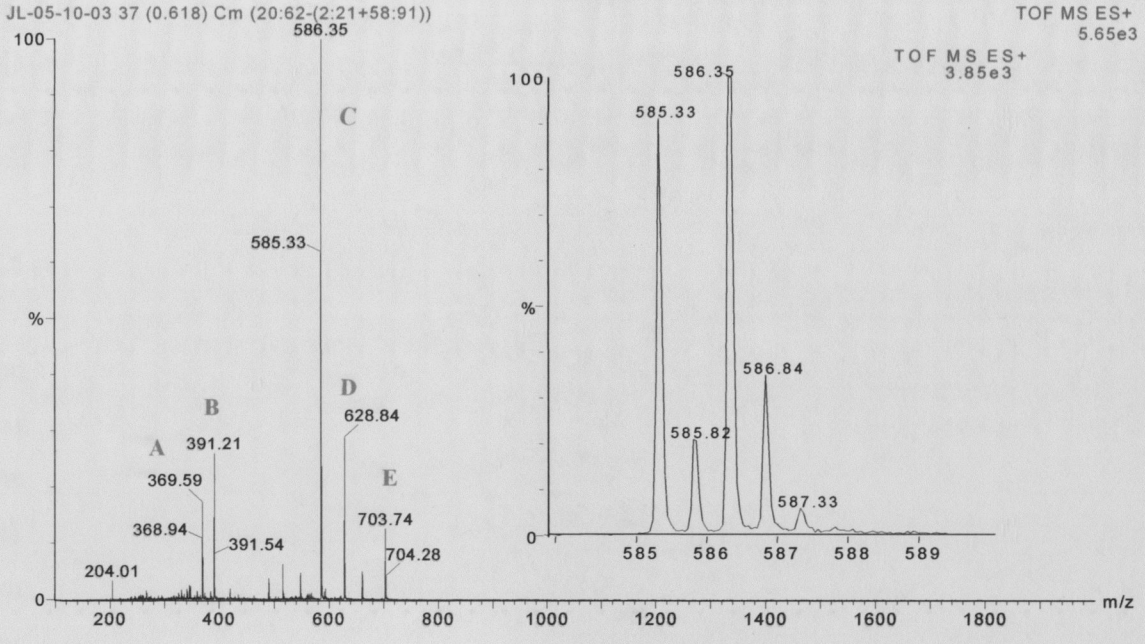


Figure 2.12 ***Mass spectrum of*** **Eu.100** ***(Uncalibrated) Selected peaks were labeled as follows:*** **A** =[M+3H]/3, **B** =[M(Triflate)$_3$+3H]/3, **C** = [MNaK +2H]/2, **D** = [M(Triflate)+2H]/2, **E** = [M(Triflate)$_2$ +2H]/2,. (Inset: **C** =[MNaK +2H]/2, indicating the isotopic pattern seen in all peaks for Eu(III) complex – Theoretical models generated with Mass Lynx®.)

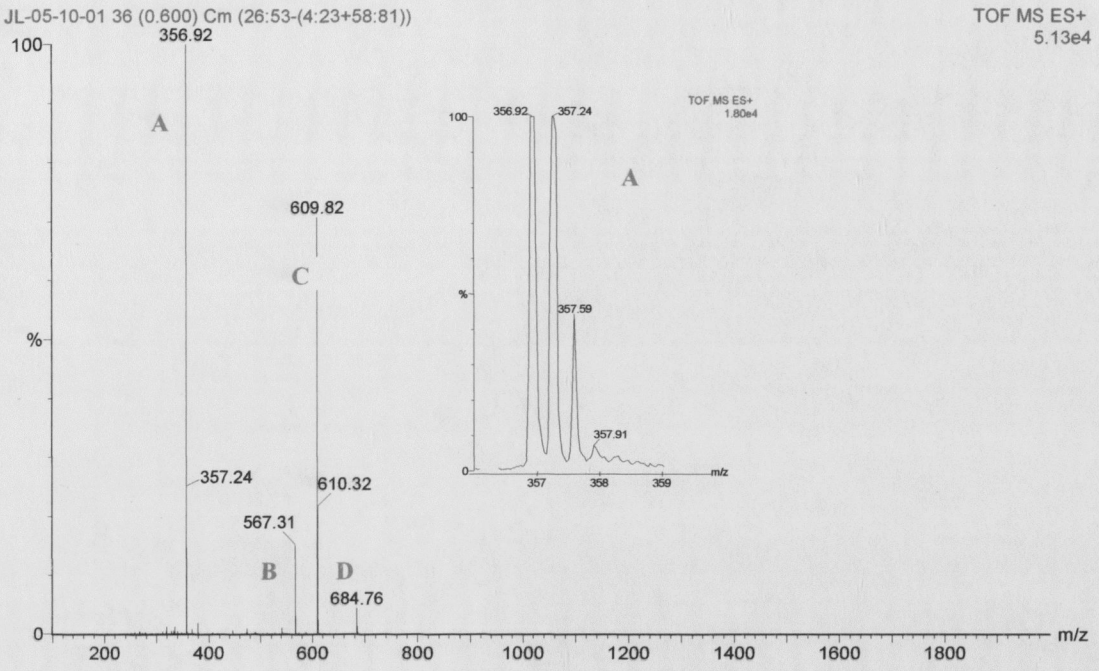


Figure 2.13 ***Mass spectrum of*** **Tb.99** ***(Uncalibrated) Selected peaks were labeled as follows:*** **A** =[M+3H]/3, **B** =[MNaK +2H]/2, **C** = [M(Triflate)+2H]/2, **D** = $[M(Triflate)_2+2H]/2$,. (Inset: **A** =[M+3H]/3, indicating the isotopic pattern seen in all peaks for Tb(III) complex – Theoretical models generated with Mass Lynx®)

2.6.1.1 Lifetime analysis of the Tb(III) and Eu(III) complexes

Ligands **99, 100, 101** and **102** are all capable of octadentate coordination with lanthanide ions. Lanthanide ions usually exist with higher coordination of 9-10.[159] For this reason it was expected in all these complexes that there would be at least one water molecule coordinated to the lanthanide ion. As discussed previously in Chapter 1, measuring the excited state lifetime (τ) of lanthanide complexes in H_2O and D_2O allows for the determination of ***q***, the number of water molecules bound directly to the metal center. Luminescent lifetime measurements were carried out using a Varian Carey Eclipse Fluorimeter. In the case of **Tb.100** the lifetime (τ) in H_2O was measured to be 0.181 ms and 0.189 ms in D_2O. Using equation 3 (Chapter 1) a ***q*** value of 0.95 was determined indicating one metal bound water molecule. Similarly, a ***q*** value of 1.23 was calculated for **Tb.99**. The Eu(III) complexes both gave longer lifetimes. In the case of **Eu.100** the lifetime in H_2O was calculated to be 0.307 ms and 0.483 ms in D_2O. Using equation 2 (Chapter 1) a ***q*** value of 1.13 was obtained, indicating that the Eu(III) complex also

had one metal bound water molecule. Similarly **Eu.99** had a q value of 1.09. The **Tb.101** and **Tb.102** complexes also produced q values indicating one bound water molecule. A comparison of the lifetimes of **Tb.101** and **Tb.102** with **Tb.100** and **Tb.99** show significant differences, possibly due to the difference in the nature of the complexing ligands, a feature observed in many studies of lanthanide complexes.[160] These results are summarised in Table 2.5 and in all cases show that there is one water molecule bound to each complex.

Table 2.5 Summary of Lifetime studies on lanthanide complexes

Complex	τ (ms) H_2O	$1/\tau$ (ms^{-1}) $k_{H2O\ (ms\text{-}1)}$	τ (ms) D_2O	$1/\tau$ (ms^{-1}) $k_{D2O\ (ms\text{-}1)}$	q ($\pm$ 0.5)
Tb.100	0.181	5.53	0.189	5.28	0.95
Tb.99	0.161	6.19	0.170	5.89	1.23
Eu.100	0.307	3.26	0.483	2.07	1.13
Eu.99	0.315	3.16	0.498	2.00	1.09
Tb.102	0.470	2.12	0.530	1.88	0.90
Tb.101	0.778	1.28	1.048	0.95	1.35

2.7 Photophysical analysis of Eu.99, Eu.100, Tb.99, Tb.100, Tb.101 and Tb.102

The six lanthanide complexes **Eu.99**, **Eu.100**, **Tb.99**, **Tb.100**, **Tb.101** and **Tb.102** were designed to operate as sensors for the detection of intracellular concentrations of cations such as Na^+ and K^+. As mentioned previously, the receptors are based on the structurally similar receptors found in **95** and **96**, both of which are successful fluorescent sensors for the detection of intracellular concentrations of Na^+ and K^+ respectively. These complexes are also similar to **Tb.89**, discussed in Chapter 1, in which binding of Zn^{2+} to the aniline nitrogen of the receptor led to a suppression of PET, resulting in an enhancement of lanthanide luminescence.[124,129,130,161] It was expected that these lanthanide complexes would function on the same basis. The following sections outline the studies performed on these lanthanide complexes to determine their ability to operate as cation sensors. The major concern of these studies was the effect on lanthanide luminescence as a function of pH or metal ion concentration. However, all of these complexes were also studied by *uv*-visible and fluorescence spectroscopy. The settings used for each study are described in detail in Chapter 6. Binding constants were determined using published methods.[144, 162]

2.7.1 Absorption investigations of Eu(III) and Tb(III) complexes

2.7.1.1 pH studies of Eu(III) and Tb(III) complexes

pH titration studies were carried out on all the lanthanide complexes in aqueous solution. In the case of **Tb.99** detailed pH titration studies were performed In all other pH experiments, the complexes were found to behave in the same manner, and so only preliminary investigations were carried out in which the absorbance spectra of the complexes at high and low pH conditions were recorded. In aqueous solution the **Eu.99**, **Eu.100**, **Tb.99** and **Tb.100** complexes displayed two absorption maxima at *ca.* 200 nm and *ca.* 275 nm. In the case of, **Tb.101** and **Tb.102** these appeared at 211 nm and 273 nm. The absorption band at *ca.* 200 nm was attributed to the amide or carboxyl moieties, while the band at 279 was attributed to the diaza crown aromatic moieties. Figure 2.14 shows the absorption spectra of **Tb.99** as a function of pH. At pH = 12, two absorption bands are present at 211 nm (log ε = 5.43) and 251 nm (log ε = 4.09) with a shoulder at 279 nm (log ε =4.03). As the pH was decreased to pH = 7, by the addition of HCl, a hypsochromic shift was observed in the 211 nm band with a concomitant hypochromic effect which resulted in the absorption band being shifted to 200 nm (log ε = 5.34). When the pH was decreased further to pH < 1, a slight bathochromic shift to 203 nm (log ε = 5.37) and concomitant hyperchromic effect were observed. Considerable changes were also observed in the 251 nm band and in the shoulder at 279 nm. The 251 nm band experienced a hypochromic effect as the pH was decreased to pH = 6. However, as the pH was decreased further a hyperchromic effect was observed. A concomitant bathochromic shift was observed in the 251 nm band as the pH decreased from pH = 12 to 8, which resulted in a shift in the maximum to 279 nm. As the pH was decreased further a hypochromic effect was observed which reached a minimum absorption at *ca.* pH = 2, resulting in a decrease in the absorbance intensity of *ca.* 54 %. A plot of absorbance at 279 nm as a function of pH is shown in Figure 2.15. The sigmoidal curves observed were consistent with a simple ion-binding equilibrium and 1:1 binding [163] From this graph two pK_a values of 11.0 (± 0.2) and 5.5 (± 0.2) were determined. The pK_a value of 11.0 was attributed to deprotonation of the aryl amide nitrogen, while the pK_a value of 5.5 was attributed to protonation of one of the two aniline nitrogen of the diaza crown. Similar pH studies were performed on all the other complexes and all showed comparable changes to those reported for **Tb.99**. However, the pK_a's for these were

not determined. The minor effect in the absorbance at 279 nm as a function of pH between pH 6 and 10 indicate that these complexes can function under physiological pH conditions.

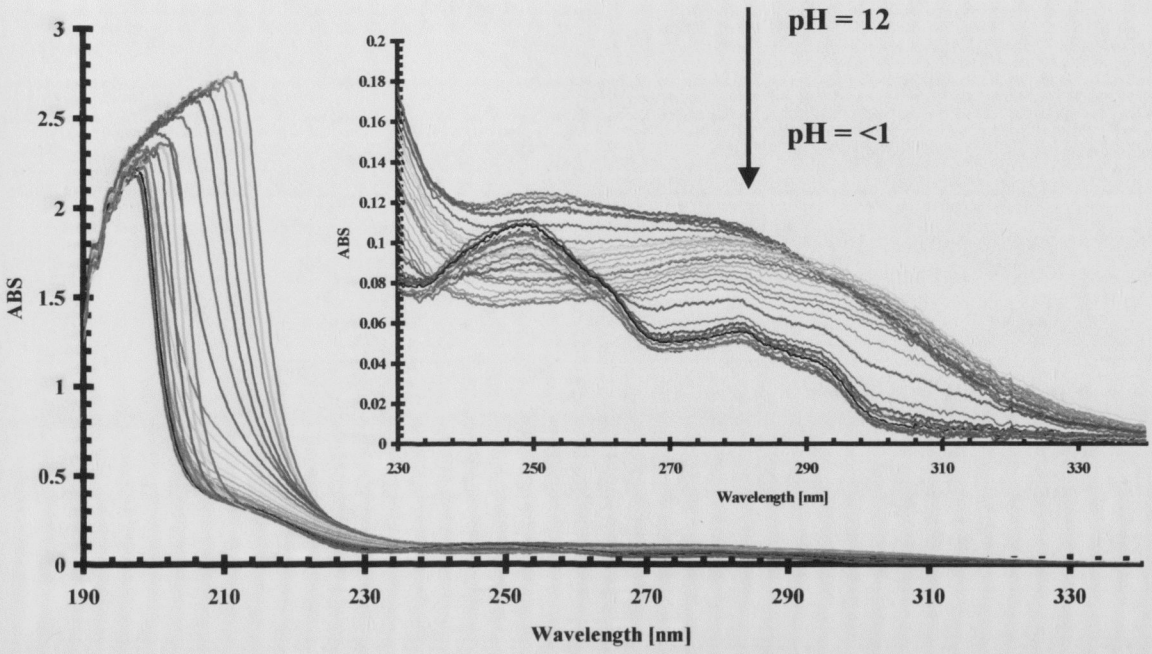


Figure 2.14 ***Absorption of*** **Tb.99** ***as a function of pH [10-μM aqueous solution. Solution basified with TMAOH and titrated with HCl] (Inset: Magnification of spectra 230-340 nm)*** Note: Absorbance is unusually high below 220 nm due to instrument sensitivity at short wavelengths.

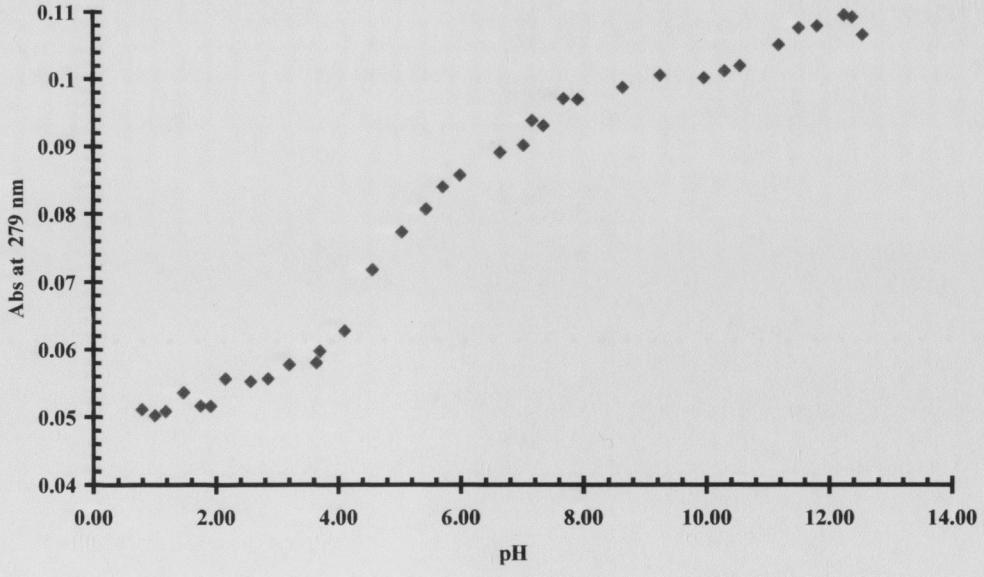


Figure 2.15 ***Absorbance of*** **Tb.99** at 279 nm ***as a function of pH [10-μM aqueous solution. Solution basified with TMAOH and titrated with HCl]***

2.7.1.2 Metal ion studies of Eu(III) and Tb(III) complexes

Metal ion studies were carried out on all the lanthanide complexes in aqueous solutions or in buffered solutions at pH 7.4. In the case of **Tb.100** a detailed metal ion titration was performed. In all the other metal ion experiments the complexes were found to behave in the same manner, and so only preliminary studies were performed. Absorption studies were carried out in the presence of physiologically important cations such as Na^+ and K^+. In the case of **Tb.100**, a Tb(III) complex designed as a sensor for K^+, a titration was performed in aqueous solution with KOAc. The effect on absorption with the addition of KOAc is shown in Figure 2.16. Two absorption bands were visible prior to the addition of KOAc, at 200 nm (log ε = 4.75) and 276 nm (log ε = 4.12) respectively. Upon addition of KOAc over a range of 1 μM to 0.8 M (pK 0.02 to 6), a bathochromic shift in the 200 nm band was observed, which was accompanied by a hyperchromic effect that resulted in a new absorption maximum at *ca.* 223 nm (log ε = 5.03). An isosbestic point was observed at *ca.* 248 nm. A concomitant hypochromic effect was also observed in the 276 nm band, which resulted in a 33 % decrease in the absorption intensity. The 276 nm band was attributed to the aniline nitrogen's of the aza crown ring. Upon cation binding the lone pair of the aniline nitrogen are involved in binding and are no longer or partially conjugated with the aromatic system. A plot of absorption at 276 nm as a function of pK is shown in Figure 2.17. In this case a sigmoidal curve was observed which occurred over two log units, an indication of simple equilibrium and 1:1 binding as previously seen during pH studies.[163] A binding constant of log β = 1.3 was determined.

In summary the absorption studies have highlighted the pH dependence of these lanthanide complexes in aqueous solution. In the case of **Tb.99**, pH dependence above pH 10 was due to deprotonation of the aryl amide were as pH dependence below pH 7 was attributed to protonation of the aniline nitrogen of the receptor. In the case of **Tb.100**, 1:1 binding of K^+ was demonstrated. Studies on all other complexes showed comparable changes in absorption in the presence of cations such as Na^+ or K^+, or when the pH was changed.

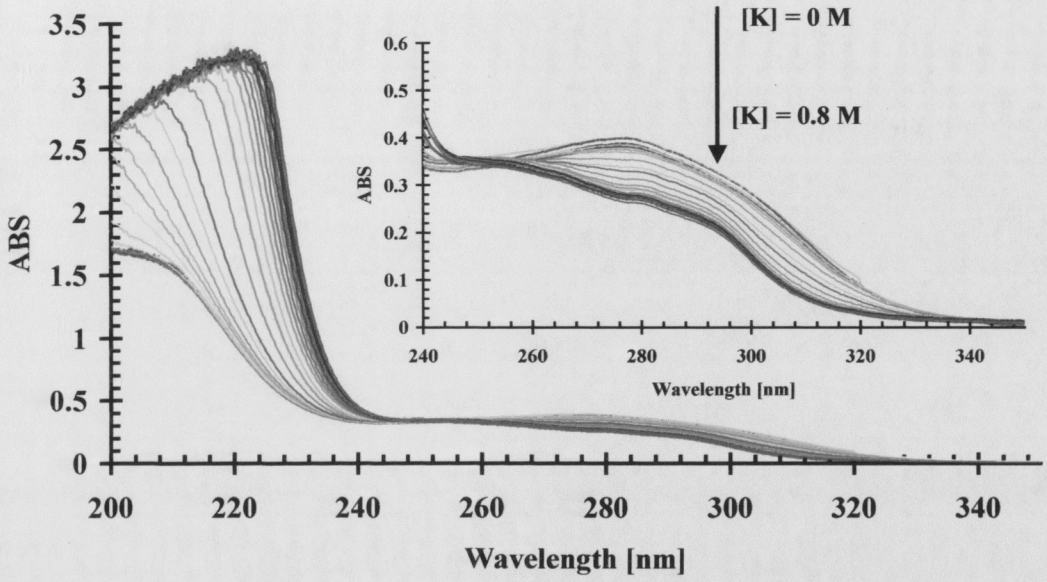


Figure 2.16 ***Absorption of*** **Tb.100** ***as a function of pK [30-μM aqueous solution. Titration with KOAc] (Inset: Magnification of the changes at 240-350 nm)*** Note: Absorbance is unusually high below 220 nm due to instrument sensitivity at short wavelengths.

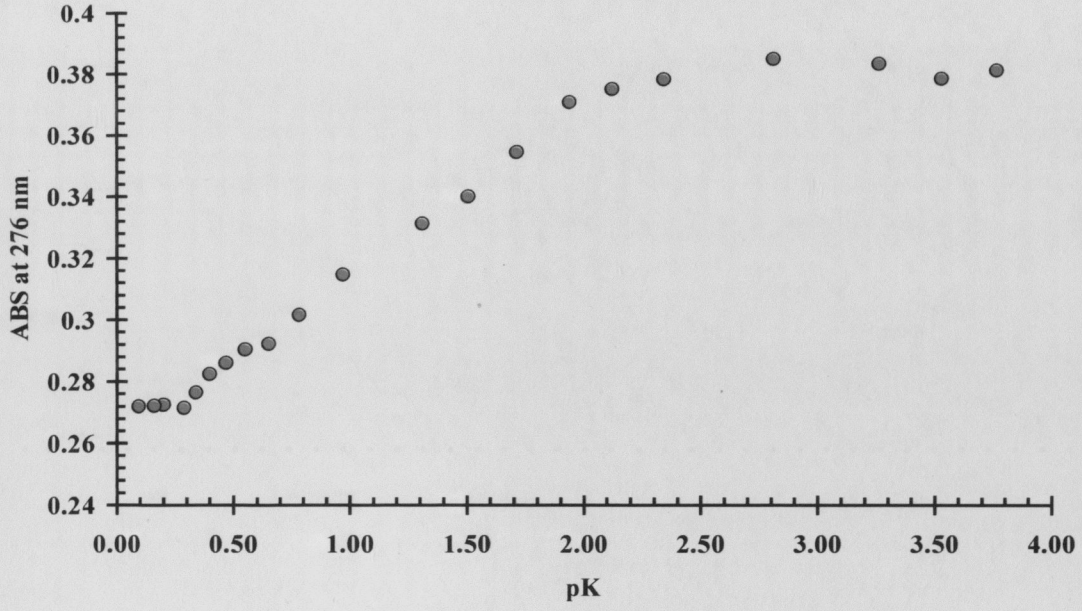


Figure 2.17 ***Absorbance of*** **Tb.100** at 279 nm ***as a function of pK [30-μM aqueous solution. Titration with KOAc]***

2.7.2 Fluorescence investigations of Eu(III) and Tb(III) complexes

Similar studies to those reported in Section 2.7.1 were performed on all the lanthanide complexes in aqueous solution or buffered solutions at pH 7.4. In these cases the fluorescent emissions of each complex were monitored as a function of pH or metal ion addition. The complexes were excited at 300 nm and emissions were observed from 315 – 585 nm.

2.7.2.1 pH studies of Eu(III) and Tb(III) complexes

A detailed pH titration was performed on **Tb.99** in aqueous solution. Figure 2.18 shows the fluorescence emission for **Tb.99** as a function of pH. The fluorescence observed was a consequence of the excitation of the aromatic moieties of the diaza crown. At pH = 7 two emission maxima were observed at 336 nm and 378 nm. Both of these bands were almost equal in intensity. Upon basification with TMAOH to pH = 12.5 the intensity of the 378 nm band increased by almost 50 %. A minor increase was also observed for the 336 nm band. Upon titration of the **Tb.99** solution with HCl, a decrease in the intensity of the 378 nm band was observed. This resulted in a total reduction in intensity of 87 % as the pH was slowly decreased from pH = 12.5 to 0.8. No significant change was seen in the emission band at 336 nm, this was determined to be due to Raman scattering and was seen in all complexes studied. The decrease in fluorescence with respect to decreasing pH may be attributed to the decrease in absorbance at 300 nm (Figure 2.14). As the pH is decreased the amount of energy being absorbed to cause excitation at 300 nm decreases, and so a weaker emission would be observed. A plot of the change in intensity at 378 nm as a function of pH is shown in Figure 2.19. Two pK_a values of approximately pK_a = 10.8 (± 0.2) and pK_a = 5.6 (± 0.2) were determined, which were comparable with the values determined experimentally in Section 2.7.1 of pK_a = 11.0 (± 0.2) and pK_a = 5.5 (± 0.2). Once again the value of pK_a 10.8 was attributed to deprotonation of the aryl amide nitrogen, were as the value of pK_a = 5.5 was attributed to protonation of one of the aniline nitrogen of the aza crown. It should be noted that at pH 4, the J = 6 and J = 5, Tb(III) emissions began to appear at 490 nm and 546 nm respectively. Similar pH experiments were also performed on **Eu.99**, **Eu.100**, **Tb.100**, **Tb.101** and **Tb.102**, in these cases only the emission at high and low pH were observed and all of these complexes showed the same trend as that discussed for **Tb.99**, that is a complete suppression in the emission intensity of the 378 nm band was observed at low pH.

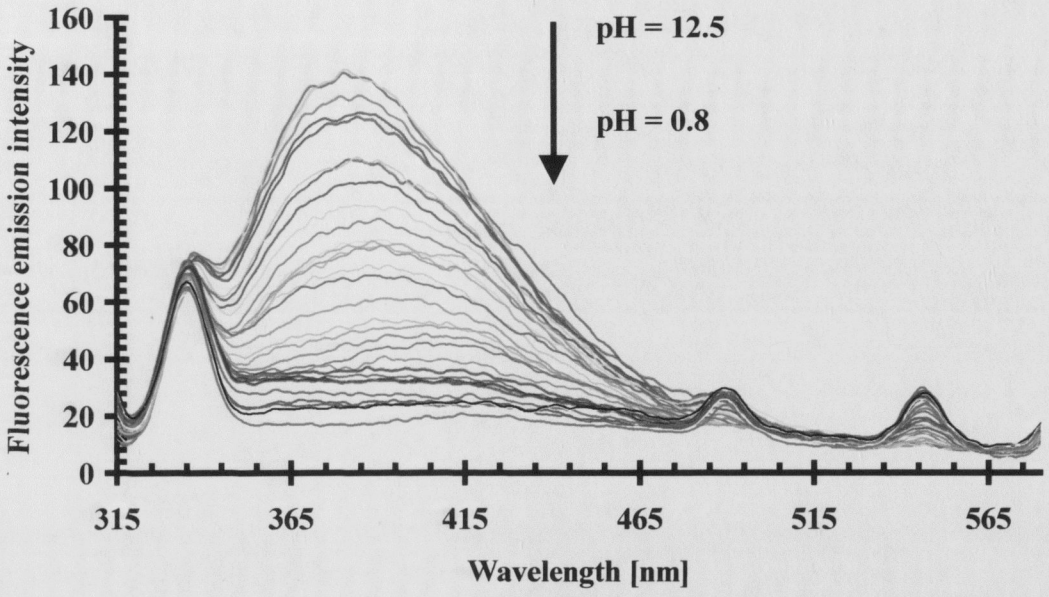


Figure 2.18. ***Fluorescence of*** **Tb.99** ***as a function of pH*** [10 μM solution slit widths 9 nm, excitation at 300 nm] (Note: The appearance of J = *6* (490 nm) and J = *5* (546 nm) Tb(III) emissions at low pH) Note: Emission band at 317 nm is due to Raman scattering

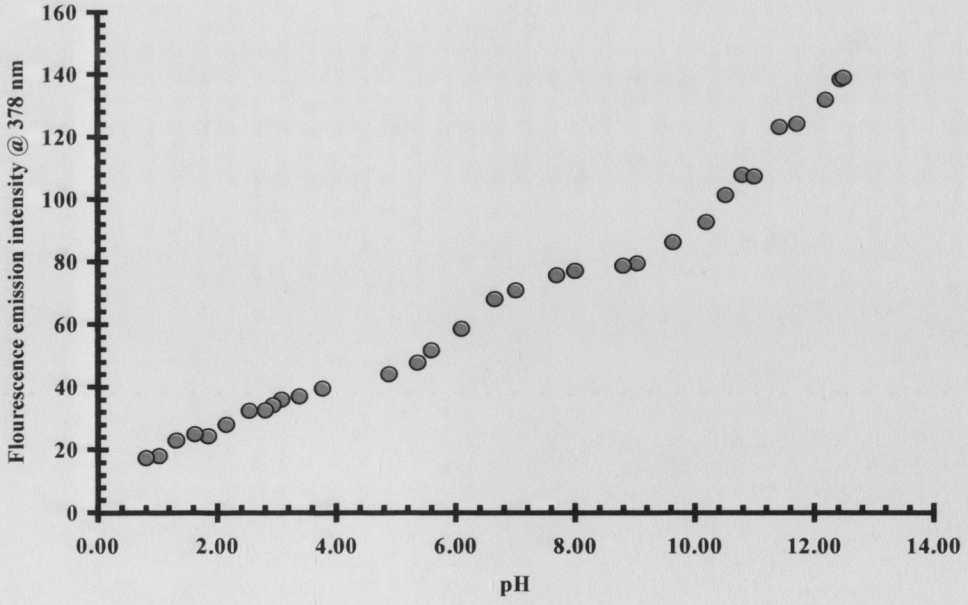


Figure 2.19. ***Fluorescence profile of*** **Tb.99** ***as a function of pH at 378 nm*** [10 μM solution slit widths 9 nm, excitation at 300 nm]

2.7.2.2 Metal ion studies of Eu(III) and Tb(III) complexes

Analysis of the fluorescent emission of all of these lanthanide complexes were also carried out in the presence of Na^+ or K^+. In all cases 10 mL solutions of each complex (8 μM) were made in buffered solutions at pH 7.4. Similar solutions of each of these complexes were then made up in buffered solutions containing 4.0 or 5.0 M of Na^+ or K^+ respectively. Excitation of the complexes was at 300 nm. The emission spectra of **Tb.99** in the presence and absence of NaOAc are shown in Figure 2.20. These show that there was no change observed in the 336 nm band in the presence of a high concentration Na^+, whereas a decrease in the emission of the 378 nm band of almost 50 % occurred. The presence of the J = *6* and J = *5* Tb(III) emissions were also observed. In this experiment the decrease in the emission intensity of the 378 nm band was attributed to cation binding with the aniline lone pair of the aza crown. The result in each of the other complexes was comparable to **Tb.99** with a decrease in the 378 nm emission band of almost 50 %, and no change in the emission band at 336 nm in the presence of a high concentration of Na^+ or K^+. In all the Tb(III) complexes the J = *6* and J = *5* Tb(III) emissions were also observed.

In summary, the fluorescence experiments of all these lanthanide complexes, mirror the results observed from the absorption studies, previously discussed. That is, these complexes show pH independence in the range pH 6.5 to 9 and a considerable change in fluorescence in the presence of metal ions, which is an indication of binding.

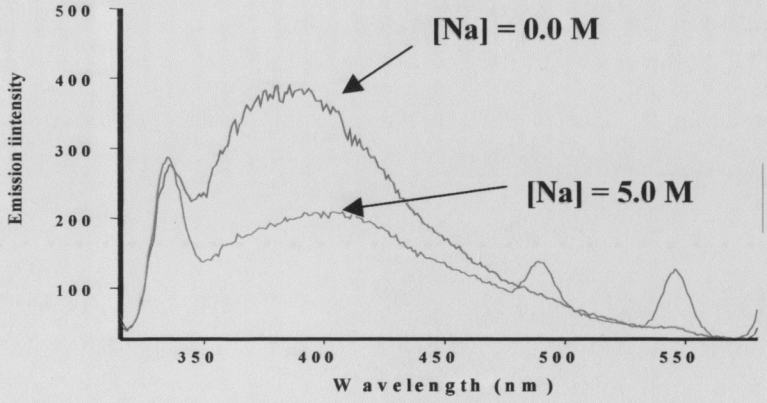


Figure 2.20. ***Fluorescence study of* Tb.99 *in the absence (brown line) or presence (red line) of NaOAc*** [8 μM solution, 0.1 M TMACl, 0.1M Tris Buffer, pH 7.4, slit widths 10 nm, λ_{excit} – 300 nm] Note: Emission band at 317 nm is due to Raman scattering

2.7.3 Lanthanide luminescence investigations of Eu(III) and Tb(III) complexes

The lanthanide complexes **Eu.99**, **Eu.100**, **Tb.99**, **Tb.100**, **Tb.101** and **Tb.102** were all analysed in terms of their lanthanide luminescence with respect to pH or metal ion addition. These investigations were all carried out on complexes in aqueous or buffered solution, with an excitation wavelength of 300 nm. All studies were performed in phosphorescence mode to account for the lanthanide emission time delay. The results of these studies are reported in the following sections.

2.7.3.1 pH studies of Eu(III) and Tb(III) complexes

The pH response of **Tb.99**, in aqueous solution is shown in Figures 2.21 and 2.22 respectively. At pH = 7, the Tb(III) emission intensity was weak, with only two Tb(III) transitions visible. These were J = 6 and J = 5, occurring at 490 nm and 547 nm respectively. The pH of this solution was adjusted using TMAOH and HCl. No changes were observed in the emission intensity in the pH range of 4.1-9.6, indicating that this complex was pH independent over this large pH range. However when the pH was increased above pH 9.6 or decreased below pH 4.1, dramatic changes were seen in the Tb(III) emission. The Tb(III) transitions, J = 6, J = 5, J = 4 and J = 3 occurring at 490 nm, 547 nm , 586 nm and 622 nm respectively were observed. At low pH a maximum emission intensity of 348 was reached at pH = 1.5, compared to 25 at pH = 7, which is a 14-fold luminescent enhancement. No significant change was observed in the Tb(III) luminescence at lower pH. A maximum emission intensity of 350 was recorded at pH 12.6, again an indication of a 14-fold enhancement. This pH response was found to be reversible, and comparable result was also found when this experiment was repeated using H_2SO_4 instead of HCl. When this experiment was performed on **Tb.100** and as shown in Figure 2.22, the same pH dependence was observed. Estimated pK_a values of 2.8 (± 0.2) and 11.2 (± 0.2) were determined for **Tb.99** and 2.5 (± 0.2) and 11.0 (± 0.2) for **Tb.100**. The high pK_a values of 11.2 and 11.0 for **Tb.99** and **Tb.100** respectively were attributed to deprotonation of the aryl amide (Scheme 12). The pK_a values of 2.8 and 2.5 for **Tb.99** and **Tb.100** respectively were attributed to the protonation of the aniline nitrogen of the aza crown (Scheme 12). As illustrated in Scheme 12 [125] protonation of the aniline nitrogen or deprotonation of the aryl amide can lead to a situation in which the aniline nitrogen lone pair is no longer conjugated. It has been reported for **Tb.89**, [130] that

deconjugation of the aniline nitrogen lone pair results in a suppression of PET, from or to the intermediate aryl singlet excited state of the aniline moiety, which leads to a luminescent enhancement. The enhancement observed for **Tb.99** and **Tb.100** in high or low pH conditions is attributed to a similar process.

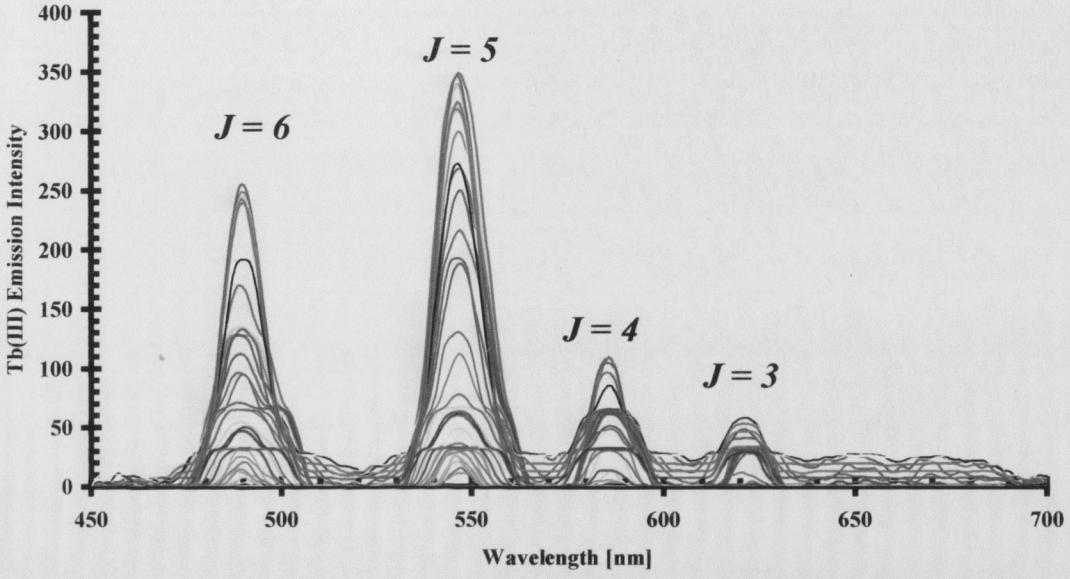


Figure 2.21. ***Lanthanide emission of*** **Tb.99** ***as a function of pH*** [10 μM aqueous solution, slit widths 9 nm, λ_{excit} – 300 nm](Results of titration using Perkin Elmer LS 50B)

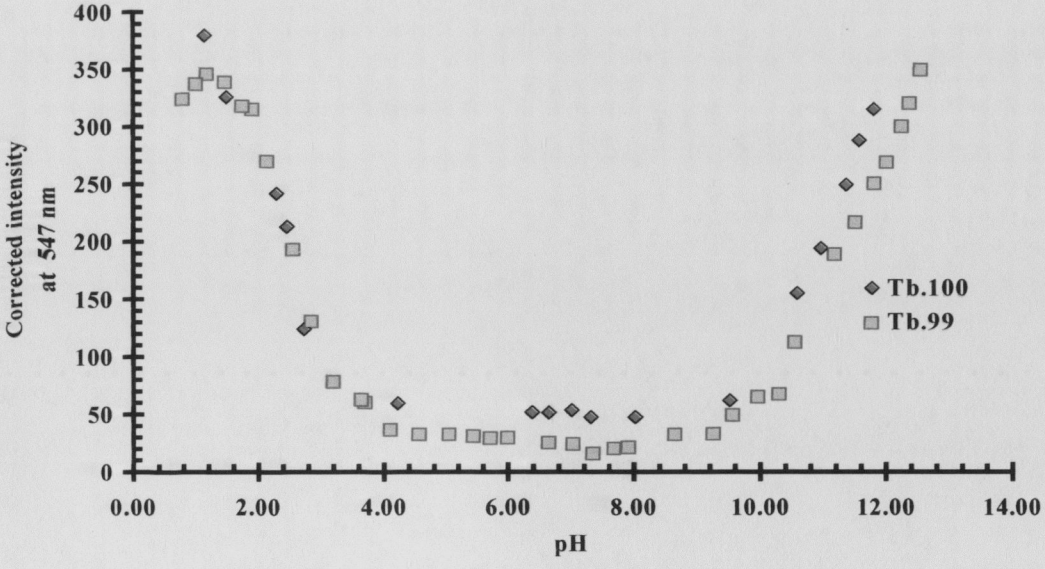
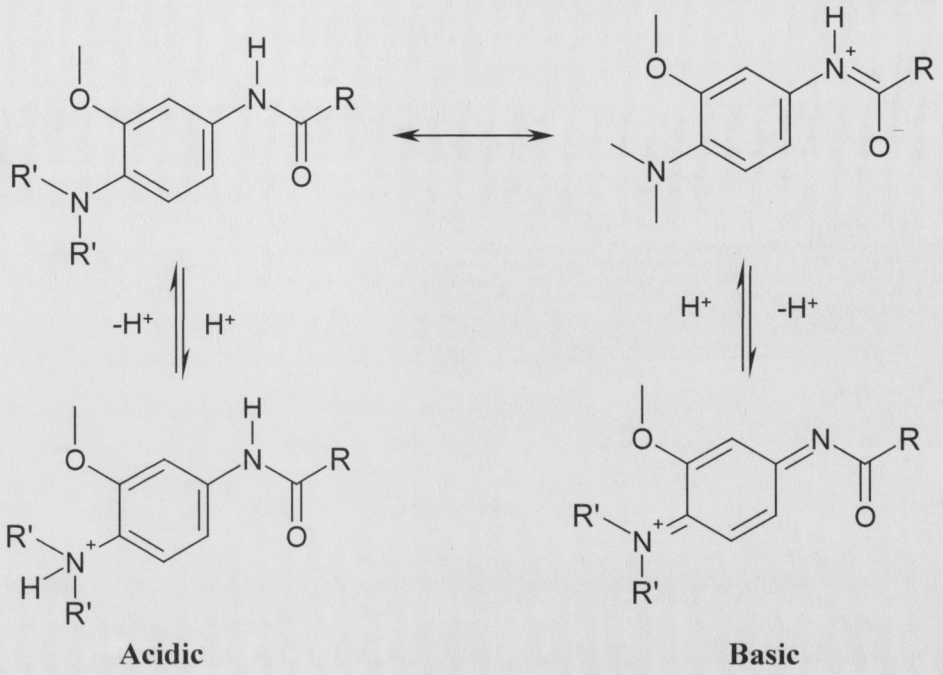


Figure 2.22. ***Lanthanide emission at 547 nm of*** **Tb.99** and **Tb.100** ***as a function of pH*** [10 μM aqueous solution, slit widths 9 nm, λ_{excit} – 300 nm](Results of titrations using Perkin Elmer LS 50B)

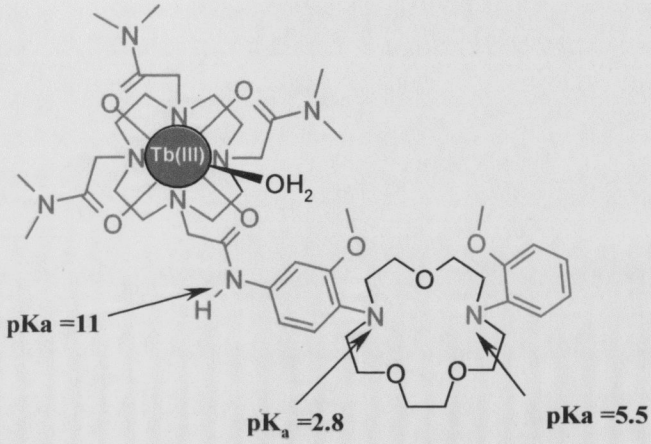


Scheme 12 ***Proposed protonated and deprotonated forms of the aryl amide moiety of*** **Tb.99** ***and*** **Tb.100** (R= lanthanide complex, R' = aza crown) [125]

The summary of the pK_a values determined for **Tb.99** from absorption, fluorescent and lanthanide luminescent measurements are shown in Table 2.6. In all three studies the pK_a value of *ca.* 11.0, was attributed to deprotonation of the aryl amide. However, two different pK_a values were determined for protonation of the aniline nitrogen's of the diaza crown, as expected. Assignment of the pK_a values are illustrated in Scheme 13, in which the value of pK_a = 5.5 was attributed to the aniline of the diaza crown furthest from the lanthanide complex. [Highlighted in **red**, Scheme 13] Upon protonation of this nitrogen efficient energy transfer to the metal center to cause sensitisation, as discussed in Section 1.5 would be prevented by the distance between the two moieties. Therefore determination of this pK_a cannot be achieved from lanthanide luminescent studies. pK_a = 2.8 was attributed to the aniline nitrogen of the aryl amide moiety. [highlighted in **green**, Scheme 13] This ligand is closer to the Tb(III) center and upon protonation an efficient energy transfer can occur to the Tb(III), resulting in a lanthanide emission. The lower pK_a of this nitrogen is attributed to enhancement of the lone pair conjugation by the electron withdrawing effect of the Tb(III) complex, which was also observed in **Tb.89**. [130]

Table 2.6 Summary of pKa values determined[162] for Tb.99

Complex	pK_a – (Abs.)	pK_a – (Fluor.)	pK_a – (Tb(III) Em.)
Tb.99	5.5 (± 0.2)	5.6 (± 0.2)	2.8 (± 0.2)
	11.0 (± 0.2)	10.8 (± 0.2)	11.2 (± 0.2)



Scheme 13 ***Assignment of pK_a values of*** **Tb.99**. (pK_a = 11- deprotonation of aryl amide, pK_a = 5.5 - protonation of aniline. [highlighted in **red**] This section of the ligand is too far from the Tb(III) center to allow for an efficient energy transfer when protonated, therefore determination of this pK_a cannot be achieved from lanthanide luminescent studies. pK_a = 2.8 - protonation of aniline nitrogen of the aryl amide [highlighted in **green**]. Protonation of this ligand, which is closer to the Tb(III) center, results in an efficient energy transfer and subsequent lanthanide luminescence. The lower pK_a is attributed to enhancement of the lone pair conjugation by the Tb(III) complex [130])

Similar pH experiments were performed on **Tb.101** and **Tb.102**. As discussed previously for **Tb.99** and **Tb.100**, at pH = 7, the Tb(III) emission intensity of both complexes was weak. However, in these complexes no luminescent enhancement was observed at high pH. This pH independence was observed from pH 4.0 – 13.5 for **Tb.101**. When the pH was decreased below pH 4.0, a significant enhancement in the luminescence intensity was observed. This steadily increased, reaching a maximum of *ca.* 920 for the J = 5 transition at pH 0.3, which was a 46-fold luminescent enhancement. These results are shown in Figure 2.23 and 2.24. The relationship between pH and the Tb(III) emission of **Tb.102** were somewhat comparable in that both showed a pH dependence below pH 4. (Figure 2.24) However, in the case of **Tb.102**,

the enhancement factor was lower, with only a 20-fold enhancement observed for the Tb(III) emission at pH 0.3. Also, between pH 4 and 7 a small but significant increase in the Tb(III) emission was observed. pK_a values of $pK_a = 2.0$ (± 0.2) and $pK_a = 1.8$ (± 0.2) were determined for **Tb.101** and **Tb.102** respectively. These values were attributed to the amine of the diaza crown closest to the lanthanide using the same explanation previously discussed for **Tb.99** and **Tb.100**. The lower pK_a values and absence of luminescent emissions corresponding to the amide deprotonation were attributed to the change in the coordinating groups of the Tb(III) complex.

pH experiments were also performed on **Eu.99** and **Eu.100**. However, in both of these complexes no Eu(III) emission was observed at any pH for either complex. These experiments were repeated at different excitation wavelengths, *e.g.*, 200 nm and 275 nm, however, no luminescence was observed. The Eu(III) emission was however observed when the complexes were excited directly at 395 nm, indicating that the Eu(III) complex was present. These observations were similar to those reported for Eu(III) complexes of **89**. [130] It is possible that the Eu(III) excited state is being quenched, as it has been shown that Eu(III) excited state can be quenched the by the presence of ligand to metal charge transfer levels[78] as well as reduction of Eu(III).[164]

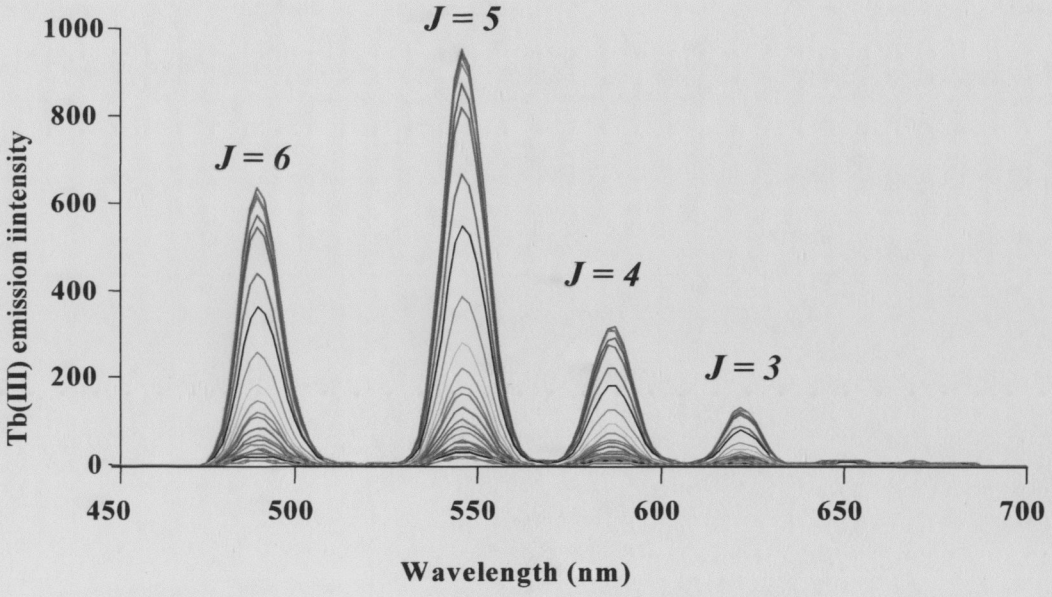


Figure 2.23. ***Lanthanide emission of*** **Tb.101** ***as a function of pH*** [4 μM aqueous solution, slit widths 10 nm, λ_{excit} – 300 nm](Results of titration using Varian Carey Eclipse)

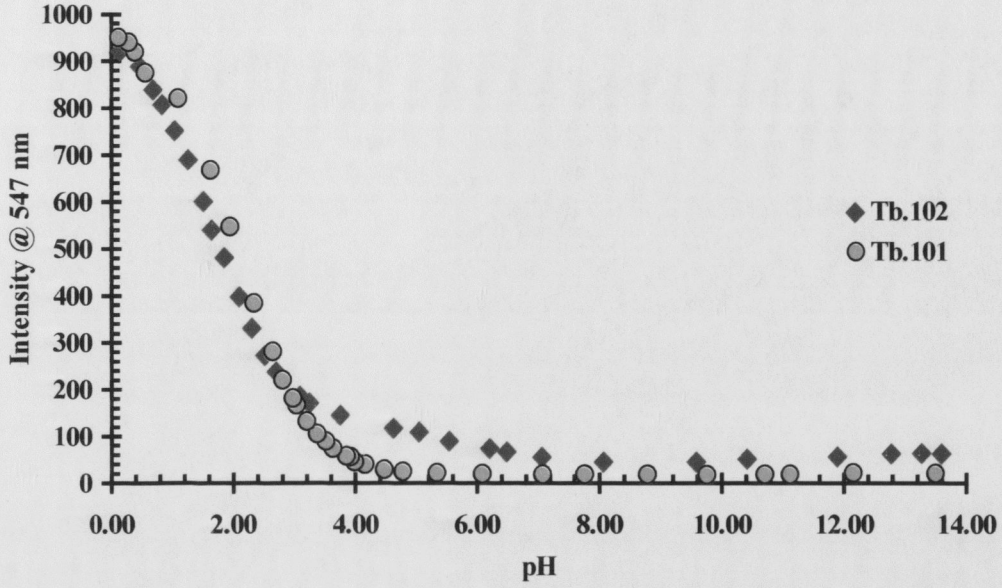


Figure 2.24. ***Lanthanide emission at 547 nm of*** **Tb.101** and **Tb.102** ***as a function of pH*** [10 μM aqueous solution, slit widths 10 nm, λ_{excit} – 300 nm](Results of titration using Varian Carey Eclipse)

2.7.3.2 Metal ion studies of Eu(III) and Tb(III) complexes

Metal ion titration experiments were performed on solutions of **Tb.99**, **Tb.100**, **Tb.101** and **Tb.102** with an excitation wavelength of 300 nm, using group I and II cations. No titrations were performed on **Eu.99** and **Eu.100** as preliminary experiments of these complexes in the presence of 5.0 M of NaOAc or 4.0 M of KOAc produced no Eu(III) emission. This was attributed to quenching of the Eu(III) excited state discussed previously. Figure 2.25 shows the result of a titration of **Tb.99** with solutions of NaCl. Prior to the addition of Na^+ a solution of **Tb.99** (buffered at pH 7.4) a weak Tb(III) emission was observed. In this case the four transitions, J = 6, J = 5, J = 4 and J = 3 were all observed. Of these the strongest emission was observed for the J = 5 transition at 547 nm with a maximum intensity of 31. Luminescent enhancement was not observed until the concentration of Na^+ in solution had reached 21 mM (pNa of 1.67). As the concentration of Na^+ was increased further, a 7-fold enhancement was observed at 1.23 M. (pNa of – 0.09) When this was repeated in an aqueous solution a comparable response was observed. The same dependence was also found when this experiment was repeated using NaOAc. Similar titration experiments were also performed on buffered solutions of **Tb.99** with KCl and LiCl as shown in Figure 2.26. In the case of K^+ a 3-

fold enhancement was observed at a K^+ concentration of 1.23 M (pK of – 0.09) , were as, a 4-fold enhancement was observed for Li^+ at the same concentration.

Structurally similar sensors such as **95** have been shown to respond to concentrations of Na^+ at intracellular levels (10-40 mM) [42] The shift in the operating range of **Tb.99** compared to **95** was attributed to enhanced conjugation of the aniline nitrogen lone pair of the aryl amide moiety caused by the close proximity of the Tb(III) complex.[130] This was shown earlier by the low pK_a value of pK_a = 2.8. Similar titration experiments were repeated on **Tb.101** (Figure 2.27), a charge neutral Tb(III) complex which incorporates the same 15-crown-5 diaza crown receptor as that found in **Tb.99** In this case the response to Na^+, K^+ and Li^+ mirrored those results presented for **Tb.99**. A summary of all the results for **Tb.99** and **Tb.100** are presented in Table 2.7.

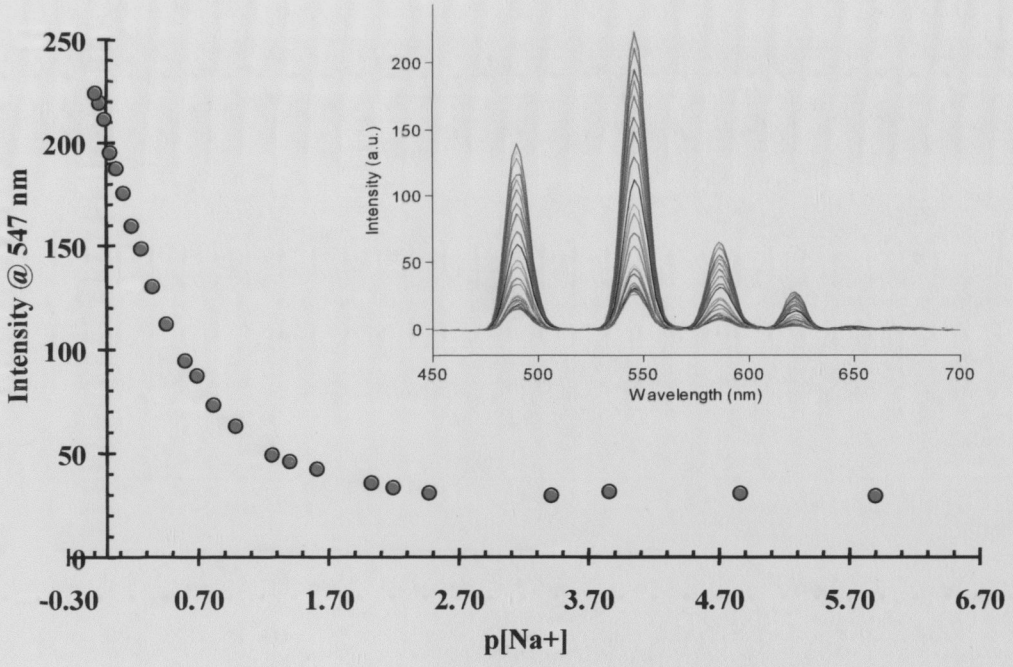


Figure 2.25. ***Lanthanide emission at 547 nm of* Tb.99 *as a function of pNa*** [8 μM solution, 0.1 M Tris Buffer, 0.1 M TMACl, pH 7.4, slit widths 10 nm, λ_{excit} – 300 nm](Inset: Tb(III) emission spectra)

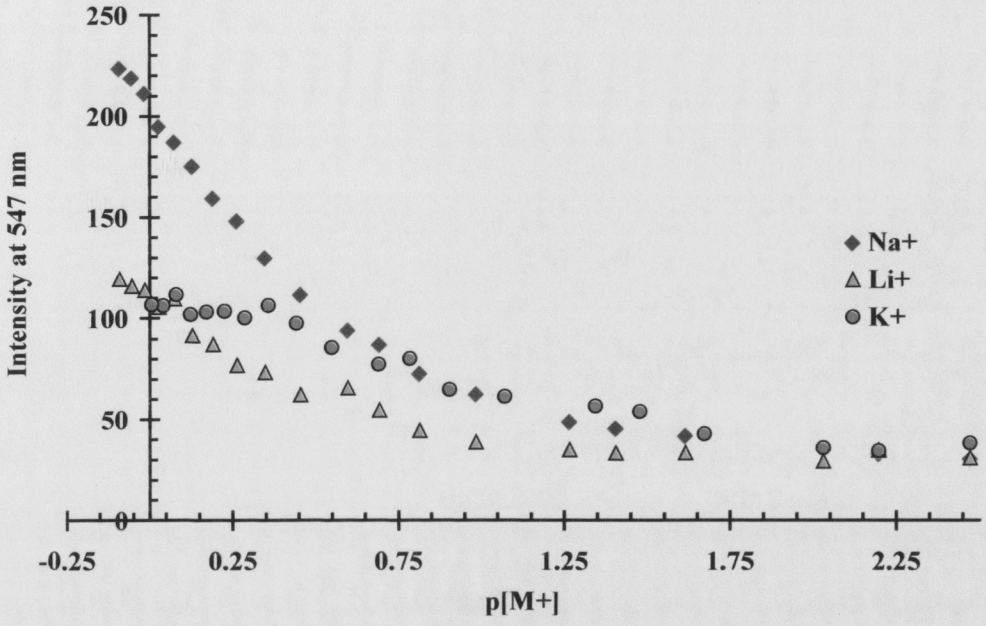


Figure 2.26. ***Comparison of Lanthanide emission at 547 nm of*** **Tb.99** ***as a function of pM*** *M= Na^+, K^+ or Li^+* [8 μM solution, 0.1 M Tris Buffer, 0.1 M TMACl, pH 7.4, slit widths 10 nm, λ_{excit} – 300 nm]

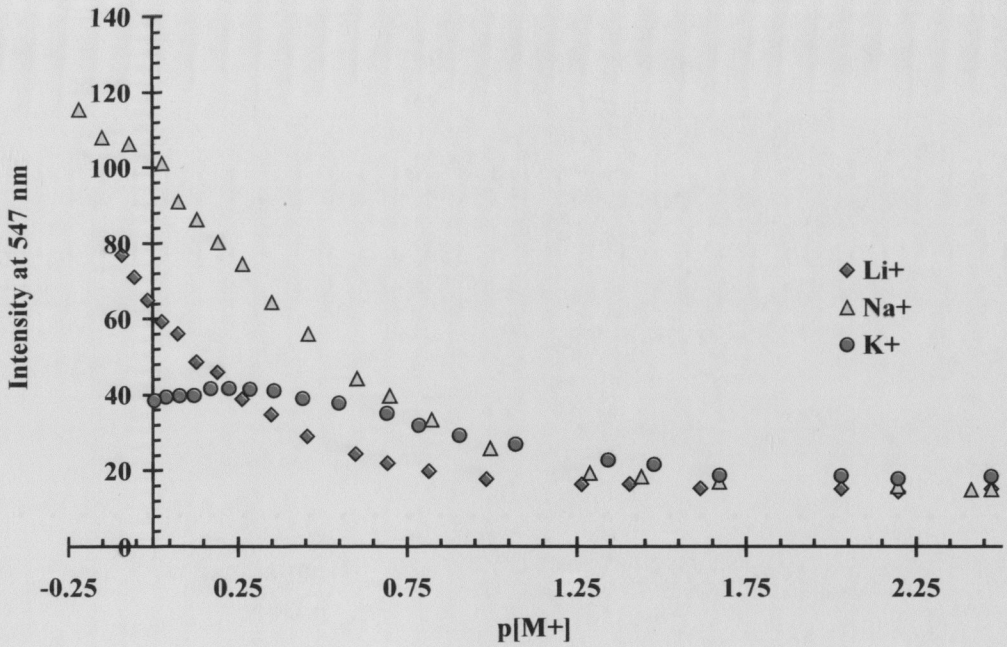


Figure 2.27. ***Comparison of Lanthanide emission at 547 nm of*** **Tb.101** ***as a function of pM,*** *M= Na^+, K^+ or Li^+* [8 μM solution, 0.1 M Tris Buffer, 0.1 M TMACl, pH 7.4, slit widths 10 nm, λ_{excit} – 300 nm]

Table 2.7 Maximum luminescent enhancement of Tb.99 and Tb.101 in the presence M^+†

Complex	Na^+	K^+	Li^+
Tb.99	7-fold	3-fold	4-fold
Tb.101	8-fold	3-fold	5-fold

† - M+ = Na^+, K^+, Li^+ at a concentration of 1.23 M. Maximum luminescence at 547 nm.

The metal ion titration experiments described previously were also performed on **Tb.100** and **Tb.102**. The results of a titration of **Tb.100** with KCl are shown in Figure 2.28. Prior to the addition of K^+ to a buffered solution of **Tb.100** a weak Tb(III) emission was observed. In this case the four transitions, J = 6, J = 5, J = 4 and J = 3 were seen. Of these, the strongest emission was observed in the J = 5 transition at 547 nm with a maximum intensity of 20. Addition of KCl in the concentration range of pK 2-6 (1μM to 10 mM) resulted in no enhancement in the Tb(III) emission. However, as the concentration of K^+ was increased beyond pK 2 (10 mM), an enhancement in the Tb(III) emission was observed, resulting in a maximum intensity of 620 at pK = 0.2 (630 mM). This represented a 31-fold enhancement in luminescence. A plot of the Tb(III) emission intensity at 547 nm as a function of pK resulted in a sigmoidal curve over two log units (pK 0.2 to 2.2), a typical indication of simple equilibrium and 1:1 binding.[163] A binding constant of log β = 0.75 was determined from these changes. The response of **Tb.100** to K^+ was found to be from 6 mM to 630 mM (pK 0.2 to 2.2), based on the titration with KCl shown above. This is well above the cellular concentration of K^+, which is typically 90-120 mM. [8] Again, this shift in the operating range of **Tb.99** compared to **96**, discussed previously, was attributed to enhanced conjugation of the aniline nitrogen lone pair of the aryl amide moiety caused by the close proximity of the Tb(III) complex.[130]

Titrations were repeated on **Tb.100** using a range of metal chloride salts such as Na^+, Li^+, Mg^{2+} and Ca^{2+}, to demonstrate the selectivity of **Tb.100** toward K^+ and the results of these are presented in Figure 2.29. No enhancement was observed in the Tb(III) emission when **Tb.100** was titrated with Li^+. This was expected as the receptor of **Tb.100** was designed for binding with K^+ and would be too big to efficiently bind Li^+. A 6-fold enhancement in the Tb(III) luminescence intensity was observed in titrations with Na^+. A plot of the Tb(III) emission

intensity at 547 nm as a function of pNa (Figure 2.29) resulted in a sigmoidal curve over two log units (pK 0.0 to 2.0), a typical indication of simple equilibrium and 1:1 binding.[163] A binding constant of log $\beta = < 0.5$ was determined indicating weaker binding than that found between **Tb.100** and K^+. Titrations of **Tb.100** with Ca^{2+} and Mg^{2+} showed 8-fold and 3-fold enhancements respectively.

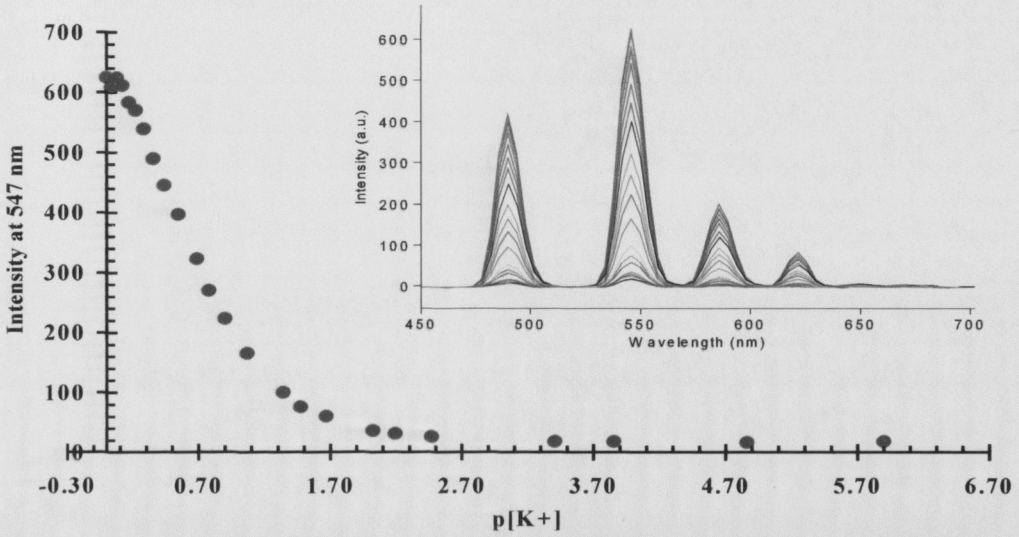


Figure 2.28. ***Lanthanide emission at 547 nm of*** **Tb.100** ***as a function of pK*** [4 μM solution, 0.1 M Tris Buffer, 0.1 M TMACl, pH 7.4, slit widths 10 nm, λ_{excit} – 300 nm](Inset: Tb(III) emission spectra)

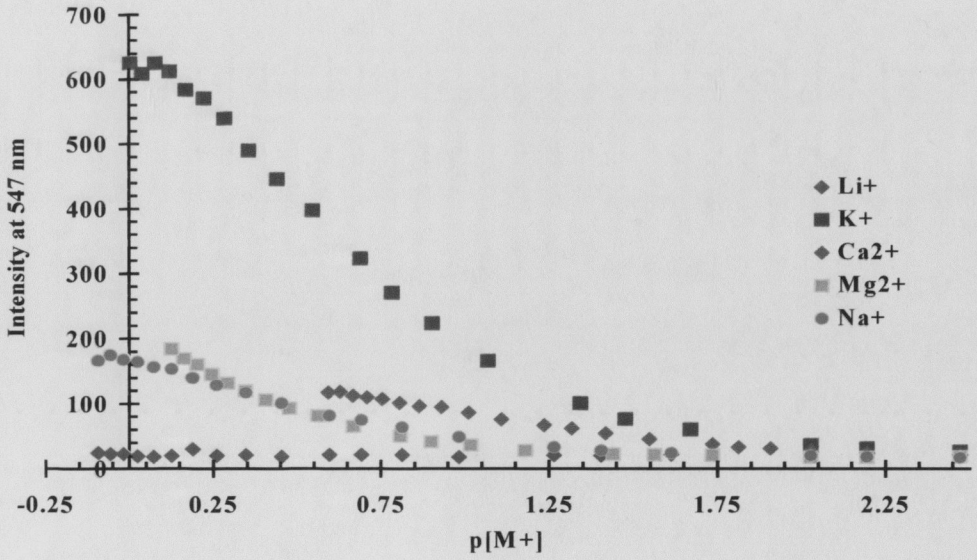


Figure 2.29. ***Comparison of Lanthanide emission at 547 nm of*** **Tb.100** ***as a function of pM*** *M= Na^+, K^+, Li^+, Ca^{2+} and Mg^{2+}*[4 μM solution, 0.1 M Tris Buffer, 0.1 M TMACl, pH 7.4, slit widths 10 nm, λ_{excit} – 300 nm]

Similar titrations experiments were performed on **Tb.102**. When a solution of **Tb.102** (buffered at pH 7.4) was titrated with KCl, a significant enhancement in the Tb(III) emission intensity occurred. At K^+ concentration levels greater than 6 mM (pK 2.2) a large increase in the emission occurred, which resulted in a 40-fold enhancement. (Figure 2.30) As observed for **Tb.100** the response was sigmoidal over two log units a typical indication of simple equilibrium and 1:1 binding.[163] A binding constant of log $\beta = 0.68$ was determined from these results. The response range for **Tb.102** was found to be the same as that of **Tb.100** occurring from 6 mM to 600 mM (pK 0.2 to 2.2). The selectivity of this sensor toward K^+ was demonstrated in titration experiments performed using Na^+, Li^+, Ca^{2+} and Mg^{2+} salts. The results are shown in Figure 2.31 and mirror the results presented earlier for **Tb.100**. A plot of the Tb(III) emission intensity at 547 nm as a function of pNa (Figure 2.31) resulted in a sigmoidal curve over two log units (pK 0.0 to 2.0), a typical indication of simple equilibrium and 1:1 binding. [163]A binding constant of log $\beta = < 0.5$ was determined for Na^+ indicating weaker binding than that found between **Tb.102** and K^+. Titrations of **Tb.102** with Ca^{2+} and Mg^{2+} both resulted in a 9-fold enhancement, whereas no change was observed for Li^+. A summary of the results for **Tb.100** and **Tb.102** are presented in Table 2.8.

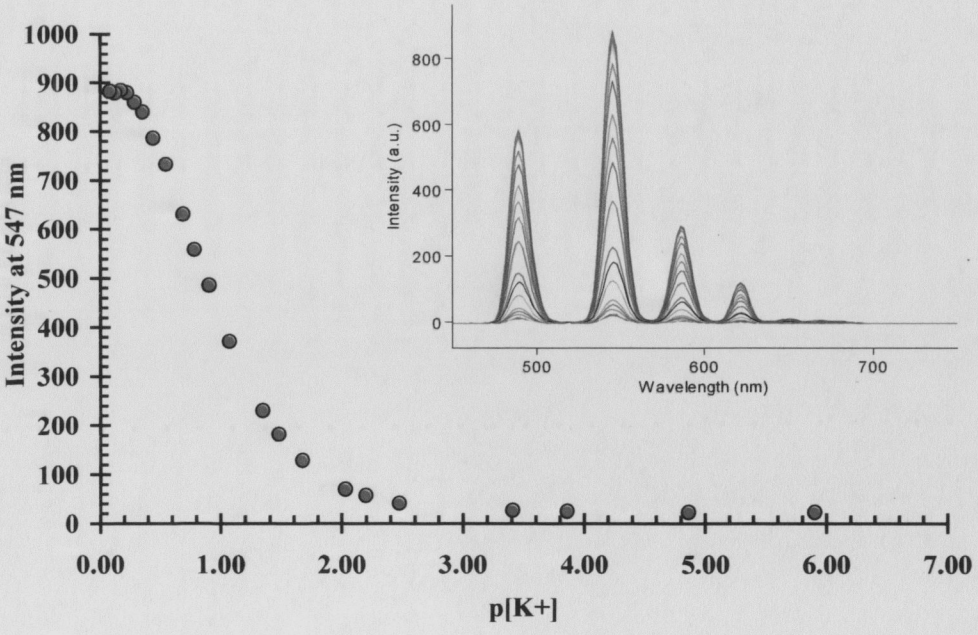


Figure 2.30. ***Lanthanide emission at 547 nm of*** **Tb.102** ***as a function of pK*** [8 μM solution, 0.1 M Tris Buffer, 0.1 M TMACl, pH 7.4, slit widths 10 nm, λ_{excit} – 300 nm](Inset: Tb(III) emission spectra)

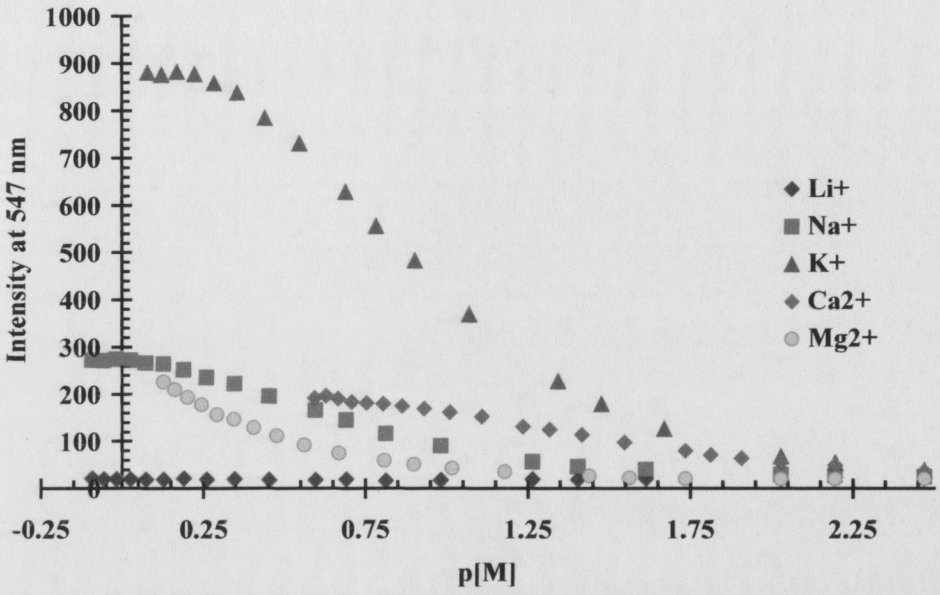


Figure 2.31. ***Comparison of Lanthanide emission at 547 nm of*** **Tb.102** ***as a function of pM*** *M= Na^+, K^+, Li^+, Ca^{2+} and Mg^{2+}* [8 μM solution, 0.1 M Tris Buffer, 0.1 M TMACl, pH 7.4, slit widths 10 nm, λ_{excit} – 300 nm]

Table 2.8 Maximum luminescent enhancement of Tb.100 and Tb.102 in the presence M^+†

Complex	Na^+	K^+	Li^+	Mg^{2+}	Ca^{2+}
Tb.100	6-fold log β = < 0.5	31-fold log β = 0.75	0	3-fold	8-fold
Tb.102	9-fold log β = < 0.5	40-fold log β = 0.68	0	9-fold	9-fold

† - $M^+ = Na^+, K^+, Li^+$. Maximum luminescence at 547 nm.

In summary, luminescence of the Tb(III) complexes was found to be independent of pH in the range pH 4-9, and shown to be dramatically enhanced at high and low pH. No luminescence was observed for the Eu(III) complexes, which was attributed to a quenching process. Luminescent enhancements were also found to occur in the presence of group I and II cations. In all cases the luminescence enhancement is believed to occur in a similar way to **Tb.89**, which involved deconjugation of the aniline nitrogen lone pair upon protonation or

cation binding, resulting in a suppression of PET, from or to the intermediate aryl singlet excited state of the aniline moiety. The lanthanide complexes **Tb.100** and **Tb.102**, designed for detecting K^+, demonstrated good selectivity over other physiologically important group I and II cations. However, the operating range for these complexes was higher than the target intracellular concentration range. This was attributed to enhanced conjugation of the aniline nitrogen lone pair of the aryl amide moiety caused by the close proximity of the Tb(III) complex to the receptor.

2.8 Conclusion

The purpose of this project was to develop lanthanide based chemosensors for the detection of intracellular concentrations of Na^+ or K^+. The synthesis and complete characterisation of lanthanide complexes **Tb.99**, **Eu.99**, **Tb.100**, **Eu.100**, **Tb.101** and **Tb.102** were successfully accomplished. These are the first examples to date of cation chemosensors that incorporate aromatic diaza crown receptors with cyclen based lanthanide complexes to form cation sensors. During the development of these chemosensors an efficient nitration method was developed for substituted aniline compounds. In addition two-monoaza crown receptors **145** and **146** were also synthesised and characterised that also have the potential to be incorporated into lanthanide complexes as potential chemosensors.

Photophysical analysis of **Tb.99**, **Eu.99**, **Tb.100**, **Eu.100**, **Tb.101** and **Tb.102** showed that all these complexes were stable in solution and in the case of the Tb(III) complexes, independent of pH with respect to their lanthanide luminescence over the pH range 4 to 9. The Tb(III) luminescence emission was found to be greatly enhanced in the presence of Na^+ or K^+. No lanthanide emission was produced in the Eu(III) complexes due to a non radiative quenching process. Evaluation of the Tb(III) complexes showed that although these complexes were photophysically responsive to Na^+ or K^+, the working range of these sensors was in the molar range and not the millimolar range as had been anticipated.

Chapter 3

Synthesis and photophysical studies of colorimetric sensors for the detection of sodium and potassium

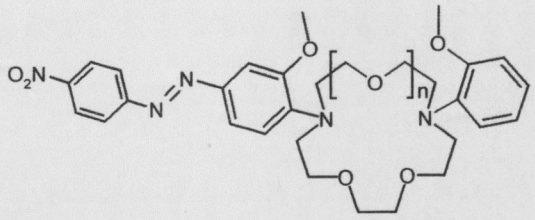
3.0 Synthesis and photophysical studies of colorimetric sensors for the detection of sodium and potassium

3.1 Introduction

As discussed in Chapter 2, Na^+ and K^+ are cations essential for maintaining life in animal cells through a number of cellular functions including nutrient uptake, regulation of intracellular ions and the transmission of electrical impulses. The concentration of Na^+ is found to exist at levels of 120-450 mM outside of cells compared to 10-40 mM within, whereas K^+ is found within cells at concentrations of 90-120 mM compared to 10 mM outside.[8, 27, 42, 138] The ability to determine these concentrations is a requirement in understanding cellular functions.[8] In recent times the focus within the field of chemosensing has resulted in the development of fluorescent and lanthanide luminescent-based sensors.[12] However, the field of colorimetric sensing still has advantages such as real time analysis on a molecular level.[165] Also colorimetric sensing is unaffected by phenomena such as autoflourescence and light scattering, both major drawbacks for fluorescent sensing as previously discussed in Chapter 1 and 2.[26, 27, 165] In recent years there have been many reports of both cation [26, 27, 166, 167, 168, 169] and anion [29, 170, 171, 172, 173] colorimetric sensors. In this chapter we will look at the synthesis and photophysical studies of colorimetric sensors **153** and **154** based on the two diaza crown receptors **111** and **112** respectively for sensing intracellular levels of Na^+ and K^+ respectively.

The judicious design of these receptors, **111** and **112** is of great importance if they are to be used for measuring cation concentrations at intracellular levels. The most important design feature is the methoxy group, as this significantly improves selectivity. For instance 15-crown-5 receptors have a high affinity for Na^+, having an ionic radius of 1.94 Å, which complements the cavity radius of 1.7 – 2.2 Å.[174] Even though K^+ has a much larger radius, at 2.66 Å it can also complex with this crown ether, but because of its size this involves 2:1 binding, therefore using a 15-crown-5 to measure intracellular levels of Na^+ would be adversely effected by the presence of K^+.[144, 174] However, this can be prevented by methoxy groups that are orientated above the cavity, thus sterically preventing the binding of K^+.[31, 144] The methoxy groups also function to aid binding. The crystal structures of **111** [144] and **112** (Chapter 2) show that the

oxygen's of the methoxy appendages coordinate to cations that are bound within the aza crown ring. This is often referred to as a 'lariat ether' effect.[20]



153: n = 1
154: n = 2

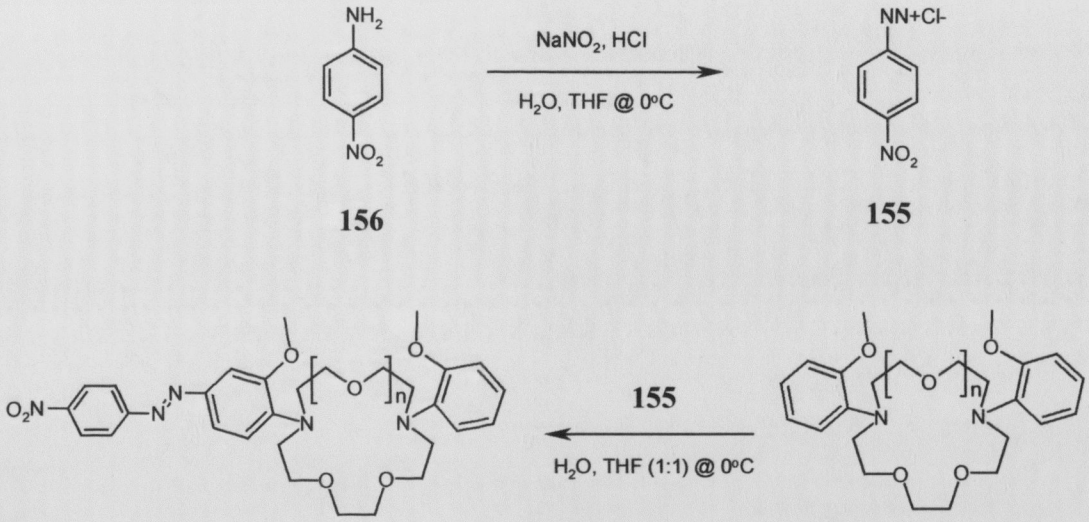
Both **153** and **154** are functionalised with azo dyes, which have been covalently attached to the receptor. Azo dyes are extremely common commercial colorants and are easy to synthesize, usually requiring no more than two synthetic steps.[175] As shown in Scheme 1, colorimetric sensors **153** and **154** are related to sensors such as **1**, previously discussed in Chapter 1, where both compounds have an internal charge transfer (ICT) excited state caused by conjugation between the electron donating aza crown nitrogen and the electron accepting NO_2 group. This system is in essence a donor/acceptor system; the aza nitrogen lone pair is donated to the electron poor azo ligand and this phenomenon leads to the colored compound. Upon cation binding by the receptor the lone pair of the nitrogen can no longer be conjugated within the aromatic system, this leads to suppression of the ICT state and a concomitant loss of color. [26, 27]

Using previous examples such as **1** as a guide, it is proposed that **153** and **154** are ideally suited for use as colorimetric sensors for Na^+ and K^+ respectively. The following sections describe the synthesis of **153** and **154** along with the various photophysical measurements used to evaluate them.

3.2 Synthesis of 153 and 154

The synthesis of receptors **111** and **112** was discussed in great detail in Chapter 2. Colorimetric sensors **153** and **154** were synthesized as shown is Scheme 1, using a synthesis that has been employed many times for monoaza crown receptors. [26, 27, 28] These sensors, **153** and **154** were made in a one-pot synthesis in which the diazonium salt, **155** was produced *in-*

situ by the addition of conc. HCl to a cold solution (0 °C) of **156** that was being stirred in a 1:1 mixture of H_2O: THF with $NaNO_2$ present. A yellow solution of **155** was formed which was then added to a stirred solution of **111** (or **112**) in a 1:1 mixture of H_2O:THF at 0 °C. A dark red solution formed and this was left stirring overnight at room temperature. The resulting solution was concentrated to dryness, dissolved in $CHCl_3$ and washed several times with water, dried over $MgSO_4$ and the solvent removed under vacuum to provide a red oil. This oil was purified on an alumina column using 70:30 Hex:EOAc as eluent, to give **153** (or **154**) as a deep red solid in yields of 50 % and 44 % respectively.



Scheme 1 - ***Synthesis of colorimetric sensors* 153 *and* 154 *based on Diaza crown receptors* 111 *and* 112** [26, 27, 28]

3.3 Characterisation of 153 and 154

153 and **154** were characterized by ^1H, ^{13}C NMR, IR, ESMS, accurate mass and elemental analysis. Both sensors are very similar in structure the only difference being an extra CH_2OCH_2 in **154**. Thus similar ^1H NMR spectra were recorded for each compound. As shown in Figure 3.1, the ^1H spectra of sensor **154** revealed two doublets at 8.43 ppm and 7.96 ppm. These were assigned to the protons of the nitro aromatic moiety that had been introduced to

112. The C_2 symmetry of the receptor, **112** was lost upon formation of **154** as seven proton signals were observed between 7.64 ppm and 6.86 ppm. These were assigned to the seven protons of the receptor aromatic moieties. Attempts to grow crystals suitable for X-ray crystallographic analysis of **153** and **154** to determine unambiguously the position of the azo dye on the sensors failed. However, NOE experiments and spectral comparison to the monoaza crown, **1**, [26, 27] suggest the azo moiety is attached *para* to the aniline nitrogen.

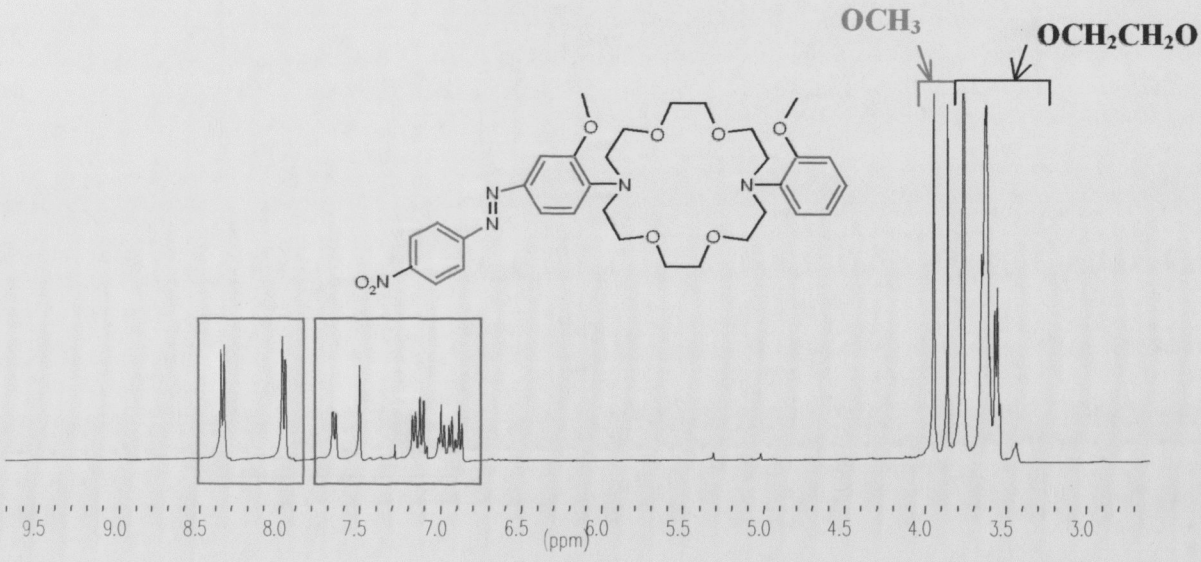


Figure 3.1 - *^{1}H NMR of* 154 - *8.34 d, 7.96 d, represent nitro aromatic protons (green box) 7.64 (d,d), 7.49 (s), 7.15 (d), 7.10 (d), 7.0 (t), 6.91 (t), 6.86 (d) represent all other aromatic protons (blue box), 3.93 (s), 3.84 (s) represent methoxy groups and 3.75 (s), 3.63-3.58 (m), 3.55 -3.52 (m) represent diaza crown ring protons.*

3.4 ^{1}H NMR complexation studies

The effect of alkali metals on sensors **153** and **154** was evaluated using ^{1}H NMR spectroscopy. In both cases 1.7 mg of the sensor was dissolved in 800 μL of $CDCl_3$ (3.4-3.6 mM). ^{1}H NMR spectra were then run in the absence of any cation and then in the presence of $NaPF_6$ for **153**, or KPF_6 for **154** in CD_3OD. These salt solutions were added in 10-20 μL aliquots (up to a maximum of 16 equivalent). Figure 3.2 shows the results of the study on **153** when titrated with Na^+. These results showed that upon addition of Na^+ to **153** the most marked changes occurred in the azacrown ring and the aromatic methoxy groups. There were

some shifts in the aromatic region, but these were not significant. As seen in Figure 3.2, the methoxy singlets experienced a considerable upfield shift with respect to every additional aliquot of Na^+. Initially the chemical shifts of the methoxy singlets were 3.91 ppm and 3.83 ppm respectively. However, after the addition of 16 equivalents of Na^+ these singlets had shifted to 3.84 ppm and 3.75 ppm respectively. Changes in the signals for the ring protons also showed considerable shifts upon addition of Na^+. Initially the proton signals appeared between 3.80 ppm and 3.40 ppm. By the addition of 16 equivalents of Na^+ these signals had shifted to 3.63-3.20 ppm. The well-defined splitting patterns observed for the free sensor were lost during this titration and only broadened signals were observed at the end. The marked chemical shifts seen during this titration study indicate the ability of the crown ether incorporated into **153** to coordinate to Na^+ successfully. These findings complement the studies already performed on **111** and **112** discussed in Chapter 2. The experiment was repeated on **154** using KPF_6 and similar results were observed.

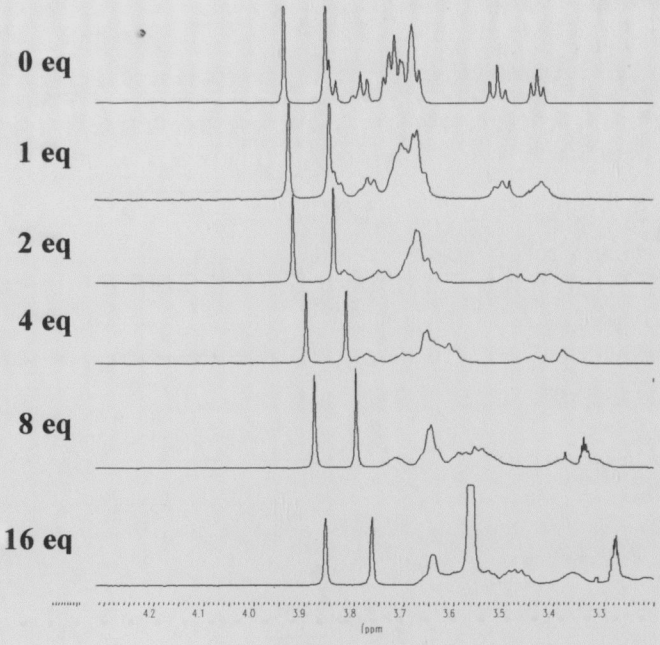


Figure 3.2. ***^1H NMR study of* 153 *($CDCl_3$), before and after the addition of $NaPF_6$ in CD_3OD***

3.5 Photophysical investigations of 111 and 112

The following sections present the findings of photophysical studies of **111** [144] and the photophysical studies performed on **112**, **153** and **154**. These studies involved analysing the

effect of pH and pM (pM = -Log M, where M = cation) on the photophysical properties of these molecules. This analysis was carried out in two stages beginning with photophysical evaluation of the receptors **111** [144] and **112** followed by the photophysical evaluation of **153** and **154**. All analysis was carried out using a Shimadzu UV-2401 PC UV-Visible spectrophotometer. Solutions were made up to an optical density of 0.2-0.25 (10 μM) in 50:50 MeOH:H_2O solutions. In experiments to investigate the detection of Na^+ and K^+ titrations were carried out in buffered solutions using 0.1M Tris buffer at pH 7.4 with 0.1M TMACl to maintain constant ionic strength.

3.5.1 pH studies of 111 and 112

The receptors **111** and **112** were designed with the intention of being able to specifically detect Na^+ and K^+ at intracellular levels respectively. In order to operate within such conditions these receptors need to be pH independent at physiological pH. Consequently, photophysical analysis began with evaluating the effect of pH. The photophysics of **111** has been reported previously; [144] the results of this study showed that this receptor was able to operate independently of pH between pH 6 and pH 9. Only one pK_a value was determined for this molecule even though there are two possible protonation sites and an averaged pK_a of 4.7 in 50:50 H_20:MeOH was determined. [144]

A similar study was performed on receptor **112**. The absorption spectrum of this receptor shown in Figure 3.3 revealed an absorption band at *ca.* 240 nm and two minor bands at 273 nm and 282 nm at pH = 12 in 50:50, MeOH:H_2O (using TMAOH). Upon titration of **112** using dilute HCl significant changes were observed in the absorbance spectra. From pH = 12–7, no major changes were observed for the 273 nm and 282 nm bands, however, a significant hypochromic effect was observed for the 240 nm band involving a 12 % reduction in absorbance as the pH was decreased. As the pH was decreased further a hypsochromic effect was observed in the 273 nm and 282 nm bands, resulting in shifts to 268 nm and 278 nm respectively. A more noticeable change was observed in the 240 nm band in which a dramatic hypochromic effect occurred. At pH = 5 the absorbance at 240 nm had decreased to *abs.* = 0.2, and at pH = 1 this had decreased further to *abs.* = 0.11. This titration was repeated a number of times and the process was found to be reversible. A graph of one such titration showing the

change in absorbance at 240 nm *vs.* pH is shown in Figure 3.4. These changes indicated the presence of two pK_a's and from the graph these were determined to be *ca.* 7.0 and *ca.* 4.9 respectively. For both **111** and **112**, the pK_a values showed that protonation of the receptors occurs at or below pH 7.0, which indicating that both the receptors can act independently of pH in the physiological range.

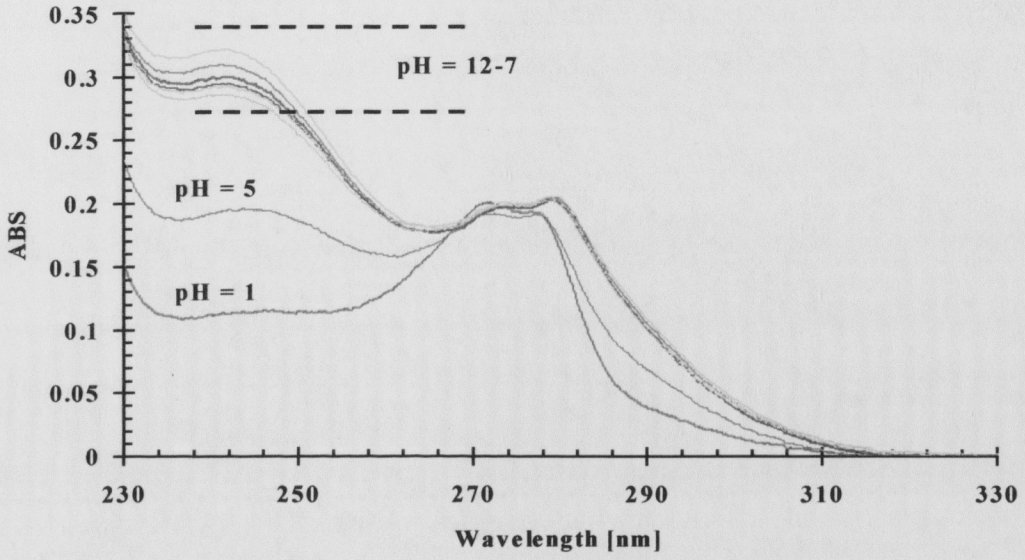


Figure 3.3 ***Absorption of* 112 *as a function of pH (Absorption at 240 nm, 50:50 MeOH:H_2O)***

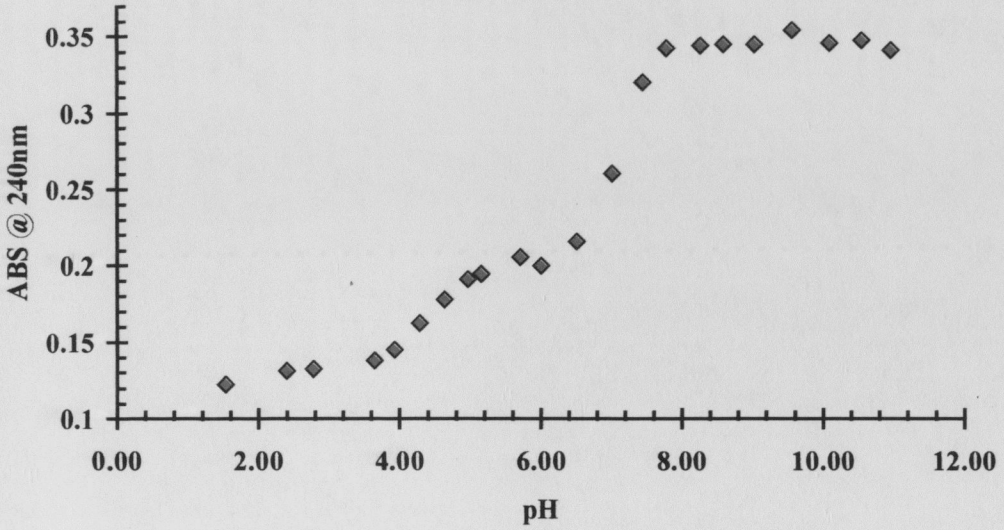


Figure 3.4 ***Absorbance vs. pH of* 112 *(Absorption at 240 nm, 50:50 MeOH:H_2O)***

3.5.2 Selectivity studies of 111 and 112 with Group I and II cations

Results of titrations carried out on **111** in 50:50 MeOH:H_2O buffered solution at pH 7.4 showed that this receptor could selectively bind Na^+ with a reported [144] binding constant log β of 3.1. The response to Na^+ occurred within a pNa range of 2-4, which was an indication of 1:1 binding and a simple equilibrium. [144] As expected this receptor also showed an ability to bind strongly with Li^+ in the same concentration range and a binding constant, log β = 2.5 was determined. This was attributed to the small size of Li^+. Such a result bears no significance in general physiological determination of cations, as Li^+ is rarely found unless deliberately administered.[13] A response to K^+ was also observed but to a lesser degree with a determined log β value of log β = 2.3. [31,144] These results indicate the strong binding of **111** to Na^+ over other cations.

Similar studies were carried out on **112** and in this case, the response of **112** to the presence of K^+ (as acetate salt) caused considerable changes in the absorption spectrum. Figure 3.5 shows these changes, in which a hypochromic effect in the absorption band at 250 nm was observed. Furthermore the absorption at 250 nm showed a bathochromic shift upon addition of K^+, eventually resulting in the loss of this band. Variation in the minor bands at 273 nm and 277 nm was not as significant. This observation is similar to that reported for **111** and was described as an indication of substantial twisting in the nitrogen-anisole bond in the bound receptor resulting from the existence of a strong conjugation between the diaza crown and the anisole π-system in the free receptor. [144] A plot of the change in absorbance at 250 nm *vs.* pK, Figure 3.6, showed a sigmoidal curve indicating a sensitivity to K^+ over two log units from pK 2-4 mirroring the results seen for **111** with Na^+. From this a binding constant value of log β = 3.9 was determined.

This titration was repeated with **112** in the presence of sodium acetate under the same experimental conditions and a similar response was observed, (Figure 3.7). The absorption spectra showed the same dramatic hypochromic effect in the band at 250 nm, indicating that Na^+ could bind to the receptor. A plot of absorption *vs.* pNa showed that the sensitivity of this interaction/ recognition was similar and in the same range as that seen for K^+. (See Figure 3.8)

Binding constants were calculated for **112** with K^+ and Na^+ at log β = 3.9 and log β = 4.0 respectively.

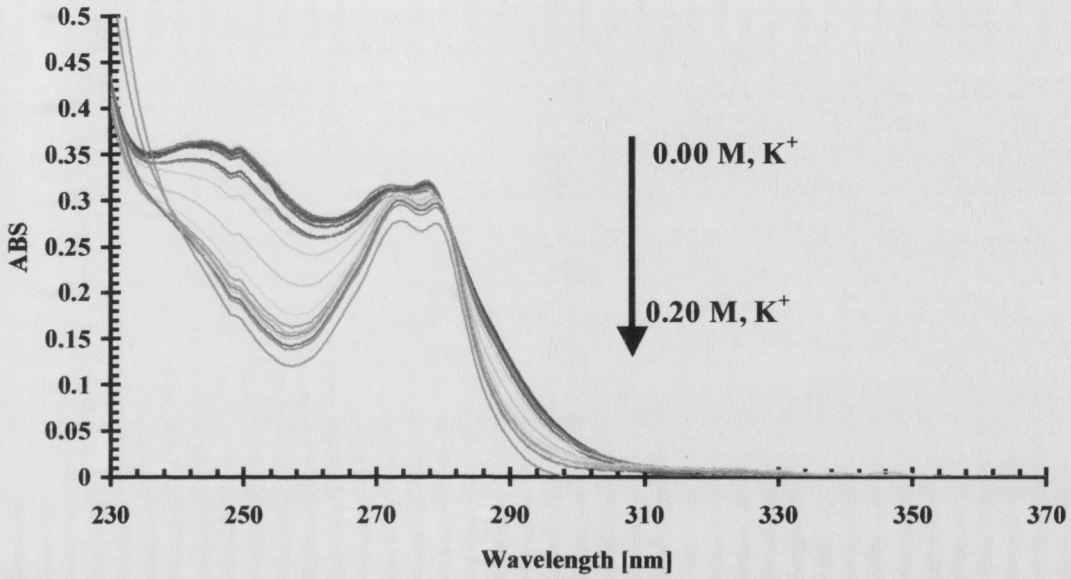


Figure 3.5 ***Absorption of* 112 *as a function of added potassium acetate, pK = 0.7-5.9 (50:50 MeOH:H_2O, 0.1M Tris buffer, 0.1M TMACl, pH 7.4)***

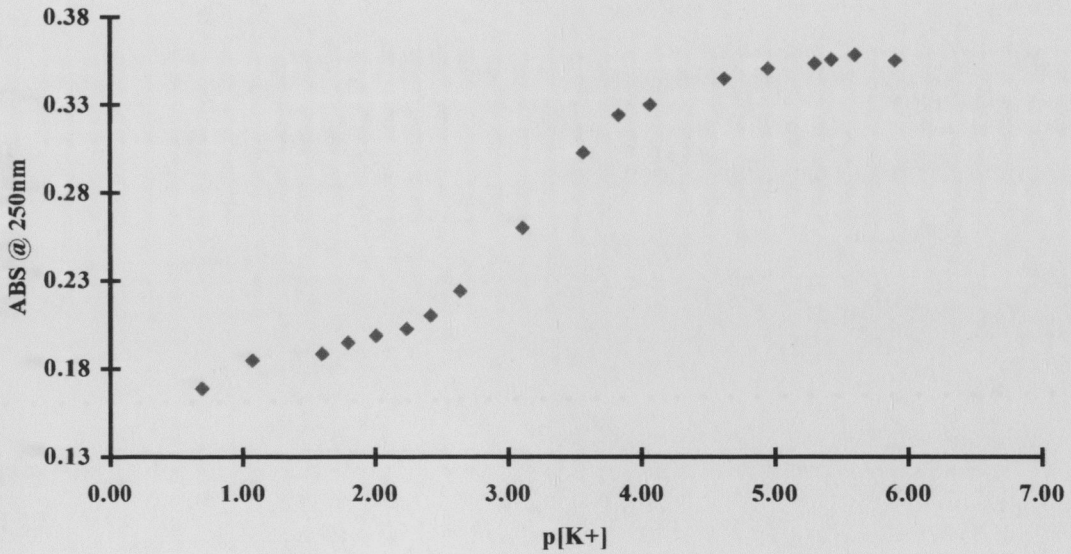


Figure 3.6 ***Absorbance vs. pK of* 112 *(50:50 MeOH:H_2O, 0.1M Tris buffer, 0.1M TMACl, pH 7.4)***

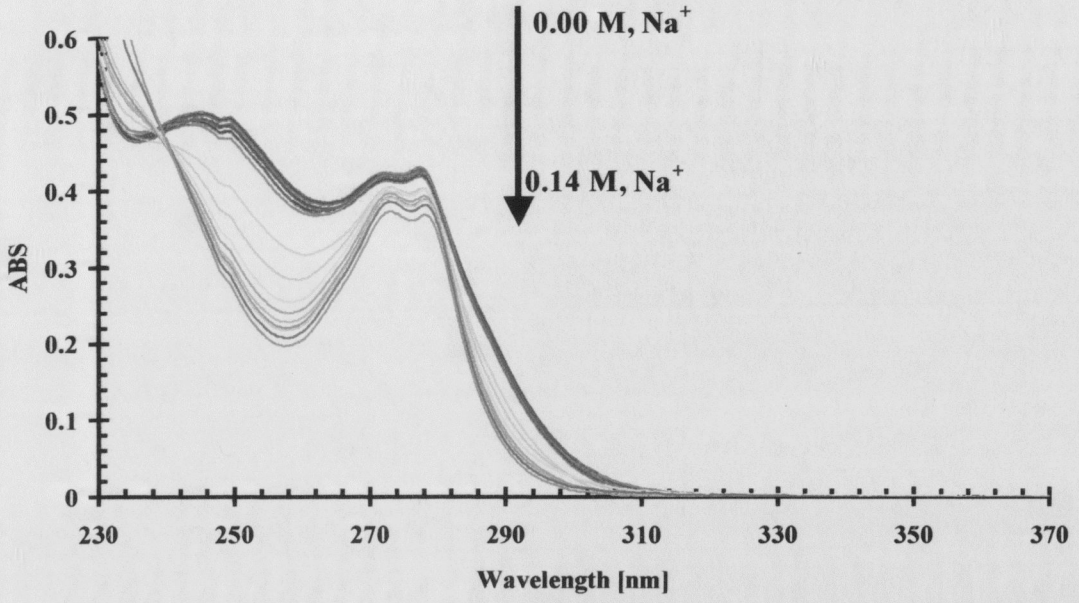


Figure 3.7 ***Absorption vs. pNa of* 112, *pNa = 0.85-5.9 (50:50 MeOH:H_2O, 0.1M Tris buffer, 0.1M TMACl, pH 7.4)***

The selectivity of **112** towards K^+ was further tested by analyzing the change in absorption of **112** with respect to the addition of acetate salts of Li^+, Ca^{2+} and Mg^{2+} using the same conditions as those reported above. For all three titrations no major changes were observed, except at very high concentrations of salt *ca.* 0.1–0.1 M. The significant hypochromic effect observed for titrations with K^+ and Na^+ were not observed and in all cases plots of absorbance at 250 nm *vs.* pM produced a roughly horizontal response. In the case of Li^+, Ca^{2+} and Mg^{2+} the responses were too small for accurate binding determination. All these results were summarised in Table 3.1 and Figure 3.8.

In summary **111** and **112** were shown to be capable of sensing cations in simulated physiological conditions. In the case of **111**, the selectivity to Na^+ was shown to exist while **112** was shown to have a similar response to both K^+ and Na^+. A similar result has been observed for **PBFI**, a fluorescent K^+ sensor [41] discussed in Chapter 2, which incorporates a structurally similar receptor.

Table 3.1 Summary of physical properties of 111 and 112

Receptor	111 *	112
λ_{max} (nm),[ε ($cm^{-1}M^{-1}$)]	253 [3.42]*, 277 [1.79]*	250 [3.4], 273 [1.80]
pK_a	~ 4.7 *	7.0 (±0.1), 4.9(±0.1)
pNa	3.1 (±0.1)*	4.0 (±0.1)
pK	<2.3 [a]*	3.9 (±0.1)
pLi	2.5 (±0.1)*	<1 [a]
pMg	<1 [a]*	<1 [a]
pCa	<1 [a]*	<1 [a]
a- Unable to determine these accurately, *-[144]		

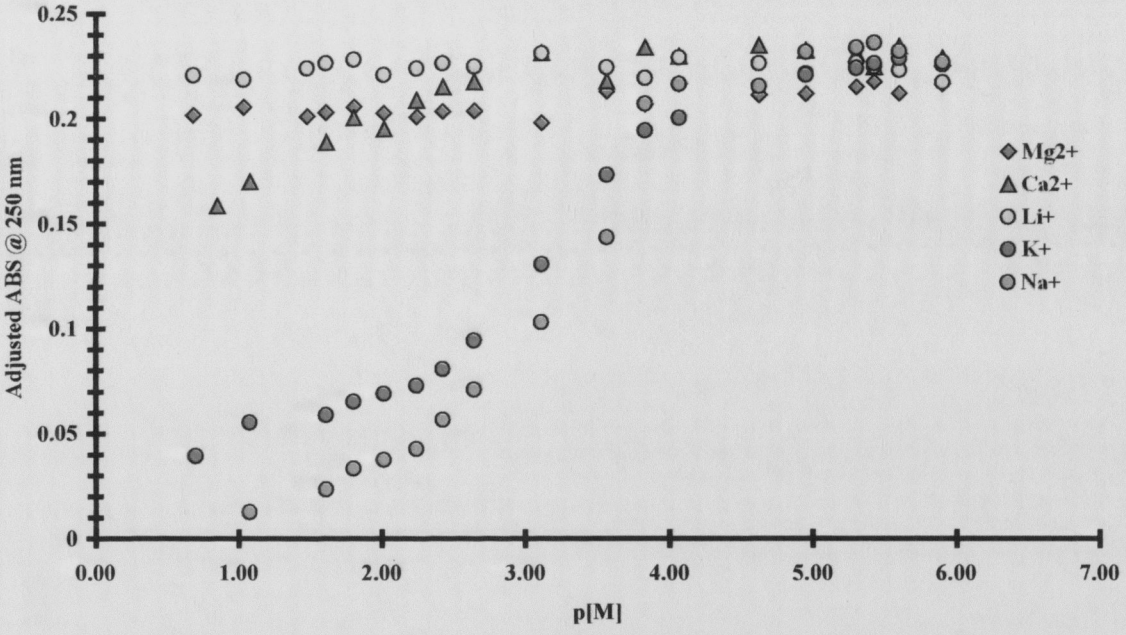


Figure 3.8 ***Absorbance vs. pM of* 112** ***(50:50 MeOH:H_2O, 0.1M Tris buffer, 0.1M TMACl, pH 7.4)***

3.6 Photophysical analysis of 153

Photophysical analysis of **153**, a colorimetric sensor designed for selective sensing of Na^+, was performed in a similar manner as described above for **111** and **112**. Analysis began with evaluation of the pH dependence of **153**. This was followed by evaluation of its response to Na^+ and its selectivity towards Na^+ over other biologically active [8] group I and II cations. All analysis was performed in 50:50 MeOH:H_2O.

3.6.1 Determination of the pH dependence of 153

The absorption spectrum of **153** in 50:50 MeOH:H_2O showed considerable differences to that of **111**. [144] In this case the spectrum consisted of a minor absorption band at 287 nm and a major absorption band at *ca.* 488 nm. The major band at 488 nm was used to determine the extinction coefficient, log ε = 4.36. [144] Upon titration of **153** with dilute HCl (following basification with TMAOH to pH 12), a hypochromic effect was observed for the absorption band at 488 nm as the pH was decreased, a with concomitant hypsochromic shift being observed until pH = 5, when a small bathochromic shift became apparent. Concurrently, the band at 287 nm was seen to decrease slightly. However, as the pH became lower the formation of a new absorption maximum at 321 nm was observed. The initial decrease in absorbance of both bands 488 nm and 287 nm was attributed to the protonation of the methoxy aniline nitrogen. The more significant changes that resulted in the formation of the new absorption maximum at 321 nm were attributed to protonation of the diaza aniline nitrogen, resulting in the suppression of the ICT state. [27] The presence of an isosbestic point at 379 nm was also clearly apparent. The results of this pH titration are summarized in Figure 3.9.

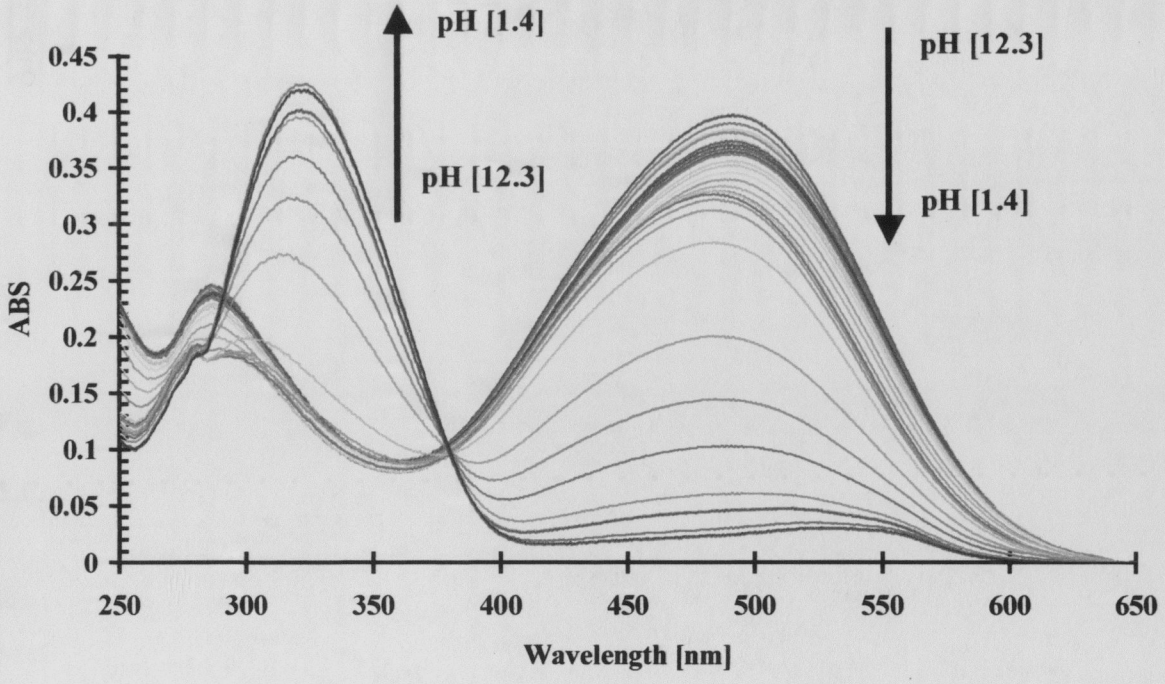


Figure 3.9 *Absorption of* **153** *as a function of pH, pH range = 1.41-12.32 (50:50 MeOH:H_2O)*

A plot of absorbance at 488 nm as a function of pH provided a sigmoidal curve. (Figure 3.10) Two pK_a values were expected, as two nitrogen atoms exist in the diaza crown ring, however, only one pK_a value could be confidently obtained. The changes in absorbance from pH 2-5 were considerable and hence the pK_a = 3.0 value was a reliable estimate. This pK_a value was attributed to the diaza crown nitrogen involved in the ICT process. This assignment was based on the observation that over the pH range from which this pK_a was determined the solution lost its red color, *i.e.*, suppression of the ICT state. Furthermore, the pK_a was expected to be low for this nitrogen; a consequence of the electron withdrawing effect of the azo dye nitro group. The overall result of this study indicates that the colorimetric sensor **153** would be able to operate independently above pH 4.

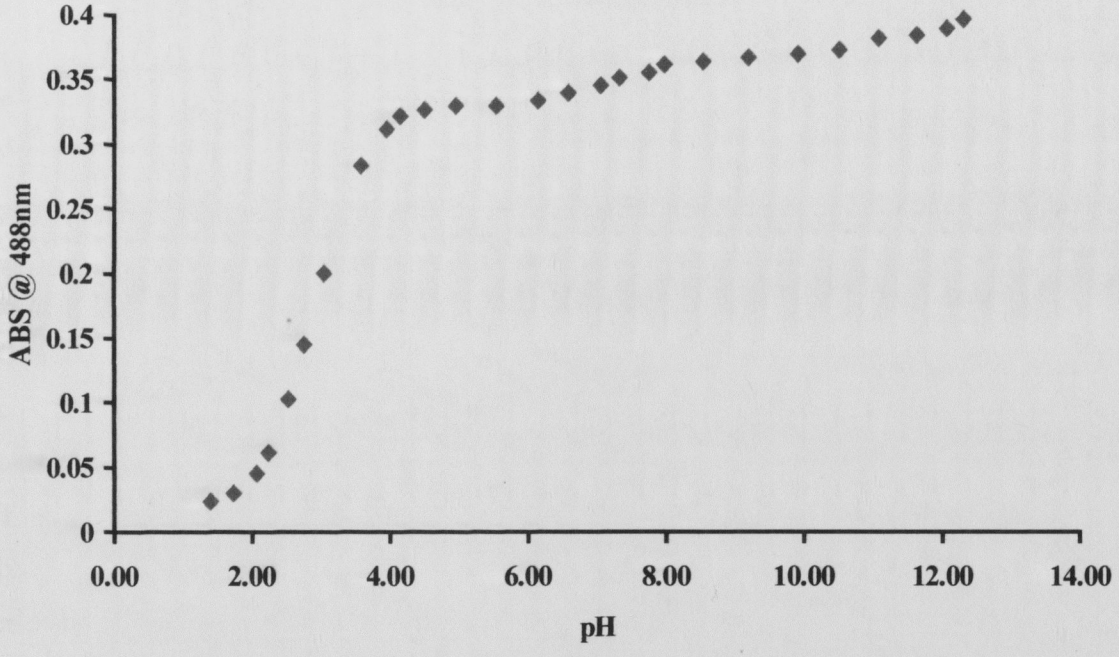


Figure 3.10 ***Absorbance vs. pH of* 153 *(50:50 MeOH:H_2O)pK_a determination studies***

3.6.2 Selectivity studies of 153 with Group I and II cations

Photophysical studies of **153** with group I and II cations began with a preliminary test of the response of **153** with the absence and presence of a large excess of sodium acetate in 50:50 MeOH:H_2O solution. The results of this test are illustrated in Figure 3.11. In this case the red colour of **153** in solution was replaced by a yellow colour upon addition of a large excess of sodium acetate, which indicated that **153** was an active colorimetric sensor for Na^+. This

preliminary test was followed by titration of **153** with Na^+, K^+, Li^+, Ca^{2+} and Mg^{2+}, with the aim determining the selectivity and sensitivity of **153** towards Na^+ over these other biologically active cations.

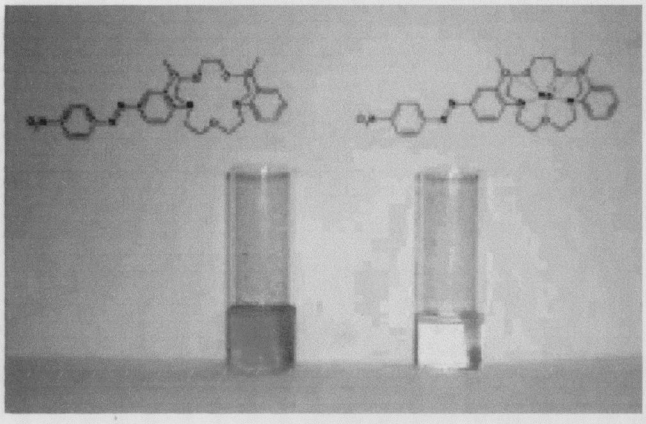


Figure 3.11 ***Illustration of* 153 *as an active colorimetric sensor for Na^+. Left hand side shows vial containing* 153. *Right hand side shows vial containing* 153 *and an excess of Na^+.***

Upon addition of Na^+ (as its acetate salt) to a buffered solution of **153** significant changes were seen in the absorption spectra similar to those observed in the pH titration. (Figure 3.12) Once again a dramatic hypochromic effect was observed for the 488 nm band with a concomitant hypsochromic shift. Concurrently a less significant hypochromic effect was observed for the 280 nm band and a new band with a maximum at *ca.* 372 nm was formed. Two isosbestic points were observed at *ca.* 402 nm and *ca.* 315 nm. The loss of the 488 nm band and formation of the 372 nm band indicated a strong interaction between **153** and Na^+ resulting in the loss of the ICT state. A plot of absorbance at 488 nm as a function of pNa showed a gradual decrease in the intensity of this band from pNa 3.5-6. From pNa 1.1 to 3.5 a dramatic drop in intensity was also observed this gave rise to the sigmoidal curve shown in Figure 3.13. From this curve a binding constant value, log $\beta = 2.8$ was estimated. From this curve it was also determined that **153** was able to detect Na^+ over the range *ca.* 0.32 mM–79 mM. This analysis was repeated with NaCl and a similar spectrum and sigmoidal response was observed. This suggests that there was no anion effect for this sensor. These results, along with the pH studies, demonstrated that **153** could successfully sense Na^+ at intracellular levels under simulated physiological conditions.

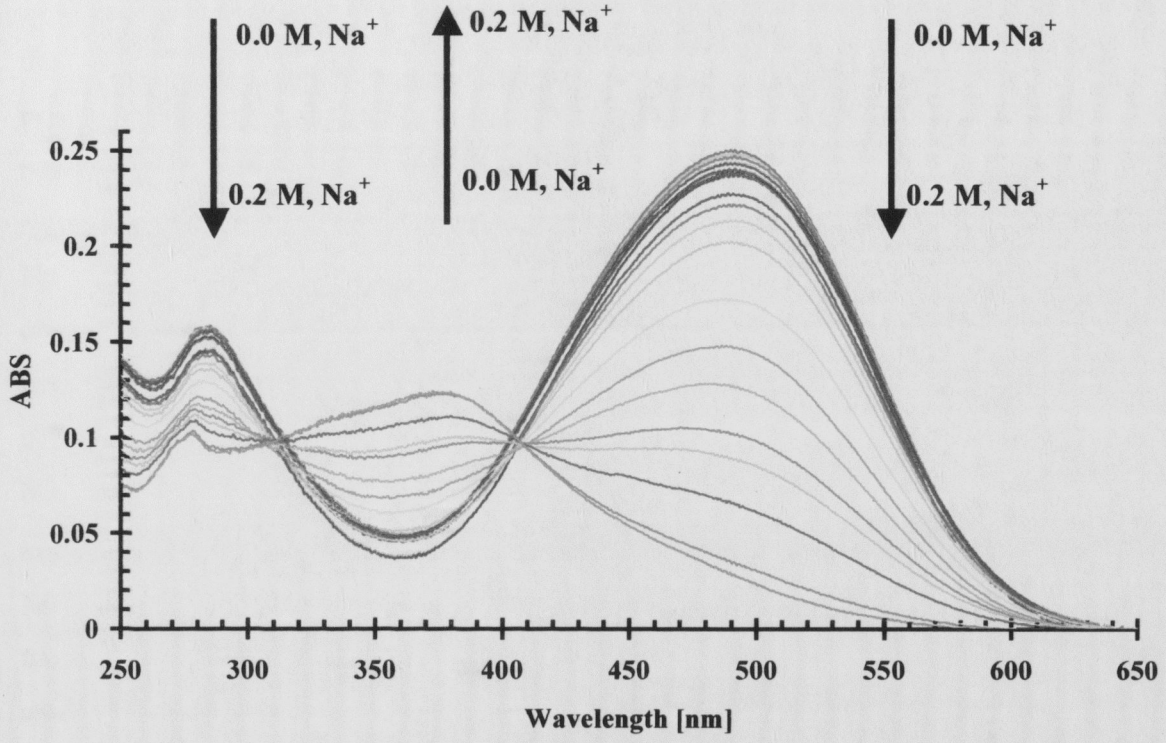


Figure 3.12 *Absorption of* **153** *as a function of added sodium acetate, pNa = 0.7-5.9 (50:50 MeOH:H_2O, 0.1M Tris buffer, 0.1M TMACl, pH 7.4)*

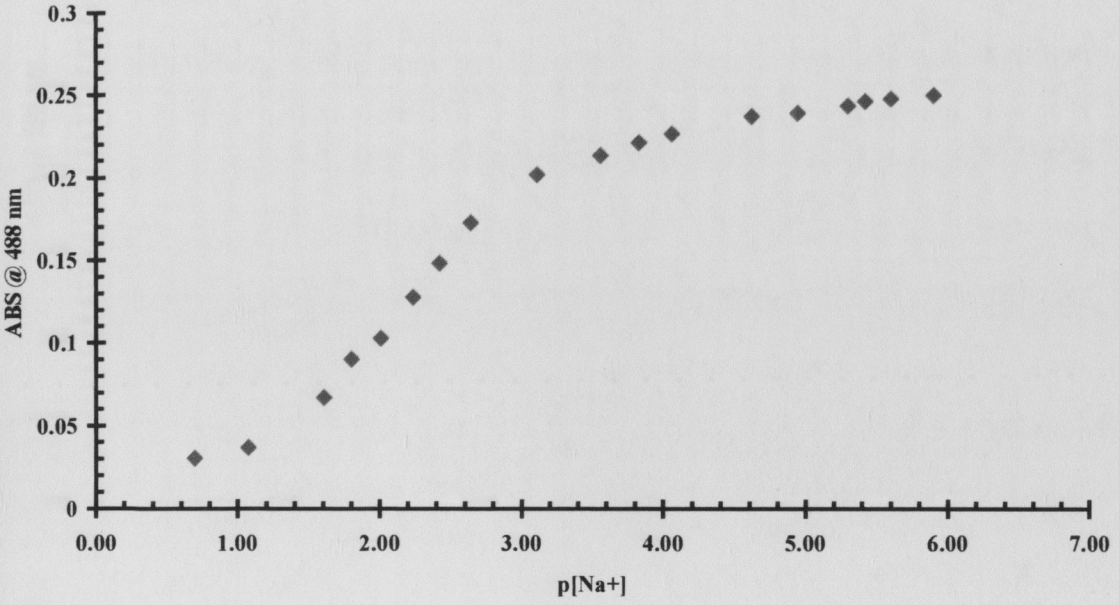


Figure 3.13 *Absorbance vs. pNa of* **153** *(50:50 MeOH:H_2O, 0.1M Tris buffer, 0.1M TMACl, pH 7.4)*

In similar studies of **153** using Ca^{2+} and Mg^{2+}, there were only minor changes observed in the absorption spectrum. No hypochromic effect was observed for the minor band at 280 nm, nor was the formation of an isosbestic point at 402 nm observed. An absorption band at 370 nm was also not observed. Only at very high cation concentration was a gradual hypochromic effect observed in the 488 nm band. These observations indicated that **153** was selective for Na^+ over both Ca^{2+} and Mg^{2+}. In studies on **153** with K^+ and Li^+ a similar response was observed for both. In these cases a hypochromic effect was observed in the 488 nm and 280 nm band. At high concentrations two isosbestic points were observed at *ca.* 380 nm and 320 nm along with the formation of a new band at 346 nm. In both cases this was an indication of binding to **153**, with binding constants roughly determined for K^+ and Li^+ to be log $\beta = 1.6$ and log $\beta = 1.8$ respectively. The binding values were considerably smaller than that found for Na^+, indicating that **153** can effectively detect Na^+ at physiological levels without interference from other cationic species. The results of all of the titrations are summarised in Figure 3.14 and a summary of binding constants can be found in Table 3.2. (Page **117**)

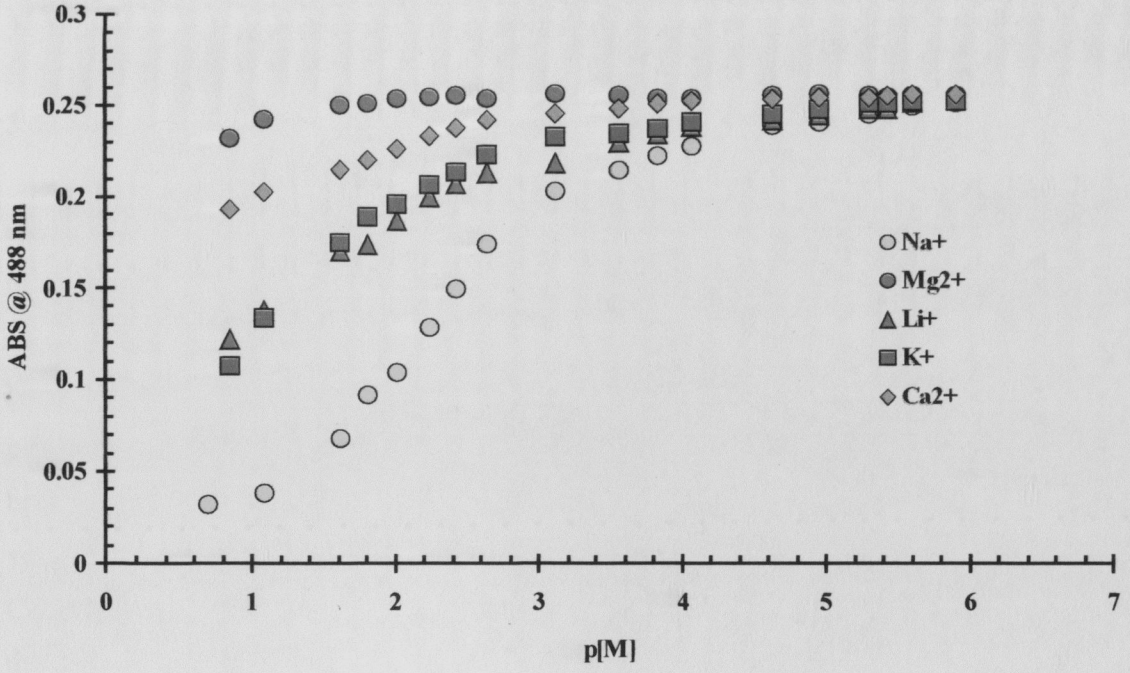


Figure 3.14 ***Absorbance vs. pM of* 153 - *Selectivity group I and II cations (50:50 MeOH:H_2O, 0.1M Tris buffer, 0.1M TMACl, pH 7.4)***

From Figure 3.14 it can be seen that **153** is selective for Na^+ and showed no response for Ca^{2+} and Mg^{2+} except at very high concentrations. Both K^+ and Li^+ also showed some response, the formation of isobestic points were an indication of binding however, this was only at high concentrations. The calculated binding constants show that the binding of **153** to Na^+ is almost a magnitude of order higher with log $\beta = 2.3$ for Na^+ compared to 1.6 and 1.8 for K^+ and Li^+ respectively. As discussed in the introduction, the selectivity for Na^+ over K^+ and Li^+ stems from the design of the receptor which has two methoxy appendages that allow stronger binding to occur with cations that fit the crown utilizing the lariat ether effect [20] and in the case of larger cations prevents binding by steric hindrance.

3.7 Photophysical analysis of 154

Photophysical analysis of **154**, a colorimetric sensor designed for selective sensing of intracellular K^+ was performed in two parts as described above for **153**. Analysis began with an evaluation of **154** in terms of its pH dependence/response. This was followed by an evaluation of its sensitivity and selectivity towards K^+ over other biologically active[8] group I and II cations. All analysis was performed in 50:50 MeOH:H_2O.

3.7.1 Determination of the pH dependence of 154

The absorption spectrum of **154** in 50:50 MeOH:H_2O was similar to that of **153**. Here the spectrum consisted of a minor absorption band at 280 nm, a major absorption band at *ca.* 473 nm and an absorption minimum at 353 nm. The major band at 473 nm was used to calculate an extinction coefficient, log $\varepsilon = 4.32$. Upon titration of an alkaline solution (TMAOH used as base) of **154** with dilute HCl the 473 nm band showed a hypochromic effect as a function of pH with a concomitant hypsochromic shift as it decreased between pH 5-6. However a bathochromic shift was then observed with a shift in the maximum from 477 nm to 527 nm. At very low pH a plateau was seen to form with two maxima at *ca.* 485 nm and *ca.* 535 nm. Concurrently the 280 nm band was seen to decrease slightly with a bathochromic shift and as the pH was lowered further the formation of a new absorption maximum at 321 nm was observed. The presence of an isobestic point at *ca.* 373 nm was also apparent. These results were similar to that of **153** indicating a similar process of protonation of the nitrogen and

suppression of the ICT state was occurring. The results of this pH titration are shown in Figure 3.15 and Figure 3.16.

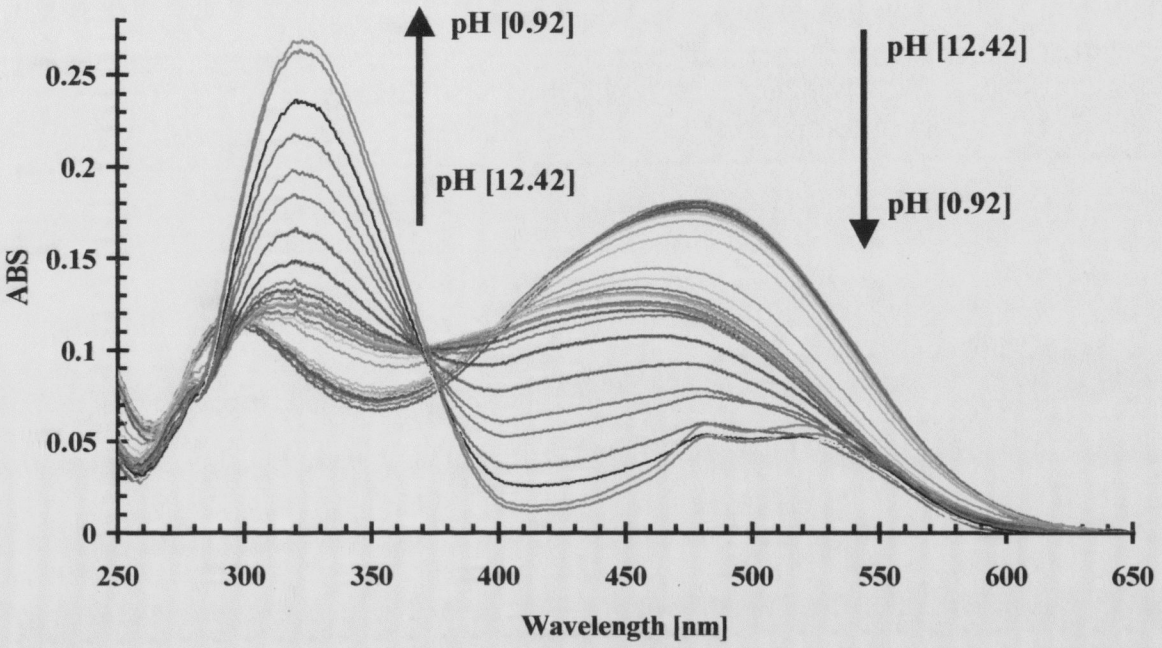


Figure 3.15 *Absorption of* **154** *as a function of pH, pH range = 0.92-12.42 (50:50 MeOH:H_2O)*

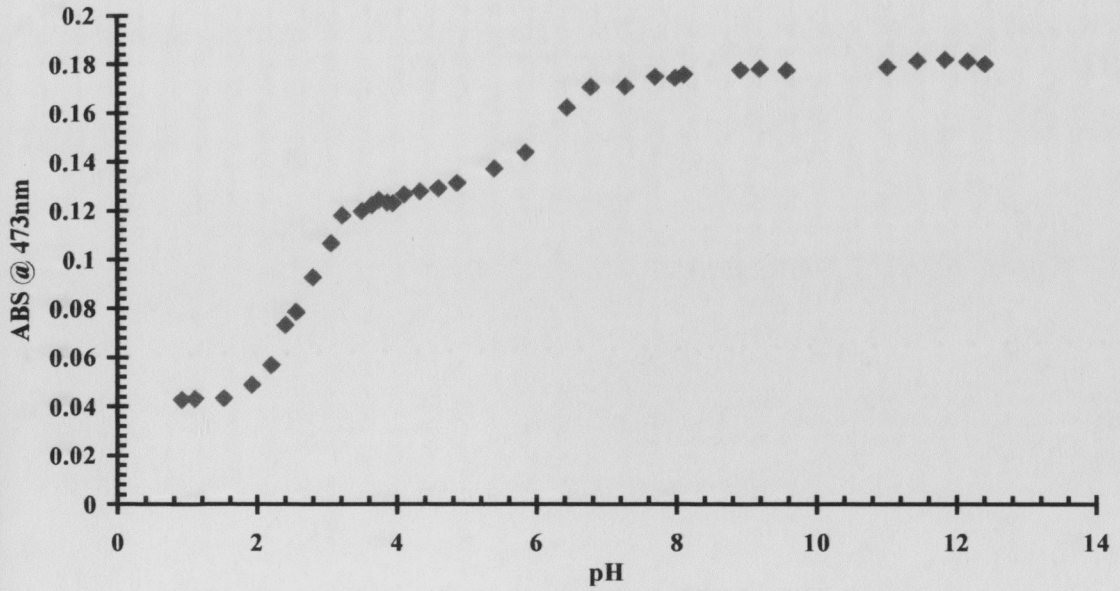
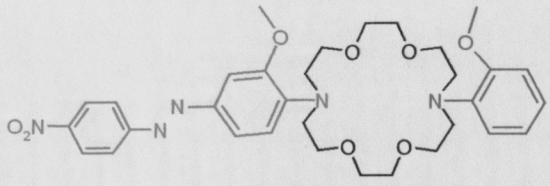


Figure 3.16 *Absorbance vs. pH of* **154** *(50:50 MeOH:H_2O)pK_a determination studies*

A plot of absorbance at 473 nm as a function of pH provided Figure 3.14, from which two pK_a values were calculated for the two nitrogen's of the diaza crown receptor, $pK_a = 6.3$ and $pK_a = 2.9$. The assignment of pK_a's was again rationalized in terms of the electron density of each nitrogen. The value of $pK_a = 2.9$ was attributed to the nitrogen involved in the ICT process, in which case an electron-withdrawing group is present that lowers the electron density of the nitrogen thus making protonation more difficult. The other aniline nitrogen has no substituents that can cause such a reduction in electron density and is thus easier to protonate. The relative electron densities are illustrated in Figure 3.17.



154

Figure 3.17 ***Illustration of* 154 *to indicate the assignment of pK_a values. Aromatic system colored red has a strongly electron withdrawing group as part of its structure, which causes a reduction in the electron density of the aniline nitrogen. This makes protonation more difficult, $pK_a = 2.9$. Aromatic system colored blue has no electron withdrawing groups so electron density is higher and protonation easier, $pK_a = 6.1$.***

3.7.2 Selectivity studies of 154 with Group I and II cations

Photophysical studies of **154** with group I and II cations were carried out in the same experimental manner as described for **153**. All titrations were carried out in 50:50 MeOH:H_20, buffered at pH 7.4. A preliminary study was again performed which showed that a solution of **154** changed from red to yellow upon addition of a large excess of K^+, indicating that **154** was an active colorimetric sensor for K^+.

This preliminary testing was followed by analysis of the selectivity and sensitivity of **154** for group I and II cations. This began with a titration of potassium acetate. These results are shown in Figure 3.18. The initial absorption spectrum showed the two characteristic absorption bands at 473 nm and 280 nm. Upon addition of K^+, a hypochromic effect was

observed for both of these bands. As this titration continued the 473 nm band decreased significantly with a concomitant hypsochromic shift. Concurrently the formation of a new band at 385 nm was observed. Two isosbestic points were also observed at *ca.* 290 nm and 413 nm. These changes were similar to those seen for **153** suggesting a similar process of ICT suppression upon binding of a cation with **154**, in this case K^+.

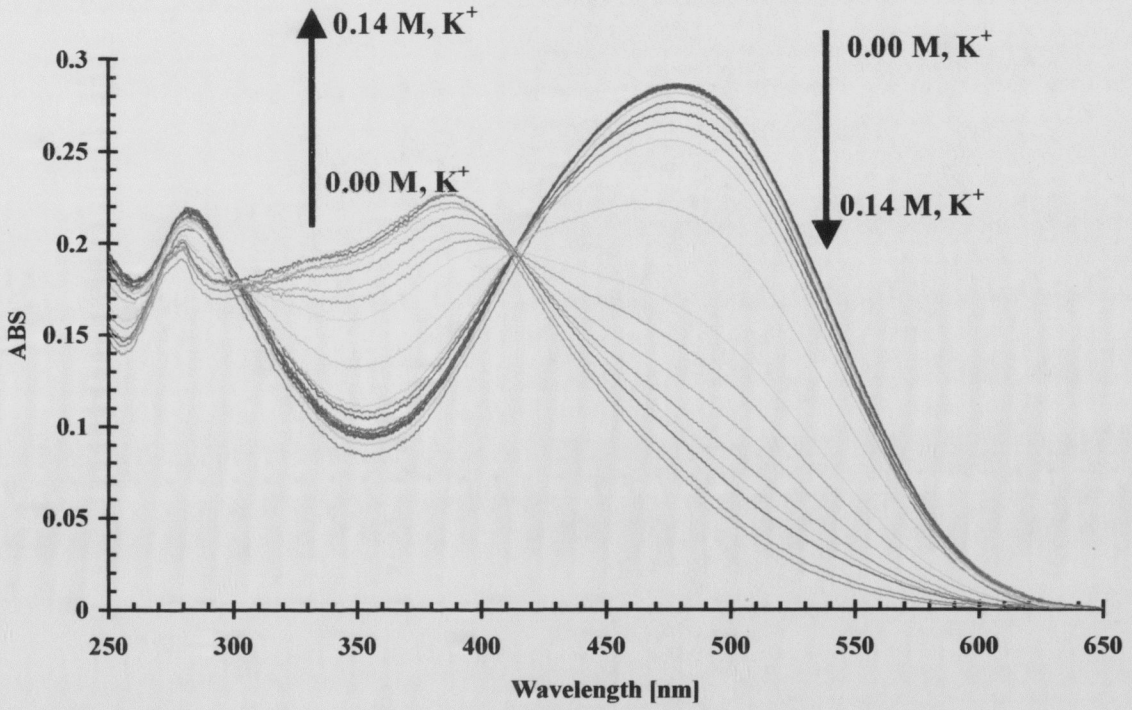


Figure 3.18 ***Absorption of* 154 *as a function of added potassium acetate, pK = 0.85-5.9 (50:50 MeOH:H_2O, 0.1M Tris buffer, 0.1M TMACl, pH 7.4)***

A plot of absorbance of **154** at 473 nm as a function of pK (Figure 3.19) showed a sigmoidal curve in which the absorption intensity was seen to decrease by almost 80 %. The detection range of **154** was found to be from pK = 1.0 to pK = 3.5, indicating the ability of this sensor to detect K^+ in the concentration range *ca.* 3.2-100 mM, which is within the physiological range of K^+. Similar titrations were performed using KCl and this resulted in a similar spectrum and sigmoidal response suggesting that there was no anion effect for this sensor.

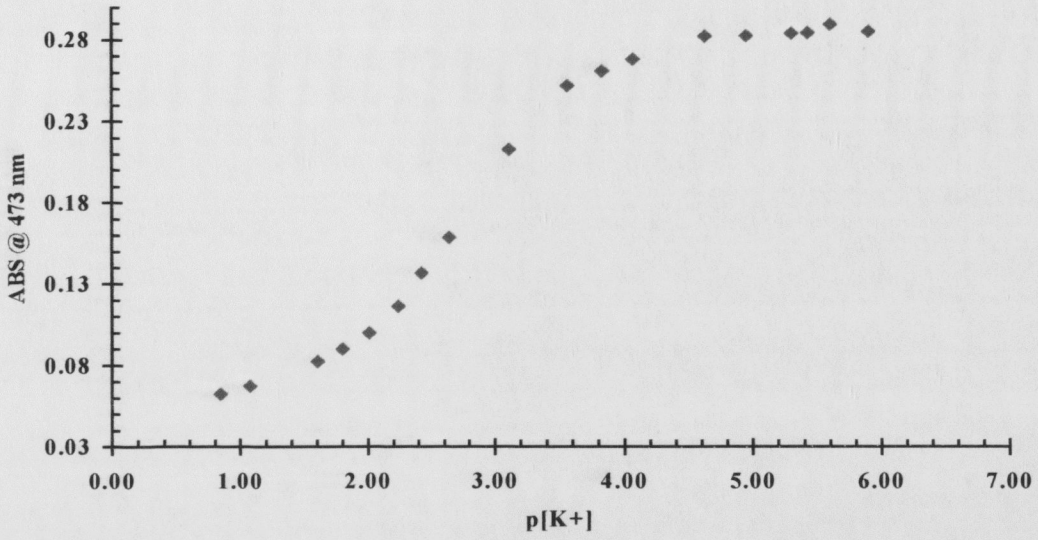


Figure 3.19 ***Absorbance vs. pK of* 154 *(50:50 MeOH:H_2O, 0.1M Tris buffer, 0.1M TMACl, pH 7.4)***

As seen before with **112** a similar response in the absorption spectrum was observed for the titration of **154** with Na^+ as shown in Figure 3.20. This response was also sigmoidal and a comparison of absorption at 473 nm as a function of pM for both Na^+ and K^+ showed that **154** was responsive to both of these cations in the same concentration range as shown in Figure 3.21.

Titrations were also carried out using Li^+, Ca^{2+} and Mg^{2+} as the cations. In the case of Ca^{2+} and Mg^{2+} **154** was unresponsive except below pM = 2 where a decrease in absorbance intensity of *ca.* 10 % was observed. When repeated for Li^+ a significant response was seen above pLi = 2 and in the final additions an isosbestic point began to form at *ca.* 410 nm. All these results are summarised in Figure 3.22. Here it was clear that **154** was only responsive to K^+ and Na^+ in the concentration range found at intracellular levels. Lack of selectivity, shown by the similar response to both Na^+ and K^+ could be thought of as a disadvantage. However, as the intracellular concentration of Na^+ is low compared to K^+, (10–40 mM for Na^+, 90–120 mM for K^+) the use of **154** for monitoring cellular levels of K^+ is still possible. From these studies **154** has been shown to have a similar response to both K^+ and Na^+, a result observed for **PBFI** a fluorescent K^+ sensor with a structurally similar receptor [41] (See Chapter 2). The results of all the studies on **153** and **154** are summarised in Table 3.2

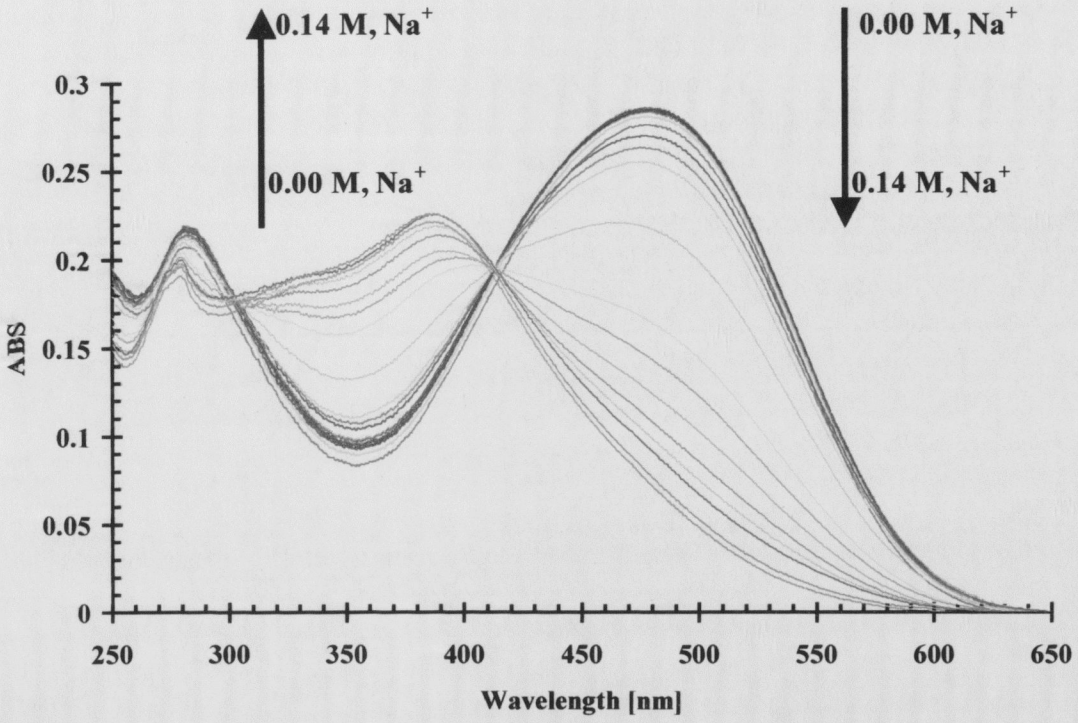


Figure 3.20 *Absorption of* **154** *as a function of added sodium acetate, pK = 0.85-5.9 (50:50 MeOH:H_2O, 0.1M Tris buffer, 0.1M TMACl, pH 7.4)*

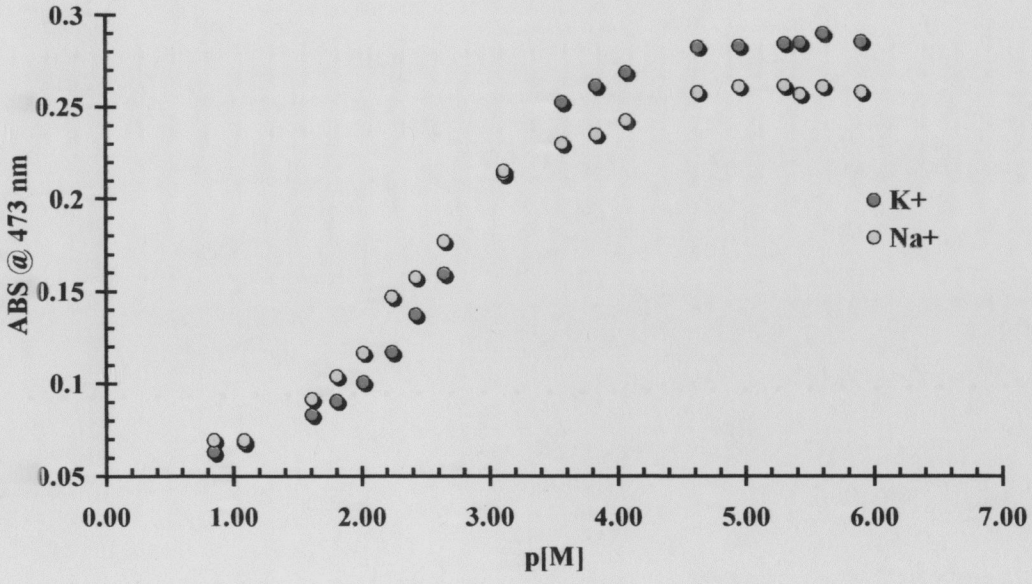


Figure 3.21 *Absorbance vs. pM of* **154** *– Comparison of response of* **154** *to Na^+ and K^+ (50:50 MeOH:H_2O, 0.1M Tris buffer, 0.1M TMACl, pH 7.4)*

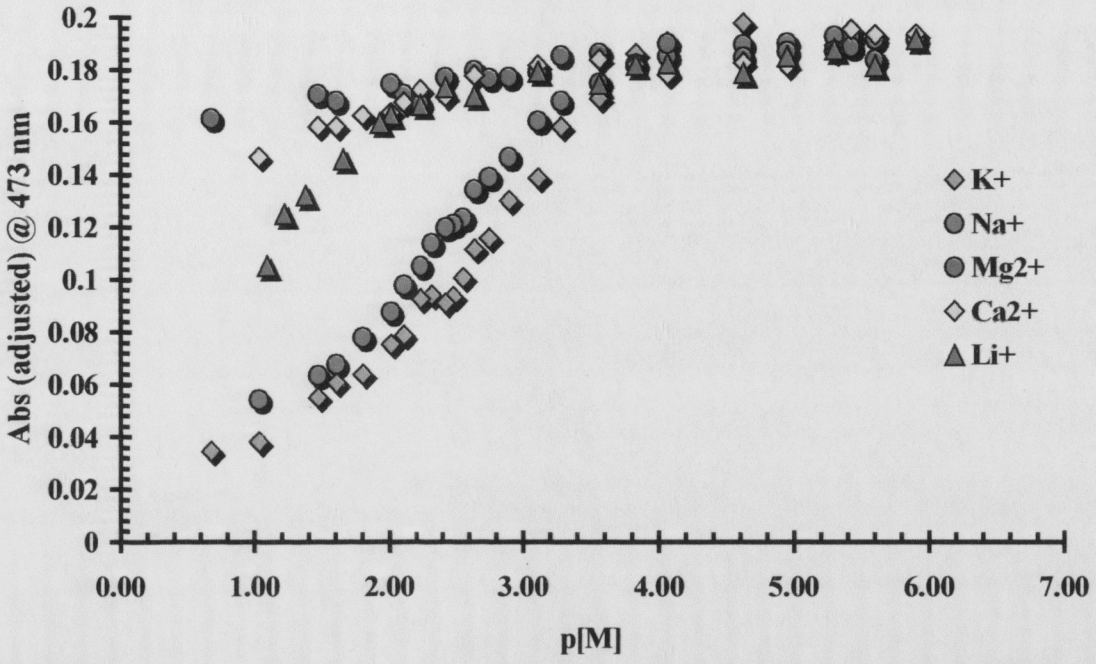


Figure 3.22 ***Absorbance vs. pM of* 154 - *Selectivity study of Group I and II cations (50:50 MeOH:H_2O, 0.1M Tris buffer, 0.1M TMACl, pH 7.4)***

Table 3.2 Summary of physical properties of 153 and 154

Sensor	153	154
λ_{max} (nm), [ε ($cm^{-1}M^{-1}$)]	491 [4.36], 287	473 [4.32], 2.82
pK_a	6.1 (±0.1), 3.0(±0.1)	6.3 (±0.1), 2.9(±0.1)
pNa	2.3 (±0.1)	2.5 (±0.1)
pK	1.6 (±0.1)	2.1(±0.1)
pLi	1.8 (±0.1)	<1 [a]
pMg	<1 [a]	<1 [a]
pCa	<1 [a]	<1 [a]
a- Unable to determine these accurately		

3.8 Comparative studies of detection ranges of 111, 112, 153 and 154

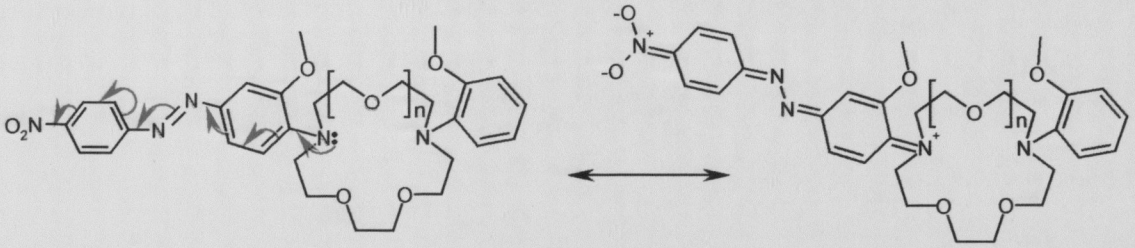
The objective of this chapter was the synthesis and evaluation of diaza crown based colorimetric sensors for the detection of Na^+ and K^+ at physiological levels. During analysis of both receptors **111**, **112** and the colorimetric sensors **153** and **154** several trends became apparent. Binding constants and the detection ranges of each receptor and sensor are shown in

Table 3.3. In the case of **111**, **153** and **112**, **154** the same trend was visible. The results show that both the receptors operated over a low concentration of 0.1-10 mM. When incorporated into the colorimetric sensors **153** and **154** a shift in the response range by an order of magnitude was observed. This shift in detection range was attributed to charge repulsion from the ICT state that exists. The formation of the ICT state leads to a situation in which the aza crown nitrogen contains a positive charge (Scheme 2) that can actively repel the cation from binding with the receptor. This theory is further supported by the decrease in binding constants.

Table 3.3 Comparison of detection ranges of sensors

Sensor / Receptor	Log β	Detection Range [mM]
111	3.1 (±0.1) [144, a]	0.1-10.0 [144, a]
153	2.3 (±0.1) [a]	0.32-79.4 [a]
112	3.9 (±0.1) [b]	0.1-10.0 [b]
154	2.1(±0.1) [b]	0.32-100 [b]

a - Titre with Na^+, **b** - Titre with K^+



153: n = 1
154: n = 2

153: n = 1
154: n = 2

Scheme 2 – ***Resonance forms of 153 and 154 to describe the charge repulsion effect proposed for the shift in detection range observed for each receptor.***

3.9 Conclusion

The design, synthesis and full characterisation of two new colorimetric sensors **153** and **154** was successfully shown. These sensors were based on the diaza crown receptors **111** and **112**. The pH dependence of **111**, **112**, **153** and **154** were all shown to be independent in the physiological pH range of 6 – 8. The selectivity of **111** a receptor specifically designed for Na^+ and its colorimetric equivalent **153** were both shown to be highly selective for Na^+ at intracellular concentrations. The high selectivity for Na^+ was attributed to the incorporation of methoxy appendages into the diaza crown receptors and the resultant lariat ether effect. A response was also seen for Li^+ but only at higher concentrations, however, this would not affect the use of **153**, as Li^+ is not a physiologically common cation. The selectivity of **112**, a receptor for K^+ and its colorimetric equivalent **154** were shown to respond in the same way for both Na^+ and K^+ at intracellular concentrations. Again this lack of discrimination is not a serious issue for intracellular sensing of K^+ as its concentration is considerably higher than that for Na^+. A change in the detection range and decrease in the binding constants of the receptors was found to occur upon addition of the azo substituents an effect that was attributed to a charge repulsion effect caused by the positive charge produced on the aza crown nitrogen due to the ICT state that had formed.

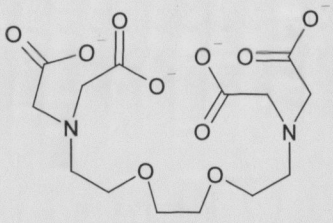
Chapter 4

Attempted synthesis of a lanthanide sensor for the detection of calcium

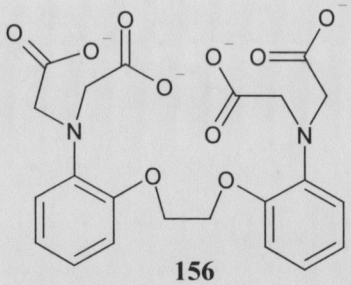
4.0 Attempted synthesis of a lanthanide luminescent chemosensor for calcium

4.1 Introduction

Along with Na^+ and K^+ discussed previously, Ca^{2+} is one of the most important cations found in living organisms. Its function and applications outside of cells include the formation of biominerals that are involved in the formation of skeletal structures. At a cellular level, Ca^{2+} is associated with fertilization and cell division as well as controlling the mechanical stability of cell walls and membranes. [8] The concentration of Ca^{2+} is typically around the 10^{-3} M range in extracellular fluids compared to 10^{-7} M within the cell cytoplasm. However, these values are somewhat dependent on the cell type and function. [8] Over the years many groups have devoted considerable efforts into the development of fluorescent chemosensors for determining cellular concentrations of Ca^{2+}. As mentioned previously in Chapter 1, Ca^{2+} receptors are typically acyclic the most common being based on the structure of EDTA and EGTA, **155**.

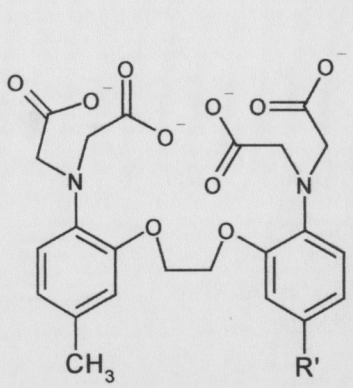


155

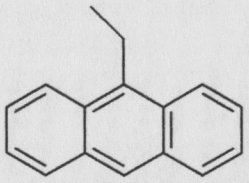


156

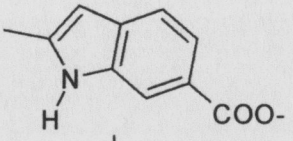
There have been many excellent examples of sensors for Ca^{2+} reported by groups such as Tsien *et al.* [176, 177, 178, 179, 180] and de Silva *et al.*[181] to name but a few. In all these examples the Ca^{2+} receptor was based on BAPTA, **156** [182] an acyclic receptor similar in structure to EGTA. The most noticeable difference being the incorporation of two aromatic moieties in **156**. The success of BAPTA in the formation of chemosensors for the determination of physiological levels of Ca^{2+} lies in its high affinity for Ca^{2+}over $Mg^{2+}$and its low pK_a's of 5 and 6 respectively for each of its nitrogen's. [42, 183] These factors and the fact that the aromatic moieties can be functionalised to incorporate various fluorophores have lead to the prominence of BAPTA in Ca^{2+} sensing resulting in reports of Ca^{2+} sensor such as **157**, [181]**158** [180] and **159** [177] Of these **158** and **159** are commercially available sensors for the determination of intracellular concentrations of Ca^{2+}.[139]



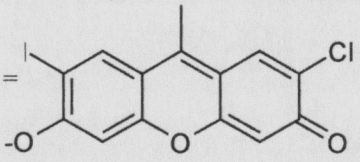
157: R' =



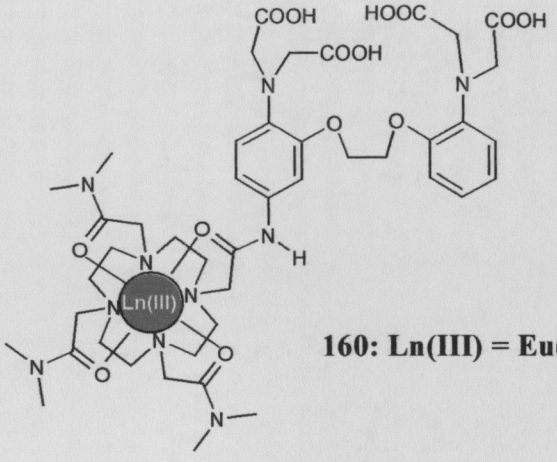
158: R' =



159: R' =



The aim of this project was to produce a lanthanide luminescent chemosensor using **160**, that could selectively sense Ca^{2+} at intracellular levels. **160** is an example of a BAPTA based ligand to which a tri substituted cyclen ligand has been attached by way of an alkyl amide linkage. The design of this ligand is the same as that discussed in Chapter 2 for **99**, **100**, **101** and **102**. In this case the BAPTA moiety acts as a Ca^{2+} receptor. The cyclen ligand acts as a luminescent signaling moiety when a lanthanide cation such as Tb(III) is complexed. These two components are attached through an amide link, which acts as a spacer group and also as part of the complexing ligand for coordination of the lanthanide.

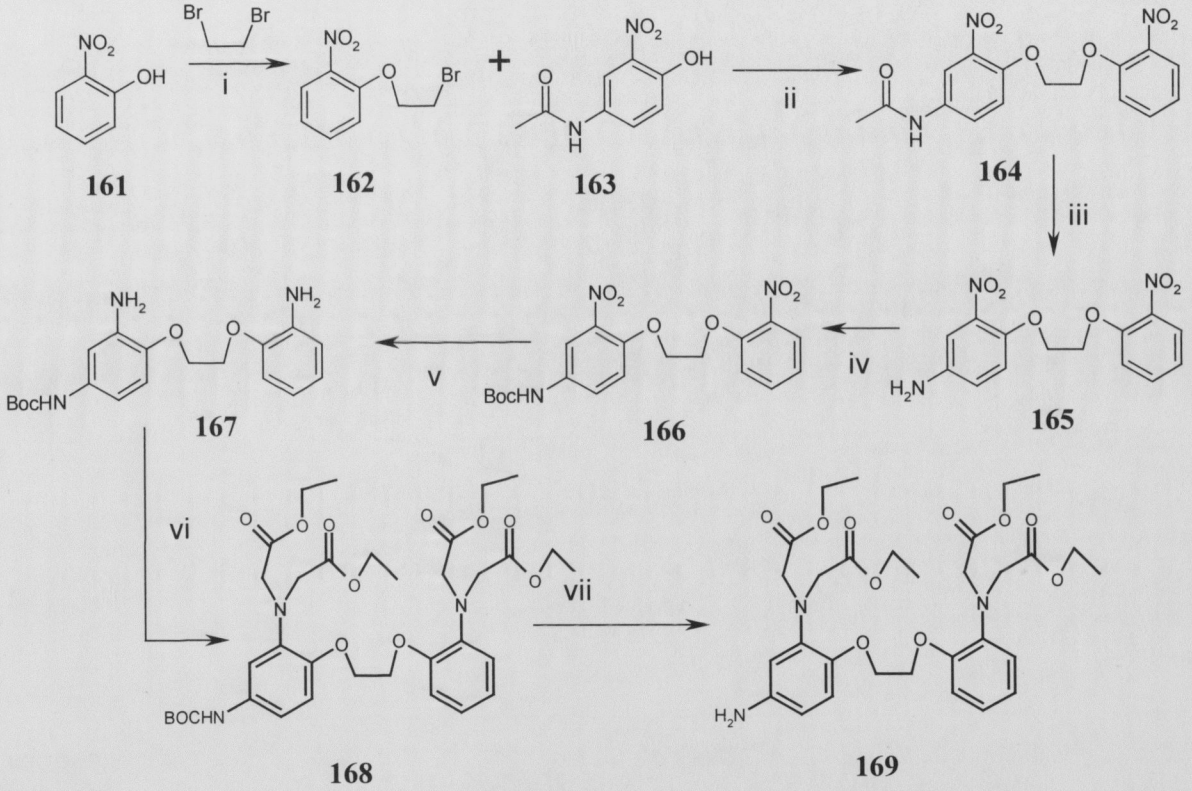


160: Ln(III) = Eu(III) or Tb(III)

4.2 Synthesis of 160

In order to make **160** the BAPTA receptor, **156** needed to be synthesized with an amino group substituted in the 4 or the 5 position so that the spacer group could be attached to the

receptor to link to the lumophore. A comprehensive literature search of amino functionalised derivatives of BAPTA resulted in only two methods, which suggested possible difficulties were involved in this synthesis. Two methods of synthesis were considered that could result in the synthesis of **156** with an amino group substituted in the 4 or 5 positions. The first method was based on a synthesis by Erdogan *et al.*. [184] Erdogan formed a 4 amino derivative of BAPTA using 4-amino, 2-nitrophenol and 4-methyl, 2-nitrophenol in a 6-step reaction involving two protection reactions on the amino, firstly by acylation and later in the synthesis by BOC. The authors quoted an overall yield of 40 % for the amino derivative. A modified version of this procedure (Scheme 1) was attempted, to produce **169**.

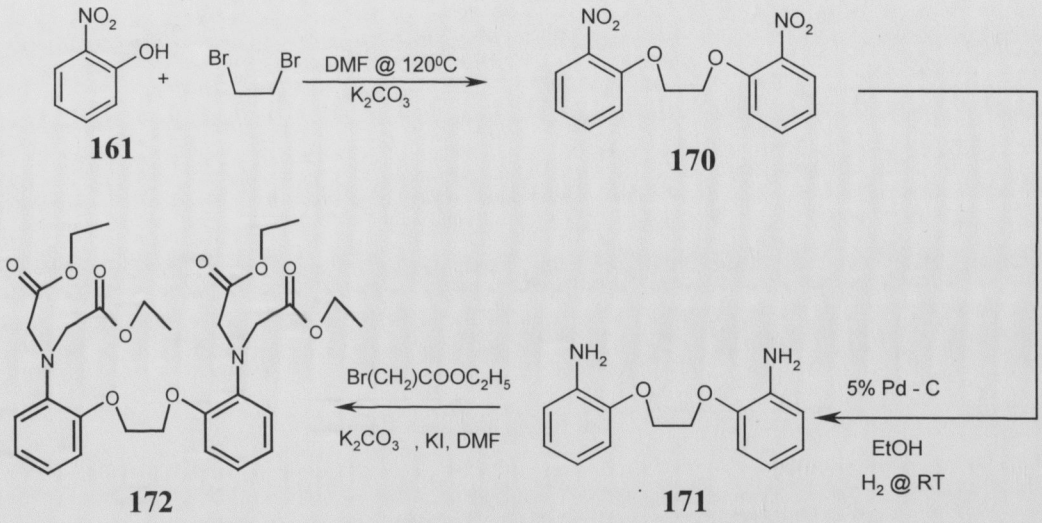


Scheme 1 - ***Proposed synthesis of 4-Amino BAPTA (169) using synthesis of*** Erdogan *et al.* [184]. *i) K_2CO_3, DMF, 120 °C; ii) K_2CO_3, DMF, 120 °C; iii) 3M HCl/ EtOH; iv) $(boc)_2O$, TEA, DCM; v) 10 % Pd-C, cyclohexene, EtOH, reflux; vi) $BrCH_2CO_2CH_2CH_3$, MeCN, base, reflux; vii) TFA/ DCM*

This proposed synthetic route was attempted. However, isolation of **164** was not possible from the substitution reaction between **163** and **162**. This was found to be due to insufficient

solubility of **162** in the reaction solvent. A number of other solvents were tested, such as MeCN, however, none were sufficient to yield **164**.

The alternative synthetic route consisted of using the original synthesis of Tsien *et al.* to produce the tetra ethyl ester derivative of BAPTA, **172**. [42] This would then be followed by nitration to yield **173**. It was foreseen that the presence of the two aromatic moieties would lead to a mixture of products at the nitration stage, which would give rise to low yields of the desired product. However, publications by Shortreed and Pethig [185, 186] indicated that selective nitration in the 5' position was possible using concentrated HNO_3 and AcOH.



Scheme 2 – *Modified synthesis of* 172 *Tetra ethyl ester – BAPTA* [42]

A number of subtle changes were made to the original synthesis of Tsien, which included using **161** instead of sodium 2-nitrophenoxide in the initial step to produce **170** and using K_2CO_3 as a base instead of 1,8-bis (dimethylamino)naphthalene, (proton sponge™) in the synthesis of **172**. The results gave comparable yields to the original synthesis. The resulting tetra ethyl ester was isolated with an overall of 55 %. Although this molecule has been published in the literature [176] it has never been fully characterised. For this reason full characterisation of **172** was carried out. Figure 4.1 shows the ^1H NMR spectra obtained for **172**. All eight aromatic protons appeared as a multiplet between 6.89 and 6.84 ppm (**A**), the ethyl esters were shown by the presence of the quartet (**D**) at *ca.* 4.0 ppm and a triplet (**E**) at

1.15 ppm. The remaining CH_2 protons were observed as two singlets at 4.29 and 4.17 ppm respectively. ^{13}C NMR showed the presence of 11 carbon signals as expected. The ester carbonyl signal appeared at 171.0 ppm, while the CH_2 and CH_3 carbon signals of the ester group appeared at 53.0 and 13.56 ppm respectively. Six signals were also observed for the aromatic moieties between 149.9 and 112.9 ppm, with the final two CH_2 signals appearing at 66.7 and 60.2 ppm. IR, ESMS, accurate mass and elemental analysis were also used to confirm the synthesis of **172**.

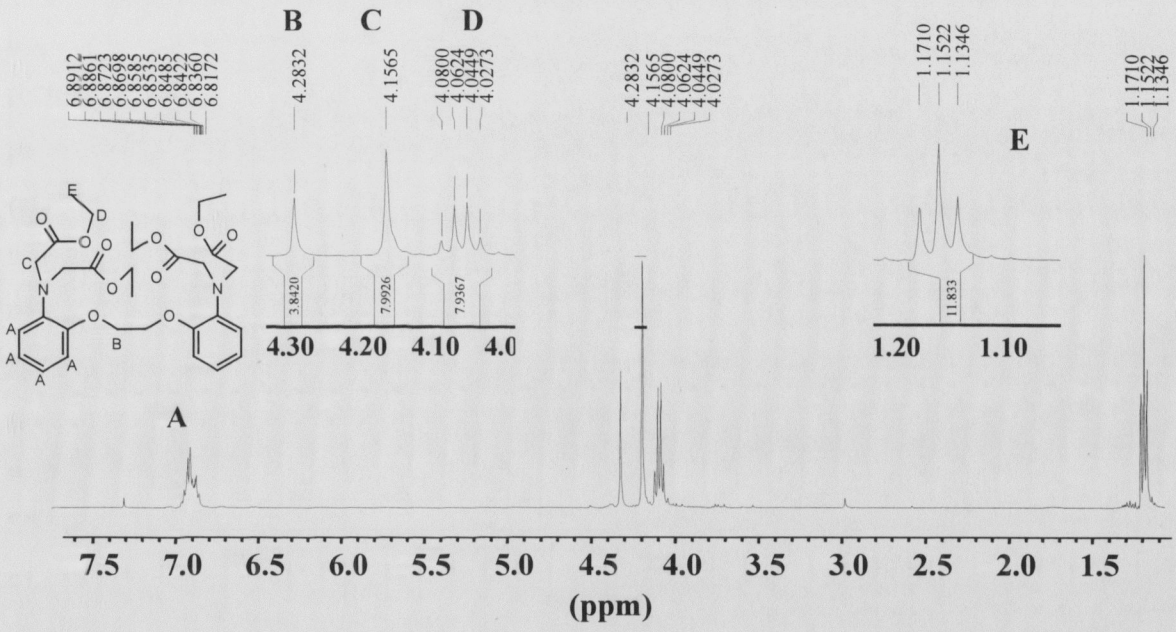
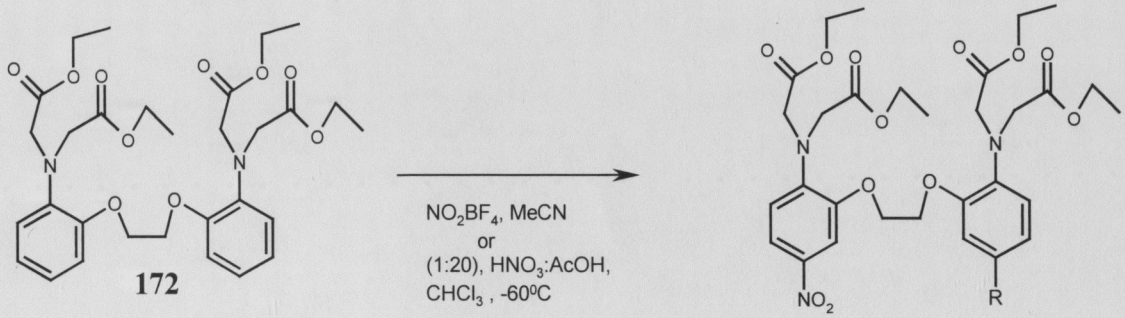


Figure 4.1 - *^{1}H NMR of 172 - (Tetra ethyl ester BAPTA)- ethyl ester shown by the presence of the quartet (D) at ca. 4.0 ppm and a triplet (E) at 1.15 ppm [Labeled structure inset]*

Following the synthesis of **172** the next step in the synthesis involved nitration at the 4 or 5 positions, to give **173**, (Scheme 3). Nitration of **172** using the published method of Shortreed and Pethig [185, 186] proved unsuccessful. This method of nitration involved adding conc. HNO_3 to a solution of **172** in glacial acetic acid. The results of this synthesis were poor with no quantifiable yield of **173** being produced. Nitration using HNO_3 and H_2SO_4 was attempted, however, analysis of the crude reaction mixture by ESMS analysis showed that multiple nitrations had occurred. This method was repeated a number of times at 0 °C using varying quantities of HNO_3 without **173** being isolated. Nitration of **172** was also attempted using

Nitronium Tetraflouroborate salt [NO_2BF_4]. A literature procedure was employed,[130] in which the salt in a solution of MeCN at -10 °C, was added to **172** in a solution of MeCN at –10 °C. The desired product, **173** was isolated from this reaction in a yield of less than 5 %. Variations of this procedure were repeated on numerous occasions. The main focus of variation was the reaction temperature and solvent quality, however no improvement was made to this yield. Over time and through observation it was found that the NO_2BF_4 salt was absorbing moisture, which appeared to be effecting the reaction. This was not expected as the salt was being stored under dry conditions. This reaction was run again at room temperature with NO_2BF_4 salt that had been dried under vacuum, in the presence of P_2O_5 for two days from which the desired product was obtained after silica column chromatography in a yield of 58 %. When this procedure was scaled up from the initial 0.169 g scale to 1.00 g the yields fell dramatically to *ca.* 30 %, and no increase was observed when this procedure was repeated with variations to the method similar to those described previously. In an attempt to improve the yield of **173** a new procedure was developed. This new method involved stirring **172** in $CHCl_3$ at -60 °C. To this a solution of 1:20 Fuming HNO_3: (Glacial) AcOH, was added in 200 µL aliquots every 60 seconds over a 60 minute duration. The result of this reaction was a reproducible yield of 56 % with a useful bis nitrated side product, **174**. A similar byproduct had been reported by Shortreed and Pethig.[185, 186] Further studies of this procedure showed that by careful addition of the acid solution the formation of this byproduct could be minimized and in cases where it was formed, efficient separation by silica gel chromatography was possible using 95:5, CH_2Cl_2:MeCN as an eluent.



173: R = H
174: R = NO_2

Scheme 3 – *Nitration of Tetra ethyl ester BAPTA,* 173 [185,186]

When this procedure was repeated with the addition of excess acid solution to ensure the synthesis of **174** yields of 79 % were achieved. These yields were reproducible even when the reaction was scaled up to 1-1.5 g. In both cases **173** and **174** were fully characterised.

The ^{1}H NMR spectrum of **173** showed considerable difference to that of **172** as illustrated in Figure 4.2. The most dramatic changes occurred in the aromatic region of the spectrum. The ^{1}H NMR of **173** consisted of a doublet at 7.83 ppm, a singlet at 7.73 ppm and a doublet at 6.68 ppm representing the protons on the nitrated aromatic system. The unnitrated aromatic system remained as a multiplet in almost the same position as the starting material, 6.91-6.84 ppm. The C_2 symmetry was lost upon nitration as shown in Figure 2 where double the number of signals were observed. NOE experiments showed that the nitration occurred in the 5' position as was reported by Shortreed and Pethig. [185, 186]

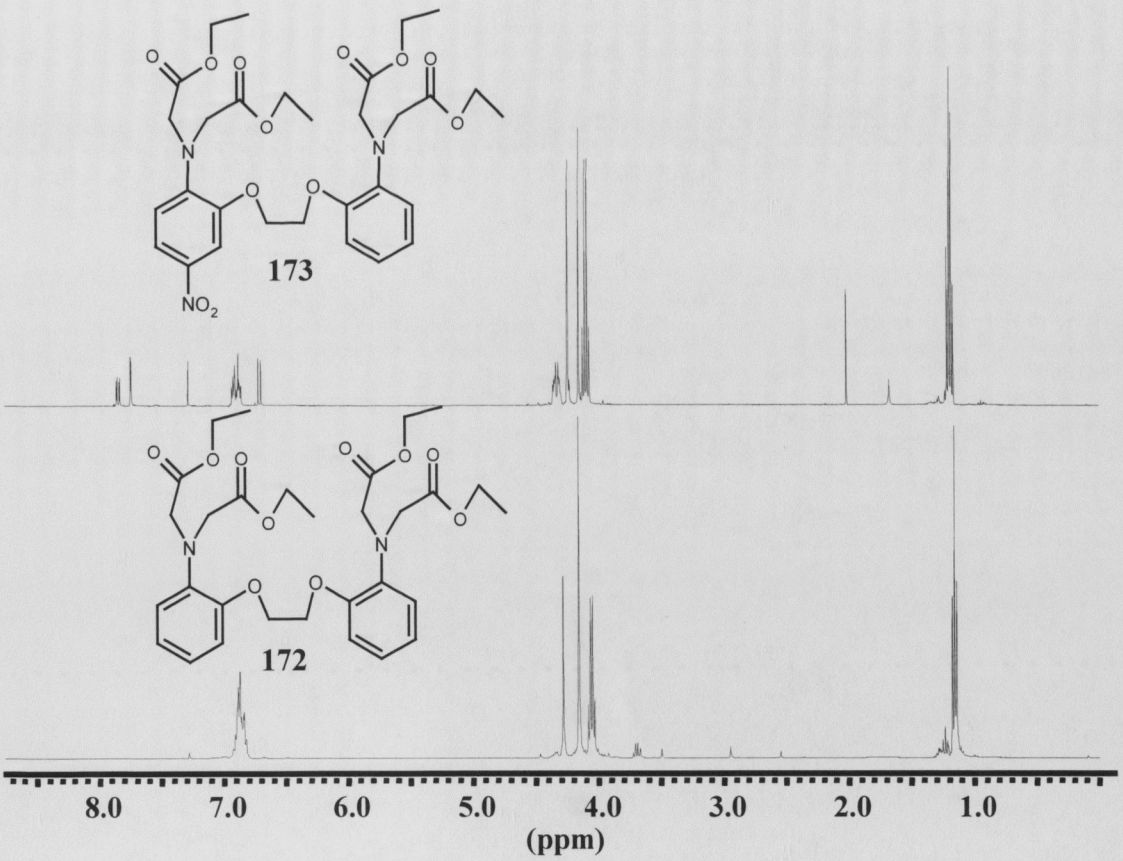
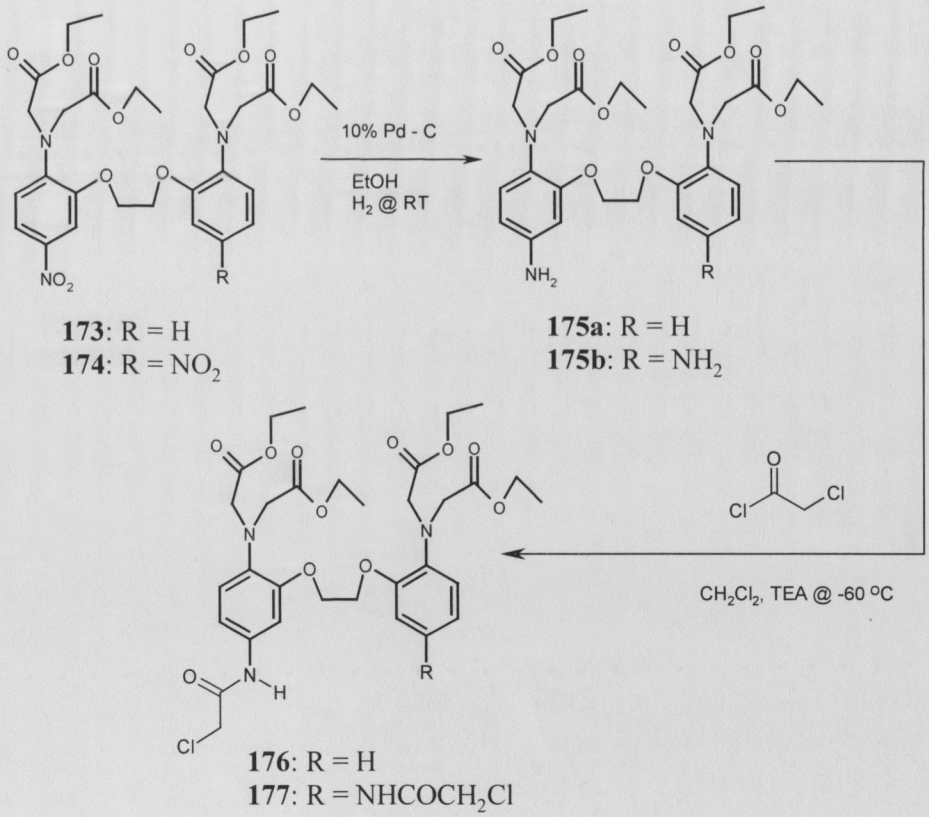


Figure 4.2 - *^{1}H NMR* comparison *173 with 172, NOE experiments show that the nitration has occurred in the 5' position* (Inset: structure of **173** with nitro group in the 5' position as determined from NOE experiments)

Following the synthesis of **173**, reduction to the amino, **175** followed by formation of the amide **176** was undertaken as described in Scheme 4. The reduction was carried out in EtOH using 10 % Pd-C as the catalyst under an atmosphere of H_2, yielding the amino product, **175** in *ca.* 80 % yield. The amide **176** was then formed by dropping a solution of chloroacetyl chloride in CH_2Cl_2 to the amine **175** in a solution of CH_2Cl_2 containing TEA at -60 °C.[130] This reaction yielded **176** in a quantitative yield. This procedure was repeated using **174**, yielding **177** in *ca.* 80 % yield. In both cases the α - chloroamides **176** and **177** were identified using ^{13}C NMR, which showed the amide carbonyl at *ca.* 163 ppm and a CH_2 signal at *ca.* 42.5 ppm. Comparison of the ESMS spectra with the calculated isotope model confirmed the presence of chlorine in the molecule due to the distinct isotope pattern produced.(Figure 4.3)



173: R = H
174: R = NO_2

175a: R = H
175b: R = NH_2

176: R = H
177: R = $NHCOCH_2Cl$

Scheme 4 - *Synthesis of* **176** *and* **177**.[130]

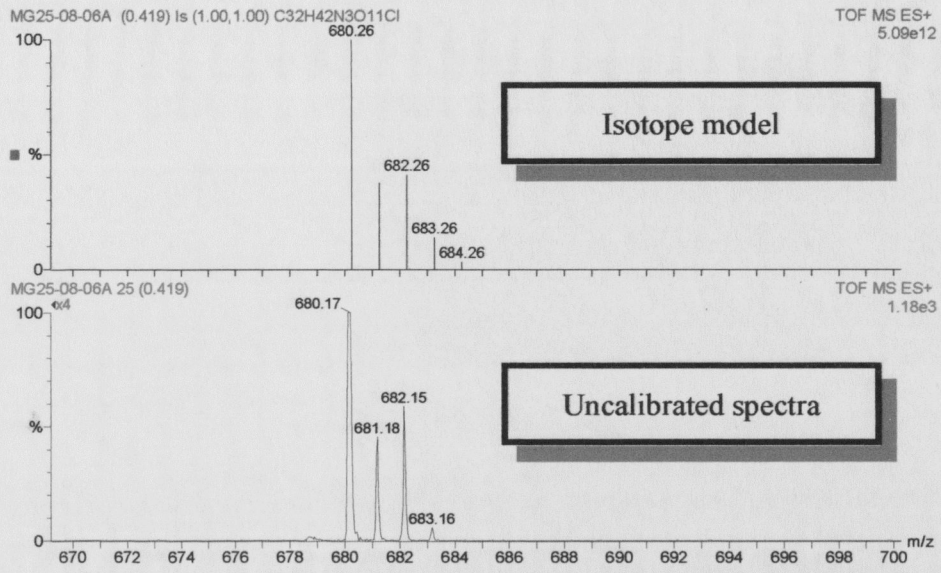
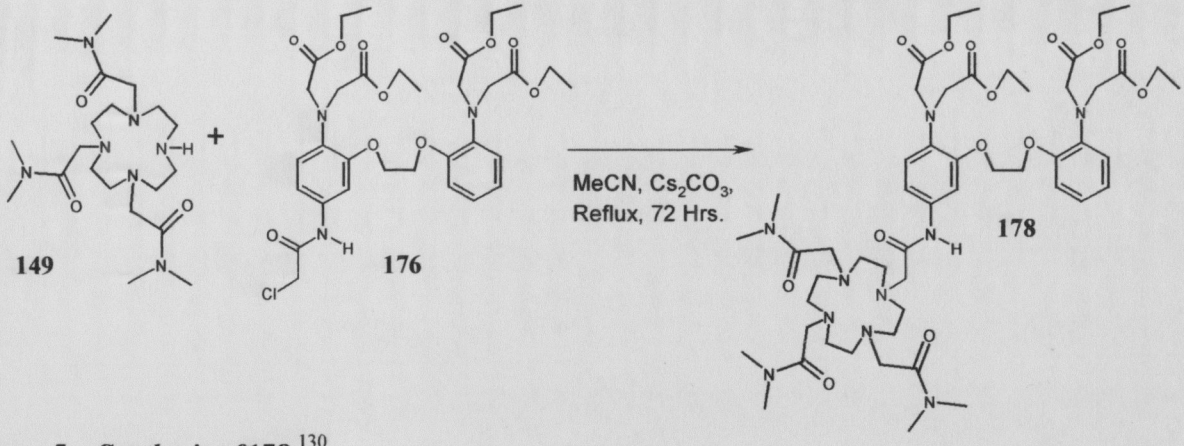


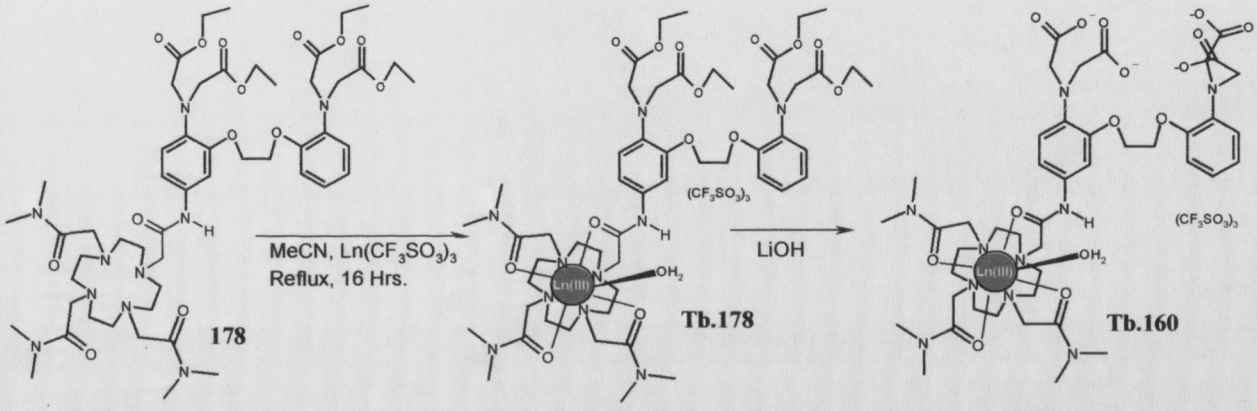
Figure 4.3- ***Comparison of ESMS spectra with the calculated isotopic model for* 176 *showing isotope spectra consistent for a molecule with one chlorine atom***



Scheme 5 - ***Synthesis of* 178** [130]

Following synthesis of the receptor-spacer system, **177**, attachment to the lumophore ligand **149** was attempted. The coupling of the two components involved a substitution reaction in MeCN at reflux in the presence of Cs_2CO_3, Scheme 5. The resulting product **178** was recovered as a crude oil that was observed by ESMS. TLC analysis revealed that there were a number of impurities, which was confirmed by ^1H NMR analysis. As described in

Chapter 2 for **99** and **100**, the purification of **178** was not possible by any conventional method of chromatography. Only partial purification was achieved, by washing a $CHCl_3$ solution of the **178** with water. The ligand was characterised by ^1H and ^{13}C NMR spectroscopy, ESMS, accurate mass and IR spectroscopy. The presence of the aromatic protons were visible as a multiplet at 6.83 ppm on ^1H NMR spectra as was the ester CH_3 peak at 1.10 ppm. ^{13}C NMR spectral analysis was useful along with DEPT experiments at distinguishing the seven aromatic C-H's expected as well as four carbonyl carbons at *ca.* 171 ppm. A number of CH_2 and CH_3 peaks were also observed including those of the ester.



Scheme 6 - *Proposed synthesis of* **Tb.178** ***and*** **Tb.160** [130]

Complexation of **178** with Tb(III) to produce **Tb.178** followed. No Eu(III) complex was synthesised. The previous results from photophysical studies on **Eu.99** and **Eu.100** (Chapter 2) indicated that the Eu(III) complex would not be emissive. The synthesis of **Tb.178** consisted of stirring the ligand and 1.1 equivalents of the Tb (III) triflate salt in freshly distilled MeCN for approximately 16 hours, under argon, Scheme 6. [130] After cooling to room temperature the reaction mixture was dropped onto ether from which a crude solid material was recovered. This was later purified by alumina column chromatography using 30:70, THF:DCM. The product was eventually isolated by increasing the polarity to 30:60:10, THF:DCM:MeOH. The Tb(III) complex, **Tb.178** was isolated in a 25 % yield. This solid produced a green emission, characteristic of Tb(III) under ultra violet light. The ^1H and ^{19}F NMR were characteristic of those seen for complexes of **99** and **100** (Chapter 2). The ^1H NMR spectra showed large shifts up and down field as far as 70 and –89 ppm respectively as a result of the paramagnetic lanthanide. The ^{19}F NMR indicated the presence of the triflate counter anions with signals at –

79.19, -167.10 and -193.92 ppm. IR analysis also showed the triflate along with C-H bands at 2956 cm^{-1}, 2926 cm^{-1} and 2854 cm^{-1} and a strong carbonyl band at 1732 cm^{-1}.

Further analysis of **Tb.178** in aqueous solution was performed using uv-visible spectroscopy and fluorimetry. These results are illustrated in Figure 4.4, Figure 4.5 and Table 4.1 respectively. The absorption spectrum (Figure 4.4) was similar to those obtained in Chapter 2 for all the lanthanide complexes. In this case there were two absorption bands at 205 nm and 282 nm respectively.

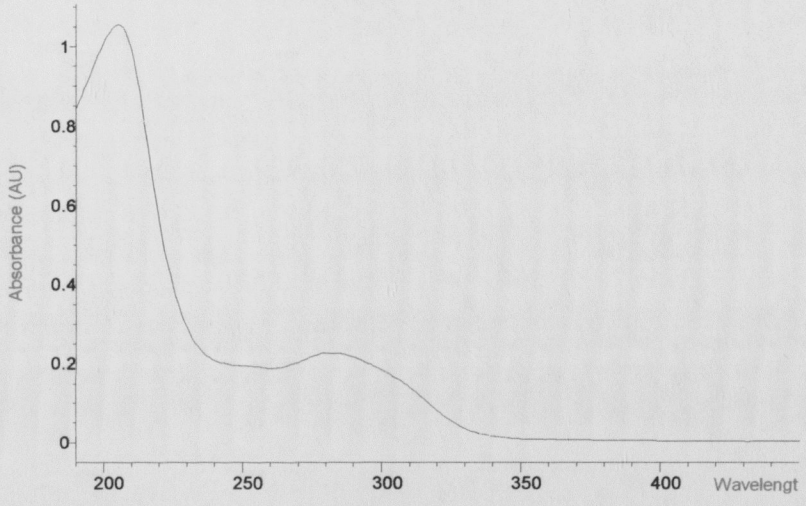


Figure 4.4- ***Absorption spectrum of*** **Tb.178** ***in aqueous solution.***

Further analysis involved excitation of the solution of **Tb.178** at different wavelengths while measuring the lanthanide emission. Four wavelengths were chosen for this experiment. These included the two absorption maxima as well as the wavelength required for direct excitation of Tb(III). When the solution was excited at 366 nm, for direct excitation of the Tb(III) metal center, a weak luminescent emission was observed with a maximum intensity of 3 for the J = 5 transition at 547 nm. This was then repeated with wavelengths of 205, 248, 284 and 300 nm respectively. In all these cases a high intensity Tb(III) emission was produced with respect to the emission produced by direct excitation. The highest emission intensity was observed when the complex was excited at 205 nm, the stronger of the two absorption bands. This resulted in a maximum emission intensity of 675 for the J = 5 transition at 547 nm.

Excitation at 248, 284 and 300 nm all resulted in a maximum emission intensity of *ca.* 500 for the J = 5 transition at 547 nm.

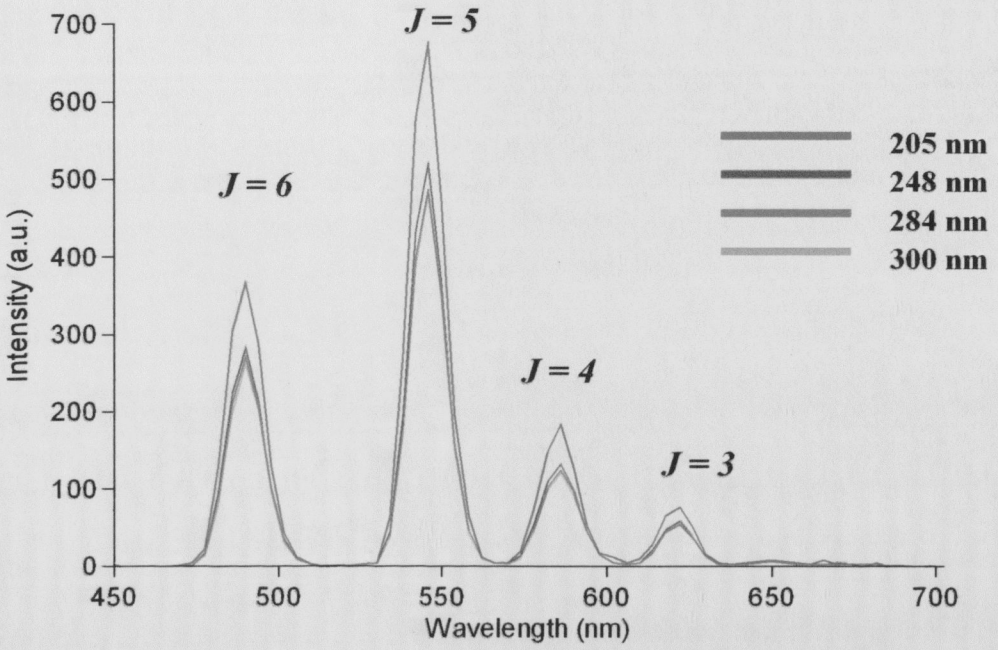


Figure 4.5- ***Lanthanide emission spectrum of*** **Tb.178** ***in aqueous solution.*** [slit widths 10 nm (Inset: Excitation wavelengths used to produce emission)]

Table 4.1 Summary of Tb.178 Emission (Max. Intensity) vs. λ_{Excite}

Excitation	*J = 6* (max) [490 nm]	*J = 5* (max) [546 nm]	*J = 4* (max) [586 nm]	*J = 3* (max) [622 nm]
λ = 205 nm	**368**	**675**	**184**	**78**
λ = 250 nm	**272**	**486**	**127**	**56**
λ = 282 nm	**283**	**520**	**132**	**59**
λ = 300 nm	**262**	**481**	**122**	**54**
λ = 366 nm	**2**	**3**	**< 1**	**< 1**

This experiment indicated that a Tb(III) complex had been formed, as indirect excitation of the complex resulted in a Tb(III) emission. The Tb(III) excited state which resulted in this

emission was produced by sensitisation of the Tb(III) metal center as discussed in Chapter 1, (Section 1.5).

Hydrolysis of **Tb.178** was attempted as shown in Scheme 6 to elucidate the final product, **Tb.160**. This involved stirring the complex in a 1.0 M solution of LiOH overnight, however, the desired product, **Tb.160** was not isolated during the workup of this reaction. Due to a lack of time and materials no further work was carried out on this synthesis.

4.3 Conclusion

The purposes of this project was to synthesis and evaluate **Tb.160** as a lanthanide luminescent chemosensor for the detection of Ca^{2+} at intracellular concentrations. The design, synthesis and characterisation of two potential Ca^{2+} receptors with amide spacers, **176** and **177** has been shown, as was the attachment of a tris alkylated cyclen ligand, **149**, with **176,** resulting in **178**. Synthesis of a Tb(III) complex, **Tb.178** was also demonstrated. Photophysical studies demonstrated that a sensitised Tb(III) emission can occur as a result of the antennae effect. The final product, **Tb.160** was not isolated following hydrolysis of **Tb.178**. However modifications to the final step should result in the desired product. This is to be a future project for the Gunnlaugsson research group.

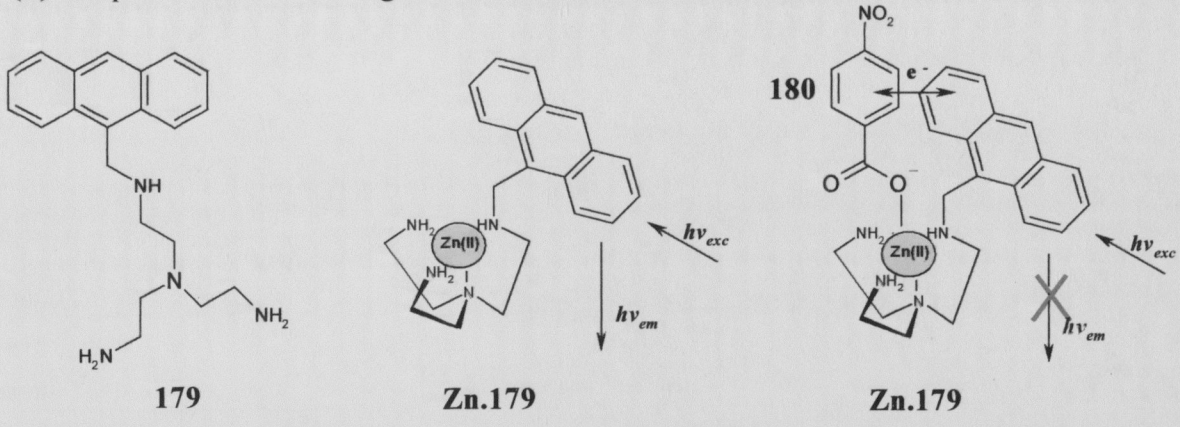
Chapter 5

Synthesis and photophysical studies of lanthanide luminescent sensors for the detection of aromatic carboxylates

5.0 Synthesis and photophysical studies of lanthanide luminescent sensors for the detection of aromatic carboxylates

5.1 Introduction

The design and synthesis of sensors for anions and neutral molecules has been an area of immense study in recent years.[187,188] The use of metal complexes as sensors in such situations has been discussed in many of these studies.[187, 188, 189] Metal complexes can form metal-ligand interactions with anions that are significantly stronger than hydrogen bonding, or other interactions commonly exploited for anion recognition[190] Fabrizzi *et al.* have demonstrated that Zn(II) complexes of **179** [190, 191] (Scheme 1) are sensors for aromatic carboxylates such as *p*-nitro benzoic acid, **180**. In this complex the zinc ion is coordinated by the tetraamine ligand **179** using the four amines, with a vacant site that could be occupied by either a solvent molecule or an anion. In MeOH a strong fluorescent emission is observed for **Zn.179** produced by the anthracence. However, in the presence of **180** electron transfer quenches this fluorescence. Another excellent example of a metal complex as an anion sensor include a Cu(II) complex with a tetraaza ligand that can detect coumarin 343.[192]



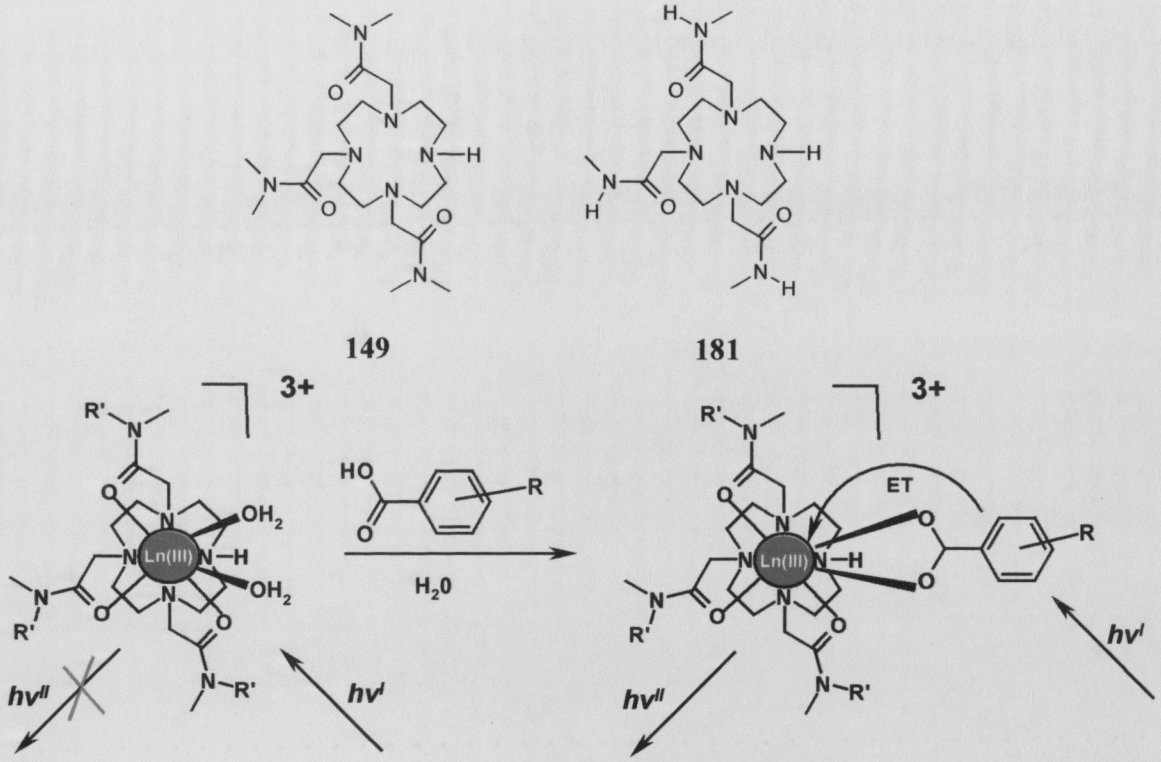
Scheme 1 - ***Illustration of* Zn.179 *as an aromatic carboxylate sensor***

The use of metal complexes for sensing anions has not been confined to transition metals alone. Over the past few decades the use of lanthanides as biological probes has been studied.[193,194, 195, 196, 197, 198, 199] Lanthanides such as Tb(III) and Eu(III) have been shown to displace cations, such as Ca(II), that can be found in the binding sites of proteins; such binding sites contain anionic groups to complex the cation. Excitation of surrounding aromatic

residues (such as tyrosine or phenylanaline) in these proteins can result in sensitisation of the lanthanide, producing a lanthanide emission.[200] Analytical chemists, in sensing the presence of drugs, have also utilized similar techniques.[201, 202, 203, 204] The formation of lanthanide complexes with a drug such as *m*-DOPA[205] occurs in a basic solution and in all cases excitation of the aromatic component of the drug, that was in close proximity to the lanthanide center, would lead to a lanthanide emission. The sensitivity of this technique has resulted in lower detection limits.[206] It has so far been shown that metal complexes can be used to detect aromatic anions and that lanthanide ions can be used in a similar fashion. However, the examples discussed for lanthanides have only involved the use of free lanthanide ions in basic solution. With the ultimate goal to detect anions *in vivo* the need for stable lanthanide complexes arises. Yu *et al.*[207] have demonstrated that stable Tb(III) [2.2.2] cryptates can be sensitized in aqueous solutions when coordinated with acac, a β-diketonate chelate . This requires the displacement of the two labile water molecules from the Tb(III) complex. Pikramenou *et al.* have shown aromatic carboxylates to act in a similar manner with Tb(III) [2.2.2] cryptates. Just like acac, the benzoic acid causes sensitization of the Tb(III) metal center upon displacement of bound water molecules and subsequent metal ion coordination.[208] In work reported by Diamandis *et al.* sensitization of Eu(III) and Tb(III) EDTA complexes at pH 11-12 using a number of aromatic carboxylate compounds such as 5- flourosalicylic acid was demonstrated.[209] Michels *et al.*[210] also showed similar results using an EDTA-bis(β-cyclodextrin) ligand showing sensitization following 1:2, complex:sensitizer adduct in aqueous solution. Parker *et al.* [135, 136] have reported the synthesis of the heptadentate cyclen based lanthanide complexes **Eu.94** and **Tb.94**. (Discussed in Chapter 1) Studies were carried out in solutions containing MES buffer with pH ranging between 6.4 and 7.3 demonstrated that stable lanthanide complexes can be produced that can detect the presence of anions under near physiological conditions. As discussed in many of the above cases, coordination to the anionic species displaces the two bound water molecules [137] from the Tb(III) or Eu(III) complexes. However, in this case the coordinating species was not a sensitizer. Instead, its presence as a coordinated species was detected by changes in the emission lifetimes of the lanthanide ion, and when the sensitizing ligands are chiral by changes in the CPL spectra.

5.1.1Project Objective

The purpose of this project was to synthesis heptadentate ligands **149** and **181** and their Eu (III) and Tb(III) complexes **Eu.149**, **Eu.181**, **Tb.149** and **Tb.181**. Furthermore these complexes were to be evaluated for their ability to coordinate and sense aromatic carboxylates. All these complexes are expected to be photophysically 'silent' upon excitation as no sensitising groups have been incorporated into the ligands, **149** and **181** and so no indirect excitation of the lanthanides can occur. However, in the presence of an aromatic carboxylate (Scheme 2) coordination could occur by displacement of any labile water molecules. After coordination, excitation of the aromatic carboxylate could result in a lanthanide ion emission by sensitisation from the triplet-excited state of the aromatic group by an energy transfer process.

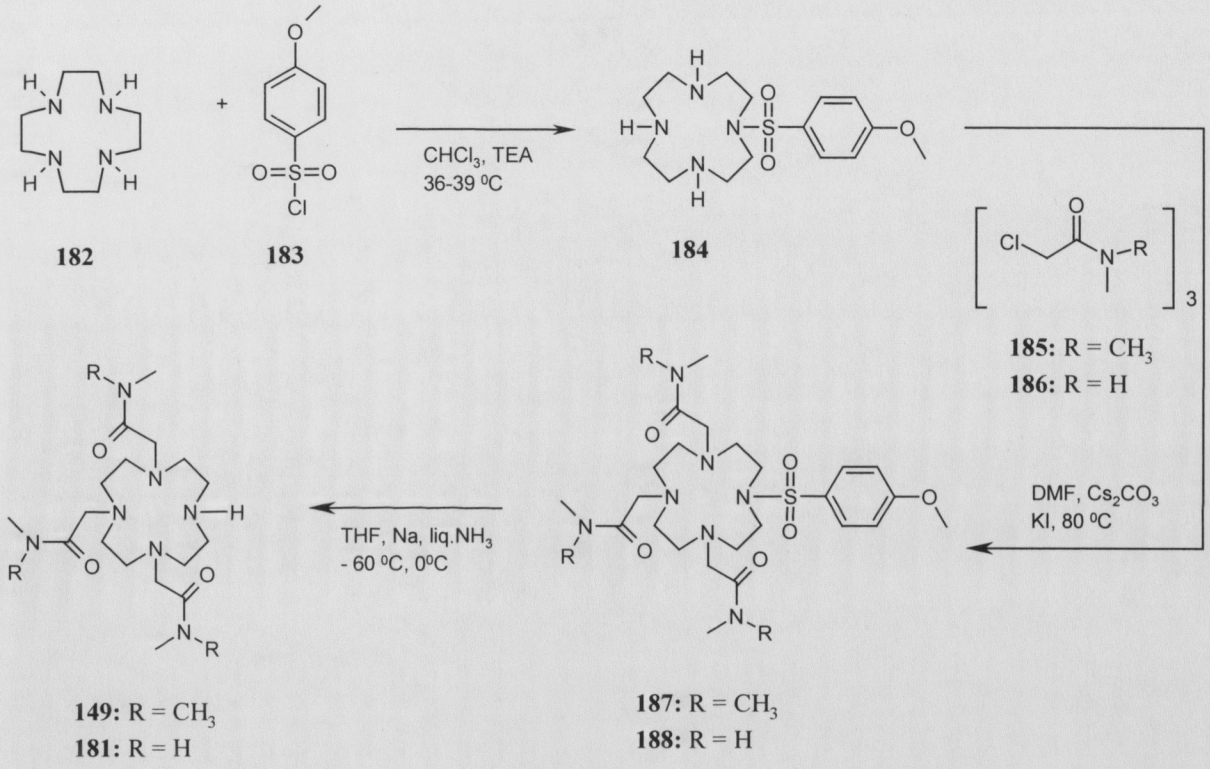


Eu.149: R' = CH_3, Ln(III) = Eu(III)
Tb.149: R' = CH_3, Ln(III) = Tb(III)
Eu.181: R' = H, Ln(III) = Eu(III)
Tb.181: R' = H, Ln(III) = Tb(III)

Scheme 2 – ***Complexes*** **Eu.149, Tb.149, Eu.181** ***and*** **Tb.181** ***and their proposed sensing function with aromatic carboxylates (R = implicit free site)***

5.2 Synthesis of 149 and 181 and their Eu(III) and Tb(III) complexes

Synthesis of ligands **149** and **181** involved tris *N*-alkylation of cyclen **182**, a macrocycle with four possible alkylation sites. In order to synthesis the proposed ligands, two possible synthetic routes were attempted. The first route (Scheme 3) involved a single *N*-protection of cyclen, **182**, in one of its four positions using one equivalent of *p*-methoxyphenylsulphonyl chloride, **183**.



Scheme 3 – ***Synthetic route 1: Synthesis of* 149 *and* 181 *by N-protection of* 182 *using p-methoxyphenylsulphonyl chloride* 183**

Synthesis of **184** involved dropwise addition of a $CHCl_3$ solution of **183** into a $CHCl_3$ solution of **182** in the presence of TEA at 36-39 °C. The resulting crude product contained a byproduct that was determined to be a bis tosylated cyclen complex. Purification by silica gel column chromatography using 90:10, MeCN:MeOH provided **184** in 53 % yield. This product was identified from its ^1H NMR spectra by the presence of two doublets at 7.72 ppm and 7.01 ppm and a singlet at 3.88 ppm resulting from the presence of the tosyl group. Alkylation of **184** using **185** or **186** was carried out in DMF at 80 °C using Cs_2CO_3 as a base

and KI to afford **187** or **188** respectively. **185** and **186** were produced from chloroacetyl chloride with the appropriate amine following published procedures.[211] Purification of **187** was achieved with alumina column chromatography using 97:3, EtOAc:MeOH giving **187** as an oil in 50 % yield whereas **188** was purified with alumina column chromatography using DCM:MeOH (1-5%) as an oil in 41 % yield. Both **187** and **188** were characterised by NMR spectroscopy, ESMS, accurate mass and infrared analysis. In the case of **188** a crystal structure was obtained in collaboration with other group members.[212] Figure 5.1 illustrates the crystal structure of **188** and clearly shows the presence of three mono methyl acetamide pendent arms attached to cyclen, along with the *p*-methoxyphenylsulphonamide protection. It was interesting to note that the crystal structure contained a single $CHCl_3$ molecule in the unit cell.

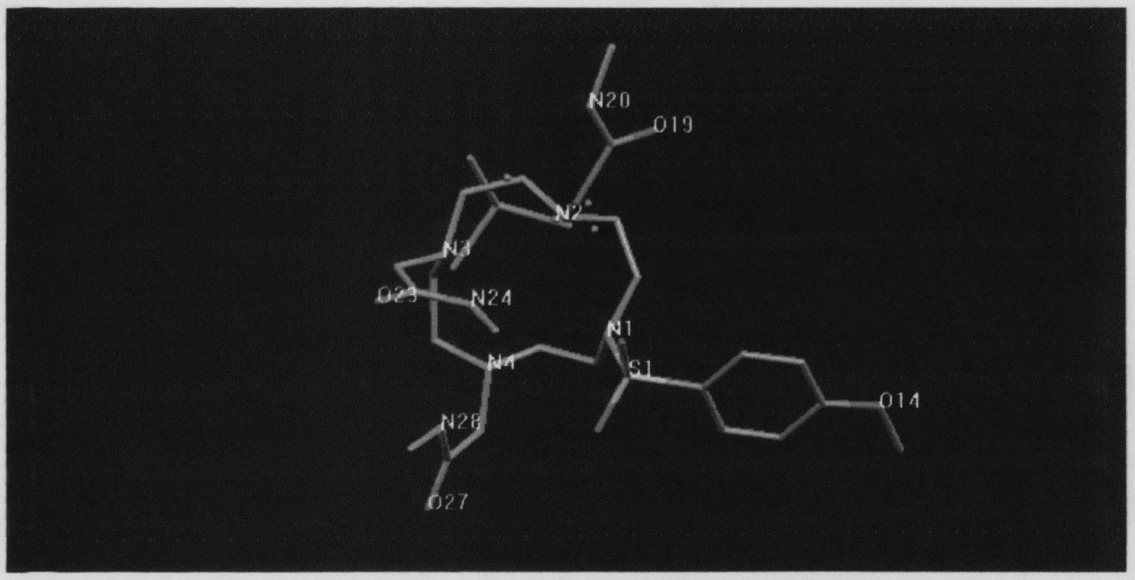


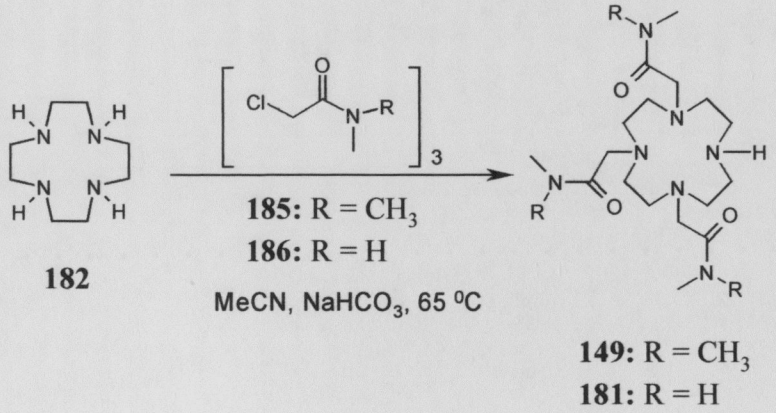
Figure 5.1 - ***X-ray crystal structure of* 188 *with* $CHCl_3$ *in unit cell (Hydrogen's omitted for clarity) – Obtained from group collaboration*** [212]

The final step in the synthesis of **149** and **181** involved deprotection of **187** and **188** using Birch conditions.[213] This was carried out by stirring a THF solution of **187** or **188** in the presence of Na metal and liquid ammonia at – 60 °C. Isolation of these products from the reaction solution involved acid base extraction, which in the case of **181** failed to give the required product even when continuous extraction techniques were used. However ligand **149**

was isolated in a low yield of 36 %. The results of this final step in the synthesis of **149** and **181** indicated that this synthetic pathway was not sufficient to synthesize the desired ligands and another method was required.

The second route attempted, involved direct alkylation (Scheme 4) of cyclen **182** with 3 equivalents of **185** or **186** to yield **149** and **181** respectively. A number of variations were attempted using this direct alkylation method, such as high dilution addition of **185** to **182**. On many occasions a number of byproducts were observed and mass spectral analysis of the reaction mixture showed the presence of mono, bis, tris and tetra alkylated cyclen. However a successful method was developed. This involved the use of cyclen, **182** that was stirred in a solution of MeCN and to this 3 equivalents of **185** (or **186**) was added directly. The resulting solution was stirred at 65 °C for 72 hours. In the case of **149**, the product was isolated as a viscous resin in a 52 % yield following purification on an alumina column using 97:3, CH_2Cl_2:MeOH(NH_3), while **181** was isolated in a 59 % yield as a white solid following precipitation from ether.

Of the two synthetic methods attempted the direct alkylation of **182** was determined to be the most efficient synthetic route for the synthesis of **149** and **181**, with yields over 50 % from a one step synthesis compared to total yields of 9.5 % for **149** and 0 % for **181** using the initial three step synthesis.



Scheme 4 – *Synthetic route 2: Synthesis of* **149** *and* **181** *by direct alkylation*

Ligands **149** and **181** were characterised using standard techniques. However, both were hygroscopic and elemental analysis of these ligands was not possible. Nevertheless, (ESMS) accurate mass spectroscopy was obtained for both. The ^{1}H NMR spectra of both ligands clearly reflect a C_2 symmetry. This C_2 symmetry runs along an axis through the unalkylated amine in position 1 and the tertiary amine in position 7 of the cyclen ring. The ^{1}H NMR spectrum of **181**, (shown in Figure 5.2) revealed the presence of two N-H singlets at 7.60 ppm and 7.30 ppm, in a ratio of 1:2 corresponding to the carboxylic amide protons. The two α-protons for the pendant arms appeared as singlets at 3.06 and 2.97 ppm (in a ratio of 4:2) respectively, whereas the N-CH_3 protons appear as two doublets in a ratio of 6:3 at 2.75 and 2.67 ppm respectively. The cyclen methyl protons were associated with the four broad singlets in the region of 2.7-2.4 ppm. The ^{1}H NMR spectrum for **149** showed similar characteristics.

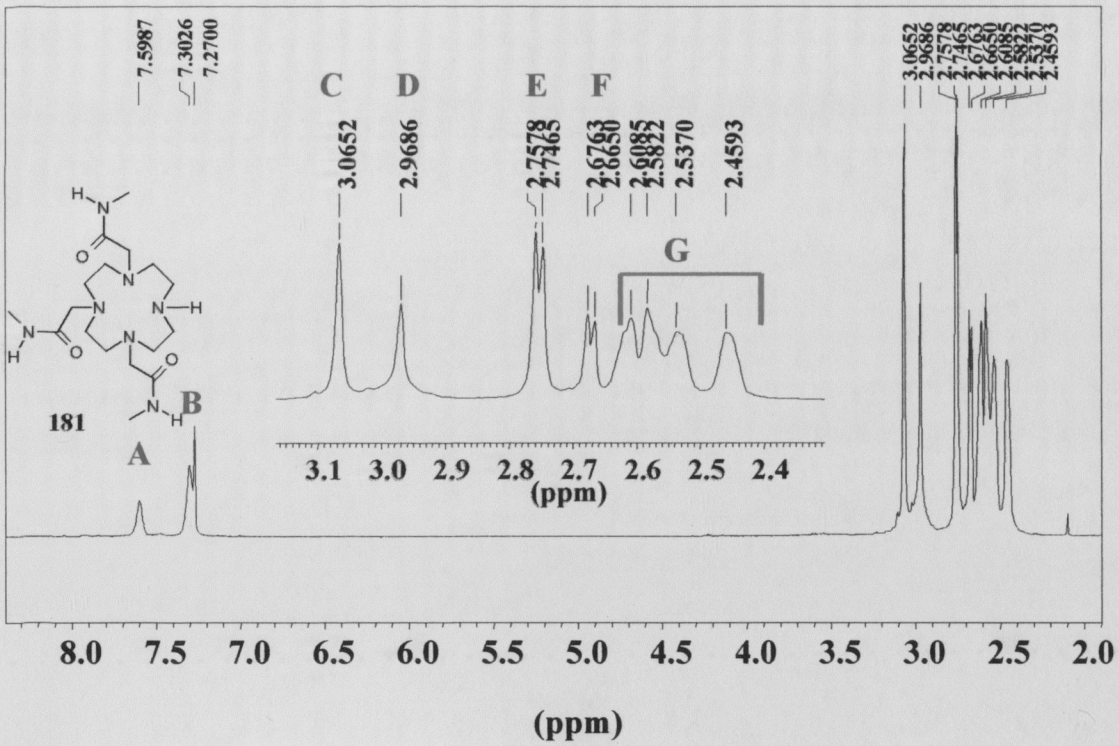
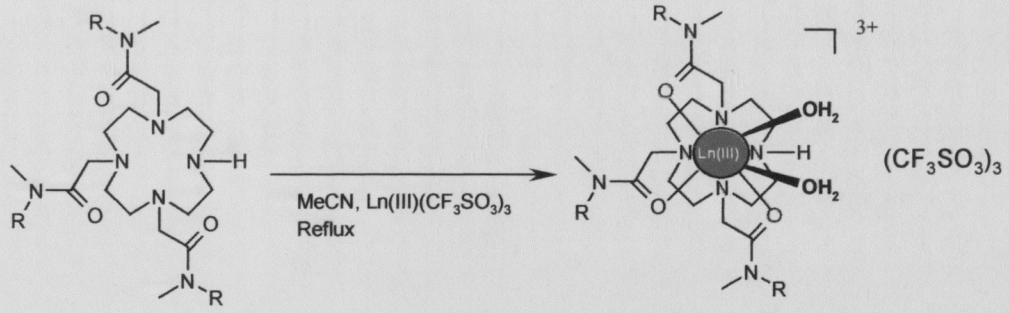


Figure 5.2 – *^{1}H NMR of* **181**, *A = N-H (1H), B = N-H (2H), C = CH_2 acetamide (4H), D = CH_2 acetamide (2H), E = CH_3 acetamide (6H), F = CH_3 acetamide (3H), G = CH_2 cyclen (16H). Cyclen N-H not observed.*

The ^{13}C NMR spectra for both **149** and **181** contained 10 signals. For **181** this consisted of two quaternary resonances at 171.5 ppm and 171.4 ppm corresponding to the carboxylic amide carbonyls of the pendant arms. Two CH_2 resonance signals at 59.54 ppm and 57.53 ppm were assigned to the pendant arms. Another four CH_2 signals observed from 53.3 ppm to 46.1 ppm correspond to the cyclen ring. The two final signals were found at 25.89 ppm and 25.72 ppm and correspond to the acetamide methyl groups. A similar ^{13}C NMR spectrum was obtained for **149**.

The synthesis of the metal complexes **Eu.149**, **Tb.149**, **Eu.181** and **Tb.181** involved refluxing **149** and **181** with Eu(III) and Tb(III) as their triflate salts in freshly dried MeCN (Scheme 5). [130] Upon cooling to room temperature the solutions were poured into stirring solutions of dry diethylether, and in all cases an oily residue was produced. These oils were collected by decanting the organic layers and the resulting residues were rinsed with either CH_2Cl_2 or $CHCl_3$. The resultant complexes were all isolated as powders in yields of *ca.* 95 % after exhaustive drying under vacuum over P_2O_5 for approximately two weeks. These complexes were characterised by elemental analysis, ESMS, accurate mass, IR and NMR spectroscopy. Similar results were observed for all of these complexes.



149: R = CH_3
181: R = H

Eu.149: R = CH_3, Ln(III) = Eu(III)
Tb.149: R = CH_3, Ln(III) = Tb(III)
Eu.181: R = H, Ln(III) = Eu(III)
Tb.181: R = H, Ln(III) = Tb(III)

Scheme 5 – *Synthesis of* Eu.149, Tb.149, Eu.181 and Tb.181 [130]

The ^1H NMR spectrum showed the presence of the paramagnetic metal centers, as indicated by several broad resonances appearing over a large ppm range. ESMS and accurate mass analysis proved very useful in characterization of these complexes. All four complexes gave similar spectra, which consisted of M+H peaks for the complex with one and two triflate counter anions present. In some instances M+H peak for the complex along with a large number of $M+H_n+Triflate_x/Z_n$ peaks. The peaks generated compared well with the theoretical isotope model, as shown below in Figure 5.3. It should be noted that the presence of the bound water molecules was not seen during analysis by mass spectroscopy. From IR spectroscopy the single carbonyl stretching frequency occurring at 1625 cm^{-1} in **149** was shifted when complexed to Eu(III) or Tb(III) to 1637 cm^{-1}, an indication that the pendent arms were indeed bound to the metal center.[211]

In summary, the synthesis of ligands **149** and **181** was shown to be achievable in modest yields in a one step synthesis. From these ligands the respective lanthanide complexes **Eu.149**, **Tb.149**, **Eu.181** and **Tb.181** were synthesised and isolated as pure compounds in high yields.

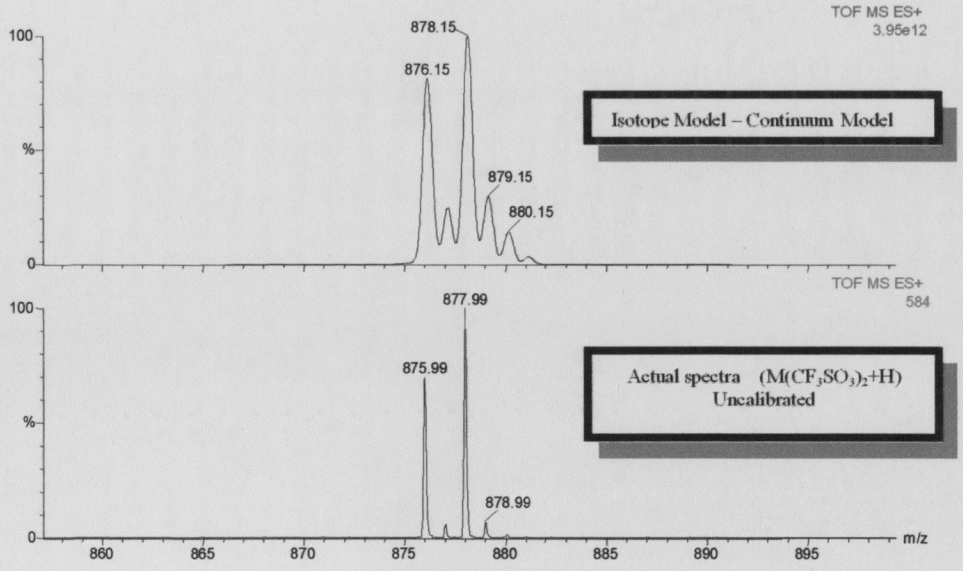


Figure 5.3 – ***ES Mass spectrum of* Eu.149 *and comparison to its theoretical isotopic model (peak shown is*** $(M(CF_3SO_3)_2+H)$ ***were*** $M = C_{20}H_{42}N_7O_3Eu$)

5.3 Determination of bound water in lanthanide complexes by lifetime analysis

The presence of two water molecules coordinated to the metal center in each of the lanthanide complexes **Eu.149**, **Tb.149**, **Eu.181**and **Tb.181** was not determined directly from characterisation, but was inferred by results obtained from elemental analysis. To determine conclusively the presence and number of these bound water molecules, estimations of ***q*** (the hydration state) were made. The luminescent emission required to measure each lifetime was produced by direct excitation of the metal center. The excited state lifetimes, τ of these complexes were measured in H_2O and in D_2O and their subsequent rates $1/\tau$ were inputed into equation 2 (Chapter 1) for Eu(III) complexes or equation 3 (Chapter 1) for Tb(III) complexes to compute the ***q*** values. The results of these studies and calculations are summarized in Table 5.1. In the case of **Eu.149** the lifetime in H_2O was calculated to be 0.281 ms and 0.855 ms in D_2O. From equation 2 (Chapter 1) a ***q*** value of 2.55 was found indicating at least two bound water molecules. A similar ***q*** value of 1.95 was calculated for **Eu.181**. The Tb(III) complexes gave longer lifetimes in both solvents. In the case of **Tb.149** the lifetime in H_2O was calculated to be 0.720 ms and 0.92 ms in D_2O. Using equation 3 (Chapter 1) a ***q*** value was calculated to be 2.01 indicating that the Tb(III) complexes also contain two bound water molecules. A similar result was determined for **Tb.181** giving a ***q*** value of 1.85. The shorter lifetimes in H_2O are attributed to quenching of the excited state of the lanthanide by O-H oscillators.[60] The results of these lifetime studies on **Eu.149**, **Tb.149**, and **Eu.181** and **Tb.181** showed that, as predicted earlier, each complex has two bound water molecules present.

Table 5.1 Measured lifetimes, rate constants and computed *q* values for Eu.149, Tb.149, Eu.181 and Tb.181†

Complex	τ_{H2O} (ms)	k_{H2O} (1/ms)	τ_{D2O} (ms)	k_{D2O} (1/ms)	q (± 0.5)
Eu.149	0.281	3.55	0.855	1.17	2.55
Eu.181	0.315	3.17	0.936	1.07	1.95
Tb.149	0.720	1.38	1.080	0.92	2.01
Tb.181	0.869	1.15	1.386	0.72	1.85

† - Lifetime measurements were carried out using a Varian Carey Eclipse Fluorimeter.

5.4 Crystallographic analysis of Eu.149, Tb.149 and Eu.181

Crystals of **Eu.149**, **Tb.149** and **Eu.181** were obtained that were suitable for X-ray crystallographic determination. The Eu(III) crystals of **Eu.149** and **Eu.181** were obtained by allowing slow evaporation from solutions of MeCN. Suitable crystals of **Tb.149** were formed by slow evaporation from a mixture of MeCN and CH_2Cl_2 (in the ratio of 1:1). The structures of **Eu.149**, **Tb.149** and **Eu.181** are shown in Figure 5.4, 5.5 and 5.6 respectively and a table of selected bond lengths and bond angles are presented in Table 5.2. All of the crystals adopted a square antiprism geometry in the solid state, a common geometry for lanthanide complexes.[214] In fact such geometry is well known for the tetra substituted octadentate lanthanide based cyclen complexes.[215, 216] All the crystal structures showed the presence of the two metal bound water molecules. After a literature examination of related structures it appears that, these were the first examples of such tri-amide lanthanide ion based cyclen complexes to show the presence of two bound water.[45] In all three complexes it was evident that the Ln(III) metal center was coordinated to the four nitrogens of the macrocycle ring and the three oxygens of the carboxylic amide pendent arms. The Ln(III) – N and Ln(III)) – O bond lengths were of similar length in all three complexes with average distances of *ca.* 2.64 Å and *ca.* 2.37 Å respectively. The Ln(III) – O1W and Ln(III) – O1W were almost identical in length within each complex. For **Eu.149**, **Tb.149** these bond lengths were similar with an average value of *ca.* 2.43 Å. This bond length was longer in **Eu.181** with an average of *ca.* 2.47 Å. The angle that these two water molecules bind to the metal centre was also of importance, since the nature of the binding mode with carboxylate anions would depend on the bite angle between the two water molecules. For **Eu.149** the O1W-Eu-O2W bite angle was measured to be 72.17 ° whereas for **Tb.149** the O1W-Tb-O2W bite angle was measured to be 71.80° and for **Eu.181** the O1W-Eu-O2W bite angle was measured to be 70.86°. Recently, Parker *et al.*[136] and Dickins *et al.* [137] have shown that related three-arm cyclen complexes can form bidentate adducts with organic anions such as acetate, citrate, glycinate, and lactate through four and five member chelates. The bite angles for all of these complexes were between 54° and 69°. In the case of acetate, this binding was bidentate and occurred through both of the carboxylate oxygens. From these reports and the bite angles calculated for **Eu.149**, **Tb.149** and **Eu.181** it was proposed that aromatic carboxylates would bind in a similar bidentate manner.

Table 5.2 Selected bond lengths and angles for Crystals of Eu.149, Tb.149 and Eu.181†

Eu.149			
Bond length label	Bond length (Å)	Bond angle Label	Bond angle (°)
Eu1 O15	2.342(5)	O25 Eu1 N10	65.39(19)
Eu1 O25	2.364(5)	O19 Eu1 N7	64.10(19)
Eu1 O19	2.378(5)	O15 Eu1 N4	65.13(19)
Eu1 O1W	2.418(5)	O1W Eu1 O2W	72.17
Eu1 O2W	2.421(5)		
Eu1 N1	2.605(6)	N-C-C-O	-2.5(11)
Eu1 N10	2.624(6)		-27.6(10)
Eu1 N7	2.625(6)		-25.4(10)
Eu1 N4	2.647(6)		
Tb.149			
Bond length label	Bond length (Å)	Bond angle Label	Bond angle (°)
Tb1 O15	2.348	O27 Tb1 N10	65.42
Tb1 O27	2.325	O20 Tb1 N7	64.54
Tb1 O20	2.368	O15 Tb1 N4	65.67
Tb1 O1W	2.429	O1W Tb1 O2W	71.80
Tb1 O2W	2.441		
Tb1 N1	2.601		
Tb1 N10	2.656	N-C-C-O	5.6(7)
Tb1 N7	2.637		25.6(6)
Tb1 N4	2.641		26.5(6)
Eu.181			
Bond length label	Bond length (Å)	Bond angle Label	Bond angle (°)
Eu1 O14	2.378		
Eu1 O22	2.394	O22 Eu1 N7	65.98
Eu1 O18	2.399	O18 Eu1 N4	65.54
Eu1 O1W	2.449	O14 Eu1 N1	66.14
Eu1 O2W	2.485	O1W Eu1 O2W	70.86
Eu1 N1	2.673		
Eu1 N10	2.617		
Eu1 N7	2.670	N-C-C-O	-30.0(7)
Eu1 N4	2.677		-32.7(1)
			-36.4(5)

† Selected parameters taken from CIF file data or generated from Mercury 1.1 ©

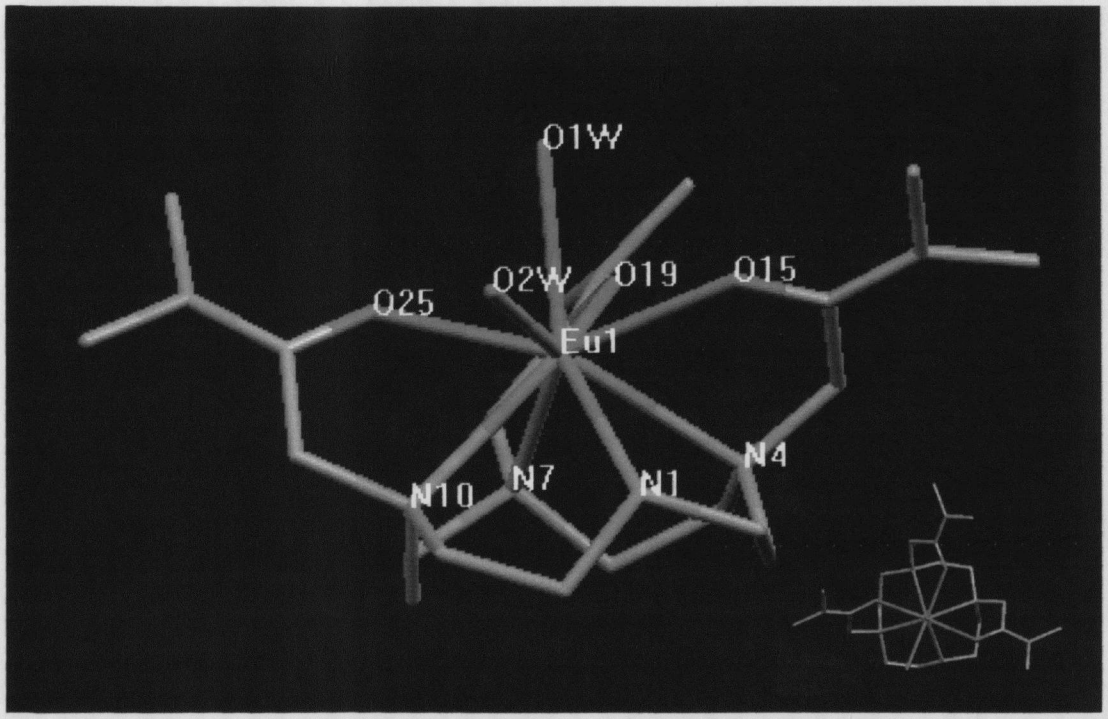


Figure 5.4. ***X-ray crystal structure of*** **Eu.149** ***showing the presence of two bound water molecules (Hydrogen's and triflates omitted for clarity)*** Inset: Top view showing square antiprism geometry

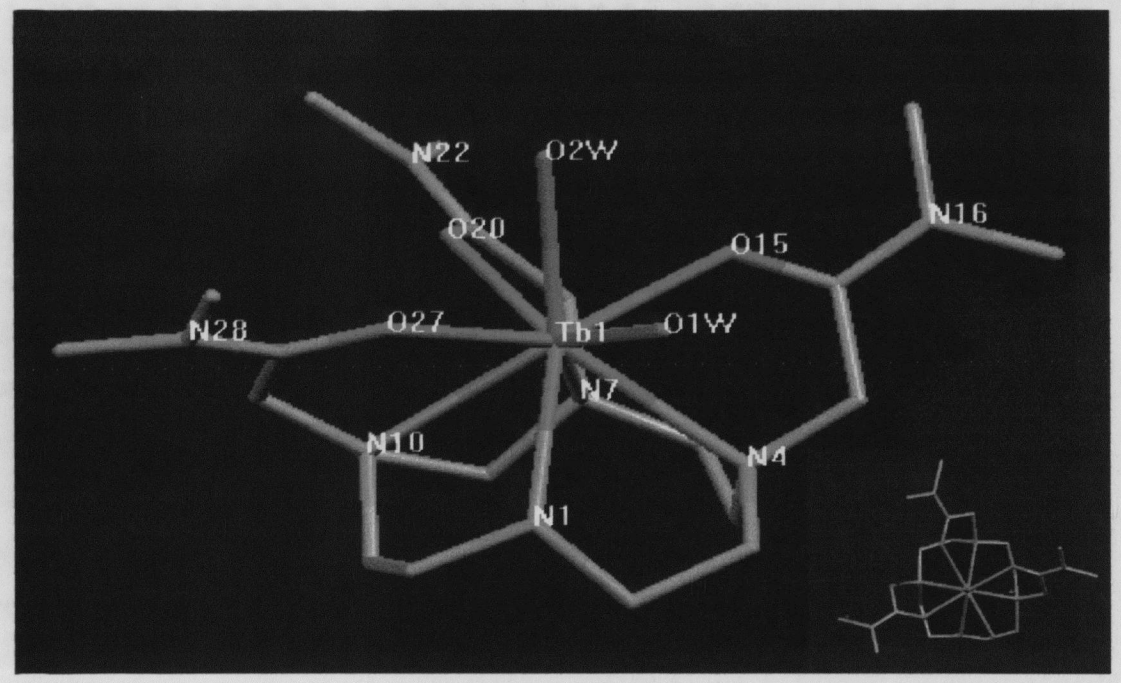


Figure 5.5. ***X-ray crystal structure of*** **Tb.149** ***showing the presence of two bound water molecules (Hydrogen's and triflates omitted for clarity)*** Inset: Top view showing square antiprism geometry

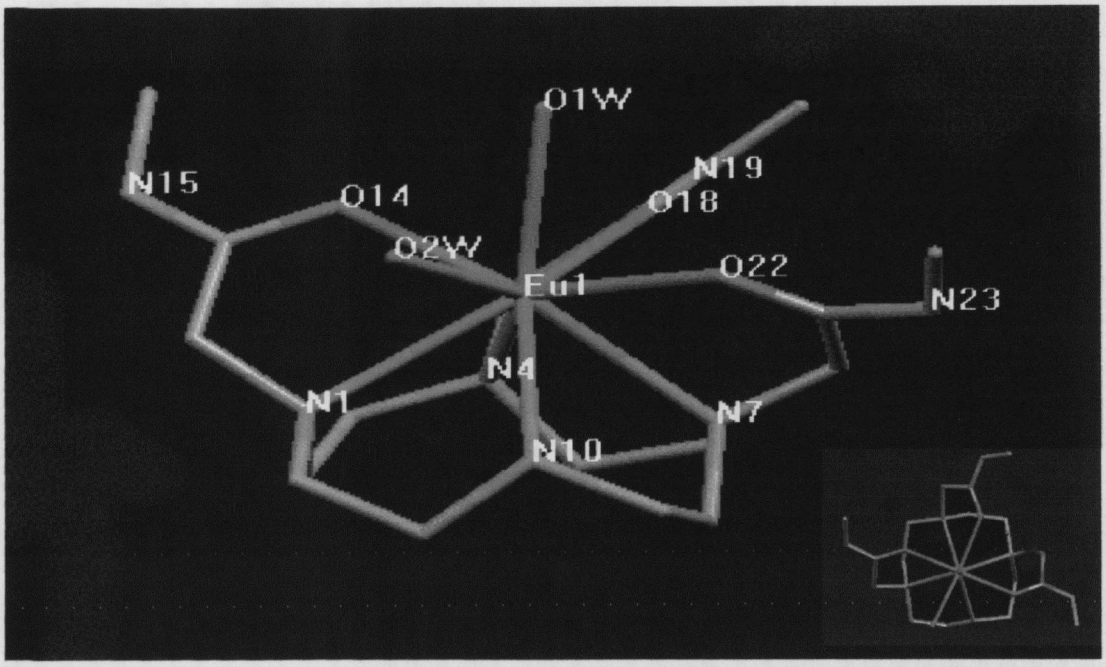
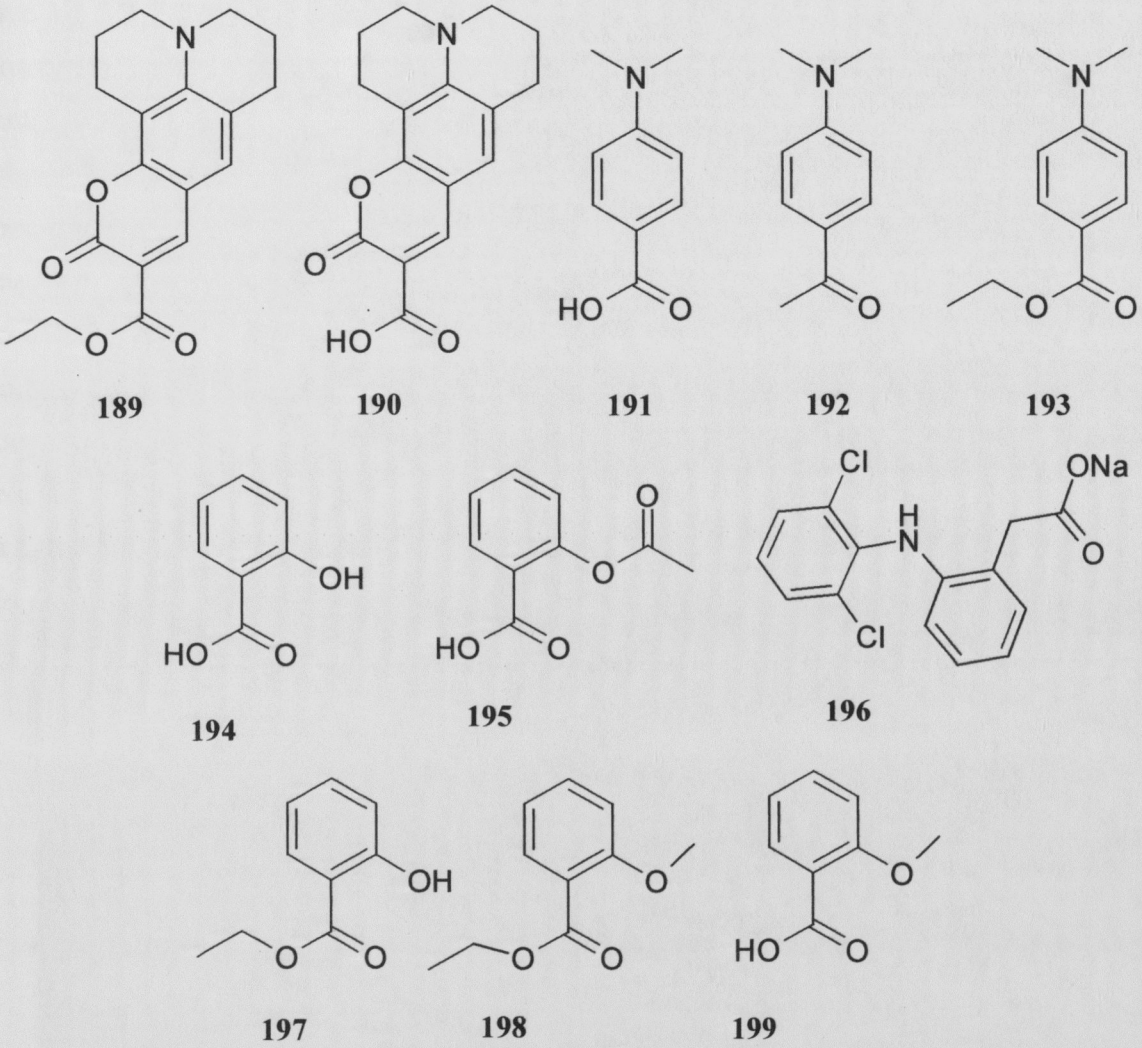


Figure 5.6. ***X-ray crystal structure of*** **Eu.181** ***showing the presence of two bound water molecules (Hydrogen's and triflates omitted for clarity)*** Inset: Top view showing square antiprism geometry

5.5 Photophysical analysis of Eu.149, Tb.149, Eu.181 and Tb.181 with aromatic carboxylates

Photophysical studies were performed on **Eu.149**, **Tb.149**, **Eu.181** and **Tb.181** using a number of aromatic carboxylates, esters and ketones (**189-199**), illustrated in Figure 5.7, to determine the sensing capability of the lanthanide complexes. For all of these compounds (**189-199**), the triplet energy was above 22,000 cm^{-1}, [217] sufficient to populate the lowest excited state, $^5D_4$ and $^5D_0$ of Tb(III) and Eu(III) respectively. (Figure 1.5 and 1.6 , Chapter 1) Photophysical studies involved titration of a lanthanide complex in aqueous or buffered solutions, at concentrations of *ca.* 16-17 μM, with solutions of **189-199**. All the lanthanide complexes were shown to be stable in solution, as indicated by comparing the results obtained from solutions made as required with the results of those obtained from stored samples. In each case the excitation wavelength chosen was the λ_{max} of each sensitiser tested (Section 6.4.3). These studies began with **189** and **190**, two coumarin based compounds, **189** containing a carboxylate and **190** its ethyl ester derivative. In titrations carried out with all four lanthanide

complexes no lanthanide emission was seen, even when 40 equivalents of **189** (or **190**) was added. These results were attributed to an inability of **189** and **190** to bind efficiently with the lanthanide complexes.



189 **190** **191** **192** **193**

194 **195** **196**

197 **198** **199**

Figure 5.7. ***Aromatic carboxylates and esters used in photophysical analysis of*** **Eu.149, Tb.149, Eu.181** ***and*** **Tb.181**

In titrations performed using **191**, lanthanide luminescent emissions were observed for the two Tb(III) complexes, **Tb.149** and **Tb.181**. However, the Eu(III) complexes **Eu.149** and **Eu.181** showed no response. The lanthanide emission spectrum of **Tb.149** produced from a titration with **191** (Figure 5.8) showed a characteristic Tb(III) emission with four emission bands observed at 491 nm (J=6), 548 nm (J=5), 587 nm (J=4), and 622 nm (J=3) reflecting

transitions $^5D_4 - {}^7F_J$, when the solution was excited at 300 nm. Before the addition of **191** to a solution of **Tb.149** no lanthanide emission was observed. However, upon addition of **191** sensitization was indicated by the appearance of the four narrow emission bands (as described above). The intensity was seen to increase as the concentration of **191** increased. A maximum intensity of 680 was reached for the emission band at 548 nm (J=5), indicating a 680-fold emission enhancement. With further additions of **191** this intensity was seen to decrease significantly. The relationship between the observed emissions and the concentration of **191** present in the **Tb.149** solution is described in Figure 5.9 and 5.10. The concentration (and equivalents) plot (Figure 5.9), shows approximately 1:1 binding occurring between the complex **Tb.149** and **191**.[163] With the addition of two equivalents of **191** maximum emission enhancement had been reached. Whereas after four equivalents the emission intensity had begun to decrease returning to zero after twelve equivalents of **191** had been added. A plot of emission intensity as a function of p**191** (where p = -log [**191**]) (Figure 5.10) showed this to be a bell shaped relationship with emission changes occurring over approximately two log units (~ 4-6) another indication of 1:1 binding. From these changes a binding constant, log β = 5.2 ($\pm$ 0.2) was determined. [162] At concentrations higher that p[**191**] = 4 , quenching was observed.

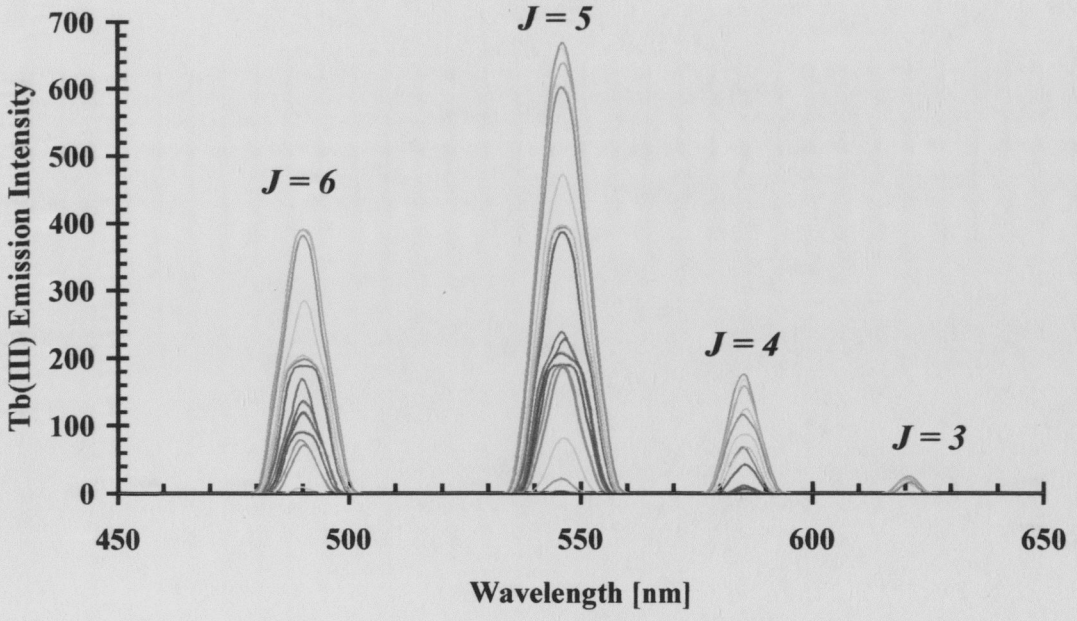


Figure 5.8. ***Lanthanide emission spectrum of* Tb.149** ***(16-17 μM) from titration with* 191** ***(0-0.4 mM) in aqueous solution. (Results of titration on Perkin Elmer LS 50B)[λ_{excite} = 300 nm]***

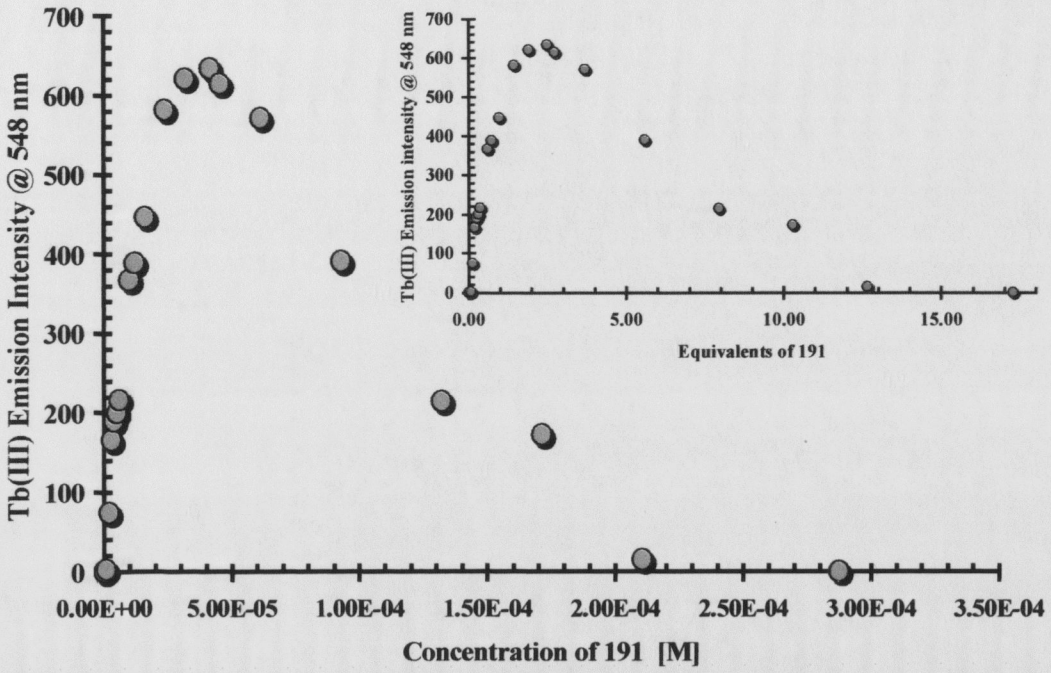


Figure 5.9. ***Tb(III) emission intensity as a function of concentration – Titration of*** **Tb.149** ***(16-17 μM) with 191 (0-0.4 mM). [λ_{excite} = 300 nm]*** (Inset: Tb(III) emission intensity *vs.* equivalents)

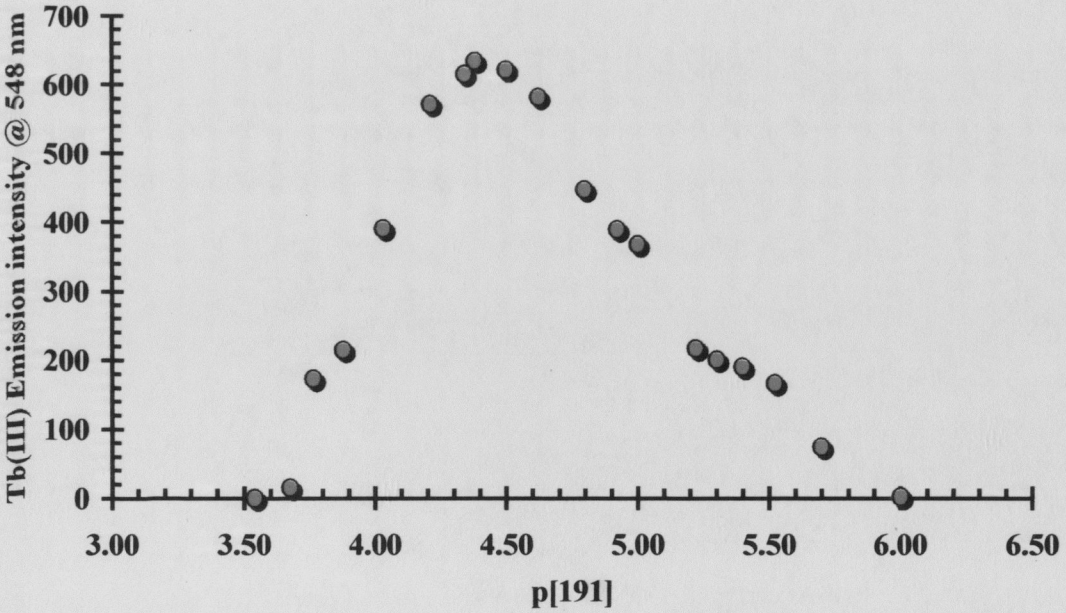


Figure 5.10. ***Tb(III) emission intensity as a function of p[191] – Titration of*** **Tb.149** ***(16-17 μM) with*** **191** ***(0-0.4 mM). [λ_{excite} = 300 nm]***

When these measurements were repeated on **Tb.181** similar results were observed. However, in this case the emission enhancement was lower. The lower intensity can be attributed to additional quenching of the Tb(III) excited state by the N-H oscillators present in the complex.[60] The maximum intensity observed at 548 nm (J=5), was 220, a 220-fold increase in emission enhancement. The equivalents plot (Figure 5.11), showed approximately 1:1 binding between the complex **Tb.181** and **191**. [162] This result was similar to that seen for **Tb.149**. With the addition of two equivalents of **191** maximum emission enhancement had been reached and this enhancement remained at a maximum intensity until four equivalents had been added whereupon the emission intensity began to decrease. From Figure 5.11 it can be seen that the 'switching off' of the emission intensity required more equivalents of **191** to "switch off" the emission than was observed for **Tb.149**. A plot of emission intensity as a function of p[**191**] (Figure 5.12) showed this to be a bell shaped relationship with emission changes occurring over approximately two log units (3.5-5.5) similar to the result observed for **Tb.149**. In this case a binding constant, log β = 4.9 ($\pm$ 0.2) was determined. The same experiments were repeated on the Eu(III) complexes **Eu.149** and **Eu.181**. In these instances no changes were observed in the emission spectra when these titrations were performed using **191**. This was unexpected, as the excited state of Eu (III) is significantly lower than that of Tb(III) and efficient population of the lanthanide $^5D_0$ excited state was anticipated. From luminescent lifetime analysis, (Section 5.4.1) this result was attributed to poor binding between **Eu.149** (or **Eu.181**) and **191**. Titrations were repeated on **Tb.149** and **Tb.181** in buffered solutions at pH 7.4 with **191**. In both titrations the lanthanide emissions were again seen upon addition of **191** but the maximum emission enhancement were lower in both cases at *ca.* 420 (Figure 5.13) and *ca.* 120 for **Tb.149** and **Tb.181** respectively. The decrease in emission enhancement was attributed to interference from the background salts, as the binding constant observed, log β = 5.0 ($\pm$ 0.2) was now lower. The experiments in buffered solutions demonstrated that the use of these complexes *in vivo* might be possible. Furthermore, the switching "on" and "off" the lanthanide emission was not due to a pH effect, that is, quenching was not due to the protonation of **191** with concomitant dissociation of the ternary complex, as this switching was observed in buffered solutions as well. From analysis of the absorption data collected during the titrations with **191** it was determined that the quenching of the lanthanide luminescence was the result of the inner filter effect. The results of this analysis

can be seen in Table 5.3 and Figure 5.14. From Table 5.3 it can be seen that as the absorbance increases with each addition of **191** the transmittance decreases significantly. Figure 5.14 shows the corrected Tb(III) emission due to the increasing absorbance value as **191** is added to the solution of **Tb.181**, in which no quenching was observed.

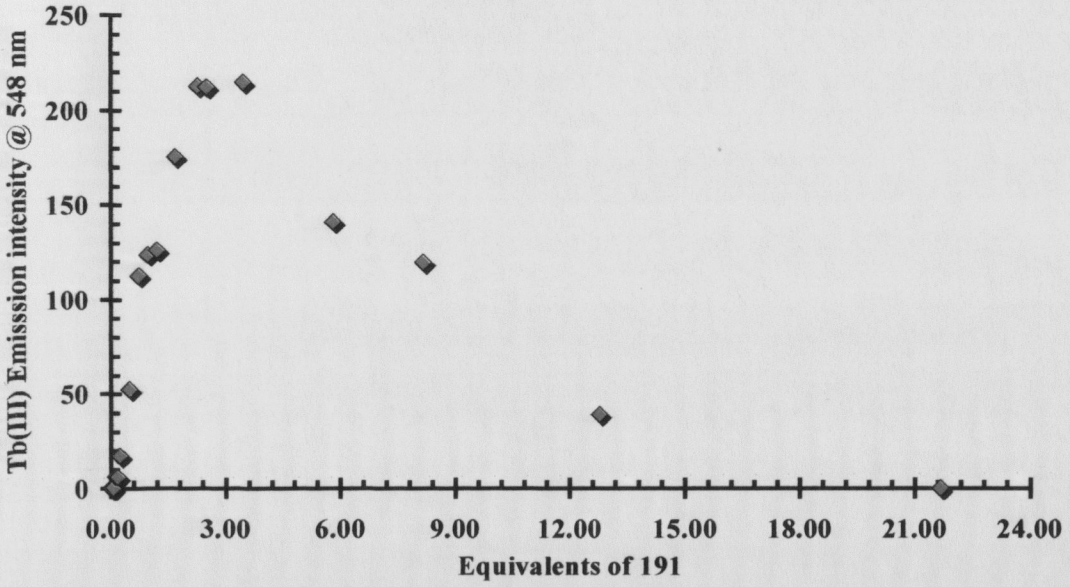


Figure 5.11. ***Tb(III) emission intensity as a function of equivalents – Titration of*** **Tb.181** ***(16-17 μM) with 191 (0-0.4 mM). [λ_{excite} = 300 nm]***

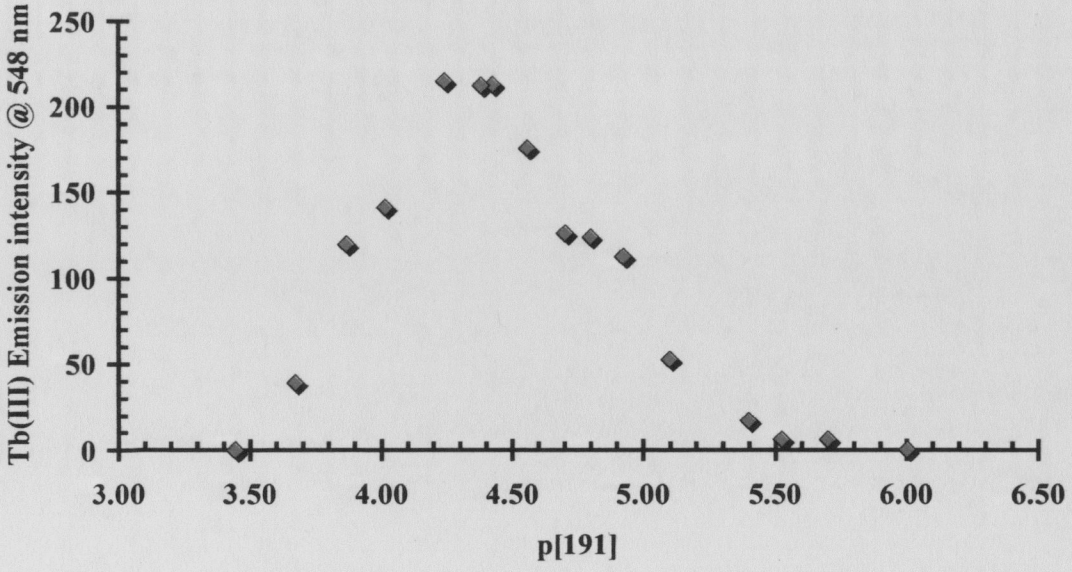


Figure 5.12. ***Tb(III) emission intensity as a function of p[191] – Titration of*** **Tb.181** ***(16-17 μM) with*** **191** ***(0-0.4 mM). [λ_{excite} = 300 nm]***

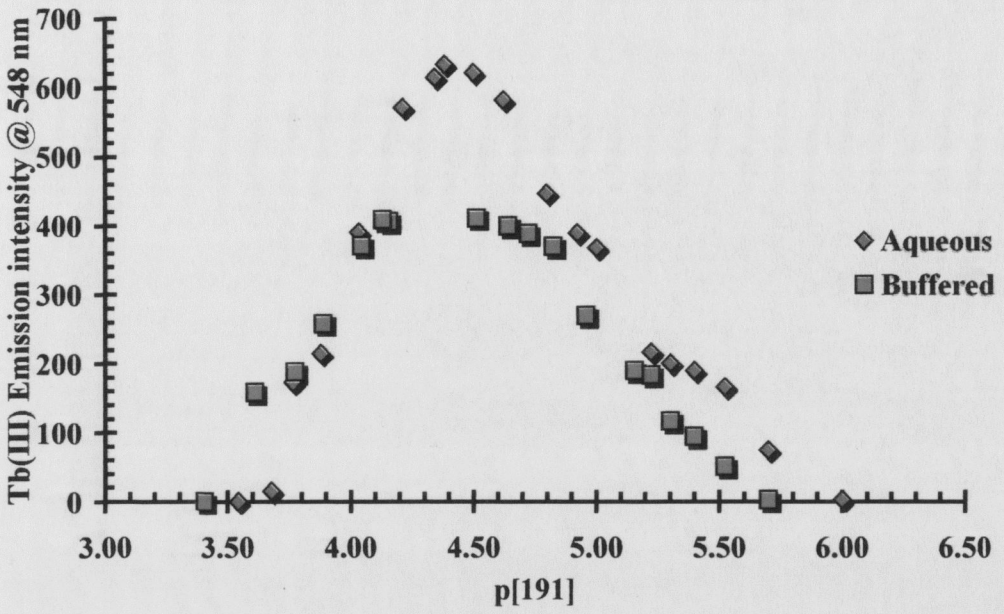


Figure 5.13. ***Effect of aqueous vs. buffered solutions on titration of*** **Tb.149** ***(16-17 μM) with*** **191** ***(0-0.4 nM). [λ_{excite} = 300 nm]***

Table 5.3 Absorption analysis Tb.181 with 191 and corrected emission (Emission/(I/I_0))

conc [191]	Abs @ 0.5 cm	$T(I/I_0)$	Tb(III) Intensity 547 nm	Tb(III) Emission / (I/I_o)
9.98E-07	0.000	1.000	17.51	17.51
2.00E-06	0.005	0.990	27.75	28.04
3.99E-06	0.009	0.979	45.6	46.57
5.98E-06	0.018	0.959	61.91	64.57
7.97E-06	0.027	0.939	77.66	82.72
1.19E-05	0.037	0.919	101.56	110.47
1.59E-05	0.055	0.882	120.51	136.69
2.39E-05	0.073	0.845	150.79	178.39
3.19E-05	0.110	0.777	172.1	221.46
3.98E-05	0.146	0.714	181.67	254.29
5.57E-05	0.183	0.657	191.77	291.97
7.94E-05	0.255	0.556	183.86	330.96
9.92E-05	0.364	0.433	174.4	403.19
1.38E-04	0.455	0.351	146.42	417.17
1.78E-04	0.634	0.232	122.08	526.09
2.17E-04	0.814	0.153	105.56	688.05
2.56E-04	0.994	0.101	95.69	943.39
3.33E-04	1.174	0.067	73.6	1097.51

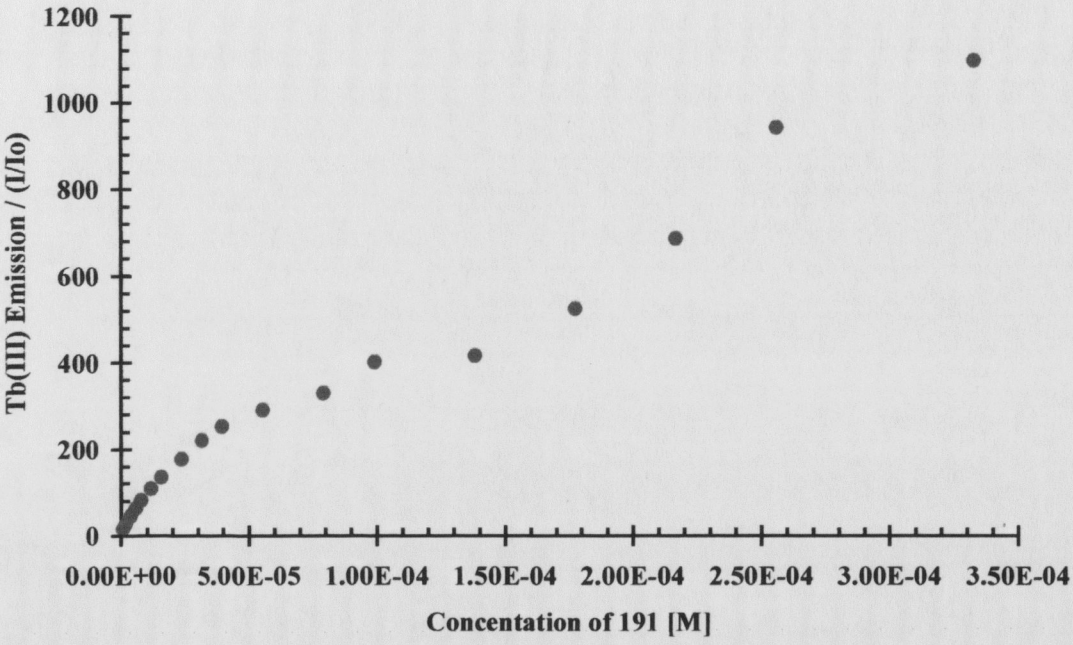


Figure 5.14. ***Corrected Tb(III) emission intensity as a function of [191] – Titration of*** **Tb.181** ***(16-17 μM Buffered solution) with*** **191** ***(0-0.35 mM). (Results of titration on Varian Cary Eclipse) [λ_{excite} = 300 nm]***

The above measurements were repeated using **192** and **193**. These were similar to **191**, **192** being a ketone and **193** an ester. No changes were seen in the emission spectra of **Tb.149**, **Eu.149**, **Tb.181** and **Tb.181** upon titration with either **192** or **193**. It was thus concluded that it was necessary to have the carboxylate present for efficient binding to the metal ion to allow sensitisation to occur.

5.5.1 Lifetime analysis of Eu.149, Tb.149, Eu.181 and Tb.181 with 191

Lifetime analysis of **Eu.149**, **Tb.149**, **Eu.181** and **Tb.181** were performed to determine the hydration state of the complexes in the presence of **191**, the results of which are summarized in Table 5.4. Initially (Section 5.2) it was determined that all of these complexes had two water molecules bound to the lanthanide metal center. When the lifetimes were measured by direct excitation in the presence of 4 equivalents of **191** significant differences were observed in the lifetimes of **Tb.149** and **Tb.181** in both H_2O and D_2O indicating a change in the

environment around the lanthanide complexes. In both complexes the lifetimes were observed to increase as a result of the removal of the bound waters whose O-H oscillations deactivate the lanthanide excited state. Using equation 3 (Chapter 1), ***q*** values were calculated to be 0.06 and 0.14 for **Tb.149** and **Tb.181** respectively which indicated that the bound waters had been displaced. The lifetimes of **Eu.149** and **Eu.181** showed no significant change in the presence of **191** from that previously determined. Estimations of the ***q*** value of each complex using equation 2 (Chapter 1) resulted in values of 2.07 and 1.80 for **Eu.149** and **Eu.181** respectively. These values clearly show that the bound waters have not been displaced from the complexes.

Table 5.4 Measured lifetimes, rate constants and computed *q* values for Eu.149, Tb.149, Eu.181 and Tb.181 in the presence of *N,N*-dimethylaminobenzoic acid (191). †

Complex	τ_{H2O} (ms)	k_{H2O} (1/ms)	τ_{D2O} (ms)	K_{D2O} (1/ms)	q (± 0.5)
Eu.149	*0.235*	*4.25*	*0.438*	*2.28*	*2.07*
Eu.181	*0.276*	*3.62*	*0.733*	1.35	1.80
Tb.149	*1.593*	*0.62*	*1.795*	*0.55*	*0.06*
Tb.181	*1.626*	*0.61*	1.895	0.52	0.14

† - 4 equivalents of **191** were used in all studies

In summary, the above results have shown that the Tb(III) complexes can bind aromatic carboxylates and in this state can be sensitised thus indicating their presence. From calculated ***q*** values it has been determined that sensitisation occurs only upon binding allowing energy transfer from the excited state of the aromatic triplet to the metal center. Photophysical inactivity in the Eu complexes was caused by inefficient binding of the carboxylates. Results in buffered solutions showed lower emission and slightly lower binding constants due to interference from background salts. Nevertheless these complexes may be suitable for *in vivo* applications.

5.6 Photophysical evaluation of Tb.149, Tb.181, Eu.149 and Eu.181 with physiological important aromatic carboxylates and their related derivatives

Lanthanide-sensitised luminescence has been shown to be possible with other aromatic carboxylates such as benzoic acid, saccharin[202,204] and salicylic acid.[205] Salicylic acid, **194** is a physiologically active molecule with analgesic and anti-inflammatory properties.[218] It is delivered into the body in its inactive form, Aspirin®, **195**, which is hydrolyzed by esterase enzymes to yield the free active drug in circulating blood.[13] The ability to measure the concentration of salicylic acid *in vivo* would be advantageous as over dosage can cause gastric bleeding that can result in fatal conditions.[218] The fatal dose of salicylic acid is estimated to be 0.2-0.5 g/Kg. [218] Toxic effects can occur at varying plasma levels depending on the duration of poisoning but are uncommon below 30 mg/dL.[218] With this in mind **Tb.149**, **Tb.181**, **Eu.149** and **Eu.181** were used to investigate the effect of binding to **194** and **195** as well as their ability to produce Eu(III) and Tb(III) emissions.

5.6.1 Photophysical evaluation of Tb.149, Tb.181, Eu.149 and Eu.181 with 194 and 195

No enhancements were observed in the Eu(III) emission using **Eu.149** and **Eu.181** in the presence of **194** or **195** when measured in either aqueous or pH 7.4 buffered solution, as was the case with **191**. Inefficient binding was believed to be the cause. In aqueous solution of both **Tb.149** and **Tb.181** enhancements were observed in the Tb (III) emission upon addition of **194**. The enhancement factor was considerably lower in both cases compared to those observed for **191**. This may have been due to a lower lying triplet state[125] in **194** compared to **191** or inefficient energy transfer, and or inefficient binding. The enhancement factor for **Tb.149** and **Tb.181** upon addition of **194** was *ca.* 50 and *ca.* 3 respectively The lower intensity for **Tb.181** can be attributed to additional quenching of the Tb(III) excited state by the N-H oscillators present in the complex.[60] When these titrations were repeated on **Tb.149** and **Tb.181** in buffered solutions the enhancement factor was found to decrease to *ca.*30, as had been observed for **191**. However, only **Tb.149** showed changes in emission intensity in the presence of **194**. **Tb.181** was inactive to **194** due to deactivation of the excited state by N-H oscillators present in the complex and lower binding efficiency in buffered solution, both of these effects had been previously noted from results with **Tb.181** and **191**. The changes in the Tb(III) emission were highly concentration dependent, though not to the same extent as seen

for **191**. As shown from Figure 5.15, the luminescence is switched on over ca. 2 log units from 5.5 to 3.5. This switching 'on' as seen before was an indication of 1:1 binding and simple equilibrium. From these changes a binding constant log $\beta = 4.5$ (± 0.2) was determined. This was lower than that found for **191**. The quenching effect was observed but was less pronounced (Figure 5.16). In Figure 5.16 the Tb(III) emission was seen to gradually increase until *ca.* 6 equivalents had been added. However, between 6 and *ca.* 15 equivalents of **194**, the emission was not dependent on the concentration. At higher concentration, *ca.* 17, the emission began to switch off but was never fully quenched. (Not shown).

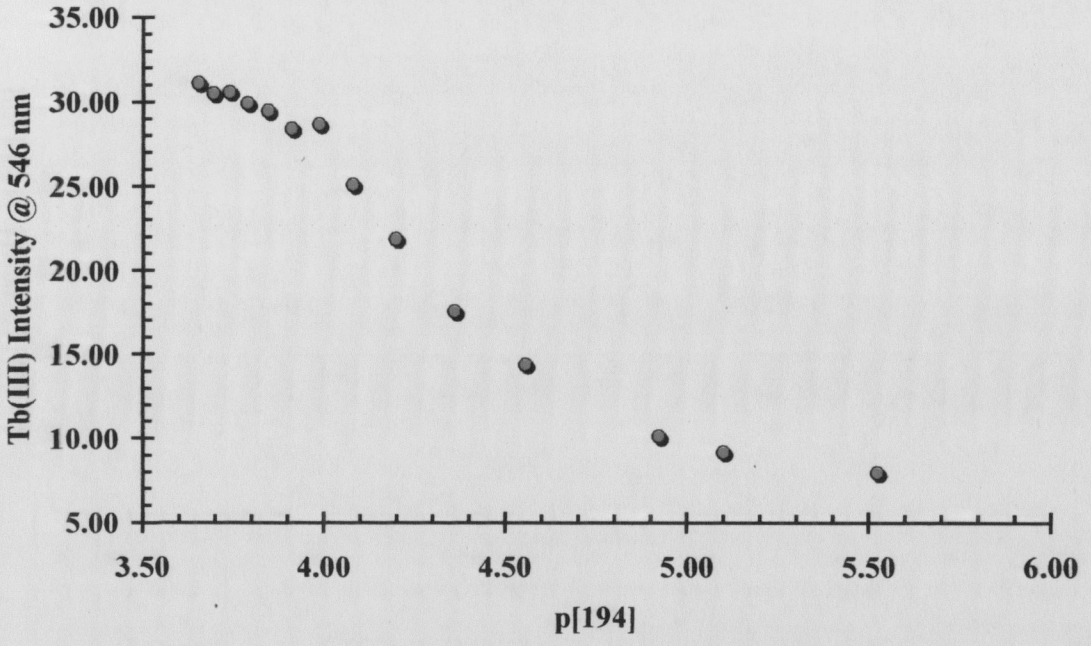


Figure 5.15. ***Tb(III) emission intensity as a function of p[194] – Titration of*** **Tb.149** ***(16-17 μM Buffered solution) with*** **194** ***(0-0.4 mM). (Results of titration on Varian Cary Eclipse) [$\lambda_{excite} = 300$ nm]***

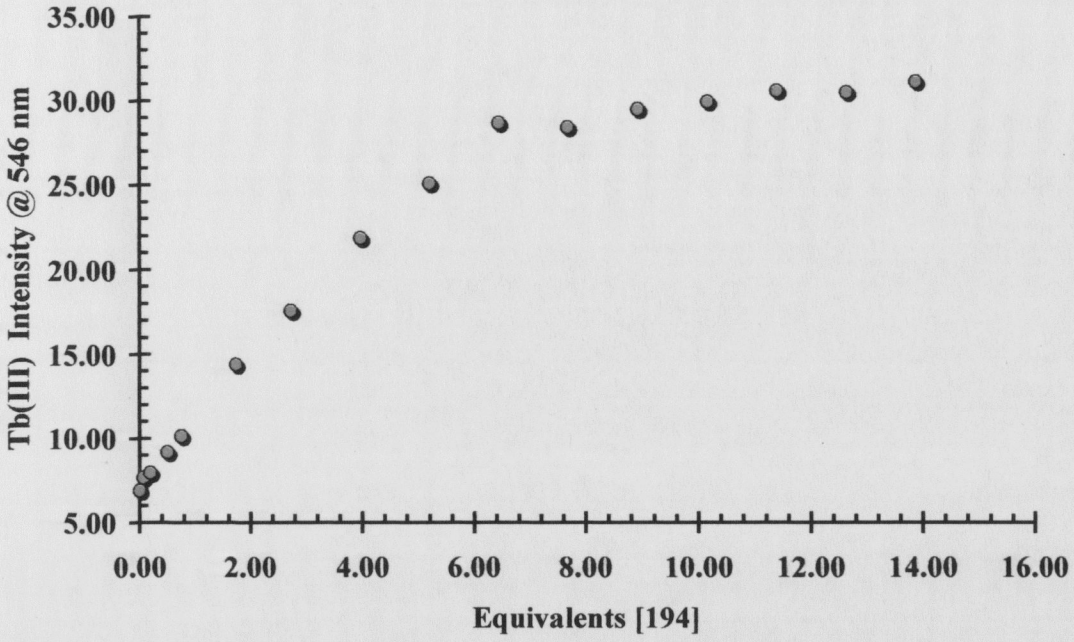


Figure 5.16. ***Tb(III) emission intensity as a function of equivalents – Titration of*** **Tb.149** ***(16-17 μM Buffered solution) with*** **194** ***(0-0.4 mM). (Results of titration on Varian Cary Eclipse) [λ_{excite} = 300 nm]***

When these titrations were repeated using **195**, in aqueous or buffered solutions no luminescent enhancements were observed in the Tb(III) emission for either **Tb.149** or **Tb.181**. This indicated that **195** was unable to bind to the metal center efficiently, if at all. It was possible that this was due to steric hindrance. (The presence of the acetate group preventing adequate access to the metal center.) These results demonstrated that in pH 7.4 buffered solution **Tb.149** could selectively detect salicylic acid, **194** the physiologically active form of Aspirin®, **195**. In a titration of **Tb.149** with **196**, another analgesic and anti-inflammatory drug no luminescent enhancements were observed, again showing **Tb.149** selectivity for salicylic acid over similarly acting drugs. In order for **Tb.149** to work *in vivo*, selectivity for **194** over other anions found *in vivo* was evaluated. A titration was carried out on **Tb.149** with **194** in a pH 7.4-buffered solution with clinical concentrations of a number of physiological anions that included $NaHCO_3$, sodium lactate, sodium citrate, and $Na_2H_2PO_4$. [127] (Section 6.4.3) Under these conditions no luminescent emission were observed. This was an indication that the binding of physiological anions with **Tb.149** was stronger. The experiment was repeated again using solutions containing each anion individually and the same result was

found each time, indicating that all of these anions bind more preferentially to **Tb.149** than **194**.

In summary, these results indicated that **Tb.149** and **Tb.181** could be sensitised by **194** in aqueous solution. However, only **Tb.149** was sensitised by **194** in pH 7.4 buffered solutions. **Tb.181** suffered from inefficient binding and a deactivation process. The application of **Tb.149** as an *in vivo* sensor for salicylic acid was shown to be impossible due to higher selectivity for other commonly found *in vivo* anions

5.7 Determination of binding mode for 194 with Tb.149

In Section 5.1.1, it was proposed that binding of carboxylates to a lanthanide metal would occur by way of a bidentate 4 membered chelate through the carboxylate oxygens. This was shown to be true for **191** with **Tb.149** and **Tb.181** (Section 5.5.1). Following the results of Section 5.6, **Tb.149** with **194** and **195,** this proposed binding mode was reviewed as **195** was shown to be inactive, even though it has a free carboxylate that has the potential to bind and a triplet energy high enough to sensitise the lowest Tb(III) excited state $^5D_4$. Steric hindrance had been considered as a reason for this result. However, following further studies with **Tb.149** and **197**, **198** and **199** alternative modes of binding were proposed. The molecular structure of **194** has two potential binding sites making three possible modes of binding possible (depicted in Figure 5.17). If binding occurs between **Tb.149** and **194** using the carboxylate alone, then [A], a bidentate four membered chelate would exist. However if the hydroxyl group was involved in binding with the carboxylate, then [B], a bidentate chelate involving a six membered chelate could exist.[137] Finally if the carboxylate was not involved in binding, then [C], a monodentate chelate could exist through the hydroxyl alone. Titrations on **Tb.149** with **197**, **198** and **199** gave mixed results. For **197** and **199**, in which the carboxylate (**197**) and the hydroxide (**198**) were blocked respectively showed large enhancements in Tb(III) emission intensity of 521 and 278 in their $J = 5$ transitions respectively, on a similar scale to that observed for **191**. As expected, **198** in which both binding sites were blocked showed no emission enhancement when added to **Tb.149**. Determination of the q value for **Tb.149** was also attempted in the presence of either **197**, **198** or **199,** but because of the $\pm$ 0.5 error associated with estimating q values, the results were inconclusive.

The results of this experiment indicated that more than one binding mode may be involved in the binding of salicylic acid, **194** to **Tb.149**. However, the exact mode for the different anions tested could not be distinguished from the data collected. A crystal structure of **Tb.149** in the presence of **194** would have clarified this issue, however no crystals suitable for X-ray analysis were obtained during these studies.

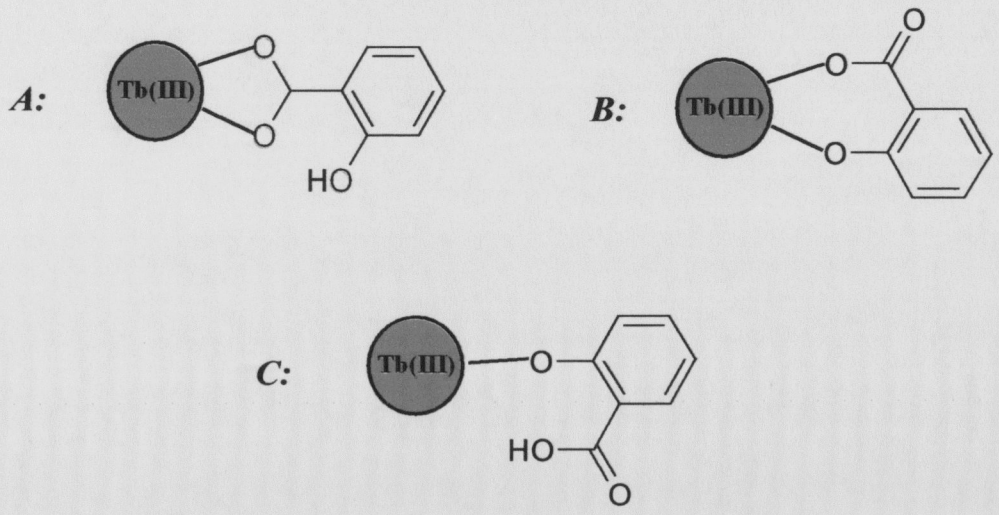


Figure 5.17. ***Methods of Binding for* 194 *with Tb(III) [A: Bidentate binding of 194 with Tb(III) through a four membered chelate with the carboxylate, B: a six membered chelate with the carboxylate and the hydroxyl., C: Monodentate binding through the hydroxyl]***

5.8 Conclusion

The synthesis and complete characterisation of heptadentate ligands **149** and **181** was successfully accomplished. Evaluation of two synthetic routes showed that **149** and **181** could be produced efficiently in a one step synthesis. The synthesis and complete characterisation of the Eu(III) and Tb(III) complexes of these ligands, **Eu.149**, **Eu.181**, **Tb.149** and **Tb.181** was also successfully accomplished. Using lifetime studies and X-ray crystallography it was shown that these complexes were bound to these heptadentate ligands along with two labile water molecules.

These complexes were designed to act as sensors for the detection of aromatic carboxylate species. Detection of such carboxylate species was predicted to arise by the formation of a ternary complex between the lanthanide complex and the carboxylate species. The presence of

such a complex could be observed by excitation of the aromatic carboxylate, which in turn can result in sensitisation of the lanthanide and a subsequent lanthanide emission. Photophysical studies on **Eu.149**, **Eu.181**, **Tb.149** and **Tb.181** showed that all these complexes were stable in solution. The complexes of **Tb.149** and **Tb.181** were shown to act as sensory systems for aromatic carboxylates in water or in buffered aqueous solution at pH 7.4. The Eu(III) complexes could not function in this capacity caused by a lower binding efficiency. Further studies on physiologically active anions showed that **194**, salicylic acid, could be detected by **Tb.149** and **Tb.181** in aqueous solution and by **Tb.149** in buffered aqueous solution at pH 7.4. **Tb.181** was not able to function in buffered solutions due to a reduction in binding efficiency and an inbuilt deactivation process.

Chapter 6

Procedures

6.0 General experimental details

Melting points were determined using an Electrothermal IA9000 digital melting point apparatus. Infrared spectra were recorded on a Mattson Genesis II FTIR spectrophotometer equipped with a Gateway 2000 4DX2-66 workstation. Oils were analysed using NaCl plates, solid samples were dispersed in KBr and recorded as clear pressed discs. ^{1}H NMR spectra were recorded at 400 MHz using a Bruker Spectrospin DPX-400 instrument. Tetramethylsilane (TMS) was used as an internal reference standard, with chemical shifts expressed in parts per million (ppm or δ) downfield from the standard. ^{13}C NMR were recorded at 100 MHz using a Bruker Spectrospin DPX-400 instrument. Mass spectroscopy was carried out using HPLC grade solvents. Mass spectra were determined by detection using Electrospray on a Micromass LCT spectrometer, using a Shimadzu HPLC or Water's 9360 to pump solvent. The whole system was controlled by MassLynx 3.5 on a Compaq Deskpro workstation. Starting materials were obtained from Sigma Aldrich, Strem Chemicals and Fluka. Columns were run using Silica gel 60 (230-400 mesh ASTM) or Aluminum Oxide (activated, Neutral, Brockmann I STD grade 150 mesh). Solvents were used at GPR grade unless otherwise stated. All data was further handled on a Dell Dimension 8100 Personal Computer (1.3GHz, Pentium IV), using Microsoft software and Isis Draw 2.2.1.

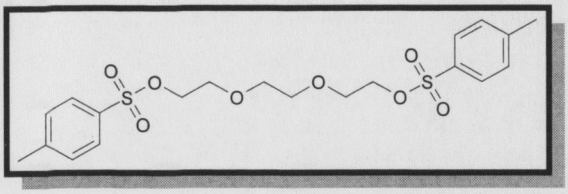
6.1 Synthesis and photophysical data for Chapter 2

General synthesis of tosylated glycerol's (108A and 108B) [145]

Sodium Hydroxide (39.997 g, 0.99 mol) was dissolved in water (150 mL) and poured into a 1L three necked round bottomed flask. The flask was cooled to 0 °C in an ice bath. A solution containing THF (200 mL), water (50 mL) and tri ethylene glycol (54.06 g, 0.36 mol) [or in the case of **108B**, tetra ethylene glycol (69.92 g, 0.36 mol)] was added. *p*-Toluenesulfonyl chloride (146.076 g, 0.766 mol) was dissolved into THF (200 mL) and placed in a dropping funnel. This solution was added to the swirling reaction solution over a period of 4 hours. (Addition over 4 hours to prevent temperature rise above 5 °C) The solution was then left to stir for a further 3 hours. At this point a white precipitate was visible in the solution. The solution was poured onto an ice water mixture. (200 g ice: 100 mL water). Toluene (300 mL)

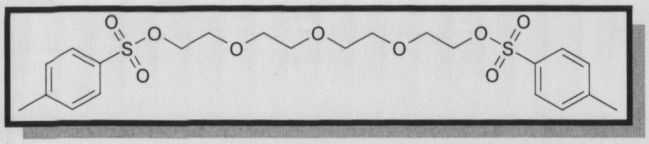
was then added and the solution was filtered producing a white crystalline product. The resulting product was dried under vacuum.

1,6 – bis (p-toluene sulfanato) triethylene glycol (108A)



134.04 g (0.292 mol), 81.2% of a white solid was collected. Calculated for $C_{20}H_{27}O_8S_2$: [M+H peak] *m/z* =459.1147, Found: 459.1141: δ_H($CDCl_3$, 400MHz) 7.79 (d, *J* = 8 Hz, 4H, Ar-H), 7.34 (d, *J* = 8 Hz, 4H, Ar-H), 4.14 (t, 4H, *J* = 3.5 Hz, CH_2), 3.65 (t, 4H, *J* = 3.0 Hz, CH_2), 3.53 (S, 4H, CH_2), 2.45 (s, 6H, Tosyl CH_3); δ_c($CDCl_3$, 100MHz) 144.81, 133.08, 129.81, 127.93, 70.67, 69.16, 68.74, 21.58; Mass Spec (MeCN, ES+) *m/z* Expected : 458.5, Found: 459.5 (M+H), 475.7 (M+H_2O), 933.5 (M_2+Na); IR υ_{max} (cm^{-1}) 2897, 1596, 1457, 1352, 1261, 1175, 1132, 1071, 982, 911, 850, 815, 779, 664, 584, 553, 489, 444.

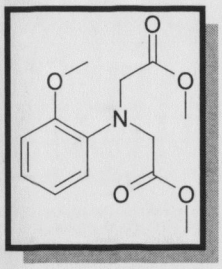
1,8 – bis (p-toluene sulfanato) tetra ethylene glycol (108B)



161.03 g (0.305 mol), 89.0% of clear oil was collected. Calculated for $C_{22}H_{31}O_9S_2$: [M+H peak] *m/z* = 503.1410, found: 503.1440: δ_H($CDCl_3$, 400MHz) 7.76 (d, *J* = 8 Hz, 4H, Ar-H), 7.32 (d, *J* = 8 Hz, 4H, Ar-H), 4.12 (t, 4H, *J* = 4.5 Hz, CH_2), 3.64 (t, 4H, *J* = 5.0 Hz, CH_2), 3.53 (S, 8H, CH_2), 2.42 (s, 6H, Tosyl – CH_3); δ_c($CDCl_3$, 100MHz) 144.71, 132.69, 129.69, 127.77, 76.47, 70.33, 69.16, 68.46, 21.46; Mass Spec (MeCN, ES+) *m/z* Expected : 502.6, Found: 502.6 (M+H), 519.6 (M+H_2O), 524.6 (M+Na); IR υ_{max} (cm^{-1}) 2874, 1597, 1495, 1452, 1355, 1293, 1248, 1188, 1097, 1017, 923, 817, 776, 664.

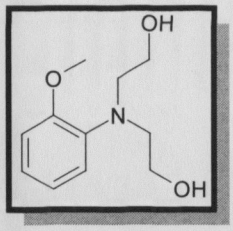
Synthesis of 3-[(2-Methoxycarbonyl-ethyl)-(2-methoxy-phenyl)-amino]-propionic acid methyl ester (109) [20, 141]

2 – Methoxyaniline (10.00 g, 81.19 mmol) was placed in a 250 mL three necked round bottomed flask. To this was added Na_2HPO_4, (23.05 g, 162.4 mmol) and KI (4.0 g, 24.1 mmol). A condenser was fitted and dry DMF (160 mL) was added. The system was placed under vacuum and the atmosphere was then replaced by argon. The solution was then heated



to 80 °C upon which bromo methyl acetate [97%] (27.33 g, 17.52 mL, 178.63 mmol) was added. The reaction was left stirring for 48 hours. The solution was then cooled and poured into a 1:1 solution of EtOAC: Water (200 mL). The two phases were separated and the water phase was washed with ethylacetate (2 x 50 mL). The combined organic layers were washed with brine (2 x 100 mL), dried over $MgSO_4$ and reduced under vacuum to produce **109** as a brown oil, 19.02g (87.6%). Calculated for $C_{13}H_{18}NO_5$: [M+H peak] *m/z* = 268.1185, Found: 268.1161; δ_H($CDCl_3$, 400 MHz) 6.94 (m, 1H, Ar-H), 6.87-6.84 (m, 3H, Ar-H), 4.16 (s, 4H, CH_2), 3.81 (s, 3H, CH_3) 3.73 (s, 6H, $COOCH_3$); δ_C($CDCl_3$, 100 MHz) 171.85, 151.31, 138.53, 122.45, 120.87, 118.99, 111.87, 55.48, 53.75, 51.67; Mass Spec (MeCN, ES+) *m/z* Expected : 267.2, Found: 267.8 (M+H), 289.8 (M+Na), 305.8 (M+K); IR υ_{max}(cm^{-1}) 2997, 2952, 2838, 1745, 1675, 1595, 1504, 1460, 1436, 1352, 1244, 1200, 1174, 1121, 1024, 747.

Synthesis of 2-[(2-Hydroxy-ethyl)-(2-methoxy-phenyl)-amino]-ethanol (110) [20, 141]



$LiAlH_4$, (5.14 g, 0.135 mol) in dry THF (500 mL) was added to a 1000 mL three necked RBF. With the temperature maintained below 0 °C a solution of 3-[(2-Methoxycarbonyl-ethyl)-(2-methoxy-phenyl)-amino]-propionic acid methyl, (17.75 g, 0.066 mol) in THF (250 mL) was added drop wise from a pressure equalising dropping funnel. The whole system was kept dry and held under an argon atmosphere. After the addition was complete the stirring solution was heated to reflux and left stirring for twenty hours. The solution was cooled down and a Saturated solution of Na_2SO_4 (100 mL) was added to neutralise the unreacted $LiAlH_4$. This solution was dried over Na_2SO_4. CH_2Cl_2 (400 mL) was added and the solution was left stirring for one hour. The solution was then passed through a celite filter. The resulting solution was reduced under vacuum to produce a resin which was run down a silica gel column using 50:50, Hex: EtOAc to produce **110** as a yellow oil. (9.154 g, 62.52% Yield) Calculated for $C_{11}H_{18}NO_3$: [M+H peak] *m/z* =212.1287, Found: 212.1267; δ_H($CDCl_3$, 400 MHz) 7.17 (d, 1H, *J* = 8.0 Hz, Ar-H), 7.10 (t, 1H, *J* = 3.5 Hz, Ar-H), 6.95-6.89 (m, 2H, Ar-H), 3.84 (s, 3H, OCH_3), 3.49(t,4H, *J* = 4.5 Hz, CH_2), 3.31 (bs, 2H, OH), 3.18 (t, 4H, *J* = 5.0 Hz, CH_2); δ_C($CDCl_3$, 100 MHz) 165.36, 138.18, 125.74, 124.98, 121.44, 115.58, 59.78, 57.19, 55.43;

Mass Spec (MeCN, ES+) *m/z* Expected : 211.3, Found: 211.9 (M+H), 233.9 (M+Na); IR $\upsilon_{max}(cm^{-1})$ 3376, 2943, 2883, 2837, 1639, 1498, 1463, 1239, 1178, 1105, 1050, 1025, 874, 750.

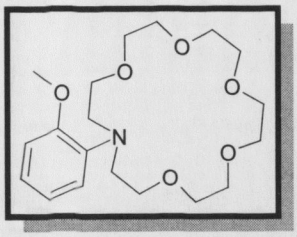
General synthesis of monoaza crown macrocycles (103 and 104) [20, 141]

NaH (1.5296 g, 0.038 mol)[60% in mineral oil] was added to a 1000 mL three necked RBF under an argon atmosphere. Hexane was added to remove the mineral oil. This was then removed and replaced with dry THF (300 mL). Two pressure equalising dropping funnels were attached containing **110**, (4.04 g, 0.019 mol) in dry THF (80 mL) and **108A or 108B** (0.019 mol) in dry THF (80 mL). The stirring solution was brought to reflux and then the two solutions were dropped simultaneously into the reaction flask over a 4 hour period. The stirring solution was then left for a further 20 hours at reflux. The reaction was then cooled down and water (50 mL) was added to destroy any unused NaH. The solution was reduced under vacuum and a 1:1 solution of H_2O:CH_2Cl_2 (300 mL) was added. The aqueous phase was washed with CH_2Cl_2 (2 x 100 mL). The organic phases were combined, dried over $MgSO_4$ and reduced to produce a pale yellow oil.

13-(2-Methoxy-phenyl)-1,4,7,10-tetraoxa-13-aza-cyclopentadecane (103) [20, 141]

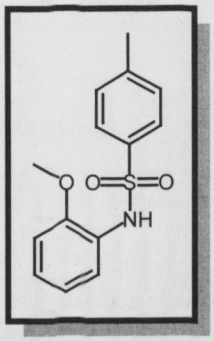
The product was purified on a silica gel column using 70:30, Hex: EtOAc to produce 13-(2-Methoxy-phenyl)-1,4,7,10-tetraoxa-13-aza-cyclopentadecane as an oil. (9.154 g, 62.52% Yield) Calculated for $C_{17}H_{28}NO_5$: [M+H peak] *m/z* =326.1967, Found: 326.1992; $\delta_H(CDCl_3, 400\ MHz)$ 7.09 (d,d 1H, J_1 = 7.5 Hz, J_2 = 1.5 Hz, Ar-H), 6.93 (t, 1H, *J* = 7.5 Hz, Ar-H), 6.88 (d, 1H, *J* = 6.5 Hz, Ar-H), 6.84 (t, 1H, *J* = 8.0 Hz, Ar-H), 3.82 (s, 3H, OCH_3) 3.69-3.63 (m, 16H, CH_2) 3.46 (t, 4H, *J* = 6.0 Hz, CH_2); $\delta_C(CDCl_3, 100\ MHz)$ 152.8, 140.1, 122.0, 120.9, 120.7, 111.8, 70.95, 70.56, 70.33, 70.18, 55.36, 53.01; Mass Spec (MeCN, ES+) *m/z* Expected : 325.41, Found: 325.84 (M+H), 347.8 (M+Na); IR $\upsilon_{max}(cm^{-1})$ 2909, 2875, 1644, 1592, 1498, 1457, 1352, 1291, 1241, 1182, 1120, 1023, 940, 828, 752.

16-(2-Methoxy-phenyl)-1,4,7,10,13-pentaoxa-16-aza-cyclooctadecane (104) [20, 141]



The organic phases were combined, dried over $MgSO_4$ and reduced to produce 16 - (2 – Methoxy - phenyl) - 1,4,7,10,13 – pentaoxa – 16 – aza -cyclooctadecane (4.0 g, 100% Yield) as a crude yellow oil. Calculated for $C_{19}H_{32}NO_6$:[M+H peak] *m/z* = 370.2230, Found: 370.2220.

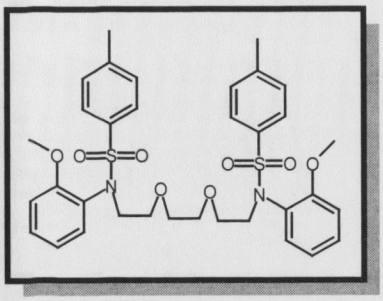
Synthesis of *N*- (2-Methoxy-phenyl)-4-methyl-benzenesulfonamide (115) [144]



In a 250 mL round bottom flask, 2-methoxyaniline (30.00 g, 248.5 mmol) and 4-toluenesulfonyl chloride (47.37 g, 248.5 mmol) in pyridine (120 mL) were refluxed for 45 minutes. The solution was left to cool to room temperature, then poured into 100 mL of ice water and stirred for one hour. The grey precipitate was filtered and washed with cold water (3 x 50 mL) and then recrystallised from ethanol and dried under vacuum to give 58.962 g (87.23% yield) of translucent crystalline **115**. M.P. = 146-147 °C. Calculated for $C_{14}H_{15}NO_3S$: C, 60.63; H, 5.45; N, 5.05, Found: C, 60.60; H, 5.40; N, 5.05; Calculated for $C_{14}H_{16}NO_3S$: [M+H peak] *m/z* = 278.0851, Found: 278.0867; δ_H($CDCl_3$, 400 MHz) 7.65 (d, *J* = 8.0 Hz, 2H, Ar-H), 7.52 (d, *J* = 8.0 Hz, 1H, Ar-H), 7.18 (d, *J* = 8.0 Hz, 2H, Ar-H), 7.05 (s, 1H, NH), 7.02 (d, *J* = 8.0 Hz,1H, Ar-H), 6.89 (t, *J* = 8.0 Hz, 1H, Ar-H), 6.74 (d, *J* = 8.0 Hz, 1H, Ar-H), 3.64 (s, 3H, Ar-O-CH_3), 2.35 (s, 3H, Ar-CH_3); δ_C($CDCl_3$, 100MHz) 149.46, 143.51, 136.29, 129.24, 127.15, 125.98, 125.21, 120.99, 120.96, 110.58, 55.54, 21.35; Mass Spec (MeCN, ES+) *m/z* Expected : 277.3, Found: 278.2 (M+H), 300.2 (M+Na), 316.1 (M+K); IR υ_{max}(cm^{-1}) 3332, 3010, 1594, 1500, 1467, 1446, 1399, 1334, 1309, 1286, 1257, 1208, 1159, 1114, 1089, 1050, 1025, 932, 916, 823, 781, 754, 707, 661, 626, 582, 556, 536.

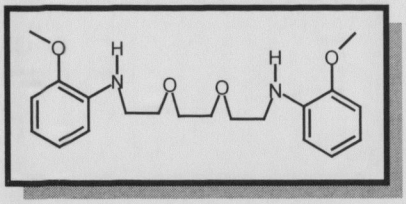
Synthesis of 1,10-bis-(2'-methoxyphenyl, 4''-methyl- benzenesulfonyl)-1,10-diaza-4,7-dioxa-decane (116) [144]

N- (2-Methoxy-phenyl)-4-methyl-benzenesulfonamide (20.00 g, 72 mmol) was placed into a 250 mL RBF containing K_2CO_3 (20.00 g, 144 mmol) and KI (4.00 g, 24 mmol) in DMF (120 mL). To this solution 1,2-bis(2-chloroethoxy)ethane (6.77 g, 5.62 mL, 36.05 mmol) was added and the mixture stirred under dry conditions for 72 hours at 70 °C. The mixture was



cooled and poured into a mixture of 1:1 water: ethyl acetate (400 mL) and the solution was shaken vigorously. The two layers were separated and the aqueous layer washed with ethyl acetate (3 x 100 mL). The combined organic layers were dried over $MgSO_4$ and then the solvent was removed under reduced pressure to give a yellow oil that was recrystalised from ethanol to produce 21.57g (90.76% Yield) of **116** as a white powder. M.P. = 142-143 °C. Calculated for $C_{34}H_{40}N_2O_8S_2$: C, 61.06; H, 6.03; N, 4.19, found: C, 60.79; H, 5.97; N, 4.12; Calculated for $C_{34}H_{41}N_2O_8S_2$: [M+H peak] *m/z* = 669.2304, Found: 669.2305; δ_H($CDCl_3$, 400 MHz) 7.56 (d, *J* = 8.0 Hz, 4H, Ar-H), 7.26 (m, 4H, Ar-H), 7.22 (d, *J* = 8.0 Hz, 4H, Ar-H), 6.90 (t, *J* = 7.5 Hz, 2H, Ar-H), 6.77 (d, 2H, *J* = 8.0 Hz, Ar-H), 3.73 (s, 4H, CH_2), 3.51 (t, *J* = 6.5 Hz, 4H, CH_2) 3.41 (s, 4H, CH_2), 3.38 (s, 6H, Ar-O-CH_3), 2.41 (s, 6H, Ar-CH_3); δ_C($CDCl_3$, 100 MHz) 156.37, 142.62, 137.51, 133.19, 129.68, 128.87, 127.57, 127.04, 120.49, 111.53, 70.10, 69.42, 54.79, 49.12, 21.39; Mass Spec (MeCN, ES+) *m/z* Expected : 668.2, Found: 669.7 (M+H), 691.7 (M+Na), 707.6 (M+K); IR υ_{max}(cm^1) 3463, 2960, 2904, 2867, 1596, 1498, 1459, 1436, 1322, 1284, 1263, 1221, 1160, 1135, 1116, 1091, 1074, 1043, 1024, 960, 914, 860, 811, 782, 757, 709, 657, 586, 553, 528, 511, 489.

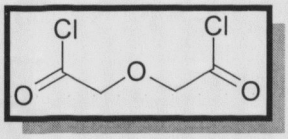
Synthesis of 1,10-Bis (2'-methoxyphenyl)-1,10-diaza-4, 7-dioxa-decane (117) [144]



To a 3:2 mixture of glacial acetic acid and sulphuric acid (70 mL: 46.6 mL) at 60 °C (exactly), 1,10-bis-(2'-methoxyphenyl, 4''-methyl- benzenesulfonyl)-1,10-diaza-4,7-dioxa-decane (5.00 g, 7.24 mmol) was added and the suspension stirred for 24 hours. The mixture was then poured hot into 400 mL of H_2O and the pH brought up to 7, by adding KOH pellets. The aqueous solution was extracted with ether (3 x 100 mL) and the combined ether layers were washed with K_2CO_3 (0.1 M) solution (2 x 100 mL) and with H_2O (2 x 100 mL). The salt was also washed with ether and combined with the organic layer. The organic layers were then dried over $MgSO_4$ and the solvent removed under reduced pressure, to give 1.85 g of a thick brown oil which was purified by flash column chromatography using 25:75, EtOAc: Hex to yield 0.85 g (31.6 % yield) of **117** as a pale yellow oil. This was later recrystalised from ethanol mp. 216-217 °C. Calculated for

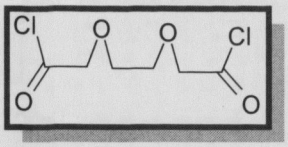
$C_{20}H_{29}N_2O_4$: C, 66.64; H, 7.83; N, 7.77, Found: C, 66.09; H, 7.78; N, 7.68; Calculated for $C_{20}H_{29}N_2O_4$: [M+H peak] *m/z* = 361.2127, Found: 361.2126; δ_H ($CDCl_3$, 400 MHz) 6.89 (t, *J* = 7.5 Hz, 2H, Ar-H), 6.79 (d, *J* = 7.5 Hz, 2H, Ar-H), 6.70 (t, *J* = 7.6 Hz, 2H, Ar-H), 6.65 (d, *J* = 7.52 Hz, 2H, Ar-H), 4.62 (s - broad, 2H, N- H), 3.85 (s, 6H, CH_2) 3.77 (t, *J* = 5.0 Hz, 4H, CH_2), 3.70 (s, 4H, CH_2), 3.37 (t, *J* = 5.0 Hz, 4H, CH_2) ; δ_C($CDCl_3$, 100 MHz) 147.07, 138.15, 121.16, 116.56, 109.91, 109.49, 70.31, 69.80, 55.32, 43.24; Mass Spec (MeCN, ES+) *m/z* Expected: 360.2, Found: 361.2 (M+H), 383.2 (M+Na), 399.2 (M+K); IR υ_{max}(cm^1) 3413, 3064, 3002, 2937, 2896, 2685, 1602, 1513, 1456, 1430, 1346, 1222, 1178, 1139, 1027, 935, 904, 738.

Attempted synthesis of Chloro carbonylmethoxy-acetyl chloride (118) [145]



Carboxymethoxy-acetic acid, (18.77g, 0.14 mol), was added to a 100 mL single necked RBF. To this was added Thionyl chloride (33.40 g, 20.48 mL, 0.28 mol). This mixture was refluxed overnight. Excess thionyl chloride was removed by distillation. Attempts at purification by vacuum distillation failed to isolate the product from the crude reaction material.

Synthesis of (2-Chlorocarbonylmethoxy-ethoxy)-acetyl chloride (119) [145]



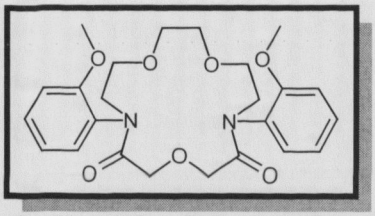
3,6-Dioxa 1,8 octanoic acid, (25.03 g, 0.14 mol), was added to a 100 mL single necked RBF. To this was added Thionyl Chloride (33.40 g, 20.48 mL, 0.28 mol). This mixture was refluxed overnight. Excess Thionyl chloride was removed by distillation. The required product was then purified by vacuum distillation at 172 °C. The product **119** was collected as a pale yellow liquid (14.051 g 0.065 mol) [48% yield] δ_H ($CDCl_3$, 400 MHz) 4.48 (s, 4H, CH_2), 3.80 (s, 4H, CH_2); δ_C ($CDCl_3$, 100 MHz); 171.83, 76.38, 71.21; Mass Spec (MeCN, ES+) *m/z*(%) Expected: 215.0, Found: 238.2 (M+Na), 431.2 (M_2+H), 453.4(M_2+Na), 476.5 (M_2+Na_2); IR υ_{max}(cm^{-1}) 2934, 2885, 1867, 1804, 1705, 1458, 1412, 1379, 1349, 1275, 1211, 1138, 1045, 939, 849, 753

General synthesis of Diaza crown macrocyclic amides (120 and 121) [144]

1,10-Bis(2'-methoxyphenyl)-1,10-diaza-4,7-dioxa-decane (7.0 g , 19.43 mmol) and diglycolyl chloride (95% purity), (3.48 g, 19.4 mmol), [or (2-Chlorocarbonylmethoxy-ethoxy)-acetyl

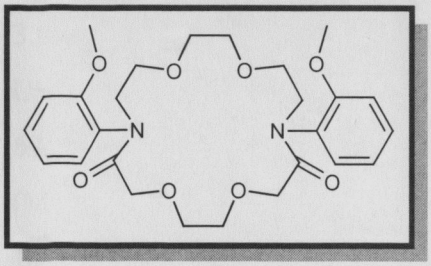
chloride, (4.176 g, 19.42 mmol),in the case of **121**] were each dissolved in dry benzene (300 mL) were placed into two pressure equalising dropping funnels, and over a period of 12 hours simultaneously dropped into a stirring mixture of dry benzene (800 mL) and dry pyridine (16 mL) in a 2000 mL, three neck, RBF under inert atmosphere. The solution was stirred for a further 12 hours at 75 °C after addition was complete. A white precipitate was produced as the reaction progressed, indicating the formation of pyridinium hydrochloride salt. The solvent was removed under vacuum, and the residues dissolved in CH_2Cl_2. The organic solution was then washed with HCl (1M) and with H_2O (2 x 50 mL). The organic layer was then dried over $MgSO_4$ and the solvent removed under reduced pressure.

7, 13-Bis-(2-methoxy-phenyl)-1, 4, 10-trioxa-7, 13-diaza-cyclopentadecane-8, 12-dione (120) [144]



A pale yellow/ clear residue (8.183 g, 17.85 mmol) of a mixture of cis and trans forms of product was produced. The product was recrystalised from EtOH to form a white solid material, (5.92g, 12.91 mmol, 66.52% Yield). Calculated for $C_{24}H_{31}N_2O_7$: [M+H peak] *m/z* = 459.2131, Found: 459.2132; Mass Spec (MeCN, ES+) *m/z* (%) Expected: 458.20, Found: 459.2 (M+H), 481.1 (M+Na), 497.2 (M+K), 916.76 (M_2+H), 938.65 (M_2+Na); IR υ_{max}(cm^{-1}) 3449, 2986, 2939, 2346, 1672, 1596, 1500, 1458, 1440, 1414, 1359, 1341, 1290, 1278, 1246, 1219, 1190, 1149, 1120, 1096, 1058, 1044, 1019, 990, 968, 926, 898, 867, 780, 763, 670, 578, 500.

7,16-Bis-(2-methoxy-phenyl)-1,4,10,13-tetraoxa-7,16-diaza-cyclooctadecane-6,17-dione (121) [144]



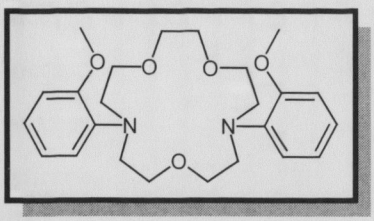
A pale yellow/ clear residue (7.09 g, 14.10 mmol) of a mixture of cis and trans forms of product was produced, which solidified on standing to give a white solid [72.64% Yield]. Calculated for $C_{26}H_{35}N_2O_8$: [M+H peak] *m/z* = 503.2393, Found: 503.2383; δ_H ($CDCl_3$, 400 MHz) 7.58 (d, 2H, *J* = 8.0 Hz, Ar-H), 7.32 (t, 2H, *J* = 8.3 Hz, Ar-H), 7.06 (t, 2H, *J* = 8.0 Hz, Ar-H), 6.90 (d, 2H, *J* = 8.0 Hz, Ar-H), 4.03 (s, 1H, CH_2), 3.99 (s, 1H, CH_2), 3.89 (s, 1H, CH_2), 3.86 (s, 1H,

$C\underline{H}_2$), 3.87 (s, 6H, Ar-O-$C\underline{H}_3$), 3.61-3.56 (m, 8H, $C\underline{H}_2$), 3.42-3.37 (m, 6H, $C\underline{H}_2$), 2.98 (t, 1H, J = 4.5 Hz , $C\underline{H}_2$), 2.95 (t, 1H, J = 4.5 Hz, $C\underline{H}_2$); δ_C ($CDCl_3$, 100 MHz) 169.85, 154.92, 132.26, 129.72, 127.75, 121.28, 111.21, 71.05, 70.50, 69.91, 67.63, 55.26, 45.72; Mass Spec (MeCN, ES+) *m/z* Expected: 502.56, Found: 503.37 (M+H), 525.42 (M+Na), 549.48 (M+K); IR $\upsilon_{max}(cm^{-1})$ 3434, 2928, 2876, 1648, 1596, 1500, 1459, 1438, 1399, 1347, 1290, 1260, 1159, 1098, 1022, 769, 584.

General synthesis of diaza crown macrocycles (111 and 112) [144]

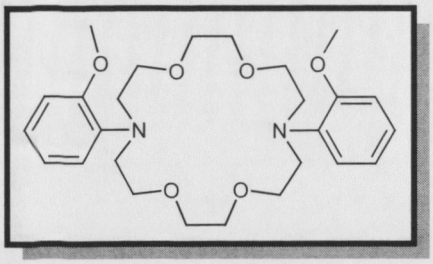
7, 13-Bis-(2-methoxy-phenyl)-1, 4, 10-trioxa-7, 13-diaza-cyclopentadecane-8, 12-dione, (4.905 g, 10.7 mmol), [or 7, 16-Bis-(2-methoxy-phenyl)-1, 4, 10, 13-tetraoxa-7, 16-diaza-cyclooctadecane-6, 17-dione, in the case of **112**] was added to stirring solution of dry THF (60 mL). To this stirred solution, at room temperature, six fold equivalents of $NaBH_4$ (2.524 g, 66.7 mmol) was added, and then over a period of two hours, eight fold equivalents of boron trifluoride triethetate (12.519 g, 88.2 mmol) in dry THF (60 mL) was added. After addition the suspension was refluxed for 4 hours and then poured into H_2O (30 mL) and the pH adjusted to 7 using KOH. The aqueous solution was extracted with CH_2Cl_2 (2 x 50 mL). The organic layer washed several times with H_2O, and then dried over $MgSO_4$.

7,13-Bis-(2-methoxy-phenyl)-1,4,10-trioxa-7,13-diaza-cyclopentadecane (111) [144]



The solvent was removed under reduced pressure to give **111** as a colourless oil. (4.502 g, 10.4mmol, 97.67% yield) Calculated for $C_{24}H_{35}N_2O_5$: [M+H peak] *m/z* = 431.2546, Found: 431.2538; δ_H ($CDCl_3$, 400 MHz) 7.05 (d, 2H, J = 7.6 Hz, Ar-$\underline{H}$), 6.95 (t, 2H, J = 6.0 Hz, Ar-$\underline{H}$), 6.87 (m, 4H, Ar-$\underline{H}$), 3.84 (s, 6H, Ar-O-$C\underline{H}_3$), 3.72 (t, 4H, J = 5.5 Hz, $C\underline{H}_2$), 3.66 (m, 8H, $C\underline{H}_2$), 3.51- 3.44 (m, 8H, $C\underline{H}_2$); δ_C ($CDCl_3$, 100 MHz) 152.96, 140.55, 122.21, 121.01, 120.75, 111.90, 71.20, 70.78, 69.80, 53.38, 53.21, 52.51; Mass Spec (MeCN, ES+) *m/z* Expected: 430.2, Found: 431.3 (M+), 453.3 (M+Na), 861.6(M_2+H), 883.7 (M_2+Na); IR $\upsilon_{max}(cm^{-1})$ 3059, 2927, 2856, 1725, 1593, 1499, 1461, 1353, 1238, 1180, 1108, 1028, 795, 744.

7,16-Bis-(2-methoxy-phenyl)-1,4,10,13-tetraoxa-7,16-diaza-cyclooctadecane (112) [144]



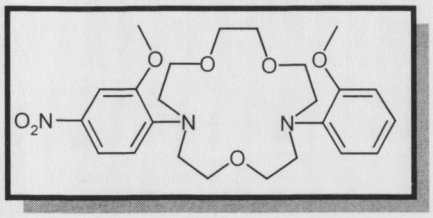
The solvent was removed to give a colourless oil (5.256g, 11.07 mmol, 91.59 % yield) of **112**. A sample was crystallized by slow evaporation from CH_2Cl_2. M.P. = 206-208 °C; Calculated for $C_{26}H_{38}N_2O_6.CH_2Cl_2$: C, 57.96; H, 7.21; N, 5.01, found: C, 57.89; H, 6.91; N, 5.04; calculated for $C_{26}H_{39}N_2O_6$: [M+H peak] m/z = 475.2808, Found: 475.2798; δ_H ($CDCl_3$, 400 MHz) 7.18 (d, 2H, J = 7.5 Hz, Ar-H), 6.98 (t, 2H, J = 7.6 Hz, Ar-H), 6.91 (t, 2H, J = 7.6 Hz, Ar-H), 6.87 (d, 2H, J = 8.0 Hz, Ar-H), 3.85 (s, 6H, Ar-O-CH_3), 3.61 (t, 8H, J = 5.5 Hz , CH_2), 3.56 (s, 8H, CH_2), 3.49 (t, 8H, J = 6.0 Hz, CH_2); δ_C ($CDCl_3$, 100 MHz) 153.07, 139.28, 122.45, 121.45, 120.72, 111.78, 70.54, 69.90, 55.37, 52.65 ; Mass Spec (MeCN, ES+) m/z Expected: 474.2, Found: 475.3 (M+H), 497.3 (M+Na), 513.3 (M+K); IR $\upsilon_{max}(cm^{-1})$ 3446, 3069, 3002, 2889, 2859, 1579, 1499, 1458, 1436, 1368, 1336, 1285, 1266, 1243, 1209, 1187, 1170, 1129, 1103, 1088, 1050, 1022, 994, 915, 880, 824, 799, 744, 718, 612, 584, 542, 479, 410.

General nitration procedure

To a 250 mL single neck RBF, (0.585 g, 1.89 mmol) of 13-(2-Methoxy-phenyl)-1,4,7,10-tetraoxa-13-aza-cyclopentadecane was added along with distilled water (60 mL) and Glacial acetic acid [100%](6 mL). The solution was stirred at room temperature. Over a ten-minute period a solution of deionised water (10 mL) containing $NaNO_2$ [97%] (0.144 g, 2.09 mmol) was added. The solution turned bright orange during this addition. The solution was then left stirring overnight. The orange solution was washed with DCM (4 x 50 mL). The organic phases were combined and dried over K_2CO_3, and the resulting solution was reduced to a yellow oil. This was purified by Alumina column chromatography using [99:1] Diethyl ether: MeOH, or by precipitation from ether.

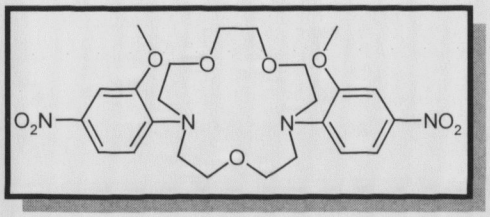
7-(2-Methoxy-4-nitro-phenyl)-13-(2-methoxy-phenyl)-1,4,10-trioxa-7,13-diaza-cyclopentadecane (124)

Isolated in 48 % yield as a yellow oil. Calculated for $C_{24}H_{34}N_3O_7$: [M+H peak] m/z = 476.2397, Found: 476.2420; δ_H ($CDCl_3$, 400 MHz) 7.81 (d,d, 1H, J_1 = 6.5 Hz, J_2 = 2.48 Hz,



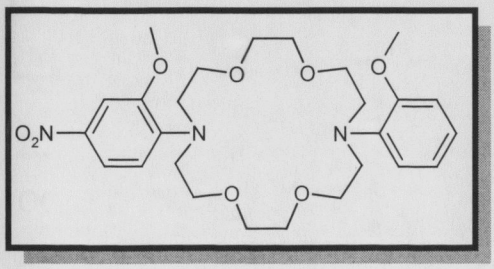
Ar-H), 7.67 (d, 1H, J = 2.5 Hz, Ar-H), 6.99 (d, 1H, J = 8.0 Hz, Ar-H), 6.94 (d, 1H, J = 7.5 Hz, Ar-H), 6.93-6.83 (m, 3H, Ar-H), 3.87 (s, 3H, OCH_3), 3.82 (s, 3H, OCH_3), 3.77 (t, 2H, J = 5.0 Hz, OCH_2CH_2), 3.71-3.61 (m, 14H, OCH_2CH_2), 3.46 (t, 2H, J = 5.5 Hz, OCH_2CH_2), 3.38 (t, 2H, J = 4.5 Hz, OCH_2CH_2); δ_C($CDCl_3$, 100 MHz) 153.19, 149.56, 146.30, 140.43, 139.46, 122.53, 121.42, 120.70, 118.34, 115.54, 111.92, 107.32, 71.44, 70.85, 70.75, 69.73, 69.38, 55.82, 55.33, 53.68, 55.35, 53.14, 52.24; Mass Spec (MeCN, ES+) m/z Expected : 475.23, Found: 476.1 (M+H); IR υ_{max}(cm^{-1}) 3431(H_2O), 2922, 2857, 1585, 1509, 1458, 1322, 1276, 1240, 1183, 1096, 1025, 862, 798, 745.

7,13-Bis-(2-methoxy-4-nitro-phenyl)-1,4,10-trioxa-7,13-diaza-cyclopentadecane (130)



Isolated in 17% yield as a yellow solid. M.P. = 130-131 °C. Calculated for $C_{24}H_{32}N_4O_9$: C, 55.38; H, 6.20; N, 10.76, Found: C, 55.63; H, 6.20; N, 10.46; Calculated for $C_{24}H_{33}N_4O_9$: [M+H peak] m/z =521.2248, Found: 521.2260; δ_H ($CDCl_3$, 400 MHz) 7.81 (d,d, 2H, J_1 = 9.0 Hz, J_2 = 2.5 Hz Ar-H), 7.68 (d, 2H, J = 2.5 Hz, Ar-H), 6.86 (d, 2H, J = 9.0 Hz, Ar-H), 3.87 (s, 6H, OCH_3), 3.73 (t, 4H, J = 5.0 Hz, OCH_2CH_2), 3.68 (m, 8H, OCH_2CH_2), 3.62 (s, 8H, OCH_2CH_2); δ_C ($CDCl_3$, 100 MHz) 149.76, 146.32, 139.79, 118.28, 115.72, 107.37, 71.35, 70.90, 69.50, 55.88, 53.67, 52.68; Mass Spec (MeCN, ES+) m/z Expected : 520.5, Found: 521.2 (M+H); IR υ_{max}(cm^{-1}) 2927, 2885, 2862, 1584, 1491, 1319, 1278, 1242, 1095, 1062, 1025, 967, 872, 798, 746, 721, 643, 593, 556.

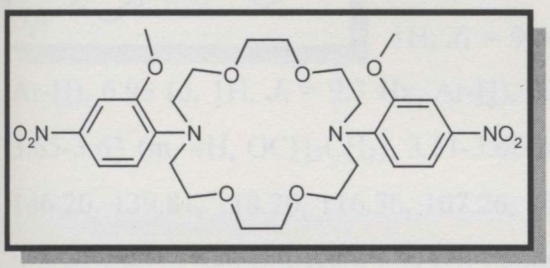
7-(2-Methoxy-4-nitro-phenyl)-16-(2-methoxy-phenyl)-1,4,10,13-tetraoxa-7,16-diaza-cyclooctadecane (125)



Isolated in 43 % yield as a yellow oil. Calculated for $C_{26}H_{37}N_3O_8$: C, 60.10; H, 7.18; N, 8.09, Found: C, 60.49; H, 7.41; N, 7.58; Calculated for $C_{26}H_{38}N_3O_8$: [M+H peak] m/z = 520.2659, Found: 520.2676; δ_H

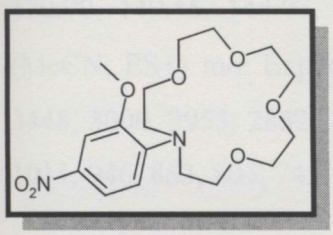
($CDCl_3$, 400 MHz) 7.82 (d,d 1H, J_1 = 6.5 Hz, J_2 = 2.5 Hz, Ar-H), 7.68 (d, 1H, J = 2.0 Hz, Ar-H), 7.11 (d, 1H, J = 6.0 Hz, Ar-H), 6.97-6.84 (m, 4H, Ar-H), 3.89 (s, 3H, OCH_3), 3.83 (s, 3H, OCH_3), 3.73-3.71 (m, 8H, OCH_2CH_2), 3.62-3.57 (m, 12H, OCH_2CH_2), 3.53-3.48 (m, 4H, OCH_2CH_2): δ_C ($CDCl_3$, 100 MHz) 153.12, 149.76, 146.16, 139.77, 139.94, 122.58, 121.41, 120.66, 118.19, 116.05, 111.84, 107.27, 70.73, 70.57, 70.08, 69.82, 55.82, 55.34, 52.70, 52.67; Mass Spec (MeCN, ES+) m/z Expected : 519.6, Found: 520.7 (M+H); IR $\upsilon_{max}(cm^{-1})$ 3434(H_2O), 2921, 2863, 1579, 1508, 1457, 1321, 1275, 1242, 1181, 1095, 800, 746, 669.

7,16-Bis-(2-methoxy-4-nitro-phenyl)-1,4,10,13-tetraoxa-7,16-diaza-cyclooctadecane (131)



Isolated in 36 % yield as a yellow solid. M.P. = 147-149 °C. Calculated for $C_{26}H_{36}N_4O_{10}$: C, 55.31; H, 6.43; N, 9.92, Found: C, 55.37; H, 6.45; N, 9.61; Calculated for $C_{26}H_{37}N_4O_{10}$: [M+H peak] m/z =565.2510, Found: 565.2507; δ_H ($CDCl_3$, 400 MHz) 7.82 (d,d, 2H, J_1 = 6.5 Hz, J_2 = 2.5 Hz, Ar-H), 7.68 (d, 2H, J = 2.5 Hz, Ar-H), 6.91 (d, 2H, J = 9.0 Hz, Ar-H), 3.89 (s, 6H, OCH_3), 3.70 (s, 12H, OCH_2CH_2), 3.60 (s, 12H, OCH_2CH_2); δ_C ($CDCl_3$, 100 MHz) 149.84, 146.11, 139.94, 118.19, 115.97, 107.34, 70.80, 70.07, 55.88, 52.76; Mass Spec (MeCN, ES+) m/z Expected : 564.2, Found: 565.2 (M+H), 586.7 (M+Na), 602.7 (M+K); IR $\upsilon_{max}(cm^{-1})$ 3434 (H_20), 2922, 2886, 2856, 1582, 1509, 1484, 1453, 1328, 1280, 1249, 1127, 1094, 1026, 991, 910, 873, 801, 728, 528, 554, 483, 431.

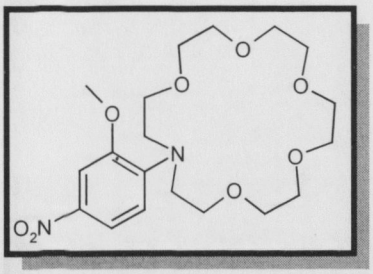
13-(2-Methoxy-4-nitro-phenyl)-1,4,7,10-tetraoxa-13-aza-cyclopentadecane (122)



Isolated as yellow oil that solidified upon standing for a few days in 89 % yield. M.P. = 75-76 °C Calculated for $C_{17}H_{26}N_2O_7$: C, 55.13; H, 7.08; N, 7.56, Found: C, 55.35; H, 7.09; N, 7.26; Calculated for $C_{17}H_{27}N_2O_7$: [M+H peak] m/z = 371.1818, found = 371.1817; δ_H ($CDCl_3$, 400 MHz) 7.77 (d,d, 1H, J_1 = 9.0 Hz, J_2 = 2.5 Hz, Ar-H), 7.63 (d, 1H, J = 2.5 Hz, Ar-H), 6.86 (d, 1H, J_1 = 9.0 Hz, Ar-H), 3.83 (s, 3H, OCH_3) 3.70 (t, 4H, J = 5.5 Hz, OCH_2CH_2) 3.64-3.59 (m, 16H, OCH_2CH_2); δ_C ($CDCl_3$, 100 MHz) 149.36, 145.96, 139.25, 118.24, 115.37, 107.21, 70.97, 70.30, 70.17, 69.72, 55.72,

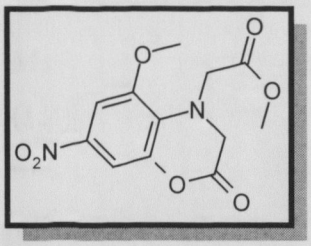
53.64; Mass Spec (MeCN, ES+) m/z Expected : 370.4, Found: 371.8 (M+H), 392.7 (M+Na); IR $\upsilon_{max}(cm^{-1})$ 2940, 2885, 2856, 1585, 1512, 1497, 1319, 1292, 1269, 1239, 1223, 1120, 1096, 1051, 1025, 992, 940, 891, 857, 800, 742, 669, 615.

16-(2-Methoxy-4-nitro-phenyl)-1,4,7,10,13-pentaoxa-16-aza-cyclooctadecane (123)



Isolated in 68% yield as a yellow oil. Calculated for $C_{19}H_{30}N_2O_8$: C, 55.06; H, 7.30; N, 6.76, Found: C, 54.57; H, 7.20; N, 6.42; Calculated for $C_{19}H_{31}N_2O_8$: [M+H peak] m/z = 415.2080, Found: 415.2066; δ_H ($CDCl_3$, 400 MHz) 7.81 (d,d, 1H, J_1 = 9.4 Hz, J_2 = 2.3 Hz, Ar-H), 7.66 (d, 1H, J = 2.9 Hz, Ar-H), 6.93 (d, 1H, J_1 = 9.3 Hz, Ar-H), 3.88 (s, 3H, OCH_3) 3.70-3.66 (m, 16H, OCH_2CH_2), 3.65-3.63 (m, 4H, OCH_2CH_2), 3.61-3.60 (m, 4H, OCH_2CH_2); δ_C ($CDCl_3$, 100 MHz) 149.85, 146.20, 139.81, 118.20, 116.36, 107.26, 70.77, 70.68, 70.53, 69.76, 55.85, 52.81; Mass Spec (MeCN, ES+) m/z Expected : 414.4, Found: 415.2 (M+H), 437.2 (M+Na), 453.2 (M+K); IR $\upsilon_{max}(cm^{-1})$ 2914, 2870, 1584, 1509, 1458, 1321, 1275, 1243, 1176, 1096, 1024, 923, 800, 748.

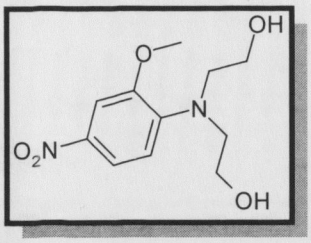
[Methoxycarbonylmethyl-(2-methoxy-4-nitro-phenyl)-amino]-acetic acid methyl ester (132)



Isolated in 44 % yield as a yellow oil. Calculated for $C_{13}H_{17}N_2O_7$: [M+H peak] m/z =313.1036, Found: 313.1038; δ_H ($CDCl_3$, 400 MHz) 7.80 (d,d, 1H, J_1 = 9.0 Hz, J_2 = 2.5 Hz, Ar-H), 7.69 (d, 1H, J = 2.5 Hz, Ar-H), 6.67 (d, 1H, J = 9.0 Hz, Ar-H), 4.20 (s, 4H, CH_2), 3.85 (S, 3H, OCH_3), 3.78 (s, 6H, $COOCH_3$); δ_C ($CDCl_3$, 100 MHz); 170.90, 149.55, 144.97, 141.21, 118.06, 115.77, 107.50, 56.11, 54.17, 52.07; Mass Spec (MeCN, ES+) m/z Expected : 312.3, Found: 313.2 (M+H), 335.2 (M+Na); IR $\upsilon_{max}(cm^{-1})$ 3448, 3000, 2953, 2852, 1750, 1685, 1588, 1515, 1458, 1329, 1289, 1249, 1207, 1176, 1101, 1011, 946, 863, 804, 745, 721, 627, 560.

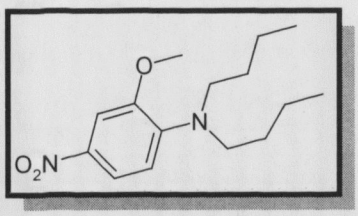
2-[(2-Hydroxy-ethyl)-(2-methoxy-4-nitro-phenyl)-amino]-ethanol (135)

Isolated in 59 % yield as a yellow oil. Calculated for $C_{11}H_{17}N_2O_5$: [M+H peak] m/z =257.1137, Found: 257.1137; δ_H ($CDCl_3$, 400 MHz) 7.82 (d,d, 1H, J_1 = 9.0 Hz, J_2 = 2.5 Hz,



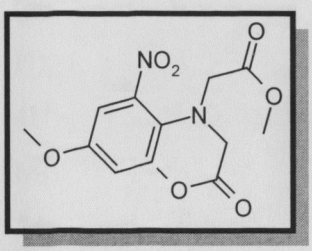
Ar-H), 7.71 (d, 1H, J = 2.5 Hz, Ar-H), 7.0 (d, 1H, J = 8.5 Hz, Ar-H), 3.93 (s, 3H, OCH_3) 3.77 (t, 4H, J = 5.0 Hz, CH_2), 3.56 (t, 4H, J = 5.0 Hz, CH_2), 2.96 (b.s 2H, OH); δ_C ($CDCl_3$, 100 MHz) 150.84, 145.42, 141.07, 117.98, 117.82, 107.39, 60.43, 55.94, 55.15; Mass Spec (MeCN, ES+) m/z Expected : 256.2, Found: 257.1 (M+H); IR $\upsilon_{max}(cm^{-1})$ 3387, 2957, 2928, 2873, 1584, 1509, 1321, 1274, 1241, 1093, 1068, 1024, 799, 745.

Dibutyl-(2-methoxy-4-nitro-phenyl)-amine (134)



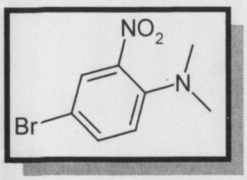
Isolated in 55 % yield as a yellow oil. Calculated for $C_{15}H_{25}N_2O_3$: [M+H peak] m/z =281.1865, Found: 281.1879; δ_H ($CDCl_3$, 400 MHz) 7.82 (d,d, 1H, J_1 = 9.0 Hz, J_2 = 2.0 Hz, Ar-H), 7.68 (d, 1H, J = 2.5 Hz, Ar-H), 6.72 (d, 1H, J = 9.0 Hz, Ar-H), 3.89 (s, 3H, OCH_3), 3.32 (t, 4H, J = 7.5 Hz, CH_2), 1.54 (m, 4H, CH_2), 1.30 (quartet, 4H, J = 7.0 Hz, CH_2), 0.92 (t, 6H, J = 7.5 Hz, CH_3); δ_C ($CDCl_3$, 100 MHz) 149.93, 146.51, 139.31, 118.31, 115.72, 107.37, 55.81, 55.24, 29.86, 20.28, 13.88; Mass Spec (MeCN, ES+) m/z Expected : 280.3, Found: 281.3 (M+H); IR $\upsilon_{max}(cm^{-1})$ 2958, 2930, 2871, 1585, 1509, 1465, 1323, 1285, 1241, 1099, 1029, 932, 864, 801, 746.

Methoxycarbonylmethyl-(4-methoxy-2-nitro-phenyl)-amino)-acetic acid methyl ester (133)



Isolated in 79 % as yellow oil. Calculated for $C_{13}H_{17}N_2O_7$: [M+H peak] m/z =313.1036, found: 313.1038; δ_H ($CDCl_3$, 400 MHz) 7.46 (d, 1H, J = 8.8 Hz, Ar-H), 7.23 (d, 1H, J = 2.9 Hz, Ar-H), 7.03 (d,d, 1H, J_1 = 9.4 Hz, J_2 = 2.9 Hz, Ar-H), 4.06 (s, 4H, CH_2), 3.81 (s, 3H, OCH_3), 3.68 (s, 6H, $COOCH_3$); δ_C ($CDCl_3$, 100 MHz) 171.00, 156.16, 147.10, 136.34, 127.88, 119.59, 109.21, 55.83, 55.40, 51.74; Mass Spec (MeCN, ES+) m/z Expected : 312.3, Found: 313.2 (M+H), 335.2 (M+Na); IR $\upsilon_{max}(cm^{-1})$ 3432, 3006, 2955, 2847, 1751, 1530, 1438, 1355, 1292, 1203, 1174, 1029, 849, 808, 624, 562.

(4-Bromo-2-nitro-phenyl)-dimethyl-amine (136)

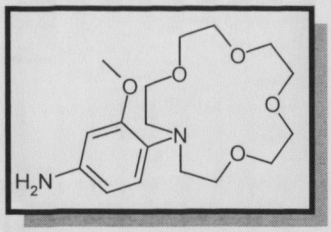


(54.66% Yield) Calculated for $C_8H_{10}N_2O_2Br$: [M+H peak] *m/z* =244.9926, found: 244.9927; δ_H ($CDCl_3$, 400 MHz) 7.90 (d, 1H, J = 2.5 Hz, Ar-H), 7.46 (d,d, 1H, J_1 = 9.0 Hz, J_2 = 2.0 Hz, Ar-H), 6.91 (d, 1H, J = 9.04 Hz, Ar-H), 2.89 (s, 6H, NCH_3); δ_C ($CDCl_3$, 100 MHz); 145.19, 138.83, 135.89, 129.02, 119.59, 108.81, 42.34; Mass Spec (MeCN, ES+) *m/z* Expected : 245.0, Found:245.38 (M+H); IR $\upsilon_{max}(cm^{-1})$ 2964, 2925, 1601, 1544, 1509, 1456, 1337, 1270, 1214, 1156, 1124, 1065, 951, 888, 803, 762, 716, 657, 616, 537.

General procedure for the reduction of nitro aromatic compounds [130]

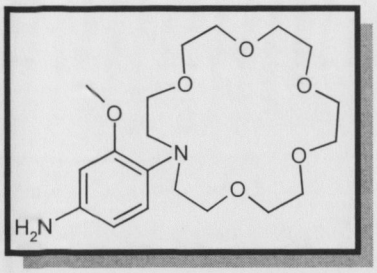
X (All nitrated aromatic compounds), was placed in 250 mL RBF. To this was added 10% Pd-C, 0.1 equivalents and EtOH (100 mL). The solution was stirred under a H_2 atmosphere until no more H_2 was consumed. The resulting solution was passed through a celite filter. The solution was then reduced under vacuum.

13-(2-Methoxy-4-amino-phenyl)-1,4,7,10-tetraoxa-13-aza-cyclopentadecane (126)



A clear resin was produced (0.448 g) which slowly turned light purple over time. This was purified by alumina column chromatography using CH_2Cl_2 to yield **126**, as a purple resin. (0.419 g, 98.24% Yield) Calculated for $C_{17}H_{29}N_2O_5$: [M+H peak] *m/z* =341.2076, Found: 341.2070; δ_H ($CDCl_3$, 400 MHz) 7.00 (d,1H, J = 6.8 Hz, Ar-H), 6.30 (s,1H, Ar-H), 6.22 (d,1H, J = 8.3 Hz, Ar-H), 5.46 (bs, 2H, N-H), 3.78 (s, 3H, OCH_3) 3.70 (s, 4H, OCH_2CH_2) 3.64 (t, 4H, J = 3.3 Hz, OCH_2CH_2); 3.53 (t, 4H, J = 4.5 Hz, OCH_2CH_2) 3.42 (s, 4H, OCH_2CH_2), 3.26 (s, 4H, OCH_2CH_2) ; δ_C ($CDCl_3$, 100 MHz) 173.35, 154.78, 145.96, 125.05, 106.85, 98.65, 68.88, 68.80, 68.83, 67.01, 54.95, 54.89; Mass Spec (MeCN, ES+) *m/z* Expected : 340.4, Found: 340.9 (M+H), 362.9 (M+Na); IR $\upsilon_{max}(cm^{-1})$ 3433, 3208, 2917, 2874, 1610, 1513, 1458, 1352, 1294, 1258, 1214, 1122, 1027, 941, 829, 631.

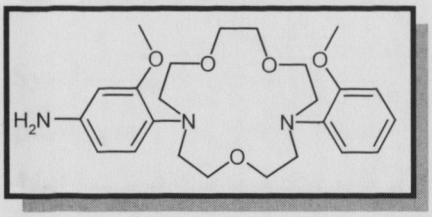
16-(2-Methoxy-4-amino-phenyl)-1,4,7,10,13-pentaoxa-16-aza-cyclooctadecane (127)



A clear resin was produced (2.408 g) which slowly turned light purple over time. This was purified by alumina column chromatography using CH_2Cl_2 to yield **127**, (1.923 g, 67.85% Yield) as a purple resin. Calculated for $C_{19}H_{33}N_2O_6$: [M+H peak] *m/z* =385.2339, found: 385.2349; δ_H ($CDCl_3$, 400 MHz) 7.28 (s,2H, N-H) 6.73(d,1H, *J* = 8.5 Hz, Ar-H), 6.33 (s,1H, Ar-H),6.19 (d,1H, *J* = 8.0 Hz, Ar-H), 3.56 (s, 3H, OCH_3) 3.41 (s, 8H, OCH_2CH_2) 3.36 (bs, 4H, OCH_2CH_2), 3.21 (bs, 4H, OCH_2CH_2) 3.10 (bs, 4H,OCH_2CH_2), 2.92 (bs, 4H,OCH_2CH_2) ; δ_C ($CDCl_3$, 100 MHz) 155.25, 127.50, 125.40, 124.02, 108.67, 99.84, 69.23, 69.06, 69.02, 68.74, 66.76, 55.14, 55.02; Mass Spec (MeCN, ES+) *m/z* Expected : 384.8, Found: 385.12 (M+H), 407.1 (M+Na); IR $\upsilon_{max}(cm^{-1})$ 3427, 2897, 1610, 1513, 1468, 1350, 1285, 1258, 1215, 1106, 1029, 956, 834, 602.

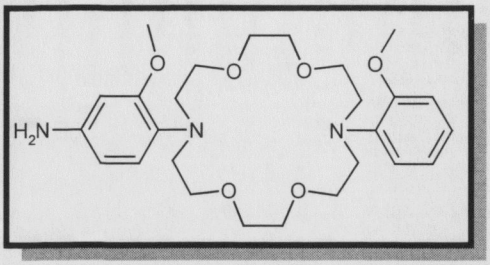
3-Methoxy-4-[13-(2-methoxy-phenyl)-1,4,10-trioxa-7,13-diaza-cyclopentadec-7-yl]-phenyl amine (128)

128, (0.7596 g) was obtained as a clear resin, which slowly turned light purple over time.



The crude resin was purified by acid/ base extraction to yield 3-Methoxy-4-[13-(2-methoxy-phenyl)-1,4,10-trioxa-7,13-diaza-cyclopentadec-7-yl]-phenyl amine. (0.4228 g, 59.0 % Yield) Calculated for $C_{24}H_{36}N_3O_5$:[M+H peak] *m/z* = 446.2655, Found: 446.2655; δ_H ($CDCl_3$, 400 MHz) 7.04 (d, 1H, *J* = 7.5 Hz, Ar-H), 6.92 (m, 2H, Ar-H), 6.87 (d, 1H, *J* = 7.5 Hz, Ar-H), 6.82 (d, 1H, *J* = 8.0 Hz, Ar-H), 6.19 (m, 2H, Ar-H), 3.80 (s, 3H, OCH_3), 3.74 (s, 3H, OCH_3), 3.70 (t, 2H, *J* = 5.5 Hz, OCH_2CH_2O), 3.62 (m, 8H, OCH_2CH_2O), 3.54 (t, 2H, *J* = 6.0 Hz, OCH_2CH_2O), 3.46 (m, 4H, OCH_2CH_2O), 3.41 (m, 4H, OCH_2CH_2O); δ_C ($CDCl_3$, 100 MHz) 155.15, 152.70, 143.20, 140.36, 131.52, 125.10, 121.93, 120.72, 120.56, 111.73, 106.49, 100.50, 70.83, 70.78, 70.52, 69.66, 69.54, 55.20, 55.03, 53.91, 53.39, 53.27, 52.96, 52.49; Mass Spec (MeCN, ES+) *m/z* Expected : 445.26, Found: 446.23 (M+H), 468.28 (M+Na); IR $\upsilon_{max}(cm^{-1})$ 3426, 2927, 2858, 1617, 1509, 1458, 1353, 1239, 1212, 1171, 1110, 1028, 950, 830, 748, 568.

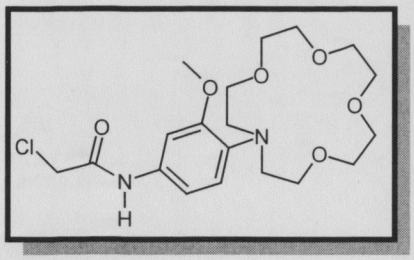
3-Methoxy-4-[16-(2-methoxy-phenyl)-1,4,10,13-tetraoxa-7,16-diaza-cyclooctadec-7-yl]-phenylamine (129)



129, (0.6322 g) was produced as a clear resin, which slowly turned light purple over time. The crude resin was purified by acid/ base extraction to yield 3-Methoxy-4-[16-(2-methoxy-phenyl)-1,4,10,13-tetraoxa-7,16-diaza-cyclooctadec-7-yl]-phenylamine. (0.487 g, 74.47% Yield) Calculated for $C_{26}H_{40}N_3O_6$: [M+H peak] *m/z* = 490.2917, Found: 490.2912; δ_H ($CDCl_3$, 400 MHz) 7.10 (d,d, 1H, J_1 = 7.5 Hz, J_2 = 1.52 Hz, Ar-H), 6.96 (d, 1H, *J* = 8.0 Hz, Ar-H), 6.91 (t, 1H, *J* = 7.5 Hz Ar-H), 6.85 (t, 1H, *J* = 7.5 Hz Ar-H), 6.80 (d, 1H, *J* = 7.5 Hz, Ar-H), 6.20 (m, 2H, Ar-H), 3.96 (bs 2H, N-H), 3.77 (s, 3H, OCH_3), 3.72 (s, 3H, OCH_3), 3.54 (t, 4H, *J* = 5.0 Hz, OCH_2CH_2O), 3.50 (m, 16H, OCH_2CH_2O), 3.35 (t, 4H, *J* = 6.0 Hz, OCH_2CH_2O); δ_C ($CDCl_3$, 100 MHz) ; 154.82, 152.89, 143.03, 139.06, 130.08, 124.40, 122.27, 121.32, 120.49, 111.63, 106.56, 99.98, 70.27, 70.23, 69.71, 69.26, 55.15, 55.04, 53.28, 52.47; Mass Spec (MeCN, ES+) *m/z* Expected : 489.61, Found: 490.16 (M+H); IR υ_{max}(cm^{-1}) 3463, 3341, 3208, 2932, 2870, 1620, 1509, 1463, 1349, 1249, 1213, 1174, 1139, 1116, 1032, 992, 927, 874, 819, 751, 635, 613, 548, 477.

Synthesis of 2-Chloro-N-[3-methoxy-4-(1,4,7,10-tetraoxa-13-aza-cyclopentadec-13-yl)-phenyl]-acetamide (145)

Method 1 [130]



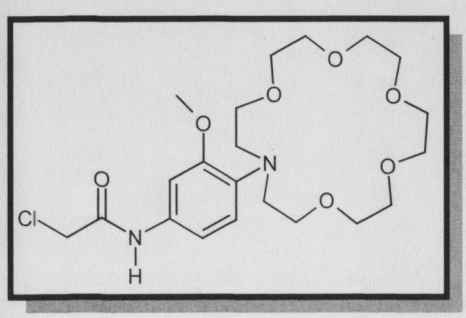
To a 250 mL 3 neck RBF, of 13 - (2 –Methoxy - 4 – amino - phenyl) - 1,4,7,10-tetraoxa-13-aza-cyclopentadecane (0.397 g, 1.16 mmol), dry CH_2Cl_2 (50 mL) and TEA (0.1416 g, 1.39 mmol) was added. This solution was then immersed into a dry ice, IPA bath kept below -60 °C. To this flask a pressure equalising dropping funnel was attached which contained a solution of dry CH_2Cl_2 (50 mL) and chloro acetyl chloride. (98%)(0.144 g, 1.28 mmol) This solution was dropped into the flask over a 2 hour period with the reaction vessel kept at -60 °C. After this addition the reaction flask was allowed to heat up to room temperature and the solution was then left stirring overnight. The resulting solution was then extracted using 1.0 M HCl (1 x 50 mL),

and then water (1 x 50 mL). The organic phase was then dried over $CaCl_2$ and reduced under vacuum. This was purified by alumina column chromatography using [99:1] DCM: MeOH to produce **145** as a purple resin. (0.193 g, 40 % yield)

Method 2 [157]

To a 25 mL single neck RBF, 13 - (2-Methoxy-4-amino-phenyl) -1,4,7,10-tetraoxa -13-aza-cyclopentadecane (0.321 g, 0.94 mmol) was added along with dry DCM (15 mL), chloro-acetic acid (0.098 g, 1.04 mmol) and 1-hydroxybenzotriazole (0.14 g, 1.04 mmol). The solution was then stirred at –10 °C. After 10 minutes EDCI (0.199 g , 1.04 mmol) was added in one portion. The resulting solution was allowed to stir overnight during which time the temperature gradually rose to room temperature. The solution was then washed with 10% $KHCO_3$ (2 x 20 mL). The organic phase was then dried over K_2CO_3 and reduced to produce a grey/purple oil. (0.288 g, 73.43 % Yield). This was purified by alumina column chromatography using [99:1] DCM: MeOH, yielding **145** as a grey resin (0.167 g, 42.53 % Yield). Calculated for $C_{19}H_{29}N_2O_6Cl$: [M+H peak] *m/z* =417.1792, Found: 417.1804; δ_H ($CDCl_3$, 400 MHz) 8.27 (s, 1H, N-H) 7.24 (d 1H, J = 2.0 Hz, Ar-H), 7.04 (d, 1H, J = 8.5 Hz, Ar-H), 6.87 (d,d, 1H, J_1 = 8.5 Hz, J_2 = 2.0 Hz, Ar-H), 4.13 (s, 2H, Cl-CH_2), 3.79 (s, 3H, OCH_3) 3.66-3.61 (m, 16H, OCH_2CH_2) 3.41 (t, 4H, J = 6.0 Hz, OCH_2CH_2); δ_C ($CDCl_3$, 100 MHz) 163.59, 152.96, 137.22, 13152, 121.12, 112.18, 104.89, 70.81, 70.39, 70.25, 70.0, 55.42, 53.03, 42.83; Mass Spec (MeCN, ES+) *m/z* Expected : 416.9, Found: 417.9 (M+H), 439.2 (M+Na); IR υ_{max}(cm^{-1}) 3276,3195, 3117, 3052, 2935, 2864, 1685, 1606, 1536, 1510, 1541, 1351, 1288, 1254, 1219, 1121, 1035, 986, 939, 846, 810, 726.

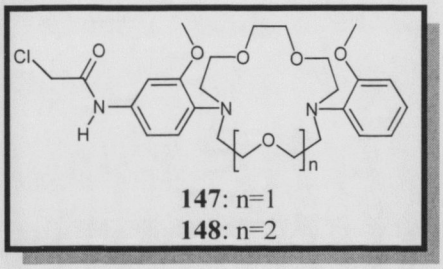
2-Chloro-N-[3-methoxy-4-(1,4,7,10,13-pentaoxa-16-aza-cyclooctadec-16-yl)-phenyl]-acetamide (146)



Synthesis carried out with Method 2, on a 2.667 mmol scale. **146** was obtained as a grey/purple oil. (0.775 g, 74.4 % yield) Calculated for $C_{21}H_{34}N_2O_7Cl$: [M+H peak] *m/z* = 461.2055, Found: 461.2043; δ_H ($CDCl_3$, 400 MHz) 9.15 (s, 1H, N-H) 7.35 (s 1H, Ar-

H), 7.00 (s, 2H, Ar-H), 4.19 (s, 2H, Cl-CH_2), 3.75 (s, 3H, OCH_3) 3.63 (s, 8H, OCH_2CH_2) 3.54(s, 4H, OCH_2CH_2) 3.47-3.42 (s, 8H, OCH_2CH_2) 3.23(s, 4H, OCH_2CH_2); Mass Spec (MeCN, ES+) *m/z* Expected : 460.19, Found: 461.30 (M+H), 483.30 (M+Na), 489.24 (M+K); IR $\upsilon_{max}(cm^{-1})$ 3434, 3235, 3180, 3103, 3040, 2884, 1750, 1689, 1607, 1542, 1511, 1458, 1408, 1650, 1253, 1219, 1107, 1032, 957, 835, 748, 551.

General procedure for the formation of α-chloroamides (147 and 148)



147: n=1
148: n=2

128, (0.559 g, 1.256 mmol) [or **129**, (0.687 g, 1.40 mmol) in the case of **148**] was placed into a 50 mL single neck RBF along with 1,4 – dioxane (99+%, ACS grade) (20 mL). To this was added 1.1 equivalents of Na_2CO_3. This solution was stirred at room temperature. To this a solution of 1,4 – dioxane (99+%, ACS grade) (10 mL), containing 1.1 equivalents of α - chloroacetic anhydride was added. The resulting solution was stirred at room temperature over night. The solution was then reduced and the resulting residue was dissolved in water (50 mL) and the pH was adjusted to pH 1 with conc. HCl. The solution was then washed with CH_2Cl_2 (2 x 30 mL). The aqueous phase pH was adjusted to pH 14 with KOH pellets and washed with CH_2Cl_2 (2 x 30 mL). The organic phase was dried over $CaCl_2$ and reduced to a crude oil. The oil was run down an alumina column using a gradient elution of CH_2Cl_2 to 30:70 CH_2Cl_2:THF

2-Chloro-N-{3-methoxy-4-[13-(2-methoxy-phenyl)-1,4,10-trioxa-7,13-diaza-cyclopentadec-7-yl]-phenyl}-acetamide (147)

147 was produced as an oil. (0.409 g, 62.26 % yield) Calculated for $C_{26}H_{37}N_3O_6Cl$: [M+H] *m/z* = 522.2371, Found: 522.2374; δ_H ($CDCl_3$, 400 MHz) 8.30 (s, 1H, N-H), 7.30(s, 1H, Ar-H), 7.03 (t, 1H, *J* = 8.0 Hz, Ar-H), 6.98 (d, 1H, *J* = 5.5 Hz, Ar-H), 6.94 – 6.83 (m, 4H, Ar-H), 4.18 (s, 2H, Cl-CH_2), 3.83 (s, 3H, OCH_3), 3.82 (s, 3H, OCH_3), 3.74-3.61 (m, 12H, -OCH_2CH_2O-), 3.49-3.40 (m, 8H, -OCH_2CH_2O-); δ_C ($CDCl_3$, 100 MHz) 163.59, 153.29, 153.0, 140.55, 137.77, 131.72, 122.24, 121.42, 121.10, 120.75, 112.25, 111.95, 105.03, 71.19, 71.05, 70.77, 69.80, 69.80, 69.71, 55.52, 55.39, 53.28, 53.25, 52.65, 52.65, 49.92; Mass Spec (MeCN, ES+) *m/z* Expected : 521.2, Found: 522.2 (M+H); IR $\upsilon_{max}(cm^{-1})$ 3033, 3199, 3116,

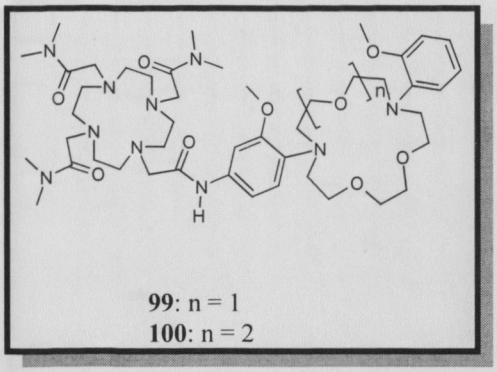
3055, 2946, 2869, 1684, 1606, 1541, 1509, 1452, 1411, 1350, 1239, 1175, 1110, 1030, 926, 857, 801, 745.

2-Chloro-N-{3-methoxy-4-[16-(2-methoxy-phenyl)-1,4,10,13-tetraoxa-7,16-diaza-cyclooctadec-7-yl]-phenyl}-acetamide (148)

148 was produced as an oil. (0.490 g, 61.67 % yield) Calculated for $C_{28}H_{41}N_3O_7Cl$: [M+H] *m/z* = 566.2633, Found: 566.2642; δ_H ($CDCl_3$, 400 MHz) 8.39 (s, 1H, N-H), 7.34 (s, 1H, Ar-H), 7.17-7.11 (m, 2H, Ar-H), 6.98-6.95 (m, 2H, Ar-H), 6.91 (t, 1H, *J* = 8.0 Hz, Ar-H), 6.85 (d, 1H, *J* = 8.0 Hz, Ar-H), 4.21 (s, 2H, Cl-CH_2), 3.85 (s, 3H, OCH_3), 3.84 (s, 3H, OCH_3), 3.60-3.51 (m, 24H, -OCH_2CH_2O-); δ_C ($CDCl_3$, 100 MHz) 163.64, 153.38, 153.15, 139.40, 136.55, 132.00, 122.50, 121.80, 121.53, 120.77, 112.29, 111.89, 104.94, 70.58, 69.98, 69.88, 55.57, 55.42, 52.79, 52.73, 42.98; Mass Spec (MeCN, ES+) *m/z* Expected : 565.2, Found: 566.2 (M+H); IR $\upsilon_{max}(cm^{-1})$ 3272, 3186, 3106, 3042, 2936, 2872, 1688, 1607, 1543, 1502, 1453, 1411, 1352, 1288, 1240, 1174, 1109, 1031, 991, 914, 858, 815, 730.

General synthesis of 99 and 100 [130]

147, (0.2815 g, 0.658 mmol) [or **148**, (0.468 g, 0.828 mmol) in the case of **100**] and 1 equivalent of **149** was placed into a 50 mL single neck RBF. To this was added 1 equivalent Cs_2CO_3 and 40 mL of dry MeCN. The solution was kept under dry conditions in an argon atmosphere and stirred at 72 °C for 72 hrs. The resulting mixture was cooled to room temperature and filtered through celite. MeCN was removed under vacuum and then dissolved in $CHCl_3$ (40 mL). This was washed with water (5 x 20 mL). The organic phase was separated dried over $MgSO_4$ and reduced to give the desired product in a relatively pure state.



99: n = 1
100: n = 2

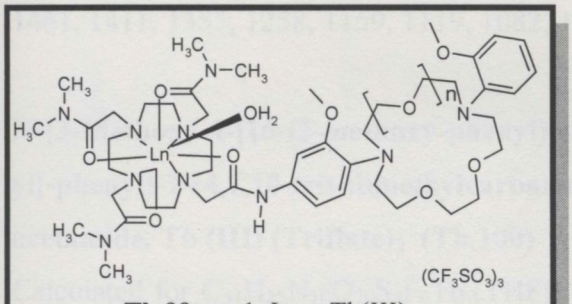
N-{3-Methoxy-4-[13-(2-methoxy-phenyl)-1,4,10-trioxa-7,13-diaza-cyclopentadec-7-yl]-phenyl}-2-(4,7,10-tris-dimethylcarbamoylmethyl-1,4,7,10tetraaza-cyclododec-1-yl)-acetamide (99)

ca. 77 % yield. Calculated for $C_{46}H_{77}N_{10}O_9$: [M+H] m/z = 913.5875, Found: 913.5858 (- 1.9 ppm); δ_C ($CDCl_3$, 100 MHz) 170.30, 170.21, 170.07, 153.0, 152.6, 151.3, 140.16, 135.60, 125.29, 122.06, 121.30, 120.66, 120.50, 111.55, 104.25, 71.01, 70.89, 70.82, 70.51, 69.47, 55.17, 54.74, 54.36, 53.13, 52.92, 52.33, 52.21, 51.84, 36.82, 36.26, 35.23, 34.92; Mass Spec (MeCN, ES+) m/z Expected: 912.5, Found: 913.1(M+H), 456.9(M+2H)/2; IR $\upsilon_{max}(cm^{-1})$ 3420, 2937, 2855, 1647, 1510, 1451, 1403, 1260, 1238, 1217, 1108, 1030, 859, 810, 747, 629, 489.

N-{3-Methoxy-4-[16-(2-methoxy-phenyl)-1,4,10,13-tetraoxa-7,16-diaza-cyclooctadec-7-yl]-phenyl}-2-(4,7,10-tris-dimethylcarbamoylmethyl-1,4,7,10tetraaza-cyclododec-1-yl)-acetamide (100)

ca. 77 % yield. Calculated for $C_{48}H_{81}N_{10}O_{10}$: [M+H] m/z = 957.6137, Found: 957.6188 (+5.3ppm); δ_C($CDCl_3$, 100 MHz) 170.28, 170.22, 170.07, 153.08, 152.80, 143.61, 138.80, 135.58, 125.27, 122.37, 121.63, 121.22, 120.47, 111.43, 104.16, 70.26, 69.54, 55.15, 54.78, 54.30, 52.93, 52.52, 52.42, 51.83, 36.82, 36.25, 35.22, 34.93; Mass Spec (MeCN, ES+) m/z Expected : 956.6 , Found: 957.0 (M+H), 979.0 (M+Na) 478.9 (M+ 2H)/2; IR $\upsilon_{max}(cm^{-1})$ 3417, 2955, 2923, 2854, 1644, 1538, 1504, 1454, 1402, 1260, 1240, 1104, 1030, 812, 750.

General synthesis of Ln(III) complexes Tb.99, Tb.100, Eu.99 and Eu.100 [130]



Tb.99: n =1, Ln = Tb(III)
Tb.100: n =2, Ln = Tb(III)
Eu.99: n =1, Ln = Eu(III)
Eu.100: n =2, Ln = Eu(III)

99 or 100 (~100 mg, ~ 0.1 mmol) and Ln (III) Triflouromethane sulphonate (0.1 mmol) were added to a 5 mL single neck RBF that contained 3 mL of freshly dried MeCN. The solution was freeze thawed three times, placed under an argon atmosphere and left stirring at reflux for 24 hrs. The resulting solution was cooled to room temperature and then dropped slowly onto dry diethyl ether (50-70 mL). The diethyl ether was decanted to leave Ln (III) complex as a crude material. This was dissolved in a small quantity of CH_2Cl_2 and placed onto a dry alumina plug that was washed with 70:30 CH_2Cl_2:THF which was slowly changed by gradient dilution to 60:30:10 CH_2Cl_2:THF:MeOH.

N-{3-Methoxy-4-[13-(2-methoxy-phenyl)-1,4,10-trioxa-7,13-diaza-cyclopentadec-7-yl]-phenyl}-2-(4,7,10-tris-dimethylcarbamoylmethyl-1,4,7,10tetraaza-cyclododec-1-yl)-acetamide. Tb(III). (Triflate)$_3$ (Tb.99)

Calculated for $C_{46}H_{77}N_{10}O_9Tb$: [M+H peak] *m/z* = 1072.5128, Found: 1072.5160 (+ 3.0 ppm); δ_H (CD_3CN, 400 MHz) 68.59, 41.76, 23.72, 18.13, 10.36, 8.69, 7.05, 6.77, 6.56, 5.58, 5.25, 4.82, 4.27, -1.42; δ_F (CD_3CN, 376 MHz) –77.68, -168.03, -196.50; Mass Spec (MeCN, ES+) *m/z* Expected: 1072.51, Found: 356.92 (M+H)/3, 609.82 (M+Triflate)/2, 684.76 (M+2[Triflate])/2; IR $\upsilon_{max}(cm^{-1})$ 3425, 2955, 2924, 2873, 1624, 1560, 1511, 1461, 1356, 1258, 1158, 1119, 1082, 1030, 957, 823, 756, 638, 573, 517.

N-{3-Methoxy-4-[13-(2-methoxy-phenyl)-1,4,10-trioxa-7,13-diaza-cyclopentadec-7-yl]-phenyl}-2-(4,7,10-tris-dimethylcarbamoylmethyl-1,4,7,10tetraaza-cyclododec-1-yl)-acetamide. Eu (III) (Triflate)$_3$ (Eu.99)

Calculated for $C_{49}H_{78}N_{10}O_{19}S_3F_9Eu.(THF)_2$: C, 40.88; H, 5.66; N, 8.36, Found: C, 41.03; H, 5.45; N, 8.42; Calculated for $C_{46}H_{77}N_{10}O_9Eu$: [M+H peak] *m/z* = 1066.5087, Found: 1066.5047 (-3.8 ppm); δ_H (CD_3CN, 400 MHz) 20.37, 18.58, 7.40-6.99 (multiplet), 4.73-2.89 (multiplet), 2.60 (b. s) 0.90, 0.28, -3.43, -8.24; δ_F (CD_3CN, 376 MHz) –79.64, -165.54, -194.95; Mass Spec (MeCN, ES+) *m/z* Expected: 1066.50, Found: 354.95 (M+H)/3, 606.82 (M+Triflate)/2, 681.76 (M+2[Triflate])/2; IR $\upsilon_{max}(cm^{-1})$ 3437, 2924, 2874, 1623, 1563, 1512, 1461, 1411, 1355, 1258, 1159, 1119, 1082, 1030, 957, 822, 756, 639, 573, 517.

N-{3-Methoxy-4-[16-(2-methoxy-phenyl)-1,4,10,13-tetraoxa-7,16-diaza-cyclooctadec-7-yl]-phenyl}-2-(4,7,10-tris-dimethylcarbamoylmethyl-1,4,7,10tetraaza-cyclododec-1-yl)-acetamide. Tb (III) (Triflate)$_3$ (Tb.100)

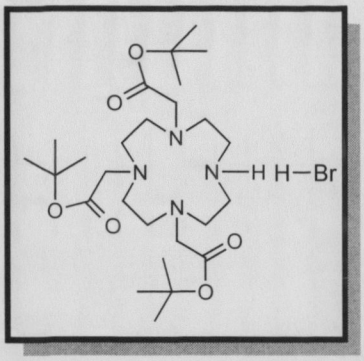
Calculated for $C_{51}H_{82}N_{10}O_{20}S_3F_9Tb.(THF)_2$: C, 41.07; H, 5.72; N, 8.12, Found: C, 40.93; H, 5.44; N, 7.63; Calculated for $C_{48}H_{81}N_{10}O_{10}Tb$: [M+H peak] *m/z* = 1116.5391, Found: 116.5390 (-0.1 ppm); δ_H (CD_3CN, 400 MHz) 77.2 (b.s), 55.7 (b.s), 46.9(b.s), 22.51 (b.s), 17.52 (b.s),15.65 (b.s), 9.31-8.62 (multiplet), 5.39 (b.s), 4.77 (b.s), 3.85 (b.s), 3.55 (b.s), 2.92 (b.s), 2.51 (b.s), 1.74 (b.s), -73.14 (s), -89.81 (s), -97.28 (s) ; δ_F (CD_3CN, 376 MHz) –78.52, -167.71, -190.58; Mass Spec (MeCN, ES+) *m/z* Expected: 1116.53, Found: 371.60 (M+H)/3,

631.84 (M+Triflate)/2, 706.74 (M+2[Triflate])/2; IR $\upsilon_{max}(cm^{-1})$ 3427, 2924, 2877, 1624, 1561, 1511, 1461, 1411, 1354, 1258, 1159, 1119, 1088, 1030, 957, 823, 756, 638, 573, 516.

N-{3-Methoxy-4-[16-(2-methoxy-phenyl)-1,4,10,13-tetraoxa-7,16-diaza-cyclooctadec-7-yl]-phenyl}-2-(4,7,10-tris-dimethylcarbamoylmethyl-1,4,7,10tetraaza-cyclododec-1-yl)-acetamide. Eu (III) (Triflate)$_3$ (Eu.100)

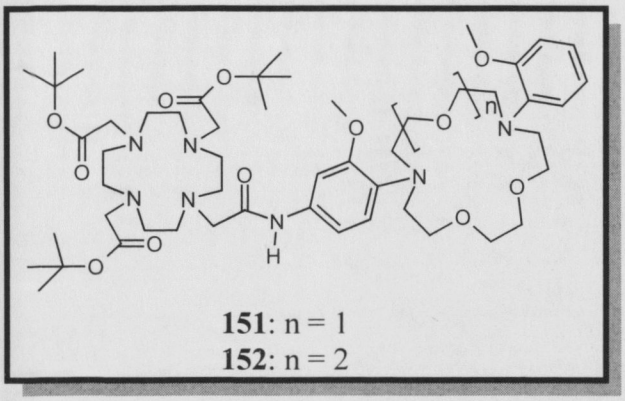
Calculated for $C_{48}H_{81}N_{10}O_{10}Eu$: [M+H peak] *m/z* = 1110.5350, Found: 1110.5302 (-4.3 ppm); δ_H (CD_3CN, 400 MHz) 19.59, 11.98, 7.95-7.00 (multiplet), 4.03, 3.71, 3.48-3.41, (multiplet), 3.17, 1.41, 1.29, -0.11, -0.43, -3.99, -4.88, -7.54, -8.12; δ_F (CD_3CN, 376 MHz) –79.70, -167.83, -197.82; Mass Spec (MeCN, ES+) *m/z* Expected: 1110.53, Found: 371.60 (M+H)/3, 631.84 (M+Triflate)/2, 706.74 (M+2[Triflate])/2; IR $\upsilon_{max}(cm^{-1})$ 3444, 2957, 2924, 2881, 1625, 1559, 1513, 1462, 1414, 1354, 1258, 1161, 1089, 1030, 957, 822, 757, 638, 573, 517.

Synthesis of (4,7-Bis-tert-butoxycarbonylmethyl-1,4,7,10tetraaza-cyclododec-1-yl)-acetic acid tert-butyl ester. Hydrobromide salt (150) [158]



1,4,7,10 tetraazacyclododecane, (98 %), (1.78 g, 10.0 mmol) was placed in a 50 mL single neck RBF. To this was added $NaHCO_3$, (2.78 g, 33.0 mmol) and dry MeCN (60 mL). Bromo-acetic acid *tert*-butyl ester (6.45 g 5.33 mL, 33.0 mmol) was added to the stirring mixture at 0 °C over a ten minute period. This solution was allowed to warm up to 20 °C and stirred for a further 48 hours. The resulting solution was then passed through a celite filter and reduced to a residue The residue was recrystalised in Toluene to give a white solid which was further purified on Silica using 100% DCM to 97:3, DCM:MeOH to give a white solid (2.803 g, 47% yield). Calculated for $C_{26}H_{51}N_4O_6$: [M+H] *m/z* = 515.3809, Found: 515.3830; δ_H ($CDCl_3$, 400 MHz) 10.03 (s, 2H, N-H•HBr), 3.37 (s, 4H, $C\underline{H}_2CO_2$), 3.29 (s, 2H, $C\underline{H}_2CO_2$), 3.10 (s, 4H, $C\underline{H}_2$), 2.93 (s, 8H, $C\underline{H}_2$), 2.88 (s, 4H, $C\underline{H}_2$), 1.46 (s, 27H *t*-butyl) ; Mass Spec (MeCN, ES+) *m/z* Expected : 514.7, Found: 515.4 (M+H);

General synthesis of 151 and 152 [130]



151: n = 1
152: n = 2

147, (0.2825 g, 0.474 mmol) [or **148**, (0.638 g, 1.12 mmol) in the case of **152**] and 1 equivalent of **150** was placed into a 50 mL single neck RBF. To this was added Cs_2CO_3 (2 equivalents) and dry MeCN (30 mL). The solution was kept under dry conditions in an Argon atmosphere and stirred at reflux for 72 hrs. The resulting mixture was cooled to room temperature and filtered through celite. MeCN was removed under vacuum to produce a crude oil. The crude oil was dissolved in a small quantity of DCM and placed onto a dry alumina column that was washed with 70:30 DCM:THF which was slowly changed by gradient dilution to 60:30:10 DCM:THF:MeOH.

[4,7-Bis-tert-butoxycarbonylmethyl-10-({3-methoxy-4-[13-(2-methoxy phenyl)-1,4,10-trioxa-7,13-diaza-cyclopentadec-7-yl]-phenylcarbamoyl}-methyl)-1,4,7,10 tetraaza-cyclododec-1-yl]-acetic acid tert-butyl ester (151)

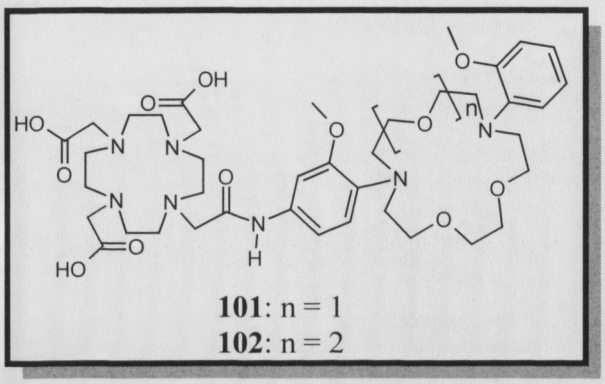
Calculated for $C_{52}H_{86}N_7O_{12}$: [M+H peak] *m/z* = 1000.6334, Found: 1000.6307 (-2.8ppm); δ_c ($CDCl_3$, 100 MHz) 172.58, 172.09, 170.18, 152.52, 151.20, 140.13, 135.48, 134.93, 122.05, 121.16, 120.64, 120.55, 112.27, 111.63, 105.35, 81.57, 81.52, 70.69, 70.41, 69.45, 67.63, 56.47, 55.50, 55.31, 55.08, 53.04, 52.72, 52.41, 52.22, 27.69, 27.62; Mass Spec (MeCN, ES+) *m/z* Expected: 999.6, Found: 1000.6 (M+H), 1022.6 (M+Na), 500.7 (M+2H)/2; IR $\upsilon_{max}(cm^{-1})$ 3428, 2975, 2854, 1728, 1681, 1607, 1504, 1454, 1368, 1312, 1228, 1166, 1106, 1008, 852, 756, 597 .

[4,7-Bis-tert-butoxycarbonylmethyl-10- ({3-methoxy-4-[16-(2-methoxy-phenyl)-1, 4, 10, 13-tetraoxa-7,16-diaza-cyclooctadec-7-yl]-phenylcarbamoyl}-methyl)-1,4,7,10 tetraazacyclododec-1-yl]-acetic acid tert-butyl ester (152)

Calculated for $C_{54}H_{90}N_7O_{13}$: [M+H peak] *m/z* = 1044.6597, found: 1044.6619 (+2.1 ppm); δ_H ($CDCl_3$, 400 MHz) [Partial NMR only] 10.82 (1H, N-H), 7.36 (d, 1H *J* = 8.52 Hz, Ar-H), 7.29 (s, 1H, Ar-H), 6.99 (d, 1H, *J* = 7.5 Hz, Ar-H), 6.82 – 6.78 (multiplet, 2H, Ar-H), 6.75 (t, 1H, *J*

= 7.5 Hz, Ar-H), 6.68 (d, 1H, J = 8.0 Hz, Ar-H), 1.32 (s, 9 H, t- butyl C$\underline{H}_3$), 1.30 (s, 18 H, t-butyl C$\underline{H}_3$); δ_c ($CDCl_3$, 100 MHz) 172.37, 171.94, 170.03, 152.60, 151.00, 135.31, 134.75, 127.67, 122.07, 120.90, 120.18, 112.02, 111.18, 104.95, 81.54, 81.31, 69.69, 69.28, 67.42, 55.30, 55.11, 54.89, 52.39, 52.14, 27.51, 27.44; Mass Spec (MeCN, ES+) *m/z* Expected: 1043.6, Found: 1044.6 (M+H), 1066.7 (M+Na), 522.8 (M+2H)/2; IR υ_{max}(cm^{-1}) 3420, 2974, 2857, 1728, 1680, 1607, 1512, 1454, 1368, 1311, 1165, 1105, 1008, 852, 755, 598.

General synthesis of 101 and 102 [158]



101: n = 1
102: n = 2

The triester, **151** (or **152**) (0.162 mmol) was placed into a 25 mL single neck RBF. To this was added DCM (12 mL) and TFA (5 mL). The solution was stirred for 24 hours at room temperature. The solvent was removed under reduced pressure and the acid chased off by the addition and evaporation of successive portions of DCM (2 x 10 mL), MeOH (2 x 10 mL) and ether (2 x 10 mL). The resulting residue was dissolved into MeOH (0.25 mL) to which ether (10 mL) was added dropwise yielding the desired product as a solid. This was filtered, washed with cold ether and dried under vacuum.

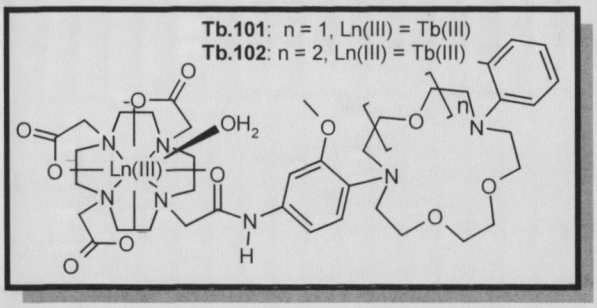
[4,7-Bis-carboxymethyl-10-({3-methoxy-4-[13-(2-methoxy-phenyl)-1,4,10-trioxa-7,13-diaza-cyclopentadec-7-yl]-phenylcarbamoyl}methyl)-1,4,7,10tetraaza-cy clododec-1-yl]-acetic acid (101)

Calculated for $C_{40}H_{62}N_7O_{12}$: [M+H peak] *m/z* = 832.4456, Found: 832.4462 (+0.6 ppm); δ_H (CD_3CN, 400 MHz) 10.88 (b.s, 1H), 8.41 (b.s, 1H), 7.57 (b.s, 2H, Ar-H), 7.51 (s, 1H, Ar-H), 7.38-7.36 (multiplet, 2H, Ar-H), 7.12-7.10 (multiplet, 1H, Ar-H), 7.04 (s, 1H, Ar-H), 3.84 (b.s, 6H), 3.61 (b.s, 10H), 3.43-3.38 (multiplet, 16H), 3.18 (b.s, 20H); Mass Spec (MeCN, ES+) *m/z* Expected: 831.44, Found: 832.3 (M+H), 854.3 (M+Na), 416.6(M+2H)/2, 278.1(M+3H)/3; IR υ_{max}(cm^{-1}) 3429, 3104, 2958, 2924, 2854, 1683, 1504, 1461, 1375, 1355, 1203, 1181, 1127, 1104, 828, 801, 721, 689, 620, 598, 516.

[4,7-Bis-carboxymethyl-10-({3-methoxy-4-[16-(2-methoxy-phenyl)-1,4,10,13-tetraoxa-7,16-diaza-cyclooctadec-7-yl]-phenylcarbamoyl}-methyl)-1,4,7,10tetraaza-cyclododec-1-yl]-acetic acid (102)

Calculated for $C_{42}H_{66}N_7O_{13}$: [M+H peak] *m/z* = 876.4719, Found: 876.4722 (+0.4 ppm); δ_H (CD_3CN, 400 MHz) 10.88 (b.s, 1H), 8.64 (b.s, 1H), 7.59 (b.s, 1H,), 7.45 (b.s, 1H), 7.27 (b.s, 3H), 7.18 (s, 1H,), 7.07-7.01 (broad multiplet, 3H, Ar-H), 4.25-4.08 (broad multiplet, 4H, Ar-H), 3.80 (b.s, 9H), 3.48 (s, 27H), 3.15 (b.s, 12H), 2.65 (b.s, 2H); δ_c (CD_3CN, 100 MHz) 173.18, 169.82, 169.43, 165.46, 154.50, 138.10, 126.41, 123.68, 121.12, 118.12, 115.26, 111.59, 102.99, 68.52, 66.62, 57.68, 56.36, 55.12, 54.45, 53.96, 53.36, 53.17, 52.84, 50.99, 49.33, 48.37, 46.80, 44.01; Mass Spec (MeCN, ES+) *m/z* Expected: 875.4, Found: 876.5 (M+H), 898.5 (M+Na), 439.1 (M+2H)/2, 298.2 (M+3H)/3; IR $\upsilon_{max}(cm^{-1})$ 3429, 3104, 2957, 2921, 2880, 1688, 1512, 1462, 1353, 1202, 1178, 1123, 1093, 827, 764, 719, 690, 618, 569, 513.

General synthesis of Ln(III) complexes Tb.101 and Tb.102 [130]



101 (or **102**) (~80 mg, ~0.1 mmol) and Tb (III) Triflouromethane sulphonate (0.1 mmol) was added to a 5 mL single neck RBF which contained freshly dried MeCN (3 mL). The solution was freeze thawed three times, placed under an argon atmosphere and left stirring at reflux for 24 hrs. The solution was cooled to room temperature and then reduced. The resulting crude was dissolved in MeCN (0.5 mL). While stirring diethyl ether (5 mL) was added leading to the formation of a white precipitate. The solvent was decanted off and the off white solid was washed with cold ether (2 x 5 mL). The resulting solid was dried under vacuum and shown by TLC, 65:30:5 (CH_2Cl_2:THF:MeOH) the product appeared to be pure indicated by one spot above the baseline. (Yields > 80%)

[4,7-Bis-carboxymethyl-10-({3-methoxy-4-[13-(2-methoxy-phenyl)-1,4,10-trioxa-7,13-diaza-cyclopentadec-7-yl]-phenylcarbamoyl}methyl)-1,4,7,10tetraaza-cy clododec-1-yl]-acetic acid. Tb(III) (Tb.101)

Calculated for $C_{40}H_{59}N_7O_{12}Tb$: [M+H peak] *m/z* = 988.3475, Found: 988.3458 (-1.7 ppm); δ_H (CD_3CN, 400 MHz) 7.13, 3.38, 1.94, 1.09, - 3.56; Mass Spec (MeCN, ES+) *m/z* Expected 987.34, Found: 988.26 (M+H), 494.67 (M+2H)/2, 1010.34 (M+Na), 505.65 (M+H)/2; IR $\upsilon_{max}(cm^{-1})$ 3481, 3111, 2987, 2927, 1612, 1504, 1460, 1408, 1276, 1257, 1165, 1086, 1030, 802, 760, 721, 639, 574, 517.

[4,7-Bis-carboxymethyl-10-({3-methoxy-4-[16-(2-methoxy-phenyl)-1,4,10,13-tetraoxa-7,16-diaza-cyclooctadec-7-yl]-phenylcarbamoyl}-methyl)-1,4,7,10tetraaza-cyclododec-1-yl]-acetic acid. Tb(III) (Tb.102)

Calculated for $C_{42}H_{63}N_7O_{13}Tb$: [M+H peak] *m/z* = 1032.3737, Found: 1032.3741 (+0.4 ppm); δ_H CD_3CN, 400 MHz) 7.65, 7.28, 6.98, 6.18, 5.48, 4.04, 3.59, 3.43, 1.34, 1.28, 1.14, 0.75, -1.47; Mass Spec (MeCN, ES+) *m/z* Expected: 1031.37, Found: 1032.23 (M+H), 516 (M+2H)/2, 344.73 (M+3H)/3; IR $\upsilon_{max}(cm^{-1})$ 3444, 2924, 2885, 1611, 1545, 1459, 1408, 1260, 1169, 1080, 1031, 841, 802, 761, 721, 640, 575, 518.

6.1.1 Photophysical studies

All studies were carried out on solutions of complexes in water or in buffered solutions at 10, 8 or 4 μM. Buffered solutions consisted of 0.1 M Tris Buffer and 0.1 M TMACl at pH 7.4. ***Uv-vis*** spectroscopy analysis was carried out on a Shimadzu UV-2401 PC UV-Vis spectrophotometer. Studies were carried out on fast scan mode with slit widths of 1.0 nm, using matched quartz cells. All absorption scans were saved as ACS II files and further processed in Excel.™ Excitations were carried out around 300 nm unless otherwise stated. Solutions were 5 mL or 10mL. Fluorescence and luminescence measurements were made on a **Perkin Elmer LS 50B** or **Varian Carey Eclipse** with general settings as indicated in Table 6.1a and Table 6.1b respectively.

Table 6.1a Fluorimeter settings for pH and pM Studies

Fluorimeter settings: Varian Cary Eclipse same on LS50B	
Mode: Fluorescence	**Flash count**: 1
Scan control: Medium	**Scan** 315nm - 580nm
Excitation: 300nm	**PMT(Voltage)**: High
Excite Slit: 10 nm	**Emission Slit**: 10 nm

Table 6.1b Fluorimeter settings (Phosphorescence mode) for pH and pM Studies

Luminescence: Perkin Elmer LS50 B Mode:	**Luminescence settings: Varian**
Phos **Delay Time**: 0.1 ms	**Mode**: Phos **Delay Time**: 0.1ms
Gate Time: 10 **Cycle**: 20	**Gate Time**: 10ms **Cycle**: 20
Flash count: 1	**Flash count**: 1 **Total decay**: 0.02s
Scan 450 nm - 750 nm (Tb(III))	**Scan** 450 nm - 700 nm (Tb(III))
550 nm - 750 nm (Eu(III))	550 nm - 750 nm (Eu(III))
Excitation: 300 nm **Scan speed**: 240nm/min	**Excitation**: 300 nm **PMT(Voltage)**: High
Excite Slit: 9 nm **Emission Slit**: 9 nm	**Excite Slit**: 10 nm **Emission Slit**: 10 nm

6.1.2 Lanthanide complexes – Life time studies

Solutions were made in H_2O and D_2O (~ 1-2 mg/2 mL). Lifetimes were measured on a Varian Carey Eclipse Fluorescence spectrophotometer using with general settings as indicated in Table 6.2.

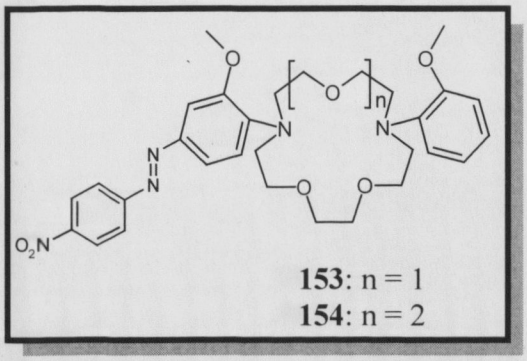
Table 6.2 Flourimeter settings for lifetime analysis

Fluorimeter settings: Lifetime measurements - Varian Carey Eclipse
Direct excitation: Eu(III) @ 395 nm, Tb(III) @ 366 nm
Emission: Eu(III) @ 615 nm, Tb(III) @ 545 nm
Mode: Phos **Delay Time**: 0.1ms **Gate Time**: 0.1ms
Cycle: 1000 **Flash count**: 1 **No. Cycles**: 1000
Total decay: 1.5 – 3.0 ms **PMT (voltage)**: High
Excitation Slit width: 5 nm **Emission Slit width**: 5 nm

6.2 Synthesis and photophysical data for Chapter 3

General synthesis of 153 and 154 [27, 28]

To a 50 mL RBF, p-nitro aniline (0.104 g, 0.766 mmol) was added containing a solution of 1:1, THF: H_2O (10 mL) and $NaNO_2$, (0.053 g 0.766 mmol). To the solution, which was, being stirred at 0 °C, HCl, (0.15 mL, 12 M), was slowly added. This solution was added drop wise to a 100 mL single neck RBF which contained **111** (0.300 g, 0.696 mmol) [or **112** (0.300 g, 0.632 mmol) in the case of **154**] in a solution of 1:1 THF:H_2O (20 mL). This solution was stirred at 0 °C for approximately 2 hours. This solution was left stirring overnight at room temperature. The resulting dark red solution was reduced down, dissolved into $CHCl_3$ (60 mL) and washed with water, (2 x 30 mL). The organic phase was dried over $MgSO_4$ and reduced to deep red oil. The crude material was purified on an alumina column using 70:30 Hex: EtOAc, to produce **153** or **154** as a deep red solid.



153: n = 1
154: n = 2

{3-Methoxy-4-[13-(2-methoxy-phenyl)-1,4,10-trioxa-7,13-diaza-cyclopentadec-7-yl]-phenyl}-(4-nitro-phenyl)-diazene (153)

0.199 g, [49.27 % Yield] of a deep red solid was collected. M.P. = 137-139 °C. Calculated for $C_{30}H_{37}N_5O_7.(H_20)_{3/2}$: C, 59.39; H, 6.65; N, 11.54, Found: C, 59.63; H, 6.37; N, 11.14; Calculated for $C_{30}H_{38}N_5O_7$: [M+H peak] *m/z* = 580.2771, Found: 580.2770; δ_H ($CDCl_3$, 400 MHz) 8.34 (d, 2H, *J* = 9.0 Hz, Ar-H), 7.95 (d, 2H, *J* = 9.0 Hz, Ar-H), 7.61 (d,d, 1H, J_1 = 8.5 Hz, J_2 = 2.0 Hz, Ar-H), 7.48 (d,1H, *J* = 2.0 Hz, Ar-H), 7.02 (d, 2H, *J* = 8.5 Hz, Ar-H), 6.96 (t,d, 1H, J_1 = 7.5 Hz, J_2 = 1.48 Hz, Ar-H), 6.86 (t,d, 2H, J_1 = 7.5 Hz, J_2 = 1.5 Hz, Ar-H), 3.91 (s, 3H, OCH$_3$), 3.83 (s, 3H, OCH$_3$), 3.76 (t, 2H, *J* = 5.5 Hz, OCH$_2$ CH$_2$O), 3.74 -3.67 (m, 6H, OCH$_2$ CH$_2$O), 3.66-3.64 (m, 6H, OCH$_2$ CH$_2$O), 3.49 (t, 4H, *J* = 4.0 Hz, OCH$_2$ CH$_2$O), 3.41 (t, 2H, *J* = 4.5 Hz, OCH$_2$ CH$_2$O); δ_C($CDCl_3$, 100 MHz) ; 156.53, 153.18, 151.36, 147.75, 146.30, 145.19, 140.54, 124.68, 123.01, 122.80, 122.50, 121.36, 120.77, 116.74, 111.96, 102.85, 71.49, 71.17, 70.94, 70.83, 69.82, 69.69, 55.59, 55.41, 53.68, 53.37, 53.09, 52.03; Mass Spec (MeCN, ES+) *m/z* Expected : 579.65, Found: 580.23 (M+H); IR

$\upsilon_{max}(cm^{-1})$ 2950, 2904, 2859, 1587, 1509, 1448, 1376, 1334, 1241, 1103, 1058, 1022, 860, 798, 768, 686, 615.

{3-Methoxy-4-[16-(2-methoxy-phenyl)-1,4,10,13-tetraoxa-7,16-diaza-cyclooctadec-7-yl]-phenyl}-(4-nitro-phenyl)-diazene (154)

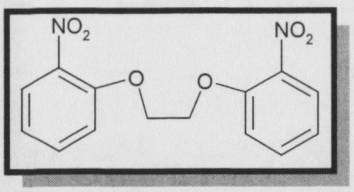
0.175 g, [44.41 % Yield] of a deep red solid was collected. M.P. = 95-97 °C. Calculated for $C_{32}H_{41}N_5O_8$: C, 61.62; H, 6.63; N, 11.23, Found: C, 61.89; H, 6.82; N, 10.84; Calculated for $C_{32}H_{42}N_5O_8$: [M+H peak] *m/z* = 624.3047, Found: 624.3041; δ_H ($CDCl_3$, 400 MHz) 8.34 (d, 2H,*J* = 9.0 Hz, Ar-H), 7.96 (d, 2H, *J* = 8.5 Hz, Ar-H), 7.64 (d,d, 1H, J_1= 8.5 Hz, J_2 = 2.0 Hz Ar-H),), 7.49 (s,1H, Ar-H), 7.15 (d, 1H, *J* = 7.5 Hz, Ar-H), 7.10 (d, 1H, *J* = 8.0 Hz, Ar-H), 7.0 (t, 1H, *J* = 7.5 Hz, Ar-H), 6.91 (t, 1H, *J* = 7.5 Hz, Ar-H), 6.86 (d, 1H, *J* = 7.5 Hz, Ar-H), 3.93 (s, 3H, OCH_3), 3.84 (s, 3H, OCH_3), 3.75 (s, 8H, OCH_2 CH_2O), 3.63-3.58 (m, 12H, OCH_2 CH_2O), 3.55-3.52 (m, 4H, OCH_2 CH_2O); δ_C($CDCl_3$, 100 MHz) 156.45, 153.12, 151.55, 147.76, 146.54, 144.77, 139.38, 124.65, 122.80, 122.71, 122.57, 121.44, 120.72, 117.42, 111.85, 102.87, 70.75, 70.62, 70.09, 70.0, 55.57, 55.39, 52.78, 52.70; Mass Spec (MeCN, ES+) *m/z* Expected : 623.7, Found: 624.3 (M+H); IR $\upsilon_{max}(cm^{-1})$ 2929, 2871, 1587, 1519, 1500, 1457, 1394, 1344, 1251, 1139, 1093, 1027, 923, 862, 738, 688, 626.

6.2.1 Photophysical studies

Uv-vis spectroscopy analysis was carried out on a Shimadzu UV-2401 PC UV-Vis spectrophotometer. Studies were carried out on fast scan mode with slit widths of 1.0 nm, using matched quartz cells. Studies were carried out in 50:50, H_2O:MeOH and/or buffered conditions. When buffered conditions were used the solutions contained 0.1M TMACl and 0.1M Tris Buffer, at pH 7.4. Test solutions were 5 mL or 10 mL for metal titrations and 10 mL or 20 mL for pH studies. All absorption scans were saved as ACS II files and further processed in Excel™ to produce all graphs shown in this thesis.

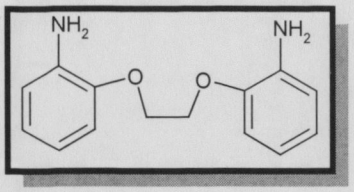
6.3 Synthesis and photophysical data for Chapter 4

Synthesis of 1,2 Bis (2-nitrophenoxy) ethane (170) [42]



Ortho nitro phenol (10.00 g, 71.88mmol) was added to a 250 mL single neck RBF. To this was added K_2CO_3 (10.00 g, 72.46 mmol) and dry DMF (120 mL). The air was removed under vacuum and replaced by an argon atmosphere. To this solution 1,2 dibromo ethane (3.2 mL, 7.04 g, 72.46mmol) was added. The solution was heated to 120 °C overnight by which time the orange solution had turned bright red, and a solid had formed. The solution was then passed through a buchner funnel were a solid material was collected. The solid was washed with water (2 x 50 mL) and EtOH (2 x 50 mL). The white solid produced was then dried under vacuum after which 5.226 g (47.79% yield) of **170** as a yellow solid was collected. M.P. = 167-169 °C. Calculated for $C_{14}H_{13}N_2O_6$: [M+H peak] *m/z* = 305.0774, Found: 305.0767; δ_H ($CDCl_3$, 400 MHz) 7.84 (d, *J* = 6.5 Hz, 2H, Ar-H), 7.58 (t, *J* = 7.6 Hz, 2H, Ar-H), 7.25 (d, *J* = 8.0 Hz, 2H, Ar-H), 7.10 (t, *J* = 6.5 Hz, 2H, Ar-H), 4.56 (s, 4H); δ_C ($CDCl_3$, 100 MHz) 151.42, 133.76, 125.08, 120.92, 115.49, 68.27; Mass Spec (MeCN, ES+) *m/z* Expected: 304.0, Found: 305.1 (M+H), 327.1 (M+Na), 343.1 (M+K), 421.1 ($M+K_3$), 631.2 (M_2+Na); IR υ_{max}(cm^{-1}) 3448, 3085, 2956, 2875, 1606, 1583, 1517, 1484, 1450, 1355, 1276, 1249, 1162, 1089, 1058, 944, 852, 771, 746, 676, 620, 557, 518, 470.

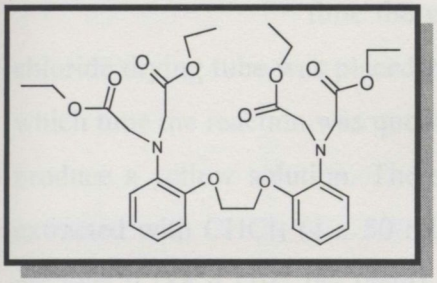
Synthesis of 1,2 Bis (2-amino phenoxy) ethane (171) [42]



1,2 Bis (2-nitrophenoxy) ethane, (4.00 g, 13.14 mmol) was placed in 100 mL RBF. To this was added 5% Pd-C, (0.40 g) and EtOH (50 mL). The solution was stirred under a H_2 atmosphere until no more H_2 was consumed. The resulting solution was passed through a celite filter, which was then washed with $CHCl_3$ (200 mL) [some of the product had precipitated from the reaction solution and was washed with $CHCl_3$ to separate from the catalyst]. The solution was then reduced under vacuum to produce 2.119 g (84.25 %) of **171** as a cream crystalline solid. M.P. = 88-89 °C. calculated for $C_{14}H_{17}N_2O_2$: [M+H peak] *m/z* = 245.1290, Found: 245.1314; δ_H ($CDCl_3$, 400 MHz) 6.90-6.84 (multiplet, 4H, Ar-H), 6.77 – 6.73 (m, 4H, Ar-H), 4.38 (s, 4H, CH_2), 3.73 (s [broad], 4H, N-H); δ_C ($CDCl_3$, 100

MHz) 145.82, 136.47, 121.50, 117.90, 114.92, 112.19, 67.09; Mass Spec (MeCN, ES+) *m/z* Expected: 244.1, Found: 245.1 (M+H), 267.1 (M+Na), 489.2 (M_2+H), 511.2 (M_2+Na); IR $\upsilon_{max}(cm^{-1})$ 3442, 3361, 3060, 2956, 2933, 2879, 1880, 1758, 1610, 1504, 1459, 13386, 1338, 1274, 1214, 1141, 1081, 943, 833, 736, 619, 565, 451.

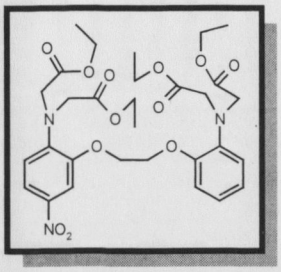
Synthesis of [(2-{2-[2-(Bis – ethoxycarbonylmethyl - amino) – phenoxy] - ethoxy} - phenyl)-ethoxycarbonylmethyl - amino]- acetic acid ethyl ester (172) [42]



1,2 Bis (2-amino phenoxy) ethane (1.00 g, 4.1 mmol) was placed in a 100 mL three necked RBF. To this was added K_2CO_3, (2.259 g, 16.37 mmol) and KI (2.72 g, 16.4 mmol). A condenser was fitted and dry DMF (60 mL) was added. The system was placed under vacuum and the atmosphere was then replaced by argon. The solution was then heated to 120 °C upon which bromo ethyl acetate, 1.8 mL (2.73 g, 16.4 mmol) was added. The reaction was left stirring for 24 hours. The solution was then cooled and poured into a solution of 1:1, EtOAc:H_2O (200 mL). The two phases were separated and the water phase was washed with EtOAc (2 x 50 mL). The combined organic layers were washed with brine (2 x 100 mL), dried over $MgSO_4$ and reduced under vacuum to a brown oil. This was dried further under vacuum to produce a brown solid, 2.39 g (99.52%). This brown solid was recrystalised from EtOH to produce **172** as yellow/ brown crystals 1.32 g (54.6% yield). M.P. = 93-94 °C; Calculated for $C_{30}H_{40}N_2O_{10}$: C, 61.21; H, 6.85; N, 4.76, Found: C, 61.00; H, 6.84; N, 4.77, Calculated for $C_{30}H_{41}N_2O_{10}$: [M+H peak] *m/z* = 589.2761, Found: 589.2756; δ_H ($CDCl_3$, 400 MHz) 6.89 – 6.84 (multiplet, 8H, Ar-H), 4.29 (s, 4H, CH_2), 4.17 (s, 8H, CH_2), 4.06 (quartet, J = 7.6 Hz, 8H, CH_2) 1.16 (triplet, J = 7.6 Hz, 12H, CH_3); δ_C ($CDCl_3$, 100 MHz) 171.0, 149.9, 139.0, 121.7, 121.0, 118.6, 112.9, 66.7, 60.2, 53.0, 13.56; Mass Spec (MeCN, ES+) *m/z* Expected: 588.6, Found: 589.2 (M+H), 611.4 (M+Na); IR $\upsilon_{max}(cm^{-1})$ 3461, 3064, 2979, 2913, 2867, 1741, 1596, 1506, 1465, 1415, 1371, 1240, 1187, 1126, 1066, 1027, 975, 941, 850, 744, 642, 554, 476.

Synthesis of [(2-{2-[2-(Bis-ethoxycarbonylmethyl-amino)-phenoxy]-ethoxy}-4-nitro-phenyl)-ethoxycarbonylmethyl-amino]-acetic acid ethyl ester (173)

Method A: [130]



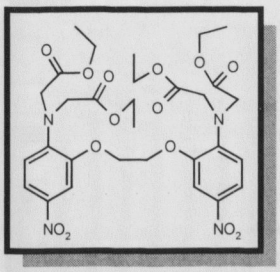
1,2 Bis [-(Bis[ethoxy carbonyl methyl]) amino phenoxy] ethane, (0.161 g, 0.27 mmol) was placed in a 100 mL single neck RBF with dry MeCN (20 mL). This solution was stirred at room temperature in an oil bath. Nitronium tetrafluoroborate [dried for 48 hours under vacuum in a P_2O_5 dessicator], (0.056 g, 0.41mmol, 1.5 eq) in MeCN (20 mL) was added drop-wise over a 15-minute period, during which time the pale yellow solution turned a dark green colour. A calcium chloride drying tube was placed on the RBF and the solution was left stirring overnight upon which time the reaction was quenched by pouring the solution into deionised water (50 mL) to produce a yellow solution. The solution was left to stir for 20 minutes upon which it was extracted with $CHCl_3$ (4 x 50 mL). The combined organic layers were dried over $MgSO_4$ to produce 0.185 g (107.1% yield) of **173** as a yellow solid that showed up on TLC as three distinct spots. The desired product was purified by silica column chromatography using 1:99, EtOAc: CH_2Cl_2, to yield 0.101 g (58.72 % yield) of a yellow solid.

Method B: **Modified version of procedure by Shortreed and Pethig** [185, 186]

1,2 Bis [-(Bis[ethoxy carbonyl methyl]) amino phenoxy] ethane (1.00 g, 1.69 mmol) was placed in a 250 mL single necked RBF with $CHCl_3$ (100 mL). This solution was stirred at -60 ^oC in a dry ice-IPA bath. 48.8 mL of solution of 1:20 Fuming HNO_3: Glacial Acetic acid, was added in 200 µL aliquots every 60 seconds. The solution was left to stir for 60 minutes upon which it was quenched with 1.0 M $NaHCO_3$ (100 mL). The yellow solution was extracted with $CHCl_3$ (4 x 50 mL). The combined organic layers were dried over $MgSO_4$ to produce 1.158 g of a yellow/ brown solid that showed up on TLC as three distinct spots. The desired product was purified by flash column chromatography using CH_2Cl_2, followed by a gradient elution to CH_2Cl_2: MeCN (95:5), to yield 0.600g (55.76% yield) of **173** as a yellow solid. MP = 128-129 ^oC; Calculated for $C_{30}H_{40}N_3O_{12}$: C, 56.87; H, 6.20; N, 6.63, Found: C, 56.80; H, 6.17; N, 6.50; Calculated for $C_{30}H_{40}N_3O_{12}$: [M+H peak] m/z = 634.2612, Found = 634.2586; δ_H ($CDCl_3$, 400 MHz; 7.83 (d,d, 1H, J_1 = 9.0 Hz, J_1 = 2.5 Hz Ar-H), 7.73 (s, 1H, Ar-H), 6.86 (m, 4H, Ar-H), 6.69 (d, 1H, J = 9.0 Hz, Ar-H), 4.32 (m, 2H, CH_2), 4.29 (m, 2H, CH_2), 4.23 (s, 4H, CH_2), 4.14 (s, 4H, CH_2), 4.08 (q, 8H, J = 7.0 Hz, CH_2), 1.16 (overlapping triplets, 12H, CH_3);

δ_C($CDCl_3$, 100 MHz); 171.4, 170.4, 150.2, 148.6, 145.4, 140.9, 139.7, 122.2, 121.9, 119.4, 118.3, 115.9, 113.9, 108.0, 67.8, 66.8, 61.2, 60.7, 53.8, 53.5, 14.04, 13.96; Mass Spec (MeCN, ES+) *m/z* Expected : 633.6, Found: 634.3 (M+H), 656.32 (M+Na), 672.33 (M+K); IR υ_{max}(cm^{-1}) 3435, 3088, 2978, 2986, 1740, 1587, 1508, 1458, 1419, 1373, 1338, 1241, 1196, 1102, 1024, 976, 933, 867, 805, 744, 725, 623, 567.

Synthesis of [(2-{2-[2-(Bis-ethoxycarbonylmethyl-amino)-5-nitro-phenoxy]-ethoxy}-4-nitro-phenyl)-ethoxycarbonylmethyl-amino]-acetic acid ethyl ester (174)



1,2 Bis [-(Bis[ethoxy carbonyl methyl]) amino phenoxy] ethane (1.50 g, 2.54 mmol) was placed in a 250 mL single neck RBF with $CHCl_3$ (100 mL). This solution was stirred at -60 °C in a dry ice – IPA bath. A solution of fuming HNO_3 [0.32 mmole/mL] in glacial acetic acid (8.00 mL), was added in 100 μL aliquots every 60 seconds. The solution was left to stir for 60 minutes upon which it was quenched with 1.0 M $NaHCO_3$ (100 mL). The yellow solution was extracted with $CHCl_3$ (4 x 50 mL). The combined organic layers were dried over $MgSO_4$ to produce 1.599 g of a yellow/ brown solid that showed up on TLC as three distinct spots. The desired product was purified by flash column chromatography using CH_2Cl_2 – CH_2Cl_2: MeCN (95:5), to yield 1.2917 g (78.72% yield) of **174** as a yellow solid. M.P. = 155-157 °C; Calculated for $C_{30}H_{38}N_4O_{14}$: C, 53.10; H, 5.64; N, 8.26, Found: C, 52.86; H, 5.54; N, 7.97; Calculated for $C_{30}H_{39}N_4O_{14}$: [M+H peak] *m/z* = 679.2463, found = 679.2458; δ_H ($CDCl_3$, 400 MHz) 7.86 (d,d 2H, J_1 = 9.0 Hz, J_2 = 2.0 Hz, Ar-H), 7.74 (s, 2H, Ar-H), 6.72 (d, 2H, J = 8.5 Hz, Ar-H), 4.36 (s, 4H, [ether]C$\underline{H_2}$), 4.23 (s, 8H, C$\underline{H_2}$), 4.12 (q, 8H, J_1 = 7.0 Hz, [ethyl] C$\underline{H_2}$), 1.20 (t, 12H, J_1 = 7.5 Hz [ethyl] CH_3); δ_C ($CDCl_3$, 100 MHz) 169.85, 147.94, 145.01, 140.45, 118.17, 115.7, 107.86, 66.94, 60.87, 53.42, 13.59 Mass Spec (MeCN, ES+) *m/z* Expected : 678.2, Found: 679.2 (M+H), 696.2(M+H_3O), 701.2 (M+Na), 717.2 (M+K); IR υ_{max}(cm^{-1}) 3349, 3084, 2986, 2928, 1749, 1586, 1511, 1419, 1373, 1331, 1290, 1244, 1199, 1179, 1101, 1056, 1025, 967, 804, 726, 623, 558, 460.

General synthesis of 175A and 175B [130]

173, (0.9748 g, 1.54 mmol) [or **174**, 1(0.9536 g, 1.41 mmol) in the case of **175B**] was placed in 250 mL RBF. To this was added 10% Pd-C, 0.10g and ethanol (100 mL). The solution was stirred under a H_2 atmosphere until no more H_2 was consumed. The resulting solution was passed through a celite filter. The solution was then reduced under vacuum to produce **175A** or **175B**.

[(4-Amino-2-{2-[2-(bis-ethoxycarbonylmethyl-amino)-phenoxy]-ethoxy}-phenyl)-ethoxycarbonylmethyl-amino]-acetic acid ethyl ester (175A)

0.7526 g (81.04%) of **175A**, was isolated as a clear resin , which slowly turned light purple over time. Dissolved the resin in $CHCl_3$ and carried out an acid base extraction. The resulting organic solution was separated dried over $MgSO_4$ and reduced to a purple resin. Calculated for $C_{30}H_{41}N_3O_{10}.CHCl_3$: C, 51.42; H, 5.71; N, 5.80, found: C, 51.63; H, 5.86; N, 5.89; calculated for $C_{30}H_{42}N_3O_{10}$: [M+H peak] *m/z* = 604.2870, Found: 604.2861; δ_H($CDCl_3$, 400 MHz) 6.84 (m, 4H, Ar-H), 6.75 (d, 1H, J = 8.5 Hz, Ar-H), 6.29 (s, 1H, Ar-H) 6.22 (d, 1H, J = 8.0 Hz, Ar-H) 4.27 (s, 4H, CH_2), 4.16 (s, 4H, CH_2), 4.06(m, 12H, CH_2) 1.16(overlapping triplets, 12H, CH_3) ; δ_C($CDCl_3$, 100 MHz); 171.46, 171.36, 151.16, 150.09, 139.01, 135.15, 134.26, 122.00, 121.15, 120.18, 118.71, 112.93, 110.79, 104.14, 67.04, 66.81, 60.69, 60.48, 53.46, 53.29, 13.81, 13.79; Mass Spec (MeCN, ES+) *m/z* Expected 603.6:, Found: 604.2 (M+H), 626.2 (M+Na), 642.16 (M+K); IR υ_{max}(cm^{-1}) 3461, 3357, 2977, 2931, 2873, 1746, 1624, 1508, 1458, 1415, 1372, 1247, 1181, 1067, 1025, 975, 933, 797, 749, 668, 625.

[(4-Amino-2-{2-[5-amino-2-(bis-ethoxycarbonylmethyl-amino)-phenoxy]-ethoxy}-phenyl)-ethoxycarbonylmethyl-amino]-acetic acid ethyl ester (175B)

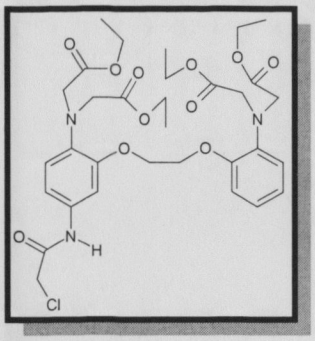
0.6358g (73.1 %) of **175B**, was isolated as a clear resin, which slowly turned light purple over time. Calculated for $C_{30}H_{43}N_4O_{10}$: [M+H peak] *m/z* = 619.2974, found: 619.2982; δ_H ($CDCl_3$, 400 MHz) 6.79 (s, 2H, Ar-H), 6.31 (s, 2H, Ar-H), 6.14 (s, 2H, Ar-H), 4.26 (s, 4H, CH_2),

4.08 (m, 16H, C$\underline{H}_2$), 1.18 (t, 12H, J = 7.0 Hz, C$\underline{H}_3$); δ_C ($CDCl_3$, 100 MHz) 171.3, 151.68, 142.23, 130.79, 121.33, 107.2, 101.66, 66.76, 60.08, 53.51, 13.66; Mass Spec (MeCN, ES+) *m/z* Expected 618.6, Found: 619.5 (M+H), 641.4 (M+Na); IR υ_{max}(cm^{-1}) 3435, 2978, 2927, 1742, 1618, 1516, 1458, 1373, 1290, 1180, 1096, 1026, 973, 802, 728, 619, 569.

General synthesis of 176 and 177 [130]

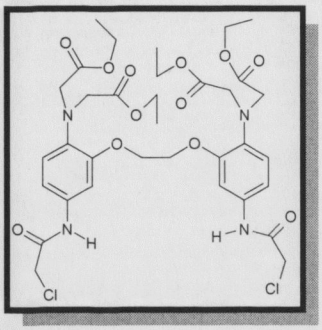
To a 250 mL 3 neck RBF **175A** (0.713 g, 1.18 mmol) [or **175B**, (10.5873 g, 0.948 mmol) in the case of **177**] was added. To this was added CH_2Cl_2 (75 mL) and (0.119 g, 0.118 mmol) of TEA. This solution was then immersed into a dry ice, IPA bath. To this flask a pressure equalising dropping funnel was attached which contained a solution of CH_2Cl_2 (75 mL) and 1.1 equivalent of chloro acetyl chloride (98%) [or 2.2 equivalents in the case of **177**]. This solution was dropped into the flask over a 2 hour period with the reaction vessel kept at –60 °C. After this addition the reaction flask was allowed to heat up to room temperature and the solution was then left stirring overnight. The resulting solution was then washed with 1.0M HCl (1 x 50 mL), and then with water (1 x 50 mL). The organic phase was then dried over $CaCl_2$ and reduced under vacuum, to produce **176** or **177**.

{[2-{2-[2-(Bis-ethoxycarbonylmethyl-amino)-phenoxy]-ethoxy}-4-(2-chloro-acetylamino)-phenyl]-ethoxycarbonylmethyl-amino}-acetic acid ethyl ester (176)



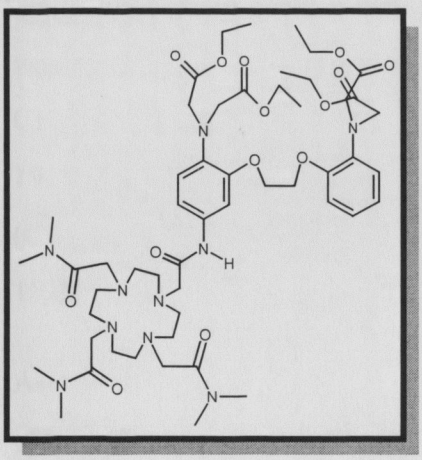
0.80g of **176** was produced as a light brown resin. Calculated for $C_{32}H_{43}N_3O_{11}Cl$: [M+H peak] *m/z* = 680.2586, found: 680.2571; δ_H($CDCl_3$, 400 MHz) 8.44 (s, 1H, N-H), 7.19 (s,1H, Ar-H), 7.04 (d, 1H, J = 8.6 Hz, Ar-H), 6.84 (m, 4H, Ar-H), 6.74 (d, 1H, J = 9.0 Hz, Ar-H), 4.21 (s, 4H, C$\underline{H}_2$), 4.12 (s, 6H, C$\underline{H}_2$), 4.09 (s, 4H, C$\underline{H}_2$) 1.12 (m, [overlapping triplet] 12H, C$\underline{H}_3$); δ_C($CDCl_3$, 100 MHz); 171.13, 170.97, 163.40, 149.9, 149.8, 138.8, 159.9, 131.3, 121.8, 121.0, 118.6, 118.5, 112.8, 112.5, 105.6, 66.82, 66.48, 60.33, 53.05, 42.56, 13.56; Mass Spec (MeCN, ES+) *m/z* Expected 679.16:, Found: 680.12 (M+H), 702.07 (M+Na), 718.12 (M+K); IR υ_{max}(cm^{-1}) 3433(H_2O), 2982, 2927, 1742, 1518, 1457, 1420, 1374, 1243, 1181, 1024, 972, 856, 805, 746, 652.

{[2-{2-[2-(Bis-ethoxycarbonylmethyl-amino)-5-(2-chloro-acetylamino)-phenoxy]-ethoxy}-4-(2-chloro-acetylamino)-phenyl]-ethoxycarbonylmethyl-amino}-acetic acid ethyl ester (177)



0.7588 g of **177** was produced as a brown resin. Calculated for $C_{34}H_{44}N_4O_{12}Cl_2.H_2O$: C, 51.72; H, 5.87; N, 7.09, found: C, 51.68; H, 5.30; N, 7.45; calculated for $C_{34}H_{45}N_4O_{12}Cl_2$: [M+H peak] *m/z* = 771.2411, found: 771.2421; δ_H ($CDCl_3$, 400 MHz) 8.41 (s, 2H, N-H), 7.22 (s, 2H Ar-H), 7.09 (d, 2H, *J* = 7.5 Hz, Ar-H), 6.82 (d, 2H, *J* = 8.5 Hz, Ar-H), 4.26 (s, 4H, Cl-C$\underline{H_2}$), 4.17 (s, 4H, C$\underline{H_2}$), 4.12 (s, 8H, C$\underline{H_2}$), 4.07 (q, 8H, *J* = 7.5 Hz, C$\underline{H_2}$) 1.12 (t, 12H, *J* = 7.5 Hz, C$\underline{H_3}$); δ_C ($CDCl_3$, 100 MHz); 170.96, 170.77, 163.30, 150.0, 119.0, 112.8, 106.3, 68.87, 60.39, 53.14, 42.53, 13.62; Mass Spec (MeCN, ES+) *m/z* Expected :770.2, Found:771.24 (M+H), 794.5 (M+Na) ; IR $\upsilon_{max}(cm^{-1})$ 3393(H_2O), 2984, 2935, 1736, 1700, 1685, 1617, 1523, 1421, 1373, 1291, 1261, 1204, 1127, 1021, 854, 790, 701, 620, 560.

Synthesis of ({2-{2-[2-(Bis-ethoxycarbonylmethyl-amino)-phenoxy]-ethoxy}-4-[2-(4,7,10-tris-dimethylcarbamoylmethyl-1,4,7,10tetraaza-cyclododec-1-yl)-acetylamino]-phenyl} ethoxycarbonylmethyl -amino)-acetic acid ethyl ester (178) [130]

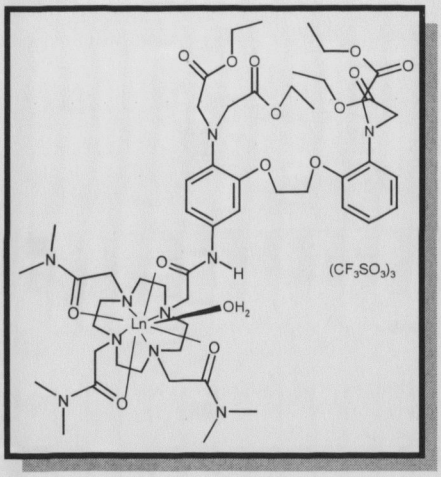


176, (0.5394 g, 0.793 mmol), and **149**, (0.3391g, 0.793 mmol), were placed into a 50 mL single neck RBF. To this was added Cs_2CO_3 (0.516 g, 1.586 mmol) and dry MeCN (30 mL). The solution was kept under dry conditions in an argon atmosphere and stirred at reflux for 72 hrs. The resulting mixture was cooled to room temperature and filtered through celite. The acetonitrile was removed under vacuum to produce 0.7376 g (86.82 % Yield) of a crude resin. The crude resin was dissolved in $CHCl_3$ (40 mL) and washed with water. (5 x 20 mL) The organic phase was separated dried over $MgSO_4$ and reduced to give the desired product, **178** in a relatively pure state. Calculated for $C_{52}H_{83}N_{10}O_{14}$:[M+H peak] *m/z* = 1071.6090 , found: 1071.6140 (4.7ppm) ; δ_H ($CDCl_3$, 400 MHz) 6.83 (m, 7 H), 4.26-4.21 (m, 6 H), 4.10-3.94 (m, 20H), 3.54-3.26 (m, 9 H), 3.02-2.69

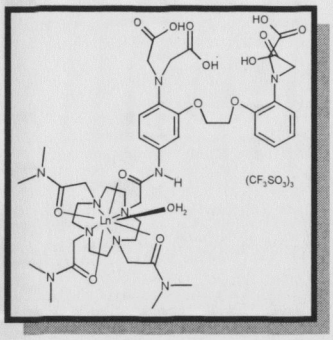
(m, 28 H), 1.10 (broad s, 12 H); δ_C ($CDCl_3$, 100 MHz) 171.45 cq, 171.36 cq, 170.88 cq, 169.81 cq, 149.72 cq, 138.78 cq, 134.55 (C-H), 130.44 (C-H), 128.23 (C-H), 121.50 (C-H), 120.80 (C-H), 118.34 (C-H), 111.36 (C-H), 66.52, 60.10, 54.48, 52.93, 51.0 (CH_2), 36.41, 36.15, 36.00, 35.01, 34.86, 34.56, 13.49 (CH_3); Mass Spec (MeCN, ES+) *m/z* Expected :1070.6, Found:1071.6 (M+H), 1093.6 (M+Na) ; IR $\upsilon_{max}(cm^{-1})$ 3450, 2976, 2933, 1742, 1649, 1513, 1453, 1413, 1244, 1179, 1062, 1026, 972, 733.

Synthesis of ({2-{2-[2-(Bis-ethoxycarbonylmethyl-amino)-phenoxy]-ethoxy}-4-[2-(4,7,10-tris-dimethylcarbamoylmethyl-1,4,7,10tetraaza-cyclododec-1-yl)-acetylamino]-phenyl} ethoxycarbonylmethyl -amino)-acetic acid ethyl ester. Tb(III) Triflate (Tb.178) [130]

~100 mg, (~ 0.1 mmol) of **178** and 0.1 mmol of Ln (III) Triflouromethane sulphonate was added to a 5 mL single necked RBF which contained 3 mL of freshly dried MeCN. The solution was freeze thawed three times, placed under an argon atmosphere and left stirring at reflux for 24 hrs. The resulting solution was cooled to room temperature and then dropped slowly onto 50-70 mL of dry diethyl ether. The diethyl ether was poured off to leave of Ln(III) complex as a crude material. This was dissolved in a small quantity of CH_2Cl_2 and placed onto a dry Alumina plug which was washed with 70:30 CH_2Cl_2:THF which was slowly changed by gradient elution to 65:30:5 CH_2Cl_2:THF:MeOH. (43.0 mg, 25 % yield) δ_H (CD_3CN, 400 MHz) 70.49, 45.32, 42.91, 19.70, 8.04, 6.13, 5.23, 4.95, 4.86, 4.50, 3.90, 2.83, 2.32,1.03, -68.06, -80.84, -89.57 ; δ_F (CD_3CN, 376 MHz) –79.19, -167.10, -193.92; IR $\upsilon_{max}(cm^{-1})$ 3444, 2956, 2926, 2854, 1732, 1626, 1516, 1455, 1261, 1171, 1261, 1171, 1034, 959, 762, 642, 519.



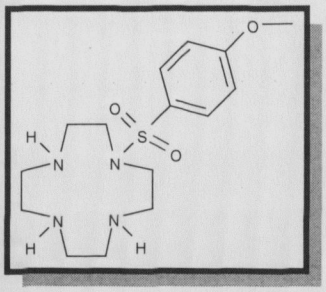
Attempted synthesis of ({2-{2-[2-(Bis-carboxymethyl-amino)-phenoxy]-ethoxy}-4-[2-(4,7,10 tris-dimethylcarbamoylmethyl-1,4,7,10tetraaza-cyclododec-1-yl)-acetylamino]-phenyl}-carboxymethyl-amino)-acetic acid. Tb(III) Triflate (Tb.160) [130]



20 mg, (11.8 μmol) of **Tb.178** was added to a 5 mL single necked RBF that contained 2 mL of 1.0 M LiOH. The solution was left stirring at room temperature overnight under an argon atmosphere. The reaction was neutralized using HCl and then passed down a Dowex 50 W ion exchange column eluting with a dilute ammonium solution. However, no product was collected.

6.4 Synthesis and photophysical data for Chapter 5

Synthesis of 1-(4-Methoxy-benzenesulphonyl) –1,4,7,10 – tetraazacyclododecane (184) [212]

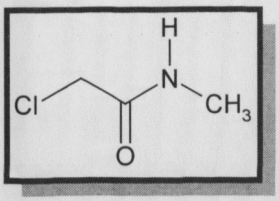


To a 500 mL three neck RBF, 1,4,7,10 tetraazacyclododecane (1.00 g, 5.8 mmol) was added along with $CHCl_3$ (50 mL). To this was added TEA (4.11 g, 40 mmol) which was heated at 36-39 °C. 4-methoxy phenyl sulphonyl chloride (1.20 g, 5.8 mmol) in $CHCl_3$ (100 mL) was added dropwise over a five-hour period. The solution was then left stirring overnight. The solution temperature was maintained at 36-39 °C. This solution was reduced to approximately 50 mL upon which a white solid was produced. This was removed by filtration and the resulting organic solution was reduced to dryness under vacuum to produce a white solid, 1.6 g (80.0 %). This was then purified by silica column chromatography using 90:10, MeCN: MeOH (53.4% recovery), to yield 0.56 g (28.0 % Yield) of **184** as a white solid. Calculated for $C_{15}H_{27}N_4O_3S$: [M+H peak] *m/z* = 343.1804, Found: 343.1806; δ_H ($CDCl_3$, 400 MHz) 7.72 (d, *J* = 9.0 Hz, 2H, Ar -H), 7.01 (d, *J* = 8.6 Hz, 2H, Ar -H), 3.88 (s, 3H), 3.40 (d, *J* = 4.5 Hz, 4H, CH_2), 3.18 (d, *J* = 5.0 Hz, 4H, CH_2), 3.00 (d, *J* = 4.0 Hz, 4H, CH_2), 2.87 (d, *J* = 5.0 Hz, 4H, CH_2); δ_C ($CDCl_3$, 100 MHz) 162.98, 128.85, 114.15, 55.23, 49.31, 48.49, 48.21, 45.47; Mass Spec (MeCN, ES+) *m/z* Expected: 342.2, Found: 343.3 (M+H); 365.1 (M+Na); IR υ_{max}(cm^{-1}) 3432, 3095, 3008, 2842, 1712, 1594, 1492, 1438, 1363, 1261, 1222, 1155, 1091, 1052, 1024, 927, 890, 842, 804, 761, 701, 561, 530, 466.

General synthesis of 185 and 186 [211]

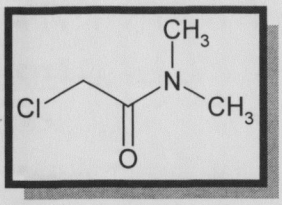
To a 250 mL 3 necked RBF, NaOH (8.00 g , 0.2 mole) was added. To this was added 150 mL of CH_2Cl_2 and methyl amine (17.22 mL, 15.500 g, 0.199 mole) (40%) [or dimethyl amine (0.2 mole) in the case of **186**) . To this flask a pressure equalising dropping funnel was attached which contained a solution of 50 mL of CH_2Cl_2 and chloro acetyl chloride (16.17 mL, 22.925 g, 0.202 mole) (98%). This solution was dropped into the flask over a 2 hour period with the reaction vessel kept at –60 °C. The solution was then left stirring overnight at room temperature. The resulting brown solution was filtered to remove the precipitate formed and then extracted using 1.0M HCl (1 x 50 mL), and washed with water (1 x 50 mL). The organic phase was then dried over K_2CO_3, and reduced under vacuum.

2-Chloro – *N*-methyl – acetamide (185) [211]



9.82 g (45.9 %) of a whitish solid was produced. δ_H ($CDCl_3$, 400 MHz) 6.67 (s 1H, N-H), 4.03 (s, 2H, CH_2), 2.87 (s, 3H, CH_3); δ_C ($CDCl_3$, 100MHz) 166.02, 42.10, 26.02; Mass Spec (MeCN, ES+) *m/z* Expected : 107 , Found: 107 (GCMS - analysis); IR $\upsilon_{max}(cm^{-1})$ 3332, 2958, 1654, 1550, 1409, 1290, 1263, 1157, 1081, 929, 989, 796, 757, 709, 626, 566, 414.

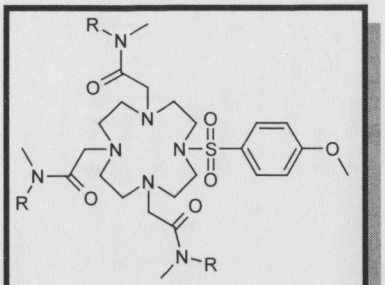
2-Chloro – *N, N*- dimethyl - acetamide (186) [211]



28.0 g (96.1 %) of 2-Chloro – *N, N*- dimethyl - acetamide as a colourless liquid was produced. δ_H($CDCl_3$, 400 MHz) 4.02 (s, 2H, CH_2), 3.02 (s, 3H, CH_3), 2.90 (s, 3H, CH_3); δ_C($CDCl_3$, 100 MHz) 166.01, 40.67, 37.00, 35.36 ; Mass Spec (MeCN, ES+) *m/z* Expected : 121, Found: 121 (GCMS - analysis); IR $\upsilon_{max}(cm^{-1})$ 3490, 2942, 1729, 1658, 1500, 1444, 1402, 1257, 1021, 1120, 1060, 979, 929, 794, 748, 657.

General synthesis of 187 and 188 [130]

184, 0.68 g (2.0 mmol) of was placed in a 100 mL three neck RBF. To this was added **185**, (0.64 g, 6.0 mmol) [or **186**, 3.1 equivalents in the case of **188**], Cs_2CO_3 (1.95 g, 6.0 mmol) and KI (1.0 g, 5.3 mmol). To this was added dry DMF (12 mL). The reaction was freeze thawed twice. The flask was then filled with argon and the reaction was stirred at 80°C



187: R = CH_3
188: R = H

overnight. The resulting solution was then filtered through a celite filter and reduced by rotatory evaporation. The resulting residue was dissolved in $CHCl_3$ and washed with water (2 x 50 mL), and brine (2 x 50 mL). The organic layer was isolated, dried over K_2CO_3, and reduced under vacuum, to produce a resin. This was then purified by alumina column chromatography using CH_2Cl_2: MeOH (1-5%).

2-[4,7-Bis-dimethylcarbamoylmethyl-10-(4-methoxy-benzenesulfonyl)-1,4,7,10 tetraaza-cyclododec-1-yl]-N,N-dimethyl-acetamide (187)

600 mg was purified by alumina column chromatography using 97:3, EtOAc: MeOH, to yield 320 mg of **187** as a pale yellow resin. Calculated for $C_{27}H_{48}N_7O_6S$: [M+H peak] *m/z* = 598.3387, found: 598.3389; δ_H ($CDCl_3$, 400 MHz) 7.62 (d, *J* = 9.0 Hz, 2H, Ar -H), 6.94 (d, *J* = 9.0 Hz, 2H, Ar -H), 3.79 (s, 6H), 3.56 (m, 6H), 3.26 (m, 8H), 3.08 – 2.90 (m, 12H), 2.87 – 2.81 (m, 10H); δ_C ($CDCl_3$,100 MHz) 173.6, 169.3, 163.1, 129.4, 114.18, 55.28, 55.21, 54.5, 53.8, 53.6, 53.2, 51.1, 36.3, 36.1, 34.9; Mass Spec (MeOH, ES+) *m/z* Expected : 597.78 , Found: 598.6 (M+H), 620.6 (M+Na); IR υ_{max}(cm^{-1}) 3438, 2962, 2923, 2854, 1735, 1646, 1508, 1457, 1398, 1340, 1261, 1155, 1091, 1022, 867, 804, 701, 559, 474.

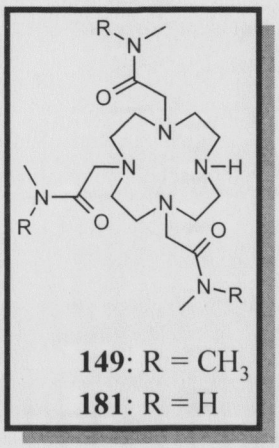
2-[4-(4-Methoxy-benzenesulfonyl)-7,10-bis-methylcarbamoylmethyl-1,4,7,10 tetraaza-cyclododec-1-yl]-*N* -methyl-acetamide (188)

455 mg of **188** was produced as a resin. Calculated for $C_{24}H_{42}N_7O_6S$: [M+H peak] *m/z* = 556.2917, found: 556.2906; δ_H ($CDCl_3$, 400 MHz) ; 7.91 (bs, 1H N-H), 7.72 (d, *J* = 8.5 Hz, 2H), 7.63 (bs, 2H, N-H), 7.02 (d, *J* = 9.0 Hz, 2H), 3.88 (s, 3H, OCH_3), 3.47 (s, 4H, CH_2), 3.42 (s, 2H, CH_2) 3.18 (bs, 8H, CH_2), 2.96 (s, 6H), 2.82 (m, 8H, CH_2), 2.08 (s, 3H); δ_C($CDCl_3$, 100 MHz) 171.5, 171.2, 129.4, 114.4, 58.51, 58.10, 55.58, 53.74, 53.33, 53.04, 49.46, 36.35, 31.31, 25.9, 25.8; Mass Spec (MeOH, ES+) *m/z* Expected : 555.3, Found: 556.6, (M+H), 578.6 (M+Na); IR υ_{max}(cm^{-1}) 3421, 3077, 2925, 2854, 1654, 1596, 1542, 1457, 1409, 1338, 1261, 1155, 1093, 1022, 841, 840, 728, 698, 559.

Synthesis of 149 and 181

Method 1: [213]

188, 0.39 g (0.70 mmole) [or **187** in the case of **149**] was placed in a 100 mL 3 necked RBF. To this was added dry THF (30 mL), ethanol (0.3 mL). This was attached to a cold finger condenser and the apparatus was placed into a dry ice/ IPA bath were the temperature was dropped to -60 °C. Dry ice and IPA was also added to the condenser. Liquid NH_3 was added to the reaction vessel through the cold finger condenser (approximately 40 mL). Sodium metal (1.2 g, 0.05 mol) was added to this solution. The reaction was left stirring at -60 °C for 4 hours during which time the yellow solution turned dark blue. The solution was allowed to warm up to room temperature and left stirring overnight. To this solution THF (20 mL) was added to dissolve the excess (unused) sodium present. Concentrated HCl was added until the solution was at pH 1 and then extracted with DCM. The pH of the solution was then adjusted to pH 14 using KOH pellets and then extracted with chloroform and reduced to yield the desired product.



149: R = CH_3
181: R = H

(**149**) 100 mg (36.2 % yield) of **181** was isolated as a clear residue. A continuous extraction was attempted on the aqueous solution without any success.

(**181**) This extraction was found to be unsuccessful with no isolation of **181**. A continuous extraction was attempted without any success. The reaction was abandoned.

Method 2

1,4,7,10 tetraazacyclododecane (98%) (0.375 g, 2.13 mmol) was placed in a 50 mL single neck RBF. To this was added $NaHCO_3$ (0.537 g, 6.39 mmol) and dry MeCN (15 mL). **185** (0.706 g, 6.6 mmol) [or **186** (0.804 g, 6.6 mmol) in the case of **149**] was added and the mixture was stirred at 65 °C for a further 72 hours.

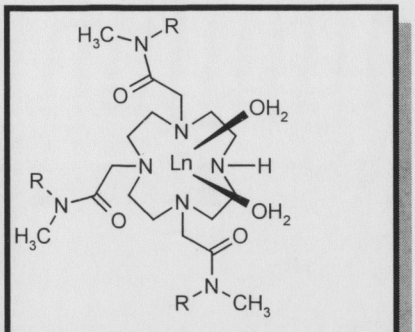
2-(4,10-Bis-dimethylcarbamoylmethyl-1,4,7,10tetraaza-cyclododec-1-yl)-*N*,*N*-dimethyl-acetamide (149)

The resulting solution was then cooled and passed through a celite filter. The pale yellow solution was reduced to a yellow residue and dried under vacuum for 1 hour to produce 0.829 g (90.89 % yield) of a mixture of products as shown by TLC. Mass spec shows mono, bis, tris and tetra substituted cyclen, TLC shows the tris complex to be the major product. The product was purified by alumina column using 100% CH_2Cl_2, with a gradient elution to 97:3 CH_2Cl_2:MeOH(NH_3) mobile phase. 0.470 g (1.1 mmole), [51.52 % Yield] of **149** was collected as a white foam after drying under vacuum which returned to a residue state over time. Calculated for $C_{20}H_{42}N_7O_3$:[M+H peak] *m/z* = 428.3344, found: 428.3349; δ_H($CDCl_3$, 400 MHz) 10.00 (broad s, 1H, N-H), 3.61(s, 2H, CH_2- acetamide), 3.58 (s, 4H, CH_2-acetamide), 3.09 (s, 8H), 3.04 (s, 3H), 2.96 (s, 6H), 2.90 (s, 10H), 2.84 (s, 7H); δ_C($CDCl_3$, 100 MHz) 170.25, 170.15, 55.51, 53.80, 51.70, 50.57, 49.72, 46.70, 36.39, 35.27; Mass Spec (MeOH, ES+) *m/z* Expected : 427.59, Found: 428.33 (M+H), 450.30(M+Na), 472.30 (M+K); IR υ_{max}(cm^{-1}) 3434, 2927, 2852, 1637, 1508, 1475, 1402, 1338, 1261, 1103, 1064, 1022, 881, 806, 769, 667, 649, 574, 484.

2-(4, 7-Bis-methylcarbamoylmethyl- 1, 4, 7, 10 tetraaza-cyclododec-1-yl)-*N*-methyl-acetamide (181)

The resulting filtered solution was dissolved in EtOH. **181** was isolated as a solid by precipitation by dropping onto ether. (59.0 % yield) Calculated for $C_{17}H_{36}N_7O_3$:[M+H peak] *m/z* = 386.2880, found: 386.2874 ; δ_H($CDCl_3$, 400 MHz) 7.59 (s, 1H, N-H), 7.30 (s,2H, N-H), 3.06 (s, 4H, CH_2 acetamide), 2.96 (s, 2H, CH_2 acetamide), 2.75 (d, 6H, *J* = 4.52, N-CH_3), 2.67 (d, 3H, *J* = 4.52, N-CH_3), 2.60 (s, 4H, CH_2), 2.58 (s, 4H, CH_2), 2.53 (s, 4H, CH_2), 2.49 (s, 4H, CH_2); δ_C($CDCl_3$, 100 MHz) 171.51, 171.41, 59.54, 57.53, 53.31, 52.63, 51.18, 46.15, 25.89, 25.72; Mass Spec (MeOH, ES+) *m/z* Expected : 385.51, Found: 386.3(M+H), 408.4 (M+Na), 424.4 (M+K); IR υ_{max}(cm^{-1}) 3430, 2846, 2103, 1643, 1567, 1456, 1415, 1367, 1311, 1257, 1164, 1110, 989, 482.

General synthesis Tb.149, Eu.149, Tb.181 and Eu.181 [130]



Eu.149: R = CH_3, Ln(III) = Eu(III)
Tb.149: R = CH_3, Ln(III) = Tb(III)
Eu.181: R = H, Ln(III) = Eu(III)
Tb.181: R = H, Ln(III) = Tb(III)

149 or 181 (0.23 mmol) and Ln (III) Triflouromethane sulphonate (0.26 mmol) was added to a 25 mL single neck RBF that contained freshly dried MeCN (10 mL). The solution was freeze thawed three times, placed under an argon atmosphere and left stirring at reflux for 24 hrs. The resulting solution was cooled to room temperature and then dropped slowly onto dry diethyl ether (100 mL). The diethyl ether was poured off to leave of **Tb.149**, **Eu.149**, **Tb.181** or **Eu.181** as an oil that was washed with CH_2Cl_2 or $CHCl_3$ and dried under vacuum. Yields > 95% achieved in all complexes. Characterisation shows that all complexes contain triflate counter anions and at least two water molecules.

2-(4,10-Bis-dimethylcarbamoylmethyl-1,4,7,10tetraaza-cyclododec-1-yl)-N,N-dimethyl-acetamide Tb(III) (Tb.149)

Calculated for $C_{23}H_{41}N_7O_{12}F_9S_3Tb.(H_20)_2(CHCl_3)_2$: C, 22.95; H, 3.62; N, 7.49, Found: C, 22.23; H, 3.71; N, 7.36; Calculated for $C_{22}H_{42}N_7O_6F_3STb$:[M[Triflate]+H peak] *m/z* = 736.2123, Found: 736.2148; δ_H (CD_3OCD_3, 400 MHz) 39.92, 32.70, 9.00, 3.95, 3.02, 1.02; δ_F (CD_3OCD_3, 376 MHz) – 78.74; Mass Spec (MeCN, ES+) *m/z* Expected: 586.5, Found: 884.15 ($M[Triflate]_2$+H), 736.21 (M[Triflate]+H) ; IR $\upsilon_{max}(cm^{-1})$ 3434, 2957, 2927, 2856, 1625, 1508, 1465, 1438, 1412, 1279, 1256, 1171, 1084, 1171, 1084, 1030, 960, 824, 761, 640, 574, 518.

2-(4,10-Bis-dimethylcarbamoylmethyl-1,4,7,10tetraaza-cyclododec-1-yl)-N,N-dimethyl-acetamide Eu(III) (Eu.149)

Calculated for $C_{23}H_{41}N_7O_{12}F_9S_3Eu.(H_20)_2(CHCl_3)_2$: C, 23.07; H, 3.64; N, 7.53, Found: C, 22.67; H, 3.74; N, 7.55; Calculated for $C_{21}H_{42}N_7O_6F_3SEu$:[M[Triflate]+H peak] *m/z* = 730.2082, Found: 730.2045 ; δ_H(CD_3OCD_3, 400 MHz) 13.91, 3.24, 2.60, 2.06, 1.30, 0.89, 0.01, -1.32, -4.95, -8.95, -12.87, -17.65; δ_F (CD_3OCD_3, 376 MHz) – 78.74; Mass Spec (MeCN, ES+) *m/z* Expected :579.56, Found: 878.15 ($M[Triflate]_2$+H), 730.20 (M[Triflate]+H) ; IR

$\upsilon_{max}(cm^{-1})$ 3434, 2982, 2927, 2884, 1625, 1508, 1459, 1438, 1413, 1280, 1258, 1173, 1084, 1031, 960, 824, 762, 641, 573, 518.

2-(4, 10-Bis-methylcarbamoylmethyl-1, 4, 7, 10 tetraaza-cyclododec-1-yl)-N-methyl-acetamide Tb (III) (Tb.181)

Calculated for $C_{20}H_{35}N_7O_{12}F_9S_3Tb.(H_20)_2(CH_2Cl_2)_2$: C, 22.07; H, 3.62; N, 8.19, Found: C, 21.61; H, 3.59; N, 7.85; Calculated for $C_{19}H_{36}N_7O_9F_6S_2Tb$:[M[Triflate]$_2$+H peak] *m/z* = 843.1174, Found: 843.1171; Calculated for $C_{18}H_{36}N_7O_6F_3STb$:[M[Triflate]+H peak] *m/z* = 694.1653, Found: 694.1674; δ_H(MeOD, 400 MHz) 121.87, 107.11, 78.35, 71.89, 68.58, 39.94, 14.52, 7.75, 6.28, 4.26, 1.96, 1.78, 1.49, 1.07, - 7.21 ; δ_F (MeOD, 376 MHz) – 85.54; Mass Spec (MeCN, ES+) *m/z* Expected :544.4, Found: 272.3 (M+H/2), 843.1(M[Triflate]$_2$+H), 694.16 (M[Triflate]+H) ; IR $\upsilon_{max}(cm^{-1})$ 3435, 3137, 2960, 2924, 1637, 1420, 1259, 1169, 1087, 1030, 994, 974, 798, 639, 574, 519.

2-(4, 10-Bis-methylcarbamoylmethyl-1, 4, 7, 10 tetraaza-cyclododec-1-yl)-N-methyl-acetamide Eu (III) (Eu.181)

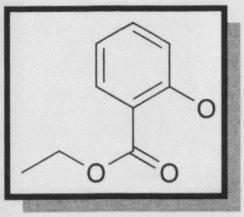
Calculated for $C_{20}H_{35}N_7O_{12}F_9S_3Eu.(H_20)_2(CH_2Cl_2)_2$: C, 22.19; H, 3.64 ; N, 8.24 , Found: C, 22.29; H, 3.74; N, 8.38; Calculated for $C_{17}H_{36}N_7O_3Eu$:[M+H peak] *m/z* = 539.2092, Found: 539.2087; Calculated for $C_{18}H_{36}N_7O_6F_3SEu$:[M[Triflate]+H peak] *m/z* = 688.1612, Found: 688.1548; Calculated for $C_{19}H_{36}N_7O_9F_6S_2Eu$: [M[Triflate]$_2$+H peak] *m/z* = 837.1133, found: 837.1181; δ_H(MeOD, 400 MHz) 27.04, 14.96, 11.44, 5.20, 3.68, 2.76, 2.41, 1.55, -0.09, -1.84, -4.93, -7.35, -10.77, - 12.31, -16.66 ; δ_F(MeOD, 376 MHz) – 80.45; Mass Spec (MeCN, ES+) *m/z* Expected :539.2, Found: 539.2(M+H), 668.1 (M[Triflate] +H), 837.1 (M[Triflate]$_2$+H); IR $\upsilon_{max}(cm^{-1})$ 3455, 3386, 3297, 3143, 3000, 2933, 2885, 1639, 1587, 1465, 1419, 1288, 1245, 1160, 1091, 1027, 725, 638, 576, 516.

General synthesis of esters 197 and 198

2-Methoxy-benzoic acid (5.00 g, 32.8 mmol) [or 2-Hydroxy-benzoic acid (5.00 g, 36.19 mmole) in the case of **197**] was added to a 50 mL single neck RBF. To this was added absolute ethanol (20 mL) and conc. H_2SO_4 (2 mL, 98%). The solution was refluxed for 4 hours, cooled and added to deionised water (50 mL). The resulting solution was washed with

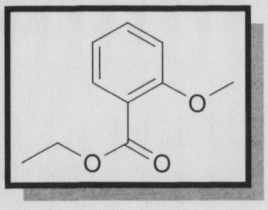
$CHCl_3$ (2 x 40 mL). The $CHCl_3$ phase was then washed with 20% Na_2CO_3 (30 mL) and deionised water (30 mL). The $CHCl_3$ phase was dried over $MgSO_4$ and reduced to produce ester product.

2-Hydroxy-benzoic acid ethyl ester (197)



4.848 g (80.59 % yield) of **197** was produced as a clear oil. Calculated for $C_9H_{11}O_3$: [M+H peak] *m/z* = 167.0708, found: 167.0723 (8.7 ppm); δ_H ($CDCl_3$, 400 MHz); 10.87 (s, 1H, OH), 7.80 (d, 1H J = 7.5 Hz, Ar-H), 7.39 (t, 1H J = 7.5 Hz, Ar-H), 6.95 (d, 1H J = 8.5 Hz, Ar-H), 6.82 (t, 1H J = 7.0 Hz, Ar-H), 4.36 (q, 2H, J = 7.0 Hz, $OC\underline{H}_2CH_3$), 1.37 (t, 3H, J = 7.0 Hz, $OCH_2C\underline{H}_3$); δ_C ($CDCl_3$, 100 MHz) : 169.89, 161.55, 135.19, 129.62, 118.71, 117.22, 112.38, 61.06, 13.81 ; Mass Spec (MeOH, ES+) *m/z* Expected :166.18, Found: 166.97 (M+H); IR $\upsilon_{max}(cm^{-1})$ 3183, 3154, 2984, 2908, 1675, 1614, 1585, 1485, 1397, 1373, 1324, 1302, 1250, 1215, 1158, 1091, 1017, 860, 817, 756, 701, 666.

2-Methoxy-benzoic acid ethyl ester (198)



5.343 g (90.22 % yield) of **198** was produced as a clear oil. Calculated for $C_{10}H_{13}O_3$: [M+H peak] *m/z* = 181.0865, Found: 181.0859 (-3.0ppm); δ_H ($CDCl_3$, 400 MHz); 7.71 (d, 1H J = 7.5 Hz, Ar-H), 7.36 (s, 1H, Ar-H), 6.88 (m, 2H, Ar-H), 4.30 (q, 2H, J = 6.0 Hz, $OC\underline{H}_2CH_3$), 3.80 (s, 3H, OCH_3), 1.30 (t, 3H, J = 7.0 Hz, $OCH_2C\underline{H}_3$): δ_C ($CDCl_3$, 100 MHz) ; 165.79, 158.75, 132.90, 131.02, 120.32, 119.73, 111.81, 60.30, 55.58, 13.92 ; Mass Spec (MeOH, ES+) *m/z* Expected : 180.08, Found: 181.08 (M+H), 202.92 (M+Na), 218.96 (M+K); IR $\upsilon_{max}(cm^{-1})$ 3077, 2980, 2838, 1711, 1600, 1491, 1465, 1437, 1389, 1366, 1300, 1251, 1165, 1132, 1081, 1050, 1024, 948, 855, 756, 706, 659.

6.4.1 Lanthanide complexes – Photo physical studies

Studies were carried out in aqueous solution or in aqueous solution with a buffer and high ionic strength at pH 7.4. Buffered solutions were made up in aqueous phase with 0.01 M (or 0.1 M) TMACl, 0.01 M (or 0.1 M) Tris Buffer, at pH 7.4. Solution concentrations ~16.7 μM. Test solutions were 5 mL or 10 mL Sensitising chromophore solutions were made up in water

2.0×10^{-3} M and 5.0×10^{-4} M. Luminescence measurements were made on a Perkin Elmer LS 50B with general settings as indicated in Table 6.3. All fluorescence scans were saved as ACS II files and processed in Excel™ to produce all graphs shown in Chapter 5.

Table 6.3 General settings for luminescence studies (Perkin Elmer LS 50B)

Luminescence settings:	
Mode: Phos	**Delay Time**: 0.1
Gate Time: 10	**Cycle**: 20
Flash count: 1 **Start**: 450nm	**End**: 700 - 750nm
Excitation: 300nm	**Scan speed**: 240nm/min
Excitation Slit width: 8nm	**Emission Slit width**: 8nm

6.4.2 Lanthanide complexes – Life time studies

Solutions of all complexes (~ 2-3 mg/2 mL) were made in H_2O and D_2O. Lifetimes were measured on a Varian Carey Eclipse Fluorescence spectrophotometer using with general settings as indicated in Table 6.4.

Table 6.4 General settings for lifetime studies (Varian Carey Eclipse)

Flourimeter settings: Lifetime measurements		
Direct excitation: Eu(III) @ 395nm, Tb(III) @ 366nm		
Emission: Eu(III) @ 615nm, Tb(III) @ 545nm		
Mode: Phos	**Delay Time**: 0.1ms	**Gate Time**: 0.1
Cycle: 20	**Flash count**: 1	**No. Cycles**: 1000
Total decay: 1.5 – 3.0 ms		**PMT (voltage)**: High
Excitation Slit width: 5nm		**Emission Slit width**: 5nm

6.4.3 Anion selectivity experiment [127]

Concentration of anions used in selectivity experiment are shown in Table 6.5

Table 6.5 Anion concentrations for selectivity studies

Anion	Concentration [mM]
$NaHCO_3$	30
Na lactate	2.3
Na citrate	0.13
$Na_2H_2PO_4$	0.9

6.4.4 Aromatic carboxylate absorption max values

UV-Vis spectroscopic analysis was carried out on a Shimadzu UV-2401 PC UV-Vis spectrophotometer. Studies were carried out on fast scan mode with slit widths of 1.0 nm, using matched quartz cells All solutions were tested in water. All absorption scans were saved as ACS II files and further processed in Excel™. The wavelengths for maximum absorption are presented in Table 6.6

Table 6.6 λ max (H_2O) of aromatic carboxylates 189-199

Compound	λ max (H_2O) – [nm]	λ Excitation (H_2O) - [nm]
189	447	447
190	428	428
191	300 (ε = 7,200 cm^{-1} M^{-1})	300
192	342	342
193	308	308
194	296	300
195	269	269
196	280-320	300
197	302	302
198	293	293
199	310	310

Chapter 7

References

7.0 References

[1] L. Fabbrizzi, *Coord. Chem. Rev.*, **2000**, 205, 1-2.
[2] A.P. de Silva, D.B. Fox, A.J.M. Huxley, T.S. Moody, *Coord. Chem. Rev.*, **2000**, 205, 41-57.
[3] R.A.Bissell, A.P. de Silva, H.Q. Nimal Gunaratine, P.L.M Lynch, G.E.M. Maguire, C.P. McCoy and K.R.A. Samankumara Sandanayake, *Topics in Current Chemistry*, **1993**, Vol. 168, Springer - Verlag Berlin Hiedelberg .
[4] A.P. de Silva, H.Q. Nimal Gunaratane, A. J.M. Huxley, C.P. McCoy, J.T. Rademacher and T.E. Rice, *Advances in Supramolecular Chemistry Vol. 4,* **1997**, 1-53, JAI press Inc. ISBN 1-55938-794-7
[5] A.P. de Silva, H.Q. Nimal Gunaratne , T. Gunnlaugsson, A.J.M. Huxley, C.P. Mc Coy, J.T. Rademacher and T.E. Rice, *Coord. Chem. Rev.*, **1997**, 97, 1515-1566.
[6] K. Rurack, *Spectrochim. Acta Part A*, **2001**, 57, 2161-2195.
[7] H-F. Ji, R. Dabestani, G. M. Brown and R.L. Hettich, *Photochem. Photobiol.*, **1999**, 69(5), 513-516
[8] J.J.R. Frausto da Silva and R.J.P. Williams, *The Biological Chemistry of the Elements - The Inorganic Chemistry of Life*, **1993**, Oxford University Press, ISBN 0-19-855802-3.
[9] E. Hodgson and P.E. Levi, **1987**, Elsevier Science Publishing Co., Inc. ISBN 0-444-01131-5
[10] Rosenberg, B., van Camp, L. Trosk, J.E., Mansour, V.H., *Nature*, **1969**, 222, 385-386.
[11] Rosenberg, B., T.G. Spiro, Ed. John Wiley and sons, Inc., New York, **1980**, 1, 1-29.
[12] B. Valeur and I. Leray, *Coord. Chem. Rev.*, **2000**, 205, 3-40.
[13] G. L. Patrick, *An Introduction to Medicinal Chemistry 2nd Ed.*, **2001**, Oxford University Press ISBN 0-19-850533-7.
[14] A. P. de Silva, H.Q. Nimal Gunaratne and T.E. Rice, *Angew. Chem., Int. Ed. Engl.*, **1996**, 35, 18, 2116-2121.
[15] I.M. Atkinson, AM. Groth, L.F. Lindoy, O.A. Mathews and G.V. Meehan, *Pure Appl. Chem.*, **1996**, 68, 6, 1231-1236
[16] Y.A. Zolotv, **1997**, Wiley & Sons ISBN - 0-471-17262-6.
[17] C.-Y. Zhu, R.M Izatt, T.-M. Wang, P. Huszthy, and J.S. Bradshaw, **1993**, *IUPAC*, 1485-1491.
[18] L. F. Lindoy, *Pure Appl. Chem.*, **1997**, 69, 10, 2179-2186.
[19] P. Comba, *Coord. Chem. Rev.*, **1999**, 185-186, 81-98.
[20] R. A. Schultz, B. D. White, D. M. Dishong, K. A. Arnold and G. W. Gokel, *J. Am. Chem. Soc.* **1985**, 107, 6659-6668.
[21] J.J.R. Frausto da SILVA and R.J.P. Williams, *The biological Chemistry of the Elements - The Inorganic Chemistry of Life 2nd Ed.*, **2001**, Oxford University Press ISBN 0-19-850847-6.
[22] M. Glynn, Ph.D. Thesis, University of Dublin, TCD, **2003**.
[23] C.H. Park and H.E. Simmons, *J. Am. Chem. Soc.*, **1968**, 90, 2431.
[24] E. Graf and J.M. Lehn, *J. Am. Chem. Soc.*, **1976**, 98, 6403.
[25] J. H. Hartley, T. D. James and C. J. Ward, *J. Chem. Soc., Perkin Trans. 1,* **2000**, 3155-3184.
[26] T. Gunnlaugsson, M. Nieuwenhuyzen, L. Richard and V. Thoss, *Tetrahedron Lett.*, **2001**, 42, 4725-4728.
[27] T. Gunnlaugsson, M. Nieuwenhuyzen, L. Richard and V. Thoss, *J. Chem. Soc. Perkin Trans.2,* **2002**, 141-150.
[28] (a) J. P. Dix and F. Vogtle, *Angew. Chem. Int. Ed. Engl.*, **1978**, 17, 11, 857; (b) J. P. Dix and F. Vogtle, *Chem. Ber.*, **1980**, 113, 457.
[29] D. H. Lee, K. H. Lee and J.I. Hong, *Org. Lett.*, **2001**, 3, 1, 5-8.
[30] A. P. de Silva and S. A. de Silva, *J. Chem. Soc., Chem. Commun.*, **1986**, 1709-1710.
[31] A. P. de Silva, H.Q. Nimal Gunaratne, T. Gunnlaugsson and M. Nieuwenhuyzen, *J. Chem. Soc., Chem. Commun.*, **1996**, 1967-1968.
[32] T. Gunnlaugsson, A. P. Davis and M. Glynn, *J. Chem. Soc., Chem. Commun.*, **2001**, 2556-2557.
[33] T. Gunnlaugsson, A. P. Davis, J. E. O' Brien and M. Glynn, Org. lett., **2002**, 4, 15, 2449-2452.
[34] F. Barigelletti, L. Flamigni, G. Calogero, L. Hammarstrom, J. -P. Sauvage and J.-P. Collin, *J. Chem. Soc., Chem. commun.*, **1998**, 2333-2334.
[35] M. H. Keefe, K. D. Benkstein, J. T. Hupp, *Coord. Chem. Rev.*, **2000**, 205, 201-228.
[36] Y. Shen and B. P. Sullivan, *J. Chem. Educ.*, **1997**, 74, 6, 685-689.
[37] a) P. D. Beer, S. W. Dent and T. J. West, *J. Chem. Soc., Dalton Trans.*, **2001**, 2341-2346, b)G.F. de Sa, O.L. Malta, C. de Mello Donega, A.M. Simas, R.L. Longo, P.A., Santa-Cruz, E.F. da Silva Jr., *Coord. Chem. Rev.*, **2000**, 196, 165-195.
[38] P. G. Sammes and G. Yahioglu, Natural products reports **1996**, 1-28.
[39] J. R. Lakowicz, **1999**, Kluwer Academic ISBN 0306460939.
[40] A. Mayer and S. Neuenhofer, *Agnew. Chem. Int. Ed. Engl.*, **1994**, 33, 1044-1072.

[41] A. Minta and R. Y. Tsien, *J. Biol. Chem.*, **1989**, 264, 32, 19449- 19457.
[42] R. Y. Tsien, *Biochemistry*, **1980**, 19, 11, 2396-2404.
[43] E.F Gudgin Dickson et al., *J. Photochem. Photobiol. B:*, **1995**, 27, 3-19.
[44] D. Plancherel, *Inorg. Chim. Acta,* **1987**, 139, 297-298.
[45] D. Parker, R. S. Dickins, H. Puschmann, C. Crossland, and J. A.K. Howard, *Chem. Rev.*, **2002**, 102(6); 1977-2010.
[46] D. Parker, *Coord. Chem. Rev.*, **2000**, 205,109-130.
[47] B.Alpha, J.- M. Lehn , R. Ballardini, V. Balzani, S. Perathoner and N. Sabbatini, *Photochem. Photobiol.*, **1990**, 52, 2, 299-306.
[48] D. Parker and J A G. Williams, *J. Chem. Soc., Dalton Trans.*, **1996**, 3613-3628.
[49] N. Sabbatini, M.Guardigli and J.-M. Lehn, *Coord. Chem. Rev.*, **1993**, 123, 201-228.
[50] A. Beeby, S. Faulkner, D. Parker, J. A. G. Williams, *J. Chem. Soc., Perkin Trans, 2,* **2001**, 1268-1273.
[51] M.H.V. Werts, Ph.D. Thesis, University of Amsterdam, **2000**.
[52] D.L. Dexter, *J. Chem. Phys.*, **1953**, 215, 836-850.
[53] TH. Forster, Discuss. Faraday Soc., **1959**, 27, 7.
[54] M. P. O. Wolbers, F. C.J.M. van Veggel, B. H.M. Snellink - Ruel, J.W. Hofstraat, F.A.J. Geurts and D. N. Reinhoudt, *J. Chem. Soc., Perkin Trans. 2*, **1998**, 2141-2149.
[55] F.S. Richardson, *Chemical Rev.*, **1982**, 82, 5, 541-552.
[56] S. Aime, M. Botta, D. Parker and J.A.G. Williams, *J. Chem. Soc., Dalton Trans.*, **1996**, 17-23.
[57] R.S. Dickens, D. Parker, A.S. de Sousa and J.A.G. Williams, *J. Chem. Soc., Chem. Commun.*, **1996**, 697-698.
[58] Y. Hass and G. Stein, *J. Phys. Chem.*, **1971**, 75, 24, 1093-1104.
[59] G. Stein and E. Wurzberg, *J. Chem. Phys.*, **1975**, 62, 1, 208-213.
[60] A. Beeby, I. M. Clarkson, R.S. Dickens, S. Faulkner, D. Parker, L. Royle, A.S. de Soussa, J.A.G. Williams and M. Woods, *J. Chem. Soc, Perkin Trans.*, 2, **1999**, 493-503.
[61] W. D. Horrocks, Jr., and D. R. Sundick, *Acc. Chem. Res.*, **1981**, 14, 384-392.
[62] *The Chemistry of Contrast Agents in Medical Magnetic Resonance Imaging*, Ed. Andre E. Merbach & Eva Toth, **2001**, Wiley & Sons ISBN - 0-471-60778-9.
[63] V. Balzani, E. Berghmans, J.-M. Lehn, N. Sabbatini, R. Terode, and R. Ziessel, *Helv. Chim. Acta,* **1990**, 73, 2083-2089.
[64] R. Ziessel and J.-M. Lehn, *Helv. Chim. Acta,* **1990**, 73, 1149-1162.
[65] J.-M. Lehn and R. Ziessel, *J. Chem. Soc. Chem. Commun.*, **1987**, 1292-1294.
[66] J.M.Lehn and J.P. Sauvage, *J. Am. Chem. Soc.*, **1975**, 97:23, 6700-6707.
[67] B. Dietrich, J.M. Lehn and J.P. Sauvage, *Tetrahedron Lett.*, **1969**, 34, 2889-2892.
[68] B. Dietrich, J.M. Lehn and J.P. Sauvage, *Tetrahedron Lett.*, **1969**, 34, 2885-2888.
[69] N. Sabbatini, S. Dellonte, M. Ciano, A. Bonazzi and V. Balzani, *Chem. Phys. Lett.*, **1984**, 107, 2, 212-216.
[70] N. Sabbatini, S. Dellonte, and G. Blasse, *Chem. Phys. Lett.*, **1986**, 129, 541-545.
[71] G. Blasse, M. Buys, and N. Sabbatini, *Chem. Phys. Lett.*, **1986**, 124, 538-542.
[72] N. Sabbatini, S. Perathoner, G. Lattanzi, S. Dellonte, and V. Balzani, *J. Phys. Chem.*, **1987**, 91, 6136-6139.
[73] J.-C. Rodriguez-Ubis, B. Alpha. D. Plancheral, and J.-M. Lehn, *Helv. Chem. Acta,* **1984**, 67, 2264 –2269.
[74] B. Alpha, J.-M. Lehn and G. Mathis, *Agnew. Chem. Int. Ed. Engl.*, **1987**, 26, 3, 266-267.
[75] J.-M. Lehn and C.O. Roth, *Helv. Chim. Acta,* **1991**, 74, 572-578.
[76] G. Blasse, G. J. Dirksen, D. van der Voort, N. Sabbatini, S. Perathoner, J.-M. Lehn, and B. Alpha, *Chem. Phys Lett.*, **1988**,146, 347-351.
[77] B. Alpha, V. Balzani, J.-M. Lehn, S. Perathoner, and N. Sabbatini, *Angew. Chem. Int. Ed. Engl.*, **1987**, 26, 1266-1267.
[78] B. Alpha, R. Ballardini, V. Balzani, J.-M. Lehn, S. Perathoner and N. Sabbatini, *Photochem. Photobiol.*, **1990**, 52, 2, 299-306.
[79] J.-M. Lehn, *Agnew. Chem. Int. Ed. Engl.*, **1988**, 27, 89-112.
[80] I.Bkouche-Waksman, J. Guilhem, C. Pascard, B. Alpha, R. Deschenaux and J.-M. Lehn, *Helv. Chem. Acta,* **1991**, 1161-1169.
[81] J.-M. Lehn, M. Pietraszkiewicz, and J Karpiuk, *Helv. Chim. Acta,* **1990**, 73, 106-111.
[82] B. Alpha, E. Anklam, R. Deschenaux, J-M. Lehn, and M. Pietraskiewicz, *Helv.Chim. Acta,* **1988**, 71, 1042 – 1052.
[83] M. Pietraszkiewicz, J. Karpiuk and A. Kumar Rout, *Pure Appl. Chem.*, **1993**, 65, 3, 563-566.
[84] C. O. Paul-Roth, J.-M. Lehn, J. Guilhem and C. Pascard, *Helv. Chim. Acta.*, **1995**, 78, 1895-1903.

[85] L. Prodi, M. Maestri, V. Balzani, *Chem. Phys. Lett.*, **1991**, 180, 1-2, 45-50.
[86] C. Galaup, C. Picard, B. Cathala, L. Cazaux and P. Tisnes, *Helv. Chem. Acta,* **1999**,.82, 543-560.
[87] G. Xue, J. S. Bradshaw, N. Kent Dalley, P. B. Savage, R. M. Izatt, L. Prodi, M. Monalti and N. Zaccheroni, *Tetrahedron*, **2002**, 58, 4809 – 4815.
[88] Comprehensive Supramolecular Chemistry – Vol.1, ed. J. L. Atwood, J. E. D. Davies D. D Macnicol, F. Vogtle, J.- M. Lehn,
[89] N. Sabbatini, M. Guardigli, A. Mecati, V. Balzani, R. Ungaro, E. Ghidini, A. Casnati, and A. Pochini, *J. Chem. Soc., Chem. Commun.*, **1990**, 878-879.
[90] N. Sato and S. Shinkai, *J. Chem. Soc., Perkin Trans. 2,* **1993**, 621- 624.
[91] H. Matsumoto and S. Shinkai, *Chem. Lett.*, **1994**, 901-904.
[92] N. Sato, I. Yoshida, and S. Shinkai, *Chem. Lett.*, **1993**, 1261-1264.
[93] G. Ulrich and R. Ziessel, *Tetrahedron Lett.*, **1994**, 35, 34, 6299 - 6302.
[94] L. Prodi, S. Pivari, F. Bolletta, M. Hissler and R. Ziessel, *Eur. J. Inorg. Chem.*, **1998**, 1959-1965.
[95] D. M. Rudkevich, W. Verboom, E. van der Tol, C. J. van Straveren, F. M. Kaspersen, J. W. Verhoeven and D. N. Reinhoudt, *J. Chem. Soc. Perkin Trans. 2,* **1995**, 131-134.
[96] F. J. Steemers, W. Verboom, D. N. Reinhoudt, E. B.vand der tol and J. W. Verhoeven, *J. Am. Chem. Soc.*, **1995**, 9408-9414.
[97] A. Casnati, C. Fischer, M. Guardigli, A Isernia, I. Manet, N. Sabbatini, *J. Chem. Soc., Perkin Trans 2*, **1995**, 395-399.
[98] C. J. Pedersen, *Agnew. Chem. Int. Ed. Engl.*, **1988**, 27, 1021-1027.
[99] C. J. Pedersen, *J. Am. Chem. Soc.*, **1967**, 2495-2496.
[100] C. J. Pedersen, *J. Am. Chem. Soc.*, **1967**, 7017-7036.
[101] R. D. Hancock, H. Maumela, A. S. de Sousa, *Coord. Chem. Rev.* **1996**, 148, 315-347.
[102] Y. Liu, B.-H. Han, Y.-T. Chen, *Coord. Chem. Rev.*, **2000**, 200-202, 53-73.
[103] S. T. Frey, C. A. Chang, J. F Carvalho, A Varadarajan, L M. Schultze, KL. Pounds, and W. De W. Horrocks Jr., *Inorg. Chem.*, **1994**, 33, 2882-2889.
[104] C. Galup , J. M. Couchet, C. Picard and P. Tisnes, *Tetrahedron Lett.*, **2001**, 42 6275-6278.
[105] R. Ziessel and J.-M. Lehn, *Helv. Chim. Acta*, **1990**, 73, 1149-1162.
[106] R. Ziessel, M. Maestri, L. Prodi, V. Balzani and A. Van Dorsselaer, *Inorg. Chem.*, **1993**, 32, 1237-1241.
[107] L. Prodi, M. Maestri, R. Ziessel & V. Balzani, *Inorg. Chem.*, **1991**, 30, 3798-3802.
[108] G. Ulrich, M. Hissler and R. Ziessel, *New J. Chem.*, **1997**, 21, 147-150.
[109] V. Balzani, J.-M. Lehn, J van de Loosdrecht, A. Mecati, N. Sabbatini, and R Ziessel, *Angew. Chem. Int. Ed. Engl.*, **1991**, 30, 190-191.
[110] N. Sabbatini, M. Guardigli, Ilse and F. Bolletta, *Inorg.Chem.*, **1994**, 33, 955-959.
[111] D. Parker and J.A.G. Williams, *J. Chem. Soc., Perkin Trans. 2,* **1996,** 1581-1586.
[112] A. Beeby, L. M. Bushby, D. Maffeo and J.A.G. Williams, *J. Chem. Soc., Perkin Trans. 2,* **2000**, 1281-1283.
[113] S. Quici, G. Marzanni, M. Cavazzini, P. L. Anelli, M. Botta, E. Gianolio, G. Accorsi, N. Araroli and F. Barigelletti, *Inorg. Chem.*, **2002**, 41, 2777-2784.
[114] G. Bobba, J. C. Frias and D. Parker, *J. Chem. Soc. Chem. Commun.*, **2002**, 890-891.
[115] Y. Habata, S. Akabori, *Coord. Chem. Rev.*, **1996**, 148, 97-113.
[116] N. Sato, M. Goto, S. Matsumoto, and S. Shinkai, *Tetrahedron Lett,*, **1993**, 34, 30, 4847-4850.
[117] M. Murru, D. Parker, J.A.G. Williams and A. Beeby, *J. Chem. Soc. Chem. Commun.*, **1993**, 1116-1119.
[118] N. Sabbatini, M. Guardigli, F. Bolletta, I. Manet and R. Ziessel, *Agnew. Chem. Int. Ed. Engl.*, **1994**, 33 1501-1503
[119] A. P. de Silva, H.Q. Nimal Gunartane, T. Gunnlaugsson, A. J.M. Huxley, Jude T. Rademacher and T. E. Rice, NATO ASI Press, ISBN: 0-7923-4555-X
[120] A.P. de Silva, D. B. Fox, A. J.M. Huxley, N. D. McClenaghan, and J. Roiron, *Coord. Chem. Rev.*, **1999**, 185-186, 297-306.
[121] A. P. de Silva, H.Q. Nimal Gunaratne and T. E. Rice, *Angew. Chem. Int. Ed. Engl.*, **1996**, 35, 18 2116-2121.
[122] A.K. Saha, K. Kross, E. D. Kloszewski, D. A. Upson, J. L. Toner, R. A. Snow, C.D.V. Black and V.C. Desai, J. *Am. Chem. Soc.*, **1993**, 115, 11032-11033.
[123] A. P. de Silva, H.Q. Nimal Gunaratne, T. E. Rice and S. Stewart, *J. Chem. Soc., Chem. Commun.*, **1997**, 1891-1892.
[124] D.Parker, P. K. Senanayake and J.A.G. Williams, *J. Chem. Soc., Perkin Trans. 2,* **1998**, 1777.
[125] T. Gunnlaugsson, D. A. Mac Donaill and D. Parker, *J. Am. Chem. Soc.*, **2001**,123, 12866-12876.

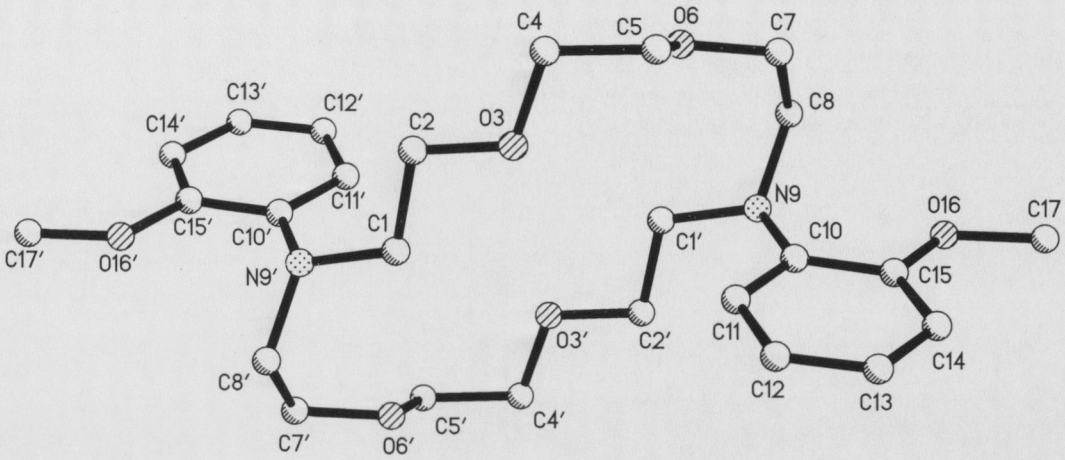
[126] T. Gunnlaugsson, *Tetrahedron*, **2001**, 42, 8901-8905.
[127] M. P. Lowe and D. Parker, *J. Chem. Soc., Chem. Commun.*, **2000**, 707-708.
[128] M. P. Lowe and D. Parker, *Inorg. Chim. Acta,* **2001**, 317, 163-173.
[129] O. Reany, T. Gunnlaugsson and D. Parker, *J. Chem. Soc. Chem. Commun.*, **2000**, 473-474.
[130] O. Reany, T. Gunnlaugsson and D. Parker, *J. Chem. Soc., Perkin Trans. 2,* **2000**, 1819-1831.
[131] C. Bazzicalupi, A. Bencini, A. Bianchi, C. Giogi, V. Fusi, A. Masotti, B. Valtancoli, A. Roque and F. Pina, *J. Chem. Soc. Chem. Commun.*, **2000**, 561-562.
[132] T. Yamada, S. Shinoda and H. Tskube, *J. Chem. Soc. Chem. Commun.*, **2002**, 1218-1219.
[133] M. Montalti , L. Prodi, N. Zaccheroni, L.Charonniere, L. Douce and R. Ziessel, *J. Am. Chem. Soc.*, **2001**, 123, 12694-12695.
[134] L. J. Charbonniere, R. Ziessel, M. Monalti, L. Prodi, N. Zacheroni, C. Boehme and G. Wipff, *J. Am. Chem. Soc.*, **2002**, 124, 7779 – 7788.
[135] J.I. Bruce, R.S. Dickens, L.J. Govenlock, T. Gunnlaugsson, S. Lopinski, M.P.Lowe, D. Parker, R.D. Peacock, J.J.B. Perry, S. Aime and M. Botta, *J. Am. Chem. Soc.*, **2000**, 122, 9674-9684.
[136] R. S. Dickins, T. Gunnlaugsson, D. Parker and R. D. Peacock, *J. Chem. Soc. Chem. Commun.*, **1998**, 1643-1644.
[137] R. S. Dickins, C. S. Love and H. Puschmann, *J. Chem. Soc. Chem. Commun.*, **2001**, 2308-2309.

[138] A. E. Bruno, S. Barnard, M. Rouilly, A. Waldner, J. Berger and M. Ehrat, *Anal. Chem.*, **1997**, 69, 507-513.
[139] R. P. Haugland, *Handbook of Fluorescent Probes and Research products [Eight Edition], Molecular Probes,* **2001**, ISBN 0-9652240-7-4.
[140] M.J. Calverley and J. Dale, *Acta Chem. Scand., Ser B*, **1982**, 36, 241-247.
[141] R. A. Schultz, D. M. Dishong and G. W. Gokel, *Tetrahedron lett.*, **1981**, 22, 28, 2623-2626.
[142] X.-X. Zhang and S.L. Buchwald, *J. Org. Chem,*. **2000**, 65, 8027-8031.
[143] H. Tsukube, H. Minatogawa, M. Munakata, M. Toda and K. Matsumoto, *J. Org. Chem.*, **1992**, 57, 542-547.
[144] T. Gunnlaugsson, PhD Thesis, Queens University of Belfast, **1996**.
[145] L.M. Harwood and C.J. Moody (Series editors), *Macrocycle Synthesis, A practical approach* Ed. by D. Parker, **1996**,
[146] J. March, *Advanced organic chemistry, Reactions, Mechanisms and structures 4th Ed.,***1992**, Wiley & Sons, USA, ISBN 0-471-60180-2
[147] J. McMurry, *Organic Chemistry 4th Ed.,***1996**, Brooks/Cole Publishing company, USA, ISBN 0-534-23832-7.
[148] R.M. Silverstien, G.C. Bassler & T.C. Morrill, *Spectrometric identification of organic compounds*, **1991**, Wiley & Sons Inc., ISBN 0-471-63404-2.
[149] *J. Org. Chem. USSR* (Eng. Transl.) **1983**, 4, 689-696.
[150] Piccard, *Chem. Ber.*, **1926**, 59, 1655.
[151] L. Grimaux, *Bull. Soc. Chim. Fr.*, **1891**, 3, 6, 415.
[152] *Justus Liebegs Ann. Chem.*, **1889**,255, 188.
[153] J. J. D'Amico, C. C. Tung and L. A. Walker, *J. Am. Chem. Soc.*, **1959**, 81, 5957-5960.
[154] R. N. Loeppky, S. P. Singh, S. Elomari, R. Hastings and T. E. Theiss, *J. Am. Chem. Soc.*, **1998**, 120, 5193-5202.
[155] a) J. K. Kochi, *Acc. Chem. Res.*, **1992**, 25, 39-47., b) U. Al-Obaidi and R. B. Moodie, *J. Chem. Soc., Perkin Trans. 2,* **1985**, 467-472., c) L. R. Dix and R. B. Moodie, *J. Chem. Soc., Perkin Trans. 2*, **1986**, 1097-1101., d) M. Colonna, L. Greci and M. Poloni, *J. Chem. Soc., Perkin Trans. 2,* **1984**, 165-169., e) G. Verardo, A. G. Giumanini and P. Strazzolini, *Tetrahedron,* **1990**, 46, 12, 4303-4332., f) A. H. Clemens, P. Helsby, J. H. Ridd and F. Al-Omran, *J. Chem. Soc., Perkin Trans. 2,* **1985**, 1217-1225.,
[156] a) J. C. Giffney, D. J. Mills and J. H. Ridd, *J. Chem. Soc., Chem. Commun.*, **1976**, 19-20; b) J. H. Ridd and J.P.B. Sandall, *J. Chem. Soc., Chem. Commun.*, **1981**, 402-403, c) R. N. Loeppky and L. Yu, *Tetrahedron Lett.*, 1990, 31, 23, 3263-3266, d) F. Al-Omran, K. Fujiwara, J. C. Giffney, J. H. Ridd and S. R. Robinson, *J. Chem. Soc., Perkin Trans. 2,* **1981**, 518-525, e) J. C. Giffney and J. H. Ridd, *J. Chem. Soc., Perkin Trans. 2,* **1979**, 618-623.
[157] M. Bodansky and A. Bodansky, *The practice of peptide synthesis 2nd ed.,* **1994**, Springer-Verlay, Berlin, ISBN-0-387-57505-7.
[158] A. Dadabhoy, S. Faulkner and P. G. Sammes, *J. Chem. Soc., Perkin Trans, 2,* **2002**, 348-357.
[159] D. Parker, R. S. Dickins, H. Puschmann, C. Crossland, and J. A.K. Howard, *Chem. Rev.*, **2002**, 102(6); 1977-2010.

[160] a) J. S. Prasad, F. J. Okuniexicz, E. J. Delaney and D. D. Dishino, J. Chem. Soc., Perkin Trans. 1, **1991,** 3329-3332; b) A. Beeby, R. S. Dickens, S. Faulkner, D. Parker and J.A G. Williams, *J. Chem. Soc., Chem. Commun.,* **1997**, 1401-1402; c) G. Ligner, R. Mohan, S. Knittle and G. Duportail, *Spectrochim. Acta, Part A,* **1990**, 46A, 5, 797-802.
[161] a) D. Parker and J.A G. Williams, *J. Chem. Soc., Chem. Commun.,* **1998**, 245-246; b) T. Gunnlaugsson and D. Parker, *J. Chem. Soc., Chem. Commun.,* **1998**, 511-512.
[162] K.A. Connors, *Binding constants*, **1987**, John Wiley & Sons, New York, 1st Ed..
[163] D. A. Skoog, D. M. West and F. J. Holler, *Fundamentals of Analytical chemistry 5th ed.,* **1988**, Saunders College publishing , New York ISBN 0-03-142828-6.
[164] D. Parker and J.A.G. Williams, *J. Chem. Soc., Perkin Trans. 2,* **1995**, 1305-1314.
[165] A. P. de Silva, H.Q. Nimal Gunaratne, T. Gunnlaugsson, A. J.M. Huxley, J.T. Rademacher and T.E. Rice, *Chemosensors of Ion and Molecule Recognition, Ed.* J.P. Desvergne and A.W. Czarnik, **1996**, NATO ASI Press, ISBN: 0-7923-4555-X.
[166] O. Brummer, J. J. La Clair and K. D. Janda, *Org. Lett.,* **1999**, 3, 3, 415-418.
[167] E. Hirayama, T. Sugiyama, H. Hisamoto and K. Suzuki, *Anal. Chem.*, **2000**, 72, 465-474.
[168] S.-H. Kim, J.-W. Kim, J.-H. Kim, K.-N. Koh, S.-W. Kang, *Dyes and Pigments*, **2000**, 46, 49-53.
[169] K. Wilcox and G.E. Pacey, *Talanta*, **1991**, 38, 11, 1315-1324.
[170] F. Sancenon, A. B. Descalzo, R. Martinez-Manez, M. A. Miranda, and J. Soto, *Agnew. Chem. Int. Ed.,* **2001**, 40, 14, 2640-2643.
[171] D. Jimenez, R. Martinez-Manez, F. Sancenon and J. Soto, *Tetrahedron Lett.,* **2002**, 43, 2823-2825.
[172] C. Lee, D. H. Lee and J. -I. Hong, *Tetrahedron Lett.,* **2001**, 42, 8665-8668.
[173] S. C. McCleskey, A. Metzger, C. S. Simmons and E. V. Anslyn, *Tetrahedron Lett.*, **2002**, 58, 621-628.
[174] P. D. Beer, P. A. Gale, and D. K. Smith, *Oxford chemistry Primers - Supramolecular Chemistry,* **1999**, Oxford Science Publications - ISBN 0 19 850447 0 (Pbk).
[175] R.M. Christie, *Colour Chemistry*, **2001**, Royal Society of Chemistry, ISBN 0-85404-573-2.
[176] A. Minta,, J. P.Y. Kao, and R. Tsien, *J. Biol. Chem.,* **1989**, 264, 14, 8171-8178.
[177] R. Y. Tsien, TINS, **1988**, 11, 10, Elsevier publications, Cambridge, 419-424.
[178] S. R Adams, V. Lev-Ram and R. Y. Tsien, *Chemistry & Biology,* **1997**, 4, 11, 867-878.
[179] S.R. Adams, J.P.Y. Kao and R. Y. Tsien, *J. Am. Chem. Soc.*, **1989**, 111, 7957-7968.
[180] G. Grynkiewicz, M. Poenie, and R. Y. Tsien, *J. Biol. Chem.,* **1985**, 260, 3440-3450.
[181] A.P. de Silva, H.Q. Nimal Gunaratane, A. T.M. Kane and G.E.M. Maguire, *Chem. Lett,*. **1995**, 125-126.
[182] R. Y. Tsien, *Nature,* **1981**, 290, 527.
[183] R. Y. Tsien, *American Physiological Society*, **1992**, C722-C728.
[184] B. Erdogan and E. U. Akkaya, *Tetrahedron Lett.,* **1998**, 39, 9107-9108.
[185] M. Shortreed, R. Kopelman, M. Kuhn and B. Hoyland, *Anal. Chem.,* **1996**, 68, 1414-1418.
[186] R. Pethig, M. Kuhn, R. Payne, E. Adler, T.-H. Chen and L.F. Jaffe, *Cell Calcium*, **1989**, 10, 491-498.
[187] P. D. Beer, J. Cadman, *Coord. Chem. Rev.*, **2000**, 205, 131-155.
[188] H. Tsukube, S. Shinoda, H. Tamiaki, *Coord. Chem. Rev.*, **2001**, 226, 227-234.
[189] G. R. Deviprasad, B. Keshavan, and F. D'Souza, *J. Chem. Soc., Perkin Trans. 1,* **1998**, 3133-3135.
[190] G. De Santis, L. Fabbrizzi, M. Licchelli, A. Poggi and A. Taglietti, *Angew. Chem., Int. Ed. Engl.,* **1996**, 35, No. 2, 202-204.
[191] L. Fabbrizzi, M. Licchelli, L. Parodi, A. Poggi, A. Taglietti, Eur. *J. Inorg. Chem.,* **1999**, 35-39.
[192] P. Pallavicini, V. Amendola, C. Massera, E. Mundum and A. Taglietti, *J. Chem. Soc., Chem. Commum.,* **2002**, 2452-2453.
[193] S. G. Schulman, *Molecular Luminescence Spectroscopy, Methods and applications: Part 1*, Wiley & Sons ISBN - 0-471-86848-5
[194] P. B O'Hara, *Photochem. Photobiol.,* **1987**, 46, 6, 1067-1070.
[195] M. Elbanowski and B. Makowska, *J. Photochemistry and Photobiology A: Chemistry*, **1996**, 99, 85-92.
[196] F.S. Richardson and A. Das Gupta, *J. Am. Chem. Soc.,* **1981**, 103, 19, 5716-5724.
[197] W. D. Horrocks, Jr., and D. R. Sudnick, *Acc. Chem. Res.,* **1981**, 14, 384-392.
[198] L. F. Lindoy, *Coord. Chem. Rev.*, **1996**, 148, 349-368.
[199] W. D. Horrocks, Jr., and D. R. Sudnick, *J. Am. Chem. Soc.,* **1979**, 101, 2, 334-340.
[200] H. G. Brittain, F. S. Richardson and R. B. Martin, *J. Am. Chem. Soc.,* **1976**, 98, 8255-8260.
[201] L.M Perry and J.D. Winefordner, *Talanta*, **1990**, 37, 10, 965-969.
[202] J. Georges, *Analyst*, **1993**, 118, 1481-1486.

[203] A. Rieutord, P. Prognon, F.Brion and G. Mahuzier, *Analyst*, **1997**, 122, 59R-66R.
[204] M.P. Aguilar - Caballos, A. Gomez - Hens and D. Perez – Bendito, *Analyst*, **1999**,124, 1079-11084.
[205] S. V. Beltyukova, E. I. Tselik, A. V. Egorova, *J. Pharm. Biomed. Anal.*, **1998**, 18, 261-266.
[206] N. Arnaud and J. Georges, *Analyst*, **1999**, 124, 1075-1078.
[207] J. A Yu, R.B. Lessard, L. E. Bowman and D. G. Nocera, *Chem. Phys. Lett.*, **1991**, 187, 3, 263- 268.
[208] Z. Pikramenou, J.A Yu, R. B. Lessard, A. Ponce, P. A. Wong, and D. G. Nocera, *Coord. Chem. Rev.*, **1994**, 132, 181-194.
[209] E. P. Diamandas, *Analyst*. **1992**, 117, 1879-1883.
[210] J. J Michels, J. Huskens and D. N. Reinhoudt, *J. Am. Chem. Soc.*, **2002**, 124, 9, 2056-2064.
[211] D. Parker and J.A.G Williams, *J. Chem. Soc., Perkin Trans. 2*, **1995**, 1305-1314.
[212] S. Mulready, PhD. Thesis, University of Dublin, Trinity College, **2003**.
[213] F. A. Carey and R. J. Sundberg, *Advanced Organic chemistry*, **1977**, Plenum Press, New York. ISBN 0-306025004-7 (pt. B)
[214] J. D. Lee, *Concise Inorganic Chemistry, 4th ed.*, **1991**, Chapman and Hall, ISBN 0412402904.
[215] J.A. K. Howard, A. M. Kenwright, J. M. Moloney, D. Parker, M. Port, M. Navet, O. Rousseau and M. Woods, *J. Chem. Soc., Chem. Commun.*, **1998**, 1381-1382.
[216] R. S. Dickens, J. A. K. Howard, C. L. Maupin, J. M. Moloney, D. Parker, R. D. Peacock, J. P. Riehl and G. Siligardi, *New J. Chem.*, **1998**, 891-899.
[217] S. L. Murov, I. Carmichael and G. L. Hug, *Handbook of Photochemistry, 2nd Ed.*, **1993**, Marcel Dekker, New York, ISBN 0-8247-7911-8.
[218] R. H. Dreisbach and W. O. Robertson, *Handbook of poisoning*, **1986**, Appelton & Lange ISBN 0-8385-3643-3.

Appendix



Crystallography data for 112

```
data_

_audit_creation_method            SHELXL-97
_chemical_name_systematic
;
 ?
;
_chemical_name_common             ?
_chemical_melting_point           ?
_chemical_formula_moiety          ?
_chemical_formula_sum
 'C26 H38 N2 O6'
_chemical_formula_weight          474.58

loop_
 _atom_type_symbol
 _atom_type_description
 _atom_type_scat_dispersion_real
 _atom_type_scat_dispersion_imag
 _atom_type_scat_source
 'C'  'C'   0.0033   0.0016
 'International Tables Vol C Tables 4.2.6.8 and 6.1.1.4'
 'H'  'H'   0.0000   0.0000
 'International Tables Vol C Tables 4.2.6.8 and 6.1.1.4'
 'N'  'N'   0.0061   0.0033
 'International Tables Vol C Tables 4.2.6.8 and 6.1.1.4'
 'O'  'O'   0.0106   0.0060
 'International Tables Vol C Tables 4.2.6.8 and 6.1.1.4'

_symmetry_cell_setting            Monoclinic
_symmetry_space_group_name_H-M    P2(1)/c
```

```
loop_
 _symmetry_equiv_pos_as_xyz
 'x, y, z'
 '-x, y+1/2, -z+1/2'
 '-x, -y, -z'
 'x, -y-1/2, z-1/2'

_cell_length_a                    7.218(2)
_cell_length_b                    7.852(2)
_cell_length_c                    21.449(6)
_cell_angle_alpha                 90.00
_cell_angle_beta                  93.011(4)
_cell_angle_gamma                 90.00
_cell_volume                      1213.9(6)
_cell_formula_units_Z             2
_cell_measurement_temperature     153(2)
_cell_measurement_reflns_used     ?
_cell_measurement_theta_min       ?
_cell_measurement_theta_max       ?

_exptl_crystal_description        plate
_exptl_crystal_colour             colourless
_exptl_crystal_size_max           0.65
_exptl_crystal_size_mid           0.54
_exptl_crystal_size_min           0.16
_exptl_crystal_density_meas       not_measured
_exptl_crystal_density_diffrn     1.298
_exptl_crystal_density_method     'not measured'
_exptl_crystal_F_000              512
_exptl_absorpt_coefficient_mu     0.092
_exptl_absorpt_correction_type    Empirical
_exptl_absorpt_correction_T_min   0.556
_exptl_absorpt_correction_T_max   1.000
_exptl_absorpt_process_details    SADABS

_exptl_special_details
;
 ?
;

_diffrn_ambient_temperature       153(2)
_diffrn_radiation_wavelength      0.71073
_diffrn_radiation_type            MoK\a
_diffrn_radiation_source          'fine-focus sealed tube'
_diffrn_radiation_monochromator   graphite
_diffrn_measurement_device_type   'CCD area detector'
_diffrn_measurement_method        'phi and omega scans'
_diffrn_detector_area_resol_mean  ?
_diffrn_standards_number          ?
_diffrn_standards_interval_count  ?
_diffrn_standards_interval_time   ?
_diffrn_standards_decay_%         ?
_diffrn_reflns_number             13480
_diffrn_reflns_av_R_equivalents   0.0999
_diffrn_reflns_av_sigmaI/netI     0.1157
```

```
_diffrn_reflns_limit_h_min        -9
_diffrn_reflns_limit_h_max        9
_diffrn_reflns_limit_k_min        -10
_diffrn_reflns_limit_k_max        10
_diffrn_reflns_limit_l_min        -28
_diffrn_reflns_limit_l_max        27
_diffrn_reflns_theta_min          1.90
_diffrn_reflns_theta_max          28.53
_reflns_number_total              2810
_reflns_number_gt                 1420
_reflns_threshold_expression      >2sigma(I)

_computing_data_collection        'Bruker SMART'
_computing_cell_refinement        'Bruker SMART'
_computing_data_reduction         'Bruker SHELXTL'
_computing_structure_solution     'SHELXS-97 (Sheldrick, 1990)'
_computing_structure_refinement   'SHELXL-97 (Sheldrick, 1997)'
_computing_molecular_graphics     'Bruker SHELXTL'
_computing_publication_material   'Bruker SHELXTL'

_refine_special_details
;
 Refinement of F^2^ against ALL reflections.  The weighted R-factor wR and
 goodness of fit S are based on F^2^, conventional R-factors R are based
 on F, with F set to zero for negative F^2^. The threshold expression of
 F^2^ > 2sigma(F^2^) is used only for calculating R-factors(gt) etc. and is
 not relevant to the choice of reflections for refinement.  R-factors based
 on F^2^ are statistically about twice as large as those based on F, and R-
 factors based on ALL data will be even larger.
;

_refine_ls_structure_factor_coef  Fsqd
_refine_ls_matrix_type            full
_refine_ls_weighting_scheme       calc
_refine_ls_weighting_details
 'calc w=1/[\s^2^(Fo^2^)+(0.0436P)^2^+0.0000P] where P=(Fo^2^+2Fc^2^)/3'
_atom_sites_solution_primary      direct
_atom_sites_solution_secondary    difmap
_atom_sites_solution_hydrogens    geom
_refine_ls_hydrogen_treatment     mixed
_refine_ls_extinction_method      none
_refine_ls_extinction_coef        ?
_refine_ls_number_reflns          2810
_refine_ls_number_parameters      230
_refine_ls_number_restraints      0
_refine_ls_R_factor_all           0.1098
_refine_ls_R_factor_gt            0.0483
_refine_ls_wR_factor_ref          0.1052
_refine_ls_wR_factor_gt           0.0886
_refine_ls_goodness_of_fit_ref    0.837
_refine_ls_restrained_S_all       0.837
_refine_ls_shift/su_max           0.000
_refine_ls_shift/su_mean          0.000

loop_
```

```
 _atom_site_label
 _atom_site_type_symbol
 _atom_site_fract_x
 _atom_site_fract_y
 _atom_site_fract_z
 _atom_site_U_iso_or_equiv
 _atom_site_adp_type
 _atom_site_occupancy
 _atom_site_symmetry_multiplicity
 _atom_site_calc_flag
 _atom_site_refinement_flags
 _atom_site_disorder_assembly
 _atom_site_disorder_group
C1 C 0.7208(3) 0.5805(3) 0.56514(10) 0.0239(5) Uani 1 1 d . . .
H1A H 0.652(2) 0.497(2) 0.5383(8) 0.023(5) Uiso 1 1 d . . .
H1B H 0.814(2) 0.642(2) 0.5391(8) 0.025(5) Uiso 1 1 d . . .
C2 C 0.5808(3) 0.7091(3) 0.58559(10) 0.0258(5) Uani 1 1 d . . .
H2A H 0.645(2) 0.806(2) 0.6084(8) 0.019(5) Uiso 1 1 d . . .
H2B H 0.493(2) 0.658(3) 0.6173(9) 0.028(5) Uiso 1 1 d . . .
O3 O 0.47966(17) 0.76238(17) 0.53044(6) 0.0265(4) Uani 1 1 d . . .
C4 C 0.3379(3) 0.8819(3) 0.54142(10) 0.0253(5) Uani 1 1 d . . .
H4A H 0.392(3) 1.002(3) 0.5538(9) 0.039(6) Uiso 1 1 d . . .
H4B H 0.263(2) 0.844(2) 0.5787(8) 0.019(5) Uiso 1 1 d . . .
C5 C 0.2156(3) 0.8978(3) 0.48303(10) 0.0246(5) Uani 1 1 d . . .
H5A H 0.136(2) 1.009(3) 0.4853(8) 0.027(5) Uiso 1 1 d . . .
H5B H 0.293(3) 0.905(2) 0.4458(9) 0.030(6) Uiso 1 1 d . . .
O6 O 0.09952(17) 0.75171(17) 0.47822(6) 0.0252(4) Uani 1 1 d . . .
C7 C -0.0118(3) 0.7398(3) 0.42155(10) 0.0256(5) Uani 1 1 d . . .
H7B H -0.142(3) 0.774(2) 0.4285(8) 0.024(5) Uiso 1 1 d . . .
H7A H 0.038(2) 0.819(2) 0.3880(9) 0.024(5) Uiso 1 1 d . . .
C8 C -0.0115(3) 0.5587(3) 0.39747(10) 0.0245(5) Uani 1 1 d . . .
H8A H -0.058(2) 0.484(2) 0.4291(7) 0.007(4) Uiso 1 1 d . . .
H8B H -0.102(2) 0.553(2) 0.3593(8) 0.014(5) Uiso 1 1 d . . .
N9 N 0.1727(2) 0.4952(2) 0.38186(7) 0.0214(4) Uani 1 1 d . . .
C10 C 0.2709(3) 0.6028(2) 0.34187(9) 0.0201(5) Uani 1 1 d . . .
C11 C 0.4441(3) 0.6718(3) 0.35941(10) 0.0237(5) Uani 1 1 d . . .
H11 H 0.501(2) 0.649(2) 0.4009(8) 0.020(5) Uiso 1 1 d . . .
C12 C 0.5396(3) 0.7735(3) 0.31864(10) 0.0287(5) Uani 1 1 d . . .
H12 H 0.667(3) 0.820(3) 0.3312(9) 0.037(6) Uiso 1 1 d . . .
C13 C 0.4623(3) 0.8117(3) 0.26092(11) 0.0303(6) Uani 1 1 d . . .
H13 H 0.526(2) 0.882(3) 0.2320(9) 0.031(6) Uiso 1 1 d . . .
C14 C 0.2908(3) 0.7455(3) 0.24211(10) 0.0251(5) Uani 1 1 d . . .
H14 H 0.231(2) 0.774(2) 0.2019(9) 0.027(6) Uiso 1 1 d . . .
C15 C 0.1958(3) 0.6417(2) 0.28160(9) 0.0223(5) Uani 1 1 d . . .
O16 O 0.02797(18) 0.56894(18) 0.26521(6) 0.0291(4) Uani 1 1 d . . .
C17 C -0.0621(4) 0.6191(3) 0.20708(11) 0.0347(6) Uani 1 1 d . . .
H17A H -0.078(3) 0.749(3) 0.2035(9) 0.049(7) Uiso 1 1 d . . .
H17B H 0.015(3) 0.585(3) 0.1720(9) 0.035(6) Uiso 1 1 d . . .
H17C H -0.186(3) 0.558(3) 0.2065(9) 0.039(6) Uiso 1 1 d . . .

loop_
 _atom_site_aniso_label
 _atom_site_aniso_U_11
 _atom_site_aniso_U_22
 _atom_site_aniso_U_33
```

```
 _atom_site_aniso_U_23
 _atom_site_aniso_U_13
 _atom_site_aniso_U_12
C1 0.0271(11) 0.0226(12) 0.0215(12) 0.0038(10) -0.0021(10) 0.0009(10)
C2 0.0312(12) 0.0231(12) 0.0224(12) 0.0005(10) -0.0050(10) 0.0052(10)
O3 0.0281(8) 0.0262(8) 0.0246(8) 0.0007(6) -0.0049(6) 0.0095(7)
C4 0.0216(11) 0.0224(13) 0.0318(14) -0.0024(10) 0.0008(10) 0.0044(10)
C5 0.0213(10) 0.0192(12) 0.0330(14) 0.0017(10) -0.0003(10) 0.0014(10)
O6 0.0262(8) 0.0239(8) 0.0249(8) 0.0018(7) -0.0048(6) -0.0039(7)
C7 0.0223(11) 0.0294(13) 0.0245(12) 0.0016(10) -0.0040(10) 0.0061(10)
C8 0.0234(11) 0.0266(12) 0.0234(13) 0.0012(10) -0.0010(10) -0.0007(10)
N9 0.0215(9) 0.0217(9) 0.0206(9) 0.0036(8) -0.0017(7) 0.0046(8)
C10 0.0222(10) 0.0177(11) 0.0203(12) -0.0004(9) 0.0005(9) 0.0041(9)
C11 0.0266(11) 0.0244(12) 0.0195(12) -0.0014(10) -0.0021(10) 0.0018(10)
C12 0.0249(11) 0.0287(13) 0.0323(14) -0.0010(11) -0.0019(10) -0.0009(11)
C13 0.0336(13) 0.0278(13) 0.0298(14) 0.0063(11) 0.0042(11) -0.0027(10)
C14 0.0297(11) 0.0230(12) 0.0224(12) 0.0036(10) -0.0010(10) 0.0009(10)
C15 0.0218(10) 0.0200(11) 0.0244(12) -0.0015(9) -0.0037(9) 0.0028(9)
O16 0.0306(8) 0.0292(9) 0.0263(9) 0.0063(7) -0.0108(7) -0.0065(7)
C17 0.0409(15) 0.0331(15) 0.0286(15) 0.0091(11) -0.0127(12) -0.0039(12)

_geom_special_details
;
 All esds (except the esd in the dihedral angle between two l.s. planes)
 are estimated using the full covariance matrix.  The cell esds are taken
 into account individually in the estimation of esds in distances, angles
 and torsion angles; correlations between esds in cell parameters are only
 used when they are defined by crystal symmetry.  An approximate
(isotropic)
 treatment of cell esds is used for estimating esds involving l.s. planes.
;

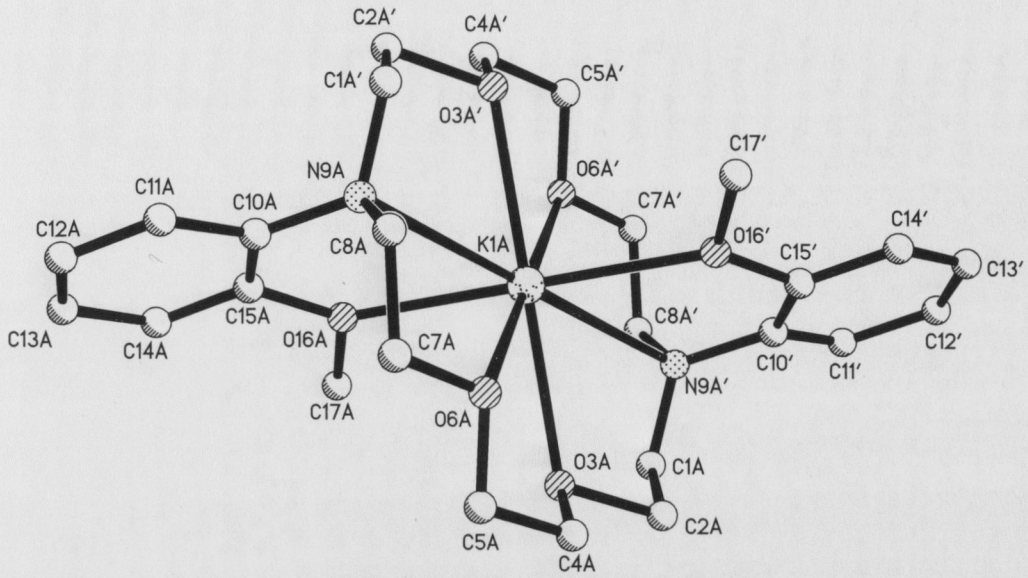
loop_
 _geom_bond_atom_site_label_1
 _geom_bond_atom_site_label_2
 _geom_bond_distance
 _geom_bond_site_symmetry_2
 _geom_bond_publ_flag
C1 N9 1.465(2) 3_666 ?
C1 C2 1.509(3) . ?
C2 O3 1.420(2) . ?
O3 C4 1.417(2) . ?
C4 C5 1.499(3) . ?
C5 O6 1.421(2) . ?
O6 C7 1.425(2) . ?
C7 C8 1.513(3) . ?
C8 N9 1.475(2) . ?
N9 C10 1.420(2) . ?
N9 C1 1.465(2) 3_666 ?
C10 C11 1.396(3) . ?
C10 C15 1.409(3) . ?
C11 C12 1.393(3) . ?
C12 C13 1.365(3) . ?
C13 C14 1.383(3) . ?
C14 C15 1.382(3) . ?
```

```
C15 O16 1.369(2) . ?
O16 C17 1.431(2) . ?

loop_
 _geom_angle_atom_site_label_1
 _geom_angle_atom_site_label_2
 _geom_angle_atom_site_label_3
 _geom_angle
 _geom_angle_site_symmetry_1
 _geom_angle_site_symmetry_3
 _geom_angle_publ_flag
N9 C1 C2 112.23(17) 3_666 . ?
O3 C2 C1 106.12(16) . . ?
C4 O3 C2 113.62(15) . . ?
O3 C4 C5 108.36(17) . . ?
O6 C5 C4 108.18(17) . . ?
C5 O6 C7 114.77(15) . . ?
O6 C7 C8 110.00(16) . . ?
N9 C8 C7 114.40(17) . . ?
C10 N9 C1 116.86(16) . 3_666 ?
C10 N9 C8 114.87(16) . . ?
C1 N9 C8 113.83(16) 3_666 . ?
C11 C10 C15 117.30(18) . . ?
C11 C10 N9 122.46(17) . . ?
C15 C10 N9 120.24(17) . . ?
C12 C11 C10 121.3(2) . . ?
C13 C12 C11 120.2(2) . . ?
C12 C13 C14 119.9(2) . . ?
C15 C14 C13 120.5(2) . . ?
O16 C15 C14 123.31(18) . . ?
O16 C15 C10 115.94(17) . . ?
C14 C15 C10 120.74(18) . . ?
C15 O16 C17 117.68(17) . . ?

_diffrn_measured_fraction_theta_max    0.910
_diffrn_reflns_theta_full              28.53
_diffrn_measured_fraction_theta_full   0.910
_refine_diff_density_max    0.262
_refine_diff_density_min   -0.234
_refine_diff_density_rms    0.052

#===END
```



Crystallography data for 112•KPF_6

```
data_

_audit_creation_method            SHELXL-97
_chemical_name_systematic
;
 ?
;
_chemical_name_common             ?
_chemical_melting_point           ?
_chemical_formula_moiety          ?
_chemical_formula_sum
 'C26 H38 F6 K N2 O6 P'
_chemical_formula_weight          658.65

loop_
 _atom_type_symbol
 _atom_type_description
 _atom_type_scat_dispersion_real
 _atom_type_scat_dispersion_imag
 _atom_type_scat_source
 'C'  'C'   0.0033   0.0016
 'International Tables Vol C Tables 4.2.6.8 and 6.1.1.4'
 'H'  'H'   0.0000   0.0000
 'International Tables Vol C Tables 4.2.6.8 and 6.1.1.4'
 'N'  'N'   0.0061   0.0033
 'International Tables Vol C Tables 4.2.6.8 and 6.1.1.4'
 'O'  'O'   0.0106   0.0060
 'International Tables Vol C Tables 4.2.6.8 and 6.1.1.4'
 'F'  'F'   0.0171   0.0103
 'International Tables Vol C Tables 4.2.6.8 and 6.1.1.4'
 'P'  'P'   0.1023   0.0942
 'International Tables Vol C Tables 4.2.6.8 and 6.1.1.4'
 'K'  'K'   0.2009   0.2494
 'International Tables Vol C Tables 4.2.6.8 and 6.1.1.4'
```

```
_symmetry_cell_setting              Triclinic
_symmetry_space_group_name_H-M      P-1

loop_
 _symmetry_equiv_pos_as_xyz
 'x, y, z'
 '-x, -y, -z'

_cell_length_a                      11.908(3)
_cell_length_b                      12.219(3)
_cell_length_c                      12.268(3)
_cell_angle_alpha                   86.206(3)
_cell_angle_beta                    70.910(3)
_cell_angle_gamma                   64.190(3)
_cell_volume                        1512.5(6)
_cell_formula_units_Z               2
_cell_measurement_temperature       153(2)
_cell_measurement_reflns_used       ?
_cell_measurement_theta_min         ?
_cell_measurement_theta_max         ?

_exptl_crystal_description          block
_exptl_crystal_colour               colourless
_exptl_crystal_size_max             0.28
_exptl_crystal_size_mid             0.18
_exptl_crystal_size_min             0.16
_exptl_crystal_density_meas         not_measured
_exptl_crystal_density_diffrn       1.446
_exptl_crystal_density_method       'not measured'
_exptl_crystal_F_000                688
_exptl_absorpt_coefficient_mu       0.308
_exptl_absorpt_correction_type      Empirical
_exptl_absorpt_correction_T_min     0.794
_exptl_absorpt_correction_T_max     1.000
_exptl_absorpt_process_details      SADABS

_exptl_special_details
;
 ?
;

_diffrn_ambient_temperature         153(2)
_diffrn_radiation_wavelength        0.71073
_diffrn_radiation_type              MoK\a
_diffrn_radiation_source            'fine-focus sealed tube'
_diffrn_radiation_monochromator     graphite
_diffrn_measurement_device_type     'CCD area detector'
_diffrn_measurement_method          'phi and omega scans'
_diffrn_detector_area_resol_mean    ?
_diffrn_standards_number            ?
_diffrn_standards_interval_count    ?
_diffrn_standards_interval_time     ?
_diffrn_standards_decay_%           ?
_diffrn_reflns_number               17315
```

```
_diffrn_reflns_av_R_equivalents   0.0565
_diffrn_reflns_av_sigmaI/netI     0.1000
_diffrn_reflns_limit_h_min        -15
_diffrn_reflns_limit_h_max        14
_diffrn_reflns_limit_k_min        -15
_diffrn_reflns_limit_k_max        15
_diffrn_reflns_limit_l_min        -15
_diffrn_reflns_limit_l_max        15
_diffrn_reflns_theta_min          1.76
_diffrn_reflns_theta_max          28.60
_reflns_number_total              6681
_reflns_number_gt                 3364
_reflns_threshold_expression      >2sigma(I)

_computing_data_collection        'Bruker SMART'
_computing_cell_refinement        'Bruker SMART'
_computing_data_reduction         'Bruker SHELXTL'
_computing_structure_solution     'SHELXS-97 (Sheldrick, 1990)'
_computing_structure_refinement   'SHELXL-97 (Sheldrick, 1997)'
_computing_molecular_graphics     'Bruker SHELXTL'
_computing_publication_material   'Bruker SHELXTL'

_refine_special_details
;
 Refinement of F^2^ against ALL reflections.  The weighted R-factor wR and
 goodness of fit S are based on F^2^, conventional R-factors R are based
 on F, with F set to zero for negative F^2^. The threshold expression of
 F^2^ > 2sigma(F^2^) is used only for calculating R-factors(gt) etc. and is
 not relevant to the choice of reflections for refinement.  R-factors based
 on F^2^ are statistically about twice as large as those based on F, and R-
 factors based on ALL data will be even larger.
;

_refine_ls_structure_factor_coef  Fsqd
_refine_ls_matrix_type            full
_refine_ls_weighting_scheme       calc
_refine_ls_weighting_details
 'calc w=1/[\s^2^(Fo^2^)+(0.0981P)^2^+0.0000P] where P=(Fo^2^+2Fc^2^)/3'
_atom_sites_solution_primary      direct
_atom_sites_solution_secondary    difmap
_atom_sites_solution_hydrogens    geom
_refine_ls_hydrogen_treatment     mixed
_refine_ls_extinction_method      none
_refine_ls_extinction_coef        ?
_refine_ls_number_reflns          6681
_refine_ls_number_parameters      429
_refine_ls_number_restraints      0
_refine_ls_R_factor_all           0.1238
_refine_ls_R_factor_gt            0.0593
_refine_ls_wR_factor_ref          0.1924
_refine_ls_wR_factor_gt           0.1488
_refine_ls_goodness_of_fit_ref    0.921
_refine_ls_restrained_S_all       0.921
_refine_ls_shift/su_max           0.198
_refine_ls_shift/su_mean          0.005
```

```
loop_
 _atom_site_label
 _atom_site_type_symbol
 _atom_site_fract_x
 _atom_site_fract_y
 _atom_site_fract_z
 _atom_site_U_iso_or_equiv
 _atom_site_adp_type
 _atom_site_occupancy
 _atom_site_symmetry_multiplicity
 _atom_site_calc_flag
 _atom_site_refinement_flags
 _atom_site_disorder_assembly
 _atom_site_disorder_group
K1A K -0.5000 0.5000 1.0000 0.0581(4) Uani 1 2 d S . .
C1A C -0.7234(13) 0.3651(12) 1.1223(12) 0.036(3) Uani 0.50 1 d P . 1
H1A1 H -0.7672 0.3166 1.1690 0.044 Uiso 0.50 1 calc PR . 1
H1A2 H -0.6997 0.3417 1.0393 0.044 Uiso 0.50 1 calc PR . 1
C2A C -0.8161(7) 0.5039(7) 1.1519(7) 0.0289(16) Uani 0.50 1 d P A 1
H2AA H -0.9086 0.5225 1.1614 0.035 Uiso 0.50 1 calc PR A 1
H2AB H -0.8132 0.5354 1.2228 0.035 Uiso 0.50 1 calc PR A 1
C1' C -0.7576(13) 0.4059(13) 1.1683(12) 0.045(3) Uani 0.50 1 d P . 2
H1'1 H -0.7952 0.3474 1.1976 0.054 Uiso 0.50 1 calc PR . 2
H1'2 H -0.8033 0.4775 1.2261 0.054 Uiso 0.50 1 calc PR . 2
C2' C -0.7765(10) 0.4434(10) 1.0603(10) 0.063(3) Uani 0.50 1 d P A 2
H2'A H -0.8674 0.4624 1.0637 0.076 Uiso 0.50 1 calc PR A 2
H2'B H -0.7127 0.3788 0.9968 0.076 Uiso 0.50 1 calc PR A 2
O3A O -0.7533(3) 0.5550(3) 1.0425(3) 0.0751(11) Uani 1 1 d . A .
C4A C -0.8391(4) 0.6774(5) 1.0751(4) 0.0662(15) Uani 1 1 d . A .
H4AA H -0.8434 0.6999 1.1529 0.079 Uiso 1 1 calc R . .
H4AB H -0.9291 0.6925 1.0787 0.079 Uiso 1 1 calc R . .
C5A C -0.7922(4) 0.7522(4) 0.9901(3) 0.0453(10) Uani 1 1 d . . .
H5AA H -0.7796 0.7244 0.9112 0.054 Uiso 1 1 calc R B .
H5AB H -0.8586 0.8387 1.0073 0.054 Uiso 1 1 calc R . .
O6A O -0.6709(3) 0.7408(2) 0.9961(2) 0.0415(7) Uani 1 1 d . B .
C7A C -0.6220(4) 0.8150(4) 0.9189(4) 0.0488(11) Uani 1 1 d . . .
H7AA H -0.6765 0.9020 0.9485 0.059 Uiso 1 1 calc R B .
H7AB H -0.6272 0.8046 0.8416 0.059 Uiso 1 1 calc R . .
C8A C -0.4826(5) 0.7784(4) 0.9094(4) 0.0591(13) Uani 1 1 d . B .
H8AA H -0.4534 0.8379 0.8663 0.071 Uiso 1 1 calc R . .
H8AB H -0.4772 0.7804 0.9880 0.071 Uiso 1 1 calc R . .
N9A N -0.3934(3) 0.6557(3) 0.8502(3) 0.0518(10) Uani 1 1 d . . .
C10A C -0.3903(4) 0.6463(4) 0.7319(4) 0.0488(11) Uani 1 1 d . . .
C11A C -0.3706(5) 0.7273(5) 0.6544(5) 0.0746(15) Uani 1 1 d . B .
H11A H -0.3574 0.7919 0.6784 0.089 Uiso 1 1 calc R . .
C12A C -0.3692(6) 0.7178(6) 0.5416(5) 0.0857(18) Uani 1 1 d . . .
H12A H -0.3529 0.7743 0.4893 0.103 Uiso 1 1 calc R B .
C13A C -0.3906(5) 0.6302(5) 0.5068(5) 0.0708(15) Uani 1 1 d . B .
H13A H -0.3907 0.6240 0.4301 0.085 Uiso 1 1 calc R . .
C14A C -0.4126(5) 0.5482(6) 0.5837(5) 0.0790(16) Uani 1 1 d . . .
H14A H -0.4274 0.4850 0.5593 0.095 Uiso 1 1 calc R B .
C15A C -0.4132(5) 0.5569(5) 0.6955(5) 0.0650(14) Uani 1 1 d . B .
O16A O -0.4628(10) 0.4951(12) 0.7851(12) 0.065(4) Uani 0.50 1 d P B 1
C17A C -0.5150(11) 0.4179(10) 0.7553(9) 0.069(3) Uiso 0.50 1 d P B 1
```

```
H17A H -0.6001 0.4692 0.7445 0.103 Uiso 0.50 1 calc PR B 1
H17B H -0.5274 0.3657 0.8178 0.103 Uiso 0.50 1 calc PR B 1
H17C H -0.4526 0.3668 0.6834 0.103 Uiso 0.50 1 calc PR B 1
O16' O -0.3936(14) 0.4569(13) 0.7572(13) 0.099(5) Uani 0.50 1 d P B 2
C17' C -0.4145(19) 0.3579(17) 0.7249(16) 0.152(7) Uiso 0.50 1 d P B 2
H17D H -0.4843 0.3897 0.6897 0.228 Uiso 0.50 1 calc PR B 2
H17E H -0.4410 0.3179 0.7940 0.228 Uiso 0.50 1 calc PR B 2
H17F H -0.3324 0.2986 0.6691 0.228 Uiso 0.50 1 calc PR B 2
K1B K 0.0000 0.0000 0.5000 0.0372(3) Uani 1 2 d S . .
C1B C -0.0144(6) -0.0317(4) 0.7895(4) 0.0658(15) Uani 1 1 d . . .
H1B1 H -0.0343 -0.0512 0.8712 0.079 Uiso 1 1 calc R . .
H1B2 H -0.0573 0.0582 0.7892 0.079 Uiso 1 1 calc R . .
C2B C 0.1332(5) -0.0775(4) 0.7343(4) 0.0579(13) Uani 1 1 d . . .
H2BA H 0.1674 -0.0451 0.7813 0.070 Uiso 1 1 calc R . .
H2BB H 0.1773 -0.1678 0.7301 0.070 Uiso 1 1 calc R . .
O3B O 0.1602(3) -0.0378(2) 0.6204(2) 0.0456(7) Uani 1 1 d . . .
C4B C 0.2998(5) -0.0888(4) 0.5571(4) 0.0611(13) Uani 1 1 d . . .
H4BA H 0.3363 -0.1786 0.5445 0.073 Uiso 1 1 calc R . .
H4BB H 0.3459 -0.0701 0.6020 0.073 Uiso 1 1 calc R . .
C5B C 0.3211(5) -0.0363(5) 0.4446(5) 0.0804(18) Uani 1 1 d . C .
H5BA H 0.2796 0.0539 0.4569 0.096 Uiso 1 1 calc R . .
H5BB H 0.4169 -0.0652 0.4031 0.096 Uiso 1 1 calc R . .
O6B O 0.2642(3) -0.0730(4) 0.3782(3) 0.0929(14) Uani 1 1 d . . .
C7B C 0.2816(8) 0.0219(9) 0.2852(7) 0.046(2) Uani 0.50 1 d P C 1
H7BA H 0.2433 0.1053 0.3228 0.055 Uiso 0.50 1 calc PR C 1
H7BB H 0.3758 -0.0035 0.2389 0.055 Uiso 0.50 1 calc PR C 1
C8B C 0.2053(16) 0.0143(16) 0.2127(14) 0.043(3) Uani 0.50 1 d P C 1
H8BA H 0.2331 0.0448 0.1365 0.051 Uiso 0.50 1 calc PR C 1
H8BB H 0.2235 -0.0717 0.1995 0.051 Uiso 0.50 1 calc PR C 1
C7# C 0.3022(8) -0.0845(7) 0.2498(7) 0.0423(19) Uani 0.50 1 d P C 2
H7#A H 0.2735 -0.1399 0.2236 0.051 Uiso 0.50 1 calc PR C 2
H7#B H 0.3989 -0.1146 0.2124 0.051 Uiso 0.50 1 calc PR C 2
C8# C 0.2293(17) 0.0436(15) 0.2251(17) 0.041(3) Uani 0.50 1 d P C 2
H8#A H 0.2608 0.0506 0.1408 0.050 Uiso 0.50 1 calc PR C 2
H8#B H 0.2474 0.0990 0.2648 0.050 Uiso 0.50 1 calc PR C 2
N9B N 0.0707(3) 0.0843(3) 0.2692(3) 0.0434(9) Uani 1 1 d . . .
C10B C 0.0151(3) 0.2154(3) 0.2728(3) 0.0345(9) Uani 1 1 d . C .
C11B C -0.0117(4) 0.2790(4) 0.1794(3) 0.0419(10) Uani 1 1 d . . .
H11B H 0.0111 0.2347 0.1085 0.050 Uiso 1 1 calc R C .
C12B C -0.0705(4) 0.4045(4) 0.1868(4) 0.0483(11) Uani 1 1 d . C .
H12B H -0.0901 0.4461 0.1224 0.058 Uiso 1 1 calc R . .
C13B C -0.1005(4) 0.4689(4) 0.2875(4) 0.0477(11) Uani 1 1 d . . .
H13B H -0.1410 0.5556 0.2929 0.057 Uiso 1 1 calc R C .
C14B C -0.0723(4) 0.4085(4) 0.3818(4) 0.0501(11) Uani 1 1 d . C .
H14B H -0.0925 0.4538 0.4512 0.060 Uiso 1 1 calc R . .
C15B C -0.0149(4) 0.2826(4) 0.3749(3) 0.0421(10) Uani 1 1 d . . .
O16B O 0.0164(3) 0.2159(2) 0.4645(2) 0.0592(9) Uani 1 1 d . C .
C17B C -0.0028(7) 0.2830(4) 0.5662(4) 0.089(2) Uani 1 1 d . . .
H17G H 0.0449 0.3336 0.5441 0.134 Uiso 1 1 calc R C .
H17H H 0.0310 0.2258 0.6203 0.134 Uiso 1 1 calc R . .
H17I H -0.0973 0.3354 0.6034 0.134 Uiso 1 1 calc R . .
P1 P -0.73270(10) 1.17357(9) 0.82810(8) 0.0330(3) Uani 1 1 d . . .
F11 F -0.6380(2) 1.2335(2) 0.7576(2) 0.0644(7) Uani 1 1 d . . .
F12 F -0.6634(2) 1.1420(2) 0.9239(2) 0.0606(7) Uani 1 1 d . . .
F13 F -0.8015(3) 1.2035(2) 0.7317(2) 0.0620(7) Uani 1 1 d . . .
```

```
F14 F -0.8375(2) 1.30315(19) 0.8961(2) 0.0540(7) Uani 1 1 d . . .
F15 F -0.6277(2) 1.04386(19) 0.7595(2) 0.0521(6) Uani 1 1 d . . .
F16 F -0.8276(2) 1.11398(19) 0.8981(2) 0.0480(6) Uani 1 1 d . . .

loop_
 _atom_site_aniso_label
 _atom_site_aniso_U_11
 _atom_site_aniso_U_22
 _atom_site_aniso_U_33
 _atom_site_aniso_U_23
 _atom_site_aniso_U_13
 _atom_site_aniso_U_12
K1A 0.0283(7) 0.0392(8) 0.1009(12) 0.0376(8) -0.0176(7) -0.0166(6)
C1A 0.031(7) 0.033(7) 0.049(8) 0.004(5) -0.011(6) -0.019(6)
C2A 0.026(4) 0.039(5) 0.032(4) 0.004(4) -0.012(3) -0.022(4)
C1' 0.030(7) 0.047(10) 0.066(10) 0.027(6) -0.023(7) -0.023(7)
C2' 0.054(6) 0.080(7) 0.087(8) 0.033(7) -0.040(6) -0.047(6)
O3A 0.0458(18) 0.060(2) 0.145(3) 0.064(2) -0.055(2) -0.0367(17)
C4A 0.037(2) 0.109(4) 0.046(3) 0.029(3) -0.016(2) -0.027(3)
C5A 0.042(2) 0.036(2) 0.041(2) 0.0035(19) -0.019(2) 0.0006(19)
O6A 0.0555(17) 0.0303(15) 0.0470(16) 0.0138(12) -0.0296(14) -0.0184(13)
C7A 0.074(3) 0.031(2) 0.048(3) 0.0154(19) -0.030(2) -0.023(2)
C8A 0.095(4) 0.052(3) 0.077(3) 0.038(3) -0.056(3) -0.058(3)
N9A 0.053(2) 0.050(2) 0.082(3) 0.035(2) -0.043(2) -0.0382(19)
C10A 0.033(2) 0.049(3) 0.072(3) 0.023(2) -0.024(2) -0.023(2)
C11A 0.086(4) 0.065(4) 0.074(4) 0.023(3) -0.014(3) -0.045(3)
C12A 0.086(4) 0.085(4) 0.063(4) 0.035(3) -0.007(3) -0.034(4)
C13A 0.043(3) 0.081(4) 0.066(4) 0.005(3) -0.011(3) -0.012(3)
C14A 0.089(4) 0.092(4) 0.082(4) 0.020(4) -0.044(3) -0.052(4)
C15A 0.075(4) 0.067(3) 0.078(4) 0.027(3) -0.042(3) -0.044(3)
O16A 0.077(7) 0.067(8) 0.062(5) -0.009(5) 0.006(5) -0.060(6)
O16' 0.184(15) 0.082(10) 0.111(12) 0.048(8) -0.104(11) -0.097(11)
K1B 0.0326(6) 0.0480(7) 0.0323(6) 0.0128(5) -0.0145(5) -0.0174(6)
C1B 0.120(5) 0.037(3) 0.027(2) 0.0043(19) -0.033(3) -0.018(3)
C2B 0.107(4) 0.048(3) 0.054(3) 0.022(2) -0.060(3) -0.044(3)
O3B 0.064(2) 0.0390(16) 0.0544(18) 0.0186(13) -0.0409(16) -0.0276(15)
C4B 0.060(3) 0.057(3) 0.088(4) 0.013(3) -0.051(3) -0.027(3)
C5B 0.042(3) 0.093(4) 0.119(5) 0.061(4) -0.038(3) -0.039(3)
O6B 0.0374(18) 0.184(4) 0.048(2) 0.046(2) -0.0186(16) -0.043(2)
C7B 0.026(4) 0.061(6) 0.039(5) 0.008(4) -0.003(4) -0.015(4)
C8B 0.038(8) 0.051(9) 0.026(5) 0.006(6) -0.005(5) -0.012(6)
C7# 0.040(4) 0.026(4) 0.049(5) -0.002(4) -0.008(4) -0.008(4)
C8# 0.032(7) 0.044(8) 0.046(8) 0.001(6) -0.006(5) -0.018(5)
N9B 0.045(2) 0.039(2) 0.0255(17) 0.0033(15) -0.0095(15) -0.0015(16)
C10B 0.0295(19) 0.038(2) 0.032(2) 0.0111(17) -0.0090(16) -0.0129(17)
C11B 0.041(2) 0.056(3) 0.039(2) 0.018(2) -0.0155(19) -0.029(2)
C12B 0.049(3) 0.052(3) 0.059(3) 0.033(2) -0.030(2) -0.030(2)
C13B 0.039(2) 0.033(2) 0.061(3) 0.019(2) -0.012(2) -0.0121(19)
C14B 0.052(3) 0.037(2) 0.042(2) 0.0063(19) -0.004(2) -0.012(2)
C15B 0.044(2) 0.036(2) 0.030(2) 0.0098(17) -0.0080(18) -0.0072(19)
O16B 0.091(2) 0.0338(16) 0.0289(15) 0.0027(12) -0.0213(16) -0.0053(16)
C17B 0.157(6) 0.050(3) 0.035(3) 0.001(2) -0.037(3) -0.019(3)
P1 0.0373(5) 0.0304(5) 0.0360(6) 0.0083(4) -0.0160(4) -0.0171(4)
F11 0.0650(17) 0.0582(17) 0.0781(18) 0.0163(14) -0.0111(14) -0.0444(14)
F12 0.0762(18) 0.0610(16) 0.0673(17) 0.0168(13) -0.0518(15) -0.0314(14)
```

```
F13 0.0796(19) 0.0691(18) 0.0538(15) 0.0184(13) -0.0441(14) -0.0331(15)
F14 0.0600(16) 0.0287(13) 0.0595(15) -0.0015(11) -0.0113(12) -0.0127(11)
F15 0.0477(14) 0.0372(13) 0.0597(15) -0.0039(11) -0.0057(12) -0.0160(11)
F16 0.0467(13) 0.0374(13) 0.0573(15) 0.0084(11) -0.0083(11) -0.0232(11)

_geom_special_details
;
 All esds (except the esd in the dihedral angle between two l.s. planes)
 are estimated using the full covariance matrix.  The cell esds are taken
 into account individually in the estimation of esds in distances, angles
 and torsion angles; correlations between esds in cell parameters are only
 used when they are defined by crystal symmetry.  An approximate
(isotropic)
 treatment of cell esds is used for estimating esds involving l.s. planes.
;

loop_
 _geom_bond_atom_site_label_1
 _geom_bond_atom_site_label_2
 _geom_bond_distance
 _geom_bond_site_symmetry_2
 _geom_bond_publ_flag
K1A O16A 2.527(15) . ?
K1A O16A 2.527(15) 2_467 ?
K1A O3A 2.659(3) 2_467 ?
K1A O3A 2.659(3) . ?
K1A O6A 2.763(2) . ?
K1A O6A 2.763(2) 2_467 ?
K1A O16' 2.813(14) . ?
K1A O16' 2.813(14) 2_467 ?
K1A N9A 2.953(3) . ?
K1A N9A 2.953(3) 2_467 ?
K1A C17A 3.310(10) 2_467 ?
K1A C4A 3.474(5) . ?
C1A N9A 1.449(15) 2_467 ?
C1A C2A 1.554(14) . ?
C2A O3A 1.547(8) . ?
C1' C2' 1.429(18) . ?
C1' N9A 1.559(14) 2_467 ?
C2' O3A 1.494(10) . ?
O3A C4A 1.386(6) . ?
C4A C5A 1.474(6) . ?
C5A O6A 1.416(5) . ?
O6A C7A 1.429(5) . ?
C7A C8A 1.484(6) . ?
C8A N9A 1.468(6) . ?
N9A C1A 1.449(15) 2_467 ?
N9A C10A 1.451(6) . ?
N9A C1' 1.559(14) 2_467 ?
C10A C15A 1.368(6) . ?
C10A C11A 1.368(6) . ?
C11A C12A 1.391(7) . ?
C12A C13A 1.328(8) . ?
C13A C14A 1.379(7) . ?
C14A C15A 1.380(7) . ?
```

```
C15A O16' 1.365(15) . ?
C15A O16A 1.407(14) . ?
O16A C17A 1.454(17) . ?
O16' C17' 1.44(2) . ?
K1B O3B 2.650(2) 2_556 ?
K1B O3B 2.650(2) . ?
K1B O16B 2.725(3) 2_556 ?
K1B O16B 2.725(3) . ?
K1B O6B 2.754(3) 2_556 ?
K1B O6B 2.754(3) . ?
K1B N9B 2.932(3) . ?
K1B N9B 2.932(3) 2_556 ?
K1B C5B 3.484(5) 2_556 ?
K1B C5B 3.484(5) . ?
K1B C1B 3.502(4) 2_556 ?
K1B C1B 3.502(4) . ?
C1B N9B 1.460(6) 2_556 ?
C1B C2B 1.508(7) . ?
C2B O3B 1.429(5) . ?
O3B C4B 1.439(5) . ?
C4B C5B 1.475(7) . ?
C5B O6B 1.413(6) . ?
O6B C7# 1.487(8) . ?
O6B C7B 1.603(9) . ?
C7B C8B 1.496(15) . ?
C8B N9B 1.393(17) . ?
C7# C8# 1.49(2) . ?
C8# N9B 1.631(16) . ?
N9B C10B 1.441(5) . ?
N9B C1B 1.460(6) 2_556 ?
C10B C11B 1.387(5) . ?
C10B C15B 1.400(5) . ?
C11B C12B 1.376(6) . ?
C12B C13B 1.367(6) . ?
C13B C14B 1.386(6) . ?
C14B C15B 1.380(5) . ?
C15B O16B 1.377(4) . ?
O16B C17B 1.437(5) . ?
P1 F12 1.584(2) . ?
P1 F13 1.587(2) . ?
P1 F14 1.592(2) . ?
P1 F16 1.595(2) . ?
P1 F15 1.596(2) . ?
P1 F11 1.597(2) . ?

loop_
 _geom_angle_atom_site_label_1
 _geom_angle_atom_site_label_2
 _geom_angle_atom_site_label_3
 _geom_angle
 _geom_angle_site_symmetry_1
 _geom_angle_site_symmetry_3
 _geom_angle_publ_flag
O16A K1A O16A 180.000(2) . 2_467 ?
O16A K1A O3A 90.1(3) . 2_467 ?
```

```
O16A K1A O3A 89.9(3) 2_467 2_467 ?
O16A K1A O3A 89.9(3) . . ?
O16A K1A O3A 90.1(3) 2_467 . ?
O3A K1A O3A 180.0 2_467 . ?
O16A K1A O6A 82.6(3) . . ?
O16A K1A O6A 97.4(3) 2_467 . ?
O3A K1A O6A 117.85(9) 2_467 . ?
O3A K1A O6A 62.15(9) . . ?
O16A K1A O6A 97.4(3) . 2_467 ?
O16A K1A O6A 82.6(3) 2_467 2_467 ?
O3A K1A O6A 62.15(9) 2_467 2_467 ?
O3A K1A O6A 117.85(9) . 2_467 ?
O6A K1A O6A 180.0 . 2_467 ?
O16A K1A O16' 14.2(4) . . ?
O16A K1A O16' 165.8(4) 2_467 . ?
O3A K1A O16' 77.2(3) 2_467 . ?
O3A K1A O16' 102.8(3) . . ?
O6A K1A O16' 93.8(3) . . ?
O6A K1A O16' 86.2(3) 2_467 . ?
O16A K1A O16' 165.8(4) . 2_467 ?
O16A K1A O16' 14.2(4) 2_467 2_467 ?
O3A K1A O16' 102.8(3) 2_467 2_467 ?
O3A K1A O16' 77.2(3) . 2_467 ?
O6A K1A O16' 86.2(3) . 2_467 ?
O6A K1A O16' 93.8(3) 2_467 2_467 ?
O16' K1A O16' 180.000(2) . 2_467 ?
O16A K1A N9A 58.1(3) . . ?
O16A K1A N9A 121.9(3) 2_467 . ?
O3A K1A N9A 62.55(9) 2_467 . ?
O3A K1A N9A 117.45(9) . . ?
O6A K1A N9A 61.59(9) . . ?
O6A K1A N9A 118.41(9) 2_467 . ?
O16' K1A N9A 57.0(3) . . ?
O16' K1A N9A 123.0(3) 2_467 . ?
O16A K1A N9A 121.9(3) . 2_467 ?
O16A K1A N9A 58.1(3) 2_467 2_467 ?
O3A K1A N9A 117.45(9) 2_467 2_467 ?
O3A K1A N9A 62.55(9) . 2_467 ?
O6A K1A N9A 118.41(9) . 2_467 ?
O6A K1A N9A 61.59(9) 2_467 2_467 ?
O16' K1A N9A 123.0(3) . 2_467 ?
O16' K1A N9A 57.0(3) 2_467 2_467 ?
N9A K1A N9A 180.00(9) . 2_467 ?
O16A K1A C17A 155.5(3) . 2_467 ?
O16A K1A C17A 24.5(3) 2_467 2_467 ?
O3A K1A C17A 74.7(2) 2_467 2_467 ?
O3A K1A C17A 105.3(2) . 2_467 ?
O6A K1A C17A 87.7(2) . 2_467 ?
O6A K1A C17A 92.3(2) 2_467 2_467 ?
O16' K1A C17A 148.8(3) . 2_467 ?
O16' K1A C17A 31.2(3) 2_467 2_467 ?
N9A K1A C17A 97.6(2) . 2_467 ?
N9A K1A C17A 82.4(2) 2_467 2_467 ?
O16A K1A C4A 93.9(3) . . ?
O16A K1A C4A 86.1(3) 2_467 . ?
```

```
O3A K1A C4A 158.74(11) 2_467 . ?
O3A K1A C4A 21.26(11) . . ?
O6A K1A C4A 42.45(11) . . ?
O6A K1A C4A 137.55(11) 2_467 . ?
O16' K1A C4A 108.0(3) . . ?
O16' K1A C4A 72.0(3) 2_467 . ?
N9A K1A C4A 102.28(11) . . ?
N9A K1A C4A 77.72(11) 2_467 . ?
C17A K1A C4A 94.0(2) 2_467 . ?
N9A C1A C2A 106.0(8) 2_467 . ?
O3A C2A C1A 100.5(7) . . ?
C2' C1' N9A 108.8(10) . 2_467 ?
C1' C2' O3A 104.8(9) . . ?
C1' C2' K1A 86.5(6) . . ?
O3A C2' K1A 45.2(3) . . ?
C4A O3A C2' 131.2(5) . . ?
C4A O3A C2A 97.3(4) . . ?
C2' O3A C2A 47.3(5) . . ?
C4A O3A K1A 114.6(3) . . ?
C2' O3A K1A 111.2(4) . . ?
C2A O3A K1A 114.8(3) . . ?
O3A C4A C5A 109.4(4) . . ?
O3A C4A K1A 44.10(18) . . ?
C5A C4A K1A 80.3(2) . . ?
O6A C5A C4A 109.0(3) . . ?
O6A C5A K1A 46.60(15) . . ?
C4A C5A K1A 75.5(2) . . ?
C5A O6A C7A 112.1(3) . . ?
C5A O6A K1A 111.5(2) . . ?
C7A O6A K1A 118.8(2) . . ?
O6A C7A C8A 109.2(3) . . ?
N9A C8A C7A 112.3(3) . . ?
C1A N9A C10A 122.1(6) 2_467 . ?
C1A N9A C8A 99.6(5) 2_467 . ?
C10A N9A C8A 112.8(3) . . ?
C1A N9A C1' 25.2(5) 2_467 2_467 ?
C10A N9A C1' 100.2(6) . 2_467 ?
C8A N9A C1' 122.6(6) . 2_467 ?
C1A N9A K1A 104.3(7) 2_467 . ?
C10A N9A K1A 112.9(2) . . ?
C8A N9A K1A 102.9(2) . . ?
C1' N9A K1A 105.5(6) 2_467 . ?
C15A C10A C11A 117.4(5) . . ?
C15A C10A N9A 120.0(4) . . ?
C11A C10A N9A 122.6(4) . . ?
C10A C11A C12A 121.9(5) . . ?
C13A C12A C11A 120.3(5) . . ?
C12A C13A C14A 119.0(6) . . ?
C13A C14A C15A 120.9(6) . . ?
O16' C15A C10A 117.0(7) . . ?
O16' C15A C14A 119.2(8) . . ?
C10A C15A C14A 120.5(5) . . ?
O16' C15A O16A 29.9(7) . . ?
C10A C15A O16A 114.4(7) . . ?
C14A C15A O16A 123.8(7) . . ?
```

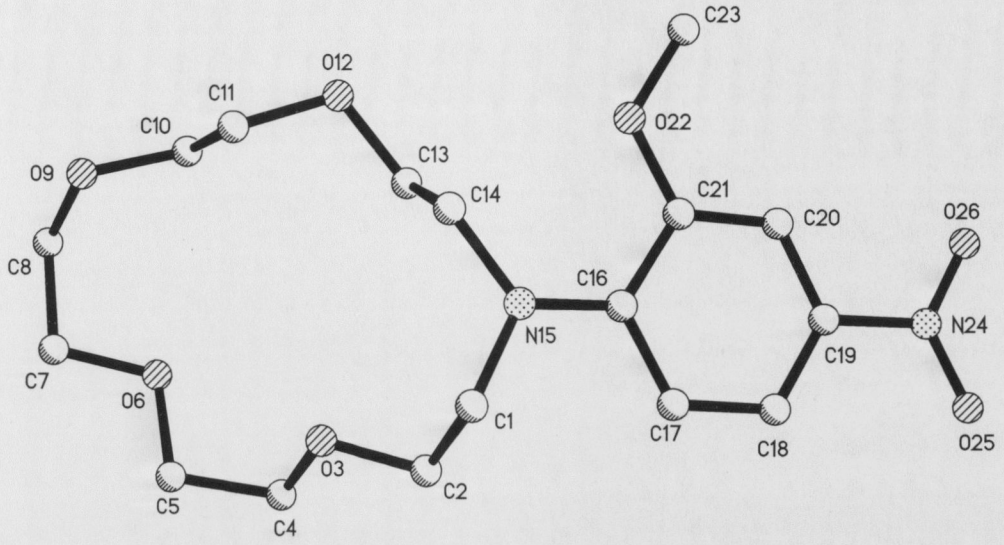
```
C15A O16A C17A 116.7(12) . . ?
C15A O16A K1A 133.5(8) . . ?
C17A O16A K1A 109.5(8) . . ?
C15A O16' C17' 120.9(13) . . ?
C15A O16' K1A 117.0(8) . . ?
C17' O16' K1A 107.5(11) . . ?
O3B K1B O3B 180.0 2_556 . ?
O3B K1B O16B 83.98(8) 2_556 2_556 ?
O3B K1B O16B 96.02(8) . 2_556 ?
O3B K1B O16B 96.02(8) 2_556 . ?
O3B K1B O16B 83.98(8) . . ?
O16B K1B O16B 180.000(19) 2_556 . ?
O3B K1B O6B 62.41(10) 2_556 2_556 ?
O3B K1B O6B 117.59(10) . 2_556 ?
O16B K1B O6B 77.13(12) 2_556 2_556 ?
O16B K1B O6B 102.87(12) . 2_556 ?
O3B K1B O6B 117.59(10) 2_556 . ?
O3B K1B O6B 62.41(10) . . ?
O16B K1B O6B 102.87(12) 2_556 . ?
O16B K1B O6B 77.13(12) . . ?
O6B K1B O6B 180.0 2_556 . ?
O3B K1B N9B 62.90(9) 2_556 . ?
O3B K1B N9B 117.10(9) . . ?
O16B K1B N9B 122.93(9) 2_556 . ?
O16B K1B N9B 57.07(9) . . ?
O6B K1B N9B 117.96(9) 2_556 . ?
O6B K1B N9B 62.04(9) . . ?
O3B K1B N9B 117.10(9) 2_556 2_556 ?
O3B K1B N9B 62.90(9) . 2_556 ?
O16B K1B N9B 57.07(9) 2_556 2_556 ?
O16B K1B N9B 122.93(9) . 2_556 ?
O6B K1B N9B 62.04(9) 2_556 2_556 ?
O6B K1B N9B 117.96(9) . 2_556 ?
N9B K1B N9B 180.0 . 2_556 ?
O3B K1B C5B 42.94(11) 2_556 2_556 ?
O3B K1B C5B 137.06(11) . 2_556 ?
O16B K1B C5B 68.16(11) 2_556 2_556 ?
O16B K1B C5B 111.84(11) . 2_556 ?
O6B K1B C5B 22.52(12) 2_556 2_556 ?
O6B K1B C5B 157.48(12) . 2_556 ?
N9B K1B C5B 104.44(11) . 2_556 ?
N9B K1B C5B 75.56(11) 2_556 2_556 ?
O3B K1B C5B 137.06(11) 2_556 . ?
O3B K1B C5B 42.94(11) . . ?
O16B K1B C5B 111.84(11) 2_556 . ?
O16B K1B C5B 68.16(11) . . ?
O6B K1B C5B 157.48(12) 2_556 . ?
O6B K1B C5B 22.52(12) . . ?
N9B K1B C5B 75.56(11) . . ?
N9B K1B C5B 104.44(11) 2_556 . ?
C5B K1B C5B 180.0 2_556 . ?
O3B K1B C1B 42.92(12) 2_556 2_556 ?
O3B K1B C1B 137.08(12) . 2_556 ?
O16B K1B C1B 101.78(10) 2_556 2_556 ?
O16B K1B C1B 78.22(10) . 2_556 ?
```

```
O6B K1B C1B 104.39(12) 2_556 2_556 ?
O6B K1B C1B 75.61(12) . 2_556 ?
N9B K1B C1B 24.21(11) . 2_556 ?
N9B K1B C1B 155.79(11) 2_556 2_556 ?
C5B K1B C1B 85.85(14) 2_556 2_556 ?
C5B K1B C1B 94.15(14) . 2_556 ?
O3B K1B C1B 137.09(12) 2_556 . ?
O3B K1B C1B 42.92(12) . . ?
O16B K1B C1B 78.22(10) 2_556 . ?
O16B K1B C1B 101.78(10) . . ?
O6B K1B C1B 75.61(12) 2_556 . ?
O6B K1B C1B 104.39(12) . . ?
N9B K1B C1B 155.79(11) . . ?
N9B K1B C1B 24.21(11) 2_556 . ?
C5B K1B C1B 94.15(14) 2_556 . ?
C5B K1B C1B 85.85(14) . . ?
C1B K1B C1B 180.0 2_556 . ?
N9B C1B C2B 113.2(3) 2_556 . ?
N9B C1B K1B 55.42(19) 2_556 . ?
C2B C1B K1B 81.5(2) . . ?
O3B C2B C1B 108.6(3) . . ?
C2B O3B C4B 112.1(3) . . ?
C2B O3B K1B 121.2(2) . . ?
C4B O3B K1B 117.1(2) . . ?
O3B C4B C5B 109.2(3) . . ?
O6B C5B C4B 108.8(4) . . ?
O6B C5B K1B 48.3(2) . . ?
C4B C5B K1B 80.2(2) . . ?
C5B O6B C7# 127.3(5) . . ?
C5B O6B C7B 91.4(5) . . ?
C7# O6B C7B 49.2(4) . . ?
C5B O6B K1B 109.2(3) . . ?
C7# O6B K1B 116.1(4) . . ?
C7B O6B K1B 110.0(3) . . ?
C8B C7B O6B 101.3(8) . . ?
N9B C8B C7B 109.4(11) . . ?
O6B C7# C8# 102.2(9) . . ?
C7# C8# N9B 110.7(10) . . ?
C8B N9B C10B 119.9(7) . . ?
C8B N9B C1B 100.8(6) . 2_556 ?
C10B N9B C1B 113.3(3) . 2_556 ?
C8B N9B C8# 21.0(7) . . ?
C10B N9B C8# 102.9(6) . . ?
C1B N9B C8# 120.9(6) 2_556 . ?
C8B N9B K1B 108.2(8) . . ?
C10B N9B K1B 112.1(2) . . ?
C1B N9B K1B 100.4(2) 2_556 . ?
C8# N9B K1B 107.5(7) . . ?
C11B C10B C15B 118.1(4) . . ?
C11B C10B N9B 122.8(3) . . ?
C15B C10B N9B 119.1(3) . . ?
C12B C11B C10B 121.7(4) . . ?
C13B C12B C11B 119.6(4) . . ?
C12B C13B C14B 120.4(4) . . ?
C15B C14B C13B 120.1(4) . . ?
```

```
O16B C15B C14B 123.7(4) . . ?
O16B C15B C10B 116.2(3) . . ?
C14B C15B C10B 120.1(4) . . ?
C15B O16B C17B 116.8(3) . . ?
C15B O16B K1B 121.6(2) . . ?
C17B O16B K1B 115.6(3) . . ?
F12 P1 F13 179.28(14) . . ?
F12 P1 F14 90.82(14) . . ?
F13 P1 F14 89.84(14) . . ?
F12 P1 F16 89.89(14) . . ?
F13 P1 F16 89.81(14) . . ?
F14 P1 F16 90.42(13) . . ?
F12 P1 F15 89.40(14) . . ?
F13 P1 F15 89.94(14) . . ?
F14 P1 F15 179.77(15) . . ?
F16 P1 F15 89.66(12) . . ?
F12 P1 F11 90.38(15) . . ?
F13 P1 F11 89.93(15) . . ?
F14 P1 F11 89.55(14) . . ?
F16 P1 F11 179.73(15) . . ?
F15 P1 F11 90.37(14) . . ?

_diffrn_measured_fraction_theta_max    0.864
_diffrn_reflns_theta_full              28.60
_diffrn_measured_fraction_theta_full   0.864
_refine_diff_density_max    0.713
_refine_diff_density_min   -0.351
_refine_diff_density_rms    0.075

#===END
```



Crystallography data for 122

```
data_

_audit_creation_method            SHELXL-97
_chemical_name_systematic
;
 ?
;
_chemical_name_common             ?
_chemical_melting_point           ?
_chemical_formula_moiety          ?
_chemical_formula_sum
 'C17 H26 N2 O7'
_chemical_formula_weight          370.40

loop_
 _atom_type_symbol
 _atom_type_description
 _atom_type_scat_dispersion_real
 _atom_type_scat_dispersion_imag
 _atom_type_scat_source
 'C'  'C'   0.0033   0.0016
 'International Tables Vol C Tables 4.2.6.8 and 6.1.1.4'
 'H'  'H'   0.0000   0.0000
 'International Tables Vol C Tables 4.2.6.8 and 6.1.1.4'
 'N'  'N'   0.0061   0.0033
 'International Tables Vol C Tables 4.2.6.8 and 6.1.1.4'
 'O'  'O'   0.0106   0.0060
 'International Tables Vol C Tables 4.2.6.8 and 6.1.1.4'

_symmetry_cell_setting            Triclinic
_symmetry_space_group_name_H-M    P-1
```

```
loop_
 _symmetry_equiv_pos_as_xyz
 'x, y, z'
 '-x, -y, -z'

_cell_length_a                    8.696(3)
_cell_length_b                    8.943(4)
_cell_length_c                    12.098(5)
_cell_angle_alpha                 83.932(6)
_cell_angle_beta                  71.217(6)
_cell_angle_gamma                 76.937(6)
_cell_volume                      867.1(6)
_cell_formula_units_Z             2
_cell_measurement_temperature     153(2)
_cell_measurement_reflns_used     ?
_cell_measurement_theta_min       ?
_cell_measurement_theta_max       ?

_exptl_crystal_description        plate
_exptl_crystal_colour             yellow
_exptl_crystal_size_max           0.52
_exptl_crystal_size_mid           0.30
_exptl_crystal_size_min           0.12
_exptl_crystal_density_meas       not_measured
_exptl_crystal_density_diffrn     1.419
_exptl_crystal_density_method     'not measured'
_exptl_crystal_F_000              396
_exptl_absorpt_coefficient_mu     0.110
_exptl_absorpt_correction_type    Empirical
_exptl_absorpt_correction_T_min   0.747
_exptl_absorpt_correction_T_max   1.000
_exptl_absorpt_process_details    SADABS

_exptl_special_details
;
 ?
;

_diffrn_ambient_temperature       153(2)
_diffrn_radiation_wavelength      0.71073
_diffrn_radiation_type            MoK\a
_diffrn_radiation_source          'fine-focus sealed tube'
_diffrn_radiation_monochromator   graphite
_diffrn_measurement_device_type   'CCD area detector'
_diffrn_measurement_method        'phi and omega scans'
_diffrn_detector_area_resol_mean  ?
_diffrn_standards_number          ?
_diffrn_standards_interval_count  ?
_diffrn_standards_interval_time   ?
_diffrn_standards_decay_%         ?
_diffrn_reflns_number             6975
_diffrn_reflns_av_R_equivalents   0.0565
_diffrn_reflns_av_sigmaI/netI     0.1665
_diffrn_reflns_limit_h_min        -11
_diffrn_reflns_limit_h_max        11
```

```
_diffrn_reflns_limit_k_min        -11
_diffrn_reflns_limit_k_max        11
_diffrn_reflns_limit_l_min        -15
_diffrn_reflns_limit_l_max        15
_diffrn_reflns_theta_min          1.78
_diffrn_reflns_theta_max          28.67
_reflns_number_total              3838
_reflns_number_gt                 1474
_reflns_threshold_expression      >2sigma(I)

_computing_data_collection        'Bruker SMART'
_computing_cell_refinement        'Bruker SMART'
_computing_data_reduction         'Bruker SHELXTL'
_computing_structure_solution     'SHELXS-97 (Sheldrick, 1990)'
_computing_structure_refinement   'SHELXL-97 (Sheldrick, 1997)'
_computing_molecular_graphics     'Bruker SHELXTL'
_computing_publication_material   'Bruker SHELXTL'

_refine_special_details
;
 Refinement of F^2^ against ALL reflections.  The weighted R-factor wR and
 goodness of fit S are based on F^2^, conventional R-factors R are based
 on F, with F set to zero for negative F^2^. The threshold expression of
 F^2^ > 2sigma(F^2^) is used only for calculating R-factors(gt) etc. and is
 not relevant to the choice of reflections for refinement.  R-factors based
 on F^2^ are statistically about twice as large as those based on F, and R-
 factors based on ALL data will be even larger.
;

_refine_ls_structure_factor_coef  Fsqd
_refine_ls_matrix_type            full
_refine_ls_weighting_scheme       calc
_refine_ls_weighting_details
 'calc w=1/[\s^2^(Fo^2^)+(0.0898P)^2^+0.0000P] where P=(Fo^2^+2Fc^2^)/3'
_atom_sites_solution_primary      direct
_atom_sites_solution_secondary    difmap
_atom_sites_solution_hydrogens    geom
_refine_ls_hydrogen_treatment     mixed
_refine_ls_extinction_method      none
_refine_ls_extinction_coef        ?
_refine_ls_number_reflns          3838
_refine_ls_number_parameters      339
_refine_ls_number_restraints      0
_refine_ls_R_factor_all           0.1572
_refine_ls_R_factor_gt            0.0640
_refine_ls_wR_factor_ref          0.1939
_refine_ls_wR_factor_gt           0.1458
_refine_ls_goodness_of_fit_ref    0.814
_refine_ls_restrained_S_all       0.814
_refine_ls_shift/su_max           0.008
_refine_ls_shift/su_mean          0.001

loop_
 _atom_site_label
 _atom_site_type_symbol
```

```
 _atom_site_fract_x
 _atom_site_fract_y
 _atom_site_fract_z
 _atom_site_U_iso_or_equiv
 _atom_site_adp_type
 _atom_site_occupancy
 _atom_site_symmetry_multiplicity
 _atom_site_calc_flag
 _atom_site_refinement_flags
 _atom_site_disorder_assembly
 _atom_site_disorder_group
C1 C -0.3049(5) 0.4305(5) 0.3536(4) 0.0279(10) Uani 1 1 d . . .
H1A H -0.420(5) 0.387(4) 0.382(3) 0.046(12) Uiso 1 1 d . . .
H1B H -0.332(4) 0.523(4) 0.333(3) 0.023(11) Uiso 1 1 d . . .
C2 C -0.2644(5) 0.4320(5) 0.4653(4) 0.0296(10) Uani 1 1 d . . .
H2A H -0.316(4) 0.531(4) 0.504(3) 0.030(11) Uiso 1 1 d . . .
H2B H -0.143(5) 0.424(4) 0.451(3) 0.030(11) Uiso 1 1 d . . .
O3 O -0.3251(3) 0.3121(3) 0.5423(2) 0.0289(7) Uani 1 1 d . . .
C4 C -0.2901(6) 0.3067(5) 0.6493(4) 0.0283(10) Uani 1 1 d . . .
H4A H -0.322(5) 0.408(5) 0.671(4) 0.048(14) Uiso 1 1 d . . .
H4B H -0.161(6) 0.276(5) 0.625(4) 0.053(14) Uiso 1 1 d . . .
C5 C -0.3820(6) 0.2002(5) 0.7331(4) 0.0308(10) Uani 1 1 d . . .
H5A H -0.505(5) 0.225(4) 0.728(3) 0.038(12) Uiso 1 1 d . . .
H5B H -0.372(5) 0.202(4) 0.800(3) 0.025(11) Uiso 1 1 d . . .
O6 O -0.3128(3) 0.0477(3) 0.6962(2) 0.0307(7) Uani 1 1 d . . .
C7 C -0.4012(6) -0.0603(5) 0.7672(4) 0.0311(11) Uani 1 1 d . . .
H7A H -0.402(5) -0.059(5) 0.837(3) 0.039(13) Uiso 1 1 d . . .
H7B H -0.527(5) -0.020(4) 0.758(3) 0.024(10) Uiso 1 1 d . . .
C8 C -0.3272(6) -0.2159(5) 0.7171(4) 0.0311(11) Uani 1 1 d . . .
H8A H -0.195(5) -0.241(4) 0.699(3) 0.036(11) Uiso 1 1 d . . .
H8B H -0.383(6) -0.284(5) 0.751(4) 0.062(16) Uiso 1 1 d . . .
O9 O -0.3493(3) -0.2219(3) 0.6064(2) 0.0306(7) Uani 1 1 d . . .
C10 C -0.2145(5) -0.1872(5) 0.5116(4) 0.0300(10) Uani 1 1 d . . .
H10A H -0.164(4) -0.118(4) 0.536(3) 0.012(9) Uiso 1 1 d . . .
H10B H -0.150(5) -0.280(5) 0.484(4) 0.049(14) Uiso 1 1 d . . .
C11 C -0.2806(5) -0.1129(5) 0.4160(4) 0.0323(11) Uani 1 1 d . . .
H11A H -0.345(5) -0.175(5) 0.403(4) 0.050(14) Uiso 1 1 d . . .
H11B H -0.363(5) -0.009(5) 0.444(3) 0.049(13) Uiso 1 1 d . . .
O12 O -0.1484(3) -0.0860(3) 0.3153(2) 0.0334(7) Uani 1 1 d . . .
C13 C -0.1058(6) 0.0594(5) 0.3166(4) 0.0281(10) Uani 1 1 d . . .
H13A H -0.129(5) 0.086(4) 0.413(4) 0.044(12) Uiso 1 1 d . . .
H13B H 0.001(4) 0.051(4) 0.282(3) 0.016(10) Uiso 1 1 d . . .
C14 C -0.2112(6) 0.1812(5) 0.2614(4) 0.0280(11) Uani 1 1 d . . .
H14A H -0.342(5) 0.178(5) 0.325(4) 0.055(13) Uiso 1 1 d . . .
H14B H -0.197(5) 0.161(5) 0.206(3) 0.029(15) Uiso 1 1 d . . .
N15 N -0.1810(4) 0.3351(3) 0.2638(3) 0.0243(8) Uani 1 1 d . . .
C16 C -0.0472(5) 0.3936(4) 0.1924(3) 0.0237(9) Uani 1 1 d . . .
C17 C -0.0263(5) 0.5386(4) 0.2147(3) 0.0236(9) Uani 1 1 d . . .
H17 H -0.116(5) 0.597(4) 0.303(3) 0.043(12) Uiso 1 1 d . . .
C18 C 0.0993(5) 0.6075(5) 0.1414(3) 0.0268(10) Uani 1 1 d . . .
H18 H 0.107(5) 0.708(5) 0.172(3) 0.045(12) Uiso 1 1 d . . .
C19 C 0.2096(4) 0.5311(4) 0.0468(3) 0.0239(9) Uani 1 1 d . . .
C20 C 0.1989(5) 0.3869(4) 0.0226(3) 0.0236(9) Uani 1 1 d . . .
H20 H 0.271(5) 0.334(5) -0.044(4) 0.049(13) Uiso 1 1 d . . .
C21 C 0.0732(5) 0.3183(4) 0.0925(3) 0.0236(9) Uani 1 1 d . . .
```

```
O22 O 0.0573(3) 0.1766(3) 0.0709(2) 0.0316(7) Uani 1 1 d . . .
C23 C 0.1819(6) 0.0971(5) -0.0251(4) 0.0342(11) Uani 1 1 d . . .
H23A H 0.157(5) -0.008(5) -0.019(3) 0.036(11) Uiso 1 1 d . . .
H23B H 0.294(5) 0.082(4) -0.012(3) 0.037(12) Uiso 1 1 d . . .
H23C H 0.192(5) 0.149(5) -0.113(4) 0.061(14) Uiso 1 1 d . . .
N24 N 0.3397(4) 0.6017(4) -0.0325(3) 0.0275(8) Uani 1 1 d . . .
O25 O 0.3477(3) 0.7324(3) -0.0129(2) 0.0358(8) Uani 1 1 d . . .
O26 O 0.4390(3) 0.5280(3) -0.1166(2) 0.0345(7) Uani 1 1 d . . .

loop_
 _atom_site_aniso_label
 _atom_site_aniso_U_11
 _atom_site_aniso_U_22
 _atom_site_aniso_U_33
 _atom_site_aniso_U_23
 _atom_site_aniso_U_13
 _atom_site_aniso_U_12
C1 0.024(2) 0.025(2) 0.030(2) -0.001(2) -0.004(2) -0.001(2)
C2 0.028(2) 0.028(2) 0.027(2) -0.008(2) 0.002(2) -0.007(2)
O3 0.0402(17) 0.0271(16) 0.0205(14) -0.0028(12) -0.0063(13) -0.0125(13)
C4 0.031(3) 0.032(3) 0.024(2) -0.004(2) -0.008(2) -0.009(2)
C5 0.031(3) 0.032(3) 0.029(3) -0.009(2) -0.008(2) -0.005(2)
O6 0.0269(16) 0.0276(16) 0.0334(16) -0.0040(13) -0.0019(13) -0.0065(13)
C7 0.032(3) 0.036(3) 0.025(2) 0.001(2) -0.005(2) -0.013(2)
C8 0.033(3) 0.031(3) 0.029(2) 0.002(2) -0.007(2) -0.011(2)
O9 0.0272(16) 0.0381(17) 0.0252(15) -0.0040(13) 0.0001(13) -0.0148(13)
C10 0.025(2) 0.028(3) 0.032(2) -0.005(2) 0.000(2) -0.008(2)
C11 0.030(3) 0.029(3) 0.035(3) 0.003(2) -0.004(2) -0.013(2)
O12 0.0391(17) 0.0235(15) 0.0300(16) -0.0031(12) 0.0007(14) -0.0068(13)
C13 0.028(3) 0.024(2) 0.029(2) 0.0012(19) -0.003(2) -0.0085(19)
C14 0.029(3) 0.028(3) 0.027(3) -0.004(2) -0.007(2) -0.0067(19)
N15 0.0219(18) 0.0229(18) 0.0215(17) -0.0057(14) 0.0023(15) -0.0022(14)
C16 0.022(2) 0.023(2) 0.025(2) -0.0028(17) -0.0064(18) -0.0016(17)
C17 0.021(2) 0.023(2) 0.024(2) -0.0052(17) -0.0046(18) -0.0011(17)
C18 0.029(2) 0.028(2) 0.027(2) -0.0046(19) -0.0128(19) -0.0047(19)
C19 0.019(2) 0.025(2) 0.025(2) 0.0041(18) -0.0061(18) -0.0039(17)
C20 0.021(2) 0.026(2) 0.020(2) -0.0043(18) -0.0017(18) -0.0006(18)
C21 0.024(2) 0.023(2) 0.023(2) -0.0043(17) -0.0079(18) -0.0007(17)
O22 0.0360(17) 0.0252(15) 0.0268(15) -0.0111(12) 0.0041(13) -0.0083(13)
C23 0.036(3) 0.027(3) 0.029(2) -0.014(2) 0.005(2) -0.003(2)
N24 0.0246(19) 0.0266(19) 0.032(2) 0.0016(16) -0.0105(17) -0.0049(15)
O25 0.0378(18) 0.0306(17) 0.0397(18) -0.0004(14) -0.0085(15) -0.0135(14)
O26 0.0292(16) 0.0377(18) 0.0297(17) -0.0052(14) 0.0014(14) -0.0064(14)

_geom_special_details
;
 All esds (except the esd in the dihedral angle between two l.s. planes)
 are estimated using the full covariance matrix.  The cell esds are taken
 into account individually in the estimation of esds in distances, angles
 and torsion angles; correlations between esds in cell parameters are only
 used when they are defined by crystal symmetry.  An approximate
(isotropic)
 treatment of cell esds is used for estimating esds involving l.s. planes.
;
```

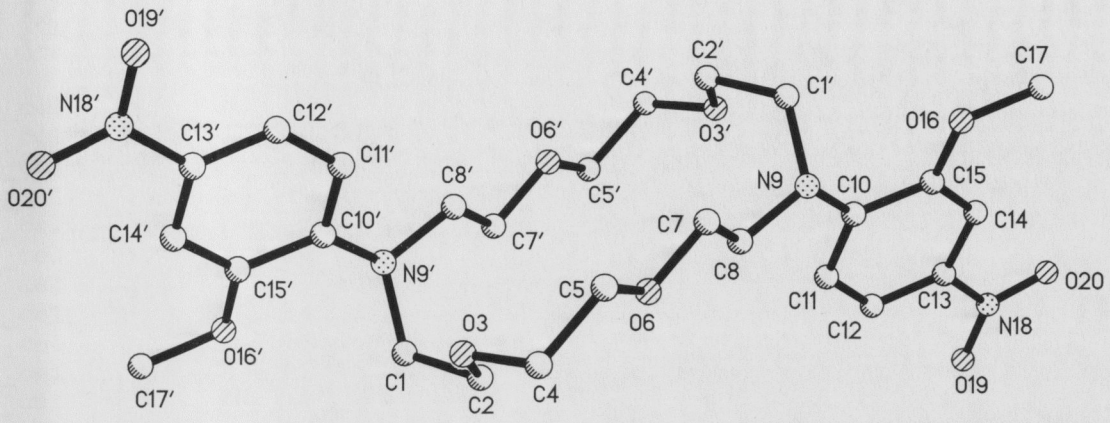
```
loop_
 _geom_bond_atom_site_label_1
 _geom_bond_atom_site_label_2
 _geom_bond_distance
 _geom_bond_site_symmetry_2
 _geom_bond_publ_flag
C1 N15 1.447(5) . ?
C1 C2 1.505(6) . ?
C2 O3 1.422(5) . ?
O3 C4 1.416(5) . ?
C4 C5 1.481(6) . ?
C5 O6 1.417(5) . ?
O6 C7 1.413(5) . ?
C7 C8 1.497(6) . ?
C8 O9 1.422(5) . ?
O9 C10 1.417(5) . ?
C10 C11 1.483(6) . ?
C11 O12 1.423(5) . ?
O12 C13 1.433(4) . ?
C13 C14 1.503(6) . ?
C14 N15 1.463(5) . ?
N15 C16 1.380(4) . ?
C16 C17 1.415(5) . ?
C16 C21 1.432(5) . ?
C17 C18 1.386(5) . ?
C18 C19 1.364(5) . ?
C19 C20 1.381(5) . ?
C19 N24 1.448(5) . ?
C20 C21 1.373(5) . ?
C21 O22 1.366(4) . ?
O22 C23 1.430(4) . ?
N24 O25 1.238(4) . ?
N24 O26 1.239(4) . ?

loop_
 _geom_angle_atom_site_label_1
 _geom_angle_atom_site_label_2
 _geom_angle_atom_site_label_3
 _geom_angle
 _geom_angle_site_symmetry_1
 _geom_angle_site_symmetry_3
 _geom_angle_publ_flag
N15 C1 C2 115.7(4) . . ?
O3 C2 C1 108.9(3) . . ?
C4 O3 C2 111.8(3) . . ?
O3 C4 C5 109.2(4) . . ?
O6 C5 C4 109.3(4) . . ?
C7 O6 C5 112.8(3) . . ?
O6 C7 C8 109.1(4) . . ?
O9 C8 C7 111.4(4) . . ?
C10 O9 C8 113.3(3) . . ?
O9 C10 C11 108.1(3) . . ?
O12 C11 C10 110.3(4) . . ?
C11 O12 C13 112.2(3) . . ?
O12 C13 C14 109.4(4) . . ?
```

```
N15 C14 C13 113.1(4) . . ?
C16 N15 C1 118.7(3) . . ?
C16 N15 C14 126.7(3) . . ?
C1 N15 C14 114.6(3) . . ?
N15 C16 C17 119.7(3) . . ?
N15 C16 C21 124.1(3) . . ?
C17 C16 C21 116.2(3) . . ?
C18 C17 C16 122.1(4) . . ?
C19 C18 C17 119.1(4) . . ?
C18 C19 C20 121.5(4) . . ?
C18 C19 N24 120.2(4) . . ?
C20 C19 N24 118.3(3) . . ?
C21 C20 C19 120.4(3) . . ?
O22 C21 C20 122.2(3) . . ?
O22 C21 C16 117.1(3) . . ?
C20 C21 C16 120.7(3) . . ?
C21 O22 C23 117.5(3) . . ?
O25 N24 O26 122.9(3) . . ?
O25 N24 C19 118.7(3) . . ?
O26 N24 C19 118.4(3) . . ?

_diffrn_measured_fraction_theta_max    0.859
_diffrn_reflns_theta_full              28.67
_diffrn_measured_fraction_theta_full   0.859
_refine_diff_density_max    0.317
_refine_diff_density_min   -0.332
_refine_diff_density_rms    0.076

#===END
```



Crystallography data for 131

```
data_

_audit_creation_method            SHELXL-97
_chemical_name_systematic
;
 ?
;
_chemical_name_common             ?
_chemical_melting_point           ?
_chemical_formula_moiety          ?
_chemical_formula_sum
 'C26 H36 N4 O10'
_chemical_formula_weight          564.59

loop_
 _atom_type_symbol
 _atom_type_description
 _atom_type_scat_dispersion_real
 _atom_type_scat_dispersion_imag
 _atom_type_scat_source
 'C'  'C'   0.0033   0.0016
 'International Tables Vol C Tables 4.2.6.8 and 6.1.1.4'
 'H'  'H'   0.0000   0.0000
 'International Tables Vol C Tables 4.2.6.8 and 6.1.1.4'
 'N'  'N'   0.0061   0.0033
 'International Tables Vol C Tables 4.2.6.8 and 6.1.1.4'
 'O'  'O'   0.0106   0.0060
 'International Tables Vol C Tables 4.2.6.8 and 6.1.1.4'

_symmetry_cell_setting            Triclinic
_symmetry_space_group_name_H-M    P-1
```

```
loop_
 _symmetry_equiv_pos_as_xyz
 'x, y, z'
 '-x, -y, -z'

_cell_length_a                    7.4201(17)
_cell_length_b                    8.1588(19)
_cell_length_c                    11.055(3)
_cell_angle_alpha                 99.130(3)
_cell_angle_beta                  100.381(3)
_cell_angle_gamma                 93.595(3)
_cell_volume                      647.1(3)
_cell_formula_units_Z             1
_cell_measurement_temperature     153(2)
_cell_measurement_reflns_used     ?
_cell_measurement_theta_min       ?
_cell_measurement_theta_max       ?

_exptl_crystal_description        block
_exptl_crystal_colour             yellow
_exptl_crystal_size_max           0.66
_exptl_crystal_size_mid           0.60
_exptl_crystal_size_min           0.42
_exptl_crystal_density_meas       not_measured
_exptl_crystal_density_diffrn     1.449
_exptl_crystal_density_method     'not measured'
_exptl_crystal_F_000              300
_exptl_absorpt_coefficient_mu     0.112
_exptl_absorpt_correction_type    Empirical
_exptl_absorpt_correction_T_min   0.760
_exptl_absorpt_correction_T_max   1.000
_exptl_absorpt_process_details    SADABS

_exptl_special_details
;
 ?
;

_diffrn_ambient_temperature       153(2)
_diffrn_radiation_wavelength      0.71073
_diffrn_radiation_type            MoK\a
_diffrn_radiation_source          'fine-focus sealed tube'
_diffrn_radiation_monochromator   graphite
_diffrn_measurement_device_type   'CCD area detector'
_diffrn_measurement_method        'phi and omega scans'
_diffrn_detector_area_resol_mean  ?
_diffrn_standards_number          ?
_diffrn_standards_interval_count  ?
_diffrn_standards_interval_time   ?
_diffrn_standards_decay_%         ?
_diffrn_reflns_number             7478
_diffrn_reflns_av_R_equivalents   0.0330
_diffrn_reflns_av_sigmaI/netI     0.0390
_diffrn_reflns_limit_h_min        -9
```

```
_diffrn_reflns_limit_h_max       9
_diffrn_reflns_limit_k_min       -10
_diffrn_reflns_limit_k_max       10
_diffrn_reflns_limit_l_min       -14
_diffrn_reflns_limit_l_max       14
_diffrn_reflns_theta_min         1.90
_diffrn_reflns_theta_max         28.57
_reflns_number_total             2884
_reflns_number_gt                2232
_reflns_threshold_expression     >2sigma(I)

_computing_data_collection       'Bruker SMART'
_computing_cell_refinement       'Bruker SMART'
_computing_data_reduction        'Bruker SHELXTL'
_computing_structure_solution    'SHELXS-97 (Sheldrick, 1990)'
_computing_structure_refinement  'SHELXL-97 (Sheldrick, 1997)'
_computing_molecular_graphics    'Bruker SHELXTL'
_computing_publication_material  'Bruker SHELXTL'

_refine_special_details
;
 Refinement of F^2^ against ALL reflections.  The weighted R-factor wR and
 goodness of fit S are based on F^2^, conventional R-factors R are based
 on F, with F set to zero for negative F^2^. The threshold expression of
 F^2^ > 2sigma(F^2^) is used only for calculating R-factors(gt) etc. and is
 not relevant to the choice of reflections for refinement.  R-factors based
 on F^2^ are statistically about twice as large as those based on F, and R-
 factors based on ALL data will be even larger.
;

_refine_ls_structure_factor_coef  Fsqd
_refine_ls_matrix_type            full
_refine_ls_weighting_scheme       calc
_refine_ls_weighting_details
 'calc w=1/[\s^2^(Fo^2^)+(0.0821P)^2^+0.0000P] where P=(Fo^2^+2Fc^2^)/3'
_atom_sites_solution_primary      direct
_atom_sites_solution_secondary    difmap
_atom_sites_solution_hydrogens    geom
_refine_ls_hydrogen_treatment     mixed
_refine_ls_extinction_method      none
_refine_ls_extinction_coef        ?
_refine_ls_number_reflns          2884
_refine_ls_number_parameters      253
_refine_ls_number_restraints      0
_refine_ls_R_factor_all           0.0595
_refine_ls_R_factor_gt            0.0460
_refine_ls_wR_factor_ref          0.1317
_refine_ls_wR_factor_gt           0.1181
_refine_ls_goodness_of_fit_ref    1.027
_refine_ls_restrained_S_all       1.027
_refine_ls_shift/su_max           0.000
_refine_ls_shift/su_mean          0.000

loop_
 _atom_site_label
```

```
 _atom_site_type_symbol
 _atom_site_fract_x
 _atom_site_fract_y
 _atom_site_fract_z
 _atom_site_U_iso_or_equiv
 _atom_site_adp_type
 _atom_site_occupancy
 _atom_site_symmetry_multiplicity
 _atom_site_calc_flag
 _atom_site_refinement_flags
 _atom_site_disorder_assembly
 _atom_site_disorder_group
C1 C -0.2726(2) -0.38498(19) -0.17160(15) 0.0206(3) Uani 1 1 d . . .
H1A H -0.232(2) -0.444(2) -0.0983(16) 0.024(4) Uiso 1 1 d . . .
H1B H -0.361(2) -0.463(2) -0.2286(16) 0.021(4) Uiso 1 1 d . . .
C2 C -0.3627(2) -0.2334(2) -0.12392(15) 0.0222(4) Uani 1 1 d . . .
H2A H -0.282(2) -0.159(2) -0.0573(16) 0.023(4) Uiso 1 1 d . . .
H2B H -0.474(2) -0.275(2) -0.0929(17) 0.029(5) Uiso 1 1 d . . .
O3 O -0.42003(15) -0.15015(13) -0.22633(10) 0.0254(3) Uani 1 1 d . . .
C4 C -0.4887(2) 0.0065(2) -0.19193(16) 0.0238(4) Uani 1 1 d . . .
H4A H -0.565(2) -0.003(2) -0.1277(17) 0.024(4) Uiso 1 1 d . . .
H4B H -0.566(2) 0.028(2) -0.2632(16) 0.023(4) Uiso 1 1 d . . .
C5 C -0.3412(2) 0.1486(2) -0.14488(15) 0.0254(4) Uani 1 1 d . . .
H5A H -0.257(2) 0.151(2) -0.1976(15) 0.021(4) Uiso 1 1 d . . .
H5B H -0.401(2) 0.258(2) -0.1384(15) 0.028(5) Uiso 1 1 d . . .
O6 O -0.24819(15) 0.13322(13) -0.02424(10) 0.0240(3) Uani 1 1 d . . .
C7 C -0.1002(2) 0.2577(2) 0.02707(15) 0.0220(3) Uani 1 1 d . . .
H7A H -0.008(2) 0.252(2) -0.0313(16) 0.021(4) Uiso 1 1 d . . .
H7B H -0.144(2) 0.369(2) 0.0366(16) 0.025(4) Uiso 1 1 d . . .
C8 C -0.0230(2) 0.21693(19) 0.15438(15) 0.0216(3) Uani 1 1 d . . .
H8A H 0.025(2) 0.105(2) 0.1395(15) 0.022(4) Uiso 1 1 d . . .
H8B H -0.122(2) 0.211(2) 0.1981(15) 0.021(4) Uiso 1 1 d . . .
N9 N 0.11493(17) 0.34590(15) 0.22996(12) 0.0194(3) Uani 1 1 d . . .
C10 C 0.1509(2) 0.34511(18) 0.35755(14) 0.0189(3) Uani 1 1 d . . .
C11 C 0.0958(2) 0.2065(2) 0.40682(16) 0.0227(4) Uani 1 1 d . . .
H11 H 0.042(2) 0.105(2) 0.3442(17) 0.030(5) Uiso 1 1 d . . .
C12 C 0.1196(2) 0.2083(2) 0.53353(15) 0.0232(4) Uani 1 1 d . . .
H12 H 0.089(3) 0.113(2) 0.5671(18) 0.032(5) Uiso 1 1 d . . .
C13 C 0.2010(2) 0.34969(19) 0.61391(14) 0.0206(3) Uani 1 1 d . . .
C14 C 0.2611(2) 0.49098(19) 0.57123(15) 0.0199(3) Uani 1 1 d . . .
H14 H 0.315(2) 0.584(2) 0.6295(17) 0.027(5) Uiso 1 1 d . . .
C15 C 0.2345(2) 0.48988(18) 0.44427(14) 0.0184(3) Uani 1 1 d . . .
O16 O 0.27808(15) 0.62565(13) 0.39366(10) 0.0226(3) Uani 1 1 d . . .
C17 C 0.3615(2) 0.7731(2) 0.47796(16) 0.0241(4) Uani 1 1 d . . .
H17A H 0.280(2) 0.810(2) 0.5360(16) 0.027(5) Uiso 1 1 d . . .
H17B H 0.374(2) 0.857(2) 0.4271(17) 0.027(5) Uiso 1 1 d . . .
H17C H 0.484(3) 0.756(2) 0.5294(18) 0.037(5) Uiso 1 1 d . . .
N18 N 0.22403(18) 0.35068(17) 0.74732(13) 0.0237(3) Uani 1 1 d . . .
O19 O 0.15584(18) 0.23022(15) 0.78320(11) 0.0340(3) Uani 1 1 d . . .
O20 O 0.31268(17) 0.47082(15) 0.81951(11) 0.0320(3) Uani 1 1 d . . .

loop_
 _atom_site_aniso_label
 _atom_site_aniso_U_11
 _atom_site_aniso_U_22
```

```
 _atom_site_aniso_U_33
 _atom_site_aniso_U_23
 _atom_site_aniso_U_13
 _atom_site_aniso_U_12
C1 0.0224(8) 0.0176(8) 0.0209(8) 0.0027(6) 0.0043(6) -0.0034(6)
C2 0.0249(8) 0.0221(8) 0.0190(8) 0.0022(7) 0.0045(7) 0.0007(7)
O3 0.0315(7) 0.0239(6) 0.0194(6) 0.0004(5) 0.0033(5) 0.0062(5)
C4 0.0230(8) 0.0242(8) 0.0212(9) 0.0007(7) -0.0011(7) 0.0040(6)
C5 0.0274(9) 0.0260(9) 0.0212(9) 0.0051(7) 0.0002(7) 0.0014(7)
O6 0.0257(6) 0.0226(6) 0.0201(6) 0.0026(5) -0.0016(5) -0.0053(5)
C7 0.0229(8) 0.0210(8) 0.0197(8) 0.0009(6) 0.0016(7) -0.0024(6)
C8 0.0220(8) 0.0200(8) 0.0210(8) 0.0017(6) 0.0027(7) -0.0038(6)
N9 0.0201(6) 0.0183(6) 0.0186(7) 0.0018(5) 0.0033(5) -0.0023(5)
C10 0.0164(7) 0.0199(8) 0.0198(8) 0.0024(6) 0.0029(6) 0.0016(6)
C11 0.0245(8) 0.0189(8) 0.0228(8) 0.0012(6) 0.0036(7) -0.0033(6)
C12 0.0240(8) 0.0204(8) 0.0260(9) 0.0061(7) 0.0061(7) -0.0019(6)
C13 0.0190(8) 0.0257(8) 0.0177(8) 0.0041(6) 0.0045(6) 0.0038(6)
C14 0.0171(7) 0.0192(8) 0.0213(8) -0.0004(6) 0.0021(6) 0.0010(6)
C15 0.0169(7) 0.0170(7) 0.0215(8) 0.0032(6) 0.0046(6) 0.0008(6)
O16 0.0306(6) 0.0157(5) 0.0193(6) 0.0017(4) 0.0022(5) -0.0031(4)
C17 0.0299(9) 0.0178(8) 0.0223(9) -0.0004(7) 0.0038(7) -0.0035(7)
N18 0.0222(7) 0.0276(7) 0.0229(7) 0.0050(6) 0.0068(6) 0.0052(6)
O19 0.0452(8) 0.0337(7) 0.0264(7) 0.0115(5) 0.0117(6) -0.0009(6)
O20 0.0344(7) 0.0369(7) 0.0204(6) -0.0020(5) 0.0027(5) -0.0043(6)

_geom_special_details
;
 All esds (except the esd in the dihedral angle between two l.s. planes)
 are estimated using the full covariance matrix.  The cell esds are taken
 into account individually in the estimation of esds in distances, angles
 and torsion angles; correlations between esds in cell parameters are only
 used when they are defined by crystal symmetry.  An approximate
(isotropic)
 treatment of cell esds is used for estimating esds involving l.s. planes.
;

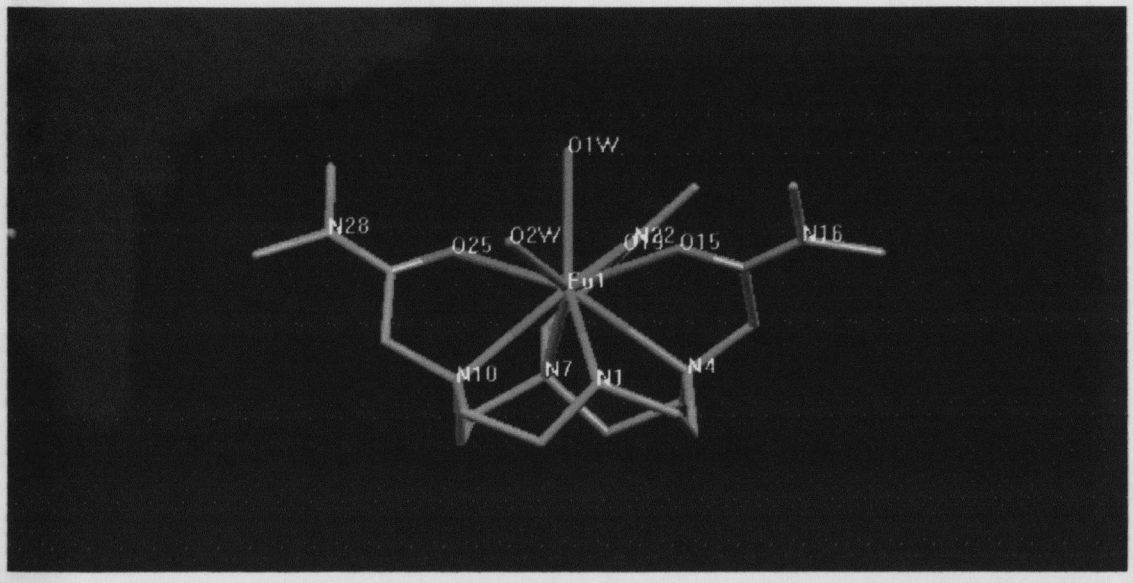
loop_
 _geom_bond_atom_site_label_1
 _geom_bond_atom_site_label_2
 _geom_bond_distance
 _geom_bond_site_symmetry_2
 _geom_bond_publ_flag
C1 N9 1.476(2) 2 ?
C1 C2 1.509(2) . ?
C2 O3 1.4251(19) . ?
O3 C4 1.4265(19) . ?
C4 C5 1.502(2) . ?
C5 O6 1.4152(19) . ?
O6 C7 1.4185(18) . ?
C7 C8 1.517(2) . ?
C8 N9 1.4598(19) . ?
N9 C10 1.3886(19) . ?
N9 C1 1.476(2) 2 ?
C10 C11 1.400(2) . ?
C10 C15 1.426(2) . ?
```

```
C11 C12 1.377(2) . ?
C12 C13 1.370(2) . ?
C13 C14 1.391(2) . ?
C13 N18 1.452(2) . ?
C14 C15 1.380(2) . ?
C15 O16 1.3643(17) . ?
O16 C17 1.4288(19) . ?
N18 O20 1.2297(17) . ?
N18 O19 1.2300(17) . ?

loop_
 _geom_angle_atom_site_label_1
 _geom_angle_atom_site_label_2
 _geom_angle_atom_site_label_3
 _geom_angle
 _geom_angle_site_symmetry_1
 _geom_angle_site_symmetry_3
 _geom_angle_publ_flag
N9 C1 C2 113.66(12) 2 . ?
O3 C2 C1 107.84(13) . . ?
C2 O3 C4 113.91(12) . . ?
O3 C4 C5 113.91(14) . . ?
O6 C5 C4 109.20(13) . . ?
C5 O6 C7 113.90(11) . . ?
O6 C7 C8 104.57(12) . . ?
N9 C8 C7 112.82(12) . . ?
C10 N9 C8 116.13(12) . . ?
C10 N9 C1 117.40(12) . 2 ?
C8 N9 C1 114.84(12) . 2 ?
N9 C10 C11 121.53(14) . . ?
N9 C10 C15 121.12(13) . . ?
C11 C10 C15 117.22(14) . . ?
C12 C11 C10 122.04(15) . . ?
C13 C12 C11 119.02(14) . . ?
C12 C13 C14 121.90(14) . . ?
C12 C13 N18 118.56(13) . . ?
C14 C13 N18 119.54(14) . . ?
C15 C14 C13 119.00(15) . . ?
O16 C15 C14 123.27(14) . . ?
O16 C15 C10 115.86(13) . . ?
C14 C15 C10 120.81(14) . . ?
C15 O16 C17 117.33(12) . . ?
O20 N18 O19 122.81(13) . . ?
O20 N18 C13 118.66(13) . . ?
O19 N18 C13 118.52(13) . . ?

_diffrn_measured_fraction_theta_max    0.876
_diffrn_reflns_theta_full              28.57
_diffrn_measured_fraction_theta_full   0.876
_refine_diff_density_max    0.284
_refine_diff_density_min   -0.315
_refine_diff_density_rms    0.064


#===END
```



Crystallography data for Eu.149

```
data_

_audit_creation_method            SHELXL-97
_chemical_name_systematic
;
 ?
;
_chemical_name_common             ?
_chemical_melting_point           ?
_chemical_formula_moiety          ?
_chemical_formula_sum
 'C23 H49 Eu F9 N7 O16 S3'
_chemical_formula_weight          1098.83

loop_
 _atom_type_symbol
 _atom_type_description
 _atom_type_scat_dispersion_real
 _atom_type_scat_dispersion_imag
 _atom_type_scat_source
 'C'  'C'   0.0033   0.0016
 'International Tables Vol C Tables 4.2.6.8 and 6.1.1.4'
 'H'  'H'   0.0000   0.0000
 'International Tables Vol C Tables 4.2.6.8 and 6.1.1.4'
 'N'  'N'   0.0061   0.0033
 'International Tables Vol C Tables 4.2.6.8 and 6.1.1.4'
 'O'  'O'   0.0106   0.0060
 'International Tables Vol C Tables 4.2.6.8 and 6.1.1.4'
 'Eu'  'Eu'  -0.1578   3.6682
```

```
 'International Tables Vol C Tables 4.2.6.8 and 6.1.1.4'
 'F'  'F'   0.0171   0.0103
 'International Tables Vol C Tables 4.2.6.8 and 6.1.1.4'
 'S'  'S'   0.1246   0.1234
 'International Tables Vol C Tables 4.2.6.8 and 6.1.1.4'

_symmetry_cell_setting            Triclinic
_symmetry_space_group_name_H-M    P-1

loop_
 _symmetry_equiv_pos_as_xyz
 'x, y, z'
 '-x, -y, -z'

_cell_length_a                    8.7196(19)
_cell_length_b                    13.147(3)
_cell_length_c                    18.427(4)
_cell_angle_alpha                 95.805(3)
_cell_angle_beta                  97.220(3)
_cell_angle_gamma                 104.013(3)
_cell_volume                      2014.3(7)
_cell_formula_units_Z             2
_cell_measurement_temperature     153(2)
_cell_measurement_reflns_used     ?
_cell_measurement_theta_min       ?
_cell_measurement_theta_max       ?

_exptl_crystal_description        block
_exptl_crystal_colour             colourless
_exptl_crystal_size_max           0.23
_exptl_crystal_size_mid           0.16
_exptl_crystal_size_min           0.14
_exptl_crystal_density_meas       not_measured
_exptl_crystal_density_diffrn     1.812
_exptl_crystal_density_method     'not measured'
_exptl_crystal_F_000              1112
_exptl_absorpt_coefficient_mu     1.828
_exptl_absorpt_correction_type    Empirical
_exptl_absorpt_correction_T_min   0.801
_exptl_absorpt_correction_T_max   1.000
_exptl_absorpt_process_details    SADABS

_exptl_special_details
;
 ?
;

_diffrn_ambient_temperature       153(2)
_diffrn_radiation_wavelength      0.71073
_diffrn_radiation_type            MoK\a
_diffrn_radiation_source          'fine-focus sealed tube'
_diffrn_radiation_monochromator   graphite
_diffrn_measurement_device_type   'CCD area detector'
_diffrn_measurement_method        'phi and omega scans'
_diffrn_detector_area_resol_mean  ?
```

```
_diffrn_standards_number          ?
_diffrn_standards_interval_count  ?
_diffrn_standards_interval_time   ?
_diffrn_standards_decay_%         ?
_diffrn_reflns_number             23924
_diffrn_reflns_av_R_equivalents   0.0788
_diffrn_reflns_av_sigmaI/netI     0.1502
_diffrn_reflns_limit_h_min        -11
_diffrn_reflns_limit_h_max        11
_diffrn_reflns_limit_k_min        -16
_diffrn_reflns_limit_k_max        17
_diffrn_reflns_limit_l_min        -23
_diffrn_reflns_limit_l_max        25
_diffrn_reflns_theta_min          1.12
_diffrn_reflns_theta_max          28.86
_reflns_number_total              9229
_reflns_number_gt                 5614
_reflns_threshold_expression      >2sigma(I)

_computing_data_collection        'Bruker SMART'
_computing_cell_refinement        'Bruker SMART'
_computing_data_reduction         'Bruker SHELXTL'
_computing_structure_solution     'SHELXS-97 (Sheldrick, 1990)'
_computing_structure_refinement   'SHELXL-97 (Sheldrick, 1997)'
_computing_molecular_graphics     'Bruker SHELXTL'
_computing_publication_material   'Bruker SHELXTL'

_refine_special_details
;
 Refinement of F^2^ against ALL reflections.  The weighted R-factor wR and
 goodness of fit S are based on F^2^, conventional R-factors R are based
 on F, with F set to zero for negative F^2^. The threshold expression of
 F^2^ > 2sigma(F^2^) is used only for calculating R-factors(gt) etc. and is
 not relevant to the choice of reflections for refinement.  R-factors based
 on F^2^ are statistically about twice as large as those based on F, and R-
 factors based on ALL data will be even larger.
;

_refine_ls_structure_factor_coef  Fsqd
_refine_ls_matrix_type            full
_refine_ls_weighting_scheme       calc
_refine_ls_weighting_details
 'calc w=1/[\s^2^(Fo^2^)+(0.0752P)^2^+0.0000P] where P=(Fo^2^+2Fc^2^)/3'
_atom_sites_solution_primary      direct
_atom_sites_solution_secondary    difmap
_atom_sites_solution_hydrogens    geom
_refine_ls_hydrogen_treatment     constr
_refine_ls_extinction_method      none
_refine_ls_extinction_coef        ?
_refine_ls_number_reflns          9229
_refine_ls_number_parameters      565
_refine_ls_number_restraints      0
_refine_ls_R_factor_all           0.1116
_refine_ls_R_factor_gt            0.0546
_refine_ls_wR_factor_ref          0.1659
```

```
_refine_ls_wR_factor_gt                0.1217
_refine_ls_goodness_of_fit_ref         0.971
_refine_ls_restrained_S_all            0.971
_refine_ls_shift/su_max                0.033
_refine_ls_shift/su_mean               0.001

loop_
 _atom_site_label
 _atom_site_type_symbol
 _atom_site_fract_x
 _atom_site_fract_y
 _atom_site_fract_z
 _atom_site_U_iso_or_equiv
 _atom_site_adp_type
 _atom_site_occupancy
 _atom_site_symmetry_multiplicity
 _atom_site_calc_flag
 _atom_site_refinement_flags
 _atom_site_disorder_assembly
 _atom_site_disorder_group
Eu1 Eu 0.63897(5) -0.10429(3) 0.74200(2) 0.02049(13) Uani 1 1 d . . .
N1 N 0.6125(8) -0.2049(5) 0.8564(4) 0.0271(16) Uani 1 1 d . . .
H1 H 0.7151 -0.2108 0.8724 0.032 Uiso 1 1 calc R . .
C2 C 0.5124(9) -0.3162(6) 0.8375(5) 0.0278(19) Uani 1 1 d . . .
H2A H 0.4836 -0.3447 0.8831 0.033 Uiso 1 1 calc R . .
H2B H 0.5737 -0.3608 0.8137 0.033 Uiso 1 1 calc R . .
C3 C 0.3648(9) -0.3190(6) 0.7865(5) 0.0274(19) Uani 1 1 d . . .
H3A H 0.2989 -0.3930 0.7744 0.033 Uiso 1 1 calc R . .
H3B H 0.3018 -0.2772 0.8118 0.033 Uiso 1 1 calc R . .
N4 N 0.3980(7) -0.2767(5) 0.7172(4) 0.0227(15) Uani 1 1 d . . .
C5 C 0.2514(9) -0.2543(6) 0.6801(5) 0.0260(19) Uani 1 1 d . . .
H5A H 0.1579 -0.3142 0.6813 0.031 Uiso 1 1 calc R . .
H5B H 0.2610 -0.2473 0.6278 0.031 Uiso 1 1 calc R . .
C6 C 0.2252(9) -0.1537(6) 0.7177(5) 0.0280(19) Uani 1 1 d . . .
H6A H 0.1259 -0.1413 0.6921 0.034 Uiso 1 1 calc R . .
H6B H 0.2103 -0.1626 0.7693 0.034 Uiso 1 1 calc R . .
N7 N 0.3616(8) -0.0587(5) 0.7181(4) 0.0234(15) Uani 1 1 d . . .
C8 C 0.3516(10) 0.0266(6) 0.7760(5) 0.029(2) Uani 1 1 d . . .
H8A H 0.4105 0.0962 0.7649 0.035 Uiso 1 1 calc R . .
H8B H 0.2383 0.0274 0.7759 0.035 Uiso 1 1 calc R . .
C9 C 0.4206(10) 0.0090(7) 0.8498(5) 0.0292(19) Uani 1 1 d . . .
H9A H 0.4059 0.0638 0.8873 0.035 Uiso 1 1 calc R . .
H9B H 0.3605 -0.0606 0.8603 0.035 Uiso 1 1 calc R . .
N10 N 0.5916(8) 0.0118(5) 0.8573(4) 0.0224(15) Uani 1 1 d . . .
C11 C 0.6394(10) -0.0317(6) 0.9252(5) 0.030(2) Uani 1 1 d . . .
H11A H 0.6065 0.0055 0.9676 0.036 Uiso 1 1 calc R . .
H11B H 0.7575 -0.0176 0.9344 0.036 Uiso 1 1 calc R . .
C12 C 0.5678(10) -0.1484(7) 0.9211(5) 0.032(2) Uani 1 1 d . . .
H12A H 0.6075 -0.1735 0.9669 0.038 Uiso 1 1 calc R . .
H12B H 0.4499 -0.1631 0.9162 0.038 Uiso 1 1 calc R . .
C13 C 0.4428(9) -0.3556(6) 0.6679(5) 0.0268(19) Uani 1 1 d . . .
H13A H 0.4169 -0.3439 0.6160 0.032 Uiso 1 1 calc R . .
H13B H 0.3805 -0.4273 0.6733 0.032 Uiso 1 1 calc R . .
C14 C 0.6188(9) -0.3481(6) 0.6856(4) 0.0235(18) Uani 1 1 d . . .
O15 O 0.7113(6) -0.2628(4) 0.7156(3) 0.0279(13) Uani 1 1 d . . .
```

```
N16 N 0.6713(8) -0.4310(5) 0.6692(4) 0.0255(15) Uani 1 1 d . . .
C17 C 0.8403(10) -0.4235(7) 0.6862(6) 0.042(2) Uani 1 1 d . . .
H17A H 0.8949 -0.3547 0.7152 0.062 Uiso 1 1 calc R . .
H17B H 0.8846 -0.4308 0.6402 0.062 Uiso 1 1 calc R . .
H17C H 0.8560 -0.4801 0.7148 0.062 Uiso 1 1 calc R . .
C18 C 0.5729(11) -0.5295(6) 0.6258(5) 0.036(2) Uani 1 1 d . . .
H18A H 0.4992 -0.5133 0.5866 0.054 Uiso 1 1 calc R . .
H18B H 0.5115 -0.5727 0.6580 0.054 Uiso 1 1 calc R . .
H18C H 0.6420 -0.5685 0.6038 0.054 Uiso 1 1 calc R . .
O19 O 0.5175(6) -0.1283(4) 0.6164(3) 0.0245(12) Uani 1 1 d . . .
C20 C 0.4093(9) -0.0880(6) 0.5918(5) 0.0247(18) Uani 1 1 d . . .
C21 C 0.3442(10) -0.0228(7) 0.6454(4) 0.0277(19) Uani 1 1 d . . .
H21A H 0.4027 0.0526 0.6493 0.033 Uiso 1 1 calc R . .
H21B H 0.2298 -0.0295 0.6276 0.033 Uiso 1 1 calc R . .
N22 N 0.3566(8) -0.0997(5) 0.5211(4) 0.0270(16) Uani 1 1 d . . .
C23 C 0.4138(11) -0.1684(8) 0.4715(5) 0.039(2) Uani 1 1 d . . .
H23A H 0.5244 -0.1670 0.4909 0.058 Uiso 1 1 calc R . .
H23B H 0.4099 -0.1444 0.4229 0.058 Uiso 1 1 calc R . .
H23C H 0.3462 -0.2408 0.4670 0.058 Uiso 1 1 calc R . .
C24 C 0.2340(10) -0.0525(7) 0.4886(5) 0.036(2) Uani 1 1 d . . .
H24A H 0.2309 0.0097 0.5219 0.055 Uiso 1 1 calc R . .
H24B H 0.1296 -0.1043 0.4808 0.055 Uiso 1 1 calc R . .
H24C H 0.2590 -0.0311 0.4411 0.055 Uiso 1 1 calc R . .
O25 O 0.6927(6) 0.0788(4) 0.7334(3) 0.0246(12) Uani 1 1 d . . .
C26 C 0.7333(9) 0.1482(6) 0.7889(5) 0.0237(18) Uani 1 1 d . . .
C27 C 0.6889(10) 0.1217(6) 0.8618(5) 0.029(2) Uani 1 1 d . . .
H27A H 0.7877 0.1322 0.8977 0.035 Uiso 1 1 calc R . .
H27B H 0.6281 0.1707 0.8803 0.035 Uiso 1 1 calc R . .
N28 N 0.8161(8) 0.2445(5) 0.7857(4) 0.0294(17) Uani 1 1 d . . .
C29 C 0.8501(11) 0.2763(7) 0.7150(5) 0.037(2) Uani 1 1 d . . .
H29A H 0.8420 0.2134 0.6798 0.055 Uiso 1 1 calc R . .
H29B H 0.9585 0.3229 0.7212 0.055 Uiso 1 1 calc R . .
H29C H 0.7727 0.3141 0.6962 0.055 Uiso 1 1 calc R . .
C30 C 0.8598(11) 0.3276(6) 0.8478(5) 0.042(2) Uani 1 1 d . . .
H30A H 0.8452 0.2966 0.8934 0.062 Uiso 1 1 calc R . .
H30B H 0.7917 0.3764 0.8415 0.062 Uiso 1 1 calc R . .
H30C H 0.9721 0.3662 0.8505 0.062 Uiso 1 1 calc R . .
O1W O 0.8454(6) -0.0669(4) 0.6651(3) 0.0263(13) Uani 1 1 d . . .
H1W1 H 0.8736 -0.1207 0.6277 0.032 Uiso 1 1 d R . .
H1W2 H 0.9200 -0.0081 0.6660 0.032 Uiso 1 1 d R . .
O2W O 0.8950(6) -0.0509(4) 0.8221(3) 0.0271(13) Uani 1 1 d . . .
H2W1 H 0.9696 0.0156 0.8482 0.032 Uiso 1 1 d R . .
H2W2 H 0.9480 -0.1068 0.8337 0.032 Uiso 1 1 d R . .
O3W O 0.9245(7) 0.8860(4) 0.3326(3) 0.0340(14) Uani 1 1 d . . .
H3W1 H 0.8945 0.8399 0.2928 0.041 Uiso 1 1 d R . .
H3W2 H 0.9036 0.8253 0.3628 0.041 Uiso 1 1 d R . .
O4W O 0.9071(8) 0.8753(5) 0.1088(3) 0.0458(18) Uani 1 1 d . . .
H4W1 H 0.8676 0.8226 0.1389 0.055 Uiso 1 1 d R . .
H4W2 H 0.9139 0.8485 0.0567 0.055 Uiso 1 1 d R . .
O11 O 0.7906(10) 0.7920(7) 0.4452(4) 0.068(2) Uani 1 1 d . . .
O12 O 0.9213(8) 0.7895(6) 0.5646(4) 0.061(2) Uani 1 1 d . . .
O13 O 0.6668(8) 0.6696(5) 0.5202(4) 0.0479(18) Uani 1 1 d . . .
S1 S 0.8113(3) 0.73320(17) 0.50355(13) 0.0323(5) Uani 1 1 d . A .
C1S C 0.9138(14) 0.6414(9) 0.4685(7) 0.051(3) Uani 1 1 d . . .
F11 F 0.846(4) 0.599(3) 0.399(2) 0.096(12) Uani 0.50 1 d P A 1
```

```
F12 F 0.896(3) 0.5589(16) 0.5037(15) 0.092(8) Uani 0.50 1 d P A 1
F13 F 1.051(5) 0.676(4) 0.462(2) 0.061(9) Uani 0.50 1 d P A 1
F11' F 0.829(3) 0.565(2) 0.423(2) 0.073(10) Uani 0.50 1 d P A 2
F12' F 0.988(3) 0.6031(16) 0.5265(13) 0.080(7) Uani 0.50 1 d P A 2
F13' F 1.043(6) 0.693(4) 0.438(2) 0.067(11) Uani 0.50 1 d P A 2
O21 O 1.3476(10) 0.4281(5) 0.7661(4) 0.060(2) Uani 1 1 d . . .
O22 O 1.4913(8) 0.2973(5) 0.7810(4) 0.056(2) Uani 1 1 d . . .
O23 O 1.2160(8) 0.2609(5) 0.7958(4) 0.0455(17) Uani 1 1 d . . .
S2 S 1.3637(3) 0.33919(17) 0.79916(13) 0.0336(5) Uani 1 1 d . . .
C2S C 1.4162(13) 0.3874(8) 0.8961(6) 0.046(3) Uani 1 1 d . . .
F21 F 1.4372(10) 0.3105(5) 0.9333(4) 0.087(3) Uani 1 1 d . . .
F22 F 1.5525(8) 0.4598(5) 0.9105(4) 0.0671(19) Uani 1 1 d . . .
F23 F 1.3090(9) 0.4262(7) 0.9212(4) 0.089(3) Uani 1 1 d . . .
O31 O 1.1974(7) 0.7892(6) 0.9716(4) 0.0511(19) Uani 1 1 d . . .
O32 O 0.9250(8) 0.7998(5) 0.9640(3) 0.0403(16) Uani 1 1 d . . .
O33 O 1.0446(8) 0.7922(5) 0.8548(3) 0.0392(16) Uani 1 1 d . . .
S3 S 1.0451(3) 0.76817(16) 0.92879(12) 0.0277(5) Uani 1 1 d . . .
C3S C 0.9763(13) 0.6255(8) 0.9144(6) 0.043(2) Uani 1 1 d . . .
F31 F 0.9615(9) 0.5885(5) 0.9772(4) 0.076(2) Uani 1 1 d . . .
F32 F 1.0758(8) 0.5835(5) 0.8819(4) 0.0665(19) Uani 1 1 d . . .
F33 F 0.8369(7) 0.5949(5) 0.8719(4) 0.0639(18) Uani 1 1 d . . .

loop_
 _atom_site_aniso_label
 _atom_site_aniso_U_11
 _atom_site_aniso_U_22
 _atom_site_aniso_U_33
 _atom_site_aniso_U_23
 _atom_site_aniso_U_13
 _atom_site_aniso_U_12
Eu1 0.0220(2) 0.0151(2) 0.0244(2) 0.00300(15) 0.00502(16) 0.00397(15)
N1 0.026(4) 0.025(4) 0.034(4) 0.008(3) 0.010(3) 0.010(3)
C2 0.026(4) 0.021(4) 0.039(5) 0.009(4) 0.011(4) 0.005(3)
C3 0.027(4) 0.018(4) 0.038(5) 0.012(4) 0.008(4) 0.002(3)
N4 0.020(3) 0.015(3) 0.032(4) 0.001(3) 0.003(3) 0.004(3)
C5 0.015(4) 0.026(4) 0.039(5) 0.009(4) 0.000(4) 0.007(3)
C6 0.021(4) 0.024(4) 0.042(6) 0.011(4) 0.008(4) 0.007(3)
N7 0.028(4) 0.019(3) 0.026(4) 0.002(3) 0.009(3) 0.010(3)
C8 0.034(5) 0.026(4) 0.035(5) 0.003(4) 0.018(4) 0.016(4)
C9 0.029(5) 0.031(5) 0.029(5) -0.002(4) 0.011(4) 0.011(4)
N10 0.025(3) 0.019(3) 0.025(4) 0.004(3) 0.011(3) 0.006(3)
C11 0.036(5) 0.024(4) 0.029(5) 0.002(4) 0.007(4) 0.003(4)
C12 0.034(5) 0.036(5) 0.029(5) 0.010(4) 0.013(4) 0.009(4)
C13 0.029(4) 0.017(4) 0.034(5) 0.007(4) 0.005(4) 0.004(3)
C14 0.024(4) 0.023(4) 0.024(5) 0.004(4) 0.003(4) 0.005(3)
O15 0.023(3) 0.022(3) 0.037(4) 0.004(3) 0.007(3) 0.002(2)
N16 0.026(4) 0.014(3) 0.034(4) 0.000(3) 0.002(3) 0.002(3)
C17 0.033(5) 0.032(5) 0.063(7) 0.004(5) 0.007(5) 0.016(4)
C18 0.046(6) 0.014(4) 0.044(6) -0.010(4) 0.007(5) 0.004(4)
O19 0.020(3) 0.029(3) 0.025(3) 0.002(3) 0.001(2) 0.009(2)
C20 0.019(4) 0.026(4) 0.029(5) 0.005(4) 0.006(4) 0.005(3)
C21 0.028(4) 0.031(5) 0.031(5) 0.016(4) 0.011(4) 0.014(4)
N22 0.025(4) 0.030(4) 0.025(4) 0.007(3) 0.000(3) 0.005(3)
C23 0.033(5) 0.049(6) 0.030(5) 0.003(5) 0.003(4) 0.004(4)
C24 0.033(5) 0.046(6) 0.030(5) 0.016(4) -0.003(4) 0.009(4)
```

```
O25 0.032(3) 0.016(3) 0.027(3) 0.001(2) 0.007(3) 0.007(2)
C26 0.021(4) 0.018(4) 0.036(5) 0.003(4) 0.007(4) 0.010(3)
C27 0.036(5) 0.026(5) 0.024(5) -0.004(4) 0.007(4) 0.006(4)
N28 0.033(4) 0.015(3) 0.036(5) 0.000(3) -0.002(3) 0.004(3)
C29 0.044(5) 0.022(4) 0.047(6) 0.016(4) 0.016(5) 0.005(4)
C30 0.048(6) 0.015(4) 0.051(7) -0.003(4) -0.004(5) -0.003(4)
O1W 0.024(3) 0.024(3) 0.033(3) 0.004(3) 0.016(3) 0.004(2)
O2W 0.024(3) 0.024(3) 0.028(3) -0.003(3) -0.006(2) 0.003(2)
O3W 0.038(4) 0.025(3) 0.036(4) 0.004(3) 0.007(3) 0.003(3)
O4W 0.054(4) 0.035(4) 0.032(4) -0.006(3) 0.012(3) -0.016(3)
O11 0.091(6) 0.085(6) 0.061(5) 0.047(5) 0.048(5) 0.049(5)
O12 0.046(4) 0.072(5) 0.050(5) -0.037(4) 0.003(4) 0.009(4)
O13 0.042(4) 0.043(4) 0.056(5) 0.002(3) 0.023(3) -0.001(3)
S1 0.0365(12) 0.0288(12) 0.0310(13) 0.0031(10) 0.0093(10) 0.0058(10)
C1S 0.049(7) 0.044(7) 0.057(8) -0.002(6) 0.008(6) 0.010(6)
F11 0.084(16) 0.09(2) 0.080(19) -0.056(16) 0.039(12) -0.030(15)
F12 0.13(2) 0.048(13) 0.13(3) 0.035(13) 0.067(18) 0.052(12)
F13 0.034(10) 0.07(2) 0.07(2) -0.016(17) 0.011(14) 0.006(11)
F11' 0.038(10) 0.045(13) 0.11(3) -0.048(14) 0.019(13) -0.015(9)
F12' 0.100(16) 0.057(13) 0.083(13) -0.013(11) -0.016(13) 0.043(11)
F13' 0.068(17) 0.071(16) 0.07(2) 0.000(15) 0.044(18) 0.019(11)
O21 0.106(6) 0.029(4) 0.048(5) 0.015(3) 0.002(4) 0.021(4)
O22 0.037(4) 0.047(4) 0.084(6) -0.001(4) 0.005(4) 0.016(3)
O23 0.040(4) 0.048(4) 0.038(4) 0.005(3) 0.001(3) -0.005(3)
S2 0.0384(13) 0.0219(11) 0.0407(14) 0.0078(10) 0.0071(11) 0.0064(9)
C2S 0.046(6) 0.030(5) 0.054(7) 0.009(5) 0.003(5) -0.004(5)
F21 0.125(6) 0.062(5) 0.050(4) 0.028(4) -0.028(4) -0.009(4)
F22 0.068(4) 0.045(4) 0.063(4) -0.002(3) -0.009(3) -0.018(3)
F23 0.063(5) 0.131(7) 0.062(5) -0.034(5) 0.014(4) 0.023(5)
O31 0.031(4) 0.059(5) 0.055(5) 0.005(4) -0.006(3) 0.005(3)
O32 0.047(4) 0.045(4) 0.033(4) 0.003(3) 0.016(3) 0.015(3)
O33 0.055(4) 0.039(4) 0.030(4) 0.009(3) 0.012(3) 0.021(3)
S3 0.0307(11) 0.0257(11) 0.0269(12) 0.0058(9) 0.0051(9) 0.0067(9)
C3S 0.051(6) 0.032(5) 0.048(7) 0.012(5) 0.006(5) 0.014(5)
F31 0.106(6) 0.053(4) 0.075(5) 0.041(4) 0.021(4) 0.016(4)
F32 0.065(4) 0.038(3) 0.103(6) 0.004(3) 0.026(4) 0.022(3)
F33 0.046(4) 0.042(4) 0.087(5) -0.005(3) -0.011(3) -0.002(3)

_geom_special_details
;
 All esds (except the esd in the dihedral angle between two l.s. planes)
 are estimated using the full covariance matrix.  The cell esds are taken
 into account individually in the estimation of esds in distances, angles
 and torsion angles; correlations between esds in cell parameters are only
 used when they are defined by crystal symmetry.  An approximate
(isotropic)
 treatment of cell esds is used for estimating esds involving l.s. planes.
;

loop_
 _geom_bond_atom_site_label_1
 _geom_bond_atom_site_label_2
 _geom_bond_distance
 _geom_bond_site_symmetry_2
 _geom_bond_publ_flag
```

```
Eu1 O15 2.342(5) . ?
Eu1 O25 2.364(5) . ?
Eu1 O19 2.378(5) . ?
Eu1 O1W 2.418(5) . ?
Eu1 O2W 2.421(5) . ?
Eu1 N1 2.605(6) . ?
Eu1 N10 2.624(6) . ?
Eu1 N7 2.625(6) . ?
Eu1 N4 2.647(6) . ?
Eu1 C26 3.219(8) . ?
Eu1 C14 3.224(8) . ?
Eu1 C20 3.263(8) . ?
N1 C12 1.484(10) . ?
N1 C2 1.491(10) . ?
C2 C3 1.486(11) . ?
C3 N4 1.477(10) . ?
N4 C13 1.466(10) . ?
N4 C5 1.480(9) . ?
C5 C6 1.511(11) . ?
C6 N7 1.500(10) . ?
N7 C21 1.467(10) . ?
N7 C8 1.494(10) . ?
C8 C9 1.479(12) . ?
C9 N10 1.471(10) . ?
N10 C27 1.476(10) . ?
N10 C11 1.481(10) . ?
C11 C12 1.499(11) . ?
C13 C14 1.505(11) . ?
C14 O15 1.241(9) . ?
C14 N16 1.303(10) . ?
N16 C17 1.444(10) . ?
N16 C18 1.460(10) . ?
O19 C20 1.248(9) . ?
C20 N22 1.307(10) . ?
C20 C21 1.495(11) . ?
N22 C23 1.436(11) . ?
N22 C24 1.457(10) . ?
O25 C26 1.252(9) . ?
C26 N28 1.307(10) . ?
C26 C27 1.496(11) . ?
N28 C30 1.444(11) . ?
N28 C29 1.451(11) . ?
O11 S1 1.404(7) . ?
O12 S1 1.396(7) . ?
O13 S1 1.421(6) . ?
S1 C1S 1.784(11) . ?
C1S F13 1.20(4) . ?
C1S F11' 1.26(3) . ?
C1S F12 1.31(2) . ?
C1S F11 1.35(4) . ?
C1S F12' 1.38(2) . ?
C1S F13' 1.39(4) . ?
O21 S2 1.399(6) . ?
O22 S2 1.416(7) . ?
O23 S2 1.431(6) . ?
```

```
S2 C2S 1.796(11) . ?
C2S F23 1.281(12) . ?
C2S F22 1.308(11) . ?
C2S F21 1.313(11) . ?
O31 S3 1.406(7) . ?
O32 S3 1.421(6) . ?
O33 S3 1.430(6) . ?
S3 C3S 1.806(10) . ?
C3S F33 1.308(11) . ?
C3S F32 1.309(11) . ?
C3S F31 1.310(11) . ?

loop_
 _geom_angle_atom_site_label_1
 _geom_angle_atom_site_label_2
 _geom_angle_atom_site_label_3
 _geom_angle
 _geom_angle_site_symmetry_1
 _geom_angle_site_symmetry_3
 _geom_angle_publ_flag
O15 Eu1 O25 147.10(19) . . ?
O15 Eu1 O19 87.51(19) . . ?
O25 Eu1 O19 85.52(19) . . ?
O15 Eu1 O1W 73.80(18) . . ?
O25 Eu1 O1W 73.54(18) . . ?
O19 Eu1 O1W 70.84(18) . . ?
O15 Eu1 O2W 83.79(19) . . ?
O25 Eu1 O2W 82.68(18) . . ?
O19 Eu1 O2W 142.98(18) . . ?
O1W Eu1 O2W 72.18(19) . . ?
O15 Eu1 N1 72.1(2) . . ?
O25 Eu1 N1 130.6(2) . . ?
O19 Eu1 N1 138.0(2) . . ?
O1W Eu1 N1 132.59(19) . . ?
O2W Eu1 N1 72.2(2) . . ?
O15 Eu1 N10 138.2(2) . . ?
O25 Eu1 N10 65.39(19) . . ?
O19 Eu1 N10 130.06(19) . . ?
O1W Eu1 N10 129.82(19) . . ?
O2W Eu1 N10 75.11(19) . . ?
N1 Eu1 N10 67.3(2) . . ?
O15 Eu1 N7 131.19(19) . . ?
O25 Eu1 N7 72.99(19) . . ?
O19 Eu1 N7 64.10(19) . . ?
O1W Eu1 N7 124.90(19) . . ?
O2W Eu1 N7 142.3(2) . . ?
N1 Eu1 N7 102.4(2) . . ?
N10 Eu1 N7 68.8(2) . . ?
O15 Eu1 N4 65.13(19) . . ?
O25 Eu1 N4 140.48(19) . . ?
O19 Eu1 N4 71.09(19) . . ?
O1W Eu1 N4 124.07(19) . . ?
O2W Eu1 N4 134.43(19) . . ?
N1 Eu1 N4 67.1(2) . . ?
N10 Eu1 N4 106.0(2) . . ?
```

```
N7 Eu1 N4 68.25(19) . . ?
O15 Eu1 C26 150.84(19) . . ?
O25 Eu1 C26 19.09(19) . . ?
O19 Eu1 C26 103.9(2) . . ?
O1W Eu1 C26 84.63(19) . . ?
O2W Eu1 C26 70.86(19) . . ?
N1 Eu1 C26 111.7(2) . . ?
N10 Eu1 C26 48.8(2) . . ?
N7 Eu1 C26 77.37(19) . . ?
N4 Eu1 C26 143.87(19) . . ?
O15 Eu1 C14 18.28(19) . . ?
O25 Eu1 C14 155.01(19) . . ?
O19 Eu1 C14 76.47(19) . . ?
O1W Eu1 C14 84.16(19) . . ?
O2W Eu1 C14 101.35(19) . . ?
N1 Eu1 C14 73.3(2) . . ?
N10 Eu1 C14 139.58(19) . . ?
N7 Eu1 C14 112.9(2) . . ?
N4 Eu1 C14 47.97(19) . . ?
C26 Eu1 C14 167.93(19) . . ?
O15 Eu1 C20 104.3(2) . . ?
O25 Eu1 C20 75.27(19) . . ?
O19 Eu1 C20 18.17(18) . . ?
O1W Eu1 C20 82.67(19) . . ?
O2W Eu1 C20 150.40(19) . . ?
N1 Eu1 C20 137.3(2) . . ?
N10 Eu1 C20 111.9(2) . . ?
N7 Eu1 C20 47.1(2) . . ?
N4 Eu1 C20 73.00(19) . . ?
C26 Eu1 C20 91.9(2) . . ?
C14 Eu1 C20 91.1(2) . . ?
C12 N1 C2 111.9(6) . . ?
C12 N1 Eu1 115.7(5) . . ?
C2 N1 Eu1 113.2(5) . . ?
N1 C2 C3 109.6(6) . . ?
N4 C3 C2 113.0(6) . . ?
C13 N4 C3 109.7(6) . . ?
C13 N4 C5 108.5(6) . . ?
C3 N4 C5 109.0(6) . . ?
C13 N4 Eu1 107.4(4) . . ?
C3 N4 Eu1 111.5(5) . . ?
C5 N4 Eu1 110.7(4) . . ?
N4 C5 C6 110.8(7) . . ?
N7 C6 C5 112.9(6) . . ?
C21 N7 C8 109.5(6) . . ?
C21 N7 C6 108.0(6) . . ?
C8 N7 C6 108.5(6) . . ?
C21 N7 Eu1 108.5(4) . . ?
C8 N7 Eu1 110.7(5) . . ?
C6 N7 Eu1 111.6(4) . . ?
C9 C8 N7 110.6(7) . . ?
N10 C9 C8 114.1(7) . . ?
C9 N10 C27 110.2(6) . . ?
C9 N10 C11 109.9(6) . . ?
C27 N10 C11 109.1(6) . . ?
```

```
C9 N10 Eu1 108.6(5) . . ?
C27 N10 Eu1 109.8(4) . . ?
C11 N10 Eu1 109.3(5) . . ?
N10 C11 C12 113.4(7) . . ?
N1 C12 C11 109.4(7) . . ?
N4 C13 C14 110.7(7) . . ?
O15 C14 N16 121.2(7) . . ?
O15 C14 C13 119.2(7) . . ?
N16 C14 C13 119.6(7) . . ?
O15 C14 Eu1 36.3(4) . . ?
N16 C14 Eu1 157.3(6) . . ?
C13 C14 Eu1 82.9(4) . . ?
C14 O15 Eu1 125.4(5) . . ?
C14 N16 C17 119.5(7) . . ?
C14 N16 C18 123.9(7) . . ?
C17 N16 C18 116.1(7) . . ?
C20 O19 Eu1 125.4(5) . . ?
O19 C20 N22 121.3(8) . . ?
O19 C20 C21 118.2(7) . . ?
N22 C20 C21 120.5(7) . . ?
O19 C20 Eu1 36.5(4) . . ?
N22 C20 Eu1 157.5(6) . . ?
C21 C20 Eu1 81.8(5) . . ?
N7 C21 C20 109.8(6) . . ?
C20 N22 C23 119.1(7) . . ?
C20 N22 C24 124.1(7) . . ?
C23 N22 C24 116.7(7) . . ?
C26 O25 Eu1 122.8(5) . . ?
O25 C26 N28 122.0(8) . . ?
O25 C26 C27 120.0(7) . . ?
N28 C26 C27 118.1(8) . . ?
O25 C26 Eu1 38.1(3) . . ?
N28 C26 Eu1 152.9(6) . . ?
C27 C26 Eu1 84.6(4) . . ?
N10 C27 C26 112.6(7) . . ?
C26 N28 C30 123.5(8) . . ?
C26 N28 C29 119.9(7) . . ?
C30 N28 C29 116.1(7) . . ?
O12 S1 O11 114.4(5) . . ?
O12 S1 O13 115.4(5) . . ?
O11 S1 O13 114.5(5) . . ?
O12 S1 C1S 101.7(5) . . ?
O11 S1 C1S 103.7(5) . . ?
O13 S1 C1S 105.0(5) . . ?
F13 C1S F11' 119(3) . . ?
F13 C1S F12 111(3) . . ?
F11' C1S F12 74.1(19) . . ?
F13 C1S F11 103(2) . . ?
F11' C1S F11 29.3(19) . . ?
F12 C1S F11 102.8(19) . . ?
F13 C1S F12' 80(2) . . ?
F11' C1S F12' 109.1(19) . . ?
F12 C1S F12' 38.7(12) . . ?
F11 C1S F12' 133(2) . . ?
F13 C1S F13' 22(3) . . ?
```

```
F11' C1S F13' 109(3) . . ?
F12 C1S F13' 130(2) . . ?
F11 C1S F13' 86(2) . . ?
F12' C1S F13' 102(2) . . ?
F13 C1S S1 117(3) . . ?
F11' C1S S1 115.5(16) . . ?
F12 C1S S1 111.7(12) . . ?
F11 C1S S1 110(2) . . ?
F12' C1S S1 109.5(12) . . ?
F13' C1S S1 110(2) . . ?
O21 S2 O22 115.2(5) . . ?
O21 S2 O23 113.9(5) . . ?
O22 S2 O23 113.9(4) . . ?
O21 S2 C2S 104.4(5) . . ?
O22 S2 C2S 104.9(5) . . ?
O23 S2 C2S 102.6(4) . . ?
F23 C2S F22 108.4(9) . . ?
F23 C2S F21 108.7(10) . . ?
F22 C2S F21 105.6(9) . . ?
F23 C2S S2 112.2(8) . . ?
F22 C2S S2 111.6(7) . . ?
F21 C2S S2 110.1(7) . . ?
O31 S3 O32 116.2(4) . . ?
O31 S3 O33 115.1(4) . . ?
O32 S3 O33 113.6(4) . . ?
O31 S3 C3S 104.1(5) . . ?
O32 S3 C3S 103.3(4) . . ?
O33 S3 C3S 102.0(4) . . ?
F33 C3S F32 107.6(9) . . ?
F33 C3S F31 108.3(9) . . ?
F32 C3S F31 108.8(8) . . ?
F33 C3S S3 110.4(6) . . ?
F32 C3S S3 110.9(7) . . ?
F31 C3S S3 110.8(7) . . ?

loop_
 _geom_torsion_atom_site_label_1
 _geom_torsion_atom_site_label_2
 _geom_torsion_atom_site_label_3
 _geom_torsion_atom_site_label_4
 _geom_torsion
 _geom_torsion_site_symmetry_1
 _geom_torsion_site_symmetry_2
 _geom_torsion_site_symmetry_3
 _geom_torsion_site_symmetry_4
 _geom_torsion_publ_flag
O15 Eu1 N1 C12 176.4(6) . . . . ?
O25 Eu1 N1 C12 24.1(6) . . . . ?
O19 Eu1 N1 C12 -118.8(5) . . . . ?
O1W Eu1 N1 C12 130.4(5) . . . . ?
O2W Eu1 N1 C12 87.3(5) . . . . ?
N10 Eu1 N1 C12 6.5(5) . . . . ?
N7 Eu1 N1 C12 -54.0(6) . . . . ?
N4 Eu1 N1 C12 -113.7(6) . . . . ?
C26 Eu1 N1 C12 27.2(6) . . . . ?
```

```
C14 Eu1 N1 C12 -164.5(6) . . . . ?
C20 Eu1 N1 C12 -91.7(6) . . . . ?
O15 Eu1 N1 C2 -52.6(5) . . . . ?
O25 Eu1 N1 C2 155.1(4) . . . . ?
O19 Eu1 N1 C2 12.2(6) . . . . ?
O1W Eu1 N1 C2 -98.6(5) . . . . ?
O2W Eu1 N1 C2 -141.7(5) . . . . ?
N10 Eu1 N1 C2 137.5(5) . . . . ?
N7 Eu1 N1 C2 77.0(5) . . . . ?
N4 Eu1 N1 C2 17.3(5) . . . . ?
C26 Eu1 N1 C2 158.2(5) . . . . ?
C14 Eu1 N1 C2 -33.5(5) . . . . ?
C20 Eu1 N1 C2 39.3(6) . . . . ?
C12 N1 C2 C3 87.6(8) . . . . ?
Eu1 N1 C2 C3 -45.2(7) . . . . ?
N1 C2 C3 N4 58.9(9) . . . . ?
C2 C3 N4 C13 77.1(8) . . . . ?
C2 C3 N4 C5 -164.1(7) . . . . ?
C2 C3 N4 Eu1 -41.7(8) . . . . ?
O15 Eu1 N4 C13 -27.9(5) . . . . ?
O25 Eu1 N4 C13 125.3(5) . . . . ?
O19 Eu1 N4 C13 68.3(5) . . . . ?
O1W Eu1 N4 C13 18.9(5) . . . . ?
O2W Eu1 N4 C13 -79.5(5) . . . . ?
N1 Eu1 N4 C13 -108.1(5) . . . . ?
N10 Eu1 N4 C13 -164.2(5) . . . . ?
N7 Eu1 N4 C13 137.2(5) . . . . ?
C26 Eu1 N4 C13 156.2(4) . . . . ?
C14 Eu1 N4 C13 -20.3(4) . . . . ?
C20 Eu1 N4 C13 87.3(5) . . . . ?
O15 Eu1 N4 C3 92.3(5) . . . . ?
O25 Eu1 N4 C3 -114.6(5) . . . . ?
O19 Eu1 N4 C3 -171.5(5) . . . . ?
O1W Eu1 N4 C3 139.1(5) . . . . ?
O2W Eu1 N4 C3 40.7(6) . . . . ?
N1 Eu1 N4 C3 12.1(5) . . . . ?
N10 Eu1 N4 C3 -44.0(5) . . . . ?
N7 Eu1 N4 C3 -102.7(5) . . . . ?
C26 Eu1 N4 C3 -83.7(6) . . . . ?
C14 Eu1 N4 C3 99.9(5) . . . . ?
C20 Eu1 N4 C3 -152.5(5) . . . . ?
O15 Eu1 N4 C5 -146.2(6) . . . . ?
O25 Eu1 N4 C5 7.0(7) . . . . ?
O19 Eu1 N4 C5 -50.0(5) . . . . ?
O1W Eu1 N4 C5 -99.4(5) . . . . ?
O2W Eu1 N4 C5 162.2(5) . . . . ?
N1 Eu1 N4 C5 133.6(5) . . . . ?
N10 Eu1 N4 C5 77.5(5) . . . . ?
N7 Eu1 N4 C5 18.9(5) . . . . ?
C26 Eu1 N4 C5 37.9(7) . . . . ?
C14 Eu1 N4 C5 -138.6(6) . . . . ?
C20 Eu1 N4 C5 -31.0(5) . . . . ?
C13 N4 C5 C6 -164.2(6) . . . . ?
C3 N4 C5 C6 76.3(8) . . . . ?
Eu1 N4 C5 C6 -46.6(7) . . . . ?
```

```
N4 C5 C6 N7 59.4(9) . . . . ?
C5 C6 N7 C21 79.9(8) . . . . ?
C5 C6 N7 C8 -161.5(7) . . . . ?
C5 C6 N7 Eu1 -39.3(8) . . . . ?
O15 Eu1 N7 C21 -90.5(5) . . . . ?
O25 Eu1 N7 C21 63.6(5) . . . . ?
O19 Eu1 N7 C21 -29.8(5) . . . . ?
O1W Eu1 N7 C21 8.6(6) . . . . ?
O2W Eu1 N7 C21 115.7(5) . . . . ?
N1 Eu1 N7 C21 -167.4(5) . . . . ?
N10 Eu1 N7 C21 133.2(5) . . . . ?
N4 Eu1 N7 C21 -108.6(5) . . . . ?
C26 Eu1 N7 C21 82.8(5) . . . . ?
C14 Eu1 N7 C21 -90.6(5) . . . . ?
C20 Eu1 N7 C21 -21.9(5) . . . . ?
O15 Eu1 N7 C8 149.4(4) . . . . ?
O25 Eu1 N7 C8 -56.6(5) . . . . ?
O19 Eu1 N7 C8 -149.9(5) . . . . ?
O1W Eu1 N7 C8 -111.5(5) . . . . ?
O2W Eu1 N7 C8 -4.5(6) . . . . ?
N1 Eu1 N7 C8 72.4(5) . . . . ?
N10 Eu1 N7 C8 13.0(5) . . . . ?
N4 Eu1 N7 C8 131.3(5) . . . . ?
C26 Eu1 N7 C8 -37.4(5) . . . . ?
C14 Eu1 N7 C8 149.3(5) . . . . ?
C20 Eu1 N7 C8 -142.1(6) . . . . ?
O15 Eu1 N7 C6 28.4(6) . . . . ?
O25 Eu1 N7 C6 -177.6(5) . . . . ?
O19 Eu1 N7 C6 89.1(5) . . . . ?
O1W Eu1 N7 C6 127.5(5) . . . . ?
O2W Eu1 N7 C6 -125.5(5) . . . . ?
N1 Eu1 N7 C6 -48.6(5) . . . . ?
N10 Eu1 N7 C6 -108.0(5) . . . . ?
N4 Eu1 N7 C6 10.3(5) . . . . ?
C26 Eu1 N7 C6 -158.4(5) . . . . ?
C14 Eu1 N7 C6 28.3(6) . . . . ?
C20 Eu1 N7 C6 96.9(6) . . . . ?
C21 N7 C8 C9 -161.2(7) . . . . ?
C6 N7 C8 C9 81.2(8) . . . . ?
Eu1 N7 C8 C9 -41.6(7) . . . . ?
N7 C8 C9 N10 62.2(9) . . . . ?
C8 C9 N10 C27 73.5(9) . . . . ?
C8 C9 N10 C11 -166.3(7) . . . . ?
C8 C9 N10 Eu1 -46.8(8) . . . . ?
O15 Eu1 N10 C9 -112.6(5) . . . . ?
O25 Eu1 N10 C9 96.5(5) . . . . ?
O19 Eu1 N10 C9 36.4(6) . . . . ?
O1W Eu1 N10 C9 134.6(5) . . . . ?
O2W Eu1 N10 C9 -174.8(5) . . . . ?
N1 Eu1 N10 C9 -98.1(5) . . . . ?
N7 Eu1 N10 C9 16.2(5) . . . . ?
N4 Eu1 N10 C9 -42.2(5) . . . . ?
C26 Eu1 N10 C9 107.8(5) . . . . ?
C14 Eu1 N10 C9 -84.7(6) . . . . ?
C20 Eu1 N10 C9 35.6(5) . . . . ?
```

```
O15 Eu1 N10 C27 126.9(5) . . . . ?
O25 Eu1 N10 C27 -24.0(5) . . . . ?
O19 Eu1 N10 C27 -84.2(5) . . . . ?
O1W Eu1 N10 C27 14.0(6) . . . . ?
O2W Eu1 N10 C27 64.7(5) . . . . ?
N1 Eu1 N10 C27 141.3(6) . . . . ?
N7 Eu1 N10 C27 -104.4(5) . . . . ?
N4 Eu1 N10 C27 -162.7(5) . . . . ?
C26 Eu1 N10 C27 -12.7(5) . . . . ?
C14 Eu1 N10 C27 154.8(5) . . . . ?
C20 Eu1 N10 C27 -85.0(5) . . . . ?
O15 Eu1 N10 C11 7.3(6) . . . . ?
O25 Eu1 N10 C11 -143.6(5) . . . . ?
O19 Eu1 N10 C11 156.2(4) . . . . ?
O1W Eu1 N10 C11 -105.6(5) . . . . ?
O2W Eu1 N10 C11 -55.0(5) . . . . ?
N1 Eu1 N10 C11 21.7(5) . . . . ?
N7 Eu1 N10 C11 136.0(5) . . . . ?
N4 Eu1 N10 C11 77.7(5) . . . . ?
C26 Eu1 N10 C11 -132.4(6) . . . . ?
C14 Eu1 N10 C11 35.2(6) . . . . ?
C20 Eu1 N10 C11 155.4(5) . . . . ?
C9 N10 C11 C12 68.8(9) . . . . ?
C27 N10 C11 C12 -170.4(7) . . . . ?
Eu1 N10 C11 C12 -50.3(8) . . . . ?
C2 N1 C12 C11 -165.1(7) . . . . ?
Eu1 N1 C12 C11 -33.5(8) . . . . ?
N10 C11 C12 N1 57.0(9) . . . . ?
C3 N4 C13 C14 -85.1(7) . . . . ?
C5 N4 C13 C14 155.9(6) . . . . ?
Eu1 N4 C13 C14 36.2(7) . . . . ?
N4 C13 C14 O15 -25.4(10) . . . . ?
N4 C13 C14 N16 154.6(7) . . . . ?
N4 C13 C14 Eu1 -27.8(5) . . . . ?
O25 Eu1 C14 O15 80.9(8) . . . . ?
O19 Eu1 C14 O15 125.9(6) . . . . ?
O1W Eu1 C14 O15 54.2(6) . . . . ?
O2W Eu1 C14 O15 -16.2(7) . . . . ?
N1 Eu1 C14 O15 -83.6(6) . . . . ?
N10 Eu1 C14 O15 -96.5(7) . . . . ?
N7 Eu1 C14 O15 179.8(6) . . . . ?
N4 Eu1 C14 O15 -157.5(7) . . . . ?
C26 Eu1 C14 O15 32.5(13) . . . . ?
C20 Eu1 C14 O15 136.8(6) . . . . ?
O15 Eu1 C14 N16 -8.9(12) . . . . ?
O25 Eu1 C14 N16 71.9(16) . . . . ?
O19 Eu1 C14 N16 117.0(15) . . . . ?
O1W Eu1 C14 N16 45.3(15) . . . . ?
O2W Eu1 C14 N16 -25.2(15) . . . . ?
N1 Eu1 C14 N16 -92.5(15) . . . . ?
N10 Eu1 C14 N16 -105.5(15) . . . . ?
N7 Eu1 C14 N16 170.8(14) . . . . ?
N4 Eu1 C14 N16 -166.4(16) . . . . ?
C26 Eu1 C14 N16 24(2) . . . . ?
C20 Eu1 C14 N16 127.8(15) . . . . ?
```

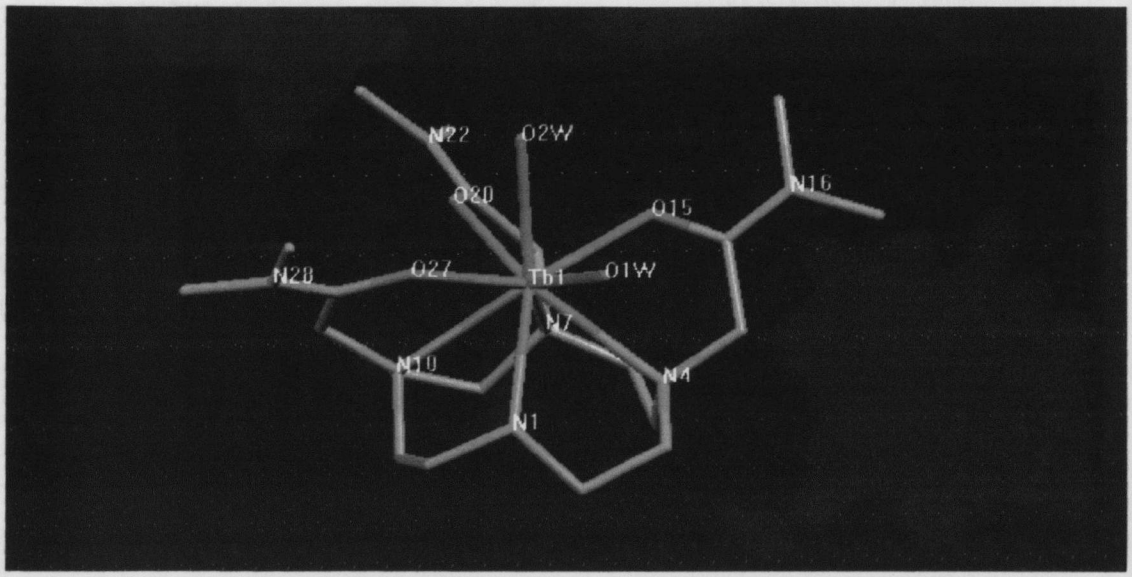
```
O15 Eu1 C14 C13 176.5(9) . . . . ?
O25 Eu1 C14 C13 -102.7(6) . . . . ?
O19 Eu1 C14 C13 -57.6(4) . . . . ?
O1W Eu1 C14 C13 -129.3(5) . . . . ?
O2W Eu1 C14 C13 160.3(4) . . . . ?
N1 Eu1 C14 C13 92.9(5) . . . . ?
N10 Eu1 C14 C13 80.0(5) . . . . ?
N7 Eu1 C14 C13 -3.7(5) . . . . ?
N4 Eu1 C14 C13 19.0(4) . . . . ?
C26 Eu1 C14 C13 -151.0(9) . . . . ?
C20 Eu1 C14 C13 -46.7(5) . . . . ?
N16 C14 O15 Eu1 176.0(5) . . . . ?
C13 C14 O15 Eu1 -4.0(10) . . . . ?
O25 Eu1 O15 C14 -129.8(6) . . . . ?
O19 Eu1 O15 C14 -52.0(6) . . . . ?
O1W Eu1 O15 C14 -122.8(7) . . . . ?
O2W Eu1 O15 C14 164.0(6) . . . . ?
N1 Eu1 O15 C14 90.7(6) . . . . ?
N10 Eu1 O15 C14 104.7(7) . . . . ?
N7 Eu1 O15 C14 -0.3(7) . . . . ?
N4 Eu1 O15 C14 18.2(6) . . . . ?
C26 Eu1 O15 C14 -166.7(6) . . . . ?
C20 Eu1 O15 C14 -45.0(6) . . . . ?
O15 C14 N16 C17 0.0(12) . . . . ?
C13 C14 N16 C17 179.9(7) . . . . ?
Eu1 C14 N16 C17 6.1(19) . . . . ?
O15 C14 N16 C18 -172.1(8) . . . . ?
C13 C14 N16 C18 7.9(12) . . . . ?
Eu1 C14 N16 C18 -165.9(11) . . . . ?
O15 Eu1 O19 C20 157.5(6) . . . . ?
O25 Eu1 O19 C20 -54.6(6) . . . . ?
O1W Eu1 O19 C20 -128.7(6) . . . . ?
O2W Eu1 O19 C20 -126.2(6) . . . . ?
N1 Eu1 O19 C20 98.0(6) . . . . ?
N10 Eu1 O19 C20 -2.3(7) . . . . ?
N7 Eu1 O19 C20 18.6(6) . . . . ?
N4 Eu1 O19 C20 93.0(6) . . . . ?
C26 Eu1 O19 C20 -49.6(6) . . . . ?
C14 Eu1 O19 C20 142.8(6) . . . . ?
Eu1 O19 C20 N22 175.4(5) . . . . ?
Eu1 O19 C20 C21 -2.9(10) . . . . ?
O15 Eu1 C20 O19 -23.2(6) . . . . ?
O25 Eu1 C20 O19 122.8(6) . . . . ?
O1W Eu1 C20 O19 48.0(6) . . . . ?
O2W Eu1 C20 O19 79.6(7) . . . . ?
N1 Eu1 C20 O19 -102.2(6) . . . . ?
N10 Eu1 C20 O19 178.1(6) . . . . ?
N7 Eu1 C20 O19 -156.9(7) . . . . ?
N4 Eu1 C20 O19 -81.1(6) . . . . ?
C26 Eu1 C20 O19 132.3(6) . . . . ?
C14 Eu1 C20 O19 -36.0(6) . . . . ?
O15 Eu1 C20 N22 -33.5(15) . . . . ?
O25 Eu1 C20 N22 112.5(14) . . . . ?
O19 Eu1 C20 N22 -10.3(12) . . . . ?
O1W Eu1 C20 N22 37.7(14) . . . . ?
```

```
O2W Eu1 C20 N22 69.4(16) . . . . ?
N1 Eu1 C20 N22 -112.4(14) . . . . ?
N10 Eu1 C20 N22 167.8(14) . . . . ?
N7 Eu1 C20 N22 -167.2(15) . . . . ?
N4 Eu1 C20 N22 -91.3(14) . . . . ?
C26 Eu1 C20 N22 122.0(14) . . . . ?
C14 Eu1 C20 N22 -46.3(14) . . . . ?
O15 Eu1 C20 C21 154.3(4) . . . . ?
O25 Eu1 C20 C21 -59.7(4) . . . . ?
O19 Eu1 C20 C21 177.5(9) . . . . ?
O1W Eu1 C20 C21 -134.6(4) . . . . ?
O2W Eu1 C20 C21 -102.9(5) . . . . ?
N1 Eu1 C20 C21 75.3(5) . . . . ?
N10 Eu1 C20 C21 -4.5(5) . . . . ?
N7 Eu1 C20 C21 20.6(4) . . . . ?
N4 Eu1 C20 C21 96.4(4) . . . . ?
C26 Eu1 C20 C21 -50.2(4) . . . . ?
C14 Eu1 C20 C21 141.5(4) . . . . ?
C8 N7 C21 C20 160.3(7) . . . . ?
C6 N7 C21 C20 -81.7(8) . . . . ?
Eu1 N7 C21 C20 39.4(7) . . . . ?
O19 C20 C21 N7 -27.6(10) . . . . ?
N22 C20 C21 N7 154.1(7) . . . . ?
Eu1 C20 C21 N7 -29.3(6) . . . . ?
O19 C20 N22 C23 5.9(11) . . . . ?
C21 C20 N22 C23 -175.9(7) . . . . ?
Eu1 C20 N22 C23 13.0(18) . . . . ?
O19 C20 N22 C24 -178.2(7) . . . . ?
C21 C20 N22 C24 0.0(12) . . . . ?
Eu1 C20 N22 C24 -171.1(11) . . . . ?
O15 Eu1 O25 C26 -116.7(6) . . . . ?
O19 Eu1 O25 C26 164.9(6) . . . . ?
O1W Eu1 O25 C26 -123.7(6) . . . . ?
O2W Eu1 O25 C26 -50.2(6) . . . . ?
N1 Eu1 O25 C26 8.8(7) . . . . ?
N10 Eu1 O25 C26 26.7(5) . . . . ?
N7 Eu1 O25 C26 100.7(6) . . . . ?
N4 Eu1 O25 C26 112.2(6) . . . . ?
C14 Eu1 O25 C26 -151.4(5) . . . . ?
C20 Eu1 O25 C26 149.7(6) . . . . ?
Eu1 O25 C26 N28 154.9(6) . . . . ?
Eu1 O25 C26 C27 -24.4(9) . . . . ?
O15 Eu1 C26 O25 95.2(7) . . . . ?
O19 Eu1 C26 O25 -15.5(6) . . . . ?
O1W Eu1 C26 O25 53.2(6) . . . . ?
O2W Eu1 C26 O25 126.2(6) . . . . ?
N1 Eu1 C26 O25 -172.8(5) . . . . ?
N10 Eu1 C26 O25 -147.1(6) . . . . ?
N7 Eu1 C26 O25 -74.4(6) . . . . ?
N4 Eu1 C26 O25 -92.4(6) . . . . ?
C14 Eu1 C26 O25 75.0(12) . . . . ?
C20 Eu1 C26 O25 -29.2(6) . . . . ?
O15 Eu1 C26 N28 42.8(15) . . . . ?
O25 Eu1 C26 N28 -52.4(12) . . . . ?
O19 Eu1 C26 N28 -67.9(13) . . . . ?
```

```
O1W Eu1 C26 N28 0.8(13) . . . . ?
O2W Eu1 C26 N28 73.8(13) . . . . ?
N1 Eu1 C26 N28 134.8(13) . . . . ?
N10 Eu1 C26 N28 160.5(14) . . . . ?
N7 Eu1 C26 N28 -126.8(13) . . . . ?
N4 Eu1 C26 N28 -144.8(12) . . . . ?
C14 Eu1 C26 N28 23(2) . . . . ?
C20 Eu1 C26 N28 -81.6(13) . . . . ?
O15 Eu1 C26 C27 -105.8(5) . . . . ?
O25 Eu1 C26 C27 159.0(8) . . . . ?
O19 Eu1 C26 C27 143.5(4) . . . . ?
O1W Eu1 C26 C27 -147.8(5) . . . . ?
O2W Eu1 C26 C27 -74.8(5) . . . . ?
N1 Eu1 C26 C27 -13.9(5) . . . . ?
N10 Eu1 C26 C27 11.9(4) . . . . ?
N7 Eu1 C26 C27 84.6(5) . . . . ?
N4 Eu1 C26 C27 66.6(6) . . . . ?
C14 Eu1 C26 C27 -126.1(10) . . . . ?
C20 Eu1 C26 C27 129.7(5) . . . . ?
C9 N10 C27 C26 -96.8(8) . . . . ?
C11 N10 C27 C26 142.5(7) . . . . ?
Eu1 N10 C27 C26 22.7(8) . . . . ?
O25 C26 C27 N10 -2.5(11) . . . . ?
N28 C26 C27 N10 178.2(7) . . . . ?
Eu1 C26 C27 N10 -17.3(6) . . . . ?
O25 C26 N28 C30 177.5(7) . . . . ?
C27 C26 N28 C30 -3.2(12) . . . . ?
Eu1 C26 N28 C30 -147.3(10) . . . . ?
O25 C26 N28 C29 6.1(12) . . . . ?
C27 C26 N28 C29 -174.7(7) . . . . ?
Eu1 C26 N28 C29 41.3(16) . . . . ?
O12 S1 C1S F13 -47(2) . . . . ?
O11 S1 C1S F13 72(2) . . . . ?
O13 S1 C1S F13 -168(2) . . . . ?
O12 S1 C1S F11' 164.8(18) . . . . ?
O11 S1 C1S F11' -76.2(18) . . . . ?
O13 S1 C1S F11' 44.3(19) . . . . ?
O12 S1 C1S F12 82.7(18) . . . . ?
O11 S1 C1S F12 -158.4(17) . . . . ?
O13 S1 C1S F12 -37.9(18) . . . . ?
O12 S1 C1S F11 -163.8(13) . . . . ?
O11 S1 C1S F11 -44.9(14) . . . . ?
O13 S1 C1S F11 75.6(14) . . . . ?
O12 S1 C1S F12' 41.2(13) . . . . ?
O11 S1 C1S F12' 160.2(13) . . . . ?
O13 S1 C1S F12' -79.3(13) . . . . ?
O12 S1 C1S F13' -70(2) . . . . ?
O11 S1 C1S F13' 49(2) . . . . ?
O13 S1 C1S F13' 169(2) . . . . ?
O21 S2 C2S F23 59.8(8) . . . . ?
O22 S2 C2S F23 -178.7(7) . . . . ?
O23 S2 C2S F23 -59.3(8) . . . . ?
O21 S2 C2S F22 -62.1(9) . . . . ?
O22 S2 C2S F22 59.4(8) . . . . ?
O23 S2 C2S F22 178.8(7) . . . . ?
```

```
O21 S2 C2S F21 -179.0(8) . . . . ?
O22 S2 C2S F21 -57.4(8) . . . . ?
O23 S2 C2S F21 61.9(8) . . . . ?
O31 S3 C3S F33 -177.1(7) . . . . ?
O32 S3 C3S F33 61.0(8) . . . . ?
O33 S3 C3S F33 -57.0(8) . . . . ?
O31 S3 C3S F32 -58.0(8) . . . . ?
O32 S3 C3S F32 -179.9(7) . . . . ?
O33 S3 C3S F32 62.1(8) . . . . ?
O31 S3 C3S F31 62.9(8) . . . . ?
O32 S3 C3S F31 -58.9(8) . . . . ?
O33 S3 C3S F31 -177.0(7) . . . . ?

_diffrn_measured_fraction_theta_max    0.874
_diffrn_reflns_theta_full              28.86
_diffrn_measured_fraction_theta_full   0.874
_refine_diff_density_max    0.985
_refine_diff_density_min   -1.534
_refine_diff_density_rms    0.224
```



Crystallography data for Tb.149

```
data_


_audit_creation_method            SHELXL-97
_chemical_name_systematic
;
 ?
;
_chemical_name_common             ?
_chemical_melting_point           ?
_chemical_formula_moiety          ?
_chemical_formula_sum
 'C23 H49 F9 N7 O16 S3 Tb'
_chemical_formula_weight          1105.79

loop_
 _atom_type_symbol
 _atom_type_description
 _atom_type_scat_dispersion_real
 _atom_type_scat_dispersion_imag
 _atom_type_scat_source
 'C'  'C'   0.0033   0.0016
 'International Tables Vol C Tables 4.2.6.8 and 6.1.1.4'
 'H'  'H'   0.0000   0.0000
 'International Tables Vol C Tables 4.2.6.8 and 6.1.1.4'
 'N'  'N'   0.0061   0.0033
 'International Tables Vol C Tables 4.2.6.8 and 6.1.1.4'
 'O'  'O'   0.0106   0.0060
 'International Tables Vol C Tables 4.2.6.8 and 6.1.1.4'
 'F'  'F'   0.0171   0.0103
 'International Tables Vol C Tables 4.2.6.8 and 6.1.1.4'
```

```
 'S'  'S'   0.1246   0.1234
 'International Tables Vol C Tables 4.2.6.8 and 6.1.1.4'
 'Tb'  'Tb'  -0.1723   4.1537
 'International Tables Vol C Tables 4.2.6.8 and 6.1.1.4'

_symmetry_cell_setting            Triclinic
_symmetry_space_group_name_H-M    P1

loop_
 _symmetry_equiv_pos_as_xyz
 'x, y, z'
 '-x, -y, -z'

_cell_length_a                    8.930(2)
_cell_length_b                    13.321(3)
_cell_length_c                    18.691(4)
_cell_angle_alpha                 95.615(4)
_cell_angle_beta                  97.542(4)
_cell_angle_gamma                 104.149(4)
_cell_volume                      2117.6(9)
_cell_formula_units_Z             2
_cell_measurement_temperature     298(2)
_cell_measurement_reflns_used     885
_cell_measurement_theta_min       2.50
_cell_measurement_theta_max       26.35

_exptl_crystal_description        'large plate'
_exptl_crystal_colour             colourless
_exptl_crystal_size_max           0.70
_exptl_crystal_size_mid           0.40
_exptl_crystal_size_min           0.18
_exptl_crystal_density_meas       'not measured'
_exptl_crystal_density_diffrn     1.734
_exptl_crystal_density_method     'not measured'
_exptl_crystal_F_000              1116
_exptl_absorpt_coefficient_mu     1.928
_exptl_absorpt_correction_type    empirical
_exptl_abs_corr_T_min_T_max_ratio 0.738
_exptl_absorpt_process_details    SADABS

_exptl_special_details
;
 ?
;

_diffrn_ambient_temperature       298(2)
_diffrn_radiation_wavelength      0.71073
_diffrn_radiation_type            MoK\a
_diffrn_radiation_source          'fine-focus sealed tube'
_diffrn_radiation_monochromator   graphite
_diffrn_measurement_device_type   'CCD area detector'
_diffrn_measurement_method        'phi and omega scans'
_diffrn_detector_area_resol_mean  ?
_diffrn_standards_number          ?
_diffrn_standards_interval_count  ?
```

```
_diffrn_standards_interval_time   ?
_diffrn_standards_decay_%         ?
_diffrn_reflns_number             18996
_diffrn_reflns_av_R_equivalents   0.0275
_diffrn_reflns_av_sigmaI/netI     0.0437
_diffrn_reflns_limit_h_min        -11
_diffrn_reflns_limit_h_max        11
_diffrn_reflns_limit_k_min        -17
_diffrn_reflns_limit_k_max        16
_diffrn_reflns_limit_l_min        -24
_diffrn_reflns_limit_l_max        24
_diffrn_reflns_theta_min          1.11
_diffrn_reflns_theta_max          28.30
_reflns_number_total              9140
_reflns_number_gt                 7839
_reflns_threshold_expression      >2sigma(I)

_computing_data_collection        'Bruker SMART'
_computing_cell_refinement        'Bruker SMART'
_computing_data_reduction         'Bruker SAINT'
_computing_structure_solution     'SHELXS-97 (Sheldrick, 1990)'
_computing_structure_refinement   'SHELXL-97 (Sheldrick, 1997)'
_computing_molecular_graphics     'Bruker SHELXTL'
_computing_publication_material   'Bruker SHELXTL'

_refine_special_details
;
 Refinement of F^2^ against ALL reflections.  The weighted R-factor wR and
 goodness of fit S are based on F^2^, conventional R-factors R are based
 on F, with F set to zero for negative F^2^. The threshold expression of
 F^2^ > 2sigma(F^2^) is used only for calculating R-factors(gt) etc. and is
 not relevant to the choice of reflections for refinement.  R-factors based
 on F^2^ are statistically about twice as large as those based on F, and R-
 factors based on ALL data will be even larger.
;

_refine_ls_structure_factor_coef  Fsqd
_refine_ls_matrix_type            full
_refine_ls_weighting_scheme       calc
_refine_ls_weighting_details
 'calc w=1/[\s^2^(Fo^2^)+(0.0582P)^2^+1.0532P] where P=(Fo^2^+2Fc^2^)/3'
_atom_sites_solution_primary      direct
_atom_sites_solution_secondary    difmap
_atom_sites_solution_hydrogens    geom
_refine_ls_hydrogen_treatment     mixed
_refine_ls_extinction_method      none
_refine_ls_extinction_coef        ?
_refine_ls_number_reflns          9140
_refine_ls_number_parameters      532
_refine_ls_number_restraints      0
_refine_ls_R_factor_all           0.0498
_refine_ls_R_factor_gt            0.0406
_refine_ls_wR_factor_ref          0.1069
_refine_ls_wR_factor_gt           0.1012
_refine_ls_goodness_of_fit_ref    1.061
```

```
_refine_ls_restrained_S_all      1.061
_refine_ls_shift/su_max          0.001
_refine_ls_shift/su_mean         0.000

loop_
 _atom_site_label
 _atom_site_type_symbol
 _atom_site_fract_x
 _atom_site_fract_y
 _atom_site_fract_z
 _atom_site_U_iso_or_equiv
 _atom_site_adp_type
 _atom_site_occupancy
 _atom_site_symmetry_multiplicity
 _atom_site_calc_flag
 _atom_site_refinement_flags
 _atom_site_disorder_assembly
 _atom_site_disorder_group
Tb1 Tb -0.13762(2) -0.394766(13) 0.256545(10) 0.03464(8) Uani 1 1 d . . .
N1 N -0.1202(5) -0.2969(3) 0.1429(2) 0.0473(9) Uani 1 1 d . . .
H1A H -0.2195 -0.2925 0.1285 0.057 Uiso 1 1 calc R . .
C2 C -0.0802(7) -0.3527(4) 0.0782(3) 0.0583(13) Uani 1 1 d . . .
H2A H 0.0326 -0.3377 0.0818 0.070 Uiso 1 1 calc R . .
H2B H -0.1208 -0.3281 0.0345 0.070 Uiso 1 1 calc R . .
C3 C -0.1482(6) -0.4686(4) 0.0731(3) 0.0543(12) Uani 1 1 d . . .
H3A H -0.1157 -0.5035 0.0322 0.065 Uiso 1 1 calc R . .
H3B H -0.2614 -0.4838 0.0641 0.065 Uiso 1 1 calc R . .
N4 N -0.0976(5) -0.5108(3) 0.1413(2) 0.0455(8) Uani 1 1 d . . .
C5 C 0.0704(6) -0.5082(4) 0.1470(3) 0.0562(12) Uani 1 1 d . . .
H5A H 0.1271 -0.4416 0.1351 0.067 Uiso 1 1 calc R . .
H5B H 0.0820 -0.5627 0.1113 0.067 Uiso 1 1 calc R . .
C6 C 0.1425(6) -0.5231(4) 0.2214(3) 0.0554(12) Uani 1 1 d . . .
H6A H 0.0873 -0.5900 0.2334 0.066 Uiso 1 1 calc R . .
H6B H 0.2507 -0.5239 0.2208 0.066 Uiso 1 1 calc R . .
N7 N 0.1360(4) -0.4384(3) 0.2780(2) 0.0422(8) Uani 1 1 d . . .
C8 C 0.2673(6) -0.3461(4) 0.2767(3) 0.0557(12) Uani 1 1 d . . .
H8A H 0.2788 -0.3386 0.2264 0.067 Uiso 1 1 calc R . .
H8B H 0.3632 -0.3580 0.3007 0.067 Uiso 1 1 calc R . .
C9 C 0.2450(5) -0.2447(4) 0.3135(3) 0.0547(12) Uani 1 1 d . . .
H9A H 0.2414 -0.2496 0.3647 0.066 Uiso 1 1 calc R . .
H9B H 0.3335 -0.1873 0.3100 0.066 Uiso 1 1 calc R . .
N10 N 0.0981(4) -0.2233(3) 0.2790(2) 0.0440(8) Uani 1 1 d . . .
C11 C 0.1248(6) -0.1818(4) 0.2097(3) 0.0563(13) Uani 1 1 d . . .
H11A H 0.1851 -0.2211 0.1847 0.068 Uiso 1 1 calc R . .
H11B H 0.1861 -0.1096 0.2206 0.068 Uiso 1 1 calc R . .
C12 C -0.0257(6) -0.1872(3) 0.1596(3) 0.0538(12) Uani 1 1 d . . .
H12A H -0.0842 -0.1446 0.1829 0.065 Uiso 1 1 calc R . .
H12B H -0.0018 -0.1603 0.1148 0.065 Uiso 1 1 calc R . .
C13 C -0.1931(6) -0.6196(4) 0.1382(3) 0.0541(12) Uani 1 1 d . . .
H13A H -0.1366 -0.6673 0.1195 0.065 Uiso 1 1 calc R . .
H13B H -0.2897 -0.6299 0.1045 0.065 Uiso 1 1 calc R . .
C14 C -0.2316(5) -0.6454(3) 0.2113(3) 0.0441(10) Uani 1 1 d . . .
O15 O -0.1934(4) -0.5743(2) 0.26541(17) 0.0457(7) Uani 1 1 d . . .
N16 N -0.3068(5) -0.7404(3) 0.2167(2) 0.0520(10) Uani 1 1 d . . .
C17 C -0.3526(8) -0.8268(4) 0.1564(4) 0.0817(19) Uani 1 1 d . . .
```

```
H17A H -0.3242 -0.8011 0.1125 0.123 Uiso 1 1 calc R . .
H17B H -0.4637 -0.8564 0.1497 0.123 Uiso 1 1 calc R . .
H17C H -0.2998 -0.8795 0.1675 0.123 Uiso 1 1 calc R . .
C18 C -0.3429(7) -0.7693(4) 0.2871(3) 0.0684(15) Uani 1 1 d . . .
H18A H -0.3091 -0.7085 0.3231 0.103 Uiso 1 1 calc R . .
H18B H -0.2896 -0.8206 0.3009 0.103 Uiso 1 1 calc R . .
H18C H -0.4537 -0.7978 0.2834 0.103 Uiso 1 1 calc R . .
C19 C 0.1550(6) -0.4733(4) 0.3505(3) 0.0521(11) Uani 1 1 d . . .
H19A H 0.2651 -0.4653 0.3678 0.063 Uiso 1 1 calc R . .
H19B H 0.1010 -0.5467 0.3468 0.063 Uiso 1 1 calc R . .
C21 C 0.0898(5) -0.4105(3) 0.4037(3) 0.0459(10) Uani 1 1 d . . .
O20 O -0.0151(4) -0.3699(2) 0.37954(17) 0.0476(7) Uani 1 1 d . . .
N22 N 0.1420(5) -0.3999(3) 0.4739(2) 0.0541(10) Uani 1 1 d . . .
C23 C 0.2617(7) -0.4487(5) 0.5059(4) 0.0780(18) Uani 1 1 d . . .
H23A H 0.2897 -0.4914 0.4681 0.117 Uiso 1 1 calc R . .
H23B H 0.2206 -0.4913 0.5410 0.117 Uiso 1 1 calc R . .
H23C H 0.3526 -0.3953 0.5294 0.117 Uiso 1 1 calc R . .
C24 C 0.0848(7) -0.3327(5) 0.5248(3) 0.0718(16) Uani 1 1 d . . .
H24A H 0.0068 -0.3059 0.4984 0.108 Uiso 1 1 calc R . .
H24B H 0.1704 -0.2757 0.5488 0.108 Uiso 1 1 calc R . .
H24C H 0.0399 -0.3726 0.5604 0.108 Uiso 1 1 calc R . .
C25 C 0.0554(5) -0.1454(3) 0.3293(3) 0.0537(12) Uani 1 1 d . . .
H25A H 0.1138 -0.0756 0.3240 0.064 Uiso 1 1 calc R . .
H25B H 0.0825 -0.1571 0.3792 0.064 Uiso 1 1 calc R . .
C26 C -0.1179(5) -0.1543(3) 0.3127(2) 0.0412(9) Uani 1 1 d . . .
O27 O -0.2085(3) -0.2404(2) 0.28392(17) 0.0450(7) Uani 1 1 d . . .
N28 N -0.1702(4) -0.0734(3) 0.3290(2) 0.0478(9) Uani 1 1 d . . .
C29 C -0.0738(7) 0.0252(4) 0.3717(4) 0.0726(17) Uani 1 1 d . . .
H29A H 0.0339 0.0234 0.3791 0.109 Uiso 1 1 calc R . .
H29B H -0.1078 0.0341 0.4180 0.109 Uiso 1 1 calc R . .
H29C H -0.0847 0.0825 0.3458 0.109 Uiso 1 1 calc R . .
C30 C -0.3383(6) -0.0830(4) 0.3130(4) 0.0672(15) Uani 1 1 d . . .
H30A H -0.3899 -0.1495 0.2848 0.101 Uiso 1 1 calc R . .
H30B H -0.3561 -0.0282 0.2859 0.101 Uiso 1 1 calc R . .
H30C H -0.3793 -0.0775 0.3578 0.101 Uiso 1 1 calc R . .
O1W O -0.3926(4) -0.4462(2) 0.17977(18) 0.0509(8) Uani 1 1 d . . .
O2W O -0.3372(4) -0.4306(2) 0.33494(18) 0.0502(8) Uani 1 1 d . . .
O3W O -0.5754(5) -0.6093(3) 0.3314(2) 0.0694(10) Uani 1 1 d . . .
O4W O 0.4065(5) -0.6206(3) 0.1097(2) 0.0872(14) Uani 1 1 d . . .
O11 O -0.2929(5) -0.7035(4) -0.0382(3) 0.1039(17) Uani 1 1 d . . .
O12 O -0.5553(6) -0.6961(4) -0.0312(3) 0.0930(15) Uani 1 1 d . . .
O13 O -0.4716(6) -0.7120(3) -0.1462(2) 0.0866(14) Uani 1 1 d . . .
S1 S -0.44947(15) -0.73007(9) -0.07182(7) 0.0493(3) Uani 1 1 d . . .
C1S C -0.5073(9) -0.8707(5) -0.0796(4) 0.0807(18) Uani 1 1 d . . .
F11 F -0.5033(10) -0.9025(4) -0.0177(4) 0.182(3) Uani 1 1 d . . .
F12 F -0.6544(6) -0.9059(4) -0.1138(4) 0.152(2) Uani 1 1 d . . .
F13 F -0.4266(7) -0.9139(3) -0.1205(3) 0.1279(18) Uani 1 1 d . . .
O21 O 0.1598(10) -0.9232(4) 0.2322(3) 0.136(2) Uani 1 1 d . . .
O22 O 0.0170(7) -0.7964(5) 0.2201(4) 0.128(2) Uani 1 1 d . . .
O23 O 0.2815(6) -0.7559(4) 0.2030(3) 0.0933(14) Uani 1 1 d . . .
S2 S 0.1417(2) -0.83701(11) 0.19938(9) 0.0714(4) Uani 1 1 d . . .
C2S C 0.0892(10) -0.8853(5) 0.1038(4) 0.089(2) Uani 1 1 d . . .
F21 F 0.1900(9) -0.9201(8) 0.0784(4) 0.206(4) Uani 1 1 d . . .
F22 F 0.0641(9) -0.8102(5) 0.0672(3) 0.179(3) Uani 1 1 d . . .
F23 F -0.0415(7) -0.9591(4) 0.0891(3) 0.141(2) Uani 1 1 d . . .
```

```
O31 O -0.1704(6) -0.1732(4) 0.4818(3) 0.0980(15) Uani 1 1 d . . .
O32 O -0.3018(9) -0.2933(5) 0.5543(3) 0.127(2) Uani 1 1 d . . .
O33 O -0.4215(6) -0.2882(4) 0.4335(3) 0.0992(16) Uani 1 1 d . . .
S3 S -0.31535(19) -0.23486(11) 0.49692(8) 0.0658(4) Uani 1 1 d . . .
C3S C -0.4115(9) -0.1408(6) 0.5302(4) 0.0843(19) Uani 1 1 d . . .
F31 F -0.4250(13) -0.0772(7) 0.4858(5) 0.235(5) Uani 1 1 d . . .
F32 F -0.3392(7) -0.0832(6) 0.5882(4) 0.191(4) Uani 1 1 d . . .
F33 F -0.5488(6) -0.1799(5) 0.5424(4) 0.177(3) Uani 1 1 d . . .

loop_
 _atom_site_aniso_label
 _atom_site_aniso_U_11
 _atom_site_aniso_U_22
 _atom_site_aniso_U_33
 _atom_site_aniso_U_23
 _atom_site_aniso_U_13
 _atom_site_aniso_U_12
Tb1 0.03580(11) 0.02815(10) 0.03950(12) 0.00394(7) 0.00698(8) 0.00724(7)
N1 0.050(2) 0.045(2) 0.049(2) 0.0151(17) 0.0087(17) 0.0125(16)
C2 0.064(3) 0.065(3) 0.050(3) 0.021(2) 0.016(2) 0.015(2)
C3 0.068(3) 0.058(3) 0.038(2) 0.005(2) 0.015(2) 0.017(2)
N4 0.054(2) 0.0420(19) 0.043(2) 0.0041(16) 0.0124(17) 0.0158(17)
C5 0.061(3) 0.064(3) 0.055(3) 0.009(2) 0.024(2) 0.029(2)
C6 0.056(3) 0.056(3) 0.065(3) 0.010(2) 0.021(2) 0.029(2)
N7 0.042(2) 0.0412(19) 0.049(2) 0.0096(16) 0.0128(16) 0.0164(15)
C8 0.040(2) 0.054(3) 0.078(4) 0.014(2) 0.014(2) 0.016(2)
C9 0.032(2) 0.048(3) 0.079(4) 0.009(2) 0.001(2) 0.0037(19)
N10 0.0303(17) 0.0360(18) 0.062(2) 0.0052(16) 0.0044(16) 0.0034(14)
C11 0.049(3) 0.042(2) 0.077(4) 0.019(2) 0.016(2) 0.001(2)
C12 0.062(3) 0.040(2) 0.066(3) 0.023(2) 0.020(2) 0.014(2)
C13 0.067(3) 0.041(2) 0.053(3) -0.005(2) 0.014(2) 0.012(2)
C14 0.048(2) 0.036(2) 0.052(3) 0.0049(19) 0.009(2) 0.0170(18)
O15 0.0578(19) 0.0332(14) 0.0470(17) 0.0038(13) 0.0114(15) 0.0122(13)
N16 0.061(2) 0.0308(17) 0.059(2) 0.0018(16) 0.002(2) 0.0082(16)
C17 0.094(5) 0.040(3) 0.095(5) -0.014(3) 0.003(4) 0.002(3)
C18 0.080(4) 0.047(3) 0.079(4) 0.022(3) 0.013(3) 0.011(3)
C19 0.055(3) 0.056(3) 0.054(3) 0.015(2) 0.010(2) 0.027(2)
C21 0.043(2) 0.044(2) 0.050(3) 0.009(2) 0.006(2) 0.0104(19)
O20 0.0464(18) 0.0534(18) 0.0447(17) 0.0021(14) 0.0054(14) 0.0190(14)
N22 0.050(2) 0.064(3) 0.048(2) 0.0131(19) -0.0010(18) 0.0156(19)
C23 0.065(4) 0.086(4) 0.081(4) 0.031(3) -0.012(3) 0.020(3)
C24 0.068(4) 0.094(4) 0.046(3) 0.001(3) 0.003(3) 0.013(3)
C25 0.043(2) 0.036(2) 0.075(3) -0.004(2) 0.002(2) 0.0045(18)
C26 0.042(2) 0.032(2) 0.047(2) 0.0025(17) 0.0051(19) 0.0076(17)
O27 0.0370(16) 0.0337(14) 0.0604(19) 0.0018(13) 0.0016(14) 0.0068(12)
N28 0.046(2) 0.0328(18) 0.062(2) 0.0018(16) 0.0059(18) 0.0077(15)
C29 0.075(4) 0.036(2) 0.098(5) -0.015(3) 0.015(3) 0.009(2)
C30 0.057(3) 0.054(3) 0.093(4) 0.000(3) 0.009(3) 0.026(2)
O1W 0.0452(18) 0.0456(17) 0.0562(19) 0.0038(14) 0.0006(15) 0.0064(14)
O2W 0.0495(18) 0.0443(17) 0.0543(19) -0.0011(14) 0.0181(15) 0.0052(14)
O3W 0.063(2) 0.056(2) 0.084(3) 0.0094(19) 0.012(2) 0.0052(17)
O4W 0.089(3) 0.067(2) 0.085(3) -0.017(2) 0.024(2) -0.013(2)
O11 0.065(3) 0.097(3) 0.130(4) -0.012(3) -0.014(3) 0.008(2)
O12 0.113(4) 0.086(3) 0.093(3) 0.006(2) 0.054(3) 0.031(3)
O13 0.146(4) 0.075(3) 0.055(2) 0.020(2) 0.024(3) 0.051(3)
```

```
S1 0.0533(7) 0.0459(6) 0.0471(6) 0.0058(5) 0.0091(5) 0.0098(5)
C1S 0.090(5) 0.060(3) 0.090(5) 0.016(3) 0.016(4) 0.010(3)
F11 0.312(9) 0.101(4) 0.145(5) 0.082(4) 0.047(6) 0.042(5)
F12 0.107(4) 0.091(3) 0.217(6) -0.015(4) 0.012(4) -0.030(3)
F13 0.141(4) 0.064(2) 0.190(5) 0.009(3) 0.049(4) 0.040(3)
O21 0.226(8) 0.070(3) 0.113(4) 0.027(3) 0.011(5) 0.045(4)
O22 0.098(4) 0.122(5) 0.168(6) -0.005(4) 0.036(4) 0.037(4)
O23 0.091(3) 0.087(3) 0.084(3) 0.004(2) 0.008(3) -0.004(3)
S2 0.0777(10) 0.0480(7) 0.0868(11) 0.0163(7) 0.0128(8) 0.0109(7)
C2S 0.098(5) 0.066(4) 0.085(5) 0.018(4) 0.002(4) -0.011(4)
F21 0.140(5) 0.330(11) 0.124(5) -0.096(6) 0.011(4) 0.069(6)
F22 0.245(8) 0.122(4) 0.122(4) 0.053(4) -0.051(5) -0.018(5)
F23 0.140(4) 0.093(3) 0.137(4) -0.001(3) -0.027(3) -0.040(3)
O31 0.076(3) 0.095(3) 0.119(4) 0.004(3) 0.032(3) 0.010(3)
O32 0.172(6) 0.137(5) 0.111(4) 0.063(4) 0.060(4) 0.075(5)
O33 0.093(3) 0.099(3) 0.087(3) -0.041(3) 0.011(3) 0.013(3)
S3 0.0780(10) 0.0548(7) 0.0636(8) 0.0004(6) 0.0178(7) 0.0147(7)
C3S 0.088(5) 0.068(4) 0.094(5) -0.009(4) 0.023(4) 0.018(4)
F31 0.405(14) 0.198(7) 0.223(8) 0.082(7) 0.164(9) 0.228(9)
F32 0.133(5) 0.187(6) 0.201(7) -0.144(6) 0.009(4) 0.018(4)
F33 0.090(3) 0.153(5) 0.270(8) -0.074(5) 0.077(4) 0.012(3)

_geom_special_details
;
 All esds (except the esd in the dihedral angle between two l.s. planes)
 are estimated using the full covariance matrix.  The cell esds are taken
 into account individually in the estimation of esds in distances, angles
 and torsion angles; correlations between esds in cell parameters are only
 used when they are defined by crystal symmetry.  An approximate
(isotropic)
 treatment of cell esds is used for estimating esds involving l.s. planes.
;

loop_
 _geom_bond_atom_site_label_1
 _geom_bond_atom_site_label_2
 _geom_bond_distance
 _geom_bond_site_symmetry_2
 _geom_bond_publ_flag
Tb1 O27 2.326(3) . ?
Tb1 O15 2.348(3) . ?
Tb1 O20 2.368(3) . ?
Tb1 O1W 2.429(3) . ?
Tb1 O2W 2.441(3) . ?
Tb1 N1 2.600(4) . ?
Tb1 N7 2.637(4) . ?
Tb1 N4 2.642(4) . ?
Tb1 N10 2.656(3) . ?
N1 C12 1.479(6) . ?
N1 C2 1.487(7) . ?
C2 C3 1.502(7) . ?
C3 N4 1.502(6) . ?
N4 C5 1.482(6) . ?
N4 C13 1.482(6) . ?
C5 C6 1.507(7) . ?
```

```
C6 N7 1.487(6) . ?
N7 C19 1.477(6) . ?
N7 C8 1.482(6) . ?
C8 C9 1.524(7) . ?
C9 N10 1.489(6) . ?
N10 C11 1.483(6) . ?
N10 C25 1.484(6) . ?
C11 C12 1.516(7) . ?
C13 C14 1.504(7) . ?
C14 O15 1.265(5) . ?
C14 N16 1.300(5) . ?
N16 C18 1.461(7) . ?
N16 C17 1.469(7) . ?
C19 C21 1.503(7) . ?
C21 O20 1.248(5) . ?
C21 N22 1.315(6) . ?
N22 C24 1.466(7) . ?
N22 C23 1.473(7) . ?
C25 C26 1.511(6) . ?
C26 O27 1.253(5) . ?
C26 N28 1.300(6) . ?
N28 C30 1.463(7) . ?
N28 C29 1.471(6) . ?
O11 S1 1.399(5) . ?
O12 S1 1.415(5) . ?
O13 S1 1.431(4) . ?
S1 C1S 1.803(6) . ?
C1S F11 1.271(8) . ?
C1S F13 1.302(8) . ?
C1S F12 1.331(9) . ?
O21 S2 1.387(5) . ?
O22 S2 1.432(6) . ?
O23 S2 1.427(5) . ?
S2 C2S 1.798(8) . ?
C2S F21 1.234(10) . ?
C2S F23 1.306(8) . ?
C2S F22 1.312(9) . ?
O31 S3 1.432(5) . ?
O32 S3 1.395(5) . ?
O33 S3 1.421(5) . ?
S3 C3S 1.790(7) . ?
C3S F31 1.258(10) . ?
C3S F32 1.263(9) . ?
C3S F33 1.270(8) . ?

loop_
 _geom_angle_atom_site_label_1
 _geom_angle_atom_site_label_2
 _geom_angle_atom_site_label_3
 _geom_angle
 _geom_angle_site_symmetry_1
 _geom_angle_site_symmetry_3
 _geom_angle_publ_flag
O27 Tb1 O15 145.59(11) . . ?
O27 Tb1 O20 86.85(11) . . ?
```

```
O15 Tb1 O20 86.04(11) . . ?
O27 Tb1 O1W 82.94(11) . . ?
O15 Tb1 O1W 82.43(11) . . ?
O20 Tb1 O1W 142.40(11) . . ?
O27 Tb1 O2W 72.70(11) . . ?
O15 Tb1 O2W 73.17(11) . . ?
O20 Tb1 O2W 70.60(11) . . ?
O1W Tb1 O2W 71.80(11) . . ?
O27 Tb1 N1 72.74(12) . . ?
O15 Tb1 N1 130.40(11) . . ?
O20 Tb1 N1 138.46(12) . . ?
O1W Tb1 N1 71.65(12) . . ?
O2W Tb1 N1 131.89(12) . . ?
O27 Tb1 N7 131.19(10) . . ?
O15 Tb1 N7 74.33(11) . . ?
O20 Tb1 N7 64.53(11) . . ?
O1W Tb1 N7 143.23(11) . . ?
O2W Tb1 N7 125.43(11) . . ?
N1 Tb1 N7 102.51(12) . . ?
O27 Tb1 N4 138.74(11) . . ?
O15 Tb1 N4 65.68(11) . . ?
O20 Tb1 N4 130.59(11) . . ?
O1W Tb1 N4 75.58(12) . . ?
O2W Tb1 N4 129.93(11) . . ?
N1 Tb1 N4 67.23(12) . . ?
N7 Tb1 N4 69.04(12) . . ?
O27 Tb1 N10 65.41(11) . . ?
O15 Tb1 N10 141.66(11) . . ?
O20 Tb1 N10 71.26(11) . . ?
O1W Tb1 N10 133.79(11) . . ?
O2W Tb1 N10 123.74(11) . . ?
N1 Tb1 N10 67.40(12) . . ?
N7 Tb1 N10 68.14(11) . . ?
N4 Tb1 N10 106.28(12) . . ?
C12 N1 C2 111.9(4) . . ?
C12 N1 Tb1 113.7(3) . . ?
C2 N1 Tb1 116.0(3) . . ?
N1 C2 C3 110.7(4) . . ?
C2 C3 N4 112.2(4) . . ?
C5 N4 C13 110.2(4) . . ?
C5 N4 C3 109.4(4) . . ?
C13 N4 C3 108.9(4) . . ?
C5 N4 Tb1 108.8(3) . . ?
C13 N4 Tb1 109.6(3) . . ?
C3 N4 Tb1 109.9(3) . . ?
N4 C5 C6 113.5(4) . . ?
N7 C6 C5 111.4(4) . . ?
C19 N7 C8 108.6(4) . . ?
C19 N7 C6 109.4(4) . . ?
C8 N7 C6 108.5(4) . . ?
C19 N7 Tb1 107.7(3) . . ?
C8 N7 Tb1 112.1(3) . . ?
C6 N7 Tb1 110.5(3) . . ?
N7 C8 C9 113.4(4) . . ?
N10 C9 C8 111.1(4) . . ?
```

```
C11 N10 C25 110.1(4) . . ?
C11 N10 C9 108.7(4) . . ?
C25 N10 C9 109.0(4) . . ?
C11 N10 Tb1 111.1(3) . . ?
C25 N10 Tb1 107.0(2) . . ?
C9 N10 Tb1 110.9(2) . . ?
N10 C11 C12 113.1(4) . . ?
N1 C12 C11 109.3(4) . . ?
N4 C13 C14 112.7(4) . . ?
O15 C14 N16 121.7(4) . . ?
O15 C14 C13 119.6(4) . . ?
N16 C14 C13 118.7(4) . . ?
C14 O15 Tb1 124.2(3) . . ?
C14 N16 C18 120.4(4) . . ?
C14 N16 C17 124.5(5) . . ?
C18 N16 C17 115.0(4) . . ?
N7 C19 C21 110.4(4) . . ?
O20 C21 N22 121.5(4) . . ?
O20 C21 C19 118.3(4) . . ?
N22 C21 C19 120.2(4) . . ?
C21 O20 Tb1 125.5(3) . . ?
C21 N22 C24 119.6(4) . . ?
C21 N22 C23 124.0(5) . . ?
C24 N22 C23 116.4(5) . . ?
N10 C25 C26 110.2(4) . . ?
O27 C26 N28 121.4(4) . . ?
O27 C26 C25 118.9(4) . . ?
N28 C26 C25 119.7(4) . . ?
C26 O27 Tb1 126.1(3) . . ?
C26 N28 C30 119.2(4) . . ?
C26 N28 C29 124.0(4) . . ?
C30 N28 C29 116.2(4) . . ?
O11 S1 O12 116.1(3) . . ?
O11 S1 O13 114.3(3) . . ?
O12 S1 O13 113.0(3) . . ?
O11 S1 C1S 103.8(3) . . ?
O12 S1 C1S 105.1(3) . . ?
O13 S1 C1S 102.5(3) . . ?
F11 C1S F13 111.5(7) . . ?
F11 C1S F12 106.9(7) . . ?
F13 C1S F12 104.4(6) . . ?
F11 C1S S1 111.9(6) . . ?
F13 C1S S1 112.2(5) . . ?
F12 C1S S1 109.4(5) . . ?
O21 S2 O23 115.4(4) . . ?
O21 S2 O22 113.9(5) . . ?
O23 S2 O22 111.5(4) . . ?
O21 S2 C2S 104.6(4) . . ?
O23 S2 C2S 103.4(3) . . ?
O22 S2 C2S 106.9(4) . . ?
F21 C2S F23 107.3(8) . . ?
F21 C2S F22 108.1(8) . . ?
F23 C2S F22 105.3(7) . . ?
F21 C2S S2 113.4(6) . . ?
F23 C2S S2 112.4(6) . . ?
```

```
F22 C2S S2 109.9(6) . . ?
O32 S3 O33 115.6(4) . . ?
O32 S3 O31 115.1(4) . . ?
O33 S3 O31 113.7(3) . . ?
O32 S3 C3S 103.6(4) . . ?
O33 S3 C3S 102.3(3) . . ?
O31 S3 C3S 104.3(3) . . ?
F31 C3S F32 103.8(8) . . ?
F31 C3S F33 105.8(9) . . ?
F32 C3S F33 105.8(7) . . ?
F31 C3S S3 111.7(6) . . ?
F32 C3S S3 114.4(6) . . ?
F33 C3S S3 114.4(5) . . ?

loop_
 _geom_torsion_atom_site_label_1
 _geom_torsion_atom_site_label_2
 _geom_torsion_atom_site_label_3
 _geom_torsion_atom_site_label_4
 _geom_torsion
 _geom_torsion_site_symmetry_1
 _geom_torsion_site_symmetry_2
 _geom_torsion_site_symmetry_3
 _geom_torsion_site_symmetry_4
 _geom_torsion_publ_flag
O27 Tb1 N1 C12 51.9(3) . . . . ?
O15 Tb1 N1 C12 -157.7(3) . . . . ?
O20 Tb1 N1 C12 -12.2(4) . . . . ?
O1W Tb1 N1 C12 140.0(3) . . . . ?
O2W Tb1 N1 C12 97.7(3) . . . . ?
N7 Tb1 N1 C12 -77.7(3) . . . . ?
N4 Tb1 N1 C12 -138.4(3) . . . . ?
N10 Tb1 N1 C12 -18.1(3) . . . . ?
O27 Tb1 N1 C2 -176.3(4) . . . . ?
O15 Tb1 N1 C2 -25.8(4) . . . . ?
O20 Tb1 N1 C2 119.7(3) . . . . ?
O1W Tb1 N1 C2 -88.1(3) . . . . ?
O2W Tb1 N1 C2 -130.5(3) . . . . ?
N7 Tb1 N1 C2 54.1(3) . . . . ?
N4 Tb1 N1 C2 -6.5(3) . . . . ?
N10 Tb1 N1 C2 113.8(4) . . . . ?
C12 N1 C2 C3 166.5(4) . . . . ?
Tb1 N1 C2 C3 33.8(5) . . . . ?
N1 C2 C3 N4 -55.7(6) . . . . ?
C2 C3 N4 C5 -70.8(5) . . . . ?
C2 C3 N4 C13 168.7(4) . . . . ?
C2 C3 N4 Tb1 48.6(5) . . . . ?
O27 Tb1 N4 C5 113.4(3) . . . . ?
O15 Tb1 N4 C5 -97.5(3) . . . . ?
O20 Tb1 N4 C5 -36.7(3) . . . . ?
O1W Tb1 N4 C5 174.4(3) . . . . ?
O2W Tb1 N4 C5 -135.1(3) . . . . ?
N1 Tb1 N4 C5 98.5(3) . . . . ?
N7 Tb1 N4 C5 -15.8(3) . . . . ?
N10 Tb1 N4 C5 42.3(3) . . . . ?
```

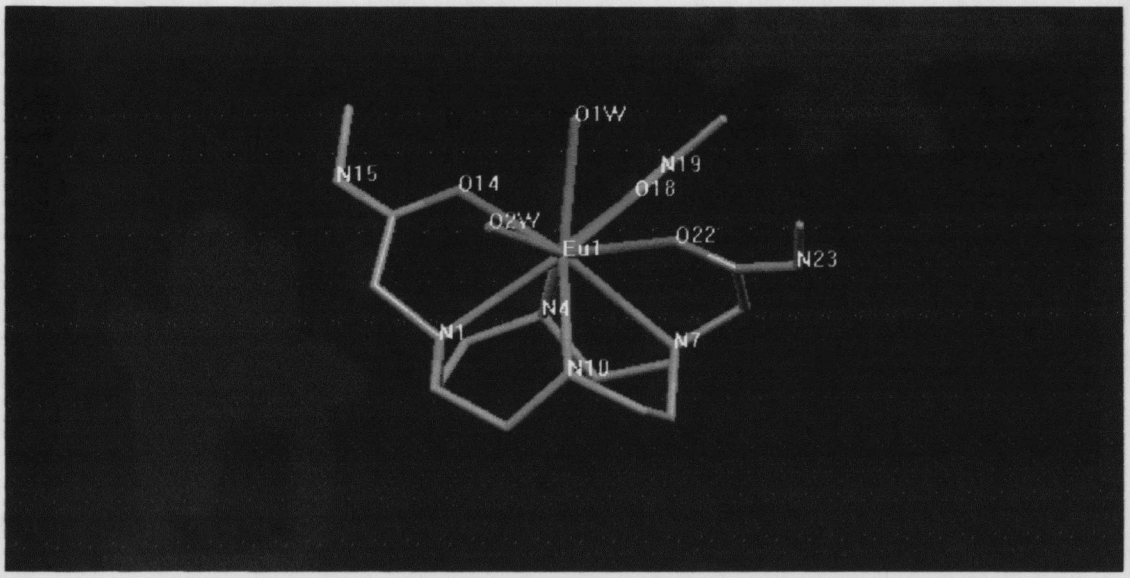
```
O27 Tb1 N4 C13 -126.1(3) . . . . ?
O15 Tb1 N4 C13 23.0(3) . . . . ?
O20 Tb1 N4 C13 83.9(3) . . . . ?
O1W Tb1 N4 C13 -65.1(3) . . . . ?
O2W Tb1 N4 C13 -14.6(4) . . . . ?
N1 Tb1 N4 C13 -141.0(3) . . . . ?
N7 Tb1 N4 C13 104.7(3) . . . . ?
N10 Tb1 N4 C13 162.9(3) . . . . ?
O27 Tb1 N4 C3 -6.4(4) . . . . ?
O15 Tb1 N4 C3 142.7(3) . . . . ?
O20 Tb1 N4 C3 -156.5(3) . . . . ?
O1W Tb1 N4 C3 54.6(3) . . . . ?
O2W Tb1 N4 C3 105.1(3) . . . . ?
N1 Tb1 N4 C3 -21.3(3) . . . . ?
N7 Tb1 N4 C3 -135.6(3) . . . . ?
N10 Tb1 N4 C3 -77.5(3) . . . . ?
C13 N4 C5 C6 -74.7(5) . . . . ?
C3 N4 C5 C6 165.6(4) . . . . ?
Tb1 N4 C5 C6 45.5(5) . . . . ?
N4 C5 C6 N7 -61.7(6) . . . . ?
C5 C6 N7 C19 160.4(4) . . . . ?
C5 C6 N7 C8 -81.3(5) . . . . ?
C5 C6 N7 Tb1 42.0(4) . . . . ?
O27 Tb1 N7 C19 89.8(3) . . . . ?
O15 Tb1 N7 C19 -63.5(3) . . . . ?
O20 Tb1 N7 C19 29.6(3) . . . . ?
O1W Tb1 N7 C19 -116.3(3) . . . . ?
O2W Tb1 N7 C19 -8.1(3) . . . . ?
N1 Tb1 N7 C19 167.7(3) . . . . ?
N4 Tb1 N7 C19 -133.0(3) . . . . ?
N10 Tb1 N7 C19 108.5(3) . . . . ?
O27 Tb1 N7 C8 -29.6(4) . . . . ?
O15 Tb1 N7 C8 177.2(3) . . . . ?
O20 Tb1 N7 C8 -89.7(3) . . . . ?
O1W Tb1 N7 C8 124.3(3) . . . . ?
O2W Tb1 N7 C8 -127.5(3) . . . . ?
N1 Tb1 N7 C8 48.3(3) . . . . ?
N4 Tb1 N7 C8 107.7(3) . . . . ?
N10 Tb1 N7 C8 -10.8(3) . . . . ?
O27 Tb1 N7 C6 -150.7(3) . . . . ?
O15 Tb1 N7 C6 56.0(3) . . . . ?
O20 Tb1 N7 C6 149.1(3) . . . . ?
O1W Tb1 N7 C6 3.2(4) . . . . ?
O2W Tb1 N7 C6 111.3(3) . . . . ?
N1 Tb1 N7 C6 -72.8(3) . . . . ?
N4 Tb1 N7 C6 -13.5(3) . . . . ?
N10 Tb1 N7 C6 -132.0(3) . . . . ?
C19 N7 C8 C9 -79.7(5) . . . . ?
C6 N7 C8 C9 161.4(4) . . . . ?
Tb1 N7 C8 C9 39.1(5) . . . . ?
N7 C8 C9 N10 -58.0(6) . . . . ?
C8 C9 N10 C11 -77.7(5) . . . . ?
C8 C9 N10 C25 162.3(4) . . . . ?
C8 C9 N10 Tb1 44.8(5) . . . . ?
O27 Tb1 N10 C11 -92.3(3) . . . . ?
```

```
O15 Tb1 N10 C11 115.6(3) . . . . ?
O20 Tb1 N10 C11 172.5(3) . . . . ?
O1W Tb1 N10 C11 -41.0(4) . . . . ?
O2W Tb1 N10 C11 -137.9(3) . . . . ?
N1 Tb1 N10 C11 -11.7(3) . . . . ?
N7 Tb1 N10 C11 103.2(3) . . . . ?
N4 Tb1 N10 C11 44.4(3) . . . . ?
O27 Tb1 N10 C25 27.9(3) . . . . ?
O15 Tb1 N10 C25 -124.2(3) . . . . ?
O20 Tb1 N10 C25 -67.3(3) . . . . ?
O1W Tb1 N10 C25 79.1(3) . . . . ?
O2W Tb1 N10 C25 -17.8(3) . . . . ?
N1 Tb1 N10 C25 108.5(3) . . . . ?
N7 Tb1 N10 C25 -136.7(3) . . . . ?
N4 Tb1 N10 C25 164.6(3) . . . . ?
O27 Tb1 N10 C9 146.6(3) . . . . ?
O15 Tb1 N10 C9 -5.5(4) . . . . ?
O20 Tb1 N10 C9 51.4(3) . . . . ?
O1W Tb1 N10 C9 -162.1(3) . . . . ?
O2W Tb1 N10 C9 101.0(3) . . . . ?
N1 Tb1 N10 C9 -132.7(3) . . . . ?
N7 Tb1 N10 C9 -17.9(3) . . . . ?
N4 Tb1 N10 C9 -76.7(3) . . . . ?
C25 N10 C11 C12 -77.7(5) . . . . ?
C9 N10 C11 C12 163.0(4) . . . . ?
Tb1 N10 C11 C12 40.6(5) . . . . ?
C2 N1 C12 C11 -88.4(5) . . . . ?
Tb1 N1 C12 C11 45.4(5) . . . . ?
N10 C11 C12 N1 -58.4(6) . . . . ?
C5 N4 C13 C14 96.6(5) . . . . ?
C3 N4 C13 C14 -143.3(4) . . . . ?
Tb1 N4 C13 C14 -23.1(5) . . . . ?
N4 C13 C14 O15 5.6(7) . . . . ?
N4 C13 C14 N16 -175.8(4) . . . . ?
N16 C14 O15 Tb1 -158.3(3) . . . . ?
C13 C14 O15 Tb1 20.2(6) . . . . ?
O27 Tb1 O15 C14 119.1(3) . . . . ?
O20 Tb1 O15 C14 -162.4(4) . . . . ?
O1W Tb1 O15 C14 53.5(4) . . . . ?
O2W Tb1 O15 C14 126.7(4) . . . . ?
N1 Tb1 O15 C14 -4.5(4) . . . . ?
N7 Tb1 O15 C14 -97.7(4) . . . . ?
N4 Tb1 O15 C14 -24.0(3) . . . . ?
N10 Tb1 O15 C14 -109.7(4) . . . . ?
O15 C14 N16 C18 -3.1(7) . . . . ?
C13 C14 N16 C18 178.4(5) . . . . ?
O15 C14 N16 C17 -179.0(5) . . . . ?
C13 C14 N16 C17 2.4(8) . . . . ?
C8 N7 C19 C21 83.2(5) . . . . ?
C6 N7 C19 C21 -158.5(4) . . . . ?
Tb1 N7 C19 C21 -38.3(4) . . . . ?
N7 C19 C21 O20 25.6(6) . . . . ?
N7 C19 C21 N22 -155.0(4) . . . . ?
N22 C21 O20 Tb1 -173.9(3) . . . . ?
C19 C21 O20 Tb1 5.5(6) . . . . ?
```

```
O27 Tb1 O20 C21 -159.4(3) . . . . ?
O15 Tb1 O20 C21 54.3(3) . . . . ?
O1W Tb1 O20 C21 126.5(3) . . . . ?
O2W Tb1 O20 C21 127.9(4) . . . . ?
N1 Tb1 O20 C21 -100.0(4) . . . . ?
N7 Tb1 O20 C21 -20.2(3) . . . . ?
N4 Tb1 O20 C21 1.4(4) . . . . ?
N10 Tb1 O20 C21 -94.3(4) . . . . ?
O20 C21 N22 C24 -4.7(7) . . . . ?
C19 C21 N22 C24 176.0(5) . . . . ?
O20 C21 N22 C23 177.9(5) . . . . ?
C19 C21 N22 C23 -1.5(7) . . . . ?
C11 N10 C25 C26 84.3(4) . . . . ?
C9 N10 C25 C26 -156.5(4) . . . . ?
Tb1 N10 C25 C26 -36.5(4) . . . . ?
N10 C25 C26 O27 26.5(6) . . . . ?
N10 C25 C26 N28 -154.0(4) . . . . ?
N28 C26 O27 Tb1 -176.8(3) . . . . ?
C25 C26 O27 Tb1 2.7(6) . . . . ?
O15 Tb1 O27 C26 131.4(3) . . . . ?
O20 Tb1 O27 C26 53.1(4) . . . . ?
O1W Tb1 O27 C26 -163.2(4) . . . . ?
O2W Tb1 O27 C26 123.8(4) . . . . ?
N1 Tb1 O27 C26 -90.2(4) . . . . ?
N7 Tb1 O27 C26 1.5(4) . . . . ?
N4 Tb1 O27 C26 -104.6(4) . . . . ?
N10 Tb1 O27 C26 -17.7(3) . . . . ?
O27 C26 N28 C30 -0.3(7) . . . . ?
C25 C26 N28 C30 -179.7(5) . . . . ?
O27 C26 N28 C29 171.2(5) . . . . ?
C25 C26 N28 C29 -8.2(7) . . . . ?
O11 S1 C1S F11 64.1(7) . . . . ?
O12 S1 C1S F11 -58.3(7) . . . . ?
O13 S1 C1S F11 -176.6(7) . . . . ?
O11 S1 C1S F13 -62.1(6) . . . . ?
O12 S1 C1S F13 175.4(6) . . . . ?
O13 S1 C1S F13 57.1(6) . . . . ?
O11 S1 C1S F12 -177.6(6) . . . . ?
O12 S1 C1S F12 60.0(6) . . . . ?
O13 S1 C1S F12 -58.3(6) . . . . ?
O21 S2 C2S F21 -60.9(8) . . . . ?
O23 S2 C2S F21 60.3(8) . . . . ?
O22 S2 C2S F21 178.0(7) . . . . ?
O21 S2 C2S F23 61.1(8) . . . . ?
O23 S2 C2S F23 -177.8(6) . . . . ?
O22 S2 C2S F23 -60.0(7) . . . . ?
O21 S2 C2S F22 178.0(7) . . . . ?
O23 S2 C2S F22 -60.8(7) . . . . ?
O22 S2 C2S F22 56.9(7) . . . . ?
O32 S3 C3S F31 176.2(8) . . . . ?
O33 S3 C3S F31 -63.3(8) . . . . ?
O31 S3 C3S F31 55.4(9) . . . . ?
O32 S3 C3S F32 58.7(8) . . . . ?
O33 S3 C3S F32 179.1(7) . . . . ?
O31 S3 C3S F32 -62.2(8) . . . . ?
```

```
O32 S3 C3S F33 -63.7(8) . . . . ?
O33 S3 C3S F33 56.8(8) . . . . ?
O31 S3 C3S F33 175.5(7) . . . . ?

_diffrn_measured_fraction_theta_max    0.869
_diffrn_reflns_theta_full              28.30
_diffrn_measured_fraction_theta_full   0.869
_refine_diff_density_max    1.159
_refine_diff_density_min   -0.455
_refine_diff_density_rms    0.104
```



Crystallography data for Eu.181

```
data_

_audit_creation_method            SHELXL-97
_chemical_name_systematic
;
 ?
;
_chemical_name_common             ?
_chemical_melting_point           ?
_chemical_formula_moiety          ?
_chemical_formula_sum
 'C20 H35 Eu F9 N7 O16 S3'
_chemical_formula_weight          1048.69

loop_
 _atom_type_symbol
 _atom_type_description
 _atom_type_scat_dispersion_real
 _atom_type_scat_dispersion_imag
 _atom_type_scat_source
 'C'  'C'   0.0033   0.0016
 'International Tables Vol C Tables 4.2.6.8 and 6.1.1.4'
 'H'  'H'   0.0000   0.0000
 'International Tables Vol C Tables 4.2.6.8 and 6.1.1.4'
 'N'  'N'   0.0061   0.0033
 'International Tables Vol C Tables 4.2.6.8 and 6.1.1.4'
 'O'  'O'   0.0106   0.0060
 'International Tables Vol C Tables 4.2.6.8 and 6.1.1.4'
 'Eu'  'Eu'  -0.1578   3.6682
 'International Tables Vol C Tables 4.2.6.8 and 6.1.1.4'
 'S'  'S'   0.1246   0.1234
 'International Tables Vol C Tables 4.2.6.8 and 6.1.1.4'
 'F'  'F'   0.0171   0.0103
```

```
 'International Tables Vol C Tables 4.2.6.8 and 6.1.1.4'

_symmetry_cell_setting            Triclinic
_symmetry_space_group_name_H-M    P-1

loop_
 _symmetry_equiv_pos_as_xyz
 'x, y, z'
 '-x, -y, -z'

_cell_length_a                    8.992(4)
_cell_length_b                    13.112(5)
_cell_length_c                    17.623(7)
_cell_angle_alpha                 79.370(6)
_cell_angle_beta                  82.503(6)
_cell_angle_gamma                 71.816(6)
_cell_volume                      1934.3(14)
_cell_formula_units_Z             2
_cell_measurement_temperature     153(2)
_cell_measurement_reflns_used     ?
_cell_measurement_theta_min       ?
_cell_measurement_theta_max       ?

_exptl_crystal_description        plate
_exptl_crystal_colour             colourless
_exptl_crystal_size_max           0.36
_exptl_crystal_size_mid           0.23
_exptl_crystal_size_min           0.10
_exptl_crystal_density_meas       not_measured
_exptl_crystal_density_diffrn     1.800
_exptl_crystal_density_method     'not measured'
_exptl_crystal_F_000              1048
_exptl_absorpt_coefficient_mu     1.899
_exptl_absorpt_correction_type    Empirical
_exptl_absorpt_correction_T_min   0.547
_exptl_absorpt_correction_T_max   0.928
_exptl_absorpt_process_details    SADABS

_exptl_special_details
;
 ?
;

_diffrn_ambient_temperature       153(2)
_diffrn_radiation_wavelength      0.71073
_diffrn_radiation_type            MoK\a
_diffrn_radiation_source          'fine-focus sealed tube'
_diffrn_radiation_monochromator   graphite
_diffrn_measurement_device_type   'CCD area detector'
_diffrn_measurement_method        'phi and omega scans'
_diffrn_detector_area_resol_mean  ?
_diffrn_standards_number          ?
_diffrn_standards_interval_count  ?
_diffrn_standards_interval_time   ?
_diffrn_standards_decay_%         ?
```

```
_diffrn_reflns_number              13494
_diffrn_reflns_av_R_equivalents    0.0618
_diffrn_reflns_av_sigmaI/netI      0.0865
_diffrn_reflns_limit_h_min         -10
_diffrn_reflns_limit_h_max         10
_diffrn_reflns_limit_k_min         -15
_diffrn_reflns_limit_k_max         15
_diffrn_reflns_limit_l_min         -20
_diffrn_reflns_limit_l_max         20
_diffrn_reflns_theta_min           1.18
_diffrn_reflns_theta_max           25.00
_reflns_number_total               6732
_reflns_number_gt                  4972
_reflns_threshold_expression       >2sigma(I)

_computing_data_collection         'Bruker SMART'
_computing_cell_refinement         'Bruker SMART'
_computing_data_reduction          'Bruker SHELXTL'
_computing_structure_solution      'SHELXS-97 (Sheldrick, 1990)'
_computing_structure_refinement    'SHELXL-97 (Sheldrick, 1997)'
_computing_molecular_graphics      'Bruker SHELXTL'
_computing_publication_material    'Bruker SHELXTL'

_refine_special_details
;
 Refinement of F^2^ against ALL reflections.  The weighted R-factor wR and
 goodness of fit S are based on F^2^, conventional R-factors R are based
 on F, with F set to zero for negative F^2^. The threshold expression of
 F^2^ > 2sigma(F^2^) is used only for calculating R-factors(gt) etc. and is
 not relevant to the choice of reflections for refinement.  R-factors based
 on F^2^ are statistically about twice as large as those based on F, and R-
 factors based on ALL data will be even larger.
;

_refine_ls_structure_factor_coef  Fsqd
_refine_ls_matrix_type            full
_refine_ls_weighting_scheme       calc
_refine_ls_weighting_details
 'calc w=1/[\s^2^(Fo^2^)+(0.1092P)^2^+0.0000P] where P=(Fo^2^+2Fc^2^)/3'
_atom_sites_solution_primary      direct
_atom_sites_solution_secondary    difmap
_atom_sites_solution_hydrogens    geom
_refine_ls_hydrogen_treatment     mixed
_refine_ls_extinction_method      none
_refine_ls_extinction_coef        ?
_refine_ls_number_reflns          6732
_refine_ls_number_parameters      491
_refine_ls_number_restraints      57
_refine_ls_R_factor_all           0.0874
_refine_ls_R_factor_gt            0.0623
_refine_ls_wR_factor_ref          0.1688
_refine_ls_wR_factor_gt           0.1523
_refine_ls_goodness_of_fit_ref    0.980
_refine_ls_restrained_S_all       0.982
_refine_ls_shift/su_max           0.003
```

```
_refine_ls_shift/su_mean          0.000

loop_
 _atom_site_label
 _atom_site_type_symbol
 _atom_site_fract_x
 _atom_site_fract_y
 _atom_site_fract_z
 _atom_site_U_iso_or_equiv
 _atom_site_adp_type
 _atom_site_occupancy
 _atom_site_symmetry_multiplicity
 _atom_site_calc_flag
 _atom_site_refinement_flags
 _atom_site_disorder_assembly
 _atom_site_disorder_group
Eu1 Eu 0.92897(5) 0.67890(3) 0.73894(2) 0.03022(16) Uani 1 1 d . . .
N1 N 1.0133(8) 0.8577(6) 0.6805(4) 0.0343(16) Uani 1 1 d . . .
C2 C 1.1846(10) 0.8406(7) 0.6831(5) 0.038(2) Uani 1 1 d . . .
H2A H 1.2043 0.9120 0.6760 0.046 Uiso 1 1 calc R . .
H2B H 1.2428 0.8025 0.6397 0.046 Uiso 1 1 calc R . .
C3 C 1.2460(10) 0.7744(7) 0.7591(5) 0.0362(19) Uani 1 1 d . . .
H3A H 1.3600 0.7645 0.7581 0.043 Uiso 1 1 calc R . .
H3B H 1.1926 0.8142 0.8025 0.043 Uiso 1 1 calc R . .
N4 N 1.2175(8) 0.6654(6) 0.7719(4) 0.0355(16) Uani 1 1 d . . .
C5 C 1.3433(9) 0.5932(7) 0.7248(5) 0.0365(19) Uani 1 1 d . . .
H5A H 1.4431 0.5714 0.7499 0.044 Uiso 1 1 calc R . .
H5B H 1.3589 0.6341 0.6728 0.044 Uiso 1 1 calc R . .
C6 C 1.3022(9) 0.4925(7) 0.7164(5) 0.038(2) Uani 1 1 d . . .
H6A H 1.3876 0.4476 0.6845 0.045 Uiso 1 1 calc R . .
H6B H 1.2938 0.4490 0.7682 0.045 Uiso 1 1 calc R . .
N7 N 1.1527(8) 0.5194(6) 0.6800(4) 0.0326(15) Uani 1 1 d . . .
C8 C 1.1815(10) 0.5479(8) 0.5952(5) 0.040(2) Uani 1 1 d . . .
H8A H 1.2304 0.4800 0.5728 0.048 Uiso 1 1 calc R . .
H8B H 1.2575 0.5905 0.5852 0.048 Uiso 1 1 calc R . .
C9 C 1.0359(10) 0.6122(7) 0.5543(5) 0.0358(19) Uani 1 1 d . . .
H9A H 1.0648 0.6303 0.4984 0.043 Uiso 1 1 calc R . .
H9B H 0.9627 0.5680 0.5600 0.043 Uiso 1 1 calc R . .
N10 N 0.9574(8) 0.7138(6) 0.5874(4) 0.0354(16) Uani 1 1 d . . .
H10 H 0.8555 0.7372 0.5721 0.043 Uiso 1 1 calc R . .
C11 C 1.0272(11) 0.8012(7) 0.5530(5) 0.041(2) Uani 1 1 d . . .
H11A H 0.9971 0.8280 0.4992 0.049 Uiso 1 1 calc R . .
H11B H 1.1431 0.7720 0.5511 0.049 Uiso 1 1 calc R . .
C12 C 0.9738(11) 0.8940(7) 0.5988(5) 0.039(2) Uani 1 1 d . . .
H12A H 1.0245 0.9505 0.5748 0.046 Uiso 1 1 calc R . .
H12B H 0.8588 0.9268 0.5974 0.046 Uiso 1 1 calc R . .
C13 C 0.9211(11) 0.9438(7) 0.7270(5) 0.040(2) Uani 1 1 d . . .
H13A H 0.8163 0.9790 0.7070 0.048 Uiso 1 1 calc R . .
H13B H 0.9755 1.0000 0.7223 0.048 Uiso 1 1 calc R . .
C14 C 0.9026(11) 0.8956(7) 0.8106(5) 0.040(2) Uani 1 1 d . . .
O14 O 0.8926(7) 0.8004(5) 0.8293(3) 0.0383(14) Uani 1 1 d . . .
N15 N 0.8926(11) 0.9565(6) 0.8639(4) 0.052(2) Uani 1 1 d . . .
H15 H 0.9041 1.0216 0.8492 0.062 Uiso 1 1 calc R . .
C16 C 0.8630(18) 0.9203(9) 0.9466(6) 0.071(4) Uani 1 1 d . . .
H16A H 0.7808 0.8840 0.9540 0.106 Uiso 1 1 calc R . .
```

```
H16B H 0.8288 0.9831 0.9741 0.106 Uiso 1 1 calc R . .
H16C H 0.9596 0.8693 0.9669 0.106 Uiso 1 1 calc R . .
C17 C 1.2288(11) 0.6202(8) 0.8552(5) 0.042(2) Uani 1 1 d . . .
H17A H 1.1813 0.6793 0.8867 0.051 Uiso 1 1 calc R . .
H17B H 1.3406 0.5883 0.8660 0.051 Uiso 1 1 calc R . .
C18 C 1.1455(11) 0.5341(7) 0.8782(5) 0.040(2) Uani 1 1 d . . .
O18 O 1.0299(7) 0.5392(5) 0.8440(3) 0.0364(13) Uani 1 1 d . . .
N19 N 1.1961(9) 0.4585(7) 0.9361(4) 0.050(2) Uani 1 1 d . . .
H19 H 1.2778 0.4599 0.9580 0.060 Uiso 1 1 calc R . .
C20 C 1.1249(13) 0.3715(9) 0.9669(6) 0.059(3) Uani 1 1 d . . .
H20A H 1.0162 0.3939 0.9529 0.089 Uiso 1 1 calc R . .
H20B H 1.1264 0.3566 1.0234 0.089 Uiso 1 1 calc R . .
H20C H 1.1846 0.3057 0.9450 0.089 Uiso 1 1 calc R . .
C21 C 1.0921(10) 0.4236(7) 0.6981(5) 0.039(2) Uani 1 1 d . . .
H21A H 1.1059 0.3904 0.7529 0.046 Uiso 1 1 calc R . .
H21B H 1.1518 0.3685 0.6650 0.046 Uiso 1 1 calc R . .
C22 C 0.9183(10) 0.4591(8) 0.6836(5) 0.037(2) Uani 1 1 d . . .
O22 O 0.8326(6) 0.5482(5) 0.6986(3) 0.0381(14) Uani 1 1 d . . .
N23 N 0.8703(8) 0.3876(6) 0.6580(4) 0.0391(17) Uani 1 1 d . . .
H23 H 0.9395 0.3272 0.6465 0.047 Uiso 1 1 calc R . .
C24 C 0.7057(11) 0.4062(10) 0.6484(6) 0.057(3) Uani 1 1 d . . .
H24A H 0.6498 0.3936 0.6991 0.085 Uiso 1 1 calc R . .
H24B H 0.6959 0.3563 0.6155 0.085 Uiso 1 1 calc R . .
H24C H 0.6603 0.4813 0.6239 0.085 Uiso 1 1 calc R . .
O1W O 0.7053(7) 0.6608(5) 0.8301(4) 0.0420(15) Uani 1 1 d . . .
O2W O 0.6877(7) 0.8212(5) 0.6947(3) 0.0414(14) Uani 1 1 d . . .
O11 O 1.5429(10) 1.3220(7) 0.4771(6) 0.088(3) Uani 1 1 d D . .
O12 O 1.4277(14) 1.2118(8) 0.4262(5) 0.113(4) Uani 1 1 d D . .
O13 O 1.3061(9) 1.2870(6) 0.5386(6) 0.092(3) Uani 1 1 d D . .
S1 S 1.4476(3) 1.25180(18) 0.49196(13) 0.0391(5) Uani 1 1 d D . .
C1S C 1.5611(13) 1.1305(9) 0.5503(6) 0.069(3) Uani 1 1 d D . .
F11 F 1.6869(9) 1.0763(7) 0.5058(5) 0.113(3) Uani 1 1 d D . .
F12 F 1.6101(17) 1.1527(10) 0.6077(6) 0.174(6) Uani 1 1 d D . .
F13 F 1.4843(10) 1.0610(6) 0.5758(5) 0.104(3) Uani 1 1 d D . .
O3W O 0.0942(8) 0.1821(5) 0.6332(4) 0.0499(16) Uani 1 1 d . . .
O21 O 0.828(2) 0.3389(13) 0.8547(9) 0.063(4) Uiso 0.50 1 d P A 2
O22 O 0.6704(19) 0.4670(13) 0.9361(10) 0.067(4) Uiso 0.50 1 d P A 2
O23 O 0.5499(17) 0.3997(12) 0.8455(9) 0.059(4) Uiso 0.50 1 d P A 2
S2 S 0.6736(8) 0.3806(6) 0.8923(5) 0.044(2) Uiso 0.50 1 d P A 2
C2S C 0.653(2) 0.2737(16) 0.9672(12) 0.049(5) Uiso 0.50 1 d P A 2
F21 F 0.5200(18) 0.3038(12) 1.0125(9) 0.080(4) Uiso 0.50 1 d P A 2
F22 F 0.7706(17) 0.2357(11) 1.0133(8) 0.077(4) Uiso 0.50 1 d P A 2
F23 F 0.6470(15) 0.1890(10) 0.9374(8) 0.066(3) Uiso 0.50 1 d P A 2
O21' O 0.5290(16) 0.3396(11) 0.9311(8) 0.051(3) Uiso 0.50 1 d P B 1
O22' O 0.7350(18) 0.3942(13) 0.9742(9) 0.060(4) Uiso 0.50 1 d P B 1
O23' O 0.6393(16) 0.4702(11) 0.8467(8) 0.049(3) Uiso 0.50 1 d P B 1
S2' S 0.6637(7) 0.3821(5) 0.9112(4) 0.0352(18) Uiso 0.50 1 d P B 1
C2S' C 0.811(2) 0.2697(15) 0.8701(10) 0.037(4) Uiso 0.50 1 d P B 1
F21' F 0.7676(16) 0.2465(11) 0.8095(8) 0.067(3) Uiso 0.50 1 d P B 1
F22' F 0.8417(17) 0.1792(12) 0.9207(8) 0.077(4) Uiso 0.50 1 d P B 1
F23' F 0.9423(16) 0.2953(10) 0.8490(7) 0.063(3) Uiso 0.50 1 d P B 1
O4W O 0.4545(18) 0.2150(12) 1.0651(9) 0.062(4) Uiso 0.50 1 d P C 1
O31 O 1.299(2) 0.9820(15) 0.8911(8) 0.069(6) Uiso 0.50 1 d PD D 2
O32 O 1.4201(13) 0.9576(9) 0.7595(7) 0.037(3) Uiso 0.50 1 d PD D 2
O33 O 1.1575(14) 1.0795(11) 0.7803(8) 0.055(3) Uiso 0.50 1 d PD D 2
```

```
S3 S 1.3047(6) 1.0241(4) 0.8103(3) 0.0398(10) Uiso 0.50 1 d PD D 2
C3S C 1.389(2) 1.1349(13) 0.8096(11) 0.078(8) Uiso 0.50 1 d PD D 2
F31 F 1.3895(18) 1.1943(11) 0.7383(8) 0.086(4) Uiso 0.50 1 d PD D 2
F32 F 1.3120(19) 1.2015(12) 0.8545(10) 0.088(5) Uiso 0.50 1 d PD D 2
F33 F 1.535(2) 1.0984(14) 0.8278(12) 0.103(6) Uiso 0.50 1 d PD D 2
O31' O 1.5179(19) 0.8934(12) 0.8302(11) 0.087(5) Uiso 0.50 1 d PD E 1
O32' O 1.3418(18) 1.0217(13) 0.7397(7) 0.067(4) Uiso 0.50 1 d PD E 1
O33' O 1.2596(18) 0.9857(13) 0.8765(9) 0.051(5) Uiso 0.50 1 d PD E 1
S3' S 1.3901(7) 0.9898(5) 0.8196(3) 0.0527(13) Uiso 0.50 1 d PD E 1
C3S' C 1.459(2) 1.0983(13) 0.8345(10) 0.065(6) Uiso 0.50 1 d PD E 1
F31' F 1.5881(15) 1.1041(11) 0.7847(8) 0.074(4) Uiso 0.50 1 d PD E 1
F32' F 1.5041(18) 1.0863(12) 0.9010(8) 0.086(4) Uiso 0.50 1 d PD E 1
F33' F 1.3583(18) 1.1944(12) 0.8121(10) 0.083(4) Uiso 0.50 1 d PD E 1
O5W O 0.9889(17) 1.1411(12) 0.8086(9) 0.057(4) Uiso 0.50 1 d P F 1

loop_
 _atom_site_aniso_label
 _atom_site_aniso_U_11
 _atom_site_aniso_U_22
 _atom_site_aniso_U_33
 _atom_site_aniso_U_23
 _atom_site_aniso_U_13
 _atom_site_aniso_U_12
Eu1 0.0284(2) 0.0346(3) 0.0235(2) -0.00417(15) 0.00280(15) -0.00559(17)
N1 0.036(4) 0.037(4) 0.023(3) 0.005(3) -0.001(3) -0.007(3)
C2 0.038(5) 0.046(5) 0.031(5) 0.001(4) 0.005(4) -0.019(4)
C3 0.035(5) 0.041(5) 0.032(5) 0.000(4) -0.004(4) -0.011(4)
N4 0.035(4) 0.039(4) 0.030(4) -0.007(3) -0.002(3) -0.007(3)
C5 0.024(4) 0.046(5) 0.040(5) -0.009(4) 0.001(4) -0.012(4)
C6 0.026(4) 0.041(5) 0.040(5) -0.009(4) 0.000(4) -0.001(4)
N7 0.024(3) 0.040(4) 0.037(4) -0.013(3) 0.000(3) -0.010(3)
C8 0.031(5) 0.049(5) 0.040(5) -0.019(4) 0.012(4) -0.010(4)
C9 0.034(4) 0.050(5) 0.024(4) -0.013(4) 0.004(3) -0.012(4)
N10 0.033(4) 0.051(4) 0.023(3) -0.010(3) 0.001(3) -0.012(3)
C11 0.042(5) 0.054(6) 0.024(4) 0.001(4) -0.003(4) -0.014(4)
C12 0.043(5) 0.040(5) 0.024(4) 0.008(4) 0.004(4) -0.009(4)
C13 0.050(5) 0.036(5) 0.030(5) -0.001(4) 0.007(4) -0.013(4)
C14 0.051(6) 0.032(5) 0.035(5) -0.002(4) -0.003(4) -0.011(4)
O14 0.044(4) 0.035(3) 0.033(3) -0.006(3) 0.008(3) -0.012(3)
N15 0.091(7) 0.033(4) 0.033(4) -0.001(3) -0.007(4) -0.022(4)
C16 0.132(12) 0.058(7) 0.026(5) -0.010(5) 0.001(6) -0.034(7)
C17 0.043(5) 0.049(6) 0.038(5) -0.003(4) -0.008(4) -0.018(4)
C18 0.043(5) 0.038(5) 0.033(5) -0.005(4) 0.002(4) -0.007(4)
O18 0.038(3) 0.040(3) 0.027(3) 0.000(2) -0.002(3) -0.009(3)
N19 0.039(4) 0.064(5) 0.037(4) 0.012(4) -0.004(3) -0.013(4)
C20 0.050(6) 0.067(7) 0.044(6) 0.021(5) 0.001(5) -0.012(5)
C21 0.030(4) 0.046(5) 0.040(5) -0.013(4) 0.003(4) -0.010(4)
C22 0.030(4) 0.055(6) 0.033(5) -0.017(4) 0.010(4) -0.020(4)
O22 0.020(3) 0.055(4) 0.037(3) -0.019(3) 0.007(2) -0.006(3)
N23 0.023(4) 0.048(4) 0.048(5) -0.020(4) 0.008(3) -0.011(3)
C24 0.035(5) 0.086(8) 0.061(7) -0.039(6) 0.006(5) -0.024(5)
O1W 0.041(3) 0.040(3) 0.043(4) -0.006(3) 0.009(3) -0.013(3)
O2W 0.032(3) 0.045(4) 0.039(3) -0.004(3) 0.003(3) -0.004(3)
O11 0.062(5) 0.079(6) 0.121(8) 0.021(5) -0.001(5) -0.040(5)
O12 0.148(10) 0.102(8) 0.069(6) -0.035(6) -0.060(6) 0.024(7)
```

```
O13 0.063(5) 0.045(4) 0.143(9) -0.010(5) 0.056(5) -0.006(4)
S1 0.0318(11) 0.0447(13) 0.0383(12) -0.0050(10) 0.0020(9) -0.0102(10)
C1S 0.053(7) 0.084(9) 0.056(7) 0.017(6) -0.004(6) -0.017(6)
F11 0.057(4) 0.110(6) 0.114(7) 0.044(5) 0.017(4) 0.014(4)
F12 0.257(16) 0.178(11) 0.112(8) 0.050(8) -0.125(10) -0.097(11)
F13 0.111(6) 0.063(5) 0.104(6) 0.019(4) 0.045(5) -0.016(4)
O3W 0.061(4) 0.052(4) 0.038(4) -0.011(3) 0.000(3) -0.018(3)

_geom_special_details
;
 All esds (except the esd in the dihedral angle between two l.s. planes)
 are estimated using the full covariance matrix.  The cell esds are taken
 into account individually in the estimation of esds in distances, angles
 and torsion angles; correlations between esds in cell parameters are only
 used when they are defined by crystal symmetry.  An approximate
(isotropic)
 treatment of cell esds is used for estimating esds involving l.s. planes.
;

loop_
 _geom_bond_atom_site_label_1
 _geom_bond_atom_site_label_2
 _geom_bond_distance
 _geom_bond_site_symmetry_2
 _geom_bond_publ_flag
Eu1 O14 2.377(6) . ?
Eu1 O22 2.393(6) . ?
Eu1 O18 2.399(6) . ?
Eu1 O1W 2.448(6) . ?
Eu1 O2W 2.485(6) . ?
Eu1 N10 2.618(7) . ?
Eu1 N7 2.670(7) . ?
Eu1 N1 2.673(7) . ?
Eu1 N4 2.678(7) . ?
Eu1 C22 3.241(9) . ?
Eu1 C14 3.248(9) . ?
Eu1 C18 3.261(9) . ?
N1 C12 1.483(10) . ?
N1 C13 1.489(11) . ?
N1 C2 1.491(11) . ?
C2 C3 1.523(12) . ?
C3 N4 1.501(11) . ?
N4 C17 1.483(11) . ?
N4 C5 1.497(10) . ?
C5 C6 1.515(12) . ?
C6 N7 1.479(11) . ?
N7 C8 1.481(11) . ?
N7 C21 1.488(11) . ?
C8 C9 1.510(12) . ?
C9 N10 1.485(10) . ?
N10 C11 1.473(11) . ?
C11 C12 1.503(12) . ?
C13 C14 1.501(12) . ?
C14 O14 1.259(10) . ?
C14 N15 1.319(11) . ?
```

```
N15 C16 1.462(12) . ?
C17 C18 1.509(13) . ?
C18 O18 1.247(11) . ?
C18 N19 1.303(12) . ?
N19 C20 1.464(13) . ?
C21 C22 1.527(12) . ?
C22 O22 1.236(10) . ?
C22 N23 1.313(11) . ?
N23 C24 1.451(11) . ?
O11 S1 1.413(8) . ?
O12 S1 1.409(8) . ?
O13 S1 1.417(7) . ?
S1 C1S 1.812(11) . ?
C1S F12 1.268(13) . ?
C1S F13 1.293(12) . ?
C1S F11 1.368(13) . ?
O21 S2 1.447(18) . ?
O22 S2 1.476(17) . ?
O23 S2 1.403(16) . ?
S2 C2S 1.78(2) . ?
C2S F22 1.33(2) . ?
C2S F23 1.33(2) . ?
C2S F21 1.34(2) . ?
O21' S2' 1.463(15) . ?
O22' S2' 1.408(16) . ?
O23' S2' 1.448(15) . ?
S2' C2S' 1.836(19) . ?
C2S' F21' 1.30(2) . ?
C2S' F23' 1.32(2) . ?
C2S' F22' 1.32(2) . ?
O31 S3 1.429(13) . ?
O32 S3 1.456(10) . ?
O33 S3 1.413(12) . ?
S3 C3S 1.833(15) . ?
C3S F32 1.265(18) . ?
C3S F33 1.316(17) . ?
C3S F31 1.351(17) . ?
O31' S3' 1.420(13) . ?
O32' S3' 1.476(12) . ?
O33' S3' 1.448(12) . ?
S3' C3S' 1.793(15) . ?
C3S' F32' 1.255(17) . ?
C3S' F33' 1.328(17) . ?
C3S' F31' 1.373(18) . ?

loop_
 _geom_angle_atom_site_label_1
 _geom_angle_atom_site_label_2
 _geom_angle_atom_site_label_3
 _geom_angle
 _geom_angle_site_symmetry_1
 _geom_angle_site_symmetry_3
 _geom_angle_publ_flag
O14 Eu1 O22 145.59(19) . . ?
O14 Eu1 O18 85.1(2) . . ?
```

```
O22 Eu1 O18 85.9(2) . . ?
O14 Eu1 O1W 72.2(2) . . ?
O22 Eu1 O1W 73.39(19) . . ?
O18 Eu1 O1W 72.7(2) . . ?
O14 Eu1 O2W 79.5(2) . . ?
O22 Eu1 O2W 88.2(2) . . ?
O18 Eu1 O2W 143.3(2) . . ?
O1W Eu1 O2W 70.9(2) . . ?
O14 Eu1 N10 130.1(2) . . ?
O22 Eu1 N10 74.3(2) . . ?
O18 Eu1 N10 139.3(2) . . ?
O1W Eu1 N10 131.1(2) . . ?
O2W Eu1 N10 72.4(2) . . ?
O14 Eu1 N7 140.3(2) . . ?
O22 Eu1 N7 65.98(19) . . ?
O18 Eu1 N7 71.9(2) . . ?
O1W Eu1 N7 127.0(2) . . ?
O2W Eu1 N7 136.8(2) . . ?
N10 Eu1 N7 67.6(2) . . ?
O14 Eu1 N1 66.1(2) . . ?
O22 Eu1 N1 140.2(2) . . ?
O18 Eu1 N1 129.4(2) . . ?
O1W Eu1 N1 128.7(2) . . ?
O2W Eu1 N1 73.3(2) . . ?
N10 Eu1 N1 66.7(2) . . ?
N7 Eu1 N1 104.2(2) . . ?
O14 Eu1 N4 74.2(2) . . ?
O22 Eu1 N4 130.5(2) . . ?
O18 Eu1 N4 65.5(2) . . ?
O1W Eu1 N4 127.7(2) . . ?
O2W Eu1 N4 138.5(2) . . ?
N10 Eu1 N4 101.2(2) . . ?
N7 Eu1 N4 67.0(2) . . ?
N1 Eu1 N4 66.9(2) . . ?
O14 Eu1 C22 154.9(2) . . ?
O22 Eu1 C22 18.6(2) . . ?
O18 Eu1 C22 76.4(2) . . ?
O1W Eu1 C22 86.0(2) . . ?
O2W Eu1 C22 105.5(2) . . ?
N10 Eu1 C22 73.9(2) . . ?
N7 Eu1 C22 48.0(2) . . ?
N1 Eu1 C22 139.0(2) . . ?
N4 Eu1 C22 112.0(2) . . ?
O14 Eu1 C14 18.9(2) . . ?
O22 Eu1 C14 155.9(2) . . ?
O18 Eu1 C14 101.1(2) . . ?
O1W Eu1 C14 86.6(2) . . ?
O2W Eu1 C14 72.2(2) . . ?
N10 Eu1 C14 111.4(2) . . ?
N7 Eu1 C14 138.1(2) . . ?
N1 Eu1 C14 47.7(2) . . ?
N4 Eu1 C14 72.6(2) . . ?
C22 Eu1 C14 172.6(2) . . ?
O14 Eu1 C18 76.0(2) . . ?
O22 Eu1 C18 102.5(2) . . ?
```

```
O18 Eu1 C18 18.5(2) . . ?
O1W Eu1 C18 85.6(2) . . ?
O2W Eu1 C18 150.3(2) . . ?
N10 Eu1 C18 137.1(2) . . ?
N7 Eu1 C18 72.1(2) . . ?
N1 Eu1 C18 111.0(2) . . ?
N4 Eu1 C18 47.8(2) . . ?
C22 Eu1 C18 90.2(2) . . ?
C14 Eu1 C18 88.9(2) . . ?
C12 N1 C13 108.7(6) . . ?
C12 N1 C2 108.2(6) . . ?
C13 N1 C2 109.9(7) . . ?
C12 N1 Eu1 110.3(5) . . ?
C13 N1 Eu1 107.1(5) . . ?
C2 N1 Eu1 112.6(5) . . ?
N1 C2 C3 112.3(7) . . ?
N4 C3 C2 110.6(7) . . ?
C17 N4 C5 109.6(7) . . ?
C17 N4 C3 108.2(6) . . ?
C5 N4 C3 107.8(6) . . ?
C17 N4 Eu1 106.5(5) . . ?
C5 N4 Eu1 112.3(5) . . ?
C3 N4 Eu1 112.3(5) . . ?
N4 C5 C6 111.9(7) . . ?
N7 C6 C5 112.1(7) . . ?
C6 N7 C8 109.0(6) . . ?
C6 N7 C21 108.8(7) . . ?
C8 N7 C21 110.3(6) . . ?
C6 N7 Eu1 112.1(5) . . ?
C8 N7 Eu1 111.3(5) . . ?
C21 N7 Eu1 105.2(4) . . ?
N7 C8 C9 114.2(7) . . ?
N10 C9 C8 110.3(7) . . ?
C11 N10 C9 111.9(6) . . ?
C11 N10 Eu1 115.0(5) . . ?
C9 N10 Eu1 112.1(5) . . ?
N10 C11 C12 111.4(7) . . ?
N1 C12 C11 111.5(7) . . ?
N1 C13 C14 110.1(7) . . ?
O14 C14 N15 120.7(8) . . ?
O14 C14 C13 120.9(7) . . ?
N15 C14 C13 118.3(8) . . ?
O14 C14 Eu1 37.6(4) . . ?
N15 C14 Eu1 158.0(6) . . ?
C13 C14 Eu1 83.5(5) . . ?
C14 O14 Eu1 123.6(5) . . ?
C14 N15 C16 122.7(8) . . ?
N4 C17 C18 111.0(7) . . ?
O18 C18 N19 122.6(9) . . ?
O18 C18 C17 120.2(8) . . ?
N19 C18 C17 117.2(9) . . ?
O18 C18 Eu1 37.7(4) . . ?
N19 C18 Eu1 160.2(7) . . ?
C17 C18 Eu1 82.5(5) . . ?
C18 O18 Eu1 123.8(6) . . ?
```

```
C18 N19 C20 123.9(9) . . ?
N7 C21 C22 109.5(7) . . ?
O22 C22 N23 124.8(8) . . ?
O22 C22 C21 119.8(7) . . ?
N23 C22 C21 115.3(8) . . ?
O22 C22 Eu1 38.1(4) . . ?
N23 C22 Eu1 162.8(6) . . ?
C21 C22 Eu1 81.8(5) . . ?
C22 O22 Eu1 123.3(5) . . ?
C22 N23 C24 121.4(8) . . ?
O12 S1 O11 114.3(7) . . ?
O12 S1 O13 113.2(7) . . ?
O11 S1 O13 115.8(6) . . ?
O12 S1 C1S 102.6(6) . . ?
O11 S1 C1S 104.9(5) . . ?
O13 S1 C1S 104.1(5) . . ?
F12 C1S F13 108.3(10) . . ?
F12 C1S F11 109.0(12) . . ?
F13 C1S F11 104.6(10) . . ?
F12 C1S S1 111.8(10) . . ?
F13 C1S S1 113.2(8) . . ?
F11 C1S S1 109.7(7) . . ?
O23 S2 O21 114.5(10) . . ?
O23 S2 O22 117.7(10) . . ?
O21 S2 O22 110.5(10) . . ?
O23 S2 C2S 105.3(10) . . ?
O21 S2 C2S 104.6(10) . . ?
O22 S2 C2S 102.4(10) . . ?
F22 C2S F23 105.9(16) . . ?
F22 C2S F21 107.1(17) . . ?
F23 C2S F21 106.6(17) . . ?
F22 C2S S2 114.4(15) . . ?
F23 C2S S2 110.6(14) . . ?
F21 C2S S2 111.8(14) . . ?
O22' S2' O23' 116.9(9) . . ?
O22' S2' O21' 115.8(10) . . ?
O23' S2' O21' 112.6(9) . . ?
O22' S2' C2S' 103.7(9) . . ?
O23' S2' C2S' 103.3(9) . . ?
O21' S2' C2S' 101.8(8) . . ?
F21' C2S' F23' 107.3(15) . . ?
F21' C2S' F22' 106.3(15) . . ?
F23' C2S' F22' 108.3(15) . . ?
F21' C2S' S2' 113.4(13) . . ?
F23' C2S' S2' 109.6(13) . . ?
F22' C2S' S2' 111.7(13) . . ?
O33 S3 O31 115.5(10) . . ?
O33 S3 O32 115.6(8) . . ?
O31 S3 O32 117.1(10) . . ?
O33 S3 C3S 102.5(8) . . ?
O31 S3 C3S 100.6(10) . . ?
O32 S3 C3S 101.5(8) . . ?
F32 C3S F33 108.3(16) . . ?
F32 C3S F31 105.6(15) . . ?
F33 C3S F31 106.5(17) . . ?
```

```
F32 C3S S3 113.4(13) . . ?
F33 C3S S3 111.9(13) . . ?
F31 C3S S3 110.8(12) . . ?
O31' S3' O33' 111.9(10) . . ?
O31' S3' O32' 113.8(10) . . ?
O33' S3' O32' 112.6(10) . . ?
O31' S3' C3S' 106.6(10) . . ?
O33' S3' C3S' 107.3(9) . . ?
O32' S3' C3S' 103.9(8) . . ?
F32' C3S' F33' 114.8(16) . . ?
F32' C3S' F31' 105.1(15) . . ?
F33' C3S' F31' 100.8(14) . . ?
F32' C3S' S3' 113.3(13) . . ?
F33' C3S' S3' 111.2(12) . . ?
F31' C3S' S3' 110.7(11) . . ?

loop_
 _geom_torsion_atom_site_label_1
 _geom_torsion_atom_site_label_2
 _geom_torsion_atom_site_label_3
 _geom_torsion_atom_site_label_4
 _geom_torsion
 _geom_torsion_site_symmetry_1
 _geom_torsion_site_symmetry_2
 _geom_torsion_site_symmetry_3
 _geom_torsion_site_symmetry_4
 _geom_torsion_publ_flag
O14 Eu1 N1 C12 -143.5(6) . . . . ?
O22 Eu1 N1 C12 7.9(7) . . . . ?
O18 Eu1 N1 C12 155.4(5) . . . . ?
O1W Eu1 N1 C12 -105.0(5) . . . . ?
O2W Eu1 N1 C12 -57.8(5) . . . . ?
N10 Eu1 N1 C12 19.8(5) . . . . ?
N7 Eu1 N1 C12 77.4(5) . . . . ?
N4 Eu1 N1 C12 134.3(5) . . . . ?
C22 Eu1 N1 C12 36.7(7) . . . . ?
C14 Eu1 N1 C12 -138.7(6) . . . . ?
C18 Eu1 N1 C12 153.4(5) . . . . ?
O14 Eu1 N1 C13 -25.4(5) . . . . ?
O22 Eu1 N1 C13 126.0(5) . . . . ?
O18 Eu1 N1 C13 -86.5(6) . . . . ?
O1W Eu1 N1 C13 13.1(6) . . . . ?
O2W Eu1 N1 C13 60.3(5) . . . . ?
N10 Eu1 N1 C13 137.9(6) . . . . ?
N7 Eu1 N1 C13 -164.5(5) . . . . ?
N4 Eu1 N1 C13 -107.6(5) . . . . ?
C22 Eu1 N1 C13 154.8(5) . . . . ?
C14 Eu1 N1 C13 -20.6(5) . . . . ?
C18 Eu1 N1 C13 -88.6(5) . . . . ?
O14 Eu1 N1 C2 95.5(5) . . . . ?
O22 Eu1 N1 C2 -113.1(5) . . . . ?
O18 Eu1 N1 C2 34.4(6) . . . . ?
O1W Eu1 N1 C2 134.0(5) . . . . ?
O2W Eu1 N1 C2 -178.8(5) . . . . ?
N10 Eu1 N1 C2 -101.2(5) . . . . ?
```

```
N7 Eu1 N1 C2 -43.6(5) . . . . ?
N4 Eu1 N1 C2 13.3(5) . . . . ?
C22 Eu1 N1 C2 -84.3(6) . . . . ?
C14 Eu1 N1 C2 100.3(6) . . . . ?
C18 Eu1 N1 C2 32.3(6) . . . . ?
C12 N1 C2 C3 -164.2(7) . . . . ?
C13 N1 C2 C3 77.2(8) . . . . ?
Eu1 N1 C2 C3 -42.0(8) . . . . ?
N1 C2 C3 N4 58.6(9) . . . . ?
C2 C3 N4 C17 -161.4(7) . . . . ?
C2 C3 N4 C5 80.2(8) . . . . ?
C2 C3 N4 Eu1 -44.0(8) . . . . ?
O14 Eu1 N4 C17 64.2(5) . . . . ?
O22 Eu1 N4 C17 -88.1(5) . . . . ?
O18 Eu1 N4 C17 -27.6(5) . . . . ?
O1W Eu1 N4 C17 12.6(6) . . . . ?
O2W Eu1 N4 C17 117.0(5) . . . . ?
N10 Eu1 N4 C17 -167.0(5) . . . . ?
N7 Eu1 N4 C17 -107.3(5) . . . . ?
N1 Eu1 N4 C17 134.6(5) . . . . ?
C22 Eu1 N4 C17 -90.0(5) . . . . ?
C14 Eu1 N4 C17 83.8(5) . . . . ?
C18 Eu1 N4 C17 -21.1(5) . . . . ?
O14 Eu1 N4 C5 -175.8(6) . . . . ?
O22 Eu1 N4 C5 31.8(6) . . . . ?
O18 Eu1 N4 C5 92.4(5) . . . . ?
O1W Eu1 N4 C5 132.5(5) . . . . ?
O2W Eu1 N4 C5 -123.1(5) . . . . ?
N10 Eu1 N4 C5 -47.1(6) . . . . ?
N7 Eu1 N4 C5 12.6(5) . . . . ?
N1 Eu1 N4 C5 -105.5(6) . . . . ?
C22 Eu1 N4 C5 29.9(6) . . . . ?
C14 Eu1 N4 C5 -156.2(6) . . . . ?
C18 Eu1 N4 C5 98.8(6) . . . . ?
O14 Eu1 N4 C3 -54.1(5) . . . . ?
O22 Eu1 N4 C3 153.5(5) . . . . ?
O18 Eu1 N4 C3 -145.9(5) . . . . ?
O1W Eu1 N4 C3 -105.8(5) . . . . ?
O2W Eu1 N4 C3 -1.4(6) . . . . ?
N10 Eu1 N4 C3 74.7(5) . . . . ?
N7 Eu1 N4 C3 134.3(6) . . . . ?
N1 Eu1 N4 C3 16.2(5) . . . . ?
C22 Eu1 N4 C3 151.7(5) . . . . ?
C14 Eu1 N4 C3 -34.5(5) . . . . ?
C18 Eu1 N4 C3 -139.4(6) . . . . ?
C17 N4 C5 C6 77.6(9) . . . . ?
C3 N4 C5 C6 -164.8(7) . . . . ?
Eu1 N4 C5 C6 -40.5(8) . . . . ?
N4 C5 C6 N7 58.3(9) . . . . ?
C5 C6 N7 C8 79.2(8) . . . . ?
C5 C6 N7 C21 -160.5(7) . . . . ?
C5 C6 N7 Eu1 -44.5(8) . . . . ?
O14 Eu1 N7 C6 3.6(7) . . . . ?
O22 Eu1 N7 C6 -147.7(6) . . . . ?
O18 Eu1 N7 C6 -54.1(5) . . . . ?
```

```
O1W Eu1 N7 C6 -104.4(6) . . . . ?
O2W Eu1 N7 C6 153.8(5) . . . . ?
N10 Eu1 N7 C6 130.1(6) . . . . ?
N1 Eu1 N7 C6 73.2(6) . . . . ?
N4 Eu1 N7 C6 16.4(5) . . . . ?
C22 Eu1 N7 C6 -141.8(7) . . . . ?
C14 Eu1 N7 C6 32.5(7) . . . . ?
C18 Eu1 N7 C6 -34.6(5) . . . . ?
O14 Eu1 N7 C8 -118.7(5) . . . . ?
O22 Eu1 N7 C8 89.9(5) . . . . ?
O18 Eu1 N7 C8 -176.4(5) . . . . ?
O1W Eu1 N7 C8 133.2(5) . . . . ?
O2W Eu1 N7 C8 31.5(6) . . . . ?
N10 Eu1 N7 C8 7.8(5) . . . . ?
N1 Eu1 N7 C8 -49.1(5) . . . . ?
N4 Eu1 N7 C8 -105.9(5) . . . . ?
C22 Eu1 N7 C8 95.9(6) . . . . ?
C14 Eu1 N7 C8 -89.9(6) . . . . ?
C18 Eu1 N7 C8 -156.9(6) . . . . ?
O14 Eu1 N7 C21 121.8(5) . . . . ?
O22 Eu1 N7 C21 -29.6(5) . . . . ?
O18 Eu1 N7 C21 64.1(5) . . . . ?
O1W Eu1 N7 C21 13.7(6) . . . . ?
O2W Eu1 N7 C21 -88.0(6) . . . . ?
N10 Eu1 N7 C21 -111.7(5) . . . . ?
N1 Eu1 N7 C21 -168.6(5) . . . . ?
N4 Eu1 N7 C21 134.5(5) . . . . ?
C22 Eu1 N7 C21 -23.7(5) . . . . ?
C14 Eu1 N7 C21 150.6(5) . . . . ?
C18 Eu1 N7 C21 83.6(5) . . . . ?
C6 N7 C8 C9 -160.4(7) . . . . ?
C21 N7 C8 C9 80.2(9) . . . . ?
Eu1 N7 C8 C9 -36.3(8) . . . . ?
N7 C8 C9 N10 57.3(10) . . . . ?
C8 C9 N10 C11 83.7(9) . . . . ?
C8 C9 N10 Eu1 -47.2(8) . . . . ?
O14 Eu1 N10 C11 29.2(7) . . . . ?
O22 Eu1 N10 C11 -178.7(6) . . . . ?
O18 Eu1 N10 C11 -114.8(6) . . . . ?
O1W Eu1 N10 C11 131.0(5) . . . . ?
O2W Eu1 N10 C11 88.1(6) . . . . ?
N7 Eu1 N10 C11 -108.7(6) . . . . ?
N1 Eu1 N10 C11 9.2(5) . . . . ?
N4 Eu1 N10 C11 -49.5(6) . . . . ?
C22 Eu1 N10 C11 -159.4(6) . . . . ?
C14 Eu1 N10 C11 26.0(6) . . . . ?
C18 Eu1 N10 C11 -87.1(6) . . . . ?
O14 Eu1 N10 C9 158.6(5) . . . . ?
O22 Eu1 N10 C9 -49.3(5) . . . . ?
O18 Eu1 N10 C9 14.6(7) . . . . ?
O1W Eu1 N10 C9 -99.6(5) . . . . ?
O2W Eu1 N10 C9 -142.5(6) . . . . ?
N7 Eu1 N10 C9 20.7(5) . . . . ?
N1 Eu1 N10 C9 138.5(6) . . . . ?
N4 Eu1 N10 C9 79.9(5) . . . . ?
```

```
C22 Eu1 N10 C9 -30.0(5) . . . . ?
C14 Eu1 N10 C9 155.4(5) . . . . ?
C18 Eu1 N10 C9 42.3(7) . . . . ?
C9 N10 C11 C12 -166.8(7) . . . . ?
Eu1 N10 C11 C12 -37.3(9) . . . . ?
C13 N1 C12 C11 -164.7(7) . . . . ?
C2 N1 C12 C11 76.0(9) . . . . ?
Eu1 N1 C12 C11 -47.5(8) . . . . ?
N10 C11 C12 N1 57.8(10) . . . . ?
C12 N1 C13 C14 156.1(8) . . . . ?
C2 N1 C13 C14 -85.6(9) . . . . ?
Eu1 N1 C13 C14 36.9(8) . . . . ?
N1 C13 C14 O14 -32.7(12) . . . . ?
N1 C13 C14 N15 149.2(9) . . . . ?
N1 C13 C14 Eu1 -28.4(6) . . . . ?
O22 Eu1 C14 O14 73.0(9) . . . . ?
O18 Eu1 C14 O14 -32.2(7) . . . . ?
O1W Eu1 C14 O14 39.4(7) . . . . ?
O2W Eu1 C14 O14 110.4(7) . . . . ?
N10 Eu1 C14 O14 172.5(7) . . . . ?
N7 Eu1 C14 O14 -107.5(7) . . . . ?
N1 Eu1 C14 O14 -166.3(8) . . . . ?
N4 Eu1 C14 O14 -92.0(7) . . . . ?
C22 Eu1 C14 O14 37(2) . . . . ?
C18 Eu1 C14 O14 -46.2(7) . . . . ?
O14 Eu1 C14 N15 11.5(16) . . . . ?
O22 Eu1 C14 N15 85(2) . . . . ?
O18 Eu1 C14 N15 -21(2) . . . . ?
O1W Eu1 C14 N15 50.9(19) . . . . ?
O2W Eu1 C14 N15 121.9(19) . . . . ?
N10 Eu1 C14 N15 -175.9(19) . . . . ?
N7 Eu1 C14 N15 -95.9(19) . . . . ?
N1 Eu1 C14 N15 -155(2) . . . . ?
N4 Eu1 C14 N15 -80.4(19) . . . . ?
C22 Eu1 C14 N15 49(3) . . . . ?
C18 Eu1 C14 N15 -34.7(19) . . . . ?
O14 Eu1 C14 C13 -174.0(10) . . . . ?
O22 Eu1 C14 C13 -101.0(7) . . . . ?
O18 Eu1 C14 C13 153.7(5) . . . . ?
O1W Eu1 C14 C13 -134.6(5) . . . . ?
O2W Eu1 C14 C13 -63.6(5) . . . . ?
N10 Eu1 C14 C13 -1.5(6) . . . . ?
N7 Eu1 C14 C13 78.5(6) . . . . ?
N1 Eu1 C14 C13 19.7(5) . . . . ?
N4 Eu1 C14 C13 94.0(5) . . . . ?
C22 Eu1 C14 C13 -136.6(17) . . . . ?
C18 Eu1 C14 C13 139.7(5) . . . . ?
N15 C14 O14 Eu1 -175.0(7) . . . . ?
C13 C14 O14 Eu1 6.9(12) . . . . ?
O22 Eu1 O14 C14 -136.2(7) . . . . ?
O18 Eu1 O14 C14 148.3(7) . . . . ?
O1W Eu1 O14 C14 -138.3(7) . . . . ?
O2W Eu1 O14 C14 -65.2(7) . . . . ?
N10 Eu1 O14 C14 -9.1(8) . . . . ?
N7 Eu1 O14 C14 94.6(7) . . . . ?
```

```
N1 Eu1 O14 C14 11.0(7) . . . . ?
N4 Eu1 O14 C14 82.4(7) . . . . ?
C22 Eu1 O14 C14 -169.4(7) . . . . ?
C18 Eu1 O14 C14 131.9(7) . . . . ?
O14 C14 N15 C16 -2.7(16) . . . . ?
C13 C14 N15 C16 175.4(10) . . . . ?
Eu1 C14 N15 C16 -11(3) . . . . ?
C5 N4 C17 C18 -83.5(9) . . . . ?
C3 N4 C17 C18 159.1(7) . . . . ?
Eu1 N4 C17 C18 38.1(8) . . . . ?
N4 C17 C18 O18 -30.2(11) . . . . ?
N4 C17 C18 N19 152.4(8) . . . . ?
N4 C17 C18 Eu1 -29.4(6) . . . . ?
O14 Eu1 C18 O18 117.7(6) . . . . ?
O22 Eu1 C18 O18 -26.9(6) . . . . ?
O1W Eu1 C18 O18 45.0(6) . . . . ?
O2W Eu1 C18 O18 82.0(8) . . . . ?
N10 Eu1 C18 O18 -107.3(6) . . . . ?
N7 Eu1 C18 O18 -86.3(6) . . . . ?
N1 Eu1 C18 O18 174.9(6) . . . . ?
N4 Eu1 C18 O18 -161.1(7) . . . . ?
C22 Eu1 C18 O18 -41.0(6) . . . . ?
C14 Eu1 C18 O18 131.6(6) . . . . ?
O14 Eu1 C18 N19 114.2(19) . . . . ?
O22 Eu1 C18 N19 -30.4(19) . . . . ?
O18 Eu1 C18 N19 -3.5(16) . . . . ?
O1W Eu1 C18 N19 41.5(19) . . . . ?
O2W Eu1 C18 N19 79(2) . . . . ?
N10 Eu1 C18 N19 -110.8(19) . . . . ?
N7 Eu1 C18 N19 -89.8(19) . . . . ?
N1 Eu1 C18 N19 171.4(18) . . . . ?
N4 Eu1 C18 N19 -165(2) . . . . ?
C22 Eu1 C18 N19 -44.5(19) . . . . ?
C14 Eu1 C18 N19 128.1(19) . . . . ?
O14 Eu1 C18 C17 -61.2(5) . . . . ?
O22 Eu1 C18 C17 154.2(5) . . . . ?
O18 Eu1 C18 C17 -178.9(9) . . . . ?
O1W Eu1 C18 C17 -133.9(5) . . . . ?
O2W Eu1 C18 C17 -96.8(6) . . . . ?
N10 Eu1 C18 C17 73.9(6) . . . . ?
N7 Eu1 C18 C17 94.8(5) . . . . ?
N1 Eu1 C18 C17 -4.0(5) . . . . ?
N4 Eu1 C18 C17 20.0(4) . . . . ?
C22 Eu1 C18 C17 140.1(5) . . . . ?
C14 Eu1 C18 C17 -47.2(5) . . . . ?
N19 C18 O18 Eu1 178.6(6) . . . . ?
C17 C18 O18 Eu1 1.3(11) . . . . ?
O14 Eu1 O18 C18 -59.6(6) . . . . ?
O22 Eu1 O18 C18 153.7(6) . . . . ?
O1W Eu1 O18 C18 -132.5(7) . . . . ?
O2W Eu1 O18 C18 -124.8(6) . . . . ?
N10 Eu1 O18 C18 93.6(7) . . . . ?
N7 Eu1 O18 C18 87.6(6) . . . . ?
N1 Eu1 O18 C18 -6.2(7) . . . . ?
N4 Eu1 O18 C18 15.3(6) . . . . ?
```

```
C22 Eu1 O18 C18 137.5(6) . . . . ?
C14 Eu1 O18 C18 -49.6(7) . . . . ?
O18 C18 N19 C20 0.6(15) . . . . ?
C17 C18 N19 C20 178.0(9) . . . . ?
Eu1 C18 N19 C20 3(2) . . . . ?
C6 N7 C21 C22 162.6(7) . . . . ?
C8 N7 C21 C22 -77.9(8) . . . . ?
Eu1 N7 C21 C22 42.2(7) . . . . ?
N7 C21 C22 O22 -36.4(11) . . . . ?
N7 C21 C22 N23 146.1(8) . . . . ?
N7 C21 C22 Eu1 -32.7(6) . . . . ?
O14 Eu1 C22 O22 75.8(9) . . . . ?
O18 Eu1 C22 O22 119.4(7) . . . . ?
O1W Eu1 C22 O22 46.2(7) . . . . ?
O2W Eu1 C22 O22 -22.6(7) . . . . ?
N10 Eu1 C22 O22 -88.6(7) . . . . ?
N7 Eu1 C22 O22 -162.8(8) . . . . ?
N1 Eu1 C22 O22 -104.8(7) . . . . ?
N4 Eu1 C22 O22 175.5(6) . . . . ?
C14 Eu1 C22 O22 48(2) . . . . ?
C18 Eu1 C22 O22 131.8(7) . . . . ?
O14 Eu1 C22 N23 85(2) . . . . ?
O22 Eu1 C22 N23 8.9(18) . . . . ?
O18 Eu1 C22 N23 128(2) . . . . ?
O1W Eu1 C22 N23 55(2) . . . . ?
O2W Eu1 C22 N23 -14(2) . . . . ?
N10 Eu1 C22 N23 -80(2) . . . . ?
N7 Eu1 C22 N23 -154(2) . . . . ?
N1 Eu1 C22 N23 -96(2) . . . . ?
N4 Eu1 C22 N23 -176(2) . . . . ?
C14 Eu1 C22 N23 57(3) . . . . ?
C18 Eu1 C22 N23 141(2) . . . . ?
O14 Eu1 C22 C21 -98.9(6) . . . . ?
O22 Eu1 C22 C21 -174.7(10) . . . . ?
O18 Eu1 C22 C21 -55.3(5) . . . . ?
O1W Eu1 C22 C21 -128.5(5) . . . . ?
O2W Eu1 C22 C21 162.6(5) . . . . ?
N10 Eu1 C22 C21 96.6(5) . . . . ?
N7 Eu1 C22 C21 22.4(4) . . . . ?
N1 Eu1 C22 C21 80.5(6) . . . . ?
N4 Eu1 C22 C21 0.8(5) . . . . ?
C14 Eu1 C22 C21 -126.5(17) . . . . ?
C18 Eu1 C22 C21 -42.9(5) . . . . ?
N23 C22 O22 Eu1 -176.8(7) . . . . ?
C21 C22 O22 Eu1 6.0(11) . . . . ?
O14 Eu1 O22 C22 -133.3(6) . . . . ?
O18 Eu1 O22 C22 -58.1(7) . . . . ?
O1W Eu1 O22 C22 -131.2(7) . . . . ?
O2W Eu1 O22 C22 158.2(7) . . . . ?
N10 Eu1 O22 C22 86.0(7) . . . . ?
N7 Eu1 O22 C22 13.9(6) . . . . ?
N1 Eu1 O22 C22 97.3(7) . . . . ?
N4 Eu1 O22 C22 -5.5(8) . . . . ?
C14 Eu1 O22 C22 -166.4(6) . . . . ?
C18 Eu1 O22 C22 -49.8(7) . . . . ?
```

```
O22 C22 N23 C24 -2.9(14) . . . . ?
C21 C22 N23 C24 174.4(9) . . . . ?
Eu1 C22 N23 C24 -10(3) . . . . ?
O12 S1 C1S F12 170.7(11) . . . . ?
O11 S1 C1S F12 50.9(11) . . . . ?
O13 S1 C1S F12 -71.1(11) . . . . ?
O12 S1 C1S F13 -66.7(10) . . . . ?
O11 S1 C1S F13 173.5(9) . . . . ?
O13 S1 C1S F13 51.5(10) . . . . ?
O12 S1 C1S F11 49.6(11) . . . . ?
O11 S1 C1S F11 -70.1(10) . . . . ?
O13 S1 C1S F11 167.8(9) . . . . ?
O23 S2 C2S F22 173.2(14) . . . . ?
O21 S2 C2S F22 52.1(17) . . . . ?
O22 S2 C2S F22 -63.2(17) . . . . ?
O23 S2 C2S F23 53.7(16) . . . . ?
O21 S2 C2S F23 -67.3(16) . . . . ?
O22 S2 C2S F23 177.4(14) . . . . ?
O23 S2 C2S F21 -64.9(16) . . . . ?
O21 S2 C2S F21 174.1(14) . . . . ?
O22 S2 C2S F21 58.8(17) . . . . ?
O22' S2' C2S' F21' -179.0(14) . . . . ?
O23' S2' C2S' F21' -56.5(15) . . . . ?
O21' S2' C2S' F21' 60.4(15) . . . . ?
O22' S2' C2S' F23' -59.1(15) . . . . ?
O23' S2' C2S' F23' 63.3(14) . . . . ?
O21' S2' C2S' F23' -179.8(13) . . . . ?
O22' S2' C2S' F22' 60.9(15) . . . . ?
O23' S2' C2S' F22' -176.7(13) . . . . ?
O21' S2' C2S' F22' -59.7(15) . . . . ?
O33 S3 C3S F32 64.2(16) . . . . ?
O31 S3 C3S F32 -55.2(17) . . . . ?
O32 S3 C3S F32 -176.0(14) . . . . ?
O33 S3 C3S F33 -173.0(15) . . . . ?
O31 S3 C3S F33 67.6(18) . . . . ?
O32 S3 C3S F33 -53.1(17) . . . . ?
O33 S3 C3S F31 -54.3(15) . . . . ?
O31 S3 C3S F31 -173.7(14) . . . . ?
O32 S3 C3S F31 65.6(14) . . . . ?
O31' S3' C3S' F32' -60.4(16) . . . . ?
O33' S3' C3S' F32' 59.6(16) . . . . ?
O32' S3' C3S' F32' 179.0(14) . . . . ?
O31' S3' C3S' F33' 168.4(15) . . . . ?
O33' S3' C3S' F33' -71.5(16) . . . . ?
O32' S3' C3S' F33' 47.9(16) . . . . ?
O31' S3' C3S' F31' 57.3(15) . . . . ?
O33' S3' C3S' F31' 177.3(13) . . . . ?
O32' S3' C3S' F31' -63.3(15) . . . . ?

_diffrn_measured_fraction_theta_max    0.988
_diffrn_reflns_theta_full              25.00
_diffrn_measured_fraction_theta_full   0.988
_refine_diff_density_max    2.051
_refine_diff_density_min   -2.021
_refine_diff_density_rms    0.169
```

Publications